Open Effective Field Theories for primordial cosmology : dissipation, decoherence and late-time resummation of cosmological inhomogeneities

Thomas Colas

université PARIS-SACLAY

Open Effective Field Theories for primordial cosmology

Dissipation, decoherence and late-time resummation of cosmological inhomogeneities

Systèmes quantiques ouverts pour la cosmologie primordiale

Dissipation, décohérence et effets séculiers des inhomogénéités cosmologiques

Thèse de doctorat de l'université Paris-Saclay

École doctorale n°564 : Physique en Île-de-France (PIF)
Spécialité de doctorat : Physique
Graduate School : Physique, Faculté des sciences d'Orsay

Thèse préparée à l'**Institut d'astrophysique spatiale** (Université Paris-Saclay, CNRS),
sous la direction de **Julien GRAIN**, chargé de recherche au CNRS,
et la co-direction de **Vincent VENNIN**, chargé de recherche au CNRS

Thèse soutenue à Paris-Saclay, le 30 août 2023, par

Thomas COLAS

Composition du jury

Membres du jury avec voix délibérative

Karim NOUI Professeur, IJClab, Université Paris-Saclay	Président
Yuko URAKAWA Maître de conférence (eq. HDR), KEK, Tsukuba University	Rapporteure et Examinatrice
Nicola BARTOLO Maître de conférence (eq. HDR), Universita di Padova	Rapporteur et Examinateur
Cliff BURGESS Professeur, McMaster University	Examinateur
Claudia DE RHAM Professeure, Imperial College London	Examinatrice
Mattia WALSCHAERS Chargé de recherche, LKB, Sorbonne Université	Examinateur

THESE DE DOCTORAT
NNT : 2023UPASP075

université PARIS-SACLAY | ÉCOLE DOCTORALE Physique en Île-de-France (PIF)

Title : Open Effective Field Theories for primordial cosmology : Dissipation, decoherence and late-time resummation of cosmological inhomogeneities

Keywords : Primordial cosmology, inflation, Effective Field Theories, Open Quantum Systems, Quantum Information Theory

Abstract : This thesis develops the implementation of Open Effective Field Theories in primordial cosmology. Offering a unique window onto unknown physics, primordial cosmology faces uncertainties regarding extensions to the minimal framework of single-field slow-roll inflation. Open Effective Field Theories aim at incorporating the effects of hidden sectors onto this minimal framework. By capturing non-unitary effects such as dissipation and decoherence, they shed new lights on the physics at play in the early universe.

In an introductary part, we provide a pedagogical introduction to the implementation of Open Effective Field Theories in cosmology. Particular highlights are made on the approximation schemes and their regime of validity. We present how to access the observables of the system and its quantum information properties and discuss the late-time resummation performed by Open Effective Field theories.

In a second part, the results obtained during the Ph.D. are gathered. First, we derive the quantum states of a linear two-field system. It allows us to discuss the dynamical generation of entanglement and provides a theoretical framework for the study of decoherence during inflation. Then, Open Effective Field Theories are benchmarked with an exactly solvable model. In particular, we evaluate their ability to implement non-perturbative resummation in cosmology. Finally, we apply these techniques to study the decoherence induced in the early universe by entropic perturbations onto the curvature perturbations observed in the cosmic microwave background.

Titre : Systèmes quantiques ouverts pour la cosmologie primordiale : Dissipation, décohérence et effets séculiers des inhomogénéités cosmologiques

Mots clés : Cosmologie primordiale, inflation, théorie effective des champs, systèmes quantiques ouverts, théorie de l'information quantique

Résumé : Cette thèse vise à l'implémentation de la théorie des systèmes quantiques ouverts en cosmologie primordiale. Si cette dernière peut nous offrir un accès sans pareil à la physique des hautes énergies, elle est également confrontée à l'heure actuelle à un ensemble d'incertitudes concernant les possibles extensions au modèle minimal d'inflation à un champs. La théorie des systèmes quantiques ouverts vise à incorporer de manière effective et systématique ces incertitudes dans la description d'un régime connu. Son implémentation nous aiderait à comprendre le rôle des phénomènes dissipatifs et de la décohérence dans l'univers primordial.

Dans une première partie, une introduction pédagogique à l'implémentation de la théorie des systèmes quantiques ouverts en cosmologie est proposée. Une attention particulière est portée sur la caractérisation des approximations. Le calcul des observables du système est expliqué et mis en relation avec des notions de théorie de l'information quantique. Une discussion des capacités de re-sommation de ces méthodes est fournie.

La seconde partie du manuscrit est dédiée aux résultats obtenus durant le doctorat. Les états quantiques des systèmes linéaires à deux champs sont caractérisés. Ce travail fournit une base théorique à la compréhension de la décohérence durant l'inflation. Dans le cadre d'un modèle intégrable, la confrontation de résultats exacts à ceux provenant d'une théorie effective nous permet d'évaluer sa capacité à implémenter une re-sommation non-perturbative en espace-temps courbe. Les méthodes acquises sont enfin utilisées pour déterminer si la présence de perturbations entropiques décohère les fluctuations adiabatiques observées dans le fond diffus cosmologique.

Acknowledgements

Most of all, I would like to thank my supervisors Julien Grain and Vincent Vennin for these three years where they have been continuously guiding me through research. I have no word to express my gratitude for their patience, kindness and support. Beyond research, they have been lively companions and examples of what could be life as a physicist and I thank them for the passion they managed to transmit.

My thoughts then go to my current collaborators Suddhasattwa Brahma, Jaime Calderón-Figueroa and Gregory Kaplanek from whom I learned a lot. I thank them for offering such a pleasant environment for doing research. I also thank my former collaborators Guido D'Amico, Leonardo Senatore and Pierre Zhang for accompanying me through my first steps in research and giving me the will to pursue my journey.

Many thanks to the ones I have met during visits, conferences, workshops and summer schools for the insightful discussions which deeply influenced my vision of physics. Especially, I would like to thank Denis Comelli, Bei-Lok Hu, Christian Käding, David Kaiser, Alberto Nicolis, Enrico Pajer, Federico Piazza, Sébastien Renaux-Petel and Marco Schirò for their consideration. Also, many thanks to my reporters Nicola Bartolo and Yuko Urakawa as well as all the members of my thesis jury Cliff Burgess, Karim Noui, Claudia de Rham and Mattia Walschaers for their time and interest in my work.

These last three years have been imprinted from the work environment in which I have been immersed and I deeply thank all the members of IAS, APC and LPENS with whom I had the chance to interact with. Especially, I would like to express my gratitude to the IAS cosmology group and administration who welcomed me from the first day of my Ph.D. to the last. Finally, my thoughts go to my office mates and fellow Ph.D. students, Danilo, Chiara and Vadim, Valentin and Pilar, Hubert and Marion, Amaury and Denis for the joy they bring everyday.

At last, some words go to the ones who share my life outside the lab. I would like to warmly thank all the teachers who showed me the fascinating aspects of physics, especially my high-school teachers Christophe Lagoute and Serge Castaing and their *Club CNRS* without whom I would not be writing this thesis. To my friends, from Castanet to Paris, thank you for the warmth you bring in my heart. To my parents, Pierre and Anne, thank you for all you gave me. To Marie, thank you for being a constant source of happiness.

Maintenant, les deux branches de la parabole se rejoignaient; la *mors philosophica* s'était accomplie: l'opérateur brûlé par les acides de la recherche était à la fois sujet et objet, alambic fragile et, au fond du réceptacle, précipité noir. L'expérience qu'on avait cru pouvoir confiner à l'officine s'était étendue à tout. S'en suivait-il que les phases subséquentes de l'aventure alchimique fussent autre chose que des songes, et qu'un jour il connaîtrait aussi la pureté ascétique de l'Œuvre au Blanc, puis le triomphe conjugué de l'esprit et des sens qui caractérise l'Œuvre au Rouge? Du fond de la lézarde naissait une Chimère.

L'Œuvre au Noir
Marguerite Yourcenar

Introduction

One of the most fascinating predictions of the standard model of cosmology is to trace back the origin of all the structures we today observe in the universe - from galaxies, clusters, voids and filaments up to the tiny temperature anisotropies of the Cosmic Microwave Background (CMB) - to quantum fluctuations of the gravitational and matter fields in the early universe. Indeed, inflation is an early phase of accelerated expansion that took place at very high energy. During this era, quantum fluctuations of the gravitational and matter fields generate small deviations from perfect homogeneity and isotropy which ultimately grow under gravitational instability into today's Large-Scale Structures (LSS) we observe in the sky.

This feature makes primordial cosmology a privileged playground to test the interface between general relativity and quantum field theory at very high energy. Since the energy scales involved in inflationary processes are many orders of magnitude above the one accessible in collider experiments, inflation offers a promising window onto beyond-standard-model physics. The intricate nature of the interactions between matter and gravitation during inflation also leads to experimentally testable predictions for a linear version of quantum gravity. Quantum aspects of inflationary model hence provide theoretical data useful in the quest for unified frameworks between quantum mechanics and gravitation.

The downside of the fact that inflation takes place at energy scales where particle physics remains mostly unknown is that the physical nature of the fields driving inflation, their number and their relations are still unclear. The tremendous improvement of cosmological data in the last decades through the exquisite measurements of the CMB and the very large volumes sampled by galaxy surveys corroborate a minimal scenario known as single-field slow-roll inflation. Despite this success and the impressive precision of modern data, they do not yet reach enough constraining power to single out a more precise scenario and a wide class of models remain compatible with these observations.

Effective Field Theories (EFTs) aim at providing a systematic way to consider extensions to a known regime, incorporating the knowledge of unknown physics in a parametrically controlled manner. New data enable to constrain the parameters of the EFTs, offering a guideline for constructing fundamental descriptions. Their implementation in primordial cosmology leads to a unified description of the class of models describing single-field slow-roll inflation. Beyond this framework, other extensions such as multifield scenarios, may require the development of new tools due to the lack of symmetries and the absence of energy conservation. In order to grasp the implications of hidden sectors at a quantum level, the formalism needs to incorporate non-unitary effects such as dissipation and decoherence. To achieve this goal, Open EFT uses techniques developed in quantum optics, in the context of Open Quantum System (OQS) theory, to parametrise poorly specified environ-

ments. It is the main purpose of this thesis to develop the implementation of Open EFTs in primordial cosmology. At the crossroads of cosmology, high-energy physics, quantum optics and quantum information theory, it aims at providing access to a so far unknown regime of the inflationary dynamics. In particular, this thesis aims at understanding how, by capturing non-unitary effects such as dissipation and decoherence, Open EFTs shed new lights on the physics at play in the early universe.

This manuscript is a thesis by publication which presents the works realised at the Institut d'Astrophysique Spatiale (IAS), the Astroparticule & Cosmologie laboratory (APC) and the Laboratoire de Physique de l'Ecole Normale Supérieure (LPENS) between September 2020 and September 2023 under the direction of Julien Grain and Vincent Vennin. Part I first contains a brief presentation of EFTs and introduces the main aspects of inflation. Then, the rest of Part I aims at motivating the use of Open EFTs in primordial cosmology and at providing the reader the conceptual and technical tools to develop these methods by his or her own. Intended to be a guided tour, this presentation serves as a basis for the understanding of the results presented in Part II. This second part collects the research articles published during the thesis.

Contents

Part I

Effective Field Theories and Cosmology

Outline

In this first part, we provide a pedagogical introduction to the implementation of Open EFTs in cosmology. Far from being exhaustive, this introduction aims at presenting the motivations for the development of Open EFTs techniques and a roadmap for those who would like to develop these methods. Chapter 1 introduces the concept of EFT and motivates its extension to non-equilibrium and open dynamics. Primordial cosmology is introduced in Chapter 2 which emphasises the role of the early universe as a window onto new physics. Finally, Chapter 3 proposes a guided tour of Open EFT techniques in primordial cosmology, illustrating computations through concrete examples. Readers familiar with either EFTs or primordial cosmology may skip Chapters 1 or 2 and directly jump into the introduction of Open EFT techniques in Chapter 3.

Chapter 1

Effective Field Theories

In this Chapter, we briefly introduce Effective Field Theories and motivate their use in the rest of the manuscript. Only a brief and partial overview of the vast literature on the topic is reviewed, based on the following articles, books and lecture notes [1–12].

Physical objects do not behave the same depending on the scales probed. For instance, dark matter is ubiquitously known as being fundamentally described by a collisionless fluid due to its weakly interacting nature. Yet, when coarse-grained on large cosmological scales, its behaviour is rather captured by a dissipative medium with the viscosity of chocolate syrup [3, 5]. This idea may seem counterintuitive, yet, it is vastly similar to the journey from H_2O molecules to the ocean water. Just as dark matter, phases of matter - liquid, solid, gazeous - share an ensemble of properties vastly independent of their fundamental components, suggesting a high degree of universality.

Effective Field Theories (EFTs) are an emphasis on these universal properties. They highlight the features shared by a class of models regardless of their microphysical details. These features are captured through a unified description organised in terms of symmetries and scale hierarchies. In this sense, EFTs look for a minimal and systematic descriptions. They allow us to understand when the microphysical details become relevant. Turned it around, they may indicate optimal strategies to probe the fundamental structure of a theory in the presence of hierarchies of scales. Hence, they have become central tools in a number of fields of research from biophysics to cosmology.

The EFT program is often considered from two complementary perspectives:

1. The *bottom-up approach* aims at understanding how unknown physics manifests itself at a given scale. Making use of the symmetries and scale hierarchies, it constructs a controllable theory in which the desired precision can be reached by including higher and higher corrections. In this sense, unknown physics is controlled by a finite number of parameters known as *Wilsonian coefficients* one has to fit to the data. These coefficients capture the imprint

of the unknown physics onto the low-energy EFT. For instance, the above-mentioned dark matter viscosity appearing in the context of the EFT of the Large-Scale Structures (EFTofLSS) has been measured in cosmological data and simulations to be of order 20 pascal-seconds [3, 5]. It encodes the complicated dynamics occurring at galactic scales that the theory does not resolve. If a better precision is required, one can push further the EFT expansion, in which case a higher number of Wilsonian coefficients is needed to be fitted to the data.

2. The *top-down approach* aims at understanding how a given theory manifests itself in a given regime of scales at low energy. For instance, even if the Standard Model of particle physics provides a more fundamental description in which the weak force is mediated through the W and Z bosons, at sufficiently low-energy, Fermi's theory of weak interactions works equally well, up to small corrections, and has a much simpler description in which gauge bosons have been integrated out. The obtained EFT captures the physics of the theory at low energy and helps us to derive observational predictions in this regime. EFTs can also capture emergent phenomena, such as collective behaviour only appearing in the low-energy description of the theory. This is for instance how, starting from a time-reversal symmetry in a microscopic theory, an arrow of time can emerge in the thermodynamic limit where the theory fulfills a positive entropy production [13].

The EFT program aims at tackling these two points. In the case where the fundamental theory is known, deriving a low energy EFT allow us to highlight the relevant physics at the scale experiments are built, which facilitates the detection protocols. When the fundamental description is unknown, EFTs allow us to apprehend how new physics will appear when we will probe new regimes of scales. In this sense, EFTs are "*dialectics*": they aim at establishing a set of rules to construct a dialogue between a known and an unknown regime.

EFTs have become central objects in the search for new physics. For instance, the *Standard Model EFT* (SMEFT) considers the SM of particle physics as a low-energy limit of a more fundamental theory. By encoding the effects of unknown physics onto the observables accessible in colliders, particle physicists explore the possible signals we might expect and help us designing new experiments. SM corrections have to fulfill many consistency constraints such as the fact that Lorentz invariance requires fermions to always come in pairs. Using similar arguments, one can construct the various building blocks of the theory from which particle physicists derive interesting phenomenological consequences [14]. Similarly, various hints suggest that *General Relativity* (GR) might correspond to the low-energy limit of some more fundamental theory [1, 6]. The *EFT of gravity* [1, 15] considers the metric $g_{\mu\nu}$ describing the geometry of space-time and apply the general covariance principle, that is the invariance of the theory under local change of coordinates, to construct the most general embedding of GR. Out of second-order derivatives of the metric $g_{\mu\nu}$, one can construct a geometrical object known as the *Riemann curvature tensor* $R_{\mu\nu\rho\sigma}[g]$ from which a generic action [1] (see also [16])

$$S = -\int \mathrm{d}^4x\sqrt{-g}\left[\Lambda + \frac{M_{\mathrm{Pl}}^2}{2}R + c_1R^2 + c_2R_{\mu\nu}R^{\mu\nu} + \cdots\right] \tag{1.1}$$

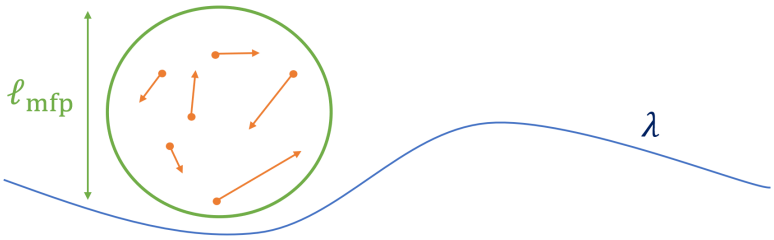

Figure 1.1: The hydrodynamical description aims at modelling the long wavelength regime where $\lambda \gg \ell_{\rm mfp}$ the mean free path, over which the probability of collision is almost certain. Because of the high probability of collisions in this regime, the microscopic description of a gas of interacting particles becomes practically unsolvable which calls for effective approaches.

is obtained out of its contractions $R_{\mu\nu} = R^{\rho}{}_{\mu\rho\nu}$ and $R = R^{\mu}{}_{\mu}$, the so-called *Ricci tensor* and *scalar*. In the above action, $M_{\rm Pl}$ is the Planck mass and Λ the cosmological constant. The point here is to illustrate that, just as the SM of particles physics, GR can be embedded into an EFT framework as it corresponds to the first two terms in the above expansion. The higher-order terms controlled by the Wilsonian coefficients c_1 and c_2 contain four derivatives of the metric and control the extensions to GR. Finally, the dots contain an infinite tower of contributions known as the *derivative expansion* which captures higher and higher number of derivatives acting on the metric. Even if the above construction might need extra work (e.g. dealing with ghosts), EFTs provide a systematic way to account for extensions around a given framework.

1.1 Hydrodynamics of a perfect fluid

Let us now illustrate the EFT construction in a concrete example by considering what is probably the oldest EFT ever made: *hydrodynamics*. More precisely, we look for the hydrodynamical description of an ensemble of weakly coupled particles in the thermodynamic (large number of particles) limit, based on A. Nicolis lectures [7]. We aim at describing the long-wavelength behaviour of the theory, for $\lambda \gg \ell_{\rm mfp}$, where $\ell_{\rm mfp}$ is the mean free path, that is the distance over which we expect one collision event, see Fig. 1.1. Along a distance $\lambda \gg \ell_{\rm mfp}$, the probability of collisions is then high and the description of the theory as a microscopic gas of interacting particles becomes intractable. Moreover, collective behaviours such as sound waves and vortices emerge of the long-wavelength description.

Making use of the symmetries obeyed by fluids, a Wilsonian EFT description is able to capture the dynamics of the hydrodynamic modes [4]. It describes a *perfect fluid*, that is a fluid with no viscosity, traditionally described in terms of the mass density $\rho(\boldsymbol{x}, t)$ and the velocity $\boldsymbol{v}(\boldsymbol{x}, t)$. For non-relativistic systems in which $|\boldsymbol{v}(\boldsymbol{x}, t)| \ll c$, the system is described by the continuity and Euler equation

$$\dot{\rho} + \boldsymbol{\nabla}.(\rho \boldsymbol{v}) = 0 \tag{1.2}$$

$$\rho \dot{\boldsymbol{v}} + \rho\,(\boldsymbol{v}.\boldsymbol{\nabla})\,.\boldsymbol{v} = -\boldsymbol{\nabla} p \tag{1.3}$$

where we assume no external forces acting on the fluid, together with an equation

of state which specifies the nature of the fluid and closes the system

$$p(\boldsymbol{x},t) = p_{\text{eq}}\left[\rho(\boldsymbol{x},t)\right]. \tag{1.4}$$

There is an approximation hidden above: the perfect fluid assumption implies the existence of an instantaneously reached local thermal equilibrium, which allows us to express the pressure $p(\boldsymbol{x},t)$ under this form.

Note that cosmologists are very familiar with the relativistic version of the above setting. Adopting the mostly-positive signature, $\rho(x)$ now represents the total energy density in the local rest frame and $u^\mu(x) = \gamma(v)(1,\boldsymbol{v})$ is the four-velocity, with $\gamma(v) \equiv (1-v^2)^{-1/2}$ the Lorentz factor in natural units where $c = 1$. The stress-energy tensor of the perfect fluid writes

$$T^{\mu\nu}_{\text{p.f.}} = \left[\rho(x) + p(x)\right] u^\mu(x) u^\nu(x) + p(x) g^{\mu\nu} \tag{1.5}$$

where $g^{\mu\nu}$ the space-time metric. Upon specifying an equation of state $p = p_{\text{eq}}(\rho)$, one can derive an equivalent set of equations using the conservation of the stress energy tensor $\nabla_\mu T^{\mu\nu} = 0$. Hence, the arguments presented in this section can be easily generalized to relativistic settings.

1.1.1 Symmetries and derivative expansion

In order to construct an EFT for the hydrodynamical modes, we need to identify the relevant degrees of freedom of the problem and the symmetries. It appears that ρ and $\boldsymbol{v}$ (or equivalently ρ and u^μ) are not the most convenient degrees of freedom as they are built-out quantities (the first two moments the Bogolyubov hierarchy) which cannot be straightforwardly embedded in a Lagrangian description. We rather look for *positional degrees of freedom* which help us keep track of infinitesimal volume elements. The idea given in [7] consists in dropping coloured confetti in the fluid then following their trajectories in order to access the deformation of the medium. It follows that the medium is completely characterised by specifying the dynamics of three scalar fields (ϕ^1,ϕ^2,ϕ^3) which define the comoving coordinate frame. This is the *Eulerian* approach of fluid mechanics where one specifies the comoving coordinates of a fluid element $\phi^I(x^i,t)$ for $I = 1,2,3$ labelling the comoving space and $i = 1,2,3$ labelling the physical space. An equivalent description, the *Lagrangian* description, consists in reverting this relation and considers $x^i(\phi^I,t)$ instead. Yet, it turns out that the Eulerian approach is particular fruitful in understanding the role played by symmetries. A convenient choice of comoving coordinates consists in considering that at rest/at equilibrium, the scalar fields are aligned with an orthogonal set of axes which matches the coordinate system under consideration, see Fig. 1.2. Formally, we write

$$\left\langle \phi^I(x) \right\rangle_{\text{eq}} = x^I \tag{1.6}$$

for $I = 1,2,3$.

It clearly appears that the dynamics of the $\phi^I(x)$ fully constrains the evolution of the fluid. Hence, we look for a least action principle based on

$$S_{\text{fluid}} = S\left[\phi^I\right]. \tag{1.7}$$

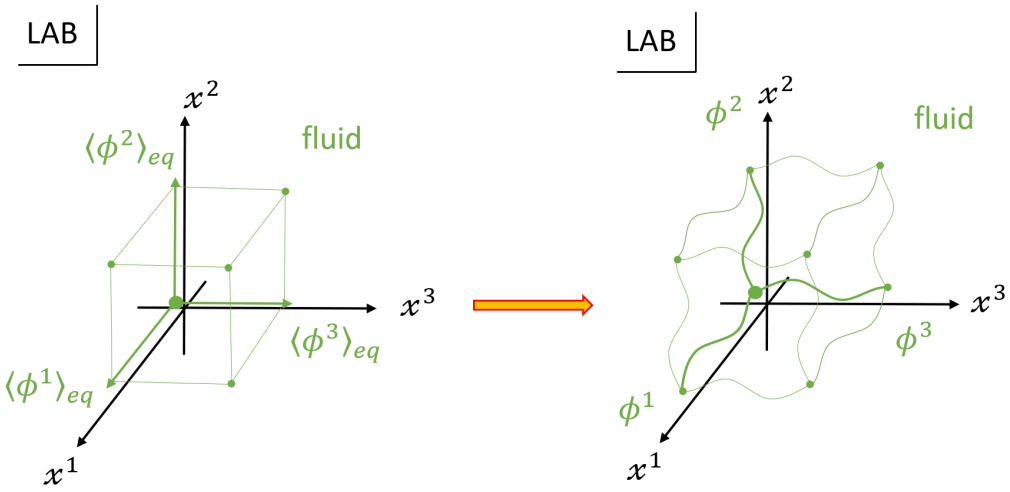

Figure 1.2: *Left:* A convenient choice of comoving coordinates consists in the ones which matches the coordinate system at equilibrium. *Right:* When the fluid experiences a deformation, it can be described in terms of the displacement of the comoving coordinates. Hence, the dynamics of the three scalar fields $\phi^I(x)$ fully characterise the evolution of the fluid.

In order to constrain this action, we now need to consider the symmetries of the system we want to describe. From the viewpoint of an observer immersed deep into the sea (far from the boundary surface of the fluid), the medium looks the same in all directions. Hence, we want Eq. (1.6) to describe a spatially *homogeneous* and *isotropic* state. Under spatial translation and rotation, the coordinate system transforms as

$$x^i \to x^i + a^i \tag{1.8}$$
$$x^i \to \boldsymbol{R}^i{}_j . x^j \tag{1.9}$$

where $a^i \in \mathbb{R}$ and $\boldsymbol{R} \in \mathrm{SO}(3)$. For Eq. (1.6) to hold, we need to impose an internal set of symmetries

$$\phi^I(x) \to \phi^I(x) + a^I \tag{1.10}$$
$$\phi^I(x) \to \boldsymbol{R}^I{}_J . \phi^J(x). \tag{1.11}$$

Indeed, if x^i translates or rotates but $\phi^I(x)$ does not, the symmetry would be broken. Hence, by imposing the existence of internal symmetries, the linear combination of x and ϕ remains unbroken. It makes that the system is now very constrained: by combining Poincaré invariance and the shift symmetry from translation invariance, a minimal building block of the theory is made of

$$B^{IJ} = \partial_\mu \phi^I \partial^\mu \phi^J. \tag{1.12}$$

If we further enforce the invariance by rotation, the operators which may appear in S_{fluid} are constrained to be[1]

$$\det B, \qquad \mathrm{Tr}B, \qquad \mathrm{Tr}B^2. \tag{1.13}$$

[1]It appears that one can at most construct 3 invariant quantities in $3+1$ dimensions [4].

At this point, there is no difference between the fluid we construct and some isotropic solid such as jelly [17]. The peculiarity of fluids consists in their ability to deform adiabatically, at no price in terms of energy, unlike solids which experience transverse stresses. How can we enforce this property in our EFT construction? Let us consider the deformed comoving coordinates

$$\phi'^I(x) = \xi^I(x) \tag{1.14}$$

where the induced deformation is volume preserving $|\det \partial\xi/\partial x| = 1$. The ability of the fluid to deform adiabatically imposes that $\phi^I(x)$ and $\xi^I(x)$ have the same energy. This suggests a much stronger symmetry through the diffeomorphism invariance [4]

$$\phi^I \to \xi^I(\phi), \qquad \frac{\partial \xi^I}{\partial \phi^J} = 1 \tag{1.15}$$

from which we observe that

$$\det B \to \det B \left(\frac{\partial \xi^I}{\partial \phi^J}\right)^2 = \det B \tag{1.16}$$

remains invariant while the traces in Eq. (1.13) do not. This feature encodes the fundamental difference between fluids and isotropic solid and we are now in a position to write an action

$$S_{\text{fluid}} = \int \mathrm{d}^4x F(\det B) + \text{higher } \partial\text{'s} \tag{1.17}$$

where F is a generic function we will relate to the properties of the fluid. Note that in this description, we worked at lowest order in derivatives. This expansion is the consequence of the initial scale hierarchy $\lambda \gg \ell_{\text{mfp}}$. Indeed, it appears that in the long-wavelength regime

$$\partial^2 \sim \mathcal{O}\left(\frac{\ell_{\text{mfp}}^2}{\lambda^2}\right) \ll 1. \tag{1.18}$$

We can then truncate the expansion and the theory becomes predictive, that is it requires a finite number of parameters to fit the data and describe the outcome of an experiment.

1.1.2 Matching

Let us map this construction in the standard ρ and u^μ language. To do so, we need to compute the stress-energy tensor of the theory $T_{\mu\nu}$. We follow the standard procedure which consists in coupling the theory to a metric g such that

$$\mathrm{d}^4x \to \sqrt{-g}\mathrm{d}^4x \tag{1.19}$$

$$B^{IJ} \to g^{\mu\nu}\partial_\mu\phi^I\partial_\nu\phi^J, \tag{1.20}$$

$\sqrt{-g}$ being the square root of the determinant of the metric $g \equiv \det g_{\mu\nu}$. The stress-energy tensor is computed by functional derivative with respect to the metric

$$T_{\mu\nu} \equiv -\frac{2}{\sqrt{-g}}\frac{\delta S_{\text{fluid}}}{\delta g^{\mu\nu}}. \tag{1.21}$$

It leads to

$$T_{\mu\nu} = -2F'BB^{-1}_{IJ}\partial_\mu\phi^I\partial_\nu\phi^J + Fg_{\mu\nu} \tag{1.22}$$

where we use the notation $B \equiv \det B^{IJ}$. In order to compare with Eq. (1.5), we need to define the four-velocity in terms of the comoving scalars ϕ^I. Along the flow, u^μ follows the trajectory. It implies that u^μ is the vector field along which the ϕ^I's do not change, that is

$$u^\mu\partial_\mu\phi^I = 0. \tag{1.23}$$

A simple way to construct the four-velocity consists in first defining the current

$$J^\mu \equiv \epsilon^{\mu\nu\rho\sigma}\partial_\nu\phi^1\partial_\rho\phi^2\partial_\sigma\phi^3 \tag{1.24}$$

$$= \frac{1}{3!}\epsilon^{\mu\nu\rho\sigma}\epsilon_{IJK}\partial_\nu\phi^I\partial_\rho\phi^J\partial_\sigma\phi^K \tag{1.25}$$

where ϵ is the Levi-Civita tensor, such that the current fulfills by definition the property $J^\mu\partial_\mu\phi^I = 0$ thanks to the complete antisymmetry of ϵ. Then, it suffices to notice that $J^2 = -B$ to construct the normalized velocity field

$$u^\mu \equiv \frac{J^\mu}{\sqrt{B}}. \tag{1.26}$$

A sanity check consists in controlling the equilibrium limit in which Eq. (1.6) holds. In that case, we find that the fluid is at rest, that is $u^\mu = (1, \mathbf{0})$.

Finally, by noticing that

$$B^{-1}_{IJ}\partial_\mu\phi^I\partial_\nu\phi^J u^\mu = 0, \tag{1.27}$$

we deduce that $B^{-1}_{IJ}\partial_\mu\phi^I\partial_\nu\phi^J$ corresponds to the projector on the hypersurface orthogonal to u^μ, that is

$$B^{-1}_{IJ}\partial_\mu\phi^I\partial_\nu\phi^J = g_{\mu\nu} + u_\mu u_\nu. \tag{1.28}$$

It follows that the stress-energy tensor obtained in Eq. (1.22) can be written in the same form as the perfect fluid case (1.5). We conclude that the density and the pressure are defined as

$$\rho = -F(B) \tag{1.29}$$

$$p = F(B) - 2F'B. \tag{1.30}$$

The equation of state (1.4) can then be rewritten as an ordinary differential equation for the free function $F(B)$, that is

$$F - 2F'B = p_{\rm eq}(-F). \tag{1.31}$$

In summary, specifying an equation of state amounts to choose a function $F(B)$. It provides a matching condition between the microphysics defined by a field theory for the scalars ϕ^I and the macrophysics specified by the hydrodynamical description of (ρ, p). Measuring these parameters in an experiment fixes the EFT coefficients of the function $F(B)$.

Useful limits:

1. *Conformal fluid:* A fluid in a CFT possesses a stress-energy tensor obeying the conformal symmetry, that is $T^{\mu}_{\ \mu} = 0$. Injecting Eq. (1.22) into this equation, we obtain

$$\frac{F'}{F} = \frac{2}{3}\frac{1}{B} \qquad \Rightarrow \qquad F(B) = F_0 B^{2/3} \tag{1.32}$$

with F_0 a constant. One can then use Eq. (1.41) introduced below to compute the speed of sound and recover with no surprises $c_s^2 = 1/3$.

2. *Cosmological fluids:* In cosmology, we often encounter generic fluids obeying the equation of state $p_{\rm eq}(\rho) = w\rho$ where w is a constant. Injecting Eqs. (1.29) and (1.30) into this expression, we obtain

$$F - 2F'B = -wF \qquad \Rightarrow \qquad F(B) = F_0 B^{\frac{1+w}{2}}. \tag{1.33}$$

Hence, for a matter dominated era in which $w \simeq 0$, $F \propto B^{1/2}$, for a radiation dominated era in which $w = 1/3$, $F \propto B^{2/3}$ and finally, for a vacuum dominated universe where $w = -1+\epsilon$ with ϵ a small parameter, $F \propto \ln B$ at leading (non-trivial) order in ϵ.

3. *Non-relativistic limit:* The non-relativistic limit is obtained when $|\boldsymbol{v}| \ll 1$, $p \ll \rho$ and $c_s^2 \ll 1$. After consistently expanding the action (1.17) in this limit, we obtain at lowest order

$$S_{\rm NR} = \int \mathrm{d}^3\phi \mathrm{d}t \left[-\rho_m^0 + \frac{1}{2}\rho_m^0 \boldsymbol{v}^2 - U\left(\det \left.\frac{\partial x^i}{\partial \phi^I}\right|_t\right)\right] \tag{1.34}$$

where $\mathrm{d}^3\phi$ is the comoving volume, ρ_m^0 the rest mass. The second term corresponds to the kinetic energy and the third term is the comoving internal energy density, which captures the compression properties of the fluid. More details can be found in [7].

1.1.3 Perturbations

The *speed of sound* is commonly defined as

$$c_s^2 = \left.\frac{\mathrm{d}p}{\mathrm{d}\rho}\right|_{\rm eq} \tag{1.35}$$

and corresponds to a small perturbation around the equilibrium distribution. Can we see how this quantity appears in our field theory for the scalars ϕ^I? We consider a small perturbation

$$\phi^I(x) = x^I + \pi^I(x) \tag{1.36}$$

around the equilibrium distribution. It follows that

$$B^{IJ} = \delta^{IJ} + \partial^I \pi^J + \partial^J \pi^I + \partial_\mu \pi^I \partial^\mu \pi^J \tag{1.37}$$

from which we expand the determinant

$$B = \det\left(\delta^{IJ} + \partial^I \pi^J + \partial^J \pi^I + \partial_\mu \pi^I \partial^\mu \pi^J\right) = 1 + 2\boldsymbol{\nabla}.\boldsymbol{\pi} + \cdots \tag{1.38}$$

Finally, injecting this expression into the expanded action

$$S_{\text{fluid}} = \int \mathrm{d}^4x \left[F(1) + F'(1)\delta B + \frac{1}{2}F''(1)\delta B^2 + \cdots\right] \tag{1.39}$$

with $\delta B \equiv B - 1$, we obtain up to second order in π the perturbed action

$$S_{\text{fluid}} = \frac{1}{2}\int \mathrm{d}^4x \left[-2F'(1)\right]\left[\dot{\boldsymbol{\pi}}^2 - c_\pi^2 \left(\boldsymbol{\nabla}.\boldsymbol{\pi}\right)^2\right] + \cdots \tag{1.40}$$

where the dots contain total derivatives and terms of order $\mathcal{O}[(\partial\pi)^3]$. The speed of sound appearing in this expression is

$$c_\pi^2 \equiv \frac{2F''(1) + F'(1)}{F'(1)} = \left.\frac{\mathrm{d}p/\mathrm{d}B}{\mathrm{d}\rho/\mathrm{d}B}\right|_{B=1} = \left.\frac{\mathrm{d}p}{\mathrm{d}\rho}\right|_{\text{eq}} = c_s^2 \tag{1.41}$$

as expected. Finally, one can also notice that $-2F'(1) = (\rho + p)|_{\text{eq}}$ in terms of the hydrodynamical quantities.

The equations of motion are given by

$$\ddot{\boldsymbol{\pi}} - c_\pi^2 \boldsymbol{\nabla}\left(\boldsymbol{\nabla}.\boldsymbol{\pi}\right) = 0. \tag{1.42}$$

In Fourier space, we can decompose the field along the linear direction $\boldsymbol{\pi}_L$ parallel to $\boldsymbol{k}$ and the transverse direction $\boldsymbol{\pi}_T$ orthogonal to $\boldsymbol{k}$. The linear component describes the emergence of sound waves obeying

$$\ddot{\boldsymbol{\pi}}_L - c_\pi^2 k^2 \boldsymbol{\pi}_L = 0. \tag{1.43}$$

The transverse component is less easy to interpret as

$$\ddot{\boldsymbol{\pi}}_T = 0, \tag{1.44}$$

yet it has a very similar physical interpretation. A solution is given by

$$\boldsymbol{\pi}_T = \boldsymbol{c} + \boldsymbol{d}t \tag{1.45}$$

with $\boldsymbol{c}$ and $\boldsymbol{d}$ constant vectors orthogonal to the wavenumber $\boldsymbol{k}$. It turns out that $\boldsymbol{\pi}_T$ are the linear version of vortices in constant rotation [7].

Physical consequences can be derived from the above equations. First, we observe that the sound wave are massless and have a dispersion relation $\omega_L^2 = c_\pi^2 k^2$: it represents the energetic price it costs to excite a wave of frequency ω. On their side, vortices have a null frequency $\omega_T = 0$ from which we conclude that it costs no energy to excite a vortex. It can be an annoying feature if one wants to design a perturbative expansion as these excitations enter easily the turbulent regime [4].

What did we learn? With this example, we observed that the identification of the relevant degrees of freedom and the use of the symmetries fulfilled by the system allow us to describe a universal behaviour shared by a variety of fluids, invariably of the diversity of their microphysical details. Higher-order corrections capture the finer details of the impact of the microphysics on the large scales. The EFT formalism is a convenient way to highlight the common properties shared by a class of models and to parametrize theoretical uncertainties.

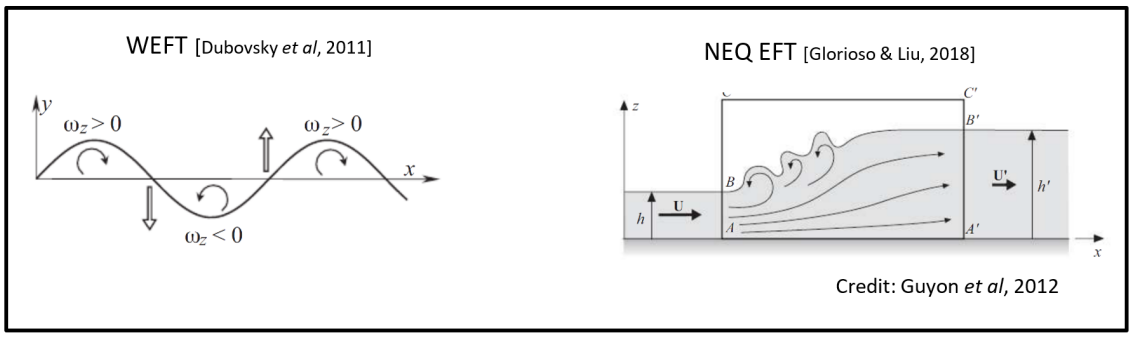

Figure 1.3: *Left:* The Wilsonian EFT approach of hydrodynamics presented in Sec. 1.1 based on [4] works remarkably well to describe the occurence of ocean waves in the deepwater regime [7]. *Right:* Yet, it is unable to describe turbulences appearing in dissipation cascades, which require the understanding of the non-equilibrium regime as developed in [8]. This manuscript aims at developing non-equilibrium and Open EFT techniques in cosmology and assess their role in the early universe. Images from [18].

1.2 Imperfect fluids and viscosity

In the previous section, we considered a perfect fluid. The instantaneously reached local thermal equilibrium, that is the immediate relaxation of the medium, allowed us to write an equation of state of the form Eq. (1.4), closing our dynamical system made of the continuity equation (1.2) and Euler equation (1.3). Yet, it is notoriously known that instantaneous equilibration is a crude approximation of the real world, in which fluids are imperfect and viscous. In general, at sufficiently long wavelength, the perfect-fluid assumption is well justified: viscosity is not an intrinsic property of the fluid but rather a kinematical property encoding the complicated reaction of the small scales onto the large wavelength regime. It implies that viscosity always vanishes at some scale [8]. Yet, it becomes a crucial ingredient for the description of turbulence, dissipation cascades and boundary layers [18], as illustrated in Fig. 1.3. A new term must be added to Euler equation, leading us to Navier-Stokes equation

$$\rho\dot{\boldsymbol{v}} + \rho\left(\boldsymbol{v}.\boldsymbol{\nabla}\right).\boldsymbol{v} = -\boldsymbol{\nabla}p + \eta\boldsymbol{\Delta}\boldsymbol{v} \tag{1.46}$$

where we again assume no external forces. The new parameter η in front of the Laplacian is the *viscosity* of the fluid. This apparently insignificant change represents in fact a tremendous challenge for theorists, as the Wilsonian EFT construction presented above is insufficient to describe this effect [8].

Dissipation has been investigated in a variety of contexts and the simplest intuitive way to describe it is through a stochastic *Langevin equation*

$$m\ddot{\phi}(t) + \gamma\dot{\phi}(t) + V'[\phi(t)] = \xi(t) \tag{1.47}$$

describing the Brownian motion [19–21] of a massive particle immersed into a medium, where ϕ the position of the Brownian particle of mass m, $V' = \partial V/\partial\phi$ the derivative of the potential energy, γ a damping coefficient and ξ a random noise acting on the particle. For the moment, let us consider $\xi(t)$ is given by a Gaussian

white noise obeying

$$\langle \xi(t) \rangle = 0, \qquad \langle \xi(t)\xi(t') \rangle = A\delta(t-t'), \tag{1.48}$$

where the brackets represent the noise average

$$\langle \mathcal{O}(\xi) \rangle = \int \mathcal{D}\xi \mathcal{P}[\xi]\mathcal{O}(\xi), \qquad \mathcal{P}[\xi] \equiv \exp\left[-\frac{1}{2A}\int \mathrm{d}t \xi^2(t)\right]. \tag{1.49}$$

The damping γ and noise ξ coefficients characterise the imprint of the surrounding medium onto the dynamics of the Brownian particle.

Let us illustrate what renders the description of dissipative dynamics hard to embed within the standard framework of Wilsonian EFT, based on [9]. When Eqs. (1.47) and (1.48) do not have explicit time dependence, the system enjoys a time-translation symmetry, that is Eq. (1.47) is covariant under $\phi(t) \to \phi'(t) = \phi(t+\epsilon)$ and $\xi(t) \to \xi'(t) = \xi(t+\epsilon)$. The authors of [9] asked what is the corresponding conserved charged associated with this time-translational symmetry. They notice that obviously, it is not the energy of the Brownian particle which is *not conserved* due to the existence of noise and dissipation, as seen in [9]

$$\frac{\mathrm{d}}{\mathrm{d}t}\left[\frac{1}{2}m\dot{\phi}^2 + V(\phi)\right] = -\gamma\dot{\phi}^2 + \xi\dot{\phi} \neq 0. \tag{1.50}$$

It is also instructive to notice that the associated Hamiltonian does not generate time-translations, as, introducing

$$H = \frac{P^2}{2m} + V(\phi) \tag{1.51}$$

where the momentum is $P = m\dot{\phi}$, the equations of motion for the canonical variables can be rewritten as

$$\dot{\phi} = \frac{\partial H}{\partial P}, \qquad \dot{P} = -\frac{\partial H}{\partial \phi} - \gamma P + \xi, \tag{1.52}$$

so that $\dot{P} \neq \{P, H\}_{\mathrm{PB}}$, where the brackets are the usual Poisson brackets which control the dynamical evolution of closed systems. Hence, dissipative dynamics do not follow the usual evolution rules of closed systems where the Hamiltonian is the generator of time-translations. It implies that the construction of an effective action as we did in Eq. (1.40) is not enough to describe the out-of-equilibrium dynamics in the presence of dissipation. The charge associated with the time-translational symmetry mentioned above is a more complicated object known as the *Fokker-Planck operator* [9] (or the *Liouvillian* for quantized systems) which effectively captures energy and information exchanges between the particle and the medium and generates the dissipative dynamics.

The understanding of *open systems* which can exchange energy and entropy with their environment is the main object of this manuscript. The ability to incorporate open and dissipative dynamics within an EFT framework is only recent, still making the object of active research under the name of *Non-Equilibrium* (see [8] for a review) or *Open EFTs* (see [22] for a review). One of the goals of this manuscript is to better understand the impact of these dynamics onto cosmological models. To do so, we

need to extend the existing tools in order to accommodate for the peculiarity of the cosmological dynamics. This is why in this thesis, we have first derived exact results in Chapter 4 to efficiently benchmark Open EFT methods in Chapter 5 and finally apply these techniques to a model of phenomenological interest in Chapter 6. Before presenting these results, we first need to introduce the physics at play in the early universe (Chapter 2) and the implementation of Open EFTs in cosmological settings (Chapter 3).

Conclusions:

Effective Field Theories aim at organising a dialogue between a known regime of scales and unknown physics. They encode new physics into a handful of EFT coefficients controlling higher-order operators organised in terms of the symmetries and the scale hierarchies of the problem. Observational constraints on these coefficients provide guidelines in constructing fundamental theories capturing the correct physics at the scale considered. In particular, it allows us to identify universal behaviours which do not depend on the microphysical details of the theory. We illustrated this principle by deriving a Wilsonian EFT describing the hydrodynamics of perfect fluids. The theory works remarkably well to describe the occurence of ocean waves in the deepwater regime and the emergence of vortices. Yet, it is unable to capture dissipative effects such as energy cascades and turbulence, that are crucial for a wide range of physical phenomena. In this case, the formalism has to be extended to capture energy and entropy exchanges between the system and its surroundings, which lead to the concept of *Non-Equilibrium* and *Open EFTs*. The goal of this thesis is to implement these techniques in cosmology and understand the role of open dynamics onto the physics of the early universe.

Chapter 2

The early-universe promise

In this Chapter, we discuss the physics at play in the early universe and its connection with new physics. Far from providing a self-contained introduction to primordial cosmology for which we refer to [6, 23–25], we rather highlight the motivations that sustain the construction of the manuscript.

The EFT perspective is reassuring: we gradually learn new physics as we probe new regimes. It can also be depressing: the only way to evade far from the known landscape seems out-of-reach. Where should we look for? Inflation, known as the main paradigm describing the early universe, might be an interesting candidate as it:

1. Takes place at high energy, which raises the hope of observing the effect of higher-order operators in the Wilsonian EFT perspective;

2. Transfers small-scale fluctuations into large-scale inhomogeneities, generating an interplay between the UV and the IR;

3. Is unconstrained enough so that it may contain hidden sectors playing the role of cosmological environments.

Hence, from the EFT perspective, inflation looks like an interesting place to look for extensions to the standard models of particle physics and cosmology. In this Section, we present an overview of "the early-universe promise". Let us first review the observational motivations for what is today known as the standard model of cosmology. We then discuss the physical picture it provides of the early universe. We finally develop possible places where to look for new physics during inflation. The discussion serves as a starting point in the perspective of constructing EFTs to handle these extensions.

2.1 A Standard Model for cosmology

Cosmology has entered a golden era where numerous experiments probe different facets of our universe and corroborate a minimal construction based on a reduced number of ingredients. Let us briefly review the conceptual steps we have to climb in order to establish the standard model of cosmology.

2.1.1 From cosmological observations to models

In order to grasp to physical implications of having a standard model of cosmology, it might be important to have in mind the few pillars it relies on. To do so, it is instructive to follow the journey from observations to physical modelling. Indeed, cosmology is a discipline which is part of astrophysics and relies on the scrutiny of the sky. It aims at connecting observations to statements about the fundamental nature of the constituents that compose our universe and their interactions. This long journey relies on turning raw data into quantities that are predictable within a theoretical framework, which is the object of the current discussion. We will first see that some efforts are needed to classify observations through the construction of *catalogues*. Then, the information is synthesized trough the construction of *statistical estimators*. These objects are finally the ones we are able to compare with quantities extracted out of theoretical constructions.

Turning raw data into model constraints: Contrarily to *experimental* sciences such as quantum optics or particle physics where we have control on both the source and the detector, cosmology is an *observational* science where we solely design the detection apparatus. Ground and space-based telescopes have been constructed to cover the wide range of signals we can receive from the cosmos. They vary in the nature of the field they detect (e.g. *IceCube* detects neutrinos, *LIGO* gravitational waves and *Planck* photons), the wavelength at which they operate (e.g. *Fermi* detects γ-rays, *JWST* in the near-visible/mid-infrared and *SKA* in the radio domain), the way they collect the signal (*SDSS* is a spectroscopic survey while *DESI* is a photometric survey) and finally their sky coverage and depth of field. From signal collection to the measurement of a physical parameter, a long journey is often ignored.

Raw data must be processed (mask application, denoising and signal subtraction, as illustrated in Fig. 2.1) to construct catalogues of objects (e.g. *supernovea* (SNe) catalogues, see [26]) which serve as the starting point for cosmological data analysis. The tremendous and astonishing amount of work from telescope design to cosmological observations is partially illustrated in Fig. 2.2 which highlights the last step of the process of constructing catalogues, from a galaxy spectrum to the Sloan Digital Sky Survey (SDSS) celestial map.

Once data is collected and sorted into catalogues, we are half-way through the journey towards constraining the physical world. Now we have access to sky maps, we can use them to construct statistics of objects. For instance, we can characterise how the temperature anisotropies of the CMB (signal in Subplot *d)* of Fig. 2.1) and the galaxy density of the Large-Scale Structure (LSS) (right panel of Fig. 2.2) vary across the sky. One can think of these signals as a draw from a statistical distribution we would like to access. To make the discussion precise, let us illustrate

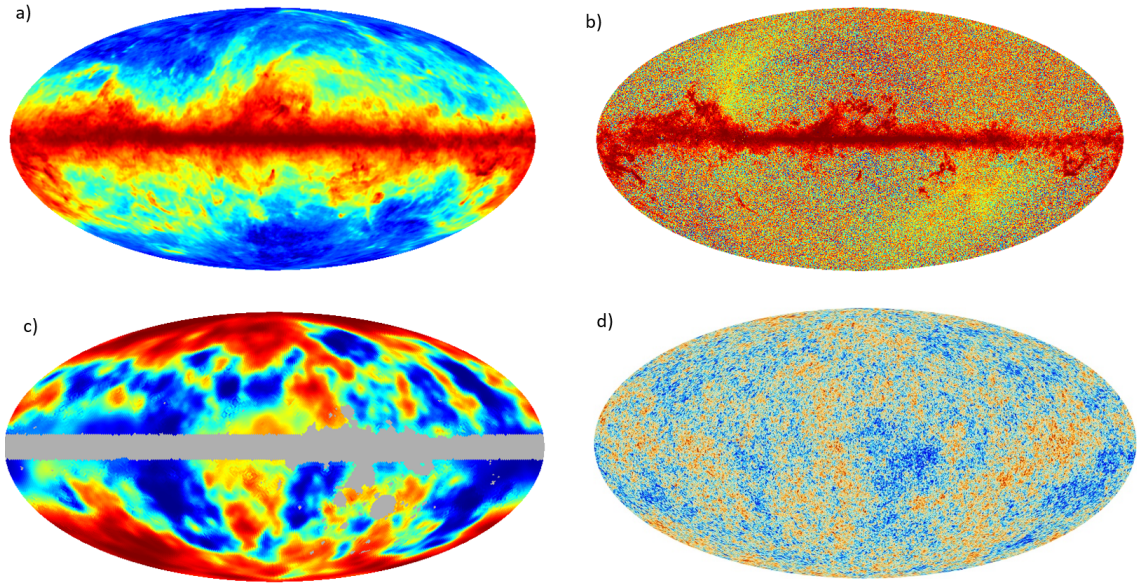

Figure 2.1: *a)* Thermal dust signal; *b)* Carbon monoxyde signal; *c)* Integrated Sachs-Wolfe (ISW) signal with a mask on the galactic plane (grey band); *d)* Cosmic Microwave Background (CMB) signal from Planck Legacy Archive. In order to obtain the CMB signal in *d)*, one must first operate component separation, foreground removal and mask application. A pedagogical introduction to the CMB signal extraction can be found [27].

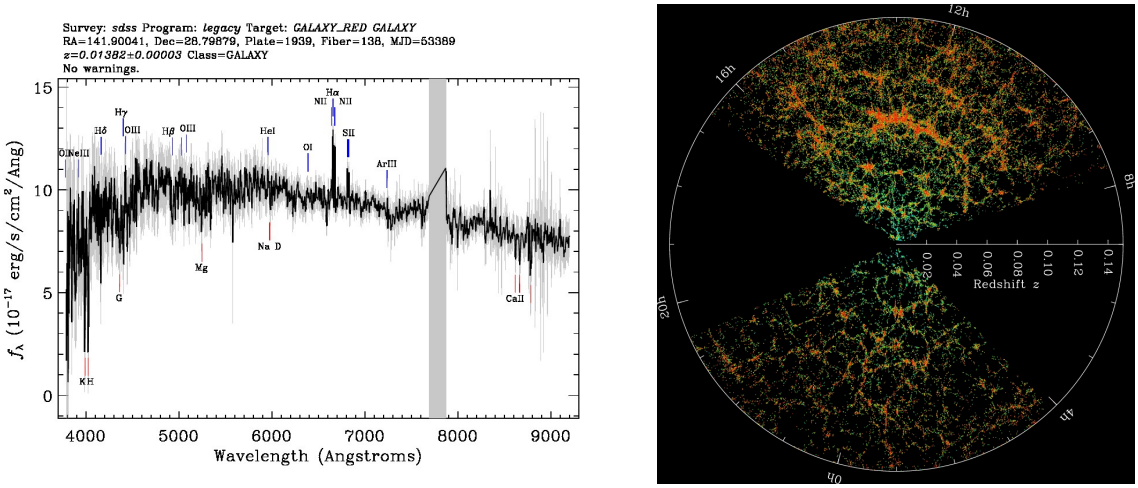

Figure 2.2: *Left:* From one of the more than four million spectra collected by the SDSS [28] to *Right:* the SDSS map of the local universe [29] where each dot is a galaxy. The construction of reliable catalogues is of prime importance for cosmologists. It relies on a long journey from raw data to cosmological observations and constitutes the starting point of statistical data analysis.

the construction of a statistical estimator used for the LSS data analysis: the *galaxy clustering power spectrum.*

Galaxy power spectrum: For the illustrative purpose of the discussion, let us consider a galaxy survey covering a cubic volume of comoving length L, on which we construct a cubic grid with $N^3_{\rm grid}$ grid points, following the approach of [23], Chapter 14. The galaxy overdensity on each of these pixels is defined as

$$\delta_g(\boldsymbol{x}_i) \equiv \frac{m_{g,i} - \bar{m}_{g,i}}{\bar{m}_{g,i}} \tag{2.1}$$

where $\boldsymbol{x}_i$ controls the position of the grid cell i, $m_{g,i}$ is the number of galaxies contained in the cell and $\bar{m}_{g,i}$ the average number of galaxies over all cells. The signal is synthesised through the discrete Fourier transform of the overdensity field

$$\delta_g(\boldsymbol{k}) = L^{3/2} \sum_i^{N^3_{\rm grid}} \delta_g(\boldsymbol{x}_i) e^{-i\boldsymbol{k}.\boldsymbol{x}_i} \quad \text{where} \quad \boldsymbol{k} \in (n_x, n_y, n_z) k_F \tag{2.2}$$

having $k_F \equiv (2\pi)/L$ the wavenumber of the fundamental mode and (n_x, n_y, n_z) a set of integers between $[-N_{\rm grid}/2; N_{\rm grid}/2]$. The Fourier modes are finally binned into equally spaced bins of wavenumber $k \equiv |\boldsymbol{k}|$. In practice, the bin α contains all modes $\boldsymbol{k}$ such that $k_\alpha - \Delta k/2 \leq |\boldsymbol{k}| \leq k_\alpha + \Delta k/2$ where Δk is the width of the bin. The number of modes in a bin $m_{k,\alpha}$ is an important quantity as it plays a major role in the statistical error of the estimator. It corresponds to the number of fundamental cells of volume k_F^3 we can order in a thin shell around k_α of volume $4\pi k_\alpha^2 \Delta k$. Explicitly,

$$m_{k,\alpha} \equiv \frac{1}{2} \frac{4\pi k_\alpha^2 \Delta k}{k_F^3} = \frac{1}{4\pi^2} V k_\alpha^2 \Delta k \tag{2.3}$$

where the $1/2$ prefactor in the first equality comes from the reality of the density field, imposing $\delta_g(-\boldsymbol{k}) = \delta_g^*(\boldsymbol{k})$ which fixes one half of the Fourier mode by knowing the value of the other half. Note that we have used the value of $k_F \equiv (2\pi)/L$ in the second equality to render explicit the role of the survey volume $V \equiv L^3$ in the number of modes accessible. The galaxy clustering power spectrum is finally constructed by averaging over all the elements of a bin

$$\widehat{P}_g(k_\alpha) = \frac{1}{m_{k,\alpha}} \sum_{\boldsymbol{k}}^{|k-k_\alpha|<\Delta k/2} |\delta_g(\boldsymbol{k})|^2 - P_N \tag{2.4}$$

where P_N is a noise term related to the grid sampling, usually assumed to be Poissonian, going as the inverse of the mean number of galaxy per cell. The power spectrum counts the variance of each bin of wavenumber k_α. It is an indicator of how the signal varies across scales. The error on the measurement

is captured by the *covariance*

$$\mathrm{Cov}_{\alpha\beta} = \frac{1}{m_{k,\alpha}} \sum_{\boldsymbol{k}}^{|k-k_\alpha|<\Delta k/2} \frac{1}{m_{k,\beta}} \sum_{\boldsymbol{k}'}^{|k'-k_\beta|<\Delta k/2} \left[\left\langle |\delta_g(\boldsymbol{k})|^2 \, |\delta_g(\boldsymbol{k}')|^2 \right\rangle - \left\langle |\delta_g(\boldsymbol{k})|^2 \right\rangle \left\langle |\delta_g(\boldsymbol{k}')|^2 \right\rangle \right] \tag{2.5}$$

where the four-point function $\left\langle |\delta_g(\boldsymbol{k})|^2 \, |\delta_g(\boldsymbol{k}')|^2 \right\rangle$ must be computed performing all possible contractions, see [23] for details. In the simplest case of Gaussian signal with no overlapping bins, it reduces to

$$\mathrm{Cov}_{\alpha\beta} = \frac{2}{m_{k,\alpha}} \left[\widehat{P}_g(k_\alpha) + P_N \right]^2 \delta_{\alpha\beta} \tag{2.6}$$

from which it appears that the error on $\widehat{P}_g(k_\alpha)$ goes as $\propto m_{k,\alpha}^{-1/2} \propto V^{-1/2}$. Hence, an intrinsic limit known as the *cosmic variance* exists due to the limitation of the finite number of modes accessible in a survey volume V. As the size of cosmological surveys increases, so does their statistical precision. All sorts of effects that were previously hidden under large error bars now generate discrepancies if not carefully accounted for.

Of course, realistic surveys integrate more ingredients such as survey geometries represented by window functions. Still, the above example highlights the main procedure of constructing statistical estimators using sky maps. An analogous construction can be made for the CMB on the celestial sphere using harmonic functions and the multipole decomposition for the temperature anisotropies. At the end of the journey, information on how is allocated the signal across scales is extracted from the data, as shown in Fig. 2.3 for the matter density and the temperature anisotropies power spectra. At first sight, one can see that this information is far from being featureless. From the dramatic oscillations observed in the CMB spectrum known as the *Baryonic Acoustic Oscillations* (BAO) to the peak in the matter density power spectrum around $k \sim 10^{-2} - 10^{-1}$ h.Mpc^{-1},[1] the imprints of underlying physical processes are manifest. We are now in a position to unravel this signal.

It is now the time where contacts between theory and observations are made. Indeed, if a theory is predictable, the quantities extracted out of the statistical estimators constructed above can be predicted within a given model for a set of parameters. We now have to understand if the theoretical expectations correctly describe the observed signal. In cosmology, this is usually made through a Bayesian inference framework [31–33] which allows us to put constraints on the parameter space of a

[1] The scale unit h.Mpc^{-1} is often used in cosmology, in particular for the LSS studies. h is the dimensionless Hubble constant

$$H_0 = 100 \; h \text{ km.s}^{-1}\text{.Mpc}^{-1} \tag{2.7}$$

such that $h = 0.674 \pm 0.005$ from the latest Planck measurements [30]. A megaparsec (Mpc) corresponds to a million of parsecs (pc), where 1 pc $\sim 3 \times 10^{16}$ m. To have a few orders of magnitude in mind, the closest star is located 1 pc away from us, the size of the Milky Way is about 30 kpc, cosmological structures such as the above mentioned BAO are ~ 150 h.Mpc^{-1} and the visible universe is made of a few Gpc.

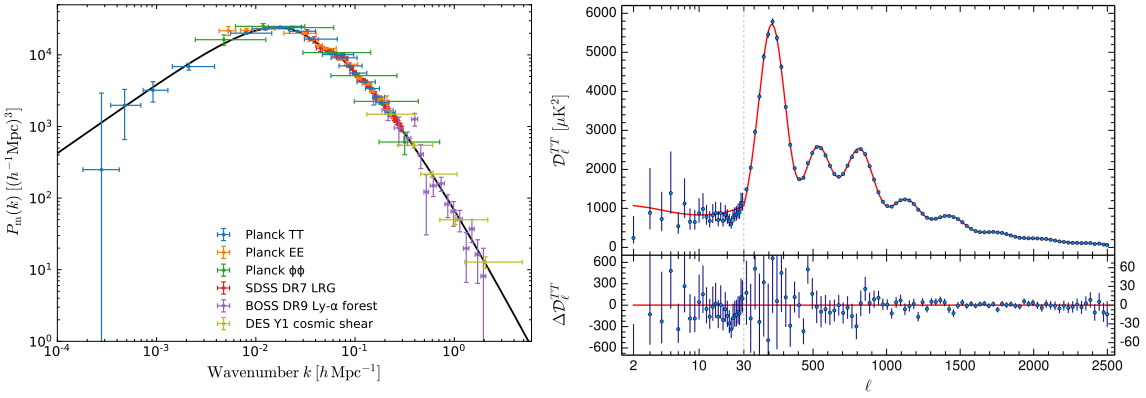

Figure 2.3: *Left:* The matter density power spectrum and *Right:* The temperature anisotropies power spectrum from Planck Image Gallery. The spectra clearly exhibit features which call for the existence of underlying physical processes explaining their occurrence. The black and red plain lines are the theoretical predictions from the Λ-CDM best fit parameters. It highlights the validity of the concordance model over a large range of scales and datasets.

theory or to compare the goodness of fit from one theory to the other [23, 34]. Let us briefly highlight the procedure, following the discussion of [35]. A quantity of central interest is the *likelihood* $\mathcal{L}(\mathcal{D}|\mathcal{M}_i, \theta_{ij})$ which is the probability of getting the data $\mathcal{D}$, given a model $\mathcal{M}_i$ and a set of parameter θ_{ij}. In the specific example of the galaxy-clustering two-point functions, assuming a Gaussian likelihood,

$$\ln \mathcal{L}(\mathcal{D}|\mathcal{M}_i, \theta_{ij}) = -\frac{1}{2}\sum_{\alpha\beta}\left[\widehat{P}_g(k_\alpha) - \widehat{P}_{\rm th.}(k_\alpha|\mathcal{M}_i, \theta_{ij})\right] \\ \mathrm{Cov}^{-1}_{\alpha\beta}\left[\widehat{P}_g(k_\beta) - \widehat{P}_{\rm th.}(k_\beta|\mathcal{M}_i, \theta_{ij})\right] \tag{2.8}$$

where $\widehat{P}_g(k_\alpha)$ is the statistical estimator from the data constructed above and $\widehat{P}_{\rm th.}(k_\beta|\mathcal{M}_i, \theta_{ij})$ is the theoretical power spectrum computed at scale k_α within the model $\mathcal{M}_i$ for the set of parameters θ_{ij}. Once the likelihood is known, Bayes theorem tells us that the posterior probability $p(\theta_{ij}|\mathcal{D}, \mathcal{M}_i)$ of a set of parameters θ_{ij} for each model $\mathcal{M}_i$ is expressed as

$$p(\theta_{ij}|\mathcal{D}, \mathcal{M}_i) = \frac{\mathcal{L}(\mathcal{D}|\mathcal{M}_i, \theta_{ij})\pi(\theta_{ij}|\mathcal{M}_i)}{\mathcal{E}(\mathcal{D}|\mathcal{M}_i)} \tag{2.9}$$

where $\pi(\theta_{ij}|\mathcal{M}_i)$ is the *prior distribution*, accounting for preestablished knowledge of the parameter space of the model $\mathcal{M}_i$ and $\mathcal{E}(\mathcal{D}|\mathcal{M}_i)$ is the *Bayesian evidence*, a normalization constant defined as

$$\mathcal{E}(\mathcal{D}|\mathcal{M}_i) = \int \mathrm{d}\theta_{ij}\mathcal{L}(\mathcal{D}|\mathcal{M}_i, \theta_{ij})\pi(\theta_{ij}|\mathcal{M}_i). \tag{2.10}$$

By sampling the parameter space through the mean of e.g. a Monte-Carlo Markov Chain (MCMC), we compute the value of the posterior for each θ_{ij} using Eq. (2.9) and infer the parameters of a given model $\mathcal{M}_i$, as in Fig. 2.4. This procedure

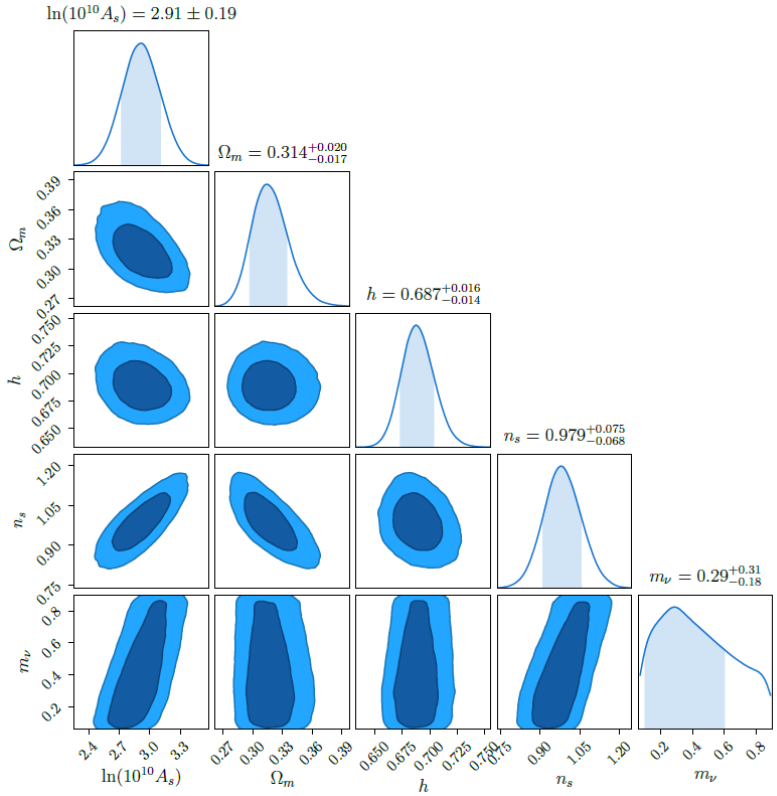

Figure 2.4: Posterior distributions for the cosmological parameters of the Λ-CDM and massive neutrinos model obtained from the analysis of the BOSS DR12 CMASS + LOWZ NGC dataset with a Big Bang Nucleosynthesis prior on Ω_b from [37]. It constitutes the first extraction of the full set of Λ-CDM parameters from the LSS with no CMB prior.

illustrates the way cosmological parameters are inferred from the data in modern cosmology.

On the top of constraining the parameter space of a given model $\mathcal{M}_i$, one can also use the Bayesian evidence defined in Eq. (2.10) to calculate the posterior probability of a model itself, $p(\mathcal{M}_i|\mathcal{D}) \propto \mathcal{E}(\mathcal{D}|\mathcal{M}_i)\pi(\mathcal{M}_i)$. Even if the normalisation constant is unknown, it provides a useful way to compare two models $\mathcal{M}_i$ and $\mathcal{M}_j$ by considering

$$\frac{p(\mathcal{M}_i|\mathcal{D})}{p(\mathcal{M}_j|\mathcal{D})} = \frac{\mathcal{E}(\mathcal{D}|\mathcal{M}_i)\pi(\mathcal{M}_i)}{\mathcal{E}(\mathcal{D}|\mathcal{M}_j)\pi(\mathcal{M}_j)} = B_{ij}\frac{\pi(\mathcal{M}_i)}{\pi(\mathcal{M}_j)} \tag{2.11}$$

where the *Bayes factor* $B_{ij} \equiv \mathcal{E}(\mathcal{D}|\mathcal{M}_i)/\mathcal{E}(\mathcal{D}|\mathcal{M}_j)$. One often assumes uninformative priors based on a principle of indifference such that $\pi(\mathcal{M}_i) = \pi(\mathcal{M}_j)$ and makes use of "Jeffreys scale" [34,36] to provide an empirical prescription for translating B_{ij} values into strengths of belief. When $\ln(B_{ij}) > 5$, $\mathcal{M}_j$ is said to be "strongly disfavored" with respect to $\mathcal{M}_i$, "moderately disfavored" if $2.5 < \ln(B_{ij}) < 5$, "weakly disfavored" if $1 < \ln(B_{ij}) < 2.5$, and the situation is said to be "inconclusive" if $\ln(B_{ij}) < 1$. This approach allows cosmologists to identify models achieving the best compromise between quality of the fit and lack of fine tuning.

This long journey from raw data to model constraints highlights the several layers of analysis required to perform a cosmological measurement, summarized in Fig. 2.5. Having these elements in mind, we can think of the way new physics

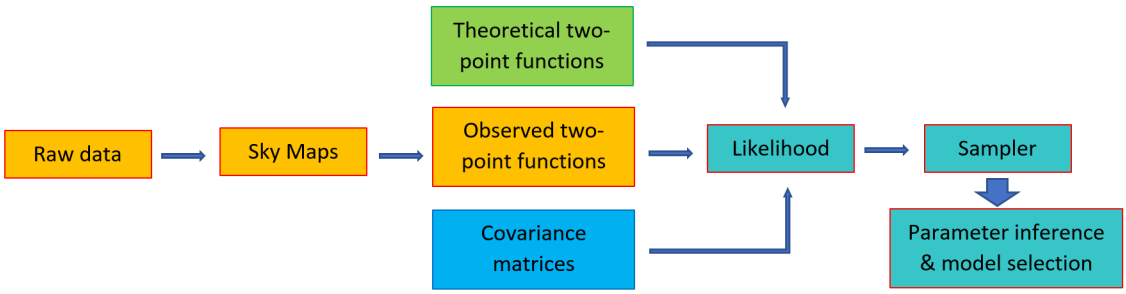

Figure 2.5: Summary of the long journey from raw data to parameter and model constraints using two-point functions and a Gaussian likelihood, adapted from [23], Chapter 14. Orange boxes represent cosmological signal, the blue box the instrumental input and the green box, on which we will focus for the rest of the manuscript, the theoretical data. The right hand side in turquoise rely on the conjunction of observations, instrumental and theoretical constraints.

could materialize itself. Given the large consistency of the concordance model we are about to describe, there are good chances that discrepancies will appear progressively through *tensions* between datasets of different nature, such as the notoriously known H_0 tension [38] or the S_8 tension [39]. These tensions arise when we measure the cosmological parameters of a model using observations of different natures made at different scales. It motivates us to further develop systematic approaches to model the incidence of new physics in a known regime in order to gain theoretical control over these occurrences. This will be the object of Sec. 2.3 in the context of primordial cosmology, but first, we need to provide a description of the known regime.

2.1.2 The Λ-CDM model

We now turn our attention to the description of what is known as the concordance model, that is the physical model gathering the most confidence within the Bayesian inference framework analysis over the widest range of data accessible. We will refer to this model as the standard model of cosmology[2] or the Λ-CDM model.

First pillar: This standard model provides a description of the cosmic history and universe content based on a few pillars, the first of which is General Relativity. In order to make the manuscript self-contained, let us briefly recap the basics of the theory which makes the space-time a dynamical object. The *metric* is a rank-2 tensor defining the spacetime interval between two infinitesimally separated space-time events in an arbitrary coordinate system

$$\mathrm{d}s^2 = g_{\mu\nu}\mathrm{d}x^\mu \mathrm{d}x^\nu. \tag{2.12}$$

$\mathrm{d}s^2$ is called the *line element* and $g_{\mu\nu}$ provides a description of the underlying geometry described by a manifold. From the metric, one can construct objects aiming at

[2]Note that contrarily to the standard model of particle physics which is a description at the level of the most "fundamental" objects today observed that are quantum fields, the standard model of cosmology is from the start an effective/fluid-like description.

describing space-time in a coordinate independent manner. The *Christoffel symbols* are defined as

$$\Gamma^{\mu}_{\alpha\beta} \equiv \frac{g^{\mu\nu}}{2}\left[\partial_\beta g_{\alpha\nu} + \partial_\alpha g_{\beta\nu} - \partial_\nu g_{\alpha\beta}\right] \tag{2.13}$$

where $g^{\mu\nu}$ is the inverse metric, that is $g^{\mu\nu}g_{\nu\lambda} = \delta^{\mu}_{\lambda}$ and $\partial_\alpha \equiv \partial/\partial x^\alpha$. From these objects, we construct the *Ricci tensor*

$$R_{\mu\nu} \equiv \partial_\alpha \Gamma^{\alpha}_{\mu\nu} - \partial_\nu \Gamma^{\alpha}_{\mu\alpha} + \Gamma^{\alpha}_{\beta\alpha}\Gamma^{\beta}_{\mu\nu} - \Gamma^{\alpha}_{\beta\nu}\Gamma^{\beta}_{\mu\alpha} \tag{2.14}$$

and the *Ricci scalar* $R \equiv R^{\mu}_{\ \mu}$. They characterise the geometry of a gravitating system. Matter and geometry are intertwined through the action

$$S = S_m + S_{\rm EH} \tag{2.15}$$

where the action for the matter sector S_m simply writes

$$S_m = -\frac{1}{2}\int \mathrm{d}^4x\sqrt{-g}\mathcal{L}_m \tag{2.16}$$

for a non-gravitating Lagrangian-density $\mathcal{L}_m$ and $\mathrm{d}^4x\sqrt{-g}$ defines the covariant volume, g in $\sqrt{-g}$ being the determinant of the metric $g_{\mu\nu}$. $S_{\rm EH}$ is the *Einstein-Hilbert action*

$$S_{\rm EH} = -\frac{M_{\rm Pl}}{2}\int \mathrm{d}^4x\sqrt{-g}\left(R + 2\Lambda\right) \tag{2.17}$$

with Λ is a constant known as the *cosmological constant*.

Units and conventions:

The *reduced Planck mass* connects with the fundamental constants as

$$M_{\rm Pl} = \frac{1}{\sqrt{8\pi}}\sqrt{\frac{\hbar c}{G_{\rm N}}} \simeq 2.10^{18}\ \text{GeV} \tag{2.18}$$

where $\hbar = 1.054 \times 10^{-34}$ J.s is the reduced Planck constant, $c = 3.10^8$ m.s^{-1} the speed of light and $G_{\rm N} = 6.67 \times 10^{-11}$ m^3.kg^{-1}.s^{-2} the Newton's constant. From now on, we work in natural units in which $\hbar = c = G_{\rm N} = 1$. Every quantity is expressed in terms of the reduced Planck mass. The metric has a mostly positive signature $(-,+,+,+)$, indices are raised and lowered using the metric $g_{\mu\nu}$ and its inverse $g^{\mu\nu}$ and summation over repeated indices apply.

From Eq. (2.15), variations with respect to the metric tensor leads to the equations of motion known as the *Einstein Field Equations* (EFE)

$$R_{\mu\nu} - \frac{R}{2}g_{\mu\nu} + \Lambda g_{\mu\nu} = \frac{1}{M_{\rm Pl}^2}T_{\mu\nu} \tag{2.19}$$

which relate the curvature of space-time to the matter content. The stress-energy tensor is constructed out of the matter sector by functional derivative with respect to the metric

$$T_{\mu\nu} \equiv -\frac{2}{\sqrt{-g}}\frac{\delta S_m}{\delta g^{\mu\nu}}. \tag{2.20}$$

Finally, defining the *Einstein tensor* as $G_{\mu\nu} \equiv R_{\mu\nu} - g_{\mu\nu}R/2$, Bianchi identities fix

$$\nabla_\mu T^{\mu\nu} = 0, \quad \nabla_\mu G^{\mu\nu} = 0 \tag{2.21}$$

which solely follows from general covariance, where the ∇_μ notation indicates covariant derivatives.

Second pillar: On large scales, for comoving observers, the universe is homogeneous and isotropic. It implies a drastic simplification of the EFE due to the introduction of 6 Killing vectors associated with the spacetime symmetries: 3 for the spatial translations and 3 for the spatial rotations. This set of symmetries is known as the *cosmological principle*. Under this assumption, the line element writes

$$\mathrm{d}s^2 = -\mathrm{d}t^2 + a^2(t)\gamma_{ij}\mathrm{d}x^i\mathrm{d}x^j \tag{2.22}$$

which defines the Friedmann-Lemaître-Robertson-Walker (FLRW) metric, the spatial part being

$$\gamma_{ij}\mathrm{d}x^i\mathrm{d}x^j = \frac{\mathrm{d}r^2}{1-\kappa r^2} + r^2\left(\mathrm{d}\theta^2 + \sin^2\mathrm{d}\varphi^2\right). \tag{2.23}$$

$a(t)$ is the scale factor which informs us on how the size of the universe is changing with time. Formally, we define a foliation along the time axis with spacelike sections. From a more formal perspective, the scale factor $a(t)$ explains how to connect neighbouring spacelike hypersurfaces. The curvature of the spacelike sections is given by $\kappa = 0, \pm 1$ (flat, sphere-like and saddle-like respectively). Therefore, this metric contains two parameters $a(t)$ and κ we constrain from physical observations.

In this framework, the matter content of the universe is given by a collection of perfect fluids. Indeed, in this minimal approach, no viscosity is allowed at the level of the *background* evolution (understood as the large-scale regime) as it would break the spacetime symmetries.[3] Therefore, the associated stress-energy tensor is

$$T_{\mu\nu} = (\rho + p)\, u_\mu u_\nu + p g_{\mu\nu} \tag{2.24}$$

with ρ is the energy density of the fluid, p its isotropic pressure and u^μ its four-velocity.

One can use these inputs to derive a cosmological history. From the FLRW metric of Eq. (2.22), we can construct the Ricci tensor using Eq. (2.14). Injecting these ingredients into the EFE, we obtain the Friedmann equations

$$H^2 = \frac{\rho}{3M_{\mathrm{Pl}}^2} - \frac{\kappa}{a^2} + \frac{\Lambda}{3} \tag{2.25}$$

$$\frac{\ddot{a}}{a} = -\frac{1}{6M_{\mathrm{Pl}}^2}(\rho + 3p) + \frac{\Lambda}{3} \tag{2.26}$$

where we defined the Hubble parameter $H \equiv \dot{a}/a$. Friedmann equations specify the evolution of the scale factor $a(t)$ as a function of the matter content, the cosmological constant and the spatial curvature.

[3] One can in fact relax this assumption by accounting for bulk viscosity while still respecting the symmetries of FLRW spacetimes. It amounts to employ the energy-momentum tensor of an imperfect fluid where the bulk viscosity would mimic an isotropic pressure term (see e.g. [40], Chapter 3).

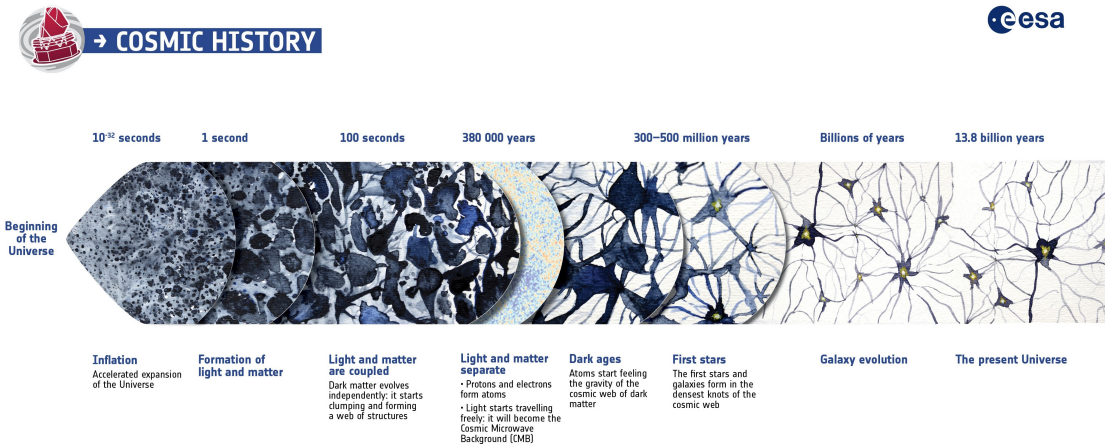

Figure 2.6: A summary of the almost 14 billion year history of the Universe from the ESA Gallery. Their description is here reproduced: "The processes depicted range from inflation, the brief era of accelerated expansion that the Universe underwent when it was a tiny fraction of a second old, to the release of the CMB, the oldest light in our Universe, imprinted on the sky when the cosmos was just 380 000 years old; and from the 'Dark Ages' to the birth of the first stars and galaxies, which reionised the Universe when it was a few hundred million years old, all the way to the present time. Tiny quantum fluctuations generated during the inflationary epoch are the seeds of future structure: the stars and galaxies of today. After the end of inflation, dark matter particles started to clump around these cosmic seeds, slowly building a cosmic web of structures. Later, after the release of the CMB, normal matter started to fall into these structures, eventually giving rise to stars and galaxies."

Validity of the cosmological pillars: General relativity, together with quantum mechanics and the standard model of particle physics, are among the most tested physical theories [41–44]. Moreover, GR can be seen as a non-renormalizable field theory well described as the low-energy limit of a more general EFT construction [1]. For both of these reasons, it provides a conservative and trustworthy framework. The cosmological principle relies on the fact that isotropy is observed in the LSS and the CMB. Homogeneity is based on the Copernician principle, that is the fact we do not occupy a privileged place in the cosmos. Giving up on this last point would be equivalent to accept a possible fine tuning related to our position, which questions modern physics at large. For these reasons, cosmological pillars lie on solid grounds.

The standard model of cosmology: The effectiveness of this minimal model is probably the most striking feature that emerged from the last few decades of research in cosmology. Though many of its ingredients remain mysterious in terms of their underlying fundamental physics, the standard model of cosmology provides a astonishing fit to an ensemble of observations ranging from the present day to about a few minutes after the Big Bang.

The Λ-CDM model is made of the conjunction of GR and a universe content which implies a certain cosmic history, the one represented in Fig. 2.6. This framework combines an initial phase of accelerated expansion known as *inflation* and a

subsequent era of decelerated expansion known as the *Hot Big Bang*. Let us briefly describe this timeline. Inflation is a high-energy phase which took place in the early universe during which the scale factor $a(t)$ underwent a nearly exponential growth. In less than a second, the universe get dilated by a factor of order e^{50}, transferring quantum fluctuations to cosmological distances. This era is described within a quantum field theoretic framework where the main component is thought to be a scalar field known as the *inflaton*. This phase ended up through a process of *reheating* during which the inflaton decayed into dark matter and particles of the standard model. By this process, inflation seeded the inhomogeneities that will later grow on under the effect of gravity. It will be the main focus of this manuscript.

Then, Hot Big Bang phase took over. It is first composed of a *radiation era*, where the formation of heavy elements occurred through the process of *Big Bang Nucleosynthesis* (BBN) within the first three minutes of our universe. The hot primordial plasma cooled down while the universe expanded, until we enter the *matter dominated era*. During this phase, *recombination* occurred, that is the physical process leading to the emission of the CMB photons, 380 000 years after the Big Bang. The temperature has dropped enough so that the protons and electrons were finally able to combine, after which photons could free stream towards us. The late evolution of the universe is characterised by the process of gravitational clustering which lasted for billions of year during which galaxies, clusters and voids were formed, generating the LSS we today observe. Recently, the universe started to accelerate again under the action of the cosmological constant Λ, entering in its last and current phase of *vacuum dominated era*. When we today observe the sky, this cosmic history provides the most consistent scenario matching the observations made so far.

The Λ-CDM model is a six-parameter model made of the baryon density Ω_b, the cold-dark-matter density Ω_c, the amplitude of the primordial power spectrum A_s and its tilt n_s and finally the optical depth τ and the angular acoustic scale $100\theta_*$ [30]. From these primary parameters, derived quantities often play a crucial role such as the expansion rate H_0, the photon density Ω_γ, the neutrino density Ω_ν or the cosmological constant density Ω_Λ. The model provides predictions we can compare to data in order to extract values for these parameters. From the measurement of supernovae or the temperature anisotropies of the CMB, we can infer the expansion rate [23]

$$H_0 = 100\ h\ \text{km.s}^{-1}.\text{Mpc}^{-1} \tag{2.27}$$

such that $h = 0.674 \pm 0.005$ from the latest Planck measurements [30]. It implies an age for the universe of about 13 Gya, a size for the observable universe of about 4 Gpc and an energy scale for the cosmological expansion of 10^{-33} eV today. To infer the rest of the parameters, the most precise approach relies on the understanding of the cosmological inhomogeneities we observe on the top of a vastly homogeneous and isotropic background. In this picture, all the structures we today observe in the universe such as galaxies, clusters, voids and filaments all originate from quantum fluctuations of the primordial vacuum produced during inflation whose statistics is (almost) fully characterised by two parameters, the amplitude of the primordial power spectrum A_s and its tilt n_s.

The initial inhomogeneities later evolve under the laws of GR and the universe content specified through the other Λ-CDM parameters. This mechanism seeds the

temperature anisotropies of the CMB and galaxy clustering in the LSS which we precisely measure today in the sky. Within the Bayesian inference framework developed above, we can test the theoretical predictions for the statistics of observables and infer the parameters of the model. It follows that the energy budget of the universe is currently shared between the cosmological constant Λ which gather 69% of the total, the cold dark matter (CDM) component which today represents about 25% of the budget and the baryons representing a remaining 5% of the budget. In its current form, the universe hosts solely about 10^{-5}% of radiation (photons and neutrinos). As a summary, the Λ-CDM model provides a description of a spatially flat universe that is dominated today by cold dark matter and a cosmological constant, with initial perturbations generated during inflation in the very early universe. Capturing the imprints of phenomena that took place at very high energy, these initial perturbations are the main motivation of this manuscript and we now aim at describing their generation.

Assumptions underlying the Λ-CDM model: As a summary, let us here reproduce the eight major assumptions listed by the Planck Collaboration in [27] on which the standard model of cosmology relies.[a] Most of them have been tested to very high level of accuracy using cosmological observations.

1. Physics is the same throughout the observable universe.
2. GR is an adequate description of gravity.
3. On large scales, the universe is statistically the same everywhere.
4. The universe was once much hotter and denser and has been expanding since early times.
5. There are five basics cosmological constituents:
   (a) Dark energy that behaves just like the energy density of the vacuum.
   (b) Dark matter that is pressureless, stable, and interacts only gravitationally with normal matter.
   (c) Regular atomic matter that behaves just like it does on Earth.
   (d) The photons we observe as the CMB.
   (e) Neutrinos that are almost massless and stream like non-interacting, relativistic particles at the time of recombination.
6. The curvature of space is very small.
7. The universe has a trivial topology, like $\mathbb{R}^3$. In particular, it is not periodic or multiply connected.
8. Variations in the density were laid down everywhere at early times, and are (almost) Gaussian, adiabatic and nearly scale invariant as predicted by inflation.

This last point will be extensively discussed in the rest of the manuscript.

[a]Note that 1. is a consequence of 2. and 3. Similarly, 4. is a consequence of 2. and 5. Here, we solely reproduce the points listed in [27].

2.2 The physics of the early universe

In the standard model of cosmology, the early universe provides the initial conditions that seed the evolution of the subsequent eras of the universe. It directly connects current observations to early universe processes taking place at very high energy. From today's sky, what can be learnt about the physics seeding these initial conditions? In order to tackle this question, we will first illustrate in Sec. 2.2.1 the modelling of the early universe commonly used within the concordance model. It provides a consistent scenario explaining the statistics of the fluctuations observed in the CMB and the LSS. In Sec. 2.2.2, we then turn our attention to the regime of validity over which this scenario has been tested. Finally, in Sec. 2.2.3, we highlight a few limits and difficulties faced by the current modelling of the early universe. The aim of this Section is to provide an overview of our current understanding of the early universe which serves as a starting point for the construction later developed in Sec. 2.3.

2.2.1 The early-universe modelling

Within the concordance model, the early universe is driven by a single scalar field ϕ, the inflaton, evolving in a flat potential. We will refer to this class of models as *single-field slow-roll inflation*. This phase is designed to permit an early era of accelerating expansion ($\ddot{a} > 0$) in order to set up the initial conditions for the subsequent Hot Big Bang. From Eq. (2.26), it turns out that having $\ddot{a} > 0$ is equivalent to consider an energy budget dominated by a perfect fluid with an equation of state $w \equiv p/\rho < -1/3$, neglecting the cosmological constant term which is assumed to be subdominant in the early universe. Let us first review how single-field slow-roll inflation can achieve this task.

The Lagrangian density for the scalar field is given by

$$\mathcal{L}_m = \frac{1}{2} g^{\mu\nu} \partial_\mu \phi \partial_\nu \phi - V(\phi) \tag{2.28}$$

from which, using Eq. (2.20), we deduce the stress-energy tensor

$$T^{(\phi)}_{\mu\nu} = \partial_\mu \phi \partial_\nu \phi - g_{\mu\nu} \left[g^{\alpha\beta} \partial_\alpha \phi \partial_\beta \phi + V(\phi) \right] \tag{2.29}$$

At the background level, for a homogeneous field configuration $\phi(\boldsymbol{x}, t) = \phi(t)$, one can assimilate the scalar field to a perfect fluid of energy density and pressure

$$\rho = \frac{1}{2}\dot{\phi}^2 + V(\phi) \tag{2.30}$$

$$p = \frac{1}{2}\dot{\phi}^2 - V(\phi) \tag{2.31}$$

When the potential energy dominates over the kinetic term, $w \simeq -1 < -1/3$ and the universe undergoes a phase of accelerating expansion. This regime in which

$\dot{\phi}^2 \ll V(\phi)$ is known as the *slow-roll* regime. It is characterised by a series of moments known as the *Hubble flow parameters* defined as

$$\varepsilon_0 = \frac{H_{\rm ini}}{H} \qquad \text{and} \qquad \varepsilon_{n+1} = \frac{\mathrm{d}}{\mathrm{d}N} \ln \varepsilon_n \tag{2.32}$$

where $H_{\rm ini}$ is some initial value for the Hubble parameter and $N = \ln a$ is the *number of efolds*. Explicitly, the first two parameters are

$$\varepsilon_1 = -\frac{\dot{H}}{H^2} = \frac{\frac{3\dot{\phi}^2}{2}}{\frac{\dot{\phi}^2}{2} + V(\phi)} \qquad \text{and} \qquad \varepsilon_2 = \frac{\dot{\varepsilon}_1}{H\varepsilon_1} = 2\left(\varepsilon_1 + \frac{\ddot{\phi}}{H\dot{\phi}}\right) \tag{2.33}$$

where we used Friedmann equations reading

$$H^2 = \frac{\frac{\dot{\phi}^2}{2} + V(\phi)}{3M_{\rm Pl}^2} \qquad \text{and} \qquad \dot{H} = -\frac{\dot{\phi}^2}{2M_{\rm Pl}^2} \tag{2.34}$$

to relate the Hubble parameter and its derivatives with the kinetic and potential energy of the field. One can easily check that $\dot{\phi}^2 \ll V(\phi)$ imposes $\varepsilon_1 \ll 1$, that is $\dot{H} \ll H^2$. Said it differently, the Hubble parameter is enforced to be almost a constant, corresponding to a nearly exponential expansion of the scale factor $a(t)$. This is the reason why inflation is often called a *quasi de-Sitter* expansion, as it only departs from the forever exponentially expanding universe (*de Sitter* spacetime) by a set of slow-roll parameters. Hence, the slow-roll expansion amounts to assume an almost frozen dynamics, for which $|\varepsilon_n| \ll 1$, $\forall n \geq 1$. In particular, it implies that the scalar field equation of motion given by the Klein-Gordon equation

$$\ddot{\phi} + 3H\dot{\phi} + V' = 0 \tag{2.35}$$

where $V' \equiv \mathrm{d}V/\mathrm{d}\phi$ simplifies to its attractor solution (independent of the initial conditions)

$$\dot{\phi} = -\frac{V'}{3H} \tag{2.36}$$

as $|\varepsilon_2| \ll 1$ amounts to neglect the acceleration of the field over the other terms of the Klein-Gordon equation. If we finally relate these slow-roll parameters to the shape of the potential using Eq. (2.36), we find

$$\varepsilon_1 \simeq \frac{M_{\rm Pl}}{2}\left(\frac{V'}{V}\right)^2 \qquad \text{and} \qquad \varepsilon_2 \simeq 2M_{\rm Pl}\left[\frac{1}{2}\left(\frac{V'}{V}\right)^2 - \frac{V''}{V}\right]. \tag{2.37}$$

To summarize, having a quasi de Sitter expansion with nearly constant H requires $\varepsilon_1 \ll 1$ which implies a flat potential. Reaching the attractor (one-dimensional phase space) trajectory of the form of Eq. (2.36) requires $|\varepsilon_2| \ll 1$ which requests a small mass for the inflaton $V'' \ll H^2$. Despite being notoriously known as a difficult task to achieve due to radiative corrections generating an inflaton mass heavier than the Hubble parameter H, the smallness of ε_2 is a well-tested observational feature.[4]

[4] In particular, it directly connects to the nearly scale invariance of the power spectrum which is tested with exquisite precision in the CMB.

What is the current observational status of inflation? There are mainly three *qualitative* features that have been tested. The first one is the spatial flatness of the universe. The first Friedmann equation given in Eq. (2.25) can be rewritten as

$$1 - \Omega = \frac{-\kappa}{(aH)^2} \tag{2.38}$$

with $\Omega \equiv \rho/3M_{\rm Pl}^2H^2$. Consequently, the deviation of the normalized density parameter Ω from unity is a measure of the curvature of the universe. Today, we observe $|1 - \Omega(a_0)| \leq 0.02$ while the inflationary prediction is $|1 - \Omega(a_0)| \leq 10^{-5}$. This is a first great success for inflation.

The peaks observed in the CMB power spectra, see the right panel of Fig. 2.3, constitute the second non-trivial qualitative feature explained by inflation. Oscillations form an highly non-trivial signal as it suggests that all Fourier modes have the same phase. In general, Fourier modes can excite both sine and cosines, so that in the case of random initial phases, their addition quickly ends up mixed into an incoherent superposition as illustrated in Fig. 2.7. Some physical mechanism must explain the phase coherence. Inflation provides such a mechanism, based on two arguments. The first one relates to the journey of a comoving scale during inflation while the second one to the peculiarity of the dynamics of the so-called *curvature perturbation* whose statistics later seed the temperature anisotropies of the CMB. Let us start with the journey of a comoving mode k^{-1} which relates to the physical distance d by $d(t) = a(t)k^{-1}$. During inflation, $a(t)$ grows almost exponentially while H is nearly frozen. It implies that the *comoving Hubble radius* (also referred as the *comoving horizon*), $(aH)^{-1}$, is decreasing. This quantity describes the size of a causal patch, as two points separated by a distance greater than (see e.g. [24])

$$\tau = \int_{a_i}^{a_f} {\rm d}a(aH)^{-1} \tag{2.39}$$

could not have communicated through a causal mechanism. If we now consider a given mode k^{-1} that is typically observed in the CMB and compare it with the evolution of the comoving Hubble radius as done in Fig. 2.8, we can easily understand that two regimes emerge depending on the scale hierarchy between the comoving mode k^{-1} and the comoving horizon $(aH)^{-1}$. When $k \gg aH$, as it is the case in the asymptotic past, the mode is said to be *sub-Hubble*. It lies well below the universe's radius of curvature, which often justifies an identification to the physics occurring in Minkowski spacetime. On the contrary, when $k \ll aH$, as it is the case in for a duration of around 50 efolds for modes observed in the CMB, the mode is said *super-Hubble*. Then, the dynamics of the expanding background plays a crucial role which affects the observables such as the curvature perturbation ζ. This quantity behaves in a dramatically different manner in the sub and super-Hubble regimes. In particular, it detains the very remarkable property of being conserved on super-Hubble scales, not only during inflation but also during the subsequent eras [23], at least for single-field models of inflation. The constraint that $\dot{\zeta} = 0$ provides a specific initial condition which aligns the phase for the modes of interest. Said it differently, the phase distribution is far from being arbitrary during inflation, which allows us to observe coherent oscillations (contrarily to some alternatives such as cosmic strings and topological defects).[5]

[5]A technical detail for cosmologists: note that the BAO oscillations in the TT spectrum of

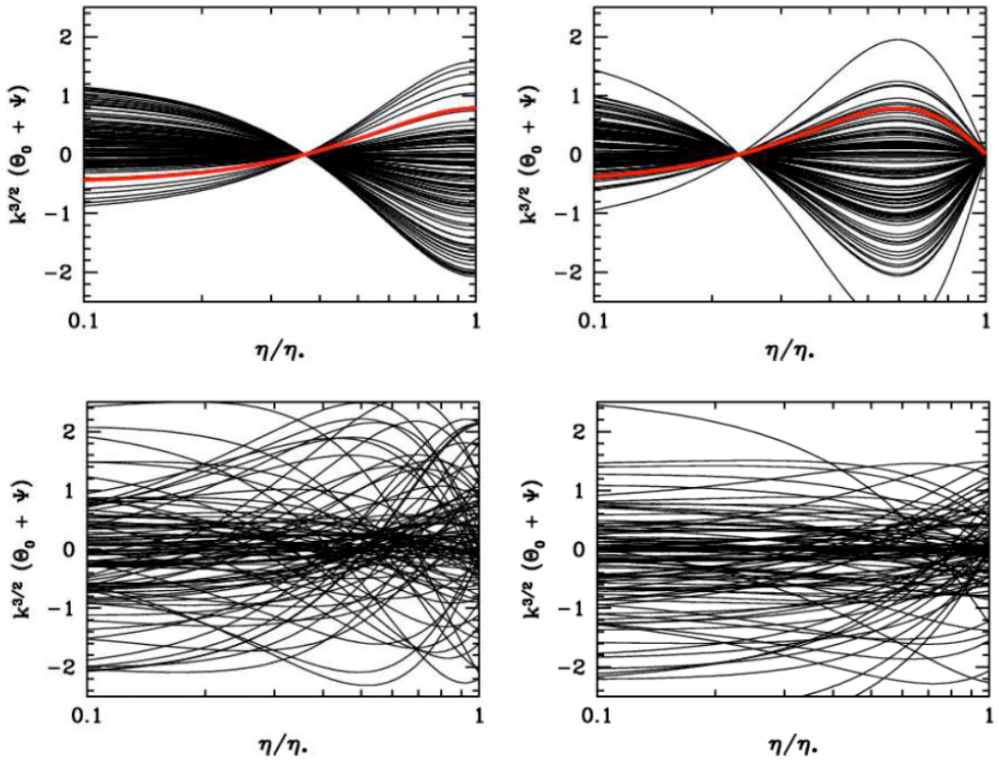

Figure 2.7: *Top:* Time evolution of modes with different initial amplitudes but the same phase, for which oscillations are observed. *Bottom:* Time evolution of modes with different initial amplitude and phases. The spectrum has no oscillations and seem featureless. Figure from [45].

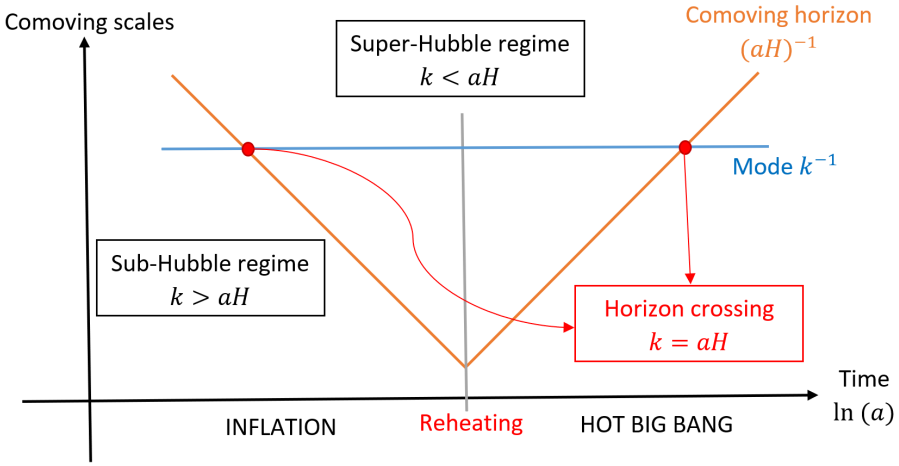

Figure 2.8: The journey of a comoving scale. A mode of interest is initially blueshifted in the deep past and so initiate its journey well below the comoving horizon $(aH)^{-1}$. As time proceeds, the scale factors grows exponentially in terms of the cosmic time, the *Hubble sphere* of radius $(aH)^{-1}$ shrinks such that at some point, the mode of interest crosses the horizon $k_* = a_* H$. During inflation, there is a continuous inflow of sub-Hubble modes on the large-scale super-Hubble dynamics which is well described within the context of stochastic inflation.

The third qualitative feature predicted by inflation is the production of primordial inhomogeneities sampled from a *nearly scale-invariant*, *Gaussian* and *adiabatic* process. Indeed, the tiny temperature anisotropies observed in the CMB directly connect to the production of primordial inhomogeneities in the early universe. These inhomogeneities correspond to the fluctuations of the curvature perturbation which seed the initial conditions for structure formation. The Gaussianity of the process implies that all the statistics is captured by the first two moments of the distribution. As the mean can always be reabsorbed by a field redefinition, we focus on the variance which is the already encountered power spectrum in Fourier space. The primordial power spectrum predicted from inflation is almost k-independent. Perfect scale invariance of the primordial power spectrum is now excluded by more than 7σ, which is consistent with the fact that inflation generates a quasi de-Sitter phase of expansion which must end at some point. The necessity for carrying a physical clock accounting for the time remaining before the end of inflation breaks the time translation symmetry which ruins the scale invariance of a perfectly de Sitter universe. The Gaussianity assumption relates to the fact that, so far, all measurements are consistent with a purely Gaussian statistics of the fluctuations. Almost perfect Gaussianity is an expected feature of single-field slow-roll inflation, even if slow-roll suppressed non-Gaussian signal is expected, see e.g. [47, 48]. It follows from the smallness of GR non-linearities [49] and the requirement that, for the inflaton potential to remain flat enough, the inflaton must be weakly self-interacting. Finally, the adiabaticity corresponds to the fact that fluctuations generated by the curvature perturbations during inflation equally affect different components during the Hot Big Bang. All perturbations of the cosmological fluids (photons, neutrinos, baryons and CDM) originate from the same curvature perturbation statistics, that is [24, 50]

$$\left(\frac{\delta\rho(\boldsymbol{x})}{\bar{\rho}+\bar{p}}\right)_a = \left(\frac{\delta\rho(\boldsymbol{x})}{\bar{\rho}+\bar{p}}\right)_b \tag{2.40}$$

where $\bar{\rho}$ and $\bar{p}$ are the spatially averaged energy density and pressure, $\delta\rho(\boldsymbol{x}) \equiv \rho(\boldsymbol{x}) - \bar{\rho}$ the local overdensity and a, b corresponds to baryons, dark matter, photons and neutrinos. Hence, all the various components of our universe are distributed in the same way at the onset of the Hot Big Bang, as predicted by single-field slow-roll inflation and observed in the CMB and the LSS [51].[6]

At the level of the *quantitative* features, inflation provides the initial conditions for each mode through a power spectrum of the form

$$\Delta_s^2(k) = A_s(k_*)\left(\frac{k}{k_*}\right)^{n_s(k_*)-1} \tag{2.41}$$

where $k_* = 0.05\ \text{Mpc}^{-1}$ is an arbitrary reference scale at which the signal is measured, known as the *pivot scale*. The latest measurements from Planck [51] indicates

the CMB are observed at scales $\ell > 200$, after horizon reentry where some other causal mechanism might explain the appearance of coherent oscillations. However, considering polarization anisotropies of the CMB, the TE spectrum exhibits the first coherent oscillations around $100 < \ell < 200$, at scales above the horizon at the time recombination occurred. It clearly calls for a causal mechanism on super-horizon scale occuring prior to the emission of the CMB. See [27,45,46] for details.

[6] Note that multifield inflation adiabatic initial conditions can also arise in specific models, see e.g. [52] for a discussion.

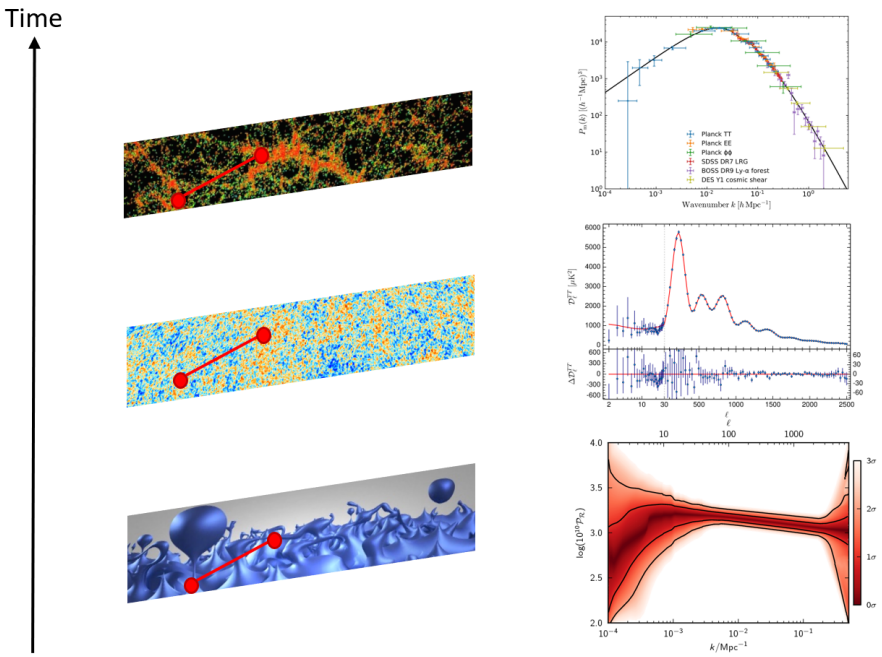

Figure 2.9: Illustration of how the correlations originating from the primordial power spectrum gets transferred to the temperature anisotropies of the CMB and the galaxy clustering data of the LSS. From the bottom to the top: primordial fluctuations of quantum mechanical origin generates a nearly scale invariant power spectrum (reconstructed from CMB observation in [27]). After inflation, the evolution of the cosmological inhomogeneities during the radiation and matter dominated era forms the temperature anisotropies of the CMB introduced in Fig. 2.3. Billion of years later, galaxies, clusters, voids and filaments of the LSS formed on the seeds of these primordial fluctuations.

an amplitude of $10^9 A_s(k_*) = 2.105 \pm 0.030$ and a tilt of $n_s(k_*) = 0.965 \pm 0.004$. This primordial seed for cosmic inhomogeneities directly relates to the physics of inflation and connects to the subsequent era of the universe later measured in the CMB and the LSS as illustrated in Fig. 2.9.

2.2.2 Unexplored regimes

From the EFT perspective, standard models exhibit their full glory solely within a certain regime. New physics hide in the dark corners[7] that have not been explored yet. For this reason, it matters to map the frontier separating the explored from the unexplored in order to construct an EFT able to describe their interplay.

[7] One may argue that dark matter and dark energy are hidden in plain sight and might be considered as new physics, in the sense that no fully satisfactory fundamental description is known so far. Yet, we may also consider them from their current status (a pressureless cosmological fluid and a cosmological constant) as indispensable ingredient of an extremely successful story that holds their name, the Λ-CDM paradigm. This form encapsulates their nature at scales we today probe. Any more fundamental description would have to mimic this behaviour at these scales in order to provide a satisfactory description. Then, distinguishing possible completions from their effective representation would necessarily require to probe new regimes where they will start departing from each other.

Current status and future surveys: So far, cosmological observations from the CMB and the LSS are all consistent on large scales with a Gaussian, nearly scale-invariant, adiabatic scalar power spectrum from quantum mechanical origin. Let us briefly highlight the regime of validity of this statement by providing existing bounds on the parameters controlling this assertion.

In order to solve the Hot Big Bang problems that are the so-called *horizon*, *flatness* and *monopole problems* [53–65], inflation must last a number of efolds [24]

$$N_{\rm inf} \equiv \frac{\ln a_{\rm end}}{\ln a_{\rm start}} \geq 50 - 60. \tag{2.42}$$

Consequently, predictions from single-field slow-roll inflation span ranges of physical scales from a few meters for modes escaping the horizon just before inflation ends up to thousands of megaparsec (Mpc), the actual size of the observable universe, for modes that spent about 50 efolds above the horizon. Indeed, we have not tested inflation over this range. The latest CMB results [51] account for a primordial power spectrum confirming a pure power law in the range of comoving scales between $0.005\ \text{Mpc}^{-1} \lesssim k \lesssim 0.2\ \text{Mpc}^{-1}$. On the LSS side, tremendous efforts have been made in the last years [37, 66–70] to push the galaxy clustering analysis down to the mildly non-linear regime $k_{\rm NL} \simeq 0.1 - 0.5\ \text{h.Mpc}^{-1}$. Hence, over the ~ 26 orders of magnitude predicted by inflation, only ~ 4 of them have been tested so far using CMB and LSS data. A wide window remains open for the existence of features at smaller scales [71, 72], even if this regime has been more and more constrained in the recent years either using gravitational waves data [51, 73] or Primordial Black Holes (PBHs) constraints [74].

The Gaussian nature of primordial inhomogeneities is a well-tested observation from the temperature anisotropies and polarization of the CMB [75] and more recently using the galaxy clustering data from spectroscopic surveys [76–80]. Deviations from Gaussianity are observationally constrained by the signal from higher-point statistics, starting with the three-point function known as the *bispectrum*.[8] In Fourier space, the bispectrum of the curvature perturbation ζ is parametrised as

$$\left\langle \widehat{\zeta}_{\boldsymbol{k}_1} \widehat{\zeta}_{\boldsymbol{k}_2} \widehat{\zeta}_{\boldsymbol{k}_3} \right\rangle = (2\pi)^3 \delta\left(\boldsymbol{k}_1 + \boldsymbol{k}_2 + \boldsymbol{k}_3\right) B_\zeta\left(\boldsymbol{k}_1, \boldsymbol{k}_2, \boldsymbol{k}_3\right) \tag{2.43}$$

Because of the spatial homogeneity, $\delta\left(\boldsymbol{k}_1 + \boldsymbol{k}_2 + \boldsymbol{k}_3\right)$ imposes to consider closed triangle configurations. One usually distinguish the equilateral $k_1 = k_2 = k_3$, the local or squeezed $k_1 \simeq k_2 \ll k_3$ and folded $k_1 = 2k_2 = 2k_3$ configurations. The amplitude of the signal from Planck in these three configurations is given by [75]

$$f_{\rm NL}^{\rm equil} = -26 \pm 47; \quad f_{\rm NL}^{\rm local} = -0.9 \pm 5.1; \quad f_{\rm NL}^{\rm ortho} = -38 \pm 24 \quad (68\%\text{CL}) \tag{2.44}$$

No significant non-zero detection from primordial origin has been made so far. Yet, non-Gaussianities remain one of the most promising probe to explore standard model extensions.

[8] Recent interests from the first detection of connected four-point correlation function in the SDSS BOSS dataset [81–83] and its relation with parity violation [84, 85] may lead to bypass the bispectrum signal in LSS data analysis and focus on even higher-order statistics for some models of interest.

Among the most robust inflationary predictions, the existence of a primordial tensor spectrum Δ_t related to the scalar spectrum Δ_s by the scalar-tensor ratio

$$r \equiv \frac{\Delta_t}{\Delta_s} = 16\varepsilon_1 \tag{2.45}$$

is a universal result of the linear perturbation theory of cosmological inhomogeneities. The slow-roll regime imposing $\varepsilon_1 \ll 1$, the signal is extremely low in vanilla inflation. Current constraints obtained by measuring polarization signal in the CMB bound $r < 0.028$ [73]. A stochastic gravitational wave background (SGWB) from primordial origin can also be generated (see e.g. [86] for a review) from a scalar-induced mechanism during or after inflation using GR non-linear couplings. Hence, the existence of a gravitational waves from primordial origin appears as an unavoidable prediction of inflationary cosmology. Yet, no direct detection has been recorded so far.

Within the scalar sector, multifield extensions beyond single-field slow-roll inflation should manifest themselves through the existence of isocurvature modes [87]. The isocurvature modes are scalar fluctuations of a different nature than the curvature perturbations which leave a distinguishable imprint on the temperature anisotropies of the CMB. The latest Planck data [51] are consistent with null detection, i.e. a pure adiabatic model, with a Bayes factor of $\ln B_{ij} < -10.9$ asserting strong confidence in the null detection, following the discussion made around Eq. (2.11).

So far, inflationary predictions have been tested through the consistency of the background dynamics they generate and the imprint they leave on the top of this background. Cosmological inhomogeneities have been successfully described in the small fluctuation regime by perturbation theory and provide a consistent scenario with the current status of cosmological observations. Yet, the quantum nature of the fluctuation do not preclude for the existence of large fluctuations [88–90] which may capture crucial information about the underlying microphysical inflationary model. By probing tails of the probability distribution associated with the local value of the curvature perturbation ζ, the large fluctuation regime could significantly impact the abundance of collapsed objects such as PBHs and dark matter halos. Unambiguous connection between the observation of collapsed objects and their primordial origin has not been successful so far (despite attempts, see for e.g. [91]) which makes of the large fluctuation regime another untested domain of the inflationary paradigm.

Lastly, the nature of the fluctuations - quantum or classical - is still an unsolved problem. Indeed, if their quantum nature is fully consistent with the observational window, a classical stochastic theory could also generate a power spectrum compatible with observations by the mean of thermally produced inhomogeneities such as string gas cosmology [92] or warm inflation [93].

As a conclusion, the inflationary framework has been tested in a limited range of scales ($0.005\ \text{Mpc}^{-1} \lesssim k \lesssim 0.2\ \text{Mpc}^{-1}$), for a limited type of species (adiabatic scalar only), in the Gaussian (null detection of higher-point statistics in the CMB) and small fluctuation regime, indistinguishable from classical counterparts (no direct evidence for the quantum nature of primordial inhomogeneities). While future CMB surveys such as *SPTpol* [94], *CMB-S4* [95] or *LiteBIRD* [96] will target B-modes of polarization and spectral distortions and strongly improve CMB constraints on primordial cosmology, *DESI* [97], *SKA* [98], *EUCLID* [99] and *Vera Rubin* [100] may

render feasible to constrain from the LSS primordial non-Gaussianities and [76–80] and parity odd theories [82] in an unprecedented manner. Lastly, pulsar-timing arrays observed by NANOGrav [101] and gravitational waves detectors such as the *LIGO/Virgo/KAGRA* collaboration [102], the *Einstein Telescope* [103] or *LISA* [104] rise promises on the possible detection of gravitational waves from primordial origin and improvement on the search for PBHs.

The existence of current tensions animating the community such as the H_0 tension [38] or the S_8 tension [39] might hint that cosmology has entered a precision era which may call for an updated paradigmatic description. Given the effective (fluid-like) nature of the concordance model, it should not come as a surprise that it might need extensions. Still, the fact that it provides a good fit of the current regime should be taken as a guideline for constructing extensions.

Inaccessible information: It is important to bear in mind the existence of inaccessible information that cannot be retrieved, independently of the technology level of astronomy in the future. Just as information hidden behind the horizon of a black-hole, the existence of inaccessible information motivates the development of frameworks able to deal with theoretical uncertainties that invariably plague any effort of theoretical construction.

A first example is given by the cosmic variance. It is associated with the inherent uncertainty on large-scale measurements due to the invariably low sampling of these regions [23]. Obviously, if we want to ask how the matter density varies between two regions of 1 Gpc^3, as we can at best only observe a few of them within the observable universe, the statistical uncertainty of the sampling will be large. On the contrary, the same question asked for boxes 1 Mpc^3 will have a much smaller statistical error as the much more data points can be collected. While large volume surveys such as MegaMapper [79] might improve the large-scale sampling, some unbeatable threshold will be reached some day due to the finiteness of the observable universe. Let us further highlight that our causal patch might be affected by soft modes of wavelength longer than the observable universe. These background effects might vary the statistics of the fluctuations in sub-volumes, rendering harder to reconstruct fundamental physics from local cosmological observations [105].

A second intrinsic observational limitation comes from the peculiarity of the inflationary dynamics. When comes the question of testing the quantum origin of primordial inhomogeneities, the most direct road to follow is the one of exhibiting correlations in the CMB or the LSS that could not been reproduced by a classical counterpart obeying local realism, in the spirit of a Bell test. Several works have developed the possibility of performing CMB Bell tests [106–112] yet most of them face a fundamental obstacle related to the unobservability of some of the inflationary correlators. Indeed, the usual way to perform a Bell test is by measuring a set of observables (spin directions for discrete variables, quadratures for continuous variables) and combining these measurements in a way that they violate a bound fulfilled by a classical theory. Within the inflationary framework, it would require to access not only the curvature perturbation two-point function $\langle\widehat{\zeta}(\boldsymbol{x},\eta)\widehat{\zeta}(\boldsymbol{y},\eta)\rangle$ but also the correlators $\langle\{\widehat{\zeta}(\boldsymbol{x},\eta),\widehat{\zeta}'(\boldsymbol{y},\eta)\}\rangle$ and $\langle\widehat{\zeta}'(\boldsymbol{x},\eta)\widehat{\zeta}'(\boldsymbol{y},\eta)\rangle$ where η is the

conformal time defined infinitesimally as $\mathrm{d}t = a\mathrm{d}\eta$ such that

$$\eta = \int_{t_0}^{t} \mathrm{d}t' \frac{1}{a(t')} = \int_{0}^{a(t)} \mathrm{d}a \frac{1}{a^2 H} \simeq -\frac{1}{a(t)H} \tag{2.46}$$

at leading order in slow-roll where H is almost a constant, primes denote derivatives with respect to it and the anticommutator is defined as $\{A, B\} \equiv AB + BA$. Unfortunately, $\widehat{\zeta}'(\boldsymbol{x}, \eta)$ is famously known as the *decaying mode* and correlators containing one insertion of this field variable are observationally inaccessible in any realistic experiment for vanilla models of inflation (counterexamples can be found, for instance in the context of ultra slow-roll phases [113] or exotic models such as the one discussed in [107]). The reason is the following.[9]

Decaying mode: The linear action for the curvature perturbations ζ writes [24]

$$S_{\zeta}^{(2)} = \int \mathrm{d}\eta \mathrm{d}^3\boldsymbol{x} a^2 \varepsilon_1 M_{\mathrm{Pl}}^2 \left[\zeta'^2 - (\partial_i \zeta)^2\right]. \tag{2.48}$$

We first introduce the time-variable $z(\eta) \equiv a(\eta)\sqrt{2\varepsilon_1} M_{\mathrm{Pl}}$ and the Mukhanov-Sasaki variables $v(\eta, \boldsymbol{x}) \equiv z(\eta)\zeta(\eta, \boldsymbol{x})$. One can Fourier transform the field variables

$$v_{\boldsymbol{k}}(\eta) \equiv \int_{\mathbb{R}^3} \frac{\mathrm{d}^3\boldsymbol{x}}{(2\pi)^{3/2}} v(\eta, \boldsymbol{x}) e^{-i\boldsymbol{k}.\boldsymbol{x}} \tag{2.49}$$

in order to take advantage of the spatial homogeneity. The equation of motion for $v_{\boldsymbol{k}}$ takes the familiar form of a parametric oscillator

$$v_{\boldsymbol{k}}'' + \left(k^2 - \frac{z''}{z}\right) v_{\boldsymbol{k}} = 0. \tag{2.50}$$

The conjugate momentum is obtained from the action and read $p_{\boldsymbol{k}} = v_{\boldsymbol{k}}' - \frac{z'}{z} v_{\boldsymbol{k}}$. Following the canonical quantisation prescription, field variables are promoted to quantum operators obeying the equal-time commutation relations

$$[\widehat{v}_{\boldsymbol{k}}(\eta), \widehat{p}_{\boldsymbol{q}}(\eta)] = i\delta(\boldsymbol{k} + \boldsymbol{q}). \tag{2.51}$$

Making use of the linear evolution, one can relate the field operators at time η to $\widehat{a}_{\boldsymbol{k}}$ and $\widehat{a}_{-\boldsymbol{k}}^{\dagger}$, the creation and annihilation operators of the Bunch-Davies

[9] The argument is often summarized through the so-called *classicalisation* mechanism which related to the fact the curvature perturbation commutator vanishes as a general feature in expanding backgrounds as [114]

$$\left[\widehat{\zeta}(\boldsymbol{x}, \eta), \widehat{\zeta}'(\boldsymbol{y}, \eta)\right] \propto \frac{1}{\sqrt{-g}} \delta(\boldsymbol{x} - \boldsymbol{y}) = \frac{1}{a^4} \delta(\boldsymbol{x} - \boldsymbol{y}) \to 0. \tag{2.47}$$

It is therefore suppressed by the volume of the universe, hiding the quantum nature of the canonical commutation relations. Note that the terminology is misleading as this mechanism can occur at the same time inflation proceeds and places cosmological inhomogeneities in a highly *quantum* state known as a *two-mode squeezed state* which saturates all quantumness criteria along the $\boldsymbol{k}/-\boldsymbol{k}$ bipartition [114–122]. Hence, rather than a fundamental erasure of the commutation relations, it highlights the experimental difficulty of observing them.

vacuum $|\emptyset\rangle$ in the asymptotic past through the mode-function decomposition

$$\widehat{v}_{\boldsymbol{k}}(\eta) = v_k(\eta)\widehat{a}_{\boldsymbol{k}} + v_k^*(\eta)\widehat{a}^\dagger_{-\boldsymbol{k}} \tag{2.52}$$

$$\widehat{p}_{\boldsymbol{k}}(\eta) = p_k(\eta)\widehat{a}_{\boldsymbol{k}} + p_k^*(\eta)\widehat{a}^\dagger_{-\boldsymbol{k}}. \tag{2.53}$$

The mode-functions obey the classical equation of motion specified in Eq. (2.50). At leading order in the slow-roll expansion, it reduces to $v_{\boldsymbol{k}}'' + (k^2 - 2/\eta^2)\, v_{\boldsymbol{k}} = 0$ which has for solution

$$v_{\boldsymbol{k}}(\eta) = \left(1 - \frac{i}{k\eta}\right)\frac{e^{-ik\eta}}{\sqrt{2k}} \quad \text{and} \quad \widehat{p}_{\boldsymbol{k}}(\eta) = -i\frac{k}{2}e^{-ik\eta}. \tag{2.54}$$

Injecting the mode function expansion to compute the primordial power spectra

$$\langle\emptyset|\, \widehat{v}^2_{\boldsymbol{k}}(\eta)\, |\emptyset\rangle = |v_{\boldsymbol{k}}(\eta)|^2 = \frac{1}{2k}\left(1 + \frac{1}{k^2\eta^2}\right) \tag{2.55}$$

$$\langle\emptyset|\, \widehat{p}^2_{\boldsymbol{k}}(\eta)\, |\emptyset\rangle = |p_{\boldsymbol{k}}(\eta)|^2 = \frac{k}{2} \tag{2.56}$$

$$\frac{1}{2}\langle\emptyset|\, \{\widehat{v}_{\boldsymbol{k}}(\eta), \widehat{p}_{\boldsymbol{k}}(\eta)\}\, |\emptyset\rangle = \Re\mathrm{e}\left[v_{\boldsymbol{k}}(\eta)p^*_{\boldsymbol{k}}(\eta)\right] = \frac{1}{2} \tag{2.57}$$

it appears that, once we move back to the original set of variables ζ and ζ', the only quantity which is not exponentially suppressed at late time where $-k\eta \sim e^{-N_{\rm inf}} \to 0$, $N_{\rm inf}$ being the duration of inflation in efolds, is

$$\left\langle\widehat{\zeta}^2(\eta)\right\rangle = \frac{1}{2\varepsilon_1 M_{\rm Pl}^2}\frac{H^2}{2k^3}\left(1 + k^2\eta^2\right) \simeq \frac{1}{2\varepsilon_1 M_{\rm Pl}^2}\frac{H^2}{2k^3}, \tag{2.58}$$

the other two spectra being suppressed by powers of $-k\eta$.

This relation propagates to the CMB, in which the temperature anisotropies relate to the curvature perturbations by the Sachs-Wolfe effect [23]

$$\frac{\delta T}{T}(\boldsymbol{e}) = \int \frac{\mathrm{d}^3\boldsymbol{k}}{(2\pi)^3}\Big\{F_{\boldsymbol{k}}\left[\zeta_{\boldsymbol{k}}(\eta_{\rm end}); \zeta'_{\boldsymbol{k}}(\eta_{\rm end})\right] + i\boldsymbol{k}.\boldsymbol{e}G_{\boldsymbol{k}}\left[\zeta_{\boldsymbol{k}}(\eta_{\rm end}); \zeta'_{\boldsymbol{k}}(\eta_{\rm end})\right]\Big\}e^{i\boldsymbol{k}.\boldsymbol{e}(\eta_{\rm lss}-\eta_0)+i\boldsymbol{k}.\boldsymbol{x}_0} \tag{2.59}$$

where $\boldsymbol{e}$ is the unit vector in the pointing direction, $\eta_{\rm lss}$ and η_0 are the conformal times at the last scattering surface and at present day respectively and $\boldsymbol{x}_0$ is the Earth location. The functions $F_{\boldsymbol{k}}$ and $G_{\boldsymbol{k}}$ are the form factors which describe the evolution of the perturbations in the post-inflationary universe. They are proportional to $\zeta_{\boldsymbol{k}}(\eta_{\rm end})$ and $\zeta'_{\boldsymbol{k}}(\eta_{\rm end})$ evaluated at the end of inflation. The relation depending linearly on the field variables at first order, we can separate the two contributions

$$\frac{\delta T}{T}(\boldsymbol{e}) = A_{\boldsymbol{k}}.\zeta_{\boldsymbol{k}}(\eta_{\rm end}) + B_{\boldsymbol{k}}.\zeta'_{\boldsymbol{k}}(\eta_{\rm end}) \to A_{\boldsymbol{k}}.\zeta_{\boldsymbol{k}}(\eta_{\rm end}) \tag{2.60}$$

as $\zeta'_{\boldsymbol{k}}(\eta_{\rm end}) \propto a^{-3}(\eta_{\rm end}) \simeq 10^{-67}$ for 50 efolds of inflation. This argument is taken from [110].

Hence, the contributions associated to $\zeta'_{\boldsymbol{k}}$ decay away, taking with them the hope of experimentally measuring information associated with the decaying mode. Therefore, in practice, information from the full set of quadratures is hidden to us, probably forever. By solely observing the curvature perturbation power spectrum $\langle\widehat{\zeta}(\boldsymbol{x},\eta)\widehat{\zeta}(\boldsymbol{y},\eta)\rangle$ in the temperature anisotropies of the CMB, we cannot distinguish their quantum origin from a classical counterpart mimicking their behaviour [120].[10] The decaying mode example, together with the cosmic variance intrinsic limitations, are here to remind us it is important to keep in mind we only have a partial access to information, motivating us to develop theoretical frameworks able to incorporate uncertainties within their construction.

2.2.3 Limits and difficulties

The current constraints on the inflationary models are well summarized by the posterior distribution in the (n_s, r) plane shown in Fig. 2.10, where we remind that n_s is the tilt of the primordial power spectrum and r the tensor-to-scalar ratio, both of which can be determined theoretically and observationally. The figure illustrates the fact that perfect scale-invariance ($n_s = 1$) is statistically disfavored by more that 7σ and that primordial gravitational waves have not been observed, such that $r < 0.056$ at 2σ. These two observations can be used to infer some information about the underlying physics within the inflationary framework, but unfortunately not enough to single-out a unique model for the early universe. Let us briefly unravel the outcomes of this Figure. The *Lyth bound* relates the tensor-to-scalar ratio r to field excursion $\Delta\Phi$, that is the range of values spanned by the scalar field rolling along its potential during inflation [24]

$$\frac{\Delta\Phi}{M_{\rm Pl}} \simeq \mathcal{O}(1)\left(\frac{r}{0.01}\right)^{1/2}. \tag{2.62}$$

Large-field models with trans-Planckian excursions $\Phi_* > M_{\rm Pl}$ tend to be disfavored compared to *small-field models* for which $\Phi_* < M_{\rm Pl}$ or *plateau models* which have a very flat potential and hence predict a smaller value for the tensor-to-scalar ratio r. Beyond this general trend, current constraints on inflation are really far from singling out a microphysical model and a wide range of options are still open (see [123] for an almost exhaustive investigation of the variety existing in the inflationary model building literature). Fig. 2.10 is not even considering examples which evade the framework of single-field slow-roll inflation with canonical kinetic terms. Well-motivated models can be found beyond this framework and perfectly fit the data, such as transient slow-roll violations (known as *features*), multifield inflation and non-canonical kinetic terms. Hence, current data remains elusive on the number of active species in the early universe (single or multi field), their nature (spin, mass) and their action (canonical or non-canonical kinetic terms).

[10] Indeed, when we evaluate expectation values,

$$\left\langle\widehat{\zeta}(\boldsymbol{x},t)\cdots\right\rangle = \int \mathrm{d}\zeta\,[\zeta(\boldsymbol{x},t)\cdots]\,|\Psi[\zeta]|^2\,, \tag{2.61}$$

$\Psi[\zeta]$ being the wavefunction of the universe, this correlator is completely equivalent to classical statistics with $|\Psi[\zeta]|^2 \to P[\zeta]$ defining a classical probability distribution function (PDF), at least at the Gaussian level.

Apart from n_s and r, the last well constrained parameter is the amplitude of the primordial power spectrum $A_s = 2.10 \times 10^{-9}$. Within the single-field slow-roll inflationary framework, it provides a direct measurement of H_*^2/ε_{1*} at the pivot scale. The lack of detection of the tensor power spectrum indicates that

$$\Delta_t < r \times A_s = 0.056 \times 2.10 \times 10^{-9} \tag{2.63}$$

from which we infer an upper bound on the energy scale of inflation, knowing that $\Delta_t \propto (H_*/M_{\rm Pl})$. We obtain the constrain $H_* < 7.6 \times 10^{-5}\ M_{\rm Pl}$. We also know that inflation occured before the Big Bang Nucleosynthesis, from which one can infer a lower bound on the energy scale of inflation, leading to the constraint

$$10^{-24}\ \text{GeV} \ll H < 10^{13}\ \text{GeV}, \tag{2.64}$$

which is arguably one of the most uncertain scale in physics currently.

Lastly, it is not even sure that inflation provides a signature of new physics, contrarily to dark matter and dark energy, as there exist proposals in which inflation is embedded within the standard model of particle physics, the Higgs field playing the role of the inflaton due to a minimalistic coupling with the Ricci scalar generated by radiative corrections, following renormalization prescriptions [124–127]. The value of this coupling is fixed by matching with the amplitude of the primordial power spectrum which leaves no free parameter at tree level. The point of this discussion is not to advocate for this class of models which face their own uncertainties, but rather to highlight that unambiguous claim of new physics from inflation is not even an easy task.

In fact, apart from the presence of a scalar degree of freedom evolving in a flat potential for a sufficiently long period of time and the apparent consistency of observations with perturbative/semiclassical version of quantum gravity, some may argue we have not learn much from inflation so far. Moreover, inflation faces conceptual challenges which may threaten its embedding in a more fundamental construction. There is an intrinsic difficulty of quantum field theory for maintaining flat potentials over a long period of time. This problem is historically known as the *η-problem* of inflation, from the name of the second slow-roll parameter $\eta \propto V''/H^2$ (proportional to a linear combination of ε_1 and ε_2 given Eq. (2.37)). In the absence of symmetries protecting the inflaton potential, its second derivative is sensible to dimension-six *Planck-suppressed operators* of the form

$$\frac{\mathcal{O}_4}{M_{\rm Pl}^2}\phi^2. \tag{2.65}$$

In the case where $\mathcal{O}_4$ acquires a non-zero vacuum expectation value comparable to the inflationary energy density $\langle \mathcal{O}_4 \rangle \sim V$, this term corrects the inflaton mass by $\Delta m \sim H$ or equivalently $\Delta\eta \sim 1$, which instantly destabilizes inflation. This phenomenon is generic: for an EFT with cutoff Λ, the mass of the scalar field runs to the cutoff scale unless it is protected by some symmetries [24]. Since we look for a theory valid at the energy scale of inflation, the cutoff must be higher than the Hubble parameter, $\Lambda > H$, which implies that having a small inflaton mass ($m_\phi \ll H$) is radiatively unstable, making that in general, η get corrected by

$$\Delta\eta = \frac{\Delta m_\phi^2}{2H^2} \geq 1. \tag{2.66}$$

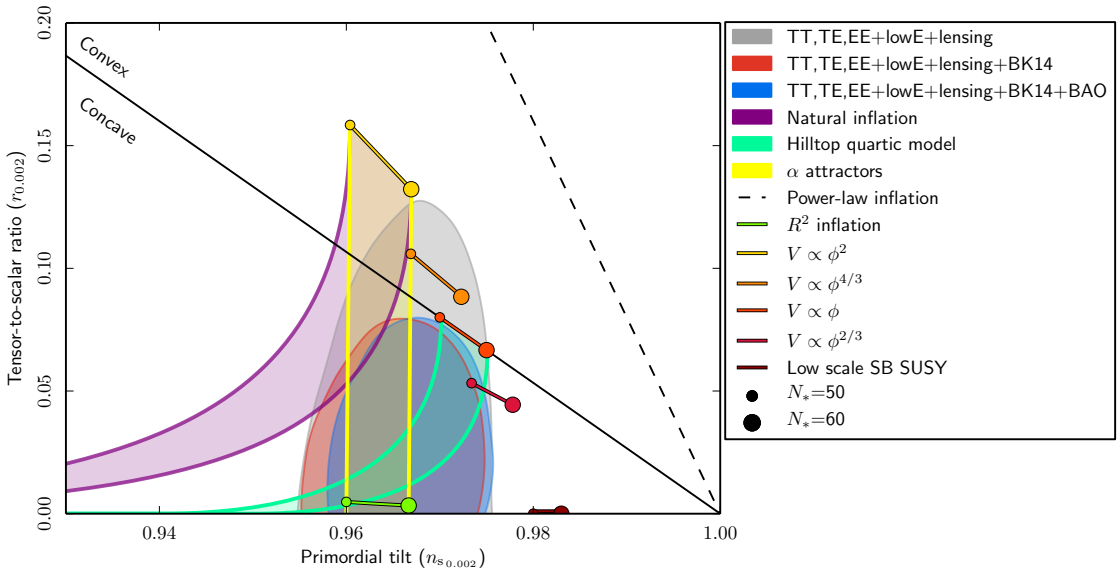

Figure 2.10: Planck 2018 results on single field slow-roll inflationary models from the Planck Image Gallery. It displays the posterior distribution of the primordial tilt n_s on the horizontal axis and of the tensor-to-scalar ratio r on the vertical axis. The grey, red and blue contours are the 1σ and 2σ allowed region of parameter space from CMB and LSS (when BAO are included) datasets. If some models are excluded from the data, current observations are far from singling out a single inflationary models.

Hence, radiative corrections prevent prolonged phases of inflation. For this reason, the understanding of the Planck-suppressed operators of the form given in Eq. (2.65) is required to address the smallness of η, that is the ability of inflation to sustain 60 efolds of expansion. One may worry about the level of fine-tuning such a slow-roll dynamics would imply. In the context of string theory, the modern expression of this *naturalness* issue is developed within the *Swampland program*, aiming at constraining low-energy EFTs that do not admit a UV completion in M-theory [128, 129]. The *de Sitter conjecture* relies on the difficulty of finding de Sitter vacua in string compactifications and has been refined to the requirements

$$\frac{|V'|}{V} > \mathcal{O}(1) \quad \text{or} \quad \frac{V''}{V} < \mathcal{O}(1). \tag{2.67}$$

It obviously provides tensions with the simplest inflationary model where the slow-roll expansions imposes $\varepsilon_1, \varepsilon_2 \ll 1$, see [130].

The above difficulties, often related to the naturalness of top-down constructions, can be overcome within the inflationary framework, for instance by considering symmetry-protected inflaton (e.g. shift symmetry such as in axion monodromy [131]) or multifield settings (see [132] for multifield inflation and the Swampland). Yet, adding to these intrinsic difficulties the failure of singling out a specific microphysical model, one might be tempted to question inflation in its position of paradigmatic theory for the early universe, in particular considering the existence of viable candidates for alternatives [92, 133, 134]. It motivates us for a deeper investigation of the phenomenology beyond single-field slow-roll inflation in the quest

for viable scenarios, the improvement of tools and techniques used within the semi-classical perspective of QFT in curved-spacetimes (far from being settled topic, see e.g. [135–137]) and the continuation of the long-standing efforts made in connecting quantum gravity candidates to observations. The next Section aims at inserting the approach developed in the manuscript within this research program.

2.3 Inflation and new physics

We saw that single-field slow-roll inflation provides a minimal framework consistent with the current observations. We also reviewed the existence of unexplored regimes which might hide signatures of new physics and motivations to go beyond this minimal framework. Let us now develop how possible extensions can be included on the top of the minimal single-field framework. To do so, we first need a unified framework to capture the phenomenology of single-field slow-roll inflation, which is the object of Sec. 2.3.1. We then discuss in Sec. 2.3.2 possible ways to extend this formalism. This discussion will serve as a basis for the Open EFT construction promoted in the rest of the manuscript.

2.3.1 A minimal setup

Among the strengths of inflation, the fact that it provides a very minimal physical setup to explain the current cosmological observations is probably one of its most remarkable features. Cosmological surveys highlight the high level of consistency of CMB and LSS data with single-field slow-roll inflation despite being unable to single out a microphysical model, as seen above. This is precisely a feature theorists must address: why so many different microphysical models end up with the same macrophysical properties? We have to identify a physical mechanism that does not depend on the details of the theory and provides consistent results with the observations. It happens that EFTs have been successful in incorporating this knowledge. As EFTs have the capacity of synthetizing the relevant physics, making it transparent, let us review the features shared by all single-field slow-roll inflationary models. The aim of this discussion is to think of inflation in the most essential way, following [6].[11]

The wide variety of models falling into the class of single-clock inflation can indeed be described at the level of the perturbations they generate in the language of an EFT. What we know about inflation at the most basic level is that it is a period of accelerated expansion. This period must reach an end to connect with the Hot Big Bang model, making it to depart from a perfectly de Sitter universe. It invariably implies that time-translations are spontaneously broken.[12] In this framework, inflation is thought as the theory of the Goldstone boson associated with this spontaneous symmetry breaking. The vacuum expectation value of this boson provides a physical clock measuring time, enforcing an end for inflation after a given duration.

By diffeomorphism invariance of GR (invariance of physical laws under coordinate redefinition), we can find a frame in which this physical clock is set to zero. It can be done by choosing spatial slices where the fluctuations of the clock vanish. For instance, let us consider a homogeneous and isotropic scalar field $\phi(\boldsymbol{x}, t) = \phi(t)$.

[11] Complementary perspectives can be found in [16, 138].

[12] Note that boosts are also broken. For the clarity of the argument, let us solely consider time-translations here.

We perform the time diffeomorphism $t \to t + \delta t(\boldsymbol{x}, t)$ such that at linear order, one can pick up a gauge in which

$$0 = \delta\phi(\boldsymbol{x}, t) - \dot{\phi}(t)\delta t(\boldsymbol{x}, t). \tag{2.68}$$

This is the so-called *unitary gauge*. The dynamical scalar mode is then included in the description of the metric, which must contain one scalar and two tensor dynamical degrees of freedom after enforcing the symmetries and constraint equations. The EFT principles aim at constructing the most generic action compatible with the symmetries for the available degrees of freedom. We solely have at our disposal the metric fluctuations as we have chosen a gauge in which the scalar field fluctuations are suppressed. Spatial homogeneity being preserved, we still have the freedom to arbitrarily change the spatial coordinates within the various spatial slices. The residual gauge symmetries are the time-dependent spatial diffeomorphisms

$$x^i \to x^i + \xi^i(\boldsymbol{x}, t) \tag{2.69}$$

We now need to understand what are the operators compatible with the remaining symmetries. Besides the usual term in Einstein-Hilbert action (2.17) which is invariant under all diffeomorphisms, there are now new terms which are allowed, the ones that are solely invariant under spatial diffeomorphisms. The simplest one is the g^{00} of the metric which transforms as a scalar under spatial diffeomorphism

$$\tilde{g}^{00} = \frac{\partial\tilde{t}}{\partial x^\mu}\frac{\partial\tilde{t}}{\partial x^\nu}g^{\mu\nu} = \delta^0_\mu\delta^0_\nu g^{\mu\nu} = g^{00} \tag{2.70}$$

as the transformation keeps the time unchanged (as it acts within a given time slice, where $\tilde{t} = t$). Polynomials of g^{00} are the only terms without derivatives, which implies they will play a leading role in the description of allowed operators. Given the existence of a preferred slicing of spacetime, we can also write operators associated with the geometric objects describing the slicing. The *extrinsic curvature* $K_{\mu\nu}$ of spatial hypersurfaces at constant time is a tensor under spatial diffeomorphisms which can be used in the action. If n^μ is the vector normal to a spatial hypersurface,

$$K_{\mu\nu} = h_\nu{}^\sigma \nabla_\sigma n_\nu \tag{2.71}$$

where ∇_σ is the *covariant derivative* and $h_{\mu\nu}$ is the *induced metric* on the spatial hypersurfaces

$$h_{\mu\nu} = g_{\mu\nu} + n_\mu n_\nu. \tag{2.72}$$

Embracing the Wilsonian EFT perspective, we can now construct the *effective action*, that is the most generic local and unitary action obeying the symmetries of the problem, keeping in mind that generic functions of time can multiply any term in the action. The most generic action takes the form

$$S = \int \mathrm{d}^4x\sqrt{-g}F(R_{\mu\nu\rho\sigma}, g^{00}, K_{\mu\nu}, \nabla_\mu, t) \tag{2.73}$$

where F is a generic functions and $R_{\mu\nu\rho\sigma}$ is the Riemann tensor. At lowest order in the fluctuations (see [2] for details)

$$\begin{aligned} S = \int \mathrm{d}^4x\sqrt{-g}\Big[&\frac{1}{2}M_{\rm Pl}^2 R - \Lambda(t) - c(t)g^{00} + \frac{1}{2}M_2^4(t)(\delta g^{00})^2 + \frac{1}{3!}M_3^4(t)(\delta g^{00})^3 \\ &- \frac{\bar{M}_1^3(t)}{2}(\delta g^{00})\delta K^\mu{}_\mu - \frac{\bar{M}_2^2(t)}{2}\left(\delta K^\mu{}_\mu\right)^2 - \frac{\bar{M}_3^2(t)}{2}\delta K^\mu{}_\nu\delta K^\nu{}_\mu + \cdots\Big] \end{aligned} \tag{2.74}$$

where the dots stand for higher-order terms in the fluctuations and derivatives. We have introduced the notations $\delta g^{00} = g^{00} - \bar{g}^{00}$ the fluctuation of the 00-component on the metric with respect to the FLRW background (in which $\bar{g}^{00} = -1$) and $\delta K_{\mu\nu} = K_{\mu\nu} - a^2 H h_{\mu\nu}$ with $h_{\mu\nu}$ defined in Eq. (2.72), which corresponds to the variation of the extrinsic curvature of spatial hypersurfaces with respect to the unperturbed FLRW metric. Only the first three terms contain linear perturbations, from which we deduce that $c(t)$ and $\Lambda(t)$ are in fact fixed by the requirement of having a specified FLRW background expansion with a given $H(t)$. Hence, the EFT of Inflation (EFTI) [2] is a theory for the inflationary fluctuations, which assumes the background dynamics as an experimental data, fixing parameters by consistency with the observed universe. The unperturbed history fixes $c(t)$ and $\Lambda(t)$ while the different physical models are encoded into different *higher-order terms*. Computing the matter stress energy tensor using Eq. (2.20) and injecting the result in Friedmann equations (2.25) and (2.26), we obtain

$$H^2 = \frac{1}{3M_{\rm Pl}^2}\left[c(t) + \Lambda(t)\right] \tag{2.75}$$

$$\frac{\ddot{a}}{a} = \dot{H} + H^2 = -\frac{1}{3M_{\rm Pl}^2}\left[2c(t) - \Lambda(t)\right] \tag{2.76}$$

which we can invert to express $c(t)$ and $\Lambda(t)$ in terms of H and $\dot{H}$, our experimental data. Injecting the result into Eq. (2.74), we obtain

$$\begin{aligned} S = \int \mathrm{d}^4x\sqrt{-g}\Big[&\frac{1}{2}M_{\rm Pl}^2 R - M_{\rm Pl}^2(3H^2 + \dot{H}) + M_{\rm Pl}^2\dot{H}g^{00} \\ &+\frac{1}{2}M_2^4(t)(\delta g^{00})^2 + \frac{1}{3!}M_3^4(t)(\delta g^{00})^3 \\ &-\frac{\bar{M}_2^2(t)}{2}\left(\delta K^\mu_{\ \mu}\right)^2 - \frac{\bar{M}_3^2(t)}{2}\delta K^\mu_{\ \nu}\delta K^\nu_{\ \mu} \\ &-\frac{\bar{M}_1^3(t)}{2}(\delta g^{00})\delta K^\mu_{\ \mu} + \cdots\Big]. \end{aligned} \tag{2.77}$$

A common assumption follows from the observation that we are interested in solutions where H and $\dot{H}$ do not vary significantly over one efold. Therefore, it is quite natural to assume the same holds for all the parameters controlling the EFT expansion. The obtained action describes the most generic dynamics for the fluctuations not only for the scalar mode but also for the two tensor degrees of freedom. If one wants to connect with a specific model of inflation, it suffices to express it in the unitary gauge where fluctuations of the clock vanish, so that

$$\int \mathrm{d}^4x\sqrt{-g}\left[-\frac{1}{2}(\partial\phi)^2 - V(\phi)\right] \to \int \mathrm{d}^4x\sqrt{-g}\left[-\frac{\dot{\bar{\phi}}^2}{2}g^{00} - V(\bar{\phi})\right] \tag{2.78}$$

As Friedmann equations give $\dot{\bar{\phi}}^2 = -2M_{\rm Pl}^2\dot{H}$ and $V(\bar{\phi}) = M_{\rm Pl}^2(3H^2 + \dot{H})$, it clearly appears that it takes the form of Eq. (2.77) where all but the three first terms are set to zero. It illustrates the fact that these three terms describe the background dynamics and all the other terms encode the possible effects of high-energy physics on this simple slow-roll model of inflation. Beyond the background level, a matching procedure allows us to connect the Wilsonian coefficients to the parameters of the microphysical model when the latter is known.

While it provides a generic description, the Lagrangian of Eq. (2.77) in the unitary gauge keeps the physics hidden. We showed that it captures the standard single-field slow-roll inflation, but the role played by the scalar degree of freedom, the one of interest for cosmological observations, is maintained cryptic. We will now make it transparent and separate it from the two graviton helicities. This procedure is known as the *Stückelberg trick*. The role played by Goldstone boson is made explicit when performing the broken gauge transformation associated with the sponteneous symmetry breaking pattern. Indeed, during the construction of the low-energy EFT, we have worked in the *unitary gauge* where the metric carries all the three dynamical degree of freedom. We rather would like the gauge field to propagates only two degrees of freedom, just at it does in the free theory. To do so, we will introduce a *Stückelberg field* which serves to restore the gauge symmetry. As the symmetry ensures the gauge field to propagate only two degrees of freedom, the Stückelberg field absorb the remaining degree of freedom. In this way, restoring the symmetry allows us to make the dynamics of the Goldstone boson explicit.

Stückelberg trick: Let us illustrate it for the $U(1)$ symmetry breaking pattern. We consider the Abelian-Higgs mechanism for electromagnetism, following [12]. This mechanism illustrates how a vector field acquires a mass dynamically. Let us start with a vector field A_μ with associated Maxwell tensor $F_{\mu\nu} = \partial_\mu A_\nu - \partial_\nu A_\mu$. The initial action

$$\mathcal{L} = -\frac{1}{4} F_{\mu\nu} F^{\mu\nu} \tag{2.79}$$

enjoys a $U(1)$ gauge symmetry, being invariant under $A_\mu \to A_\mu + \partial_\mu \xi$ for an arbitrary scalar ξ. There is initially two dynamical degrees of freedom, the two transverse modes. In general, a Proca action of the form

$$\mathcal{L}_{\text{Proca}} = -\frac{1}{4} F_{\mu\nu} F^{\mu\nu} - \frac{1}{2} m^2 A_\mu A^\mu \tag{2.80}$$

breaks the $U(1)$ gauge symmetry because of the mass term so that the longitudinal mode is now dynamical. A massive vector field thus propagates three degrees of freedom, two transverse modes and one longitudinal mode. This action naturally appears when we couple electromagnetism with a complex scalar field ϕ having a quartic potential

$$\mathcal{L}_{\text{AH}} = -\frac{1}{4} F_{\mu\nu} F^{\mu\nu} - \frac{1}{2} \left(\mathcal{D}_\mu \phi\right) \left(\mathcal{D}^\mu \phi\right)^* - \lambda \left(\phi \phi^* - v^2\right)^2 . \tag{2.81}$$

The covariant derivative, $\mathcal{D}_\mu = \partial_\mu - iqA_\mu$ ensures the existence of the $U(1)$ symmetry under which the fields transform as

$$A_\mu \to A_\mu + \partial_\mu \xi \tag{2.82}$$

$$\phi \to \phi e^{iq\xi} \tag{2.83}$$

Then, there is three dynamical degrees of freedom in the system. Splitting the complex scalar into norm and phase $\phi = \varphi e^{i\chi}$, we observe that the covariant

derivative generates a mass term for the vector field when the scalar field acquires a non-vanishing vacuum expectation value

$$\mathcal{L}_{\rm AH} = -\frac{1}{4}F_{\mu\nu}F^{\mu\nu} - \frac{1}{2}\varphi^2\left(qA_\mu - \partial_\mu\chi\right)^2 - \frac{1}{2}\left(\partial_\mu\varphi\right)^2 - \lambda\left(\varphi^2 - v^2\right)^2 . \quad (2.84)$$

By setting $\lambda \gg 1$, the Higgs field φ is made arbitrarily massive in such a way that its dynamics may be neglected, the field being frozen at $\varphi = v$. The resulting theory is that of a massive vector field

$$\mathcal{L}_{\rm AH} = -\frac{1}{4}F_{\mu\nu}F^{\mu\nu} - \frac{1}{2}v^2\left(qA_\mu - \partial_\mu\chi\right)^2 . \quad (2.85)$$

As we saw above, the vector field may propagate three dynamical degrees of freedom in the presence of a mass term breaking the $U(1)$ gauge symmetry. Yet, in the current setting, we can restore the $U(1)$ gauge symmetry under the prescription that the fields transform as

$$A_\mu \to A_\mu + \partial_\mu\xi \quad (2.86)$$

$$\chi \to \chi + q\xi \quad (2.87)$$

Hence, the gauge symmetry is restored at the price of introducing a Stückelberg field χ which transforms in a way that makes the mass term invariant. We now see that the Goldstone boson *non-linearly realizes the symmetry* (in the sense that zero is not mapped to zero). The symmetry ensures the vector field A_μ propagates solely two degrees of freedom while χ propagates the third degree of freedom. Restoring the symmetry has been a way to disentangle the dynamics of the Goldstone boson from the rest of the dynamical degrees of freedom. Its peculiarity is captured in the way it realizes the symmetry known as a *non-linear shift symmetry*. Defining the mass $m = vq$ and the canonical normalization $\chi_c \equiv m/q.\chi$, the advantage of having reintroduced the Goldstone mode is manisfest at energies $E \gg m$. In this limit, the mixing between the Goldstone and the transverse components of the gauge field becomes irrelevant and the two sectors *decouple*. Indeed, the mixing terms are of the form

$$\frac{m^2}{q}A_\mu\partial^\mu\chi = mA_\mu\partial^\mu\chi_c \quad (2.88)$$

which are irrelevant with respect to the canonical kinetic term $(\partial\chi_c)^2$ for $E \gg m$. In this high-energy window, the physics of the Goldstone χ is weakly coupled and it can be studied neglecting the mixing with the transverse components.

Similarly, in the inflationary case, despite the EFT action Eq. (2.77) might break covariance, the gauge symmetry can always be formally restored using the Stückelberg trick, after which the symmetry is non-linearly realized for the Goldstone modes and general covariance restored. The procedure to reintroduce the Goldstone is similar to the gauge theory case. To illustrate the procedure, let us

perform a time translation diffeomorphism

$$t \to \tilde{t} = t + \xi^0(x), \qquad x_i \to \tilde{x}_i = x_i \tag{2.89}$$

on the action

$$\int \mathrm{d}^4x\sqrt{-g}\left[A(t) + B(t)g^{00}(x)\right]. \tag{2.90}$$

$A(t)$ and $B(t)$ transforms as scalars under this transformation, that is $A(t) \to \tilde{A}(\tilde{t}) = A(t)$ and $B(t) \to \tilde{B}(\tilde{t}) = B(t)$ while

$$g^{00}(x) \to \tilde{g}^{00}(\tilde{x}) = \frac{\partial\tilde{t}}{\partial x^\mu}\frac{\partial\tilde{t}}{\partial x^\nu}g^{\mu\nu}(x). \tag{2.91}$$

The action after the transformation takes the form

$$\int \mathrm{d}^4\tilde{x}\sqrt{-\tilde{g}}\left[A(\tilde{t}-\xi^0) + B(\tilde{t}-\xi^0)\frac{\partial(\tilde{t}-\xi^0)}{\partial\tilde{x}^\mu}\frac{\partial(\tilde{t}-\xi^0)}{\partial\tilde{x}^\nu}\tilde{g}^{\mu\nu}(\tilde{x}).\right] \tag{2.92}$$

where we used the fact that $t = \tilde{t} - \xi^0$ and inverted Eq. (2.91) in order to express $g^{00}(x)$ in terms of $\tilde{g}^{\mu\nu}(\tilde{x})$. Whenever ξ^0 appears in the action, for a reason that will be apparent in a second, we make the substitution $\xi^0 \to -\tilde{\pi}(\tilde{x})$ in order to introduce the Stückelberg field. Dropping the tildes for clarity, we obtain the action

$$\int \mathrm{d}^4x\sqrt{-g}\left\{A[t+\pi(x)] + B[t+\pi(x)]\partial_\mu[t+\pi(x)]\partial_\nu[t+\pi(x)]g^{\mu\nu}(x)\right\}. \tag{2.93}$$

One can check that Eq. (2.93) is indeed invariant under diffeomorphisms at all order upon assigning to π the transformation rule

$$\pi(x) \to \tilde{\pi}(\tilde{x}) = \pi(x) - \xi^0, \tag{2.94}$$

that is π transforms as a scalar field plus an additional shift under time diffeomorphisms.

Applying this procedure to Eq. (2.77), all the time-dependent coefficients must be evaluated at $t + \pi$, leading to

$$\begin{aligned} S = \int \mathrm{d}^4x\sqrt{-g}\Big\{&\frac{1}{2}M_{\rm Pl}^2R - M_{\rm Pl}^2[3H^2(t+\pi) + \dot{H}(t+\pi)] \\ &+M_{\rm Pl}^2\dot{H}(t+\pi)\left[\partial_\mu(t+\pi)\partial_\nu(t+\pi)g^{\mu\nu}\right] \\ &+\frac{1}{2}M_2^4(t+\pi)\left[1+\partial_\mu(t+\pi)\partial_\nu(t+\pi)g^{\mu\nu}\right]^2 \\ &+\frac{1}{3!}M_3^4(t+\pi)\left[1+\partial_\mu(t+\pi)\partial_\nu(t+\pi)g^{\mu\nu}\right]^3 + \cdots\Big\} \end{aligned} \tag{2.95}$$

where we have neglected for simplicity the terms proportional to $\bar{M}_n$ involving the extrinsic curvature. At this point, the obtained action is complicated and there is no apparent advantage of reintroducing the Goldstone π compared to the unitary gauge Lagrangian of Eq. (2.77). Yet, a simplification occurs in the decoupling limit, just as for the gauge theory case. By comparing the mixing terms to the canonical kinetic

terms, we can estimate the energy scale at which the decoupling occurs (see [2] for details). In the regime $E \gg \varepsilon_1 H$, the action drastically simplifies to

$$S_\pi = \int \mathrm{d}^4x\sqrt{-g}\Bigg\{\frac{1}{2}M_{\rm Pl}^2 R - M_{\rm Pl}^2\dot{H}\left[\dot{\pi}^2 - \frac{(\partial_i\pi)^2}{a^2}\right] \\ +2M_2^4\left[\dot{\pi}^2 + \dot{\pi}^3 - \dot{\pi}\frac{(\partial_i\pi)^2}{a^2}\right] - \frac{4}{3}M_3^4\dot{\pi}^3 + \cdots\Bigg\} \tag{2.96}$$

Here, we are assuming that the time dependence of the coefficients is slow compared to the Hubble time such that the additional π terms coming from the Taylor expansion of the coefficients are slow-roll suppressed. The non-linear realization of the time-diffeomorphisms forces π to appear into non-linear blocks which generates intricate observational signatures. For instance, modifying M_2^4 generates an effective speed of sound which affects the power spectrum but also increases the signal of the bispectrum by changing the interactions $\dot{\pi}^3$ and $\dot{\pi}(\partial_i\pi)^2$. Finally, one may be skeptical about the usefulness of the decoupling limit only valid at high energy given our goal of computing late-time (IR) observables. Yet, the conservation of ζ on super-horizon scales makes that one can compute observables right after horizon crossing where $E \sim H \gg \varepsilon_1 H$, well within the regime of validity of the decoupling limit, then use the conservation of ζ to propagate the result at late time. Note that if it is not justified to work within the decoupling limit, one can keep interactions with the graviton helicity by working with Eq. (2.77) for instance.

The above action is simple and unifies all single-field inflationary models undergoing a slow-roll phase. It describes the theory for fluctuations which are what we actually confront to observations of the CMB and the LSS. In this language, inflation is the theory of a Goldstone boson associated to the time-translation symmetry breaking. It makes the underlying physics transparent: the existence of scalar fluctuations relates to the order parameter of a spontaneous symmetry-breaking pattern as a simple unifying principle. In particular, it explains why so many microphysical models share the same macrophysical properties. The fact that it applies to all possible single-clock inflationary models allows us to prove theorems valid for this class of theories on the possible signals to expect. In this sense, it is an appropriate formalism to confront single-field slow-roll inflation with its extensions.

2.3.2 Extensions

Now that we have a unified framework capturing the phenomenology of single-field slow-roll inflation, we are in position to discuss possible extensions around this framework.

High-energy extensions: We have seen in Eq. (2.64) that inflation could occur as high as $H \sim 10^{13}$ GeV. This energy scale is far above the highest energies we can probe on Earth, of the order of the TeV. For this reason, inflation is likely to access regimes where particle physics remains vastly elusive. From a model building perspective, high-energy extensions often amount to consider an enlarged particle sector which we might be able to connect to the fundamental structure of the theory such as in the *Minimal Supersymmetric Standard Model* (MSSM) [139, 140] or in *Grand*

Unified Theory (GUT) scenarios [141]. These *Beyond Standard Model* (BSM) extensions offer opportunities to connect particle physics and cosmology, constraining parameter spaces with both collider experiments and cosmological surveys.

Ultimately, we would like to connect inflation to an even higher energy pre-inflationary phase naturally described by a theory of *Quantum Gravity* (QG). The hope is that of an updated description which would resolve the Big Bang singularity and naturally provide a mechanism to generate inflation, constrained by observations. The possibility of embedding inflation in the context of string theory has been widely studied in the past, see [142] for a review. Popular scenarios encompass inflation from *relativistic branes* (e.g. DBI inflation, though effectively captured through the framework of Sec. 2.3.1), inflation with *axions* (e.g. axion monodromy) or inflation with *Kähler moduli*.

Multifield inflation: At a phenomenological level, both BSM and QG approaches coincide in practice with the study of multifield inflation, which provides a natural extension to single-field slow-roll inflation [25]. Let us briefly motivate the existence of multiple scalars in high-energy frameworks. Already at $d = 10$ dimensions, the low-energy limit of supersymmetric string-theory known as supergravity contains several scalars such as the *dilaton*. The closed string sector might also contain several axions enjoying a discrete shift symmetry $\theta \to \theta + (2\pi)f$ where f is the decay constant. Going from ten dimensions to the four-dimensional spacetime we observe in cosmology is made through the *compactification* of six extra dimensions that are turned into internal dimensions. The obtained EFT of the four-dimensional manifold highly depends on the compactification process, which often generates large number of moduli with an infinite tower of masses [143]. Besides approaches based on string theory, it is natural to assume the existence of a wider set of dynamical degrees of freedom at high energy: this is precisely what the EFT dictionary taught us in Chapter 1. Hence, extra fields provide a natural environment for the inflaton.

Multifield constructions often start with the fairly generic partial UV completion

$$S = \int \mathrm{d}^4x\sqrt{-g}\left[\frac{M_{\rm Pl}^2}{2}R - \frac{1}{2}g^{\mu\nu}G_{IJ}\partial_\mu\phi^I\partial_\nu\phi^J - V(\phi)\right] \tag{2.97}$$

which consists in gravity coupled to a set of scalar fields ϕ^I in a curved field space whose geometry is described by the field space metric G_{IJ}. At the level of the background, homogeneous scalar leads to the Friedmann equation

$$3M_{\rm Pl}^2H^2 = \frac{1}{2}\dot\Phi^2 + V(\phi) \quad \text{and} \quad \dot H = -\frac{\dot\Phi^2}{2M_{\rm Pl}^2} \tag{2.98}$$

where $\dot\Phi^2 = G_{IJ}\dot\phi^I\dot\phi^J$. The background equations of motion for the fields are

$$D_t\dot\phi^I + 3H\dot\phi^I + G^{IJ}V_{,J} = 0 \tag{2.99}$$

where $D_t\dot\phi^I = \ddot\phi^I + \Gamma^I_{JK}\dot\phi^J\dot\phi^K$ defines the field-space covariant time derivative, Γ^I_{JK} being the field space connections defined in an analogous manner as Eq. (2.13) and $V_{,J} = \partial V/\partial\phi^J$. The two first slow-roll parameters simply generalises the single-field case given in Eq. (2.33) by

$$\varepsilon_1 = \frac{\dot\Phi^2}{2M_{\rm Pl}^2H^2} \qquad \text{and} \qquad \varepsilon_2 = 2\left(\varepsilon_1 + \frac{\ddot\Phi}{H\dot\Phi}\right). \tag{2.100}$$

When the scalar potential is flat enough, one can define a generalised slow-roll approximation for which the slow-roll equations of motion reduce to

$$\dot{\phi}^I = -\frac{G^{IJ}V_{,J}}{3H}. \tag{2.101}$$

Yet, in general, one cannot assume the individual accelerations $D_t\dot{\phi}^I$ to be negligible, which can be large but compensate each other. It happens when the field space trajectory is bent. In that case, one must either resort to a numerical resolution or adopt a geometrical approach in which the scalar degrees of freedom are usually decomposed into a basis where one direction has a flat potential, corresponding to the inflationary valley of single-field slow-roll inflation, and the other ones are curved, corresponding to heavy directions known as *entropic* or *isocurvature modes* [144–153]. This approach is the so-called *adiabatic-entropic decomposition* of multifield inflation and relies on the introduction of veilbeins, one of which points towards the background trajectory given by the adiabatic direction and the other ones corresponding to the $N_{\rm field}-1$ orthogonal directions. Usually, one fixes the first entropic direction as being the instantaneous rate of turn of the adiabatic direction and all the other directions are defined from a wedge product of the first two directions. At the level of the perturbations, this decomposition naturally leads to a linear mixing between the adiabatic and first entropic direction. Formally, one defines a space-time foliation, adopts the ADM formalism of general relativity and perturbs the fields and the metric, as explicitly done in [153]. The gauge is fixed and the constraints solved in this gauge. Injecting the result for the constraints into the action, one finally obtains the perturbed Lagrangian, which at quadratic order in the comoving gauge where the dynamical degrees of freedom are the curvature perturbation ζ and the $N_{\rm field}-1$ entropic directions $\mathcal{F}^\alpha$ writes

$$\begin{aligned}\mathcal{L}^{(2)} = a^3\Big\{&\varepsilon_1 M_{\rm Pl}^2\left[\dot{\zeta}^2 - \frac{(\partial_i\zeta)^2}{a^2}\right] + 2\sqrt{2\varepsilon_1}M_{\rm Pl}\eta_\perp\delta_{\alpha 1}\mathcal{F}^\alpha\dot{\zeta}\\ &+\frac{1}{2}\left[(\dot{\mathcal{F}}^\alpha)^2 - \frac{(\partial_i\mathcal{F}^\alpha)^2}{a^2} - m_{\alpha\beta}\mathcal{F}^\alpha\mathcal{F}^\beta + 2\Omega_{\alpha\beta}\dot{\mathcal{F}}^\alpha\mathcal{F}^\beta\right]\Big\}.\end{aligned} \tag{2.102}$$

The parameter $\eta_\perp$ is the rate of turn of the adiabatic direction e^I_ζ defined as $D_t e^I_\zeta = \eta_\perp e^I_\zeta$. The matrices $m_{\alpha\beta}$ and $\Omega_{\alpha\beta}$ have involved expressions whose details can be found in [153] which do not matter for the purpose of this manuscript. We obtain a phenomenology driven by a linear mixing of the form $\mathcal{F}^\alpha\dot{\zeta}$ between the adiabatic direction and the entropic sector. This generic feature plays an important role in the *quantum recoherence* process [154] later discussed in this manuscript. Note that this phenomenology equally emerges from the bottom-up construction of multifield inflation, which do not assume the UV-completion (2.97) as a starting point.

Bottom-up construction of multifield inflation: Based on [155], we construct a general phenomenology of inflation in the presence of hidden sectors (note that this construction is not the first, see [25] for details on multifield phenomenology). Let us consider two scalars, one of which, Φ, enjoys an approximate shift-symmetry, while the other Σ, represents the hidden sector. Let us discuss the EFT of the $\Phi-\Sigma$ couplings. We consider a Lagrangian

density of the form

$$\mathcal{L}_\Phi = -\frac{1}{2}(\partial\Phi)^2 - V(\Phi) \tag{2.103}$$

with a flat-enough potential sustaining a phase of slow-roll. The approximate shift-symmetry $\Phi \to \Phi + \text{const.}$ constrains self-interactions in the potential to be small and the related non-Gaussianities to be unobservable, neglecting higher-derivative operators of the form $(\partial\Phi)^4$. We consider a Lagrangian density for the hidden sector of the form

$$\mathcal{L}_\Sigma = -\frac{1}{2}(\partial\Sigma)^2 - V(\Sigma), \tag{2.104}$$

yet, in the case of the hidden sector, interactions are much less constrained and in particular, self-interactions in $V(\Sigma)$ can be large. The mixing between the two sectors is expressed in terms of the most general operators allowed in the EFT

$$\mathcal{L}_{\text{mix}}[\Phi, \Sigma] = \sum_n c_n \frac{\mathcal{O}_n[\Phi, \Sigma]}{\Lambda^{\delta_n - 4}} \tag{2.105}$$

where the operators $\mathcal{O}_n$ are made out of powers of the fields Φ and Σ and their derivatives. The mass dimensions of the operators are given by δ_n and the Wilson coefficients c_n are dimensionless. The approximate shift symmetry of $\Phi \to \Phi + \text{const.}$ drastically restrict the list of accessible operators, excluding all operators involving Φ as opposed to the ones made of $\partial_\mu\Phi$. In Table 2.1, we explictly construct the list of available operators from at most first derivative, up to dimension 5, enforcing the approximate shift symmetry.

Dimension	Operators
0	V_0
1	Σ
2	Σ^2
3	Σ^3
4	Σ^4, $(\partial\Phi)^2$, $(\partial\Sigma)^2$, $\partial_\mu\Phi\partial^\mu\Sigma$
5	Σ^5, $\Sigma(\partial\Phi)^2$, $\Sigma(\partial\Sigma)^2$, $\Sigma(\partial_\mu\Phi\partial^\mu\Sigma)$

Table 2.1: List of all operators constructed from at most first derivatives, up to dimension 5, enforcing the shift symmetry $\Phi \to \Phi + \text{const.}$ The notation $(\partial\Phi)^2$ stands for $\partial_\mu\Phi\partial^\mu\Phi$

At this order, only three operators, $\partial_\mu\Phi\partial^\mu\Sigma$, $\Sigma(\partial_\mu\Phi\partial^\mu\Sigma)$ and $\Sigma(\partial\Phi)^2$ contribute to the mixing, two of which can be reabsorbed either by field redefinition or by redundancy. Indeed, we diagonalize the kinetic term $\partial_\mu\Phi\partial^\mu\Sigma$ by performing a rotation in field space $\Phi \to \cos(\theta)\Phi - \sin(\theta)\Sigma$ and $\Sigma \to \sin(\theta)\Phi + \cos(\theta)\Sigma$. It suffices to impose the shift symmetry after the diagonalizing procedure, motivated by the fact primordial fluctuations are observed to be nearly scale-invariant. The dimension 5 coupling $\Sigma(\partial_\mu\Phi\partial^\mu\Sigma)$ is removed by integrating by parts (see [155] for details on the boundary term)

$$\Sigma(\partial_\mu\Phi\partial^\mu\Sigma) \to -\Box\Phi\Sigma^2 \tag{2.106}$$

which is redundant. Indeed, using Φ's equation of motion $\Box\Phi = \partial_\Phi V$, we can rewrite it in terms of $\Phi^m\Sigma^n$ which is included in the standard EFT treatment and have to be small due to the approximate shift-symmetry. Hence, the mixing between the inflaton and the hidden sector is mediated through

$$\mathcal{L}_{\rm mix} = -\frac{1}{2}\frac{\Sigma\,(\partial\Phi)^2}{\Lambda}. \tag{2.107}$$

Cosmological inhomogeneities seeding the observables of the CMB and the LSS originate from small fluctuations around the background vacuum expectation values

$$\Phi(t,\boldsymbol{x}) = \Phi_0(t) + \varphi(t,\boldsymbol{x}) \quad \text{and} \quad \Sigma(t,\boldsymbol{x}) = \Sigma_0(t) + \sigma(t,\boldsymbol{x}). \tag{2.108}$$

In the spatially flat gauge where the spatial part of the metric is unperturbed $g_{ij} = a^2\delta_{ij}$, the primordial curvature perturbations are given by

$$\zeta(t,\boldsymbol{x}) \equiv -\frac{H}{\dot\Phi_0}\varphi(t,\boldsymbol{x}). \tag{2.109}$$

At leading order in the slow-roll expansion, the inflaton fluctuations are massless and the mixing between matter and the metric fluctuations (helicities) vanishes [155]. It follows that the complete Lagrangian for the $\varphi-\sigma$ dynamics is

$$\mathcal{L}_{\rm eff}\left[\varphi,\sigma\right] = -\frac{1}{2}\left(\partial\varphi\right)^2 - \frac{1}{2}\left(\partial\sigma\right)^2 - \frac{1}{2}m^2\sigma^2 + \rho\dot\varphi\sigma - \frac{1}{2}\frac{\left(\partial\varphi\right)^2\sigma}{\Lambda} - \mu\sigma^3 + \cdots \tag{2.110}$$

where we stopped at the first non-linear operator σ^3 in the hidden sector. The linear mixing $\rho\dot\varphi\sigma$ with coupling constant $\rho \equiv \dot\Phi/\Lambda$ plays a crucial role in the dynamics of the mixing between the inflaton and the hidden sector.

Already at linear order, the existence of a massive degree of freedom during inflation generates an interesting phenomenology. Note that Planck results strongly constrained isocurvature perturbations (see e.g. [87]) which sets upper bounds on ρ. Environmental self-interactions $\mu\sigma^3$ affect the system by coupling with the linear mixing $\rho\dot\varphi\sigma$ which generates primordial non-Gaussianities for the curvature perturbations. It leads to the famous *cosmological collider* signature [156] on the squeezed limit of the bispectrum which directly relates to the mass of the environmental field, providing a potential smoking-gun for multifield inflation.

The phenomelogy of multifield inflation has been motivated by the search for signatures of new physics in the early universe signal [105, 147, 151, 152, 155]. This research program aims at characterising the precise number of fields together with their spin, masses and interactions. It includes the understanding of the inflationary dynamics in the presence of multiple scalars as described above but also the effect of spinning particles during inflation and the inclusion of higher orders in derivatives in the context of modified gravity. Unravelling the particle content of the early universe is often referred to as the *cosmological collider program* [156].

The understanding of hidden sectors has been well developed within the past few years and most of their possible observational signatures discussed. Just as we did in Sec. 2.3.1, it would be valuable to encompass the variety of possible extensions within a minimal set of physical principles. Unfortunately, we face the difficulty that extensions to single-field slow-roll inflation are *a priori* much less symmetric than the single-field construction. Given the lack of observational guidance, there is no reason to expect the existence of non-linearly realised symmetry which usually provides the best control over the theory. Hence arises the question of knowing how we can develop systematic extensions around single-field slow-roll inflation in a model-independent manner.

Short and soft modes: From a hydrodynamical perspective, new physics can also be understood as the accounting for the role of the small-scale physics on the large-scale dynamics probed in the CMB and the LSS. This interplay between scales separates into two distinct mechanisms, one of which is specific to the inflationary dynamics, corresponding to the inflow of UV mode into the IR continuum, and the other common among all gravitational settings, due to the fact that GR is a fundamentally non-linear theory. It provides two distinct manners for the small scales to generate imprints on the large-scale dynamics, that is two distinct manners for inflation to mix scales and generate interplay between regimes.

During inflation, Fig. 2.8 illustrates the existence of a natural scale separation between modes within the horizon (sub-Hubble) that do not feel the background curvature and the super-Hubble modes which we today observe. We can then define a fundamental bipartition by schematically separating

$$\zeta(\boldsymbol{x},t)=\int_{k>aH}\frac{\mathrm{d}^3\boldsymbol{k}}{(2\pi)^3}e^{i\boldsymbol{k}\boldsymbol{x}}\zeta(\boldsymbol{k},t)+\int_{k<aH}\frac{\mathrm{d}^3\boldsymbol{k}}{(2\pi)^3}e^{i\boldsymbol{k}\boldsymbol{x}}\zeta(\boldsymbol{k},t). \tag{2.111}$$

The first term corresponds to the UV scales we want to integrate out in order to solely describes the hydrodynamical/coarse-grained dynamics of the IR scales of the second term. The subtlety follows from the fact that as time proceed, there is a continuous inflow of sub-Hubble modes that cross the horizon and become super-Hubble, as described in Fig. 2.8. Classically, this phenomenon is well described within the framework of *stochastic inflation* [157–172] which aims at providing a description of the long-wavelength part of the quantum fields *coarse grained* over a physical scale larger than the Hubble radius. In this framework, the small wavelength fluctuations impact the long-wavelength dynamics as a classical noise arising when they cross the coarse-graining horizon so that the IR theory is described in terms of a classical stochastic framework (Langevin equation for the field values, Fokker-Planck equation for the dynamics of their probability distribution and Martin-Siggia-Rose path integral for their field theoretic path integral representation).[13]

Beyond the peculiar inflationary dynamics, GR remains a highly non-linear theory such that all scales couple together and the careful accounting for the effect

[13]The embedding of stochastic inflation within a quantum framework has been the object of recent studies [173–175] which provide a concrete application for the Open EFT program [173, 176, 177]. It seems fair to admit that so far, no complete understanding (in the sense of a rigurous derivation of stochastic inflation from within the Open EFT framework) is known. The recent developments of hybrid quantum-classical dynamics [178–180] might provide the missing cornerstone to encompass stochastic inflation and Open EFTs within the same language, combined with the Non-Equilibrium EFT approaches of [8, 9].

of non-linearities may be crucial for precision cosmology. Mode coupling induced by GR can also turn into a precision test to confront it against alternative theories. The null detection of primordial non-Gaussianities in the *squeezed limit* (a super-Hubble scale coupled to two sub-Hubble modes) of the bispectrum [75] is in agreement with the so-called *consistency relations* emerging from the study of the cubic self-interactions of GR, as done in the seminal paper [49]. The idea is that the soft limit of an IR mode generates a very long wavelength modulation of the background, which, combined with the symmetry prescriptions of the theory, induces stringent constraints on the squeezed limit of the bispectrum of any single-clock model [49, 181–183]. New physics could materialise itself through violation of these consistency conditions, and so their intense investigation in the CMB (see e.g. [184]) and the LSS (see e.g. [185]), which necessitates a careful treatment of the post-inflationary contamination of the signal (see e.g. [186, 187]).

Conclusions:

The early-universe promise is the one of a new window towards unknown physics. After reviewing the Bayesian inference framework at the heart of model discrimination in cosmology, we presented the Λ-CDM model which today gathers the most confidence. Turning our attention to the early-universe content of the concordance model, we saw the crucial role played by single-field slow-roll inflation. After discussing the regime probed by current experiments which sustains it, we highlighted a few difficulties to embed it in a wider UV picture. We then presented a framework that serves as a basis for the rest of the manuscript. We introduced an EFT construction synthesizing a variety of microphysical models into a few universal properties which provides a minimal framework compatible with the current observations. From a fundamental perspective, this construction often has to be supplemented by new ingredients called extensions which represent the inclusion of new physics. They may correspond to high-energy extensions which are often phenomenologically modelled in the context of multifield inflation by hidden sectors. In the rest of this manuscript, we aim at implementing Open EFT techniques to model the impact of hidden sectors onto the dynamics of single-field slow-roll inflation.

Chapter 3

Open EFTs for primordial cosmology

In this Chapter, we propose an overview of Open EFTs and a guide to their implementation in cosmology. Further details can be found in reviews [10, 22] or textbooks partially covering this topic [13, 188].

In the previous Chapter, we identified a minimal framework, the one of single-field slow-roll inflation, on which we would like to incorporate extensions of new physics. To tackle this problem, we develop the **Open EFT formalism**, defined as the application of *Open Quantum System (OQS) theory* to QFT settings.[1] OQS theory was first developed in the context of quantum optics and it might be unclear why it has the ability to tackle problems in cosmology. We first review this aspect in Sec. 3.1. We then discuss in Sec. 3.2 the general method sustaining the application of these tools in cosmology. Finally, in Sec. 3.3, we provide a detailed roadmap to their implementation and discuss open problems in Sec. 3.4.

3.1 Motivation

Clearly, Open EFTs are not the only techniques existing to incorporate the effects of hidden sectors onto a given physical description, as seen from the variety of EFT descriptions we already encountered. Among the various existing procedures, what renders Open EFTs interesting for cosmology?

3.1.1 The quantum-to-classical transition

One of the most fascinating aspects of inflation relies in its ability to trace back the origin of all the structures we today observe in the universe to quantum fluc-

[1] The application of Open EFTs in cosmology is sometimes referred to as *Cosmological OQS* or as *Cosmological Open EFTs*.

tuations of the primordial vacuum. In order to understand the full implications of this statement, we need to develop a formalism able to keep track of the quantum information properties of the system. In general, this is a hard task, in particular in the presence of unknowns related to the elusiveness of the physics at high energy. In quantum optics, a device is often embedded in a wider environment that is not very well specified, for instance the laboratory room. If one wants to make precise measurements, one needs to model the way a poorly specified environment may affect the observables. OQS have been precisely designed for this purpose. If we manage to implement OQS techniques in cosmology, we might be able to model the impact of an almost unknown cosmological extension onto the dynamics of single-field slow-roll inflation in a systematic manner.

Among the motivations for the use of Open EFTs in cosmology, their ability to keep track of the quantum information properties of the system is certainly one of the most remarkable. In order to understand the interest of the community for this aspect, we need to review a decade-old debate known as the so-called *quantum-to-classical* transition of cosmological inhomogeneities. Reviewing this topic is far from being an easy task, given the fuzzy nature of the debate which encompasses several questions such as:

1. Can we model inflation from within a classical stochastic theory? [117–119]

2. Can we prove the quantum nature of cosmic inhomogeneities? [106, 107, 110]

3. Can we explain the appearance of classical geometry from within a quantum realm? [189, 190]

where we here solely provide for a few references in order to illustrate the various positions.

We organise this section in the following manner. We first argue that 1. and 2., far from being incompatible, are in fact the two faces of a same coin: the peculiarity of the inflationary dynamics, through the process of *quantum squeezing*, generates a dynamics which can be seen by some aspects as highly 'classical' and by others as highly 'quantum'. Indeed, the very high level of quantum squeezing induces the suppression of the decaying mode we observed in Eq. (2.60). It renders possible to mimick inflation with a classical stochastic theory [120] in the sense that a classical construction can be obtained such that it reproduces the observed primordial power spectrum. At the same time, the cosmological inhomogeneities are placed in a quantum state known as a *two-mode squeezed state* [114, 116, 121] which exhibits very large amounts of quantum correlations along a certain bipartition we will soon specify. This is the reason why cosmological inhomogeneities can be seen as highly classical and highly quantum at the same time.

We then turn our attention to 2. and highlight that, once the question of proving the quantum nature of cosmological inhomogeneities is posed, a plethora of technical and conceptual obstructions arise [110]. Some of these obstructions might be answered by the Open EFT program which motivates its implementation in cosmology. In particular, the mechanism of quantum decoherence [191–193], well-modelled within the OQS framework, provides a fundamental obstruction to the exhibition of quantum correlations in the sky and this manuscript aims at providing a toolbox to explore the phenomenology of this physical process during inflation.

Finally, in relation with 3., we argue that depending on the perspective we adopt, the knowledge of decoherence may or may not be sufficient to explain why cosmological perturbations appear classical to us. From the semiclassical point of view, if cosmological perturbations initially exhibit genuine quantum correlations which might be revealed through a Bell test, decoherence "classicalizes" the system, in the sense it obstructs our ability to exhibit the genuine quantum correlations. Yet, from a quantum gravity perspective, quantum decoherence by itself is not sufficient to explain the emergence of a classical geometry from within a quantum realm as one still has to go through the measurement problem as raised by Sudarsky in [189]. Hence, one has to work harder and find ways to circumvent this problem such as, e.g., Quantum Darwinism [194, 195].

Quantum-squeezing: Let us consider the quadratic evolution of single-field slow-roll inflation described in Eq. (2.48). We already saw that it generates a power spectrum for the curvature perturbations of the form

$$P_\zeta(k) \simeq \frac{1}{2\varepsilon_1 M_{\rm Pl}^2}\frac{H^2}{2k^3}, \tag{3.1}$$

and that correlators containing $\dot\zeta$ insertions are exponentially suppressed by $e^{-\Delta N_*(k)}$ at the end of inflation, $\Delta N_*(k)$ being the number of efolds spent by a mode above the horizon. In order to gain insight on the structure of the quantum correlations generated during inflation, it is instructive to characterise the quantum state in which cosmological inhomogeneities are placed.

Two-mode squeezed states: Starting from the quadractic action for the curvature perturbations given in Eq. (2.48), let us first introduce the rescaled Mukhanov-Sasaki variable $v(\eta,\boldsymbol{x}) \equiv z(\eta)\zeta(\eta,\boldsymbol{x})$ where $z(\eta) \equiv a(\eta)\sqrt{2\varepsilon_1}M_{\rm Pl}$ is a time-dependent variable of the background. At linear order, the action for the perturbations writes

$$S_v^{(2)} = \frac{1}{2}\int {\rm d}\eta {\rm d}^3\boldsymbol{x}\left[(v')^2 - (\partial_i v)^2 + \frac{z''}{z}v^2\right], \tag{3.2}$$

which is the action for a free scalar field with a time dependent mass $m_{\rm eff}^2 = -z''/z$. One can add a total derivative term to obtain the equivalent action

$$S_v^{(2)} = \frac{1}{2}\int {\rm d}\eta {\rm d}^3\boldsymbol{x}\left[(v')^2 - (\partial_i v)^2 - 2\frac{z'}{z}vv' + \left(\frac{z'}{z}\right)^2 v^2\right]. \tag{3.3}$$

The Hamiltonian of the system writes

$$H = \frac{1}{2}\int {\rm d}^3\boldsymbol{x}\left[p^2 + (\partial_i v)^2 + 2\frac{z'}{z}vp\right], \tag{3.4}$$

where p is the impulsion associated to the v-variable. Following the canonical quantization procedure, fields are promoted to quantum operators and

decomposed in their Fourier representation

$$\widehat{v} = \int \frac{\mathrm{d}^3 k}{(2\pi)^{3/2}} \widehat{v}_{\boldsymbol{k}} e^{i\boldsymbol{k}.\boldsymbol{x}}, \tag{3.5}$$

$$\widehat{p} = \int \frac{\mathrm{d}^3 k}{(2\pi)^{3/2}} \widehat{p}_{\boldsymbol{k}} e^{i\boldsymbol{k}.\boldsymbol{x}}. \tag{3.6}$$

For each mode, we obtain the two-mode Hamiltonian operator

$$\widehat{\mathcal{H}}_{\boldsymbol{k}} = \widehat{p}_{-\boldsymbol{k}}\widehat{p}_{\boldsymbol{k}} + k^2 \widehat{v}_{-\boldsymbol{k}}\widehat{v}_{\boldsymbol{k}} + \frac{z'}{z}\left(\widehat{p}_{-\boldsymbol{k}}\widehat{v}_{\boldsymbol{k}} + \widehat{v}_{-\boldsymbol{k}}\widehat{p}_{\boldsymbol{k}}\right). \tag{3.7}$$

Introducing creation and annihilation operators in the usual way

$$\widehat{v}_{\boldsymbol{k}} = \frac{1}{\sqrt{2k}}\left(\widehat{a}_{\boldsymbol{k}} + \widehat{a}^{\dagger}_{-\boldsymbol{k}}\right), \tag{3.8}$$

$$\widehat{p}_{\boldsymbol{k}} = -i\sqrt{\frac{k}{2}}\left(\widehat{a}_{\boldsymbol{k}} - \widehat{a}^{\dagger}_{-\boldsymbol{k}}\right), \tag{3.9}$$

the two-mode Hamiltonian operator can be written in a simple form

$$\widehat{\mathcal{H}}_{\boldsymbol{k}} = F_k\left(\widehat{a}^{\dagger}_{\boldsymbol{k}}\widehat{a}_{\boldsymbol{k}} + \widehat{a}^{\dagger}_{-\boldsymbol{k}}\widehat{a}_{-\boldsymbol{k}} + 1\right) + iR_k\left(e^{-2i\Theta_{\boldsymbol{k}}}\widehat{a}_{\boldsymbol{k}}\widehat{a}_{-\boldsymbol{k}} - \text{h.c.}\right) \tag{3.10}$$

where [116]

$$F_k = \frac{k}{2}, \tag{3.11}$$

$$R_k = \left[\left(\frac{k}{2}\right)^2 + \left(\frac{z'}{z}\right)^2\right]^{1/2}, \tag{3.12}$$

$$\Theta_k = -\frac{\pi}{2} + \frac{1}{2}\arctan\left(\frac{k}{2}\frac{z}{z'}\right). \tag{3.13}$$

This Hamiltonian has a *harmonic* part associated with the frequency F_k and a *parametric amplification* part associated with R_k. The parametric amplification is caused by the curvature of the background which generates a time-dependent mass $m^2_{\text{eff}} = -z''/z$ to the field. The evolution operator produced by this Hamiltonian can be factorized into [196]

$$\widehat{\mathcal{U}}(\eta, \eta_0) = \widehat{\mathcal{R}}(\varphi_k)\widehat{\mathcal{Z}}(r_k)\widehat{\mathcal{R}}(\theta_k) \tag{3.14}$$

where $\widehat{\mathcal{R}}$ is the *phase-shift*

$$\widehat{\mathcal{R}}(\varphi_k) = \exp\left(i\varphi_k\left[\widehat{a}^{\dagger}_{\boldsymbol{k}}\widehat{a}_{\boldsymbol{k}} + \widehat{a}^{\dagger}_{-\boldsymbol{k}}\widehat{a}_{-\boldsymbol{k}} + 1\right]\right), \tag{3.15}$$

and $\widehat{\mathcal{Z}}$ the *squeezer*

$$\widehat{\mathcal{Z}}(r_k) = \exp\left[r_k\left(\widehat{a}^{\dagger}_{\boldsymbol{k}}\widehat{a}^{\dagger}_{-\boldsymbol{k}} - \text{h.c.}\right)\right]. \tag{3.16}$$

Eq. (3.14) is expressed in terms of the so-called *squeezing parameters* $(\varphi_k, r_k, \theta_k)$ which depend on the details of the dynamics and can be found in [116].

Let us now apply this dynamics to evolve the quantum state of the system. Starting from a Bunch-Davies vacuum annihilated by the two annihilation operators $\widehat{a}_{\boldsymbol{k}}$ and $\widehat{a}_{-\boldsymbol{k}}$ such that it contains no excitation

$$|\emptyset(\eta_0)\rangle = \prod_{\boldsymbol{k}\in\mathbb{R}^{3+}} |0_{\boldsymbol{k}},\ 0_{-\boldsymbol{k}}\rangle\,, \tag{3.17}$$

one can apply the evolution operator (3.14) to obtain the evolved vacuum at any time η. It amounts to operate on each mode $\boldsymbol{k}$ the quantum circuit

$$|0_{\boldsymbol{k}},\ 0_{-\boldsymbol{k}}\rangle \text{—} \boxed{\widehat{\mathcal{R}}(\varphi_k)} \text{—} \boxed{\widehat{\mathcal{Z}}(r_k)} \text{—} \boxed{\widehat{\mathcal{R}}(\theta_k)} \text{—} |2\mathrm{MSS}_{\boldsymbol{k}}\rangle$$

where the quantum gates are specified above. We notice that the vacuum state becomes populated by an infinite tower of particles under the action of $\widehat{\mathcal{Z}}(r_k)$, that is

$$\prod_{\boldsymbol{k}\in\mathbb{R}^{3+}} |2\mathrm{MSS}_{\boldsymbol{k}}\rangle = \prod_{\boldsymbol{k}\in\mathbb{R}^{3+}} \left[\frac{e^{i\varphi_k}}{\cosh r_k} \sum_{n=0}^{\infty} (-1)^n e^{2in\theta_k} \tanh^n r_k\, |n_{\boldsymbol{k}},\ n_{-\boldsymbol{k}}\rangle\right], \tag{3.18}$$

where

$$|n_{\boldsymbol{k}},\ n_{-\boldsymbol{k}}\rangle = \frac{1}{n!}\left(\widehat{a}^{\dagger}_{\boldsymbol{k}}\right)^n \frac{1}{n!}\left(\widehat{a}^{\dagger}_{-\boldsymbol{k}}\right)^n |0_{\boldsymbol{k}}, 0_{-\boldsymbol{k}}\rangle\,. \tag{3.19}$$

This class of quantum states are known as *two-mode squeezed states*. $\widehat{\mathcal{Z}}(r_k)$ is responsible for the amplification of the vacuum fluctuations, $\widehat{a}^{\dagger}_{\boldsymbol{k}}\widehat{a}^{\dagger}_{-\boldsymbol{k}}$ creating pairs of quanta. This amplification explains the statistics of the inhomogeneities in the matter distribution at the end of inflation which ultimately seeds the CMB temperature anisotropies and the LSS of the universe. Indeed, once the state is known, it is a matter of writing to obtain the two point correlation function

$$\langle 2\mathrm{MSS}_{\boldsymbol{k}}|\, \widehat{v}_{\boldsymbol{k}}\widehat{v}_{-\boldsymbol{k}}\, |2\mathrm{MSS}_{\boldsymbol{k}}\rangle = \frac{1}{2k}\left[\cosh(2r_k) + \sinh(2r_k)\cos(2\theta_k)\right] \tag{3.20}$$

$$\to \frac{1}{2k}\left[1 + \cos(2\theta_k)\right] e^{2r_k} \tag{3.21}$$

when $r_k \to \infty$. Comparing it with Eq. (2.55) which asymptotically scales as $a^2/(2k)$, we conclude that r_k grows as the number of efolds N_{inf} and that θ_k gets aligned with $\pi/4$ [116].

Hence, the inflationary dynamics generates a very peculiar quantum state at the end of inflation, that is a two-mode squeezed state with a squeezing parameter of order $r_k \sim 50 - 60$ for the modes appearing in the CMB. This level of squeezing is extremely high compared to the squeezed states constructed in quantum optics for which $r_k \sim \mathcal{O}(1-10)$ is already challenging to reach [197, 198]. While squeezed

states are known as prototypical example of 'nonclassical' states in quantum optics (see [198] for a review), their appearance in cosmology has been first interpreted as generating the 'classicalization' of cosmological inhomogeneities [117–119]. In order to make this argument clear, let us follow [199] and first adopt an alternative representation of the quantum state. Indeed, the quantum state can be represented in the Fock space as in Eq. (3.18) but also has a phase-space representation in terms of the so-called *Wigner function* (see [200] for a pedagogical introduction to the topic). In this case, the quantum state is a function of the phase-space variables $(v_{\boldsymbol{k}}, p_{\boldsymbol{k}})$. Explicitly, the Wigner function is defined as the *Wigner-Weyl transform* of the density matrix, that is, for the two-mode squeezed state $|2\mathrm{MSS}_{\boldsymbol{k}}\rangle$

$$W_{\boldsymbol{k}}\left[v_{\boldsymbol{k}}, p_{\boldsymbol{k}}\right] = \int \mathrm{d}x e^{-ip_{\boldsymbol{k}}x} \left\langle v_{\boldsymbol{k}} + \frac{x}{2} | 2\mathrm{MSS}_{\boldsymbol{k}} \right\rangle \left\langle 2\mathrm{MSS}_{\boldsymbol{k}} | v_{\boldsymbol{k}} - \frac{x}{2} \right\rangle, \tag{3.22}$$

where $|v_{\boldsymbol{k}}\rangle$ is an eigenstate of the position operator $\widehat{v}_{\boldsymbol{k}}$. The Wigner function of Gaussian states is nothing but a Gaussian distribution [201]

$$W_{\boldsymbol{k}}\left[v_{\boldsymbol{k}}, p_{\boldsymbol{k}}\right] = \frac{1}{(2\pi)^2\sqrt{\det \mathbf{Cov}}} \exp\left[-\frac{1}{2}\begin{pmatrix} v_{\boldsymbol{k}} & p_{\boldsymbol{k}}\end{pmatrix} \mathbf{Cov}^{-1} \begin{pmatrix} v_{\boldsymbol{k}} \\ p_{\boldsymbol{k}}\end{pmatrix}\right], \tag{3.23}$$

where the covariance matrix is constructed out of the power spectra, that is

$$\mathbf{Cov} = \begin{pmatrix} \langle 2\mathrm{MSS}_{\boldsymbol{k}}| \widehat{v}_{\boldsymbol{k}}\widehat{v}_{-\boldsymbol{k}} |2\mathrm{MSS}_{\boldsymbol{k}}\rangle & \frac{1}{2}\langle 2\mathrm{MSS}_{\boldsymbol{k}}| \{\widehat{v}_{\boldsymbol{k}}, \widehat{p}_{-\boldsymbol{k}}\} |2\mathrm{MSS}_{\boldsymbol{k}}\rangle \\ \frac{1}{2}\langle 2\mathrm{MSS}_{\boldsymbol{k}}| \{\widehat{v}_{\boldsymbol{k}}, \widehat{p}_{-\boldsymbol{k}}\} |2\mathrm{MSS}_{\boldsymbol{k}}\rangle & \langle 2\mathrm{MSS}_{\boldsymbol{k}}| \widehat{p}_{\boldsymbol{k}}\widehat{p}_{-\boldsymbol{k}} |2\mathrm{MSS}_{\boldsymbol{k}}\rangle \end{pmatrix}. \tag{3.24}$$

One can inject the expression of the two-mode squeezed state in order to express the power spectra in terms of the squeezing parameters as we did in Eq. (3.20). In the large-squeezing limit, one finally obtains a highly elongated ellipse with the large axis oriented along the line defined by the classical solutions for the momenta $p_{\boldsymbol{k}} = p_{cl}(\widehat{v}_{\boldsymbol{k}})$. In this limit, the width becomes negligible as shown in Figure 3.1. This mechanism has been proposed as a way to visualize the system as an effective classical stochastic behaviour [199]. The position variables $\widehat{v}_{\boldsymbol{k}}$ can take any value corresponding to quasi-probability distribution provided by the Wigner function $W_{\boldsymbol{k}}\left[v_{\boldsymbol{k}}, p_{\boldsymbol{k}}\right]$. On the contrary, for a given realization of the perturbation $v_{\boldsymbol{k}}$, the corresponding momentum is (almost) fixed and equal to the classical one. Consequently, the system behaves as it follows an infinite number of classical trajectories with a definite probability on each of them, which defines a classical stochastic system. Yet, this interpretation has to be tempered by the fact that conjointly, the state remains pure and highly coherent, hence, this form of 'classicalization' is solely a question of how is organised the saturation of the minimal uncertainty

$$\Delta\widehat{v}_{\boldsymbol{k}}.\Delta\widehat{p}_{\boldsymbol{k}} = \frac{1}{2}. \tag{3.25}$$

In the case of a squeezed state, $\Delta\widehat{v}_{\boldsymbol{k}} \sim e^{r}$ while $\Delta\widehat{p}_{\boldsymbol{k}} \sim e^{-r}$, rendering challenging to keep track of the correlators associated to the momentum $\widehat{p}_{\boldsymbol{k}}$. In this sense, what has been understood as a form of 'classicalization' by the authors of [199] is just the recasting of the existence of a decaying mode in inflation, expressed in the language of quantum squeezing. In fact, beyond [199], even in the absence of quantum squeezing, the fact that Gaussian states have a positive Wigner function makes that once marginalised over all variables but the position, it can always be seen it as a classical

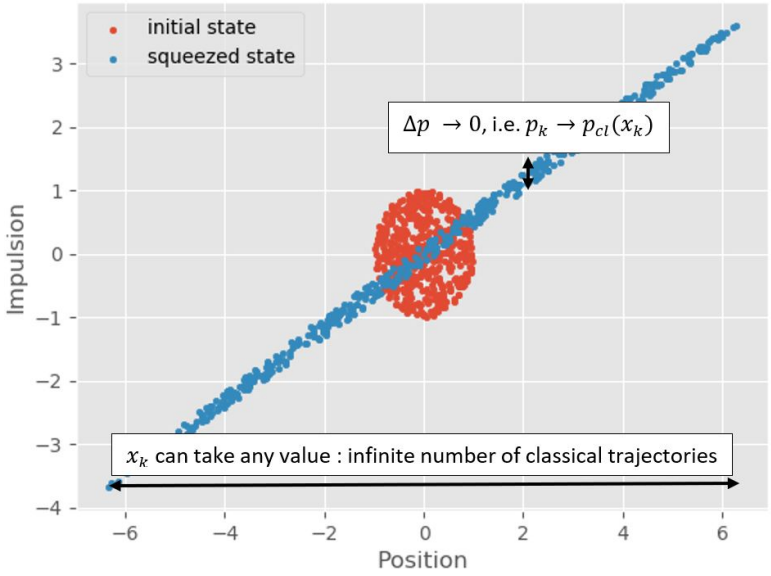

Figure 3.1: Sampling of the Gaussian Wigner function $W_{\boldsymbol{k}}[v_{\boldsymbol{k}}, p_{\boldsymbol{k}}]$ for the initial vacuum $|0_{\boldsymbol{k}},\, 0_{-\boldsymbol{k}}\rangle$ in red and the two-mode squeezed state $|2\mathrm{MSS}_{\boldsymbol{k}}\rangle$ in blue. The minimal uncertainty $\Delta\widehat{v}_{\boldsymbol{k}}.\Delta\widehat{p}_{\boldsymbol{k}} = 1/2$ is elongated into an ellipse that makes the system effectively looking like a classical stochastic theory in the high squeezing limit according to [199]. Yet, this interpretation has to be tempered by the fact that highly squeezed states also exhibit large non-classical features [198]. In particular, in the inflationary context, a large amount of non-classical correlations is generated along the $\boldsymbol{k}/-\boldsymbol{k}$ bipartition.

PDF. Hence, the 'stochastisation' of the theory is far from being specific to quantum squeezing but apply to any linearly evolving Gaussian state [121]. We would like to now argue that the quantum states in which the cosmological inhomogeneities are placed, that are the so-called two-mode squeezed states, in fact exhibit a very large amount of entanglement along a certain bipartition. Hence, we conclude that cosmological inhomogeneites can be seen by some aspects be seen as highly 'classical' and by others as highly 'quantum'.

CMB Bell tests and their obstructions: In Eq. (3.18), it appears that a crucial ingredient in the appearance of highly squeezed states is the pair creation process $\widehat{a}^{\dagger}_{\boldsymbol{k}}\widehat{a}^{\dagger}_{-\boldsymbol{k}}$. This mechanism generates very large amount of entanglement between the $\boldsymbol{k}$ and $-\boldsymbol{k}$ sectors which can be traced through the mean of the *quantum discord* [120, 202]. Quantum discord is an entanglement tracer which aims at quantifying the amount of information present in a quantum system that cannot be reproduced by a classical counterpart. Let us illustrate the existence of quantum correlations in cosmic inhomogeneities following [120]. Quantum discord is constructed out of two different ways of calculating the mutual information between the $\boldsymbol{k}$ and $-\boldsymbol{k}$ sectors which coincide for classical correlations but not necessarily for quantum ones. The first measure is given by

$$\mathcal{I}(\boldsymbol{k}, -\boldsymbol{k}) = S\left[\widehat{\rho}(\boldsymbol{k})\right] + S\left[\widehat{\rho}(-\boldsymbol{k})\right] - S\left[\widehat{\rho}(\boldsymbol{k}, -\boldsymbol{k})\right] \tag{3.26}$$

where S is the von-Neumann entropy defined by $S = -\mathrm{Tr}(\widehat{\rho}\log_2\widehat{\rho})$ with $\widehat{\rho}$ being the density matrix of the system under consideration. $\widehat{\rho}(\boldsymbol{k}, -\boldsymbol{k})$ is constructed out of

$|2\mathrm{MSS}_{\boldsymbol{k}}\rangle$ through

$$\widehat{\rho}(\boldsymbol{k},-\boldsymbol{k}) \equiv |2\mathrm{MSS}_{\boldsymbol{k}}\rangle \langle 2\mathrm{MSS}_{\boldsymbol{k}}| \tag{3.27}$$

and the reduced density matrix of the subsystems $\boldsymbol{k}$ and $-\boldsymbol{k}$ are obtained by tracing over the other sector, that is $\widehat{\rho}(-\boldsymbol{k}) \equiv \mathrm{Tr}_{\boldsymbol{k}}[\widehat{\rho}(\boldsymbol{k},-\boldsymbol{k})]$ and $\widehat{\rho}(\boldsymbol{k}) = \mathrm{Tr}_{-\boldsymbol{k}}[\widehat{\rho}(\boldsymbol{k},-\boldsymbol{k})]$. The second measure is obtained by assuming that a projective measurement is operated in the subsystem $-\boldsymbol{k}$ while we observe the $\boldsymbol{k}$ sector. It projects the state into

$$\widehat{\rho}(\boldsymbol{k},\widehat{\Pi}_j) = \mathrm{Tr}_{-\boldsymbol{k}}\left[\widehat{\rho}(\boldsymbol{k},-\boldsymbol{k})\widehat{\Pi}_j\right] \tag{3.28}$$

up to a normalization factor (see [120] for details) where $\widehat{\Pi}_j$ is the normalised projector operator.[2] If one performs all possible measurements through a complete set of measurements $\{\widehat{\Pi}_j\}$, an alternative definition of the mutual information is given by [120]

$$\mathcal{J}(\boldsymbol{k},-\boldsymbol{k}) = S\left[\widehat{\rho}(\boldsymbol{k})\right] - \sum_j \widehat{\rho}(\boldsymbol{k},\widehat{\Pi}_j). \tag{3.29}$$

Classically, thanks to Bayes theorem, the two measures coincide, that is $\mathcal{J}(\boldsymbol{k},-\boldsymbol{k}) = \mathcal{I}(\boldsymbol{k},-\boldsymbol{k})$. Quantum mechanically however, the two measure can depart. Indeed, quantum entanglement tells us that if Alice performs a measurement on the state

$$|\Psi\rangle = \frac{1}{\sqrt{2}}\left(|\uparrow\rangle_{\mathrm{A}} \otimes |\downarrow\rangle_{\mathrm{B}} - |\downarrow\rangle_{\mathrm{A}} \otimes |\uparrow\rangle_{\mathrm{B}}\right), \tag{3.30}$$

where $|\uparrow\rangle$ and $|\downarrow\rangle$ are eigenstates of a spin operator $\widehat{S}_z$, it projects the state in one of the two possible outcomes, which instantaneously affects the result observed by Bob. This property, known as the *non-locality* of quantum entanglement (see, e.g. [203, 204]), opens the door for *quantum steering* which aims at monitoring a subsystem by performing projective measurements on another entangled subsystem [205], a useful property for the development of quantum technologies and quantum communications. Hence, a characterisation of the amount of non-classical correlations in a system is given by the quantum discord

$$\delta(\boldsymbol{k},-\boldsymbol{k}) \equiv \min_{\{\widehat{\Pi}_j\}}\left[\mathcal{I}(\boldsymbol{k},-\boldsymbol{k}) - \mathcal{J}(\boldsymbol{k},-\boldsymbol{k})\right] \tag{3.31}$$

where we minimize over all possible sets of measurements in order to avoid the dependence on the projectors. For a two-mode squeezed state $|2\mathrm{MSS}_{\boldsymbol{k}}\rangle$, it has been shown in [120] that the discord grows as

$$\delta(\boldsymbol{k},-\boldsymbol{k}) = \cosh^2 r_k \log_2\left(\cosh^2 r_k\right) - \sinh^2 r_k \log_2\left(\sinh^2 r_k\right) \tag{3.32}$$

$$\simeq \frac{1}{\ln 2}\left(2r_k+1\right) - 2 + \mathcal{O}\left(e^{-2r_k}\right), \tag{3.33}$$

where in the second line we took the large r_k limit. Remembering that r_k scales as the number of efolds during inflation, we observe that $\delta(\boldsymbol{k},-\boldsymbol{k})$ grows and reaches high

[2] For instance, the Pauli matrices are normalised projector operators corresponding to the measurement of a qubit in different directions.

values (above a hundred) by the end of inflation, which illustrates the generation of entanglement by the pair creation process during inflation.

This observation, which accounts for the existence of a large amount of quantum correlations generated during inflation, has been at the heart of a research program aiming at understanding if it may be possible to exhibit the non-classical nature of the cosmological inhomogeneities observed in the CMB and the LSS. The most direct proposal follows from the construction of Bell observables in the sky [106–108, 110]. Bell tests aim at defining bounds that classical theories (obeying local realism) cannot violate. In quantum theories, these bounds can be bypassed thanks to the richer correlation structure allowed by quantum entanglement, leading to the famous Bell inequality violation [203]. Let us briefly review the *Clauser, Horne, Shimony and Holt* (CHSH) *setup* [206]. We consider a bipartite system $\mathcal{H} = \mathcal{H}_{\rm A} \otimes \mathcal{H}_{\rm B}$ prepared in the entangled Einstein–Podolsky–Rosen (EPR) state (3.30). We define a Bell operator

$$\widehat{\mathcal{B}}_{\rm CHSH} = \widehat{S}_{\rm A} \otimes \widehat{S}_{\rm B} + \widehat{S}_{\rm A} \otimes \widehat{S}_{\rm B'} + \widehat{S}_{\rm A'} \otimes \widehat{S}_{\rm B} - \widehat{S}_{\rm A'} \otimes \widehat{S}_{\rm B'} \tag{3.34}$$

where A, A′, B and B′ correspond to the measurement of four different spin directions. Averaging over many experimental outcomes, one obtains the expectation value $\langle \widehat{\mathcal{B}}_{\rm CHSH} \rangle = E(\theta_{\rm A}, \theta_{\rm B}) + E(\theta_{\rm A}, \theta_{\rm B'}) + E(\theta_{\rm A'}, \theta_{\rm B}) - E(\theta_{\rm A'}, \theta_{\rm B'})$ where it can be shown that $E(\theta_{\rm A}, \theta_{\rm B}) = -\cos(\theta_{\rm A} - \theta_{\rm B})$, the measurement angles being defined with respect to the z-axis (see e.g. [120]). If one chooses $\theta_{\rm A} - \theta_{\rm B} = \pi/4$, $\theta_{\rm A} - \theta_{\rm B'} = \theta_{\rm A'} - \theta_{\rm B} = -\pi/4$ and $\theta_{\rm A'} - \theta_{\rm B'} = -3\pi/4$, then $\langle \widehat{\mathcal{B}}_{\rm CHSH} \rangle = -2\sqrt{2}$. Since $|\langle \widehat{\mathcal{B}}_{\rm CHSH} \rangle| > 2$, Bell inequality is violated and the statistics of this quantum system cannot be accounted for in a theory obeying local realism. This system has been widely tested experimentally, from the initial experiments (see e.g. [204]) to the closure of many *loopholes* [207], for instance by using the polarization of photons coming from distant quasars in order to select the spin measurement directions, pushing the "freedom-of-choice" loophole of having an influenced spin angle selection to more than 7.8 Gya [208, 209].

If one wants to design a similar experiment for the primordial inhomogeneties, a first difficulty consists in going beyond the discrete (dichotomic) variable paradigm. For continuous variable systems such as the one constructed out of the Mukhanov-Sasaki variables $\widehat{v}_{\boldsymbol{k}}$, one can construct pseudo-spin operators such as *Banaszek-Wodkiewicz operators* which obey the same algebra as the usual spin operators [210]. Explicitly, following [110], we construct

$$\widehat{S}_x(\boldsymbol{k}) = \sum_{n=0}^{\infty} \left(|2n_{\boldsymbol{k}} + 1\rangle \langle 2n_{\boldsymbol{k}}| + |2n_{\boldsymbol{k}}\rangle \langle 2n_{\boldsymbol{k}} + 1| \right) \tag{3.35}$$

$$\widehat{S}_y(\boldsymbol{k}) = i \sum_{n=0}^{\infty} \left(|2n_{\boldsymbol{k}}\rangle \langle 2n_{\boldsymbol{k}} + 1| - |2n_{\boldsymbol{k}} + 1\rangle \langle 2n_{\boldsymbol{k}}| \right) \tag{3.36}$$

$$\widehat{S}_z(\boldsymbol{k}) = \sum_{n=0}^{\infty} \left(|2n_{\boldsymbol{k}} + 1\rangle \langle 2n_{\boldsymbol{k}} + 1| - |2n_{\boldsymbol{k}}\rangle \langle 2n_{\boldsymbol{k}}| \right) \tag{3.37}$$

where the $|n_{\boldsymbol{k}}\rangle$ are the eigenstates of the particle number operator $\widehat{N}_{\boldsymbol{k}} = \widehat{a}^{\dagger}_{\boldsymbol{k}} \widehat{a}_{\boldsymbol{k}}$, and similarly for the $-\boldsymbol{k}$ sector. These operators obey the usual $SU(2)$ algebra such that $\widehat{S}_x$, $\widehat{S}_y$ and $\widehat{S}_z$ satisfy all the properties of a spin operators system. We can use

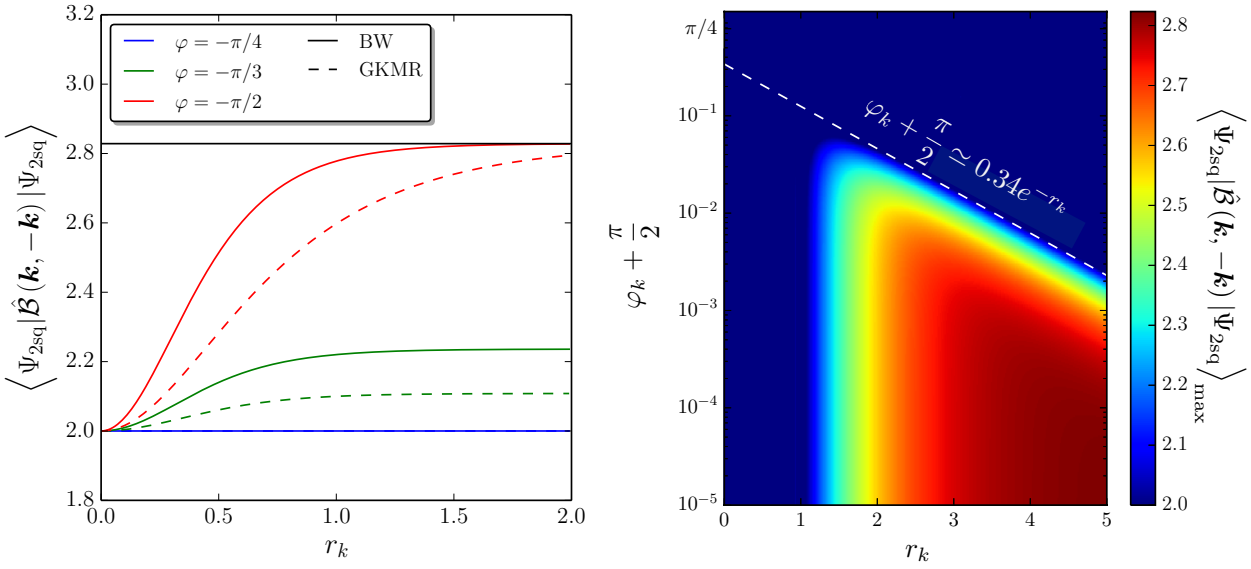

Figure 3.2: Bell inequality violation as a function of the squeezing parameters. *Left:* Mean value $\langle \widehat{\mathcal{B}}_{\mathrm{CHSH}} \rangle$ of the Bell operator for the Banaszek-Wodkiewicz operators (solid lines) and an alternative definition of the pseudo-spin operators (dashed lines, see [110] for details), when the system is placed in the two-mode squeezed state (3.18), as a function of the squeezing parameter r_k, for different values of the squeezing angle φ_k. The horizontal black line represents the Cirel'son bound $2\sqrt{2}$. *Right:* Maximum Bell operator expectation value $\langle \widehat{\mathcal{B}}_{\mathrm{CHSH}} \rangle$ for an alternative definition of the pseudo-spin operators, see [110] for details, as a function of the squeezing parameters r_k and φ_k. The dashed white line stands for $\varphi_k + \pi/2 = 0.34e^{-r_k}$ which delimits the Bell inequality violation domain in the large-squeezing limit. Figure taken from [110].

these variables to construct a pseudo Bell operator for the two sectors $(\boldsymbol{k}, -\boldsymbol{k})$. It has been shown in [110], for a two-mode squeezed state $|2\mathrm{MSS}_{\boldsymbol{k}}\rangle$ with parameters compatible with the super-Hubble dynamics of a mode during inflation, for which $r_k \sim N_{\mathrm{inf}}$, $\langle \widehat{\mathcal{B}}_{\mathrm{CHSH}} \rangle \to 2\sqrt{2}$ which maximally violates Bell inequality (in practice, the precise result also depends on the value of the squeezing angle, see Fig. 3.2 and [110] for details). This example can be used as a proof of principle that there exists a large amount of correlations that cannot be reproduced by a classical theory in the cosmological inhomogeneities generated during inflation, confirming the quantum discord result [122].

Can we experimentally harvest this quantum entanglement? From the time this question is paused, a plethora of obstructions arise, both at the technical and conceptual level. Among various obstructions to Bell CMB experiments [110], one can first ask if pseudo-spin operators are really measurable. It turns out that in order to be able to reconstruct pseudo-spin operators, we would need not only to access the correlators of ζ, but also the ones of $\dot{\zeta}$, which we have identified as being the decaying mode around Eq. (2.60). It poses strong constraints on the observational accessibility of these pseudo-spin variables. The problem might be circumvent by either considering peculiar dynamics in which the decaying mode is not so small in a given observational range (see Maldacena's proposal [107], or models with an

ultra-slow-roll phase), or extending the study to a wider class of inequalities such as the Leggett-Garg or temporal Bell inequalities [111, 211]. A second concern might be expressed regarding the bipartition along which the entanglement is exhibited. Indeed, violating Bell inequality in Fourier space would imply the incompatibility with local realism in Fourier space. Non-locality being ubiquitous in this dual space, the statement is weaker than its formulation in real space. Hence, efforts have been made in order to understand the entanglement structure in real space [112, 212, 213] and it appears that entanglement is much less ubiquitous in real space than in Fourier space [214], though the peculiar dynamics of the pair-creation process during inflation still generates larger entanglement than its flat space counterpart. A last obstruction we would like to highlight is fact that in general, quantum correlations are fragile, as suggests our daily experience of the classical world in which macroscopic quantum effects are rare. Hence, one of the greatest challenges is to understand if this entanglement may have survived up to the present days.

In general, when a quantum system is embedded in a wider environment, their interactions generate a leakage of information which has the tendency to wash away the desired quantum features after a very short timescale. If the system initially exhibits quantum correlations one may want to reveal through a Bell test, this information quickly ends up being delocalised into the environment, rendering impossible to account for the presence of quantum correlations in the system at late time. This phenomenon, known as *quantum decoherence* [191–193], is a fierce challenge for the development of quantum technologies and quantum communication. It explains why, in our daily life, it is so hard to maintain coherence of quantum signals for more than a few seconds. In the context of cosmology, it is generally argued [165, 177, 199, 215–229] that, due to the process of quantum decoherence, quantum signatures are likely to be erased by the presence of environmental degrees of freedom from the early time they were generated to the record of their imprints in the CMB or the LSS. This is why studying decoherence channels [179, 230–240] has become of primary importance to assess the severity of this potential obstruction. It also motivates for model-independent approaches as even if we manage to evaluate all the possible decay channels imaginable within the standard models of particle physics and cosmology, the presence of hidden/unknown physics may still ruin any hope of observing quantum correlations in the sky.

As a summary, despite being created through a quantum-mechanical process, cosmological structures have not yet revealed any sign of genuine quantum correlations. Among the obstructions to the direct detection of quantum signatures in cosmology, environmental-induced decoherence is arguably one of the most inevitable. If we want to assess decoherence in cosmology, we need to evaluate the quantum information properties of inflationary models, which motivates the introduction of Open EFT techniques.

The measurement problem: This discussion motivates the use of Open EFTs to establish a toolbox able to provide answers to some of the questions related to the so-called "quantum-to-classical" transition of cosmological inhomogeneities. Indeed, Open EFTs may help us to model decoherence channels and to understand if there is any hope for a direct experimental evidence of quantum correlations in the statistics of the curvature perturbations observed in the CMB and the LSS. Still, Open EFT techniques shall not provide a complete answer to the "quantum-to-

classical" transition. We would like to highlight that, *per se*, quantum decoherence is not able to explain the emergence of a classical geometry from a quantum gravity scenario (nor the selection of a unique classical inhomogeneity from the fluctuations of a quantum field). Indeed, while decoherence provides a mechanism to understand the appearance of a statistical mixture of classical outcomes, e.g., the decoherence of a cat state

$$|\mathrm{cat}_+\rangle = \frac{1}{\sqrt{2}}\left(|\uparrow\rangle + |\downarrow\rangle\right) \tag{3.38}$$

into the mixture

$$\frac{1}{2}\left(|\uparrow\rangle\langle\uparrow| + |\downarrow\rangle\langle\downarrow|\right), \tag{3.39}$$

it does not explain why we finally observe $|\uparrow\rangle$ or $|\downarrow\rangle$ and not a linear combination of the two, that is why the final step of a measurement consists in projecting either on the $|\uparrow\rangle$ or in the $|\downarrow\rangle$ outcome. Known as the *measurement problem*, it constitutes one of the most fundamental questions about the nature of quantum mechanics, aiming at understanding why the quantum evolution is dictated by the Schrödinger equation up to the point where a measurement is performed and the Von-Neumann postulate projects the wavefunction on an eigenvector of the observable. The measurement problem can be particularly embarrassing when seriously considered in the context of primordial cosmology, as done by Sudarsky in [189]. Hence, decoherence may explain why we are unable to exhibit genuine quantum correlations in the sky but it cannot explain why a classical geometry has been selected out of a quantum wavefunction.

3.1.2 Decoherence, dissipation and late-time resummation

Beyond the opportunity to access the quantum information properties of inflationary models, another motivation for the use of Open EFT techniques comes from the lack of energy conservation in cosmology. Indeed, in cosmology, the FLRW background is less symmetric than in Minkowski or de Sitter. Energy is not conserved which plays a crucial role in the generation of fluctuations out of the primordial vacuum. It sometimes renders the implementation of Wilsonian EFTs cumbersome as the cornerstone of these approaches is the existence of segregated energy sectors in which the evolution is unitary [1,22]. On their side, OQS techniques are particularly suited to describe energy exchanges between the system and its environment which commonly occur in quantum optics and condensed matter, for instance when one couples a quantum device to a thermal bath. OQS techniques are also useful when the lack of symmetries prevents their use as guiding principle for the construction of extensions. Even if simplifications occur when environments fulfil symmetries [241], OQS frameworks can still be derived in their absence and other type of constraints can be placed to restrict the dynamics.

OQS theory not only describes the renormalisation of the energy levels of the system by the environment but also the processes of *dissipation* and *decoherence*, that is the energy exchanges and the generation of entanglement. Thanks to this property, Open EFT techniques have been used to describe the decoherence of cosmological perturbations in the early universe (see [154, 173, 174, 177, 223, 230, 238, 242–244]

for a non-exhaustive list of references). They are also common to discuss quantum gravity effects such as gravitationally-induced decoherence (see for instance [179, 233, 234, 245, 246]). In order to capture these effects, we need to give up on the unitarity of the evolution. In this sense, Open EFTs aim at supplementing Wilsonian EFTs by adding non-unitary contributions describing dissipation and decoherence.

It is crucial to identify in which settings Open EFT techniques may be useful. When do we care about non-unitary effects? Despite being ubiquitous in hydrodynamics, condensed matter and quantum optics, the QFT literature rarely discuss dissipation [1]. The reason is that in general, scale hierarchies and symmetries makes that well-segregated UV and IR energy sectors emerge. In the in-out perspective of scattering experiments, the quantum state in the asymptotic future is known. It enforces energy conservation for the system, such that no net energy loss or gain is observed (though the IR and the UV can transiently exchange energy at finite time when an in-in perspective is adopted, see e.g. [247]). Non-unitary effects in the IR sector are discarded, energy is conserved and the quantum state of the system obey Poincaré group symmetries [241]. On the contrary, when the system and environment are not organised in terms of energy sectors but rather divided by the presence of a horizon [22], a physical separation [11] or the different nature of their constituents [188], or anytime the asymptotic state at future boundary is unknown, out-of-equilibrium QFT techniques [13] are necessary. The energy of the system is in general not anymore conserved and one has to take into account dissipative effects, as in hydrodynamics, condensed matter, quantum optics, but also in black hole mergers [11] and cosmology [22]. Hence, the introduction of Open EFT techniques may allow us to capture the non-unitary dynamics associated to the mechanisms of dissipation and decoherence and to characterise in which regime they can be discarded.

Finally, Open EFTs have long-standing history in the context of non-perturbative QFT techniques for their ability to resum *late-time effects* or '*tails*'. Let us provide an example with the *Liouvillian gap*.

The Liouvillian gap: Let us provide an example of the non-perturbative insights OQS techniques provide following the approach of spectral theory for Liouvillians developed in [248]. The quantum state of an OQS is described by a density matrix $\widehat{\rho}$ whose dynamics is governed by a Liouvillian super-operator $\mathcal{L}_{\mathcal{S}}$ such that

$$\frac{\mathrm{d}\widehat{\rho}}{\mathrm{d}t} = \mathcal{L}_{\mathcal{S}}\left[\widehat{\rho}\right]. \tag{3.40}$$

For time-independent Liouvillian and finite dimensional Hilbert space $\mathcal{H}_{\mathcal{S}}$, there is at least one steady-state $\widehat{\rho}_{\mathrm{eq}}$ [248] such that

$$\mathcal{L}_{\mathcal{S}}\left[\widehat{\rho}_{\mathrm{eq}}\right] = 0, \tag{3.41}$$

that is an eigenmatrix associated with the zero eigenvalue of the Liouvillian super-operator. In order to fully determine the dynamics of the system, the knowledge of the steady-state density matrix $\widehat{\rho}_{\mathrm{eq}}$ is not enough. Indeed, one has to know all the spectrum of the Liouvillian super-operator $\mathcal{L}_{\mathcal{S}}$

$$\mathcal{L}_{\mathcal{S}}\left[\widehat{\rho}_{\mathrm{i}}\right] = \lambda_i \widehat{\rho}_{\mathrm{i}}. \tag{3.42}$$

One can decompose the reduced density matrix in the basis formed by the eigenmatrices such that

$$\widehat{\rho}(t) = \widehat{\rho}_{\rm eq} + \sum_{i\neq 0} c_i(t) e^{\lambda_i t}\widehat{\rho}_i. \tag{3.43}$$

It can be proved that $\Re\mathrm{e}\,[\lambda_i] \leq 0$ for all i [248]. Since the real part of the eigenvalues is responsible for the relaxation to the steady state,

$$\widehat{\rho}_{\rm eq} = \lim_{t\to\infty} e^{\mathcal{L}_S t}\widehat{\rho}(t_0). \tag{3.44}$$

For convenience, let us organise the eigenvalues in such a way that $0 < |\Re\mathrm{e}\,[\lambda_1]\,| < \cdots < |\Re\mathrm{e}\,[\lambda_n]\,|$. An important quantity is the so-called *Liouvillian gap* $\lambda \equiv |\Re\mathrm{e}\,[\lambda_1]\,|$ which constitutes the asymptotic decay rate. Indeed, it corresponds to the smallest (in amplitude) non-zero eigenvalue and hence determines the slowest relaxation dynamics in the long-time limit. One can extract meaningful information about thermalization and decoherence by estimating the Liouvillian gap (at least in flat space, as new complications arise in cosmology, as we will see below). Hence, one of the strengths of the OQS formalism resides in computing quantities such as the Liouvillian gap λ perturbatively and then using this information to infer non-perturbative statements on the late-time dynamics of the system such as the decay rates, distribution tails, metastability or driven-dissipative phase transitions [248].

The idea behind the non-perturbative resummation implemented in Open EFT settings relies on deriving perturbatively an object such as the generator of the dynamical map then solving the dynamics non-perturbatively, as it is, without performing any further expansion. In a sense, the generator for the dynamical map is taken as a *bona fide* object such that its integration over time implements a resummation which allows us to accurately describe the late-time distribution [22].

Summary: Open EFT techniques were initially developed in the context of quantum optics and possess desirable features in the context of primordial cosmology. First, they allow us to synthesize the effects of complex environments into a handful of parameters. Second, they render accessible the quantum information properties of the system. Third, they are well suited to describe dissipation, decoherence and thermalization in out-of-equilibrium settings where the energy of the system is not conserved. They may also allow us to implement some form of late-time resummation and accurately described late-time dynamics. If we manage to implement OQS techniques in cosmology, we would access a so-far unexplored regime associated to the understanding of the quantum information properties of inflationary models.

3.2 Methods

This Section aims at providing a first introduction to the Open EFT techniques used in cosmology. This overview explains the basic principles of Open EFT such as the definition of a bipartition or the tracing out procedure. It highlights the various

tools at our disposal such the master equations, the influence functional and their corresponding stochastic unravelling and characterises their relationships.

3.2.1 The system/environment bipartition

The OQS approach relies on a bipartition between a *system* and an *environment*. The system is made of the degrees of freedom we can experimentally access. In the early-universe context, we could have in mind the curvature perturbations whose imprints are today observed in the CMB and the LSS. One could also consider a system made of the large scales ($0.005\ \mathrm{Mpc}^{-1} \lesssim k \lesssim 0.2\ \mathrm{Mpc}^{-1}$), the one currently probed by cosmological surveys. The environment is in general experimentally inaccessible and poorly specified. It characterises the unobservable degrees of freedom that may have played a role in the description of the system but that we do not physically access. For instance, the cosmological collider program motivates the study of heavy field and higher-spin particles which may constitute a cosmological environment. Alternatively, the reservoir of sub-Hubble modes which cross the horizon later than the scales today probed in the CMB could also constitute a natural environment.

Obviously, the bipartition definition is crucial: if one changes it, it redefines the observables we can access, the work and heat flows between the system and its environment, the entanglement and the quantum information properties we can test. For this reason, looking for physically motivated bipartitions is decisive. In this manuscript, we mainly discuss the so-called adiabatic and entropic bipartition and the sub/super Hubble bipartition introduced in Sec. 2.3.2 which constitute two observationally motivated bipartitions, as suggested above. Yet, no choice is innocent and one should keep in mind the implications of a bipartition choice, see [214, 249] for an in-depth discussion of this topic. In particular, one has to keep in mind that once the bipartition is defined, it poses a constraint on the accessible space of canonical transformations which do not affect the system properties. Indeed, as long as the canonical transformation does not affect the bipartition, the field redefinition would not affect the results.[3] Yet, no possible redefinition can change the inter-sector dynamics without affecting the OQS properties.

In order to illustrate the OQS procedure, let us introduce a follow-up problem we will use all along the next Sections. We consider a two-field system $\Phi = \zeta, \mathcal{F}$ where the two scalar fields now separate observable ζ and unobservable $\mathcal{F}$ degrees of freedom

$$S\left[\Phi\right] = S_{\zeta}\left[\zeta\right] + S_{\mathcal{F}}\left[\mathcal{F}\right] + S_{\mathrm{int}}\left[\zeta;\mathcal{F}\right]. \tag{3.45}$$

In cosmology, it would for instance represent the interactions between the curvature perturbations observed in the CMB and the LSS with an entropic sector, so far unobserved. Now that the bipartition is defined, we aim at describing the effective effect of $\mathcal{F}$ onto the dynamics of ζ.

[3] Especially if the results are expressed in terms of *symplectic eigenvalues* which are invariant quantities under field redefinition, see [250] for a discussion in the context of Gaussian states.

3.2.2 Tracing out of the environment

A general approach to deal with unknowns in physics consists in summing over, integrating out or coarse-graining our ignorance. Indeed, when initial conditions are unknown, one often sums over all possible initial states in order to obtain reliable predictions for the late-time outcomes. Alternatively, in the Bayesian inference framework presented in Sec. 2.1.1, posterior distributions are often provided after the *marginalisation* of parameters whose detailed description does not matter for the purpose of a study. A similar approach in the OQS context aims at capturing the effect of the environment onto the system while giving up the detailed description of the dynamics of the environment.

This procedure can be carried out from different perspective, depending on the representation of the quantum state of the system chosen. Let us consider that the ensemble composed of the system and its environment consists in a closed quantum system described by a pure state $|\Psi\rangle$. The *density matrix* $\widehat{\rho} \equiv |\Psi\rangle\langle\Psi|$ offers a representation of the quantum state on the Hilbert space $\mathcal{H} = \mathcal{H}_{\mathcal{S}} \otimes \mathcal{H}_{\mathcal{E}}$. In this case, the action of summing over our ignorance of the details of the environment takes the form of a *partial trace*, which allows us to define a crucial object for the rest of this manuscript, the *reduced density matrix* of the system

$$\widehat{\rho}_{\rm red} \equiv {\rm Tr}_{\mathcal{E}}\widehat{\rho}. \tag{3.46}$$

This operation can be carried out over any basis $\{|\alpha\rangle\}$ of the Hilbert space of the environment $\mathcal{H}_{\mathcal{E}}$

$$\widehat{\rho}_{\rm red} = \sum_{\alpha} \langle\alpha|\,\widehat{\rho}\,|\alpha\rangle\,, \tag{3.47}$$

the trace being invariant under basis redefinition. Two such bases are for instance the Fock basis (see e.g. [251]) and the position basis (see e.g. [228]), yet, in practice, the tracing-out procedure often serves as an intermediate to reveal the physical quantities encoding the effect of the environment onto the system. Hence, in general, one does not have to perform this step explicitly.

The quantum state also has a phase-space representation, for instance in terms of the so-called *Wigner function*, which provides an alternative description, as we have already seen for the single field case in Eq. (3.22). In the two-field case, the quantum state is a function of the phase-space variables (ζ, p_ζ) and $(\mathcal{F}, p_\mathcal{F})$ where p_ζ and $p_\mathcal{F}$ are the conjugate momenta of ζ and $\mathcal{F}$. Again, the Wigner function is defined as the *Wigner-Weyl transform* of the density matrix, that is

$$\begin{aligned} W\left[\zeta, p_\zeta; \mathcal{F}, p_\mathcal{F}\right] = \int {\rm d}a{\rm d}b e^{-ip_\zeta a - ip_\mathcal{F} b} \\ \left(\langle\zeta + \frac{a}{2}| \otimes \langle\mathcal{F} + \frac{b}{2}|\right)\widehat{\rho}\left(|\zeta - \frac{a}{2}\rangle \otimes |\mathcal{F} - \frac{b}{2}\rangle\right), \end{aligned} \tag{3.48}$$

$|\zeta\rangle$ and $|\mathcal{F}\rangle$ being eigenstates of the position operator of the system and the environment respectively. The tracing-out procedure then corresponds to the marginalization of the phase-space of the environment, that is the reduced Wigner function simply writes

$$W_{\rm red}\left[\zeta, p_\zeta\right] = \int {\rm d}\mathcal{F}{\rm d}p_\mathcal{F} W\left[\zeta, p_\zeta; \mathcal{F}, p_\mathcal{F}\right]. \tag{3.49}$$

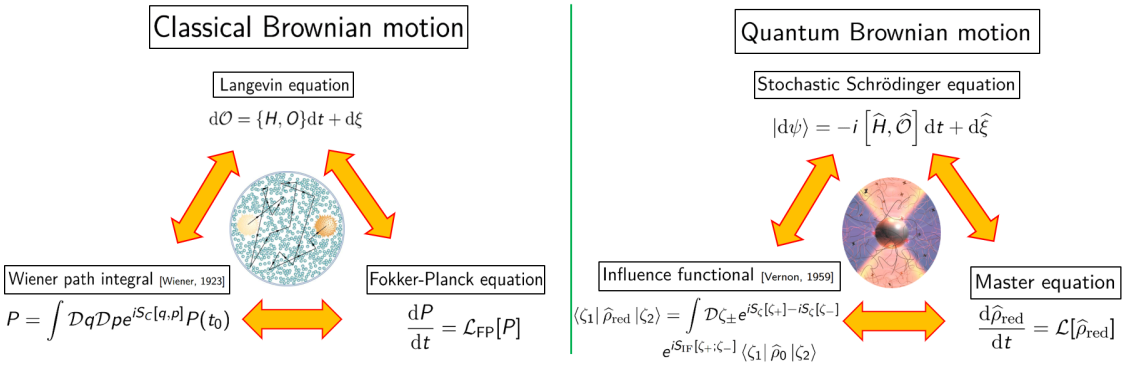

Figure 3.3: The *Holy trinity* of Open Classical and Quantum Systems. The effect of the surrounding environment is encoded through a set of stochastic variables called noises. It generates an effective dynamics which renormalizes the free evolution, dissipates energy into the environment and gets entangled through the process of decoherence. These effects are captured at the classical level by the Langevin equation, the Fokker-Planck equation or the Martin-Siggia-Rose path integral. These techniques have quantum analogues where they are replaced by the stochastic Schrödinger equation, the master equation and the influence functional respectively.

In [251], we demonstrated that Eq. (3.49) is indeed the Wigner-Weyl transform of $\widehat{\rho}_{\rm red}$, which illustrates how the tracing-out procedure can be carried out either in the phase space or in the Hilbert space, depending on what is most convenient for a given problem.

3.2.3 The *Holy trinity* of Open Quantum Systems

The objects we look for to describe the system once the environment has been integrated out are either $\widehat{\rho}_{\rm red}$ or $W_{\rm red}$. Now, how do we access these quantities? The OQS theory provides a toolbox of effective methods to describe their dynamical evolution. The origin of this toolbox is far from being recent, originating from the XIX$^{\rm th}$ century with the study of particles of pollen immersed into water by Lord Brown [19]. The investigation and theoretical modelling of *Brownian motion* lead to the discovery of atoms by Jean Perrin in 1905 [21] following the pionerring work of Albert Einstein [20]. In Fig. 3.3, we illustrate the different ways to model this long-standing problem.

The effect of the surrounding environment is encoded through a set of stochastic variables known as noises, which promote the deterministic equations of motion to stochastic differential equations such as the Langevin equation. Averaging over many realisations, we derive a dynamical equation for the probability distribution of being at a given position at a given time, known as a Fokker-Planck equation. This probability distribution also has a path integral formulation first derived by Wiener in 1923 and today mainly studied through the language of the Martin-Siggia-Rose (MSR) path integral [252]. These techniques rely on the same physics and represent different aspects of a same problem. For instance, the Langevin equation focuses on the equations of motion and is well-suited for numerical simulations. The MSR

path integral allows us to describe relativistic settings in a manifestly covariant formalism while the Fokker-Planck equation has been widely studied for its ability to implement resummations, in particular in the context of stochastic inflation [113]. One can relate these techniques one to the other, see e.g. [9] and we now aim at performing the same task at the quantum level. Indeed, as shown in the Right panel of Fig. 3.3, there exists an exact same language in the quantum framework where the Fokker-Planck equation is supplemented by master equations, the MSR path integral by the influence functional and the Langevin equation by a stochastic unravelling [188].

Master equations: As an analogue of the Fokker-Planck equation, master equations provide a generator for the dynamical map characterising the evolution of the density matrix of the system generated by

$$\frac{\mathrm{d}\widehat{\rho}_{\mathrm{red}}}{\mathrm{d}t} = \mathcal{L}_{\mathcal{S}}\left[\widehat{\rho}_{\mathrm{red}}\right] \tag{3.50}$$

where $\mathcal{L}_{\mathcal{S}}$ is the so-called Liouvillian which not only describes unitary evolution through self-adjoint Hamiltonian but also captures non-unitary effects such as dissipation and decoherence.

It is important to have in mind that there is no such thing as one single master equation: there rather exists a whole bestiary [188] depending on the level of approximation we work at. For instance, there exist exact master equations such as the Nakajima-Zwanzig (NZ) equation which are just a recasting of the full dynamics focusing on the degrees of freedom of the system. As hard to solve as the full dynamics, their main interests rely on the rewriting of the initial problem in a form that is well suited to perform systematic expansions. Then, approximation schemes allow us to simplify the effective dynamics. There are mainly two approximation schemes which depend on the way the system couples to its environment and the nature of the environment itself.

In general, the system and the environment are weakly coupled, as otherwise the mixing would be strong and we would have no reason to distinguish on the one hand the dynamics of the system and on the other the one of the environment.[4] The approximation scheme aiming at carrying out a systematic expansion in powers of the coupling constant between the system and the environment is known as the *Born approximation*. Let us consider the following Hamiltonian

$$\widehat{H} = \widehat{H}_{\mathcal{S}} + \widehat{H}_{\mathcal{E}} + g\widehat{H}_{\mathrm{int}} \tag{3.51}$$

where $\widehat{H}_{\mathcal{S}}$ and $\widehat{H}_{\mathcal{E}}$ respectively denote the Hamiltonians for the system made of ζ and the environment made of $\mathcal{F}$ in the absence of interactions, and $g\widehat{H}_{\mathrm{int}}$ is the interaction term, controlled by the coupling constant g. The setup considered is represented in Fig. 3.4.

Let us derive the simplest master equation we can consider by expanding the dynamics in powers of the coupling constant g. We work in the interaction picture which is particularly convenient to perform this type of expansion, where quantum

[4] In the context of cosmology, the consistency of observations with single-field (null detection of multifield environments) Gaussian (stringent constraints on non-Gaussianities which prevent large sub/super Hubble mixing) systems sustains this idea.

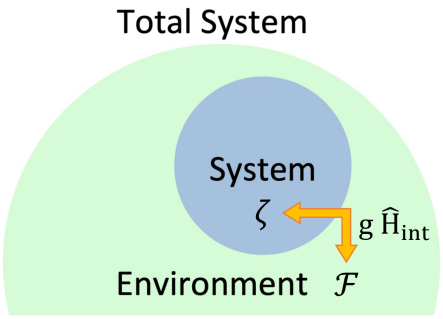

Figure 3.4: Schematic setup of the OQS considered. The system, made of the degree of freedom ζ, evolves freely according to $\widehat{H}_{\mathcal{S}}$ and is embedded in the environment made of $\mathcal{F}$ controlled by $\widehat{H}_{\mathcal{E}}$. Their interaction is specified by $g\widehat{H}_{\rm int}$. From the point of view of the system, this interaction renormalizes its energy level, generates energy losses and gains described by dissipation and information exchanges captured by decoherence. Figure adapted from [253].

states evolve with the interaction Hamiltonian $g\widehat{H}_{\rm int}$ and operators evolve with the free Hamiltonian, *i.e.* the Hamiltonian in the absence of interactions $\widehat{H}_0 \equiv \widehat{H}_{\mathcal{S}} + \widehat{H}_{\mathcal{E}}$. Operators in the interaction picture are denoted with an overall tilde, in order to make the distinction with the Schrödinger and Heisenberg pictures where they carry an overall hat. The link between the Schrödinger and the interaction picture is given by

$$\widetilde{\rho}(t) = \widehat{\mathcal{U}}_0^\dagger(t)\widehat{\rho}(t)\widehat{\mathcal{U}}_0(t) \quad \text{and} \quad \widetilde{H}_{\rm int}(t) = \widehat{\mathcal{U}}_0^\dagger(t)\widehat{H}_{\rm int}(t)\widehat{\mathcal{U}}_0(t)\,, \tag{3.52}$$

where we have introduced the free evolution operator

$$\widehat{\mathcal{U}}_0(t) = \mathcal{T}\exp\left[-i\int_{t_0}^{t}\widehat{H}_0(t')\mathrm{d}t'\right] \tag{3.53}$$

with $\mathcal{T}$ indicating time ordering (time arguments increase from right to left).

The three pictures of quantum mechanics: Let us make a brief memo on the various pictures appearing in quantum mechanics. First, we define on the top of the free evolution operator (3.53), the full evolution operator

$$\widehat{\mathcal{U}}(t) = \mathcal{T}\exp\left[-i\int_{t_0}^{t}\widehat{H}(t')\mathrm{d}t'\right]. \tag{3.54}$$

and the interaction evolution $\widehat{\mathcal{U}}_{\rm int}(t) \equiv \widehat{\mathcal{U}}_0^\dagger(t)\widehat{\mathcal{U}}(t)$. The three picture are defined as follow:

- *Schrödinger picture:* In this picture, the state $|\Psi(t)\rangle$ and density matrix $\widehat{\rho}(t) \equiv |\Psi(t)\rangle\langle\Psi(t)|$ (assuming purity) evolve while the observables $\widehat{O}$ are constant, that is

$$|\Psi(t)\rangle = \widehat{\mathcal{U}}(t)\,|\Psi(t_0)\rangle \qquad \text{and} \qquad \widehat{\rho}(t) = \widehat{\mathcal{U}}(t)\widehat{\rho}(t_0)\widehat{\mathcal{U}}^\dagger(t). \tag{3.55}$$

  This picture is the standard one taught in quantum mechanics textbooks in which the state evolves according to the *Schrödinger equation* or equivalently the density matrix according to the *Liouville–von-Neumann*

equation, that is

$$\frac{\mathrm{d}\,|\Psi(t)\rangle}{\mathrm{d}t} = -i\widehat{H}(t)\,|\Psi(t)\rangle \quad \text{and} \quad \frac{\mathrm{d}\widehat{\rho}(t)}{\mathrm{d}t} = -i\left[\widehat{H}(t), \widehat{\rho}(t)\right]. \tag{3.56}$$

- *Heisenberg picture:* In this picture, the state $|\Psi\rangle$ and density matrix $\widehat{\rho}$ are constant while the observables $\widehat{O}(t)$ evolve, that is

$$\widehat{O}(t) = \widehat{\mathcal{U}}^{\dagger}(t)\widehat{O}(t_0)\widehat{\mathcal{U}}(t). \tag{3.57}$$

  This representation is particularly useful when one wants to consider temporal correlations such as *out-of-time-ordered correlators* $\langle[\widehat{O}(t), \widehat{O}(t')]\rangle$. In this picture, operators evolve according to the *Heisenberg equation*

$$\frac{\mathrm{d}\widehat{O}(t)}{\mathrm{d}t} = i\left[\widehat{H}(t), \widehat{O}(t)\right]. \tag{3.58}$$

- *Interaction picture:* This picture represent a mixed evolution in which the state and the density matrix evolve with the interaction Hamiltonian, that is with $\widehat{\mathcal{U}}_{\mathrm{int}}$ while the observables follow the free evolution dictated by $\widehat{\mathcal{U}}_0$. Explicitly, the state evolves according to

$$|\widetilde{\Psi}(t)\rangle = \widehat{\mathcal{U}}_{\mathrm{int}}(t)\,|\Psi(t_0)\rangle \qquad \text{and} \qquad \widetilde{\rho}(t) = \widehat{\mathcal{U}}_{\mathrm{int}}(t)\widehat{\rho}(t_0)\widehat{\mathcal{U}}^{\dagger}_{\mathrm{int}}(t) \tag{3.59}$$

  while the observables follow

$$\widetilde{O}(t) = \widehat{\mathcal{U}}^{\dagger}_0(t)\widehat{O}\widehat{\mathcal{U}}_0(t). \tag{3.60}$$

  This representation is particularly convenient to implement perturbative expansions as it allows us to factorize the free dynamics and we will use it extensively in the following.

All three pictures provide an equivalent description of the dynamics. The above relations imply that we connect the interaction picture to the Schrödinger picture by $|\widetilde{\Psi}(t)\rangle = \widehat{\mathcal{U}}^{\dagger}_0(t)\,|\Psi(t)\rangle$ or equivalently $\widetilde{\rho}(t) = \widehat{\mathcal{U}}^{\dagger}_0(t)\widehat{\rho}(t)\widehat{\mathcal{U}}_0(t)$ and to the Heisenberg picture by $\widetilde{O}(t) = \widehat{\mathcal{U}}_{\mathrm{int}}(t)\widehat{O}(t)\widehat{\mathcal{U}}^{\dagger}_{\mathrm{int}}(t)$. Finally, all three picture coincide at initial time where $|\Psi(t_0)\rangle = |\Psi\rangle = |\widetilde{\Psi}(t_0)\rangle$, $\widehat{\rho}(t_0) = \widehat{\rho} = \widetilde{\rho}(t_0)$ and $\widehat{O} = \widehat{O}(t_0) = \widetilde{O}(t_0)$. Hence, if one wants to change from one picture to the other, one can evolve the quantities of interest backward in time up to t_0 where the conversion is straightforward.

As mentioned above, in the interaction picture the total density matrix evolves with the interaction Hamiltonian,

$$\frac{\mathrm{d}\widetilde{\rho}}{\mathrm{d}t} = -ig\left[\widetilde{H}_{\mathrm{int}}(t), \widetilde{\rho}(t)\right]. \tag{3.61}$$

One can formally integrate this equation from initial time t_0 to final time t, writing

$$\widetilde{\rho}(t) = \widetilde{\rho}(t_0) - ig \int_{t_0}^{t} \mathrm{d}t' \left[\widetilde{H}_{\mathrm{int}}(t'), \widetilde{\rho}(t') \right] . \tag{3.62}$$

If ones trace over the environment in order to obtain $\mathcal{O}(g)$ corrections to the quantum state of the system, it immediately appears that a result only exists if the expectation value of the environmental operator appearing in $\widetilde{H}_{\mathrm{int}}$ is non-vanishing [188, 244]. In general, these contributions can be reabsorbed by a field redefinition so that for the clarity of the argument, we first assume $\mathrm{Tr}_{\mathcal{E}}[\widetilde{H}_{\mathrm{int}}(t)\widetilde{\rho}(t)] = 0$ and rather focus on probing the effect of the environment when an exchange diagram such as

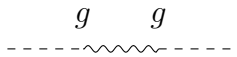

occurs, where the straight dashed line represents propagation through the system and the wiggly line propagation through the environment, which is $\mathcal{O}(g^2)$ at lowest order. One can easily relax this assumption if needed.

Injecting Eq. (3.62) in Eq. (3.61) and tracing over the environmental degrees of freedom, we obtain a first equation for the reduced density matrix $\widetilde{\rho}_{\mathrm{red}}$

$$\frac{\mathrm{d}\widetilde{\rho}_{\mathrm{red}}}{\mathrm{d}t} = -g^2 \int_{t_0}^{t} \mathrm{d}t' \mathrm{Tr}_{\mathcal{E}} \left[\widetilde{H}_{\mathrm{int}}(t), \left[\widetilde{H}_{\mathrm{int}}(t'), \widetilde{\rho}(t') \right] \right] . \tag{3.63}$$

Under this form, this equation is exact and does not yet provide a closed dynamical equation for $\widetilde{\rho}_{\mathrm{red}}$. We now have to rely on some approximation scheme in order to close the integro-differential system. For the illustrative purpose of this Section, let us consider a perturbative expansion in powers of the coupling constant g. From Eq. (3.61), it appears that the density matrix is constant in the interaction picture at lowest order in g, such that for an initial factorized state $\widehat{\rho}(t_0) \equiv \widehat{\rho}_{\mathcal{S}}^{(0)} \otimes \widehat{\rho}_{\mathcal{E}}^{(0)}$ (denoted with a hat given that at initial time, all three pictures coincide)

$$\widetilde{\rho}(t') = \widehat{\rho}_{\mathcal{S}}^{(0)} \otimes \widehat{\rho}_{\mathcal{E}}^{(0)} + \mathcal{O}(g). \tag{3.64}$$

We conclude that the second-order perturbative master equation is

$$\frac{\mathrm{d}\widetilde{\rho}_{\mathrm{red}}}{\mathrm{d}t} = -g^2 \int_{t_0}^{t} \mathrm{d}t' \mathrm{Tr}_{\mathcal{E}} \left[\widetilde{H}_{\mathrm{int}}(t), \left[\widetilde{H}_{\mathrm{int}}(t'), \widehat{\rho}_{\mathcal{S}}^{(0)} \otimes \widehat{\rho}_{\mathcal{E}}^{(0)} \right] \right] + \mathcal{O}(g^3). \tag{3.65}$$

Once integrated, this equation provides the first correction to the quantum state of the system due to the interactions with its surrounding environment. The regime of validity of this master equation is defined by the dominance of the right-hand side of Eq. (3.65) over the next-to-the-leading order correction

$$ig^3 \int_{t_0}^{t} \mathrm{d}t' \int_{t_0}^{t'} \mathrm{d}t'' \mathrm{Tr}_{\mathcal{E}} \left[\widetilde{H}_{\mathrm{int}}(t), \left[\widetilde{H}_{\mathrm{int}}(t'), \left[\widetilde{H}_{\mathrm{int}}(t''), \widehat{\rho}_{\mathcal{S}}^{(0)} \otimes \widehat{\rho}_{\mathcal{E}}^{(0)} \right] \right] \right] . \tag{3.66}$$

Let us perform one last step in order to rewrite Eq. (3.65) in a form that renders the physics more explicit and easily compares with the influence functional derived below. To do so, let us decompose the interaction Hamiltonian in terms of a local tensor product of operators acting on the system and on the environment,

$$\widehat{H}_{\mathrm{int}}(t) = \int \mathrm{d}^3\boldsymbol{x} \widehat{J}_{\mathcal{S}}(t, \boldsymbol{x}) \otimes \widehat{J}_{\mathcal{E}}(t, \boldsymbol{x}) , \tag{3.67}$$

where one can easily extend to the bi-linear combination $\sum_{ij} \boldsymbol{A}_{ij} \widehat{J}_{\mathcal{S},i} \otimes \widehat{J}_{\mathcal{E},j}$ if needed. Plugging this decomposition into Eq. (3.65) and using 4−vector $x = (t, \boldsymbol{x})$ and $y = (t', \boldsymbol{y})$ to lighten the notations, the second-order perturbative master equation reads[5]

$$\frac{\mathrm{d}\widetilde{\rho}_{\mathrm{red}}}{\mathrm{d}t} = -\, g^2 \int_{t_0}^{t} \mathrm{d}t' \int \mathrm{d}^3\boldsymbol{x} \int \mathrm{d}^3\boldsymbol{y} \Bigg\{ \left[\widetilde{J}_{\mathcal{S}}(x)\widetilde{J}_{\mathcal{S}}(y)\widehat{\rho}_{\mathcal{S}}^{(0)} - \widetilde{J}_{\mathcal{S}}(y)\widehat{\rho}_{\mathcal{S}}^{(0)}\widetilde{J}_{\mathcal{S}}(x)\right] \mathcal{K}^{>}(x,y) - \left[\widetilde{J}_{\mathcal{S}}(x)\widehat{\rho}_{\mathcal{S}}^{(0)}\widetilde{J}_{\mathcal{S}}(y) - \widehat{\rho}_{\mathcal{S}}^{(0)}\widetilde{J}_{\mathcal{S}}(y)\widetilde{J}_{\mathcal{S}}(x)\right] [\mathcal{K}^{>}(x,y)]^* \Bigg\}, \tag{3.69}$$

where

$$\mathcal{K}^{>}(x,y) \equiv \mathrm{Tr}_{\mathcal{E}}\left[\widehat{J}_{\mathcal{E}}(x)\widehat{J}_{\mathcal{E}}(y)\widehat{\rho}_{\mathcal{E}}^{(0)}\right] = \left\langle \widehat{J}_{\mathcal{E}}(x)\widehat{J}_{\mathcal{E}}(y)\right\rangle_0, \tag{3.70}$$

the '0' index meaning expectation values are evaluated with respect to the initial state of the environment. $\mathcal{K}^{>}(x,y)$, known as the *memory kernel*, is expressed in the Heisenberg picture and encodes the effect of the environment onto the system. It takes the form of a unequal time two-point correlation function of the environment current, and thus depends on the environment properties.

Typical environments contain a large number of degrees of freedom, hence behave as reservoirs in which the correlation functions quickly decay with $|t-t'|$. More precisely, if the relaxation time of the environment is small compared to the typical scales over which the system evolves, one may coarse-grain the evolution of the system on timescales larger than the environment relaxation time. The memory kernel is then sharply peaked, such that the integral over t' only receives contributions close to its upper bound t. In this limit, the past history ($t' < t$) is not involved in the dynamics anymore, which therefore becomes *Markovian*. Together with the Born approximation, the Markov approximation constitutes a second approximation scheme commonly used to simplify master equations.

Integrating Eq. (3.69) over time would allow us to capture the leading order corrections of the environment onto the quantum state of the system. Apart from organising the perturbative expansion in a sometimes favourable manner, the advantage of Eq. (3.69) is not manifest. Yet, this form provides a useful comparison with the results obtained using the influence functional and the stochastic Schrödinger equation. Moreover, this simplest form is at the basis of a vast effort made in constructing ever more powerful master equations able to go beyond this lowest order perturbative expansion [188]. Indeed, as stated at the beginning of this Section, there exist many other master equations than the one derived in Eq. (3.69). For instance, one could consider to work at a higher order in powers of the coupling constant g. Alternatively, one could make use of the properties of the environment

[5] Equivalently, for future convenience, let us rewrite

$$\frac{\mathrm{d}\widetilde{\rho}_{\mathrm{red}}}{\mathrm{d}t} = -\, g^2 \int_{t_0}^{t} \mathrm{d}t' \int \mathrm{d}^3\boldsymbol{x} \int \mathrm{d}^3\boldsymbol{y} \Bigg\{ \Re\mathrm{e}\left[\mathcal{K}^{>}(x,y)\right] \left[\widetilde{J}_{\mathcal{S}}(x), \left[\widetilde{J}_{\mathcal{S}}(y), \widehat{\rho}_{\mathcal{S}}^{(0)}\right]\right] + i\Im\mathrm{m}\left[\mathcal{K}^{>}(x,y)\right] \left[\widetilde{J}_{\mathcal{S}}(x), \left\{\widetilde{J}_{\mathcal{S}}(y), \widehat{\rho}_{\mathcal{S}}^{(0)}\right\}\right] \Bigg\}, \tag{3.68}$$

where $\{A, B\} \equiv AB + BA$ denotes the anticommutator.

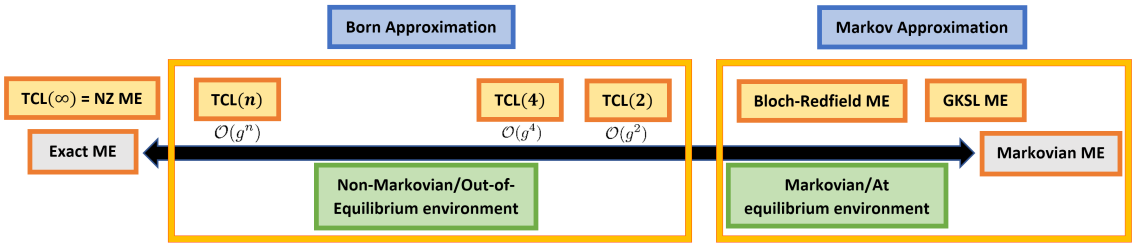

Figure 3.5: The master equation bestiary. On the left lies exact master equations such as the NZ equation, which are just a recasting of the full dynamics focusing on the degrees of freedom of the system. In general, the system and its environment are weakly coupled, which allows one for a systematic expansion in powers of the coupling constant g such as the one carried by the Time-ConvolutionLess (TCL) technique, further developed in Sec. 3.3.1. From left to right are organised schemes in terms of the power of the coupling constant considered. Finally, when the environment is not able to keep track of the past interactions with the system, for instance in the case of a thermal bath with efficient scrambling properties, one can afford for a Markovian approximation, further developed in Sec. 3.3.2. In this case, the dynamics of the system evolves according to a semi-group property and the associated master equation takes the form of a Gorini-Kossakowski-Sudarshan-Lindblad (GKSL) master equation, also known as Lindblad equation, depicted in the right hand side of the graph.

to simplify the memory kernel and derive a Markovian limit. It will be the object of Secs. 3.3.1 and 3.3.2 to develop and characterise these approximation schemes. Fig. 3.5 provides a summary of the most commonly encountered master equations and their relations one to the others. Details on the mentioned master equations can be found in [188] and a summary is provided in the beginning of [251].

Influence functional: While master equations describe the dynamics of the system in the language of super-operators (operations which map positive operators to positive operators) such as the Liouvillian superoperator $\mathcal{L}_{\mathcal{S}}$ of Eq. (3.50), relativistic quantum systems are often treated by the mean of a path integral formalism. Here, we aim at connecting the previously derived master equation to the so-called (Feynman-Vernon) influence functional [254], which is the quantum analogue of the MSR path integral. Yet, first, it is instructive to review the way observables are computed in out-of-equilibrium QFT through the Schwinger-Keldysh formalism.

Schwinger-Keldysh formalism: Also known under the name of *Closed-Time-Path* (CTP) *formalism* or *in-in formalism*, this framework provides the underlying technique used to compute cosmological correlators in primordial cosmology. It aims at describing quantum systems that are out-of-equilibrium, that is to say quantum systems initially prepared in a configuration that do not evolve towards a known state at late-time. This situation contrasts with the one familiar to particle physicists in which the late-time configuration is known to be the adiabatic vacuum of the theory, and so the name of *in-out* computations. This discussion is based on [22] and more details can be found

in [13, 255].

To illustrate the formalism, let us consider the computation of an equal-time two-point function of the system variable in the absence of environment (closed system), in the Schrödinger picture

$$\left\langle \widehat{\zeta}(t,\boldsymbol{x})\widehat{\zeta}(t,\boldsymbol{x}')\right\rangle \equiv \mathrm{Tr}\left[\widehat{\zeta}(\boldsymbol{x})\widehat{\zeta}(\boldsymbol{x}')\widehat{\rho}(t)\right] \tag{3.71}$$

$$= \int \mathrm{d}\zeta \zeta(\boldsymbol{x})\zeta(\boldsymbol{x}')\left\langle\zeta\right|\widehat{\rho}(t)\left|\zeta\right\rangle \tag{3.72}$$

where in the second line, we expanded the expression in the field basis following [22], where $|\zeta\rangle$ is an eigenstate of $\widehat{\zeta}(\boldsymbol{x})$ with eigenvalue $\zeta(\boldsymbol{x})$. In general, we solely know the initial state $\widehat{\rho}_0$ in which the quantum system is prepared. Then, the dynamics leading to $\widehat{\rho}(t)$ is rarely exactly solvable and we often have to rely on approximation schemes to access this quantity. A way to separate what is known from what is not is the following. We can evolve the quantum state using the evolution operator $\widehat{\mathcal{U}}(t,t_0)$ so that

$$\widehat{\rho}(t) = \widehat{\mathcal{U}}(t,t_0)\widehat{\rho}_0\widehat{\mathcal{U}}^\dagger(t,t_0), \tag{3.73}$$

transforming Eq. (3.71) into

$$\left\langle \widehat{\zeta}(t,\boldsymbol{x})\widehat{\zeta}(t,\boldsymbol{x}')\right\rangle = \int \mathrm{d}\zeta\mathrm{d}\zeta_1\mathrm{d}\zeta_2\left[\zeta(\boldsymbol{x})\zeta(\boldsymbol{x}')\right]$$
$$\left[\left\langle\zeta\right|\widehat{\mathcal{U}}(t,t_0)\left|\zeta_1\right\rangle\right]\left[\left\langle\zeta_1\right|\widehat{\rho}_0\left|\zeta_2\right\rangle\right]\left[\left\langle\zeta_2\right|\widehat{\mathcal{U}}^\dagger(t,t_0)\left|\zeta\right\rangle\right] \tag{3.74}$$

where we used two representations of the identity. When an action is specified, $\left\langle\zeta\right|\widehat{\mathcal{U}}(t,t_0)\left|\zeta_1\right\rangle$ has a path integral representation [22]

$$\left\langle\zeta\right|\widehat{\mathcal{U}}(t,t_0)\left|\zeta_1\right\rangle = \int_{\zeta_1}^{\zeta}\mathcal{D}\left[\zeta\right]e^{iS_\zeta[\zeta]} \tag{3.75}$$

where $S_\zeta\left[\zeta\right]$ is the single-field action.[a] One obtains the Schwinger-Keldysh/CPT/in-in formulation of the correlator

$$\left\langle \widehat{\zeta}(t,\boldsymbol{x})\widehat{\zeta}(t,\boldsymbol{x}')\right\rangle = \int \mathrm{d}\zeta\mathrm{d}\zeta_1\mathrm{d}\zeta_2\left[\zeta(\boldsymbol{x})\zeta(\boldsymbol{x}')\right]$$
$$\int_{\zeta_1}^{\zeta}\mathcal{D}\left[\zeta_+\right]\int_{\zeta_2}^{\zeta}\mathcal{D}\left[\zeta_-\right]e^{iS_\zeta[\zeta_+]-iS_\zeta[\zeta_-]}\left\langle\zeta_1\right|\widehat{\rho}_0\left|\zeta_2\right\rangle \tag{3.76}$$

A cartoon representation of the path integral is represented in the top panel of Fig. 3.6

[a] Notations on the boundary conditions are lighten for the sake of clarity, meaning $\zeta(t_0,\boldsymbol{x}) = \zeta_1(\boldsymbol{x})$ and $\zeta(t,\boldsymbol{x}) = \zeta(\boldsymbol{x})$, see [256] for details.

Let us now include a hidden sector, for which we separate observable and unobservable degrees of freedom in the action

$$S\left[\Phi\right] = S_\zeta\left[\zeta\right] + S_\mathcal{F}\left[\mathcal{F}\right] + S_{\mathrm{int}}\left[\zeta;\mathcal{F}\right]. \tag{3.77}$$

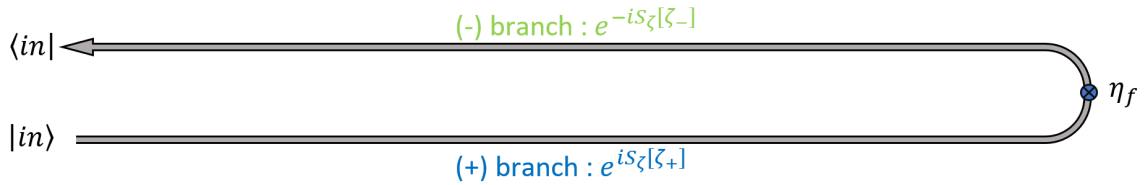

Figure 3.6: Cartoon representation of the *Schwinger-Keldysh* (closed dynamics) path integral. In the Schwinger-Keldysh/CPT/in-in formalism, solely the initial state is known. This is the reason why the dymanics is backward evolved once the final time is reached, leading to the doubling of the path integral. The + branch progates upward and the − branch propagates backward.

Assuming an initial factorisable initial state (such as the Bunch-Davies vacuum) $\widehat{\rho}_0 = \widehat{\rho}_{\mathcal{S}}^{(0)} \otimes \widehat{\rho}_{\mathcal{E}}^{(0)}$, we obtain through similar manipulations as the one presented above for the Schwinger-Keldysh formalism (see [22, 256] if needed)

$$\left\langle \widehat{\zeta}(t,\boldsymbol{x})\widehat{\zeta}(t,\boldsymbol{x}')\right\rangle = \int \mathrm{d}\zeta\mathrm{d}\zeta_1\mathrm{d}\zeta_2\,[\zeta(\boldsymbol{x})\zeta(\boldsymbol{x}')] \int_{\zeta_1}^{\zeta}\mathcal{D}\left[\zeta_+\right]\int_{\zeta_2}^{\zeta}\mathcal{D}\left[\zeta_-\right] e^{iS_\zeta[\zeta_+]-iS_\zeta[\zeta_-]+iS_{\mathrm{IF}}[\zeta_+;\zeta_-]}\left\langle\zeta_1\right|\widehat{\rho}_{\mathcal{S}}^{(0)}\left|\zeta_2\right\rangle \tag{3.78}$$

where the contributions from the unobservable degrees of freedom are captured within the so-called *Feynman-Vernon influence functional* $S_{\mathrm{IF}}\left[\zeta_+;\zeta_-\right]$

$$e^{iS_{\mathrm{IF}}[\zeta_+;\zeta_-]} = \int \mathrm{d}\mathcal{F}\mathrm{d}\mathcal{F}_1\mathrm{d}\mathcal{F}_2\int_{\mathcal{F}_1}^{\mathcal{F}}\mathcal{D}\left[\mathcal{F}_+\right]\int_{\mathcal{F}_2}^{\mathcal{F}}\mathcal{D}\left[\mathcal{F}_-\right] e^{iS_{\mathcal{F}}[\mathcal{F}_+]+iS_{\mathrm{int}}[\zeta_+;\mathcal{F}_+]-iS_{\mathcal{F}}[\mathcal{F}_-]-iS_{\mathrm{int}}[\zeta_-;\mathcal{F}_-]}\left\langle\mathcal{F}_1\right|\widehat{\rho}_{\mathcal{E}}^{(0)}\left|\mathcal{F}_2\right\rangle. \tag{3.79}$$

The influence functional generates three types of contributions which supplement the previously described closed dynamics, as illustrated in Fig. 3.7. Firstly, the influence functional generates contributions which do not mix the two branches of the path integral. These contributions correspond to the generation of an effective action from the interactions of the system with its environment. This effect is unitary and known as the *Lamb shift*, that is the renormalization of the energy levels of the system due to the system-environment coupling. On the top of this unitary effect, some other contributions mix the two branches of the path integral and cannot be recast under the form of an effectively closed quantum system. These terms represent the non-unitary contributions due to physical processes of dissipation and decoherence, that is the energy and information exchange between the system and its surrounding environment. Hence, just as the master equation, the influence functional provides a way to visualize how the unobservable environment affect the dynamics of the system.

In full generality, this object is as hard to compute as it is to solve the full theory. Yet, it is written in a form suitable to perform perturbative expansions. Following [256], let us organise the expansion in powers of S_{int}, that is in powers of the coupling constant between the system and the environment and recover the master equation result derived previously. The interaction between the system and

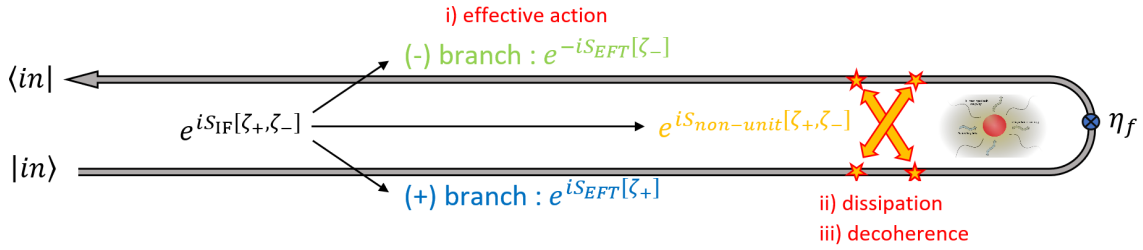

Figure 3.7: Cartoon representation of the *Feynman-Vernon* (open dynamics) path integral. In the Feynman-Vernon/influence functional formalism, the previous picture is supplement by new contributions coming from the impact of the environment onto the dynamics of the system. Some contributions change the expression of the action that propagates along the branches of the path integral. This corresponds to the renormalization of the energy level of the system due to the interactions with its environment, captured by the *Lamb shift* in the master equation language. Some other contributions mix the two branches of the path integral and cannot be captured by a unitary action. They correspond the processes of dissipation and decoherence.

its environment can always be written as a linear combinations of interactions of the form

$$S_{\rm int}\left[\zeta;\mathcal{F}\right] = g\int \mathrm{d}^4x J_{\mathcal{S}}[\zeta(x)]J_{\mathcal{E}}[\mathcal{F}(x)] \tag{3.80}$$

where $J_{\mathcal{S}}[\zeta(x)]$ and $J_{\mathcal{S}}[\mathcal{F}(x)]$ are current densities constituted out of field variables and their derivatives. At second order in g, expanding the LHS and RHS of Eq. (3.79), it becomes [256]

$$\begin{aligned} iS_{\rm IF}\left[\zeta_+;\zeta_-\right] = -\frac{g^2}{2}\int \mathrm{d}^4x\int \mathrm{d}^4y\Big[&J^+_{\mathcal{S}}(x)G_{++}(x,y)J^+_{\mathcal{S}}(y) + J^-_{\mathcal{S}}(x)G_{--}(x,y)J^-_{\mathcal{S}}(y) \\ &-J^+_{\mathcal{S}}(x)G_{+-}(x,y)J^-_{\mathcal{S}}(y) - J^-_{\mathcal{S}}(x)G_{-+}(x,y)J^+_{\mathcal{S}}(y)\Big] \end{aligned} \tag{3.81}$$

where we used the notation $J^\pm_{\mathcal{S}}(x) \equiv J_{\mathcal{S}}[\zeta_\pm(x)]$ and defined the *Wightman function* $G_{-+}(x,y)$ and the *Feynman propagator* $G_{++}(x,y)$ as

$$G_{-+}(x,y) \equiv \langle \widehat{J}_{\mathcal{E}}(x)\widehat{J}_{\mathcal{E}}(y)\rangle_0 = G^*_{+-}(x,y) \tag{3.82}$$

$$G_{++}(x,y) \equiv \langle \mathcal{T}[\widehat{J}_{\mathcal{E}}(x)\widehat{J}_{\mathcal{E}}(y)]\rangle_0 = G^*_{--}(x,y). \tag{3.83}$$

In fact, only one quantity is needed as time ordering relates

$$G_{++}(x,y) = G_{-+}(x,y)\Theta(t-t') + G_{+-}(x,y)\Theta(t'-t) \tag{3.84}$$

where Θ is the Heaviside distribution. We immediately identify $G_{-+}(x,y)$ and the memory kernel $\mathcal{K}^>(x,y)$ previously introduced. Just as for the master equation, the environment is encoded through unequal time two-point functions. Finally, note that in Eq. (3.81), we assumed $\langle \widehat{J}_{\mathcal{E}}(x)\rangle_0 = 0$ as one can often redefine $\widehat{J}_{\mathcal{E}}(x) \to \widehat{J}_{\mathcal{E}}(x) - \langle \widehat{J}_{\mathcal{E}}(x)\rangle_0$ if it is not the case.[6] This assumption can be easily relaxed if needed.

[6] This is equivalent to the previously made assumption $\mathrm{Tr}_{\mathcal{E}}[\widetilde{H}_{\rm int}(t)\widetilde{\rho}(t)] = 0$.

Let us now explicitly connect the second-order influence functional to the second order master equation, following the approach developed in [188, 256, 257]. Let us first notice that Eq. (3.78) provides an expression for the reduced density matrix in the field basis

$$\rho_{\zeta\zeta'}(t) \equiv \langle\zeta|\,\widehat{\rho}_{\rm red}(t)\,|\zeta'\rangle = \int \mathrm{d}\zeta_1\mathrm{d}\zeta_2 \int_{\zeta_1}^{\zeta} \mathcal{D}\left[\zeta_+\right] \int_{\zeta_2}^{\zeta'} \mathcal{D}\left[\zeta_-\right] e^{iS_\zeta[\zeta_+]-iS_\zeta[\zeta_-]+iS_{\rm IF}[\zeta_+;\zeta_-]}\,\langle\zeta_1|\,\widehat{\rho}_{\mathcal{S}}^{(0)}\,|\zeta_2\rangle \tag{3.85}$$

such that expectation value simply expressed as

$$\left\langle\widehat{\zeta}(t,\boldsymbol{x})\widehat{\zeta}(t,\boldsymbol{x}')\right\rangle = \int \mathrm{d}\zeta\zeta(\boldsymbol{x})\zeta(\boldsymbol{x}')\rho_{\zeta\zeta}(t). \tag{3.86}$$

From Eq. (3.85), it appears that $S_{\rm IF}\left[\zeta_+;\zeta_-\right]$ supplements the free dynamics and vanishes in the absence of coupling between the system and the environment, such that one would easily relate it to the dynamics of the interaction picture. Then, let us consider the dynamical generator of the influence functional

$$\begin{aligned}\frac{\mathrm{d}}{\mathrm{d}t}\left\{e^{iS_{\rm IF}[\zeta_+;\zeta_-]}\right\} = -g^2\int_{t_0}^{t}\mathrm{d}t'\int\mathrm{d}^3\boldsymbol{x}\int\mathrm{d}^3\boldsymbol{y}\Big\{&\left[J_{\mathcal{S}}^+(x)J_{\mathcal{S}}^+(y) - J_{\mathcal{S}}^+(y)J_{\mathcal{S}}^-(x)\right]\mathcal{K}^{>}(x,y)\\ &-\left[J_{\mathcal{S}}^+(x)J_{\mathcal{S}}^-(y) - J_{\mathcal{S}}^-(x)J_{\mathcal{S}}^-(y)\right]\left[\mathcal{K}^{>}(x,y)\right]^*\Big\}\left\{e^{iS_{\rm IF}[\zeta_+;\zeta_-]}\right\}\end{aligned} \tag{3.87}$$

where we relabelled x and y when $t' > t$ and used the fact that $G_{-+}(x,y) = \mathcal{K}^{>}(x,y)$. This form is very much reminiscent of Eq. (3.69), pointing towards the idea that the dynamical generator of the influence functional is nothing but the generator of the dynamical map of the quantum state in the interaction picture. In fact, a dictionary can be established relating the sources appearing in the path integral formulation and the operators acting of the Hilbert space of the master equation. The rules are the following:

- The quantum operator associated with a '$+$' source acts on the left of $\widetilde{\rho}_{\rm red}$;
- The quantum operator associated with a '$-$' source acts on the right of $\widetilde{\rho}_{\rm red}$.

Moreover, because of the time-ordering, first act operators that are the innermost in the nested time structure. A rigorous derivation can be found in [188], Chapter 12. This dictionary establishes a correspondence between the second order influence functional derived in Eq. (3.81) and the associated second-order master equation (3.69). The proof is generalisable at any order [257], demonstrating the equivalence between master equation and influence functional formulations which end up being two faces of a same coin, just as the Fokker-Planck equation and the MSR path integral.

Langevin equation: Let us finally highlights how to obtain a stochastic equation of motion for the field operators. First, the so-called "classical"/"quantum" (cl-q) basis (see [255] for an in-depth discussion) is defined as

$$J_{\rm cl}(x) \equiv \frac{J_{\mathcal{S}}^+(x) + J_{\mathcal{S}}^-(x)}{2}\,, \tag{3.88}$$

$$J_{\rm q}(x) \equiv J_{\mathcal{S}}^+(x) - J_{\mathcal{S}}^-(x)\,. \tag{3.89}$$

From Eq. (3.84), we use the relation between the Feynman and Wightman propagators

$$G_{++}(x,y) = \Re\mathrm{e}[\mathcal{K}^{>}(x,y)] + i\Theta\left(t-t'\right)\Im\mathrm{m}[\mathcal{K}^{>}(x,y)] \tag{3.90}$$

to rewrite the influence functional (3.81) in the cl-q basis as[7]

$$\begin{aligned} iS_{\mathrm{IF}}\left[J_{\mathrm{cl}};J_{\mathrm{q}}\right] = -\frac{g^2}{2}\int \mathrm{d}^4x \int \mathrm{d}^4y\; J_{\mathrm{q}}(x)\mathrm{Re}\left[\mathcal{K}^{>}(x,y)\right] J_{\mathrm{q}}(y) \\ -2ig^2\int \mathrm{d}^4x \int^{t} \mathrm{d}^4y\; J_{\mathrm{q}}(x)\mathrm{Im}\left[\mathcal{K}^{>}(x,y)\right] J_{\mathrm{cl}}(y) \end{aligned} \tag{3.91}$$

where the upper boundary in the second line indicates that the $\Theta\left(t-t'\right)$ distribution applies. It follows that

$$e^{iS_{\mathrm{IF}}[J_{\mathrm{cl}};J_{\mathrm{q}}]} \supset e^{-\frac{g^2}{2}\int \mathrm{d}^4x \int \mathrm{d}^4y\; J_{\mathrm{q}}(x)\mathrm{Re}[\mathcal{K}^{>}(x,y)]J_{\mathrm{q}}(y)} \tag{3.92}$$

$$= \int \mathcal{D}\xi e^{-\frac{1}{2}\int \mathrm{d}^4x \int \mathrm{d}^4y \xi(x)\sigma^{-1}(x,y)\xi(y)} e^{2i\int \mathrm{d}^4x \xi(x) J_{\mathrm{q}}(x)} \tag{3.93}$$

where in the second line we used a Bose-Stratanovich transform [255], introducing the auxiliary field ξ. The variance $\sigma(x,y)$ provides the statistic of the Gaussian noise ξ, that is

$$\langle \xi(x)\xi(y)\rangle \equiv \sigma(x,y) = \frac{g^2}{4}\mathrm{Re}\left[\mathcal{K}^{>}(x,y)\right]. \tag{3.94}$$

For this reason, the real part of the memory kernel $\mathrm{Re}\left[\mathcal{K}^{>}(x,y)\right]$ is often called the *noise kernel* [13] as it fixes the statistics of the stochastic variable encoding the effect of the environment onto the system. We finally obtain non-unitary contributions by functional differentiation

$$\left.\frac{\delta S_{\mathrm{IF}}\left[J_{\mathrm{cl}};J_{\mathrm{q}}\right]}{\delta J_{\mathrm{q}}}\right|_{J_{\mathrm{q}}=0} = 0 \tag{3.95}$$

which has to be added to the deterministic evolution specified by the action $S_\zeta\left[\zeta\right] \equiv \int \mathrm{d}^4x \mathcal{L}_\zeta$, leading to the Langevin equation

$$-\frac{\partial \mathcal{L}_\zeta}{\partial \zeta} + \frac{\mathrm{d}}{\mathrm{d}t}\frac{\partial \mathcal{L}_\zeta}{\partial \dot{\zeta}} + g^2\int \mathrm{d}^4y \mathrm{Im}\left[\mathcal{K}^{>}(x,y)\right] J_{\mathcal{S}}(y) = \xi(x) \tag{3.96}$$

where we remind that the source current $J_{\mathcal{S}}\left[\zeta\right]$ has been specified in Eq. (3.80). The non-local term in the LHS is responsible for the dissipation and so $\mathrm{Im}\left[\mathcal{K}^{>}(x,y)\right]$ is known as the *dissipation kernel*. Note that the noise and dissipation kernels are always related by the fact that they correspond to the real and imaginary part of

[7] Under this form, the influence functional is related to the master equation derived in Eq. (3.68) through the following dictionary

- The quantum operator associated with a 'cl' source acts as $\frac{1}{2}\times$ anticommutator;
- The quantum operator associated with a 'q' source acts as a commutator.

Again, time-ordering implies that the innermost operators act first. This dictionary relates the cl-q sources to quantum operators acting on the Hilbert space.

the same object which is the memory kernel. There exist situations where the real and imaginary parts are constrained such as for thermal states where the *Kubo-Martin-Schwinger* (KMS) detailed-balance condition imposes some structure on the thermal correlators

$$\left\langle \widehat{J}_{\mathcal{E}}(t,\boldsymbol{x})\widehat{J}_{\mathcal{E}}(t',\boldsymbol{y})\right\rangle_{\beta} = \left\langle \widehat{J}_{\mathcal{E}}(t',\boldsymbol{y})\widehat{J}_{\mathcal{E}}(t+i\beta,\boldsymbol{x})\right\rangle_{\beta} \tag{3.97}$$

also known as the *fluctuation-dissipation theorem*.

Let us finally mention that the formulation of Eq. (3.96) can be reexpressed in the Hilbert space in terms of a stochastic Schrödinger equation [188], that is a stochastic dynamical equation for the quantum state of the system. The study of non-Hermitian Hamiltonians might be convenient for formal purposes such as demonstrating the Complete-Positive and Trace-Preserving (CPTP) nature of a dynamical map [258–260] or for numerical implementations. Stochastic formulations of the dynamics can also be related to the previously derived master equation through the procedure of *stochastic unravelling*, see Part III of [188]. It closes the triangle presented in Fig. 3.3, illustrating the relation between OQS tools as quantum analogues of the Langevin equation, the Fokker-Planck equation and the MSR path integral.

3.3 Implementation

In this section, we review step by step the construction of Open EFTs, from the derivation of master equations to the assessment of quantum decoherence. The approximation schemes are characterised by rendering explicit the error they induce. Finally, we discuss how to access observables and quantum information properties in Open EFT settings.

3.3.1 A focus on master equations

In the previous Section, we have seen how to derive perturbative master equations, allowing us to access the quantum state of the system in the Hilbert space. The interest of master equations is twofold. First, they organise the computation in terms of objects that directly relate to the quantum information properties of the system, a feature emphasized in Sec. 3.3.4. Second, in some cases, they have the ability to resum late-time secular effects [173, 174, 243, 244, 261–264], hence to go beyond standard perturbation theory and implement non-perturbative resummations in cosmology. It will be the object of Sec. 3.4.1, based on the findings of [244]. For these reasons, master equations are promising tools in the context of the implementation of Open EFTs in cosmology and we now aim at providing some more details about their derivation and structure.

Let us first derive an exact master-equation known as the *Nakajima-Zwanzig* (NZ) equation, which serves as a starting point for the implementation of approximation schemes. We then discuss two different implementations of the Born approximation that are the *perturbative Nakajima-Zwanzig* (NZ_n) and *Time-ConvolutionLess* (TCL_n) techniques. We carefully account for their differences and highlight the merit of time-local formulations. We also characterise the higher-order dynamical generators and specify the error they generate when neglected. Both schemes lead

to non-Markovian master equations which agree at the perturbative level for the observables of the system but depart when considering the resummed terms they may include. Finally, we exhibit the structure of the master equation and the physical role played by each term. In the case of environments forming a Markovian bath, we will connect these formulations to the familiar Gorini-Kossakowski-Sudarshan-Lindblad (GKSL) master equation, also known as *Lindblad equation*. This discussion is based on [244] and provides an augmented discussion of these concepts.

The exact Nakajima-Zwanzig equation: As mentioned above in Eq. (3.61), in the interaction picture the total density matrix evolves with the interaction Hamiltonian, that is

$$\frac{\mathrm{d}\widetilde{\rho}}{\mathrm{d}t} = -ig\left[\widetilde{H}_{\mathrm{int}}(t), \widetilde{\rho}(t)\right] \equiv g\mathcal{L}(t)\widetilde{\rho}(t)\,, \tag{3.98}$$

which defines the Liouville–Von-Neumann super-operator $\mathcal{L}$. Let us now introduce the projection super-operator $\mathcal{P}$, defined as

$$\mathcal{P}\widetilde{\rho} = \mathrm{Tr}_{\mathcal{E}}\left(\widetilde{\rho}\right) \otimes \widetilde{\rho}_{\mathcal{E}}^{(0)}\,, \tag{3.99}$$

where $\widetilde{\rho}_{\mathcal{E}}^{(0)}$ is a fixed reference state in the environment. In practice, it is taken as the state of the environment in the absence of interactions with the system, which is indeed constant in the interaction picture. One can check that $\mathcal{P}$ is a projector, *i.e.* $\mathcal{P}^2 = \mathcal{P}$, and that $\mathcal{P}\widetilde{\rho}$ contains the relevant information to reconstruct the reduced state of the system $\widetilde{\rho}_{\mathrm{red}}$. Upon applying the super-projector $\mathcal{P}$ and its complementary projector $\mathcal{Q} = \mathrm{Id} - \mathcal{P}$ to Eq. (3.98), one obtains

$$\frac{\partial}{\partial t}\mathcal{P}\widetilde{\rho}(t) = g\mathcal{P}\mathcal{L}(t)\widetilde{\rho}(t), \tag{3.100}$$

$$\frac{\partial}{\partial t}\mathcal{Q}\widetilde{\rho}(t) = g\mathcal{Q}\mathcal{L}(t)\widetilde{\rho}(t). \tag{3.101}$$

Here we have used that since the reference state $\widetilde{\rho}_{\mathcal{E}}^{(0)}$ is independent of time, $\mathcal{P}$ and $\mathcal{Q}$ commute with $\partial/\partial t$. Inserting the identity $\mathrm{Id} = \mathcal{P} + \mathcal{Q}$ between the Liouville operator and the density matrix, one obtains

$$\frac{\partial}{\partial t}\mathcal{P}\widetilde{\rho}(t) = g\mathcal{P}\mathcal{L}(t)\mathcal{P}\widetilde{\rho}(t) + g\mathcal{P}\mathcal{L}(t)\mathcal{Q}\widetilde{\rho}(t), \tag{3.102}$$

$$\frac{\partial}{\partial t}\mathcal{Q}\widetilde{\rho}(t) = g\mathcal{Q}\mathcal{L}(t)\mathcal{P}\widetilde{\rho}(t) + g\mathcal{Q}\mathcal{L}(t)\mathcal{Q}\widetilde{\rho}(t). \tag{3.103}$$

A formal solution of Eq. (3.103) is given by

$$\mathcal{Q}\widetilde{\rho}(t) = \mathcal{G}_{\mathcal{Q}}(t,t_0)\mathcal{Q}\widetilde{\rho}(t_0) + g\int_{t_0}^{t}\mathrm{d}t'\mathcal{G}_{\mathcal{Q}}(t,t')\mathcal{Q}\mathcal{L}(t')\mathcal{P}\widetilde{\rho}(t'), \tag{3.104}$$

where t_0 is some initial time and $\mathcal{G}_{\mathcal{Q}}(t,t')$ is the propagator defined as

$$\mathcal{G}_{\mathcal{Q}}(t,t') \equiv \mathcal{T}\exp\left[g\int_{t'}^{t}\mathrm{d}t''\mathcal{Q}\mathcal{L}(t'')\right]. \tag{3.105}$$

Plugging Eq. (3.104) into Eq. (3.102), one then obtains a closed equation for the time evolution of the projected density matrix $\mathcal{P}\widetilde{\rho}$, namely

$$\frac{\partial}{\partial t}\mathcal{P}\widetilde{\rho}(t) = g\mathcal{P}\mathcal{L}(t)\mathcal{G}_{\mathcal{Q}}(t,t_0)\mathcal{Q}\widetilde{\rho}(t_0) + g\mathcal{P}\mathcal{L}(t)\mathcal{P}\widetilde{\rho}(t) + g^2\int_{t_0}^{t}\mathrm{d}t'\mathcal{P}\mathcal{L}(t)\mathcal{G}_{\mathcal{Q}}(t,t')\mathcal{Q}\mathcal{L}(t')\mathcal{P}\widetilde{\rho}(t'). \tag{3.106}$$

This is the Nakajima-Zwanzig equation. Although formal, it provides an exact master equation for the reduced state of the system. It can be further simplified by assuming that the initial state does not contain correlations between the system and the environment, *i.e.* $\widetilde{\rho}(t_0) = \mathrm{Tr}_{\mathcal{E}}(\widetilde{\rho}^{(0)}) \otimes \mathrm{Tr}_{\mathcal{S}}(\widetilde{\rho}^{(0)}) = \widehat{\rho}_{\mathcal{S}}^{(0)} \otimes \widehat{\rho}_{\mathcal{E}}^{(0)}$, hence $\mathcal{Q}\widetilde{\rho}(t_0) = 0$. Moreover, without loss of generality one can assume that the expectation value of the interaction Hamiltonian vanishes in the reference state, *i.e.* $\langle \widehat{H}_{\mathrm{int}}\rangle_0 = 0$ (if this is not satisfied, one simply redefines $\widehat{H}_{\mathcal{S}}$ by adding $g\langle \widehat{H}_{\mathrm{int}}\rangle_0$ to it, as discussed above). This leads to $\mathcal{P}\mathcal{L}(t)\mathcal{P} = 0$, so the Nakajima-Zwanzig equation reduces to

$$\frac{\partial}{\partial t}\mathcal{P}\widetilde{\rho}(t) = g^2\int_{t_0}^{t}\mathrm{d}t'\mathcal{K}(t,t')\mathcal{P}\widetilde{\rho}(t'), \tag{3.107}$$

where we have introduced the memory kernel $\mathcal{K}(t,t')$ defined as

$$\mathcal{K}(t,t') = \mathcal{P}\mathcal{L}(t)\mathcal{G}_{\mathcal{Q}}(t,t')\mathcal{Q}\mathcal{L}(t')\mathcal{P}. \tag{3.108}$$

In this form, the master equation is as difficult to solve as the Liouville equation (3.98) of the full setup. However, it allows efficient approximation schemes to be designed, as we shall now see. The first approximation relies on the assumption of weak coupling between the system and the environment and is discussed below, the second approximation concerns properties of the environment itself and is developed in Sec. 3.3.2.

Perturbative Nakajima-Zwanzig equations (NZ_n): An effective description of the system alone is in general possible only when it weakly couples to its environment. This naturally provides a small parameter, namely the interaction strength, in which to perform an expansion. This is the so-called *Born approximation*. Several implementation of this approximation scheme have been proposed, see [188], Chapter 9. For factorised initial-conditions, the simplest approach consists in expanding the memory kernel $\mathcal{K}(t,t')$ defined in Eq. (3.108) in powers of the coupling constant g. The second-order expansion of the Nakajima-Zwanzig equation, denoted NZ_2, writes

$$\frac{\partial}{\partial t}\mathcal{P}\widetilde{\rho}(t) = g^2\int_{t_0}^{t}\mathrm{d}t'\mathcal{P}\mathcal{L}(t)\mathcal{L}(t')\mathcal{P}\widetilde{\rho}(t'), \tag{3.109}$$

which we reexpress in terms of the interaction Hamiltonian for clarity

$$\frac{\mathrm{d}\widetilde{\rho}_{\mathrm{red}}}{\mathrm{d}t} = -g^2\int_{t_0}^{t}\mathrm{d}t'\mathrm{Tr}_{\mathcal{E}}\left[\widetilde{H}_{\mathrm{int}}(t),\left[\widetilde{H}_{\mathrm{int}}(t'),\widetilde{\rho}_{\mathrm{red}}(t')\otimes\widehat{\rho}_{\mathcal{E}}^{(0)}\right]\right]. \tag{3.110}$$

The regime of validity is defined by the dominance of the right-hand side of Eq. (3.110) over the next-to-the-leading order correction

$$ig^3\int_{t_0}^{t}\mathrm{d}t'\int_{t_0}^{t'}\mathrm{d}t''\mathrm{Tr}_{\mathcal{E}}\left[\widetilde{H}_{\mathrm{int}}(t),\left[\widetilde{H}_{\mathrm{int}}(t'),\left[\widetilde{H}_{\mathrm{int}}(t''),\widetilde{\rho}_{\mathrm{red}}(t'')\otimes\widehat{\rho}_{\mathcal{E}}^{(0)}\right]\right]\right]. \tag{3.111}$$

In practice, NZ_2 has some technical disadvantages [188]. The perturbative expansion simplifies the computation of the memory kernel which boils down to the estimation of a free Wightman function but the generator of the dynamical map remains an integro-differential system whose numerical treatment may be quite involved.

Time-ConvolutionLess master equations (TCL_n): The Time-ConvolutionLess (hereafter TCL) method, developed in [265] based on the previous cumulant expansion of Van Kampen [266, 267], allow us to remove the convolution by noticing that the non-local in time contributions are also organised in powers of the coupling constant g, which must be neglected if we consistently derive the master equation at a given order. For instance, the second-order TCL master equation, hereafter called TCL_2, reads

$$\frac{\mathrm{d}\widetilde{\rho}_{\mathrm{red}}}{\mathrm{d}t} = -g^2 \int_{t_0}^{t} \mathrm{d}t' \mathrm{Tr}_{\mathcal{E}} \left[\widetilde{H}_{\mathrm{int}}(t), \left[\widetilde{H}_{\mathrm{int}}(t'), \widetilde{\rho}_{\mathrm{red}}(t) \otimes \widehat{\rho}_{\mathcal{E}}^{(0)} \right] \right]. \tag{3.112}$$

Both Eq. (3.110) and Eq. (3.112) are second-order and it is expected they approximate the exact dynamics at the same accuracy [188]. In practice, TCL_2 is preferred as it involves a time-local generator instead of a convolutional kernel, which reduces the complexity of the differential equation. One can evaluate the leading order difference between Eq. (3.110) and Eq. (3.112) by Taylor expanding the $\widetilde{\rho}_{\mathrm{red}}(t')$ contribution, following the approach developed in [228, 236, 237, 239, 262, 268]

$$\widetilde{\rho}_{\mathrm{red}}(t') \simeq \widetilde{\rho}_{\mathrm{red}}(t) + (t'-t) \frac{\mathrm{d}\widetilde{\rho}_{\mathrm{red}}}{\mathrm{d}t} + \mathcal{O}\left[(t'-t)^2 \right]. \tag{3.113}$$

By injecting this expansion in Eq. (3.110), we recover Eq. (3.112) up to a $\mathcal{O}(g^4)$ correction reading

$$\begin{aligned} g^4 \int_{t_0}^{t} \mathrm{d}t' \, (t-t') \, \mathrm{Tr}_{\mathcal{E}} \Big[\widetilde{H}_{\mathrm{int}}(t), \Big[\widetilde{H}_{\mathrm{int}}(t'), \\ \int_{t_0}^{t} \mathrm{d}t'' \mathrm{Tr}_{\mathcal{E}} \left[\widetilde{H}_{\mathrm{int}}(t), \left[\widetilde{H}_{\mathrm{int}}(t''), \widetilde{\rho}_{\mathrm{red}}(t) \otimes \widehat{\rho}_{\mathcal{E}}^{(0)} \right] \right] \Big] \Big]. \end{aligned} \tag{3.114}$$

where we replaced $\mathrm{d}\widetilde{\rho}_{\mathrm{red}}/\mathrm{d}t$ by its lowest order expression given in Eq. (3.112) in a iterative way. As long as the right hand side of Eq. (3.112) dominates over Eq. (3.114), the deconvolution approximation holds. Note that when the perturbative expansion is well under control, Eq. (3.111) becomes dominant before Eq. (3.114) takes over, so that the localness in time remains well justified within the regime of validity of the Born approximation.

Let us stress that despite being written in a time-local form, the TCL_2 master equation (3.112) remains a *non-Markovian* master equation. Following the definition of Breuer and Petruccione [188], a dynamical map $\widetilde{\rho}(t) \to \widetilde{\rho}(t') = \mathcal{V}_{t\to t'}\widetilde{\rho}(t)$ is said to be *Markovian* if it forms a semi-group, *i.e.*

$$\mathcal{V}_{t\to t'} = \mathcal{V}_{t''\to t'}\mathcal{V}_{t\to t''}. \tag{3.115}$$

For the semi-group structure (3.115) to occur, the imprint of the environment onto the system must be the same at anytime. This feature is likely to happen solely if the environment is large enough so that it does not feel the backreaction of the system

and reaches some form of stationarity, in which case we call it a *bath*. Markovianity provides a much stronger statement on the dynamics of the system than time locality. In particular, it implies some form of *irreversibility* as no information backflow can occur in Markovian frameworks (see [188], Section 3.2.5). The system has a positive entropy production rate and obeys the H-theorem. On the contrary, non-Markovian OQS can experience memory effects and information backflow, as we showed in the context of cosmology in [154]. Non-Markovian dynamics allow us to evade the restrictive framework of Markovian bath for the environment, which turns out to be crucial in the context of cosmology where the presence of a dynamical background often ruins any hope of semi-group evolution [244, 269, 270]. It makes the TCL formalism particularly suited to tackle finite size environments, an interesting feature in the context of cosmology where symmetries of the background induce reduction of the effective number of dynamical degrees of freedom [154]. Note that a Markovian master equation is necessarily local in time, but the reverse is not necessarily true. Hence, as stressed above, there exists a fundamental difference between local-in-time and Markovian master equations. This point has been a continuous object of confusion in the community, mainly due to the various definitions 'Markovian' can handle depending on the context. For this reason, we aim at clarifying this aspect which is further developed in Sec. 3.3.2.

The TCL cumulant expansion: The TCL expansion addresses one of the difficulties inherent to the Nakajima-Zwanzig equation (3.107), namely the fact that it is non-local in time, *i.e.* the time derivative of $\mathcal{P}\widetilde{\rho}(t)$ depends on its past history $\mathcal{P}\widetilde{\rho}(t')$ for $t' < t$. By solely expanding the dynamics of the system in powers of the coupling constant g, the TCL expansion renders the equation local in time while preserving the non-Markovian nature of the dynamical map. One thus obtains an equation of the form

$$\frac{\partial}{\partial t}\mathcal{P}\widetilde{\rho}(t) = \sum_{n=2}^{\infty} g^n \mathcal{K}_n(t)\mathcal{P}\widetilde{\rho}(t)\,, \tag{3.116}$$

where the $\mathcal{K}_n$ operators are called the TCL_n operators and can be computed iteratively. This can be done by expanding Eq. (3.105) in g, and by using Eq. (3.116) to express $\mathcal{P}\widetilde{\rho}(t')$ in terms of $\mathcal{P}\widetilde{\rho}(t)$ in the right-hand side of Eq. (3.107), at the required order. Let us illustrate this so-called *cumulant expansion* in the language of Van Kampen. Following [266, 267], one can recast the exact dynamics presented in Eq. (3.107) in an infinite tower of super-operators organised in powers of the coupling constant. We introduce the notation

$$\langle \mathcal{X} \rangle \equiv \mathcal{P}\mathcal{X}\mathcal{P} \tag{3.117}$$

for any super-operator $\mathcal{X}$. The formal solution of the Liouville-von Neumann equation (3.98) for the relevant part of the density matrix can be written as

$$\mathcal{P}\widetilde{\rho}(t) = \left\langle \mathcal{T} \exp\left[g \int_{t_0}^{t} \mathrm{d}t' \mathcal{L}(t') \right] \right\rangle \mathcal{P}\widetilde{\rho}(t_0). \tag{3.118}$$

Differentiating this equation with respect to time, we obtain

$$\frac{\partial}{\partial t}\mathcal{P}\widetilde{\rho}(t) = \Bigg[g\,\langle \mathcal{L}(t)\rangle + g^2 \int_{t_0}^{t} \mathrm{d}t'\,\langle \mathcal{L}(t)\mathcal{L}(t')\rangle + g^3 \int_{t_0}^{t} \mathrm{d}t' \int_{t_0}^{t'} \mathrm{d}t''\,\langle \mathcal{L}(t)\mathcal{L}(t')\mathcal{L}(t'')\rangle + \cdots \Bigg] \mathcal{P}\widetilde{\rho}(t_0). \tag{3.119}$$

In order to write this equation in a time-local form, we can backward evolve Eq. (3.118) to express $\mathcal{P}\widetilde{\rho}(t_0)$ in terms of $\mathcal{P}\widetilde{\rho}(t)$. This property, known as the reversibility of the dynamical map, is ensured by the smallness of the coupling constant. Note that it might break down at late time [188]. Upon expanding this expression in powers of g, we obtain a cumulant expansion of the form of Eq. (3.116) where the so-called TCL_n generators $\mathcal{K}_n(t)$ are defined by

$$\mathcal{K}_n(t) \equiv \int_{t_0}^{t} \mathrm{d}t_1 \int_{t_0}^{t_1} \mathrm{d}t_2 \cdots \int_{t_0}^{t_{n-2}} \mathrm{d}t_{n-1}\,\langle \mathcal{L}(t)\mathcal{L}(t_1)\mathcal{L}(t_2)\cdots\mathcal{L}(t_{n-1})\rangle_{\mathrm{oc}} \tag{3.120}$$

with the quantities

$$\langle \mathcal{L}(t)\mathcal{L}(t_1)\mathcal{L}(t_2)\cdots\mathcal{L}(t_{n-1})\rangle_{\mathrm{oc}} \equiv \sum (-1)^q \mathcal{P}\mathcal{L}(t)\cdots\mathcal{L}(t_i)\mathcal{P}\mathcal{L}(t_j)\cdots \mathcal{L}(t_k)\mathcal{P}\mathcal{L}(t_l)\cdots\mathcal{L}(t_m)\mathcal{P}\cdots\mathcal{P} \tag{3.121}$$

known under the name of ordered cumulants and defined according to the following rules [188]. Let us consider a sequence of the form $\mathcal{P}\mathcal{L}\cdots\mathcal{L}\mathcal{P}$ with n factors of $\mathcal{L}$ in between two $\mathcal{P}$. The next step consists in inserting q factors of $\mathcal{P}$ between the $\mathcal{L}$ such that at least two $\mathcal{L}$ stand in between two successive projector operators. There is an overall $(-1)^q$ factor and the time arguments are organised such that the first one is always t and all possible permutation of the time arguments $t_1, t_2, \cdots, t_{n-1}$ must be included. The only restriction is that the time arguments in between two successice $\mathcal{P}$ must be ordered chronologically. The ordered cumulant is obtained by a summation over all possible insertions of $\mathcal{P}$ and over all allowed partitions of the time arguments. For concreteness, the first cumulants are

$$\mathcal{K}_2(t) = \int_{t_0}^{t} \mathrm{d}t'\mathcal{P}\mathcal{L}(t)\mathcal{L}(t')\mathcal{P}\,, \tag{3.122}$$

$$\mathcal{K}_3(t) = \int_{t_0}^{t} \mathrm{d}t' \int_{t'}^{t} \mathrm{d}t''\mathcal{P}\mathcal{L}(t)\mathcal{L}(t'')\mathcal{L}(t')\mathcal{P} \tag{3.123}$$

$$\mathcal{K}_4(t) = \int_{t_0}^{t} \mathrm{d}t_1 \int_{t_0}^{t_1} \mathrm{d}t_2 \int_{t_0}^{t_2} \mathrm{d}t_3 \Big[\mathcal{P}\mathcal{L}(t)\mathcal{L}(t_1)\mathcal{L}(t_2)\mathcal{L}(t_3)\mathcal{P} - \mathcal{P}\mathcal{L}(t)\mathcal{L}(t_1)\mathcal{P}\mathcal{L}(t_2)\mathcal{L}(t_3)\mathcal{P} - \mathcal{P}\mathcal{L}(t)\mathcal{L}(t_2)\mathcal{P}\mathcal{L}(t_1)\mathcal{L}(t_3)\mathcal{P} - \mathcal{P}\mathcal{L}(t)\mathcal{L}(t_3)\mathcal{P}\mathcal{L}(t_1)\mathcal{L}(t_2)\mathcal{P}\Big]. \tag{3.124}$$

This expansion can be carried on to the required level of accuracy, which allows one to work out Eq. (3.116) when truncated at the corresponding order TCL_n.

Note that, even if the TCL_2 order may be sufficient for practical purposes, the derivation of the fourth-order generator is useful to control the validity of the cumulant expansion, by evaluating the error estimate $g^2||\mathcal{K}_4||/||\mathcal{K}_2||$ and checking that it is indeed small.

Link with perturbative methods: In Sec. 3.2.3, we have derived a perturbative master equation now supplemented by the NZ_2 and TCL_2 schemes. For the sake of clarity, let us reproduce these three equations

$$\frac{\mathrm{d}\widetilde{\rho}_{\mathrm{red}}}{\mathrm{d}t} = -g^2 \int_{t_0}^{t} \mathrm{d}t' \mathrm{Tr}_{\mathcal{E}} \left[\widetilde{H}_{\mathrm{int}}(t), \left[\widetilde{H}_{\mathrm{int}}(t'), \widehat{\rho}_{\mathcal{S}}^{(0)} \otimes \widehat{\rho}_{\mathcal{E}}^{(0)}\right]\right] \qquad \text{(pert.)} \qquad (3.125)$$

$$\frac{\mathrm{d}\widetilde{\rho}_{\mathrm{red}}}{\mathrm{d}t} = -g^2 \int_{t_0}^{t} \mathrm{d}t' \mathrm{Tr}_{\mathcal{E}} \left[\widetilde{H}_{\mathrm{int}}(t), \left[\widetilde{H}_{\mathrm{int}}(t'), \widetilde{\rho}_{\mathrm{red}}(t') \otimes \widehat{\rho}_{\mathcal{E}}^{(0)}\right]\right] \qquad (\mathrm{NZ}_2) \qquad (3.126)$$

$$\frac{\mathrm{d}\widetilde{\rho}_{\mathrm{red}}}{\mathrm{d}t} = -g^2 \int_{t_0}^{t} \mathrm{d}t' \mathrm{Tr}_{\mathcal{E}} \left[\widetilde{H}_{\mathrm{int}}(t), \left[\widetilde{H}_{\mathrm{int}}(t'), \widetilde{\rho}_{\mathrm{red}}(t) \otimes \widehat{\rho}_{\mathcal{E}}^{(0)}\right]\right] \qquad (\mathrm{TCL}_2) \qquad (3.127)$$

Later on in this manuscript, we will investigate in Sec. 3.4.1 the extent to which NZ and TCL master equations go beyond perturbative effects and enable some non-perturbative resummation. At this stage however, it is important to stress that, when solved perturbatively, they all reduce to the same standard perturbative results. This is because, when deriving the NZ_2 and TCL_2 equations, no contribution of order lower than g^2 has been dropped.

More explicitly, the Liouville–Von-Neumann equation (3.98) can be formally solved as done in Eq. (3.50). By recursively evaluating $\widetilde{\rho}$ in the right-hand side with Eq. (3.50) itself, one obtains

$$\widetilde{\rho}(t) = \sum_{n=0}^{\infty} (-ig)^n \int_{t_0}^{t} \mathrm{d}t_1 \int_{t_0}^{t_1} \mathrm{d}t_2 \cdots \int_{t_0}^{t_{n-1}} \mathrm{d}t_n \qquad (3.128)$$
$$\left[\widetilde{H}_{\mathrm{int}}(t_1), \left[\widetilde{H}_{\mathrm{int}}(t_2), \cdots \left[\widetilde{H}_{\mathrm{int}}(t_n), \widehat{\rho}_{\mathcal{S}}^{(0)} \otimes \widehat{\rho}_{\mathcal{E}}^{(0)}\right] \cdots\right]\right],$$

which displays all contributions to the quantum state order-by-order in g. In turn, this allows one to compute corrections to the observables at all orders, as in the Schwinger-Keldysh/CTP/in-in formalism.[8] Let us see how this compares with a

[8] Indeed, in the Schwinger-Keldysh/CTP/in-in formalism, the expectation value of an operator $\widehat{O}$ at time t reads

$$\langle \widehat{O} \rangle(t) = \langle \Psi | \, \overline{\mathcal{T}} \left[e^{ig \int_{t_0}^{t} \mathrm{d}t' \widetilde{H}_{\mathrm{int}}(t')} \right] \widetilde{O}(t) \mathcal{T} \left[e^{-ig \int_{t_0}^{t} \mathrm{d}t'' \widetilde{H}_{\mathrm{int}}(t'')} \right] |\Psi\rangle \, . \qquad (3.129)$$

By Taylor expanding the exponential functions, one obtains

$$\langle \widehat{O} \rangle(t) = \sum_{n=0}^{\infty} (ig)^n \int_{t_0}^{t} \mathrm{d}t_1 \int_{t_0}^{t_1} \mathrm{d}t_2 \cdots \int_{t_0}^{t_{n-1}} \mathrm{d}t_n \qquad (3.130)$$
$$\langle \Psi | \left[\widetilde{H}_{\mathrm{int}}(t_n), \left[\widetilde{H}_{\mathrm{int}}(t_{n-1}), \cdots \left[\widetilde{H}_{\mathrm{int}}(t_1), \widetilde{O}(t)\right] \cdots\right]\right] |\Psi\rangle \, .$$

Using that $\langle \widehat{O} \rangle(t) = \mathrm{Tr}_{\mathcal{S}+\mathcal{E}}[\widetilde{O}(t)\widetilde{\rho}(t)]$, together with

$$\mathrm{Tr}_{\mathcal{S}+\mathcal{E}}[\widetilde{O}(t)[\widetilde{H}_{\mathrm{int}}(t_i), \widehat{\rho}_{\mathcal{S}}^{(0)} \otimes \widehat{\rho}_{\mathcal{E}}^{(0)}]] = -\langle \Psi | [\widetilde{H}_{\mathrm{int}}(t_i), \widetilde{O}(t)] | \Psi \rangle, \qquad (3.131)$$

this is indeed consistent with Eq. (3.128).

perturbative solution of NZ_n and TCL_n. At second order, since the right-hand sides of Eqs. (3.126) and (3.127) are proportional to g^2, one has

$$\widetilde{\rho}_{\mathrm{red}}(t') = \widetilde{\rho}_{\mathrm{red}}(t) + \mathcal{O}\big(g^2\big) \tag{3.132}$$

$$= \widetilde{\rho}_{\mathrm{red}}(t_0) + \mathcal{O}\big(g^2\big) \tag{3.133}$$

$$= \widehat{\rho}_{\mathcal{S}}^{(0)} \otimes \widehat{\rho}_{\mathcal{E}}^{(0)} + \mathcal{O}\big(g^2\big) \tag{3.134}$$

and all three schemes leads to

$$\widetilde{\rho}(t_f) = \widehat{\rho}_{\mathcal{S}}^{(0)} \otimes \widehat{\rho}_{\mathcal{E}}^{(0)} - g^2 \int_{t_0}^{t_f} \mathrm{d}t \int_{t_0}^{t} \mathrm{d}t' \mathrm{Tr}_{\mathcal{E}} \left[\widetilde{H}_{\mathrm{int}}(t), \left[\widetilde{H}_{\mathrm{int}}(t'), \widehat{\rho}_{\mathcal{S}}^{(0)} \otimes \widehat{\rho}_{\mathcal{E}}^{(0)}\right]\right], \tag{3.135}$$

which reduces to Eq. (3.128) when traced over the environmental degrees of freedom and truncated at order g^2. This shows that solving NZ_2 or TCL_2 at order g^2 is equivalent to standard perturbative techniques at the same order. Likewise, one can show that solving NZ_n or TCL_n perturbatively at order g^n is equivalent to standard perturbation theory. Therefore, beyond this perturbative limit, when solved as *bona fide* generators of the dynamical map (*i.e.* when taken *per se* and solved without further perturbative expansion), they contain *all* terms of order g^n, and *some* terms of order $g^{m>n}$. It provides a first example of how master equations are able to go beyond the perturbative regime by implementing some form of resummation in time.

Interpretating the master equation: We now turn our attention to the TCL_2 master equation (3.127) which has a simpler interpretation than its NZ_2 counterpart. We remind that it is formulated in the interaction picture, where the interaction Hamiltonian reads $\widehat{H}_{\mathrm{int}}(t) = \int \mathrm{d}^3\boldsymbol{x}\, \widehat{J}_{\mathcal{S}}(t,\boldsymbol{x}) \otimes \widehat{J}_{\mathcal{E}}(t,\boldsymbol{x})$. The TCL_2 master equation (3.112) thus takes a form similar to the one derived in Eq. (3.69), that is

$$\begin{aligned}\frac{\mathrm{d}\widetilde{\rho}_{\mathrm{red}}}{\mathrm{d}t} = -\, g^2 \int_{t_0}^{t} \mathrm{d}t' \int \mathrm{d}^3\boldsymbol{x} \int \mathrm{d}^3\boldsymbol{y} \Bigg\{ &\left[\widetilde{J}_{\mathcal{S}}(x)\widetilde{J}_{\mathcal{S}}(y)\widetilde{\rho}_{\mathrm{red}}(t) - \widetilde{J}_{\mathcal{S}}(y)\widetilde{\rho}_{\mathrm{red}}(t)\widetilde{J}_{\mathcal{S}}(x)\right] \mathcal{K}^{>}(x,y) \\ &- \left[\widetilde{J}_{\mathcal{S}}(x)\widetilde{\rho}_{\mathrm{red}}(t)\widetilde{J}_{\mathcal{S}}(y) - \widetilde{\rho}_{\mathrm{red}}(t)\widetilde{J}_{\mathcal{S}}(y)\widetilde{J}_{\mathcal{S}}(x)\right] [\mathcal{K}^{>}(x,y)]^* \Bigg\},\end{aligned} \tag{3.136}$$

where the only difference with Eq. (3.69) is that now, $\widehat{\rho}_{\mathcal{S}}^{(0)}$ is replaced by $\widetilde{\rho}_{\mathrm{red}}(t)$. We want to highlight the structure hidden behind this equation. For the sake of clarity, we consider localised currents $\widehat{J}_{\mathcal{S}}(x) = \widehat{J}_{\mathcal{S}}(t)\delta(\boldsymbol{x} - \boldsymbol{x}_0)$ and further simplify the discussion by focusing on bilinear interactions.[9] In this case, the most generic quadratic interaction Hamiltonian can be written as

$$\widehat{H}_{\mathrm{int}}(t) = \widehat{\boldsymbol{z}}_{\zeta}^{\mathrm{T}}(t)\boldsymbol{V}(t)\widehat{\boldsymbol{z}}_{\mathcal{F}}(t) \tag{3.137}$$

where $\boldsymbol{V}(t)$ is an arbitrary 2×2 matrix containing the linear couplings between the two fields and $\widehat{\boldsymbol{z}}_{\alpha} = (\widehat{\alpha}, \widehat{p}_{\alpha})^{\mathrm{T}}$ for $\alpha = \zeta, \mathcal{F}$ gathers the configuration and momentum operators of the system and the environment. In order to write Eq. (3.112) in the Schrödinger picture where the physics is manifest, we need to recast it in terms

[9] A general discussion for non-linear interactions is doable at the price of introducing new terms whose interpretation is less straightforward, obscuring the clear connection existing at the level of Gaussian master equations between Markovian and non-Markovian master equations.

of local-in-time operators for the system. We use the fact that in the interaction picture, operators evolve with the free Hamiltonian $\widehat{H}_0(t)$ so that

$$\widetilde{\boldsymbol{z}}_\zeta(t') = \overline{\mathcal{T}} \exp\left[i\int_t^{t'} \widehat{H}_0(t'')\mathrm{d}t''\right] \widetilde{\boldsymbol{z}}_\zeta(t) \mathcal{T} \exp\left[-i\int_t^{t'} \widehat{H}_0(t'')\mathrm{d}t''\right]. \tag{3.138}$$

This quantity can be hard to access, yet, the linearity of the dynamics greatly simplifies the computation as

$$\widetilde{\boldsymbol{z}}_\zeta(t') = \boldsymbol{G}^{(\mathcal{S})}(t',t)\widetilde{\boldsymbol{z}}_\zeta(t) \tag{3.139}$$

where $\boldsymbol{G}^{(\mathcal{S})}(t',t)$ is the Green's matrix of the unperturbed system (see e.g. [121, 251] for a discussion of the underlying symplectic structure generating this dynamics). Expressing Eq. (3.136) in terms of equal-time operators using Eq. (3.139), one finds

$$\begin{aligned}\frac{\mathrm{d}\widetilde{\rho}_{\mathrm{red}}}{\mathrm{d}t} = -\int_{t_0}^{t} \mathrm{d}t' \Big\{ &[\widetilde{\boldsymbol{z}}_{\zeta,i}(t)\widetilde{\boldsymbol{z}}_{\zeta,j}(t)\widetilde{\rho}_{\mathrm{red}}(t) - \widetilde{\boldsymbol{z}}_{\zeta,j}(t)\widetilde{\rho}_{\mathrm{red}}(t)\widetilde{\boldsymbol{z}}_{\zeta,i}(t)]\, \boldsymbol{\mathcal{D}}^{>}_{ij}(t,t') \\ &- [\widetilde{\boldsymbol{z}}_{\zeta,i}(t)\widetilde{\rho}_{\mathrm{red}}(t)\widetilde{\boldsymbol{z}}_{\zeta,j}(t) - \widetilde{\rho}_{\mathrm{red}}(t)\widetilde{\boldsymbol{z}}_{\zeta,j}(t)\widetilde{\boldsymbol{z}}_{\zeta,i}(t)]\, \boldsymbol{\mathcal{D}}^{>*}_{ij}(t,t') \Big\},\end{aligned} \tag{3.140}$$

where implicit summation over repeated indices apply. The kernel $\boldsymbol{\mathcal{D}}^{>}(t,t')$ is defined by

$$\boldsymbol{\mathcal{D}}^{>}(t,t') \equiv \boldsymbol{V}(t)\boldsymbol{\mathcal{K}}^{>}(t,t')\boldsymbol{V}^{\mathrm{T}}(t')\boldsymbol{G}^{(\mathcal{S})}(t',t) \tag{3.141}$$

where $\boldsymbol{\mathcal{K}}^{>}(t,t') \equiv \mathrm{Tr}[\widehat{\boldsymbol{z}}^{\mathrm{T}}_{\mathcal{F}}(t)\widetilde{\boldsymbol{z}}_{\mathcal{F}}(t')\widehat{\rho}^{(0)}_{\mathcal{E}}]$ is the generalized 2×2 memory kernel, that is the Wightman function of the free environment. Eq. (3.140) is expressed in terms of equal time operators, which renders the final transfer in the Schrödinger picture straightforward. We finally decompose the memory kernel in real and imaginary parts $\boldsymbol{\mathcal{D}}^{>}(t,t') \equiv \boldsymbol{\mathcal{D}}^{\mathrm{Re}}(t,t') + i\boldsymbol{\mathcal{D}}^{\mathrm{Im}}(t,t')$ and perform some simple manipulations in order to obtain

$$\begin{aligned}\frac{\mathrm{d}\widehat{\rho}_{\mathrm{red}}}{\mathrm{d}t} = &-i\left[\widehat{H}_{\mathcal{S}}(t) + \widehat{H}_{\mathrm{LS}}(t), \widehat{\rho}_{\mathrm{red}}(t)\right] \\ &+\boldsymbol{\gamma}_{ij}(t)\left(\widehat{\boldsymbol{z}}_{\zeta,i}\widehat{\rho}_{\mathrm{red}}(t)\widehat{\boldsymbol{z}}_{\zeta,j} - \frac{1}{2}\left\{\widehat{\boldsymbol{z}}_{\zeta,j}\widehat{\boldsymbol{z}}_{\zeta,i}, \widehat{\rho}_{\mathrm{red}}(t)\right\}\right).\end{aligned} \tag{3.142}$$

This form encompasses all Gaussian master equations where the system linearly couples to its environment. Let us now interpret the various terms appearing in this decomposition. The *Lamb-shift Hamiltonian* is a quadratic form $\widehat{H}_{\mathrm{LS}}(t) = \frac{1}{2}\widehat{\boldsymbol{z}}^{\mathrm{T}}_{\zeta}\boldsymbol{\Delta}(t)\widehat{\boldsymbol{z}}_\zeta$ where

$$\boldsymbol{\Delta}_{ij}(t) = 2\int_{t_0}^{t} \mathrm{d}t' \boldsymbol{\mathcal{D}}^{\mathrm{Im}}_{(ij)}(t,t') \tag{3.143}$$

and we used the symmetric and antisymmetric decomposition of 2×2 matrices

$$\boldsymbol{A}_{ij} = \boldsymbol{A}_{(ij)} + A_{-}\boldsymbol{\omega}_{ij} \quad \text{where} \quad \boldsymbol{\omega} = \begin{pmatrix} 0 & 1 \\ -1 & 0 \end{pmatrix} \tag{3.144}$$

and $\boldsymbol{A}_{(ji)} = \boldsymbol{A}_{(ij)}$. The *dissipator matrix* is the time-dependent 2×2 matrix

$$\boldsymbol{\gamma}_{ij}(t) \equiv \boldsymbol{D}_{ij}(t) - i\Delta_{-}(t)\boldsymbol{\omega}_{ij} \tag{3.145}$$

where the *noise* and *dissipation kernels* are respectively defined as

$$\boldsymbol{D}_{ij}(t) = 2\int_{t_0}^{t} \mathrm{d}t' \boldsymbol{\mathcal{D}}^{\mathrm{Re}}_{(ij)}(t,t') \tag{3.146}$$

$$\Delta_{-}(t) = 2\int_{t_0}^{t} \mathrm{d}t' \mathcal{D}^{\mathrm{Im}}_{-}(t,t'). \tag{3.147}$$

The first term in the right-hand side of Eq. (3.142) provides a unitary contribution, which renormalises the energy levels of the system due to the interactions with the environment [188, 253, 271]. This contribution, when expressed in terms of local operators, can be captured by a Wilsonian EFT and has a proper diagrammatic representation. The second and the third terms in Eq. (3.142) are of a different nature, since they capture the non-unitary evolution of the system and thus cannot be described by an effective Lagrangian. This is due to dissipation and decoherence, which are related respectively to the imaginary part $\Delta_{-}(t)$ and the real part $\boldsymbol{D}_{ij}(t)$ of the dissipator matrix $\boldsymbol{\gamma}_{ij}(t)$ in Eq. (3.142). The fact that the real and the imaginary part of the memory kernel lead to distinct physical effects has already been encountered in Sec. 3.2.3 when we discussed the influence-functional approach and the Langevin equation it generates. Importantly, when the environment obeys fluctuation-dissipation relations, the two quantities are related [255].

Phase-space representation of Gaussian master equations: In phase space, the TCL_2 master equation (3.142) takes the form of a Fokker-Planck equation for the reduced Wigner function W_{red}. Indeed, an alternative representation of the quantum state is given in the phase-space by the Wigner function (see [200] for a brief introduction). It provides a quantum analogue of a phase-space quasi probability distribution encoding the statistics of the quantum system. For Gaussian states, the Wigner function takes the simple form of a multivariate Gaussian [272], which makes it particularly convenient to work with. The Wigner function is defined as the inverse Wigner-Weyl transform of the density matrix given in Eq. (3.22). For a generic quantum operator $\widehat{O}$, the inverse Wigner-Weyl transform has a similar definition

$$W_{\widehat{O}}(\zeta, p_\zeta) \equiv 2\int_{-\infty}^{\infty} \mathrm{d}y e^{-2ip_\zeta y} \left\langle \zeta + y \right| \widehat{O} \left| \zeta - y \right\rangle \tag{3.148}$$

and is a function of the phase-space variables ζ and p_ζ. The above formula is written in the configuration representation, it can also be written in the momentum representation,

$$W_{\widehat{O}}(\zeta, p_\zeta) \equiv 2\int_{-\infty}^{\infty} \mathrm{d}k e^{2ik\zeta} \left\langle p_\zeta + k \right| \widehat{O} \left| p_\zeta - k \right\rangle . \tag{3.149}$$

In this way, commutators of quantum operators are mapped to the Poisson brackets of their phase-space representations. Indeed, using the above formu-

las, one finds

$$W_{[\widehat{\zeta},\widehat{O}]} = i\frac{\partial}{\partial p_\zeta} W_O \quad \text{and} \quad W_{[\widehat{p}_\zeta,\widehat{O}]} = -i\frac{\partial}{\partial \zeta} W_O \,, \tag{3.150}$$

$$W_{\{\widehat{\zeta},\widehat{O}\}} = 2\zeta W_O \quad \text{and} \quad W_{\{\widehat{p}_\zeta,\widehat{O}\}} = 2p_\zeta W_O \,. \tag{3.151}$$

This leads to

$$i\boldsymbol{\omega}_{ij} W_{[\widehat{\boldsymbol{z}}_{\zeta,j},\widehat{O}]} = \frac{\partial W_O}{\partial \boldsymbol{z}_{\zeta,i}} \,, \tag{3.152}$$

$$\frac{1}{2} W_{\{\widehat{\boldsymbol{z}}_{\zeta,i},\widehat{O}\}} = \boldsymbol{z}_{\zeta,i} W_O \,. \tag{3.153}$$

These relations can be used to compute the inverse Weyl transform of the TCL_2 master equation (3.142). Using that $\boldsymbol{\omega}$ is antisymmetric, one finds

$$\begin{aligned} \frac{\mathrm{d}W_{\mathrm{red}}}{\mathrm{d}t} &= \left\{ \widetilde{H}_{\mathcal{S}} + \widetilde{H}_{\mathrm{LS}}, W_{\mathrm{red}} \right\} \\ &\quad - \boldsymbol{\Delta}_- \sum_i \frac{\partial}{\partial \boldsymbol{z}_{\zeta,i}} \left(\boldsymbol{z}_{\zeta,i} W_{\mathrm{red}} \right) - \frac{1}{2} \sum_{i,j} \left[\boldsymbol{\omega} \boldsymbol{D} \boldsymbol{\omega} \right]_{ij} \frac{\partial^2 W_{\mathrm{red}}}{\partial \boldsymbol{z}_{\zeta,i} \partial \boldsymbol{z}_{\zeta,j}} \,, \end{aligned} \tag{3.154}$$

where $W_{\mathrm{red}} = W_{\widehat{\rho}_{\mathrm{red}}}$ is the reduced Wigner function, *i.e.* the inverse Wigner-Weyl transform of the reduced density matrix $\widehat{\rho}_{\mathrm{red}}$. The curly brackets now represent Poisson's brackets, not to be confused with the anticommutators for quantum operators. The first term in Eq. (3.154) corresponds to the free evolution dressed by the Lamb-shift Hamiltonian $\widetilde{H}_{\mathrm{LS}}$. This part of the equation only captures the unitary evolution. The second term proportional to $\boldsymbol{\Delta}_-$ is dissipative: it is a drift (or friction) term that accounts for the energy transfer from the system into the environment [177]. Finally, the last term proportional to $\boldsymbol{\omega}\boldsymbol{D}\boldsymbol{\omega}$ corresponds to diffusion and leads to decoherence. These last two terms can be combined into a single second-order differential operator involving the dissipator matrix $\boldsymbol{\gamma}_{ij}$ defined in Eq. (3.145), and they induce the non-unitary evolution. Finally, one can show that Eq. (3.154) admits Gaussian solutions, hence the reduced state of the system is still Gaussian.

3.3.2 On Markovianity

Among the concepts encountered in the OQS literature, Markovianity is certainly the one that has been the most passionately discussed during my Ph.D. While ubiquitous in quantum optics and condensed matter [188], its generalisation in curved spacetime is far from being obvious [154,268,270]. It is also fair to recognize that Markovianity might refer to different concepts as:

- A *Markovian master equation* is a master equation that fulfils the semi-group property;
- A *Markovian approximation* is an expansion that neglects variations of the environment in the derivation of a master equation;

- A *Markovian environment* is a bath that dissipates information fast compared to the dynamical evolution of the system.

Rather than providing a definitive answer on the status of Markovianity in Open EFTs, this Section delivers a partial vision which is likely to evolve and aims at illustrating how this concept has been used in the situations we encountered so far. We first present the bottom-up construction of Markovian master equations induced by Lindblad theorem. We then reconcile this result with the non-Markovian master equation we obtained in Eq. (3.142) by illustrating how the Markovian limit can be reached. We finally present a systematic approach to non-Markovian corrections and discuss tracers of non-Markovianity.

Lindblad theorem: The semi-group evolution (3.115) imposes strong constraints on the available physical dynamical maps, as first notice by Lindblad in his seminal paper [273].

A bottom-up construction of Markovian ME: Let us illustrate from [188, 253] the construction of the most general form for the generator of a quantum dynamical semi-group. For simplicity, let us consider a finite dimensional Hilbert space for the system $\mathcal{H}_{\mathcal{S}}$ of dimension N. The space of super-operators is then of dimension N^2, spanned by a complete basis of orthonormal operators F_i for $i = 1, 2, \cdots N^2$. The mapping of operators acting on the Hilbert space to super-operators acting on the doubled Hilbert space (the Fock-Liouville space) is known as the *Choi isomorphism* [274] which often appears in ThermoField Dynamics (TFD) [275, 276]. The orthonormality prescription is defined through the Hilbert-Schmidt product

$$(F_i, F_j) \equiv \mathrm{Tr}_{\mathcal{S}} \left\{ F_i^\dagger F_j \right\} = \delta_{ij}. \tag{3.155}$$

One can always choose one of the basis operators to be the identity, namely $F_{\mathbb{I}} = \mathbb{I}/\sqrt{N}$ such that the other basis operators are traceless.

Let us construct a dynamical map $\mathcal{V}(t)$ out of these operators, such that

$$\widehat{\rho}_{\mathcal{S}}^{(0)} \mapsto \widehat{\rho}_{\rm red}(t) = \mathcal{V}(t)\widehat{\rho}_{\mathcal{S}}^{(0)} \equiv \mathrm{Tr}_{\mathcal{E}} \left\{ \widehat{\mathcal{U}}(t) \left[\widehat{\rho}_{\mathcal{S}}^{(0)} \otimes \widehat{\rho}_{\mathcal{E}}^{(0)} \right] \widehat{\mathcal{U}}^\dagger(t) \right\} \tag{3.156}$$

which follows from tracing out the environmental degrees of freedom in Eq. (3.55), that is

$$\begin{array}{ccc} \widehat{\rho}_{\mathcal{S}}^{(0)} \otimes \widehat{\rho}_{\mathcal{E}}^{(0)} & \xrightarrow{\text{unit. evol.}} & \widehat{\mathcal{U}}(t) \left[\widehat{\rho}_{\mathcal{S}}^{(0)} \otimes \widehat{\rho}_{\mathcal{E}}^{(0)} \right] \widehat{\mathcal{U}}^\dagger(t) \\ \Big\downarrow \mathrm{Tr}_{\mathcal{E}} & & \Big\downarrow \mathrm{Tr}_{\mathcal{E}} \\ \widehat{\rho}_{\mathcal{S}}^{(0)} & \xrightarrow{\text{dyn. map}} & \widehat{\rho}_{\rm red}(t) = \mathcal{V}(t)\widehat{\rho}_{\mathcal{S}}^{(0)}. \end{array}$$

$\mathcal{V}(t)$ defines a map from the space $\mathcal{S}(\mathcal{H}_{\mathcal{S}})$ of reduced density matrices into itself

$$\mathcal{V}(t) : \mathcal{S}(\mathcal{H}_{\mathcal{S}}) \to \mathcal{S}(\mathcal{H}_{\mathcal{S}}). \tag{3.157}$$

Such a dynamical map can be characterised entirely in terms of operators pertaining to the open system's Hilbert space $\mathcal{H}_\mathcal{S}$. Indeed, let us use the spectral decomposition for the density matrix of the environment

$$\widehat{\rho}_\mathcal{E}^{(0)} = \sum_\alpha \lambda_\alpha \left|\varphi_\alpha\right\rangle \left\langle\varphi_\alpha\right| \tag{3.158}$$

where the $|\varphi_\alpha\rangle$ form an orthonormal basis of the Hilbert space of the environment $\mathcal{H}_\mathcal{E}$. It immediately follows from Eq. (3.156) that

$$\mathcal{V}(t)\widehat{\rho}_\mathcal{S}^{(0)} = \sum_{\alpha\beta} W_{\alpha\beta}(t)\widehat{\rho}_\mathcal{S}^{(0)} W_{\alpha\beta}^\dagger(t) \tag{3.159}$$

where the $W_{\alpha\beta}$ are operators acting on $\mathcal{H}_\mathcal{S}$ defined as

$$W_{\alpha\beta}(t) = \sqrt{\lambda_\beta}\left\langle\varphi_\alpha\right|\widehat{\mathcal{U}}(t)\left|\varphi_\beta\right\rangle \tag{3.160}$$

This is the necessary statement made by *Choi's Theorem* which further demonstrates its sufficiency [253].

Theorem 1: *Choi's Theorem.*
A linear map of the form Eq. (3.157) is completely positive iff it can be expressed as

$$\mathcal{V}(t)\widehat{\rho}_\mathcal{S}^{(0)} = \sum_{\alpha\beta} W_{\alpha\beta}(t)\widehat{\rho}_\mathcal{S}^{(0)} W_{\alpha\beta}^\dagger(t) \tag{3.161}$$

with $W_{\alpha\beta} \in \mathcal{S}(\mathcal{H}_\mathcal{S})$.

A dynamical map of this form is the one of a generalized quantum measurement [188]. If we further require the dynamical map to be trace preserving, $\mathrm{Tr}_\mathcal{S}\left[\mathcal{V}(t)\widehat{\rho}_\mathcal{S}^{(0)}\right] = \mathrm{Tr}_\mathcal{S}\widehat{\rho}_\mathcal{S}^{(0)} = 1$, the cyclicity of the trace imposes

$$\sum_{\alpha\beta} W_{\alpha\beta}^\dagger(t) W_{\alpha\beta}(t) = \mathbb{I}. \tag{3.162}$$

Hence, CPTP dynamical maps obey *Choi-Kraus' Theorem* (again, see [253] for the demonstration of the sufficiency).

Theorem 2: *Choi-Kraus' Theorem.*
A linear map of the form Eq. (3.157) is CPTP iff it can be expressed as

$$\mathcal{V}(t)\widehat{\rho}_\mathcal{S}^{(0)} = \sum_{\alpha\beta} W_{\alpha\beta}(t)\widehat{\rho}_\mathcal{S}^{(0)} W_{\alpha\beta}^\dagger(t) \tag{3.163}$$

with $W_{\alpha\beta} \in \mathcal{S}(\mathcal{H}_\mathcal{S})$ *fulfilling*

$$\sum_{\alpha\beta} W_{\alpha\beta}^\dagger(t) W_{\alpha\beta}(t) = \mathbb{I}. \tag{3.164}$$

.

This theorem first imposes some structure on the available shapes for a physical dynamical map. When the microphysical theory is known, $W_{\alpha\beta}$ are determined by Eq. (3.160). We now seek to constrain these objects when the microphysics is unknown.

We now consider how the semi-group evolution combined with Choi-Kraus' Theorem imposes structure on $\mathcal{V}(t)$. First, we decompose the $W_{\alpha\beta}$ in the F_i basis, that is

$$W_{\alpha\beta}(t) = \sum_{i=1}^{N^2} (F_i, W_{\alpha\beta}(t))\, F_i \tag{3.165}$$

where we used the scalar product defined in Eq. (3.155). It follows that the dynamical map writes

$$\mathcal{V}(t)\widehat{\rho}_{\mathcal{S}}^{(0)} = \sum_{i,j=1}^{N^2} c_{ij}(t) F_i \widehat{\rho}_{\mathcal{S}}^{(0)} F_j^\dagger \tag{3.166}$$

with

$$c_{ij}(t) \equiv \sum_{\alpha\beta} (F_i, W_{\alpha\beta}(t))\, (F_j, W_{\alpha\beta}(t))^* \,. \tag{3.167}$$

The scalar product structure ensures that the matrix c_{ij} is Hermitian and positive [188]. The crucial point is that the semi-group property

$$\mathcal{V}(t_1)\mathcal{V}(t_2) = \mathcal{V}(t_1 + t_2) \tag{3.168}$$

implies the existence of a dynamical generator $\mathcal{L}_{\mathcal{S}}$ such that

$$\mathcal{V}(t) = \exp\left(\mathcal{L}_{\mathcal{S}}\, t\right) \tag{3.169}$$

and the reduced density matrix obeys a first-order differential equation of the form

$$\frac{\mathrm{d}\widehat{\rho}_{\mathrm{red}}}{\mathrm{d}t} = \mathcal{L}_{\mathcal{S}}\widehat{\rho}_{\mathrm{red}}(t). \tag{3.170}$$

We can then construct the dynamical generator $\mathcal{L}_{\mathcal{S}}$ by differentiating the dynamical map obtained in Eq. (3.166), that is

$$\mathcal{L}_{\mathcal{S}}\widehat{\rho}_{\mathcal{S}}^{(0)} = \lim_{\varepsilon\to 0} \frac{1}{\varepsilon}\left[\mathcal{V}(\varepsilon)\widehat{\rho}_{\mathcal{S}}^{(0)} - \widehat{\rho}_{\mathcal{S}}^{(0)}\right] \tag{3.171}$$

$$= \frac{a_{N^2N^2}}{N}\widehat{\rho}_{\mathcal{S}}^{(0)} + \frac{1}{\sqrt{N}}\sum_{i=1}^{N^2-1}\left[a_{iN^2}F_i\widehat{\rho}_{\mathcal{S}}^{(0)} + a_{iN^2}^*\widehat{\rho}_{\mathcal{S}}^{(0)}F_i^\dagger\right] + \sum_{i,j=1}^{N^2-1} a_{ij}F_i\widehat{\rho}_{\mathcal{S}}^{(0)}F_j^\dagger$$

where we defined

$$a_{N^2N^2} = \lim_{\varepsilon\to 0}\frac{c_{N^2N^2}(\varepsilon) - N}{\varepsilon} \tag{3.172}$$

$$a_{iN^2} = \lim_{\varepsilon\to 0}\frac{c_{iN^2}(\varepsilon)}{\varepsilon} \tag{3.173}$$

$$a_{ij} = \lim_{\varepsilon\to 0}\frac{c_{ij}(\varepsilon)}{\varepsilon} \tag{3.174}$$

for $i, j = 1, \cdots, N^2 - 1$. Upon defining the operators

$$F = \frac{1}{\sqrt{N}} \sum_{i=1}^{N^2-1} a_{iN^2} F_i \tag{3.175}$$

and

$$G = \frac{\mathbb{I}}{2N} a_{N^2 N^2} + \frac{1}{2} \left(F^\dagger + F \right), \tag{3.176}$$

we rewrite

$$\mathcal{L}_{\mathcal{S}} \widehat{\rho}_{\mathcal{S}}^{(0)} = -i \left[H, \widehat{\rho}_{\mathcal{S}}^{(0)} \right] + \left\{ G, \widehat{\rho}_{\mathcal{S}}^{(0)} \right\} + \sum_{i,j=1}^{N^2-1} a_{ij} F_i \widehat{\rho}_{\mathcal{S}}^{(0)} F_j^\dagger \tag{3.177}$$

where

$$H = \frac{1}{2i} \left(F^\dagger - F \right) \tag{3.178}$$

is a Hermitian operator. Since the semi-group is trace preserving, we must have $\mathrm{Tr}_{\mathcal{S}}[\mathcal{L}_{\mathcal{S}} \widehat{\rho}_{\mathcal{S}}^{(0)}] = 0$, which imposes

$$G = -\frac{1}{2} \sum_{i,j=1}^{N^2-1} a_{ij} F_j^\dagger F_i \tag{3.179}$$

where we again used the cyclicity of the trace. We conclude from the semi-group property that the dynamical generator acts on the reduced density matrix at time t in the same way it acts on $\widehat{\rho}_{\mathcal{S}}^{(0)}$, such that the RHS of Eq. (3.170) writes

$$\mathcal{L}_{\mathcal{S}} \widehat{\rho}_{\mathrm{red}}(t) = -i \left[H, \widehat{\rho}_{\mathrm{red}}(t) \right] + \sum_{i,j=1}^{N^2-1} a_{ij} \left(F_i \widehat{\rho}_{\mathrm{red}}(t) F_j^\dagger - \frac{1}{2} \left\{ F_j^\dagger F_i, \widehat{\rho}_{\mathrm{red}}(t) \right\} \right). \tag{3.180}$$

The matrix formed by the coefficients a_{ij} is Hermitian and positive, a property inherited from the structure of c_{ij}. It can then be diagonalized with the help of an appropriate unitary transformation u,

$$uau^\dagger = \mathrm{diag} \left(\gamma_1^{(M)}, \gamma_2^{(M)}, \cdots, \gamma_{N^2-1}^{(M)} \right) \tag{3.181}$$

where the eigenvalues $\gamma_i^{(M)}$ are non-negative. Introducing a new set of operators L_k through

$$F_i = \sum_{k=1}^{N^2-1} u_{ki} L_k, \tag{3.182}$$

we obtain the diagonal form of the generator

$$\mathcal{L}_{\mathcal{S}}\widehat{\rho}_{\rm red}(t) = -i\left[H, \widehat{\rho}_{\rm red}(t)\right] + \sum_{k=1}^{N^2-1} \gamma_k^{(M)} \left(L_k \widehat{\rho}_{\rm red}(t) L_k^\dagger - \frac{1}{2}\left\{ L_k^\dagger L_k, \widehat{\rho}_{\rm red}(t) \right\} \right). \tag{3.183}$$

This equation, known as the Gorini-Kossakowski-Sudarshan-Lindblad (GKSL) or Lindblad equation, is the most general form for the generator of a quantum dynamical semi-group. We can easily recognise the first term as the unitary evolution generated by the free and Lamb-shift Hamiltonians. The L_k operators are the so-called jump or Lindblad operators. When the L_k are chosen dimensionless, the $\gamma_k^{(M)}$ have dimension of the inverse of a time. When a connection with a microphysical derivation is possible, we observe that these rates relate to correlation functions of the environment that are specified by the memory kernel and play the role of relaxation rates for the different decay modes of the open system [188].

To put it in a nutshell, Lindblad theorem implies that [273]

Lindblad theorem [273]:

Semi-group evolution ⇒ Semi-positive definiteness of the dissipator.

It follows that a Markovian master equation can always be written in the form

$$\begin{aligned} \frac{\mathrm{d}\widehat{\rho}_{\rm red}}{\mathrm{d}t} &= -i\left[\widehat{H}_{\mathcal{S}}(t) + \widehat{H}_{\rm LS}(t), \widehat{\rho}_{\rm red}(t)\right] \\ &+ \sum_{ij} \boldsymbol{a}_{ij}(t) \left(\widehat{\boldsymbol{F}}_i \widehat{\rho}_{\rm red}(t) \widehat{\boldsymbol{F}}_j^\dagger - \frac{1}{2}\left\{ \widehat{\boldsymbol{F}}_j^\dagger \widehat{\boldsymbol{F}}_i, \widehat{\rho}_{\rm red}(t) \right\} \right). \end{aligned} \tag{3.184}$$

for some operators $\widehat{\boldsymbol{F}}_i$ acting on $\mathcal{H}_{\mathcal{S}}$ where the dissipator $\boldsymbol{a}_{ij}$ is now a positive semi-definite matrix. This entails the fact that it can be diagonalised by a unitary transformation (due to the hermiticity implied by the positive semi-definiteness), and in this basis Eq. (3.184) becomes

$$\begin{aligned} \frac{\mathrm{d}\widehat{\rho}_{\rm red}}{\mathrm{d}t} &= -i\left[\widehat{H}_{\mathcal{S}}(t) + \widehat{H}_{\rm LS}(t), \widehat{\rho}_{\rm red}(t)\right] \\ &+ \sum_{k} \gamma_k^{(\mathrm{M})} \left(\widehat{\boldsymbol{L}}_k \widehat{\rho}_{\rm red}(t) \widehat{\boldsymbol{L}}_k^\dagger - \frac{1}{2}\left\{ \widehat{\boldsymbol{L}}_k^\dagger \widehat{\boldsymbol{L}}_k, \widehat{\rho}_{\rm red}(t) \right\} \right) \end{aligned} \tag{3.185}$$

where $\widehat{\boldsymbol{L}}_k$ are the so-called *jump operators* and $\gamma_k^{(\mathrm{M})}$ are the *positive eigenvalues* of the dissipator matrix (be careful not to confuse them with the eigenvalues λ_i of the Liouvillian $\mathcal{L}$ which capture physical information about the decay rates [248]). This equation is called a GKSL or Lindblad equation and is the most generic form of a Markovian dynamical equation that preserves trace, Hermiticity and positivity of the density matrix [273]. Lindblad equation plays a key role when studying environmental effects in OQS. However, it physically relies on strong hypotheses which may or may not be always satisfied.

Markovian limit: How do we reconcile this bottom-up constructions of dynamical maps obeying a semi-group evolution to the microphysical construction that lead us to the TCL_2 master equation obtained in Eq. (3.142)? We remind that we only made use of the Born approximation to derive Eq. (3.142), that is the smallness of the coupling between the system and the environment. We already mentioned that despite being written in a time-local form, the TCL_2 master equation does not provide a generator for a Markovian dynamical map, that is a generator for a dynamical map obeying the semi-group property (3.115). We now aim at illustrating when this limit arises before discussing in details systematic inclusion of the non-Markovian corrections.

Typical environments encountered in quantum optics and condensed matter contain a large number of degrees of freedom, hence they behave as *reservoirs* in which correlation functions quickly decay with $|t-t'|$ [188]. More precisely, if the relaxation time of the environment $\tau_{\mathcal{E}}$ is small compared to the typical time over which the system evolves $\tau_{\mathcal{S}}$, one may coarse-grain the evolution of the system on scales larger than the environment relaxation time $\tau_{\mathcal{S}} \gg \tau_{\mathcal{E}}$. From the coarsed-grained perspective, the memory kernel $\boldsymbol{\mathcal{K}}^{>}(t,t')$ is then sharply peaked and falls off to zero in timescales much shorter than the time it needs for the Green's matrix of the system $\boldsymbol{G}^{(\mathcal{S})}(t',t)$ to significantly evolve. In this limit, one can always approximate $\boldsymbol{G}^{(\mathcal{S})}(t',t) \to \boldsymbol{G}^{(\mathcal{S})}(t,t) = \mathbb{I}$ when convolved with the memory kernel $\boldsymbol{\mathcal{K}}^{>}(t,t')$, the equal-time limit of the Green's matrix of the system being constrained to be the identity by Eq. (3.139). This manipulation has drastic consequences which are often summarized by saying that the past history ($t' < t$) of the system is not anymore involved in the dynamics, which therefore becomes Markovian.

Let us show how it arises in the simplest case where the system and its environment couple through

$$\widehat{H}_{\mathrm{int}} = \widehat{\zeta} \otimes \widehat{\mathcal{F}} \qquad \text{that is} \qquad \boldsymbol{V}(t) = \begin{pmatrix} 1 & 0 \\ 0 & 0 \end{pmatrix}. \tag{3.186}$$

In this case, the Lamb-shift Hamiltonian in Eq. (3.142) takes the form

$$\widehat{H}_{\mathrm{LS}}(t) = \frac{1}{2}\left[\boldsymbol{\Delta}_{11}(t)\widehat{\zeta}^2 + \boldsymbol{\Delta}_{12}(t)\{\widehat{\zeta},\widehat{p}_\zeta\}\right] \tag{3.187}$$

and the dissipator matrix defined in Eq. (3.145) writes

$$\boldsymbol{\gamma}_{ij}(t) = \begin{pmatrix} \boldsymbol{D}_{11}(t) & \boldsymbol{D}_{12}(t) - i\boldsymbol{\Delta}_{12}(t) \\ \boldsymbol{D}_{12}(t) + i\boldsymbol{\Delta}_{12}(t) & 0 \end{pmatrix}. \tag{3.188}$$

The four real master equation coefficients are defined through two complex quantities

$$\boldsymbol{D}_{11}(t) + i\boldsymbol{\Delta}_{11}(t) = 2g^2 \int_{t_0}^{t} \mathrm{d}t' \mathcal{K}^{>}(t,t') \boldsymbol{G}^{(\mathcal{S})}_{11}(t',t) \tag{3.189}$$

$$\boldsymbol{D}_{12}(t) + i\boldsymbol{\Delta}_{12}(t) = g^2 \int_{t_0}^{t} \mathrm{d}t' \mathcal{K}^{>}(t,t') \boldsymbol{G}^{(\mathcal{S})}_{12}(t',t), \tag{3.190}$$

where here again, we recognize the fact that the dissipation coefficients $\boldsymbol{D}$ are related to the real part of the memory kernel via

$$\mathcal{K}^{>}(t,t') \equiv \mathrm{Tr}_{\mathcal{E}}\left[\widehat{\mathcal{F}}(t)\widehat{\mathcal{F}}(t')\widehat{\rho}^{(0)}_{\mathcal{E}}\right] = \left\langle \widehat{\mathcal{F}}(t)\widehat{\mathcal{F}}(t')\right\rangle_0, \tag{3.191}$$

while the fluctuation coefficients $\boldsymbol{\Delta}$ are related to the imaginary part. We remind that the quantities $\boldsymbol{G}_{11}^{(\mathcal{S})}(t',t)$ and $\boldsymbol{G}_{12}^{(\mathcal{S})}(t',t)$ are respectively the first and second entries of the Green's matrix of the system which are real quantities.[10] The eigenvalues of the dissipator are

$$\gamma_{\pm}(t) = \frac{\boldsymbol{D}_{11}(t)}{2}\left[1 \pm \sqrt{1 + \frac{4\left[\boldsymbol{D}_{12}^2(t) + \boldsymbol{\Delta}_{12}^2(t)\right]}{\boldsymbol{D}_{11}^2(t)}}\right] \tag{3.194}$$

where it clearly appears that $\gamma_{-}(t) \leq 0$. It implies that under its current form, the TCL_2 master equation (3.142) violates Lindblad theorem, as expected from its ability to describe non-Markovian dynamics. Indeed, let us stress the fact that non-Markovian dissipators contain negative eigenvalues which do not necessarily compromise the physicality of the dynamical map (see [260, 277, 278] for a discussion of CPTP non-Markovian master equations). If the dynamical map generated by Eq. (3.142) were Markovian, then according to Lindblad theorem [273] a negative eigenvalue would imply a CPTP violation. However, Eq. (3.142) belongs to the class of so-called "Gaussian master equations", which were shown to be CPTP in [258–260]. The contrapositive of Lindblad's theorem imposes the TCL_2 master equation to be non-Markovian. In this sense, negative eigenvalues are ubiquitous in non-Markovian OQS. They encode the reversibility of the dynamics through memory effects [279] and vanish in the Markovian limit where the dynamics become irreversible, as we show below. In this sense, they are tracers of information backflow and do not jeopardise the dynamics of the system if non-Markovian effects are carefully accounted for [277]. They only become an issue when they subsist despite the Markovian limit being taken, as they capture an inconsistency in the way the coarse-graining procedure has been performed and so the CPTP violation expected from Lindblad theorem [273].

When the Green's matrix elements $\boldsymbol{G}_{11}^{(\mathcal{S})}(t',t)$ and $\boldsymbol{G}_{12}^{(\mathcal{S})}(t',t)$ vary slowly compared to $\mathcal{K}^{>}(t,t')$, we can pull them out of the integrals defined in Eqs. (3.189) and (3.190). In this limit

$$\boldsymbol{D}_{11}^{(0)}(t) + i\boldsymbol{\Delta}_{11}^{(0)}(t) = \left[2g^2\int_{t_0}^{t}\mathrm{d}t'\mathcal{K}^{>}(t,t')\right]\boldsymbol{G}_{11}^{(\mathcal{S})}(t,t) \tag{3.195}$$

$$= 2g^2\int_{t_0}^{t}\mathrm{d}t'\mathcal{K}^{>}(t,t') \tag{3.196}$$

$$\boldsymbol{D}_{12}^{(0)}(t) + i\boldsymbol{\Delta}_{12}^{(0)}(t) = \left[g^2\int_{t_0}^{t}\mathrm{d}t'\mathcal{K}^{>}(t,t')\right]\boldsymbol{G}_{12}^{(\mathcal{S})}(t,t) \tag{3.197}$$

$$= 0, \tag{3.198}$$

where we used the coincident limit of the system Green's matrix. We obtain the Markovian master equation (see Eq. (3.30) of [244] for the rewriting of the master

[10] For concreteness, when the mode functions of the system are known, we have [244]

$$\boldsymbol{G}_{11}^{(\mathcal{S})}(t',t) = -2\Im\mathrm{m}\left[p_{\zeta}(t)v_{\zeta}^{*}(t')\right] \tag{3.192}$$

$$\boldsymbol{G}_{12}^{(\mathcal{S})}(t',t) = 2\Im\mathrm{m}\left[v_{\zeta}(t)v_{\zeta}^{*}(t')\right] \tag{3.193}$$

equation in this form)

$$\frac{\mathrm{d}\widehat{\rho}_{\rm red}}{\mathrm{d}t} = -i\left[\widehat{H}_{\mathcal{S}}(t) + \frac{\boldsymbol{\Delta}_{11}^{(0)}(t)}{2}\widehat{\zeta}^2, \widehat{\rho}_{\rm red}(t)\right] - \frac{\boldsymbol{D}_{11}^{(0)}(t)}{2}\left[\widehat{\zeta}, \left[\widehat{\zeta}, \widehat{\rho}_{\rm red}(t)\right]\right], \tag{3.199}$$

only the positive value of the dissipator remains $\gamma_+^{(0)}(t) = \boldsymbol{D}_{11}^{(0)}(t)$ while the negative eigenvalue vanishes in this limit $\gamma_-^{(0)}(t) = 0$. Under this form, Eq. (3.199) do not exhibit anymore signs of apparent non-Markovianity such as negative eigenvalue and might be a good candidate for a time-dependent Lindblad equation obeying a semi-group evolution. Note that sometimes, other layers of approximation such as the rotating-wave approximation must be performed in order to reach the Markovian limit [188]. Since the evolution of the system is coarse-grained over time scales larger than those describing the dynamics of the environment, this approximation consists in removing the quickly oscillating terms appearing in the master equation, for consistency. The implementation of this approach is however challenging in cosmology, where the dynamical background prevents the existence of a natural frequency basis [268].

Non-Markovian corrections: In general, non-Markovian corrections are suppressed when the memory kernel is sharply peaked, which depends on the scrambling properties of the environment. If the environment dissipates information in a timescale $\tau_{\mathcal{E}}$ much smaller than the typical system evolution $\tau_{\mathcal{S}}$, then it is not able to keep track of the past interactions with the system and the non-Markovian effects are suppressed in powers of $\tau_{\mathcal{E}}/\tau_{\mathcal{S}}$ [188]. In this case, the environment looks the same every-time the system interacts with it, which explains why the semi-group property (3.115) holds. Our goal is now to make transparent the systematic inclusion of non-Markovian corrections. In particular, it will allow us to assess the regime of validity of the Markovian approximation derived in Eq. (3.199).

Starting from Eq. (3.189) and (3.190), we Taylor expand the coefficients

$$\boldsymbol{D}_{11}(t) + i\boldsymbol{\Delta}_{11}(t) = 2g^2\int_{t_0}^{t}\mathrm{d}t'\mathcal{K}^{>}(t,t')\sum_{s=0}^{\infty}\frac{(t'-t)^s}{s!}\,\partial_{t'}^{(s)}\boldsymbol{G}_{11}^{(\mathcal{S})}(t',t)\Big|_{t'\to t} \tag{3.200}$$

$$\boldsymbol{D}_{12}(t) + i\boldsymbol{\Delta}_{12}(t) = g^2\int_{t_0}^{t}\mathrm{d}t'\mathcal{K}^{>}(t,t')\sum_{s=0}^{\infty}\frac{(t'-t)^s}{s!}\,\partial_{t'}^{(s)}\boldsymbol{G}_{11}^{(\mathcal{S})}(t',t)\Big|_{t'\to t}. \tag{3.201}$$

If we consider that the system mode functions are known and obey a classical equation of motion of the form

$$\frac{\mathrm{d}^2 v_\zeta}{\mathrm{d}t^2} + \omega^2(t)v_\zeta = 0 \tag{3.202}$$

and $p_\zeta = \partial_t v_\zeta$ for a time dependent frequency $\omega^2(t)$,[11] then the Green's matrix entries are specified by Eqs. (3.192) and (3.193) and it follows that

$$\partial_{t'}^{(2s)}\boldsymbol{G}_{11}^{(\mathcal{S})}(t',t)\Big|_{t'\to t} = -i(-1)^s\omega^{2s}(t) \tag{3.203}$$

$$\partial_{t'}^{(2s+1)}\boldsymbol{G}_{12}^{(\mathcal{S})}(t',t)\Big|_{t'\to t} = -i(-1)^s\omega^{2s+1}(t) \tag{3.204}$$

[11] Following [121], one can always recast the single-field dynamics under this form called the *invariant representation*.

and $\partial_{t'}^{(2s+1)}\mathcal{G}^{\mathcal{S}}_{11,\boldsymbol{k}}(t',t)\Big|_{t'\to t} = \partial_{t'}^{(2s)}\mathcal{G}^{\mathcal{S}}_{12,\boldsymbol{k}}(t',t)\Big|_{t'\to t} = 0$ for all s. The non Markovian coefficients are organised in powers of $(t'-t)^s$ and reads

$$\boldsymbol{D}_{11}^{(2s)}(t) + i\boldsymbol{\Delta}_{11}^{(2s)}(t) \equiv (-1)^s 2g^2 \int_{t_0}^{t} \mathrm{d}t' \mathcal{K}^{>}(t,t') \frac{(t'-t)^{2s}}{(2s)!} \omega^{2s}(t) \tag{3.205}$$

$$\boldsymbol{D}_{12}^{(2s+1)}(t) + i\boldsymbol{\Delta}_{12}^{(2s+1)}(t) \equiv (-1)^s \frac{g^2}{\omega(t)} \int_{t_0}^{t} \mathrm{d}t' \mathcal{K}^{>}(t,t') \frac{(t'-t)^{2s+1}}{(2s+1)!} \omega^{2s+1}(t). \tag{3.206}$$

By injecting the expressions obtained in Eqs. (3.205) and (3.206) computed at a given order in $(t'-t)$ into Eqs. (3.187) and (3.188), we obtain a systematic non-Markovian expansions of the master equation coefficients.

This expansion has been proposed in [228] as a way to control the regime of validity of the Markovian limit (3.199). Indeed, at lowest order $s=0$, we recover Eq. (3.199) as already shown. The first order non-Markovian correction obtained for $s=1$ reads

$$\begin{aligned}\frac{\mathrm{d}\widehat{\rho}_{\mathrm{red}}^{(1)}}{\mathrm{d}t} = \frac{\mathrm{d}\widehat{\rho}_{\mathrm{red}}^{(0)}}{\mathrm{d}t} - i\left[\frac{1}{2}\boldsymbol{\Delta}_{12}^{(1)}(t)\{\widehat{\zeta},\widehat{p}_\zeta\},\widehat{\rho}_{\mathrm{red}}(t)\right] \\ -\frac{1}{2}\left(\boldsymbol{D}_{12}^{(1)}(t)\left[\widehat{\zeta},[\widehat{p}_\zeta,\widehat{\rho}_{\mathrm{red}}(t)]\right] + \boldsymbol{D}_{12}^{(1)}(t)\left[\widehat{p}_\zeta,\left[\widehat{\zeta},\widehat{\rho}_{\mathrm{red}}(t)\right]\right]\right) \\ -\frac{i}{2}\left(\boldsymbol{\Delta}_{12}^{(1)}(t)\left[\widehat{\zeta},\{\widehat{p}_\zeta,\widehat{\rho}_{\mathrm{red}}(t)\}\right] - \boldsymbol{\Delta}_{12}^{(1)}(t)\left[\widehat{p}_\zeta,\left\{\widehat{\zeta},\widehat{\rho}_{\mathrm{red}}(t)\right\}\right]\right)\end{aligned} \tag{3.207}$$

where we labelled the master equations in terms of the order of $(t-t')^s$ considered, $\mathrm{d}\widehat{\rho}_{\mathrm{red}}^{(0)}/\mathrm{d}t$ corresponding to the Markovian limit (3.199). In [228], the authors proposed to control the validity of the Markovian limit by schematically checking that

$$\left|\frac{\mathrm{d}\widehat{\rho}_{\mathrm{red}}^{(n)}}{\mathrm{d}t}\right| \ll \left|\frac{\mathrm{d}\widehat{\rho}_{\mathrm{red}}^{(n-1)}}{\mathrm{d}t}\right|. \tag{3.208}$$

for all integers n. In practice, at lowest order, it amounts to control that

$$\boldsymbol{D}_{12}^{(1)}(t) + i\boldsymbol{\Delta}_{12}^{(1)}(t) \ll \boldsymbol{D}_{11}^{(0)}(t) + i\boldsymbol{\Delta}_{11}^{(0)}(t) \tag{3.209}$$

in the regime of interest. Let us also mention that it is probably worth checking the validity of the Markovian hierarchy at second order by explicitly controlling that

$$\boldsymbol{D}_{11}^{(2)}(t) + i\boldsymbol{\Delta}_{11}^{(2)}(t) \ll \boldsymbol{D}_{11}^{(0)}(t) + i\boldsymbol{\Delta}_{11}^{(0)}(t) \tag{3.210}$$

as in the context of time-dependent frequencies, it is easy to find settings in which $\boldsymbol{D}_{12}^{(1)}(t) + i\boldsymbol{\Delta}_{12}^{(1)}(t) \ll \boldsymbol{D}_{11}^{(0)}(t) + i\boldsymbol{\Delta}_{11}^{(0)}(t)$ but $\boldsymbol{D}_{11}^{(2)}(t) + i\boldsymbol{\Delta}_{11}^{(2)}(t) \sim \boldsymbol{D}_{11}^{(0)}(t) + i\boldsymbol{\Delta}_{11}^{(0)}(t)$.[12] Once the Markovian hierarchy is established, one can in principle reach a desired precision by including higher and higher order non-Markovian corrections to the Markovian limit of Eq. (3.199). Note that in practice, this program has not yet

[12] Indeed, in the context of cosmology, t is replaced by the conformal time $\eta \propto a^{-1}$ during inflation. It follows that

$$\boldsymbol{D}_{12}^{(1)}(\eta) + i\boldsymbol{\Delta}_{12}^{(1)}(\eta) = -g^2 \int_{\eta_0}^{\eta} \mathrm{d}\eta' \mathcal{K}^{>}(\eta,\eta')\,(\eta'-\eta) \tag{3.211}$$

been established in cosmology and it is still an open question to understand how to properly reach the Markovian limit and how to make sense of the non-Markovian corrections [154, 228, 244, 268].

Finally, let us inject the non-Markovian expansion in the expression of dissipator eigenvalue given in Eq. (3.194) and compare the Markovian (3.199) and first non-Markovian correction (3.207) to the full TCL_2 result (3.142). In the Markovian limit, we already obtained $\gamma_-^{(0)}(t) = 0$ and $\gamma_+^{(0)}(t) = \boldsymbol{D}_{11}^{(0)}(t)$, hence the dissipator turns out to be positive semi-definite. If we assume that the Markovian hierarchy (3.209) holds, it follows that

$$\gamma_-^{(1)}(t) \simeq -\frac{\left[\boldsymbol{D}_{12}^{(1)}(t)\right]^2 + \left[\boldsymbol{\Delta}_{12}^{(1)}(t)\right]^2}{\boldsymbol{D}_{11}^{(0)}(t)} < 0 \tag{3.214}$$

$$\gamma_+^{(1)}(t) \simeq \boldsymbol{D}_{11}^{(0)}(t) + \frac{\left[\boldsymbol{D}_{12}^{(1)}(t)\right]^2 + \left[\boldsymbol{\Delta}_{12}^{(1)}(t)\right]^2}{\boldsymbol{D}_{11}^{(0)}(t)} > 0. \tag{3.215}$$

Hence, the inclusion of non-Markovian corrections gradually makes emerge a negative eigenvalue capturing the essence of the non-Markovian dynamics. The inclusion of the full tower of non-Markovian corrections should finally add up to generate Eq. (3.194).

3.3.3 Connecting with observables

Once a master equation is established, we can use this dynamical equation for the quantum state of the system to derive dynamical equations for the observables of interest, also known as *transport equations* [280–284]. In practice, in order to access this quantity, we start from the expression of the correlator in the Schrödinger picture[13]

$$\left\langle \widehat{O}(t) \right\rangle = \mathrm{Tr}_{\mathcal{S}} \left[\widehat{O} \widehat{\rho}_{\mathrm{red}}(t) \right] \tag{3.217}$$

which we differentiate with respect to time to obtain

$$\frac{\mathrm{d}}{\mathrm{d}t} \left\langle \widehat{O}(t) \right\rangle = \mathrm{Tr}_{\mathcal{S}} \left\{ \widehat{O} \mathcal{L}_{\mathcal{S}} \left[\widehat{\rho}_{\mathrm{red}}(t) \right] \right\}. \tag{3.218}$$

is a priori a^{-1} suppressed with respect to

$$\boldsymbol{D}_{11}^{(0)}(\eta) + i\boldsymbol{\Delta}_{11}^{(0)}(\eta) = 2g^2 \int_{\eta_0}^{\eta} \mathrm{d}\eta' \mathcal{K}^{>}(\eta, \eta') \tag{3.212}$$

while

$$\boldsymbol{D}_{11}^{(2)}(\eta) + i\boldsymbol{\Delta}_{11}^{(2)}(\eta) = g^2 \omega^2(\eta) \int_{\eta_0}^{\eta} \mathrm{d}\eta' \mathcal{K}^{>}(\eta, \eta') \left(\eta' - \eta\right)^2 \tag{3.213}$$

is not from the fact that $\omega^2(\eta) \propto a^2$ in general.

[13] Formally, this procedure is known as the determination of the *adjoint master equation* characterised by the *adjoint generator* $\mathcal{L}_{\mathcal{S}}^{\dagger}$, such as if the quantum state evolves according to Eq. (3.50), then the expectation value of a given operator $\widehat{O}(t)$ evolves in the Heisenberg picture as

$$\frac{\mathrm{d}}{\mathrm{d}t} \left\langle \widehat{O}(t) \right\rangle = \left\langle \mathcal{L}_{\mathcal{S}}^{\dagger} \left[\widehat{O}(t) \right] \right\rangle. \tag{3.216}$$

Injecting the derived master equation, e.g. Eq. (3.142), we obtain

$$\frac{\mathrm{d}}{\mathrm{d}t}\left\langle \widehat{O}(t)\right\rangle = \frac{i}{2}\left[\boldsymbol{H}_0(t)+\boldsymbol{\Delta}(t)\right]_{ij}\left\langle\left[\widehat{\boldsymbol{z}}_{\zeta,i}\widehat{\boldsymbol{z}}_{\zeta,j},\widehat{O}\right]\right\rangle \\ +\boldsymbol{\gamma}_{ij}\left[\frac{1}{2}\left\langle\left[\widehat{\boldsymbol{z}}_{\zeta,j},\widehat{O}\right]\widehat{\boldsymbol{z}}_{\zeta,i}\right\rangle+\frac{1}{2}\left\langle\widehat{\boldsymbol{z}}_{\zeta,j}\left[\widehat{O},\widehat{\boldsymbol{z}}_{\zeta,i}\right]\right\rangle\right], \tag{3.219}$$

that is a set of first order coupled differential equations for the observables of the system, where the parameters $\boldsymbol{\Delta}$ and $\boldsymbol{\gamma}_{ij}$ were defined in Eqs. (3.143) and (3.145). Applying this procedure to the covariance matrix

$$\boldsymbol{\Sigma}(t)=\frac{1}{2}\mathrm{Tr}_{\mathcal{S}}\left[\left\{\widehat{\boldsymbol{z}}_{\zeta},\widehat{\boldsymbol{z}}_{\zeta}^{\mathrm{T}}\right\}\widehat{\rho}_{\mathrm{red}}(t)\right], \tag{3.220}$$

the TCL_2 non-Markovian Gaussian master equation (3.142) leads to closed transport equations

$$\frac{\mathrm{d}\boldsymbol{\Sigma}}{\mathrm{d}t}=\boldsymbol{\omega}\left(\boldsymbol{H}_0+\boldsymbol{\Delta}\right)\boldsymbol{\Sigma}-\boldsymbol{\Sigma}\left(\boldsymbol{H}_0+\boldsymbol{\Delta}\right)\boldsymbol{\omega}-\boldsymbol{\omega}\boldsymbol{D}\boldsymbol{\omega}+2\boldsymbol{\Delta}_{-}\boldsymbol{\Sigma}, \tag{3.221}$$

where $\boldsymbol{D}$ and $\boldsymbol{\Delta}_{-}$ were introduced in Eqs. (3.146) and (3.147) respectively and we made use of the canonical commutation relations $[\widehat{\boldsymbol{z}}_{\zeta,l},\widehat{\boldsymbol{z}}_{\zeta,a}]=i\boldsymbol{\omega}_{la}$ leading to

$$\left[\widehat{\boldsymbol{z}}_{\zeta,l},\frac{1}{2}\left\{\widehat{\boldsymbol{z}}_{\zeta,a},\widehat{\boldsymbol{z}}_{\zeta,b}\right\}\right]=i\boldsymbol{\omega}_{la}\widehat{\boldsymbol{z}}_{\zeta,b}+(a\leftrightarrow b). \tag{3.222}$$

The first two terms in Eq. (3.221) correspond to the unitary evolution, which as stressed above receives an additional contribution from the Lamb-shift Hamiltonian. The last two terms respectively correspond to the diffusion (a source term proportional to $\boldsymbol{D}$) and the dissipation (a damping term proportional to $\boldsymbol{\Delta}_{-}$).

Solving the transport equations directly allows us to access the observable quantities such as the curvature perturbation power spectrum (2.58), which would correspond in this example to the first entry of the covariance matrix $\boldsymbol{\Sigma}_{11}=\langle\widehat{\zeta}^2\rangle$. Let us stress that, as already discussed, the perturbative limit of Eq. (3.221) is nothing but the result one would obtain from applying the second order Schwinger-Keldysh/CTP/in-in formalism on the full theory, as we explicitly demonstrated in [244]. This limit is simply obtained by noticing that $\boldsymbol{\Delta}$, $\boldsymbol{D}$ and $\boldsymbol{\Delta}_{-}$ are already of order $\mathcal{O}(g^2)$, such that anytime $\boldsymbol{\Sigma}$ multiplies these quantities, one must take the zeroth order (unperturbed) expression of the covariance matrix of the system.

Beyond the Gaussian case, non-linearities prevent the set of coupled differential equations to close. This problem is not specific to the OQS procedure and relates to the non-integrability of general non-linear systems in the absence of symmetries. Schematically, the dynamical equation of a n-point function requires the knowledge of the $n+1$-point functions,

$$\frac{\mathrm{d}}{\mathrm{d}t}\left\langle\widehat{\zeta}^n\right\rangle=F\big(\langle\widehat{\zeta}^n\rangle\big)+G\big(\langle\widehat{\zeta}^{n+1}\rangle\big), \tag{3.223}$$

where F and G are functions which depend on the details of the dynamics, hence we need the knowledge of the correlators at all order to fully specify the distribution of the state. In order for the system of ordinary differential equations to close, one must adopt an approximation scheme to truncate the series and express $G\big(\langle\widehat{\zeta}^{n+1}\rangle\big)$ in terms of lower order statistics. It has been shown in [281–283] that the Wick contractions of higher point functions is strictly equivalent to the perturbative result obtained using the Schwinger-Keldysh/CTP/in-in formalism.

3.3.4 Assessing quantum decoherence

Not only OQS techniques allow us to access the observables of the system but also to characterise its quantum information properties such as the purity of the state, the amount of entanglement with its environment or the appearance of a pointer basis [191, 192].

Entanglement measures: We first need to construct tracers of decoherence. The physical reason behind the loss of coherence of a quantum system is the delocalisation of correlations initially contained within the system into its surrounding environment [193]. A way to assess this leakage consists in measuring the evolution of the amount of information shared between the system and its environment. One can for instance compute the *entropy of entanglement* $S_{\rm ent}$, that is the von-Neumann entropy of the system once the environment have been traced over. It is defined as

$$S_{\rm ent} \equiv -{\rm Tr}_{\mathcal{S}} \left(\widehat{\rho}_{\rm red} \ln \widehat{\rho}_{\rm red}\right) \tag{3.224}$$

and is often challenging to evaluate because of the logarithm.

The *purity* γ provides a simpler measure of the level of mixedness of a quantum state, being defined as

$$\gamma = {\rm Tr}_{\mathcal{S}} \left(\widehat{\rho}^2_{\rm red}\right) \tag{3.225}$$

An associated entropy measure is defined by *linear entropy* as $S_{\rm L} \equiv 1 - \gamma$ which varies from 0 (pure) to 1 (maximally mixed). In the case of a Gaussian state where the system is made of a single dynamical degree of freedom (for instance the curvature perturbation ζ), specifying the purity is enough to fully characterise the other quantumness measures [122, 250].[14] In particular, the entanglement entropy is given by

$$S_{\rm ent} = \frac{1-\gamma}{2\gamma} \ln\left(\frac{1+\gamma}{1-\gamma}\right) - \ln\left(\frac{2\gamma}{1+\gamma}\right). \tag{3.226}$$

In this case, the entropy of entanglement is a monotonically increasing function of the linear entropy so that $S_{\rm ent}$ and $S_{\rm L}$ yields the same characterization of mixedness.

If the system remains Gaussian but now contains several dynamical degrees of freedom, the previous relation does not hold and there is no one-to-one relation between the linear and von Neumann entropy [250]. The von Neumann entropy then provides a finer characterisation of the mixedness in the case of multi-mode Gaussian states, is concave and additive and relates to the mutual information, a measure of the total amount of correlations contained in a state we used in Eq. (3.26). One can connect linear and von Neumann entropies throught the use of the Tsallis entropy

$$S_q \equiv \frac{1}{q-1} {\rm Tr}\left(\widehat{\rho}_{\rm red} - \widehat{\rho}^q_{\rm red}\right) \tag{3.227}$$

as $\lim_{q\to 1} S_q = S_{\rm ent}$ and $S_2 = S_{\rm L}$. Being constructed out of the symplectic eigenvalues of the system, these entropy measures are basis independent and invariant under

[14] The reason is that in this case, there is only one symplectic eigenvalue proportional to the purity γ. All the other quantumness measures are constructed out of this quantity which is the only invariant under field reparametrisation one can construct out of the observables.

reparametrisation of the system. Note that despite being desirable features in many situations, it also makes this formalism sometimes insufficient to describe processes such as the einselection of a pointer basis [191,192]. Future works may be dedicated to the investigation of alternative entanglement tracers providing good trade-off between computability and precision, such as the overlap [285] or the quantum Fisher information [286,287].

Gaussian states: Once a master equation is specified, it generates a dynamical evolution for the quantities introduced above. In general, even combined with the transport equations for the observables, it does not provide a close system of equations and one needs to rely on further assumptions in order to reach some results. Yet, in the Gaussian case, it turns out that there exists a simple relation between the purity γ and the observables of the system that are fully specify by the covariance matrix $\mathbf{\Sigma}$ defined in Eq. (3.220), that is [244,250,251]

$$\gamma(t) = \frac{1}{4\det\mathbf{\Sigma}}. \tag{3.228}$$

Moreover, when the system consists in a single dynamical degree of freedom, this quantity fully characterise the other entanglement measures as explained above. Hence, the problem of accessing the quantum information properties of the system reduces to the one of solving the transport equations. One can then assess decoherence by keeping track of the transition of the purity from 1 to 0.

To render Eq. (3.228) transparent, it can be instructive to show how the two-point functions of the system appear in the construction of the quantum state. In [228], it has been shown that the matrix element of a Gaussian state in the position basis,

$$\langle\zeta_1|\,\widehat{\rho}_{\rm red}(t)\,|\zeta_2\rangle = \sqrt{\frac{\Re\mathrm{e}\,(a)-b}{\pi}}\exp\left(-\frac{a}{2}\zeta_1^2-\frac{a^*}{2}\zeta_2^2+b\zeta_1\zeta_2\right), \tag{3.229}$$

is related to the power spectra through

$$\Re\mathrm{e}\,(a) = \frac{1}{\mathbf{\Sigma}_{11}}\left(\det\mathbf{\Sigma}+\frac{1}{4}\right), \quad \Im\mathrm{m}\,[a] = -\frac{\mathbf{\Sigma}_{12}}{\mathbf{\Sigma}_{11}} \tag{3.230}$$

$$b = \frac{1}{\mathbf{\Sigma}_{11}}\left(\det\mathbf{\Sigma}-\frac{1}{4}\right). \tag{3.231}$$

If the state is pure state such that $\widehat{\rho}_{\rm red}(t) = |\Psi(\eta)\rangle\langle\Psi(\eta)|$, the purity of the state imposes $\det\mathbf{\Sigma} = 1/4$, that is $b = 0$, $\Re\mathrm{e}\,(a) = 1/(2\mathbf{\Sigma}_{11})$ and $\Im\mathrm{m}\,[a] = -\mathbf{\Sigma}_{12}/\mathbf{\Sigma}_{11}$. We deduce from Eq. (3.229) that the wavefunction reads

$$\Psi\,[\zeta] = \sqrt{\frac{1}{2\pi\mathbf{\Sigma}_{11}}}\exp\left[-\frac{1}{2}\left(\frac{1}{2\mathbf{\Sigma}_{11}}-i\frac{\mathbf{\Sigma}_{12}}{\mathbf{\Sigma}_{11}}\right)\zeta^2\right]. \tag{3.232}$$

From this formula, we notice that the real part is related to $\mathbf{\Sigma}_{11}$ while the imaginary part allows us to access the two other spectra, making use of the purity relation $\det\mathbf{\Sigma} = 1/4$. Now, when $\gamma_{\boldsymbol{k}} \ll 1$, $\det\mathbf{\Sigma} \gg 1/4$, the state becomes maximally mixed such that $b \simeq \Re\mathrm{e}\,(a)$. Injecting this relation into Eq. (3.229) leads to

$$\langle\zeta_1|\,\widehat{\rho}_{\rm red}(t)\,|\zeta_2\rangle \propto \exp\left[-\frac{\Re\mathrm{e}\,(a)}{2}\left(\zeta_1-\zeta_2\right)^2\right] \tag{3.233}$$

which illustrates the diagonalisation of the density matrix under the action of quantum decoherence.

Let us finally investigate the dynamics induced on γ by the master equations found above. Starting from the TCL_2 non-Markovian master equation Eq. (3.142), we obtained the transport equations Eq. (3.221), from which one can deduce that

$$\frac{\mathrm{d}\det\boldsymbol{\Sigma}}{\mathrm{d}t} = \mathrm{Tr}\left(\boldsymbol{\Sigma}\boldsymbol{D}\right) - 4\boldsymbol{\Delta}_{-}\det\boldsymbol{\Sigma}. \tag{3.234}$$

Solving Eqs. (3.221) and (3.234) allows us to fully access the observables and the quantum information properties of the Gaussian system. One can further manipulate this expression in order to reach the Markovian limit using Eq. (3.199), leading to

$$\frac{\mathrm{d}\det\boldsymbol{\Sigma}^{(0)}}{\mathrm{d}t} = \boldsymbol{D}_{11}^{(0)}\boldsymbol{\Sigma}_{11} \tag{3.235}$$

or a given order in the non-Markovian corrections such as Eq. (3.207).

Perturbative purity: Beyond the Gaussian case, non-linearities render difficult to evaluate the purity if not in the perturbative regime. In this limit, the usefulness of the master equation reduces to its ability to organise the computation in a clear manner. Let us consider the purity $\gamma \equiv \mathrm{Tr}_{\mathcal{S}}\left(\widehat{\rho}_{\mathrm{red}}^{2}\right)$ in the perturbative framework where the reduced density matrix contains a tower of contributions

$$\widehat{\rho}_{\mathrm{red}} = \sum_{i=0}^{\infty}\widehat{\rho}_{\mathrm{red}}^{(i)} \tag{3.236}$$

where $\widehat{\rho}_{\mathrm{red}}^{(0)} \equiv \widehat{\rho}_{\mathcal{S}}^{(0)}$, the initial state of the system in the Heisenberg picture. The master equation provides a way to access the i^{th} order correction to the reduced density matrix of the system, as discussed along Eq. (3.128). We now aim at expressing the purity γ in terms of observables that are the (unequal-time) correlators of the system and the environment.

From Eq. (3.236), we obtain

$$\gamma = 1 + 2\sum_{i=1}^{\infty}\mathrm{Tr}_{\mathcal{S}}\left[\widehat{\rho}_{\mathrm{red}}^{(i)}\widehat{\rho}_{\mathcal{S}}^{(0)}\right] + \sum_{i,j=1}^{\infty}\mathrm{Tr}_{\mathcal{S}}\left[\widehat{\rho}_{\mathrm{red}}^{(i)}\widehat{\rho}_{\mathrm{red}}^{(j)}\right]. \tag{3.237}$$

If we focus on the first non-trivial term, we observe that it amounts to evaluate the free expectation value of the i^{th} order correction to the reduced density matrix of the system. For instance, at second order in the coupling constant g, we found in Eq. (3.135) that

$$\widehat{\rho}_{\mathrm{red}}^{(2)}(t_f) = -g^2\int_{t_0}^{t_f}\mathrm{d}t\int_{t_0}^{t}\mathrm{d}t'\mathrm{Tr}_{\mathcal{E}}\left[\widehat{H}_{\mathrm{int}}(t),\left[\widehat{H}_{\mathrm{int}}(t'),\widehat{\rho}_{\mathcal{S}}^{(0)}\otimes\widehat{\rho}_{\mathcal{E}}^{(0)}\right]\right] \tag{3.238}$$

such that for the interaction Hamiltonian $\widehat{H}_{\rm int}(t) = \int \mathrm{d}^3\boldsymbol{x}\widehat{J}_{\mathcal{S}}(t,\boldsymbol{x}) \otimes \widehat{J}_{\mathcal{E}}(t,\boldsymbol{x})$

$$\widehat{\rho}^{(2)}_{\rm red}(t_f) = -g^2 \int_{t_0}^{t_f} \mathrm{d}t \int_{t_0}^{t} \mathrm{d}t' \int \mathrm{d}^3\boldsymbol{x} \int \mathrm{d}^3\boldsymbol{y} \tag{3.239}$$

$$\left\{ \left[\widehat{J}_{\mathcal{S}}(x)\widehat{J}_{\mathcal{S}}(y)\widehat{\rho}^{(0)}_{\mathcal{S}} - \widehat{J}_{\mathcal{S}}(y)\widehat{\rho}^{(0)}_{\mathcal{S}}\widehat{J}_{\mathcal{S}}(x)\right] \mathcal{K}^{>}(x,y) \right.$$

$$\left. - \left[\widehat{J}_{\mathcal{S}}(x)\widehat{\rho}^{(0)}_{\mathcal{S}}\widehat{J}_{\mathcal{S}}(y) - \widehat{\rho}^{(0)}_{\mathcal{S}}\widehat{J}_{\mathcal{S}}(y)\widehat{J}_{\mathcal{S}}(x)\right] [\mathcal{K}^{>}(x,y)]^* \right\}. \tag{3.240}$$

We now use this perturbative expansion to compute the second order correction to the purity

$$\gamma(t_f) \supset 1 + 2\mathrm{Tr}_{\mathcal{S}}\left[\widehat{\rho}^{(2)}_{\rm red}(t_f)\widehat{\rho}^{(0)}_{\mathcal{S}}\right] \tag{3.241}$$

where we again assumed that $\mathrm{Tr}_{\mathcal{E}}[\widetilde{H}_{\rm int}(t)\widetilde{\rho}(t)] = 0$, such that there is no first order correction, $\widehat{\rho}^{(1)}_{\rm red}(t_f) = 0$. Injecting the above expressions into this equation, we obtain

$$\gamma(t_f) = 1 - 4g^2 \int_{t_0}^{t_f} \mathrm{d}t \int_{t_0}^{t} \mathrm{d}t' \int \mathrm{d}^3\boldsymbol{x} \int \mathrm{d}^3\boldsymbol{y} \Re\mathrm{e}\left[\mathcal{K}^{>}_{\mathcal{S}}(x,y)\mathcal{K}^{>}_{\mathcal{E}}(x,y)\right] \tag{3.242}$$

where we defined $\mathcal{K}^{>}_{\mathcal{E}}(x,y) \equiv \mathcal{K}^{>}(x,y)$ the memory kernel of the environment and

$$\mathcal{K}^{>}_{\mathcal{S}}(x,y) \equiv \mathrm{Tr}_{\mathcal{S}}\left[\widehat{J}_{\mathcal{S}}(x)\widehat{J}_{\mathcal{S}}(y)\widehat{\rho}^{(0)}_{\mathcal{S}}\right] - \mathrm{Tr}_{\mathcal{S}}\left[\widehat{J}_{\mathcal{S}}(x)\widehat{\rho}^{(0)}_{\mathcal{S}}\right]\mathrm{Tr}_{\mathcal{S}}\left[\widehat{J}_{\mathcal{S}}(y)\widehat{\rho}^{(0)}_{\mathcal{S}}\right] \tag{3.243}$$

the Wightman function of the system. Under this form, the symmetry of the purity under the exchange of the system and environment definition $\mathcal{S} \leftrightarrow \mathcal{E}$ is manifest, which is deeply reinsuring. Indeed, the purity being directly related to the linear entropy which characterises the amount of information shared between the system and the environment, it has to be a symmetric quantity. It also appears that the purity can be expressed in terms of two unequal time correlators, one which encodes the information for the system and one for the environment.

Hence, in the perturbative limit, it might be possible to access the purity in a simple manner and it is an ongoing effort to apply this approach in the context of cosmology. It may also provide a way to extract timescales associated with purity variations as, in that case, if one considers small time variations, one can Taylor expand the expression of the perturbative purity such as

$$\gamma(t_0 + \Delta t) \simeq \gamma(t_0) + \Delta t \left.\frac{\mathrm{d}\gamma(t_f)}{\mathrm{d}t_f}\right|_{t_f \to t_0} + \frac{\Delta t^2}{2}\left.\frac{\mathrm{d}^2\gamma(t_f)}{\mathrm{d}t_f^2}\right|_{t_f \to t_0} + \cdots \tag{3.244}$$

Then $\gamma(t_0) = 1$ and

$$\frac{\mathrm{d}\gamma(t_f)}{\mathrm{d}t_f} = -4g^2 \int_{t_0}^{t_f} \mathrm{d}t' \int \mathrm{d}^3\boldsymbol{x} \int \mathrm{d}^3\boldsymbol{y} \Re\mathrm{e}\left[\mathcal{K}^{>}_{\mathcal{S}}(t_f,\boldsymbol{x};t',\boldsymbol{y})\mathcal{K}^{>}_{\mathcal{E}}(t_f,\boldsymbol{x};t',\boldsymbol{y})\right] \tag{3.245}$$

$$\frac{\mathrm{d}^2\gamma(t_f)}{\mathrm{d}t_f^2} = -4g^2 \int \mathrm{d}^3\boldsymbol{x} \int \mathrm{d}^3\boldsymbol{y} \mathcal{K}^{>}_{\mathcal{S}}(t_f,\boldsymbol{x};t_f,\boldsymbol{y})\mathcal{K}^{>}_{\mathcal{E}}(t_f,\boldsymbol{x};t_f,\boldsymbol{y}) \tag{3.246}$$

from which we deduce that the first order derivative in the expansion (3.244) vanishes, the time integral having no support when $t_f \to t_0$, and we removed the real part in the expression for second order derivative as equal time correlators are by construction real. Hence,

$$\gamma(t_0 + \Delta t) \simeq 1 - \Gamma^2 \Delta t^2 \tag{3.247}$$

with the rate

$$\Gamma^2 = 2g^2 \int \mathrm{d}^3\boldsymbol{x} \int \mathrm{d}^3\boldsymbol{y} \mathcal{K}^{>}_{\mathcal{S}}(t_0, \boldsymbol{x}; t_0, \boldsymbol{y}) \mathcal{K}^{>}_{\mathcal{E}}(t_0, \boldsymbol{x}; t_0, \boldsymbol{y}) \tag{3.248}$$

It boils down to a product of equal-time correlators for the system and its environment. Note that for $\widehat{J}_{\mathcal{S}} = \widehat{\zeta}$ and $\widehat{J}_{\mathcal{S}} = \widehat{\mathcal{F}}$, once transferred in Fourier space, these quantities are nothing but the usual power spectra often computed in cosmology such that, in the case of a homogeneous and isotropic background, the decay rate for a given mode is given by the product of the free power spectra of the system and its environment

$$\Gamma^2_k(t_0) = 2g^2 \mathcal{P}^{\mathcal{S}}_k(t_0) \mathcal{P}^{\mathcal{E}}_k(t_0). \tag{3.249}$$

This setting might not correspond to any realistic situation in the context of cosmology, yet it illustrates how the investigation of the perturbative purity may allow us to connect observables to quantum information properties.

Finally, the computation of the perturbative purity paves the road towards the understanding of higher-order interactions and non-linear interactions in the system and the environment. In Eq. (3.237), $i + j$ counts the order of $\widehat{H}_{\rm int}$ insertions such that if one wants to compute the purity at order $\mathcal{O}(g^n)$, it must includes all the i, j fulfilling $i + j = n$. Then, one can also treat the non-linearities in the system and the environment perturbatively, by considering

$$\widehat{H}_{\mathcal{S}} = \widehat{H}^{(0)}_{\mathcal{S}} + \sum_{\alpha} \lambda^{(\alpha)}_{\mathcal{S}} \widehat{H}^{(\alpha)}_{\mathcal{S}} \tag{3.250}$$

$$\widehat{H}_{\mathcal{E}} = \widehat{H}^{(0)}_{\mathcal{E}} + \sum_{\beta} \lambda^{(\beta)}_{\mathcal{E}} \widehat{H}^{(\beta)}_{\mathcal{E}} \tag{3.251}$$

where α and β sum over all the non-linear interactions of the system and the environment. We obtain a triple expansion in g, $\lambda^{(\alpha)}_{\mathcal{S}}$ and $\lambda^{(\beta)}_{\mathcal{E}}$ where the fundamental quantities are unequal time correlators evaluated with respect to the initial states $\widehat{\rho}^{(0)}_{\mathcal{S}}$ and $\widehat{\rho}^{(0)}_{\mathcal{E}}$. Future work may aim at constructing a diagrammatic approach based on this expansion (see [288] for a recent study along this line).

Decoherence functional: Beyond the purity and its associated entropy measures, there exist other manner to assess decoherence such as the so-called *decoherence functional* [13, 188]. Following [188] analysis, let us consider the Markovian master equation obtained in Eq. (3.199) and solely consider the non-unitary contribution

$$\frac{\mathrm{d}\widehat{\rho}_{\rm red}}{\mathrm{d}t} \supset -\frac{\boldsymbol{D}^{(0)}_{11}(t)}{2} \left[\widehat{\zeta}, \left[\widehat{\zeta}, \widehat{\rho}_{\rm red}(t)\right]\right]. \tag{3.252}$$

If we further assume that the coefficient $\boldsymbol{D}_{11}^{(0)}$ is time independent, the role of this contribution clearly appears in the position basis where it generates a damping of the off-diagonal elements of the density matrix

$$\langle\zeta_1|\,\widehat{\rho}_{\rm red}(t)\,|\zeta_2\rangle \propto \exp\left[-\frac{\boldsymbol{D}_{11}^{(0)}}{2}\left(\zeta_1-\zeta_2\right)^2 t\right]\langle\zeta_1|\,\widehat{\rho}_{\mathcal{S}}^{(0)}\,|\zeta_2\rangle\,. \tag{3.253}$$

The *decoherence functional* is defined as

$$\Gamma(t) \equiv -\frac{\boldsymbol{D}_{11}^{(0)}}{2}\Delta_\zeta^2 t \tag{3.254}$$

where Δ_ζ the typical size of a fluctuation in the system. If we take it to be the free power spectrum such that $\Delta_\zeta^2 = \boldsymbol{\Sigma}_{11}$, a *decoherence timescale* can be extracted out of

$$\tau_D \equiv \frac{2}{\boldsymbol{D}_{11}^{(0)}\boldsymbol{\Sigma}_{11}}. \tag{3.255}$$

It straightforwardly relates to the evolution of the purity we found in Eq. (3.235). This approach is developed in [188] and some elements in the context of cosmology can be found in [223].

3.4 Developments

We close this Chapter with the presentation of two active research directions, the first one concerning the development of non-perturbative resummation techniques using the master equation formalism and the second one being related to the construction of bottom-up Open EFTs based on the influence functional. These advanced topics are less settled than the above results and constitute promising research avenues.

3.4.1 Towards non-perturbative resummations

One of the most fascinating aspects of master equations is certainly their ability to go beyond the perturbative regime by implementing some form of resummation in time. Indeed, we have seen around Eq. (3.135) that when solved as *bona fide* generators of the dynamical map (*i.e.* when taken *per se* and solved without further perturbative expansion), the NZ_n or TCL_n master equations contain *all* terms of order g^n, and *some* terms of order $g^{m>n}$. We now want to highlight where the resummation appears in practice and what sort of effects can be resummed. For the sake of clarity, let us focus on the TCL cumulant expansion.

Non-diagrammatic resummations: Let us first stress that the TCL resummation does not correspond to the resummation of a class of diagrams. In this sense, it is more comparable to the Dynamical Renormalisation Group (DRG) resummation [289–291] where diagrams are partially resummed.[15] Let us illustrate this

[15] A complete comparison between the master equation and DRG results is still lacking, see [244] Appendix E for a first comparison.

feature in the case of a linear coupling between the system and its environment. In this case, in the full theory, there is only one *one-particle irreducible* (1PI) diragram

while in the Open EFT generated by the master equation cumulant expansion, there is an infinite tower of 1PI

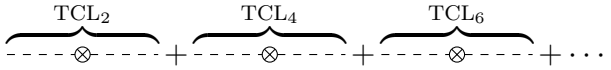

one for each of the TCL cumulants. Moreover, the Open EFT also contains non-unitary contributions originating from diffusion and dissipation which do not have any diagrammatic representation. Hence, the question of knowing which diagram has been resumed is ill-posed. This feature is shared with Wilsonian EFT and the DRG.

Gaussian transport equations: For Gaussian systems, the resummation can be easily implemented by deriving the effective transport equations of the form Eq. (3.221) and solving then non-perturbatively. In order to illustrate this procedure, let us derive the formal solution of Eq. (3.221). Let us first absorb the damping term $2\boldsymbol{\Delta}_{-}\boldsymbol{\Sigma}$ by introducing

$$\boldsymbol{\sigma} \equiv e^{\Gamma(t,t_0)}\boldsymbol{\Sigma} \qquad \text{with} \qquad \Gamma(t,t_0) \equiv -2\int_{t_0}^{t} \mathrm{d}t' \boldsymbol{\Delta}_{-}(t')\,, \tag{3.256}$$

which is solution of a damping-free transport equation, namely

$$\frac{\mathrm{d}\boldsymbol{\sigma}}{\mathrm{d}t} = \boldsymbol{\omega}\left(\boldsymbol{H}_0 + \boldsymbol{\Delta}\right)\boldsymbol{\sigma} - \boldsymbol{\sigma}\left(\boldsymbol{H}_0 + \boldsymbol{\Delta}\right)\boldsymbol{\omega} - e^{\Gamma(t,t_0)}\boldsymbol{\omega}\boldsymbol{D}\boldsymbol{\omega}\,. \tag{3.257}$$

This equation can be seen as a homogeneous part, describing the Lamb-shift corrected unitary evolution, and a source term, describing diffusion. The homogeneous part is generated by the Hamiltonian $\widehat{H}_0 + \widehat{H}_{(\mathrm{LS})}$, and, by denoting $\boldsymbol{g}_{\mathrm{LS}}(t,t_0)$ the associated Green's matrix, the solution of Eq. (3.257) expressed in terms of the original covariance reads [244]

$$\begin{aligned}\boldsymbol{\Sigma}(t) =& e^{-\Gamma(t,t_0)}\boldsymbol{g}_{\mathrm{LS}}(t,t_0)\boldsymbol{\Sigma}(t_0)\boldsymbol{g}_{\mathrm{LS}}^{\mathrm{T}}(t,t_0) \\ &- \int_{t_0}^{t} \mathrm{d}t' e^{-\Gamma(t,t')}\boldsymbol{g}_{\mathrm{LS}}(t,t')\left[\boldsymbol{\omega}\boldsymbol{D}(t')\boldsymbol{\omega}\right]\boldsymbol{g}_{\mathrm{LS}}^{\mathrm{T}}(t,t').\end{aligned} \tag{3.258}$$

The resummation is manisfest in the expression of the damping term, as $\boldsymbol{\Delta}_{-}$ has been derived at order $\mathcal{O}(g^2)$ such that $\exp[-\Gamma(t,t_0)]$ contains contributions of order $\mathcal{O}(g^n)$ with $n > 2$. $\boldsymbol{g}_{\mathrm{LS}}(t,t')$ also plays an important role in the resummation as the effective unitary dynamics is solved in a way that can generate important non-perturbative effects. For instance, we observed in Eq. (3.199) that the Markovian limit of a linear coupling between the system and its environment generates an effective mass for the system of the form $\boldsymbol{\Delta}_{11}^{(0)}\widehat{\zeta}^2/2$. The effective mode functions are obtained by solving

$$\frac{\mathrm{d}^2 v_\zeta}{\mathrm{d}t^2} + \left[\omega^2(t) + \boldsymbol{\Delta}_{11}^{(0)}(t)\right] v_\zeta = 0. \tag{3.259}$$

For an illustrative purpose, let us assume that ω^2 and $\boldsymbol{\Delta}_{11}^{(0)}$ are time independent, such that we obtain solutions of the form $\exp[\pm i(\omega^2 + \boldsymbol{\Delta}_{11}^{(0)})^{1/2}t]$. $\boldsymbol{\Delta}_{11}^{(0)}$ being of order $\mathcal{O}(g^2)$, a perturbative treatment would truncate these contributions as $\exp(\pm i\omega t)[1 \pm i(\boldsymbol{\Delta}_{11}^{(0)}/2\omega)t]$ which grows secularly. The resummation of these terms requires contributions of orders $\mathcal{O}(g^n)$ with $n > 2$ and dresses the frequency of the system which consistently accounts for the interaction with the environment. Hence, the master equation resummation can be understood as the procedure which first identifies the terms relating to the Lamb shift and dissipation in the effective dynamics generated by the master equation (that are the ones that depend on the imaginary part of the memory kernel), then to capture the effects of these terms at all order in perturbation theory.

Let us close this discussion with words of caution: while in [244], the non-perturbative resummation performed by the TCL_2 master equation dramatically improves the results on the observables and the purity compared to standard perturbation theory, in [154], the resummation does not and rather generates a tiny violation of positivity at late time, which signals a small breakdown of the effective theory. The reason behind these different behaviours might be due to the presence of secular corrections correctly resummed by the master equation in the first example while their absence in the second case aggregates unphysical corrections. Yet, a deeper investigation of master equation resummations in Markovian and non-Markovian cosmological settings seems necessary to provide a definitive answer on this open question.

Spurious terms: The investigation of non-perturbative resummation in the context of non-Markovian master equation lead us to unexpected complications. In Ref. [244], it has been shown that some terms dubbed "spurious" appear in the master-equation coefficients, that cancel out in the perturbative limit but ruin the resummation otherwise. More precisely, the second-order master-equation coefficients are expressed as integrals between t_0 and t, see Eqs. (3.143)-(3.146) and (3.147) , i.e.

$$\boldsymbol{\Delta}_- = 2\int_{t_0}^{t} \mathrm{d}t' \boldsymbol{\mathcal{D}}_-^{\mathrm{Im}}(t,t') = F_{\boldsymbol{\Delta}_-}(t,t) - F_{\boldsymbol{\Delta}_-}(t,t_0)\,, \tag{3.260}$$

where $F_{\boldsymbol{\Delta}_-}(t,\cdot)$ is the primitive of $2\boldsymbol{\mathcal{D}}_-^{\mathrm{Im}}(t,t')$, which itself might depend on t, and with similar notations for the other coefficients $\boldsymbol{\Delta}$ and $\boldsymbol{D}$. The second term in Eq. (3.260), the one that depends on the initial time t_0, is the "spurious" one. Note that in the Markovian limit, the damping of the memory kernel would prevent this term to contribute. In the exact solution, there is no such initial-time dependent term in the dynamical equations, and indeed one can show that it cancels out at all orders in perturbation theory [244]. At leading order in the coupling constant g, we have demonstrated in Eq. (3.135) that the master equation reduces to standard perturbation theory, hence again one can show that the spurious contribution vanishes [244]. At higher order however, the master equation stops being equivalent to standard perturbation theory, since it only performs resummation of the leading-order interaction. The non-diagrammatic nature of the resummation explains why the spurious term alters the result, as illustrated in Fig. 3.8. In some sense, the resummation breaks order-by-order relations that hold in standard perturbation

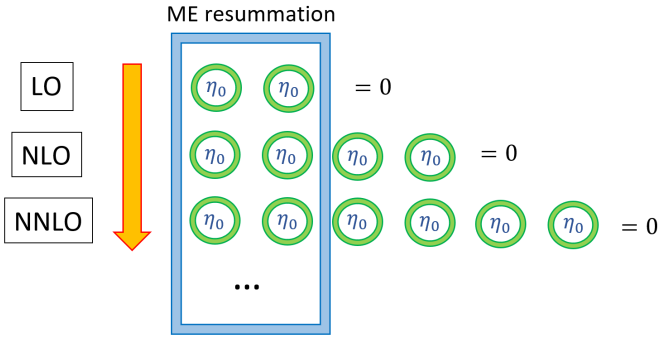

Figure 3.8: The appearance of spurious terms in non-Markovian settings might jeopardize the non-perturbative resummation if not carefully taken into account while remaining harmless in the perturbative limit. One can control that at any order in perturbation theory, these η_0 dependent terms cancel each other (here, t_0 is replaced by η_0). Hence, they do not affect the perturbative results [244]. Still, they play a crucial role as if kept, they introduce a large error compared to the exact results during the resummation [244]. Indeed, partial resummations such as the one implemented by the master equation formalism break order-by-order relations. TCL_n contains all terms at order g^n and some terms of order $g^{m>n}$. Yet, the cancellation requires all the η_0-dependent terms at a given order. In order to perform a meaningful resummation, one needs to impose the broken relation by hand before resumming. Spurious terms can be identified without ambiguity by the prescription of recovering the perturbative result at order g^n.

theory. However, since we know that it should vanish at all orders, one can simply remove it by hand, and thus restore the ability of the master equation to perform efficient resummation [244]. This is equivalent to the procedure of reintroducing by hand a symmetry that has been broken by a partial resummation scheme. One may be worried that, from Eq. (3.260), the spurious terms are only defined up to an additive constant. However, since they are known to vanish at all (and in particular at leading) orders, they can be determined without ambiguity by comparison with the perturbative theory. We concluded in [244] that master equations were able to perform late-time resummation, even though the system is far from the Markovian limit, provided spurious contributions are suppressed.

Beyond Gaussianity: The ability of master equations to perform late-time resummations beyond the Gaussian case is still an open question. A guideline might be given by what has been learnt in the context of stochastic inflation where the comparison between stochastic resummation and field-theoretic computations has been pushed to exquisite levels [90, 167, 292–296]. Given the great level of similarity existing between Fokker-Planck equations and master equations, it could provide promising directions to investigate. In particular, we have seen in Eq. (3.154) that the phase-space representation of the master equation can formally be expressed in terms of a Fokker-Planck equation for the Wigner function of the system. By looking at the equilibrium distribution towards which the generator of the dynamical map drives the system, stochastic inflation provides a non-perturbative expression for the probability distribution function for the system (a property often used in the context of stochastic inflation, see e.g. A. Starobinsky's seminal article [157]). Ap-

plying this procedure to Eq. (3.154) under the assumption of stationary coefficients, we obtain an equation for the equilibrium reduced Wigner function of the system $W_{\rm eq}$,

$$\left\{\widetilde{H}_{\mathcal{S}}+\widetilde{H}_{\rm LS},W_{\rm eq}\right\}=\boldsymbol{\Delta}_{-}\sum_{i}\frac{\partial}{\partial\boldsymbol{z}_{\zeta,i}}\left(\boldsymbol{z}_{\zeta,i}W_{\rm eq}\right)+\frac{1}{2}\sum_{i,j}\left[\boldsymbol{\omega}\boldsymbol{D}\boldsymbol{\omega}\right]_{ij}\frac{\partial^{2}W_{\rm eq}}{\partial\boldsymbol{z}_{\zeta,i}\partial\boldsymbol{z}_{\zeta,j}}\,.$$

This form of equilibrium distribution has been investigated in the context of hot accelerated qubits [236, 237, 262, 268] (see [22] for a review) but not in the context of cosmological continuous-variable systems which are often time-dependent even at late-time. Note that equilibrium distributions are insufficient to describe the processes of decoherence and thermalization which require some knowledge of the transient dynamics [22]. One of the most compelling characterisations of the generators of dynamical maps is given by the study of the Liouvillian spectrum [248] which provides non-perturbative information on the decay rates towards equilibrium. Unfortunately, little is known about the structure of the Liouvillian for continuous-variable systems or for non-Markovian dynamics [248]. Hence, this research still must be developed before being applied to the Open EFT context for the implementation of non-perturbative resummations in non-Gaussian settings. Given the similarity of the formalism with the one used in stochastic inflation, improvements might come from the importation of techniques used to find the Fokker-Planck spectrum even if similar difficulties are faced in this context.

3.4.2 Bottom-up constructions of Open EFTs

Let us close this Chapter with a brief discussion of an open research question around the bottom-up construction of Open EFTs. In Chapter 1, we presented the bottom-up EFT construction of perfect fluids and the difficulty of including viscosity and dissipation in this framework. The inclusion of these effects would require an understanding of the role of symmetries in non-equilibrium frameworks, a topic that has been partially investigated in [9]. In this article, the authors discussed the role of time-translational symmetry breaking in the influence functional describing the non-unitary evolution of a pseudo-Goldstone boson. In particular, it fixes constraints on the noise and dissipation operators appearing in the influence functional. Far from being a definitive answer to the bottom-up constructions of non-unitary dynamics, it rather provides a first concrete attempt we could use to further develop model-agnostic understanding of dissipation and decoherence. We here summarize the main arguments while referring to [9] for technical details.

Their main result is the following. There are two branches in the path integral appearing in the Schwinger-Keldysh formalism. Hence, there are initially two time-translational symmetries. The former is explicitly broken by dissipative effects while the latter in not. The conserved charges/generators associated with the symmetries are the original Hamiltonian and the Liouvillian (Fokker-Planck operator), respectively. In order to be slightly more explicit, let us consider the influence functional approach obtained in Sec. 3.2.3, for e.g. Eq. (3.85) that we reproduce here for clarity.

$$\rho_{\zeta\zeta'}(t)=\int\mathrm{d}\zeta_{1}\mathrm{d}\zeta_{2}\int_{\zeta_{1}}^{\zeta}\mathcal{D}\left[\zeta_{+}\right]\int_{\zeta_{2}}^{\zeta'}\mathcal{D}\left[\zeta_{-}\right]e^{iS_{\zeta}[\zeta_{+}]-iS_{\zeta}[\zeta_{-}]+iS_{\rm IF}[\zeta_{+};\zeta_{-}]}\left\langle\zeta_{1}\right|\widehat{\rho}_{\mathcal{S}}^{(0)}\left|\zeta_{2}\right\rangle\,. \tag{3.261}$$

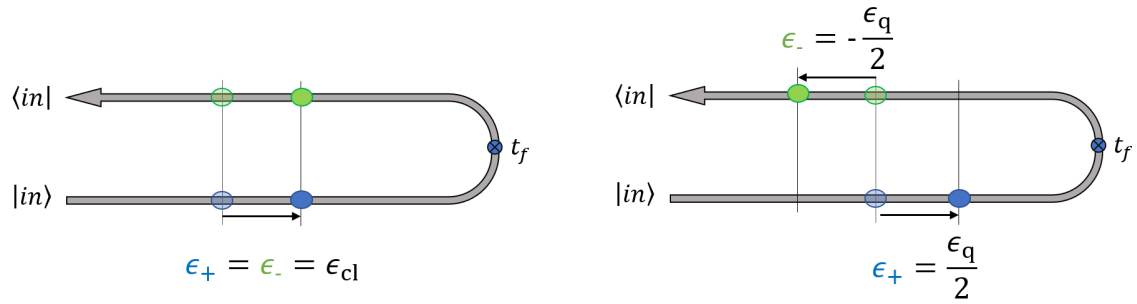

Figure 3.9: The $\epsilon_{\rm cl}$ and $\epsilon_{\rm q}$ transformations on the closed time path. The $\epsilon_{\rm cl}$ transformation translates the " $+$ " and " $-$ " variables in the same direction while $\epsilon_{\rm q}$ transformation does it in the opposite directions. While the $\epsilon_{\rm cl}$ transformation is preserved for open systems without explicit t-dependence (detailed balance), the $\epsilon_{\rm q}$ one is explicitly broken due to dissipative effects. Hence, the theory is not anymore invariant under time-reversal symmetry. Note that the formalism can also accomodate non-stationary open systems where on the top of the $\epsilon_{\rm q}$ transformation, the $\epsilon_{\rm cl}$ transformation also becomes spontaneously broken [9].

If the microscopic action $S_\zeta[\zeta_\pm]$ is invariant under the doubled time-translations labelled by $\epsilon_\pm$,

$$\zeta_+(t) \to \zeta'_+(t) = \zeta_+(t+\epsilon_+), \qquad \zeta_-(t) \to \zeta'_-(t) = \zeta_-(t+\epsilon_-), \tag{3.262}$$

the effective action $S_{\rm IF}[\zeta_+;\zeta_-]$ is not for general $\epsilon_+ \neq \epsilon_-$ due to the non-unitary effects arising from integrating out the environmental degrees of freedom. More precisely, the effective action remains invariant under the translation (see left panel of Fig. 3.9)

$$\epsilon_+ = \epsilon_- = \epsilon_{\rm cl} \tag{3.263}$$

while it is explicitly broken for the translation (see right panel of Fig. 3.9)

$$\epsilon_+ = -\epsilon_- = \frac{\epsilon_{\rm q}}{2}. \tag{3.264}$$

In this way, the two time-translational symmetries of the microscopic action are broken into a diagonal one $\epsilon_+ = \epsilon_-$ corresponding to the detailed balance in the presence of fluctuation and dissipation.

We now plan to understand the impact of the symmetry breaking at the level of the non-unitary effective action obtained from the influence functional

$$S_{\rm eff}[\zeta_+;\zeta_-] = S_\zeta[\zeta_+] - S_\zeta[\zeta_-] + S_{\rm IF}[\zeta_+;\zeta_-]\,. \tag{3.265}$$

Following [9], we work in the cl-q basis, that is defined as

$$\zeta_{\rm cl} \equiv \frac{\zeta_+ + \zeta_-}{2}\,, \tag{3.266}$$

$$\zeta_{\rm q} \equiv \zeta_+ - \zeta_-\,. \tag{3.267}$$

It can be easily shown that in this basis, the normalisation of the reduced density matrix and its self-adjointness translate into [255, 297]

$$S_{\rm eff}[\zeta_{\rm cl};\zeta_{\rm q}=0] = 0 \tag{3.268}$$

$$S_{\rm eff}[\zeta_{\rm cl};\zeta_{\rm q}] = -S_{\rm eff}[\zeta_{\rm cl};-\zeta_{\rm q}]^*\,. \tag{3.269}$$

Moreover, this second relation highlights that the effective action in general contains an imaginary part. This is a basic feature of open systems for which, after integrating out the environment, the effective dynamics contains fluctuation and dissipation in general. As the effective action $S_{\rm eff}$ weights the path integral, we may have divergent behaviour if $\Im\mathrm{m}\left[S_{\rm eff}\right] < 0$. To avoid this situation, the authors of [9] impose the positivity of the imaginary part of the effective action

$$\Im\mathrm{m}\left\{S_{\rm eff}\left[\zeta_{\rm cl};\zeta_{\rm q}\right]\right\} \geq 0. \tag{3.270}$$

These observations, together with the symmetry content of Fig. 3.9, will serve to construct the most generic open dynamics in the semi-classical limit [9].

Effective Lagrangian for closed dynamics: It is useful to have in mind the bottom-up construction of closed dynamics in the case of a scalar field breaking time-translation symmetry

$$\langle\phi(t,\boldsymbol{x})\rangle = \bar{\phi}(t) \quad \text{with} \quad \dot{\bar{\phi}} \neq 0. \tag{3.271}$$

The Nambu-Goldstone mode defined from [9]

$$\phi(t,\boldsymbol{x}) = \bar{\phi}[t+\pi(t,\boldsymbol{x})] \tag{3.272}$$

and transform under translations $(t \to t+\epsilon^0, \boldsymbol{x} \to \boldsymbol{x}+\boldsymbol{\epsilon})$ as

$$\pi(t,\boldsymbol{x}) \to \pi'(t,\boldsymbol{x}) = \pi(t+\epsilon^0, \boldsymbol{x}+\boldsymbol{\epsilon}) + \epsilon^0. \tag{3.273}$$

In addition, under Lorentz transformations, $\pi(t,\boldsymbol{x})$ transforms as

$$\pi(t,\boldsymbol{x}) \to \pi'(t,\boldsymbol{x}) = \pi\left(\Lambda^0{}_\mu x^\mu, \Lambda^i{}_\mu x^\mu\right) + \Lambda^0{}_\mu x^\mu - t \tag{3.274}$$

where we introduced $\Lambda^\mu{}_\nu \in \mathrm{SO}(1,3)$. From the fundamental definition (3.272), it appears that the effective action is constructed from $t+\pi(t,\boldsymbol{x})$ and its derivatives [2]. Indeed, one can easily show that these building blocks are invariant under the transformations (3.273)-(3.274) upon an appropriate coordinate transformation. It is convenient to introduce the quantity

$$P_\mu = \partial_\mu(t+\pi) = \delta^0{}_\mu + \partial_\mu\pi \tag{3.275}$$

which is used as a basic building block in the construction of the effective Lagrangian. In particular, the Lorentz invariant combination

$$P_\mu P^\mu = -1 - 2\dot{\pi} + (\partial_\mu\pi)^2 \tag{3.276}$$

is ubiquitous.

As for the hydrodynamical EFTs presented in Chapter 1, the authors of [9] considered a derivative expansion in which higher derivative terms with two or more derivatives acting on $\pi(x)$ are dropped. This is a standard procedure to work out the long-wavelength IR regime [4, 8]. It follows that at leading order in the derivative expansion the general action is given by [9]

$$S_{\rm eff} = -\frac{1}{2}\int \mathrm{d}^4x \left[\alpha_0(t+\pi) + \alpha_1(t+\pi)P_\mu P^\mu + \sum_{n\geq 2}\alpha_n(t+\pi)\left(P_\mu P^\mu + 1\right)^n\right] \tag{3.277}$$

where the α_n's are arbitrary functions of $t+\pi$. Imposing the shift symmetry/slow roll expansion would further constrain these coefficients to be time-independent, $\alpha_n(t+\pi)=\alpha_n$ for all n. At this point, the action contains terms linear in π

$$S_{\text{eff}} = -\frac{1}{2}\int \mathrm{d}^4x \left\{\alpha_0(t) - \alpha_1(t) + \left[\dot{\alpha}_0(t) - \dot{\alpha}_1(t)\right]\pi - 2\alpha_1(t)\dot{\pi} + \mathcal{O}(\pi^2)\right\}. \tag{3.278}$$

This tadpole contribution is absorbed by the background evolution, enforcing $\dot{\alpha}_0(t) = -\dot{\alpha}_1(t)$ [9]. Upon dropping total derivatives and choosing the integration constant of $\dot{\alpha}_0(t) = -\dot{\alpha}_1(t)$ such that $\alpha_0(t) = \alpha_1(t)$, we obtain

$$S_{\text{eff}} = -\frac{1}{2}\int \mathrm{d}^4x \left\{\alpha_1(\partial_\mu\pi)^2 + \sum_{n\geq 2}\alpha_n\left[-2\dot{\pi} + (\partial_\mu\pi)^2\right]^n\right\} \tag{3.279}$$

where we further enforced the shift-symmetry of π, rendering the Wilsonian coefficients time-independent. The α_1 coefficient characterises the symmetry breaking scale $\alpha_1 \sim E^4_{\text{SSB}}$ and note that $-2\dot{\pi}+(\partial_\mu\pi)^2$ is the combination that is invariant under boosts and not $(\partial_\mu\pi)^2$ itself. Only keeping the linear part of the effective action, we find that the π field enjoys a massless linear dispersion relation

$$\omega^2 = c_s^2 k^2 \quad \text{with} \quad c_s^2 \equiv \frac{\alpha_1}{\alpha_1 - 4\alpha_2}. \tag{3.280}$$

One immediately notices how this effective speed of sound is related to the cubic operator $\dot{\pi}(\partial_\mu\pi)^2$ by the mean of α_2.

Let us now construct the EFT for the Nambu-Goldstone modes in open systems. We work in the double-path integral Schwinger-Keldysh formalism and construct the effective action $S_{\text{eff}}[\pi_{\text{cl}};\pi_{\text{q}}]$ in the cl-q basis. In this basis, the ϵ_{cl}-transformations are (left panel of Fig. 3.9) [9]

$$\pi_{\text{cl}}(t,\boldsymbol{x}) \to \pi'_{\text{cl}}(t,\boldsymbol{x}) = \pi_{\text{cl}}(t+\epsilon^0_{\text{cl}}, \boldsymbol{x}+\boldsymbol{\epsilon}_{\text{cl}}) + \epsilon^0_{\text{cl}} \tag{3.281}$$

$$\pi_{\text{q}}(t,\boldsymbol{x}) \to \pi'_{\text{q}}(t,\boldsymbol{x}) = \pi_{\text{q}}(t+\epsilon^0_{\text{cl}}, \boldsymbol{x}+\boldsymbol{\epsilon}_{\text{cl}}), \tag{3.282}$$

whereas the Λ_{cl}-transformations follow

$$\pi_{\text{cl}}(t,\boldsymbol{x}) \to \pi'_{\text{cl}}(t,\boldsymbol{x}) = \pi_{\text{cl}}\left(\Lambda^0_{\text{cl}\ \mu}x^\mu, \Lambda^i_{\text{cl}\ \mu}x^\mu\right) + \Lambda^0_{\text{cl}\ \mu}x^\mu - t \tag{3.283}$$

$$\pi_{\text{q}}(t,\boldsymbol{x}) \to \pi'_{\text{q}}(t,\boldsymbol{x}) = \pi_{\text{q}}\left(\Lambda^0_{\text{cl}\ \mu}x^\mu, \Lambda^i_{\text{cl}\ \mu}x^\mu\right). \tag{3.284}$$

The important point is that the π_{q} field *linearly transforms* under the ϵ_{cl} and Λ_{cl}-symmetries, just as ordinary matter.

It follows that the effective non-unitary Lagrangian can be constructed out of π_{q}, $t+\pi_{\text{cl}}$ and their derivatives, just as we did for the closed case. A useful way to organise the expansion, on the top of the derivative expansion, is to notice that

$$\pi_{\text{cl}} = \mathcal{O}(\hbar^0), \quad \pi_{\text{q}} = \mathcal{O}(\hbar) \tag{3.285}$$

and so their name. It is a known fact of the Schwinger-Keldysh formalism, see e.g. [255], which allows us to organise the expansion in powers of $\hbar$,

$$\mathcal{L}_{\rm eff} = \sum_{n=1}^{\infty} \mathcal{L}_n \quad \text{with} \quad \mathcal{L}_n = \mathcal{O}(\pi_{\rm q}^n) = \mathcal{O}(\hbar^n) \tag{3.286}$$

where we used the unitarity condition (3.268) to notice that the Lagrangian starts from the first order term in $\pi_{\rm q}$. The conjugate condition (3.269) also imposes strong constraints on even and odd orders of the expansion. In particular, it will appear shortly that $\mathcal{L}_1$ contains the dissipation term and $\mathcal{L}_2$ the noise term of Brownian motion. Hence, the second order truncation $\mathcal{O}(\hbar^2)$ matches the semi-classical limit obtained through the MSR formalism [9].

Dissipation: Let us illustrate the procedure by first considering the leading order of $\mathcal{L}_1$

$$\mathcal{L}_1^{\rm LO} = \gamma_0(t+\pi_{\rm cl})\pi_{\rm q} + \gamma_1(t+\pi_{\rm cl})\left(P_\mu P^\mu + 1\right)\pi_{\rm q} - \alpha_1(t+\pi_{\rm cl})P^\mu\partial_\mu\pi_{\rm q} \tag{3.287}$$

where we introduced $P_\mu = \partial_\mu(t+\pi_{\rm cl}) = \delta^0{}_\mu + \partial_\mu\pi_{\rm cl}$. The EFT coefficients γ_0, γ_1 and α_1 are functions of $t+\pi_{\rm cl}$ which have to be real because of the conjugate condition (3.269). Just as above, we remove the linear contributions by fixing the background dynamics. Indeed, the Lagrangian contains terms linear in π that are

$$\mathcal{L}_1^{\rm LO} = \gamma_0(t)\pi_{\rm q} + \alpha_1(t)\dot\pi_{\rm q} + \mathcal{O}(\pi^2), \tag{3.288}$$

so we impose the background equation of motion to require $\gamma_0(t) = \dot\alpha_1(t)$. The Lagrangian thus reduces to

$$\mathcal{L}_1^{\rm LO} = \gamma_1\left[-2\dot\pi_{\rm cl} + \left(\partial_\mu\pi_{\rm cl}\right)^2\right]\pi_{\rm q} - \alpha_1\partial^\mu\pi_{\rm cl}\partial_\mu\pi_{\rm q}. \tag{3.289}$$

in the slow-roll regime where we assumed time-independence for the EFT coefficients.[16] The α_1 term is the usual kinetic term written in the cl-q basis. On the other hand, the γ_1 term leads to a dissipative/damping term in the $\pi_{\rm cl}$ equation of motion. Interestingly, the dissipation term $\dot\pi_{\rm cl}\pi_{\rm q}$ is accompanied by a cubic interaction $\left(\partial_\mu\pi_{\rm cl}\right)^2\pi_{\rm q}$, as first noted in [298], such that the combination is invariant under Lorentz boosts.

We now have to include higher-derivative of $\pi_{\rm cl}$ which leads to

$$\begin{aligned}\mathcal{L}_1 = \mathcal{L}_1^{\rm LO} &+ \sum_{n=2}^{\infty}\gamma_n\left[-2\dot\pi_{\rm cl} + \left(\partial_\mu\pi_{\rm cl}\right)^2\right]^n\pi_{\rm q} \\ &- \sum_{n=2}^{\infty}\alpha_n\left[-2\dot\pi_{\rm cl} + \left(\partial_\mu\pi_{\rm cl}\right)^2\right]^{n-1}\left(-\dot\pi_{\rm q} + \partial^\mu\pi_{\rm cl}\partial_\mu\pi_{\rm q}\right),\end{aligned} \tag{3.290}$$

which does not contain any term linear in π, so that the background equation of motion is unchanged. Note that only α_1, α_2 and γ_1 provide quadratic terms in π, relevant for the dispersion relation of the Goldstone mode.

[16] This assumption can be relaxed, see [9] for details.

Diffusion: Finally, the last ingredient generating quadratic terms is $\mathcal{L}_2$ (as $\mathcal{L}_n$ for $n > 2$ at least contains $\pi_{\rm q}^{n>2}$). Just as above, working with operators containing at most one derivative, in the slow-roll limit, we obtain

$$\mathcal{L}_2 \supset i\Big[\beta_1\pi_{\rm q}^2 + \beta_2\left(\partial_\mu\pi_{\rm q}\right)^2 + \beta_3\left(-\dot{\pi}_{\rm q} + \partial^\mu\pi_{\rm cl}\partial_\mu\pi_{\rm q}\right)\pi_{\rm q} + \beta_4\left(-\dot{\pi}_{\rm q} + \partial^\mu\pi_{\rm cl}\partial_\mu\pi_{\rm q}\right)^2\Big]. \tag{3.291}$$

The i in front directly follows from the conjugate condition (3.269). While the term proportional to β_1 is the standard noise term, we observe the presence of higher-order corrections such as $\left(\partial_\mu\pi_{\rm q}\right)^2$ and $\dot{\pi}_{\rm q}^2$ in the β_2 and β_4 terms which make the noise scale-dependent. Finally, as above, general operators in $\mathcal{L}_2$ can be obtained by multiplying arbitrary powers of $(P^\mu P_\mu + 1) = -2\dot{\pi}_{\rm cl} + \left(\partial_\mu\pi_{\rm cl}\right)^2$ with one of the four operators constructed above.

There exists a positivity condition on the β's coefficients due to Eq. (3.270) which imposes $\Im\mathrm{m}\left[S_{\rm eff}\right] > 0$. Making use of the derivative expansion which tells us that $\omega^2, k^2 \ll |\beta_1/\beta_{2,4}|$ (the quadratic term in β_3 can be written as a total derivative and removed), we conclude that β_1 dominates in $\mathcal{L}_2$, such that the positivity constraints imposes [9]

$$\beta_1 > 0. \tag{3.292}$$

This positivity constraint on the noise kernel directly translates into consequences for the non-Gaussian signal if we multiply this operator by higher powers of $(P^\mu P_\mu + 1) = -2\dot{\pi}_{\rm cl} + \left(\partial_\mu\pi_{\rm cl}\right)^2$.

Unitary limit: Because of the symmetry structure of the theory, retrieving the unitary limit is a rather straightforward task. First, being purely imaginary, it is clear that $\mathcal{L}_2$ describes the statistical noise, a property specific to open systems. Then, in order to identify which part of $\mathcal{L}_1$ relates to the unitary evolution, one can use the fact that in the absence of dissipation, the dynamics must be symmetric under $\epsilon_{\rm cl}$ but also $\epsilon_{\rm q}$. Because of the fact that along the two $\pm$ branches of the path integral [9]

$$\pi_\pm(t,\boldsymbol{x}) \to \pi'_\pm(t,\boldsymbol{x}) = \pi_\pm(t + \epsilon^0_\pm, \boldsymbol{x} + \boldsymbol{\epsilon}_\pm) + \epsilon^0_\pm \tag{3.293}$$

and that the $\epsilon_{\rm q}$ symmetry is given by $\epsilon^0_+ = -\epsilon^0_- = \epsilon_{\rm q}/2$ (see right panel of Fig. 3.9), we have

$$\pi_{\rm cl}(t,\boldsymbol{x}) \to \pi'_{\rm cl}(t,\boldsymbol{x}) = \pi_{\rm cl}(t,\boldsymbol{x}) + \mathcal{O}(\hbar^2) \tag{3.294}$$

$$\pi_{\rm q}(t,\boldsymbol{x}) \to \pi'_{\rm q}(t,\boldsymbol{x}) = \pi_{\rm q}(t,\boldsymbol{x}) + \dot{\pi}_{\rm q}(t,\boldsymbol{x})\epsilon_{\rm q} + \epsilon_{\rm q} + \mathcal{O}(\hbar^3), \tag{3.295}$$

where we used the fact that $\epsilon_{\rm q} = \mathcal{O}(\hbar)$. If we then consider the transformation of $\mathcal{L}_1$ under $\epsilon_{\rm q}$, we first notice the following transformation property

$$\delta_{\epsilon_{\rm q}}\left(P^\mu\partial_\mu\pi_{\rm q}\right) = \epsilon_{\rm q}P^\mu\partial_\mu\left(\dot{\pi}_{\rm q} + 1\right) = \frac{1}{2}\epsilon_{\rm q}\partial_t\left(P^\mu P_\mu + 1\right), \tag{3.296}$$

such that the $\epsilon_{\rm q}$ transformation of $\mathcal{L}_1$ is

$$\delta_{\epsilon_{\rm q}}\mathcal{L}_1 = \epsilon_{\rm q}\left[\sum_{n=1}^{\infty}\gamma_n(P^\mu P_\mu + 1)^n\left(\dot{\pi}_{\rm q} + 1\right) - \sum_{n=1}^{\infty}\frac{\alpha_n}{2n}\partial_t\left(P^\mu P_\mu + 1\right)^n\right]. \tag{3.297}$$

Because the second term is a total derivative, the authors of [9] concluded that the α_n operators are invariant under the ϵ_q time transformation. Therefore, the α_n operators may exist in closed systems while the γ_n operators are specific to open dynamics and capture dissipation. We conclude that the unitary part of the action is

$$\mathcal{L}_1^{\text{unit}} = -\alpha_1 \partial^\mu \pi_{\text{cl}} \partial_\mu \pi_{\text{q}} - \sum_{n=2}^{\infty} \alpha_n \left[-2\dot{\pi}_{\text{cl}} + (\partial_\mu \pi_{\text{cl}})^2 \right]^{n-1} \left(-\dot{\pi}_{\text{q}} + \partial^\mu \pi_{\text{cl}} \partial_\mu \pi_{\text{q}} \right) \tag{3.298}$$

which must be compared with the previously derived result (3.279). The amplitude of the EFT coefficients is then estimated from $\alpha_n \sim E_{\text{SSB}}^4$.

Energy scales and observables: One can also associate an energy scale to the dissipative effects which allows us to estimate when they play a leading role by noticing that in Eq. (3.289) $\dot{\pi}_{\text{cl}} \pi_{\text{q}}$ dominates over the unitary kinetic term when

$$E_{\text{diss}} \sim \gamma_1 / \alpha_1 \gg \omega. \tag{3.299}$$

One can then generalise to estimate $\gamma_n \sim E_{\text{diss}} E_{\text{SSB}}^4$. Restricting ourselves to the quadratic Lagrangian, we can already extract useful information out of the dispersion relations.

Dispersion relations: Supposing there is a hierarchy $E_{\text{diss}} \ll E_{\text{SSB}}$ (otherwise dissipation occurs in regime of scales beyond the regime of validity of the EFT) and that the derivative expansion $\omega^2, k^2 \ll |\beta_1/\beta_{2,4}|$ operates in $\mathcal{L}_2$ so that we drop higher-order corrections to the noise term, there exists three different dynamical regimes:

1. When $E_{\text{diss}} \ll \omega \ll E_{\text{SSB}}$, non-unitary effects are subdominant and the quadratic Lagrangian reduces to

$$\mathcal{L}_{\text{eff}} \simeq (\alpha_1 - 2\alpha_2) \left(\dot{\pi}_{\text{cl}} \dot{\pi}_{\text{q}} - c_s^2 \partial_i \pi_{\text{cl}} \partial_i \pi_{\text{cl}} \right) \tag{3.300}$$

   where we introduced

$$c_s^2 \equiv \frac{\alpha_1}{\alpha_1 - 2\alpha_2} \tag{3.301}$$

   which denotes the propagation speed of the Goldstone modes. The dispersion relation is the usual massless dispersion relation

$$\omega^2 = c_s^2 k^2. \tag{3.302}$$

2. When $\omega \ll E_{\text{diss}} \ll E_{\text{SSB}}$, we reach the low energy limit of the theory where dissipation dominates over the kinetic term. In this limit

$$\mathcal{L}_{\text{eff}} \simeq -\alpha_1 \partial_i \pi_{\text{cl}} \partial_i \pi_{\text{cl}} - 2\gamma_1 \dot{\pi}_{\text{cl}} \pi_{\text{q}} + i\beta_1 \pi_{\text{q}}^2 \tag{3.303}$$

   and the on-shell condition is satisfied when [255]

$$\det \begin{pmatrix} 0 & -\frac{1}{2}\alpha_1 k^2 - i\gamma_1 \omega \\ -\frac{1}{2}\alpha_1 k^2 + i\gamma_1 \omega & i\beta_1 \end{pmatrix} = 0. \tag{3.304}$$

We obtain the dispersion relation

$$\omega^2 = -\frac{\alpha_1^2}{4\gamma_1^2}k^4 \tag{3.305}$$

and the noise term β_1 does not affect the dispersion relation.

3. When $\omega \sim E_{\rm diss} \ll E_{\rm SSB}$, the intermediate regime requires both kinetic and dissipative contributions, such that

$$\mathcal{L}_{\rm eff} \simeq (\alpha_1 - 2\alpha_2)\left(\dot\pi_{\rm cl}\dot\pi_{\rm q} - c_s^2\partial_i\pi_{\rm cl}\partial_i\pi_{\rm cl} - \gamma\dot\pi_{\rm cl}\pi_{\rm q} + i\frac{A}{2}\pi_{\rm q}^2\right) \tag{3.306}$$

where we defined

$$\gamma \equiv \frac{2\gamma_1}{\alpha_1 - \alpha_2}, \qquad A \equiv \frac{2\beta_1}{\alpha_1 - \alpha_2}. \tag{3.307}$$

Solving the on-shell condition

$$\det\begin{pmatrix} 0 & \omega^2 - c_s^2k^2 - i\gamma\omega \\ \omega^2 - c_s^2k^2 + i\gamma\omega & iA \end{pmatrix} = 0 \tag{3.308}$$

we find

$$\omega^2 = c_s^2k^2 - \frac{\gamma^2}{2} \pm \sqrt{\frac{\gamma^4}{4} - \gamma^2c_s^2k^2}. \tag{3.309}$$

In the low-energy/large-dissipation regime $c_sk \ll \gamma \sim E_{\rm diss}$, there is a gapless and a gapped diffusive mode

$$\omega^2 \simeq -\frac{c_s^4k^4}{\gamma^2}, \qquad \omega^2 \simeq -\gamma^2 + 2c_s^2k^2. \tag{3.310}$$

On the other hand, for the short length scales satisfying $c_sk \gg \gamma \sim E_{\rm diss}$, there are two propagating modes with small dissipation

$$\omega^2 \simeq c_s^2k^2 \pm i\gamma c_sk. \tag{3.311}$$

The next step would consist in accessing the observables, starting with the equal-time correlators

$$\langle\pi_{\rm cl}(t,\boldsymbol{k})\pi_{\rm cl}(t,\boldsymbol{q})\rangle, \qquad \langle\pi_{\rm cl}(t,\boldsymbol{k}_1)\pi_{\rm cl}(t,\boldsymbol{k}_2)\pi_{\rm cl}(t,\boldsymbol{k}_3)\rangle, \qquad \cdots \tag{3.312}$$

directly relevant for cosmology. This task is harder than for closed system. Introducing the auxiliary field ξ through

$$i\frac{A}{2}\pi_{\rm q}^2 = \frac{i}{2A}\xi^2 + \xi\pi_{\rm q}, \tag{3.313}$$

in Eq. (3.306), we derive the equation of motion for $\pi_{\rm cl}$ from $\delta S_{\rm eff}/\delta\pi_{\rm q} = 0$, leading to the Langevin equation

$$\ddot\pi_{\rm cl} + 2\gamma\dot\pi_{\rm cl} + c_s^2k^2\pi_{\rm cl} = \xi \tag{3.314}$$

with the noise obeying

$$\langle \xi(t) \rangle = 0, \qquad \langle \xi(t)\xi(t') \rangle = A\delta(t-t'). \tag{3.315}$$

In order to obtain the mode functions, one needs to solve the homogeneous part of the equation to obtain a Green's function which is then convolved with the noise kernel. The observables can be computed following the method developed in [298] and recently applied in [299]. Note that in [298], the authors only considered the large-dissipation regime, having in mind applications to warm inflation [300]. Warm inflation [300] is a class of inflationary models where cosmological inhomogeneities are thermally produced, contrarily to the cold inflation paradigm where the amplification of vacuum fluctuations seed cosmological inhomogeneities. It provides a direct field of application for the formalism developed in this Section.

What did we learn? As a conclusion, this approach highlights the intricate structure connecting unitary and non-unitary evolution, relating dissipative effects to observables. Physical bounds impose constraints on the accessible EFT parameters, such as $\beta_1 > 0$. The non-linearly realised nature of the symmetries provides an interesting phenomenology to explore, relating linear dissipation and non-Gaussian features. Finally, the formalism does not impose the dynamical KMS symmetry, allowing us to access the complete out-of-equilibrium regime. In this way, it evades the main criticism against warm inflation [301] as it does not necessary require a thermal bath. Hence, the approach could potentially explore the intermediate regime between cold and warm inflation and in this way extend the results of [298] to a more sustainable regime.

Conclusions:

Open Effective Field Theories aim at capturing the effects of an unobservable environment onto the physics of a system we probe. In the context of cosmology, they provide a way to incorporate the impact of hidden sectors onto the curvature perturbations we observe in the CMB. They offer tools to better understand the quantum aspects of the early universe such as the so-called quantum-to-classical transitions of cosmological inhomogeneities. Open EFTs capture non-unitary effects such as dissipation and decoherence which make them particularly relevant to treat systems in which energy is not conserved. Their ability to perform late-time resummation of secular effects is also a desirable feature in the context of cosmology where perturbativity often breaks down at late-time. We presented the implementation of Open EFTs, from the definition of the bipartition to the development of resummation techniques. The relationship between the influence functional, the master equation and its stochastic unravelling has been established. A focus on master equations allowed us to highlight the ubiquity of non-Markovian dynamics in the presence of a non-stationary background. We also discussed the different facets of Markovianity and proposed some directions to develop this concept in cosmology. We finally explained how to compute the observables and assess quantum decoherence. Quantifying decoherence by evaluating the

purity is a way to estimate the amount of information that cannot be retrieved from a unitary EFT. Hence, it provides a way to evaluate the need for non-unitary extensions. We concluded the Chapter with the presentation of two active research directions, the first one concerning the development of non-perturbative resummation techniques and the second one investigating the bottom-up construction of Open EFTs.

Part II

Results and Publications

Outline

This second part collects the research articles published during the thesis. More precisely, in Chapter 4, we use group theoretic constructions to characterise the quantum state in which are placed cosmological inhomogeneities of two-field systems. In particular, we aim at characterising quantum decoherence when one of the fields is unobservable. In Chapter 5, we use an exactly solvable toy model in order to benchmark the master equation program in cosmology. We review the approximation schemes and regimes of validity and assess the ability of the master equation to implement a non-perturbative resummation. Finally, in Chapter 6, we apply these tools on a model of phenomonological interest in the context of primordial cosmology and account for a phenomenon of quantum recoherence. We emphasize how cosmological OQS can depart from their lab-based counterpart.

Chapter 4

Four-mode squeezed states

Preface

In this article, we derive the quantum state of a generic linear two-field system known as the four-mode squeezed states. These states constitute a multifield generalisation of the squeezing mechanism presented in Sec. 3.1.1. In particular, they allow us to discuss the dynamical generation of entanglement between two scalar degrees of freedom. In the inflationary context, it provides a theoretical framework for the study of de(re)coherence generated by entropic perturbations linearly coupled to the adiabatic sector, as we later did in [154].

The understanding of the four-mode squeezed states follows from the investigation of the group theoretic structure underlying the linear dynamics. Based on [121], we carried out a systematic study of the symplectic group $\mathrm{Sp}(4,\mathbb{R})$ which describes two-field linear canonical transformations. The understanding of its Lie algebra allowed us to write down a simple decomposition of the evolution operator in terms of elementary gates, the building blocks of the dynamical evolution, from which we can derive the four-mode squeezed states.

In the Fock space, these states can be understood as the tensor product of two two-mode squeezed states on the top of which quanta can be exchanged. In the phase space, they have a simpler representation, as they belong to the class of Gaussian states. In this representation, the non-perturbative connection between the purity and the determinant of the system covariance matrix given in Eq. (3.228) is the more apparent. Hence, working in the phase space is particular convenient for Gaussian states.

In the next pages, before exposing the article, we briefly highlight the physics at play in the study of the four-mode squeezed states which can be sometimes obscured by the mathematical formalism. We construct the discussion in light of the knowledge gained after the publication of [251], in our later articles presented in the next Chapters.

The article [251] can be found online at:

- https://link.springer.com/article/10.1140/epjc (published version);
- https://arxiv.org/abs/2104.14942 (arXiv version).

The physics behind four-mode squeezed states

This brief discussion aims at highlighting the benefit of the formulation presented in [251] which relies in providing a microphysical understanding of the mechanism of quantum decoherence. Thought as a supplemental material, notations are loosely introduced, all details being found in the article. We first review the structure of the state before we discuss its learnings about quantum decoherence. Lastly, we provide a brief description of the phenomenology depending on the mass of scalar fields.

Understanding four-mode squeezed states

Let us discuss the circuit derived in Appendix B which represents the dynamical evolution from the Bunch-Davies vacuum in the asymptotic past to the four-mode squeezed states in the asymptotic future. We reproduce it in Fig. 4.1 and discuss its various elements.

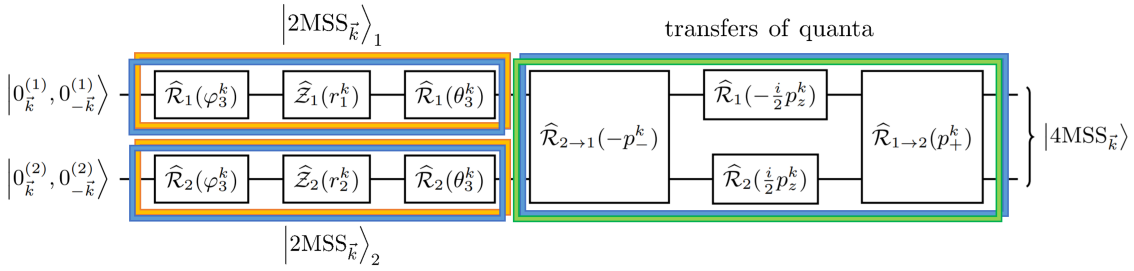

Figure 4.1: Four-mode squeezed states can be understood as two copies of the two-mode squeezed states, one for the system and one for the environment, on the top of which quanta can be exchanged. Orange boxes represent pair creation, green box represents transfers of quanta and blue boxes represent phase shifts.

The circuit is made of three elementary operations

$$\widehat{\mathcal{R}}_{i,\vec{k}}(\theta_k) \equiv \exp\left[-i\theta_k\left(\widehat{a}^\dagger_{i,\vec{k}}\widehat{a}_{i,\vec{k}} + \widehat{a}^\dagger_{i,-\vec{k}}\widehat{a}_{i,-\vec{k}} + 1\right)\right] , \tag{4.1}$$

$$\widehat{\mathcal{Z}}_{i,\vec{k}}(r_k) \equiv \exp\left[r_k\left(\widehat{a}^\dagger_{i,\vec{k}}\widehat{a}^\dagger_{i,-\vec{k}} - \widehat{a}_{i,\vec{k}}\widehat{a}_{i,-\vec{k}}\right)\right] , \tag{4.2}$$

$$\widehat{\mathcal{R}}_{i\to j,\vec{k}}(p_k) \equiv \exp\left[ip_k\left(\widehat{a}^\dagger_{j,\vec{k}}\widehat{a}_{i,\vec{k}} + \widehat{a}^\dagger_{j,-\vec{k}}\widehat{a}_{i,-\vec{k}}\right)\right] . \tag{4.3}$$

Among these operations, only Eq. (4.2) is able to modify the number of excitations. Hence, it plays a crucial role in populating the vacuum. Then, the parameters r_1^k and r_2^k appearing in Fig. 4.1 are the one controlling the occupation number in both the system and the environment. We also observe that only Eq. (4.3) is able to transfer quanta from the system to the environment (and reversely). Therefore, the parameters p_-^k and p_+^k are the one controlling the mixing between the two sectors.

Learnings about quantum decoherence

In this Manuscript, we often assess decoherence through the mean of the purity. Being related to the linear entropy by $S_\mathrm{L} \equiv 1 - \gamma$, it reminds us that decoherence

can be understood as an increase of the amount of information shared between the system and its environment that cannot be retrieved by performing measurements on the system only [193]. In order to observe such an increase, one first needs to populate the state, otherwise, there is no information to share in the vacuum. Hence, considering Fig. 4.1, it appears that a preliminary requirement for decoherence to take place consists in having r_1^k and r_2^k able to stir pairs of quanta out of the vacuum. Then, decoherence proceeds if correlations initially contained within the system are delocalised to the environment. The mixing occurs through transfers of quanta, which is controlled by p_-^k and p_+^k.

In [251], we carry an systematic small-coupling expansion which can be understood as an expansion in the number of quanta exchanged between the system and its environment. It appears that the expansion is controlled by a parameter $|\tau_k|$ such that $p_\pm^k \propto \mathcal{O}(|\tau_k|)$. Working at order $\mathcal{O}(|\tau_k|^n)$ implies we consider the exchange of n quanta between the two sectors. Using the perturbative expansion of the system's spectra and the purity, we identified in Eq. 6.21 a regime of parameters in which decoherence is effective without substantially affecting the system's observables

$$e^{-\left(r_1^k + r_2^k\right)} \ll |\tau_k| \ll 1. \tag{4.4}$$

Therefore, in the large squeezing regime, it implies that one can remain within the observational window of single-field slow roll inflation without having anymore any chance to observe genuine quantum signatures due to quantum decoherence. The larger are the squeezing parameters r_1^k and r_2^k, the larger is the window. This observation seems consistent with the above requirement of populating the state before sharing information.

Phenomenology for massive scalars

Based on the above observations, we would like to understand the behaviour of the squeezing parameters in practical situations such as the one described in [154] presented in Chapter 6. In particular, we would like to understand if the dynamics fall into the regime of Eq. (4.4). Answering this question in full generality appears to be extremely challenging, as it requires to invert the ten algebraic non-linear equations given in Eqs 5.23 to 5.32 in order to express the squeezing parameters in terms of the entries of the covariance matrix. Even in the perturbative limit, at second order in $|\tau_k|$, it remains a difficult task, beyond the scope of this brief discussion, which might be the object of future works.

Yet, some intuition about the phenomenology can be obtained by considering the decoupling limit of the theory. Working in the perturbative regime, the evolution of the system is mainly controlled by the free dynamics of massive scalar fields in a de Sitter background. Moreover, in the Open EFT approach, the properties of the environment are encoded through the memory kernel, which is the Wightman function of the environment computed in the free theory. Hence, it is insightful to consider the dynamics of the squeezing parameters of a free massive scalar in a de Sitter background. In this case, the state is given by

$$\left|2\mathrm{MSS}_{\vec{k}}\right\rangle = \frac{e^{-2i\theta_k}}{\cosh r_k} \sum_{n=0}^{\infty} (-1)^n e^{-2in\varphi_k} \tanh^n r_k \left|n_{\vec{k}}, n_{-\vec{k}}\right\rangle \tag{4.5}$$

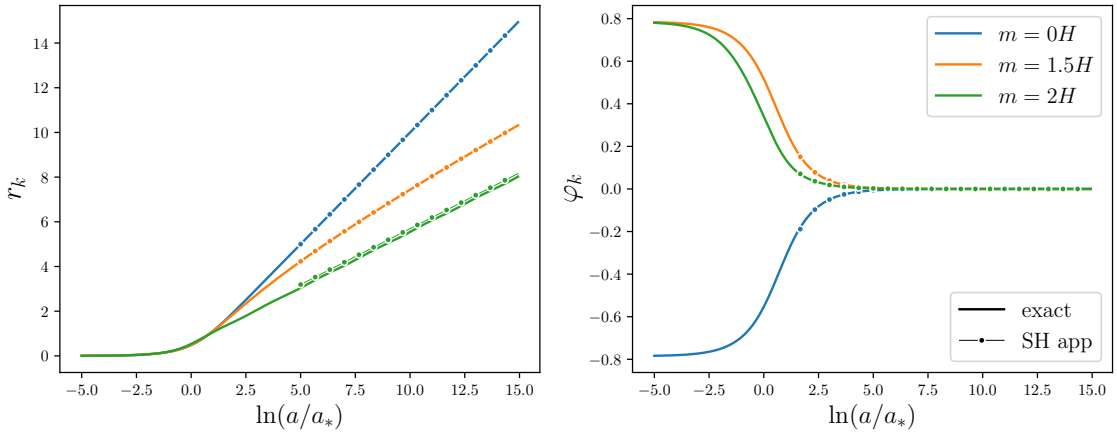

Figure 4.2: Squeezing parameters as a function of the number of efolds before and after Hubble crossing. *Left:* r_k grows in the super-Hubble regime faster for lighter environments *Right:* φ_k converges toward zero in the super-Hubble regime, with opposite sign for light ($m < 3H/2$) and heavy ($m \geq 3H/2$) environments. Dotted lines are late-time expansions in $k \ll aH$ and $m \gg H$ given in Eq. (4.10). The small mismatch between plain and dotted lines on r_k (*left* figure) for $m = 2H$ (*green* curve) is due to the fact that the assumption $m \gg H$ used to reach simple analytical expressions is not fully satisfied in this case.

where θ_k is a global phase we can discard for the discussion. The squeezing parameters r_k and φ_k are related to the two-point functions through (see e.g. [121])

$$\cosh(2r_k) = k\mathbf{Cov}_{11,k} + k^{-1}\mathbf{Cov}_{22,k} \tag{4.6}$$

$$\tan(2\varphi_k) = \frac{2\mathbf{Cov}_{12,k}}{k\mathbf{Cov}_{11,k} - k^{-1}\mathbf{Cov}_{22,k}} \tag{4.7}$$

where we use the same notations as in [251]. Therefore, once the power spectra are known (for instance using the mode functions for a massive field in de Sitter), one can deduce the squeezing parameters.

In [154], we observe that depending on the mass of the environment, curvature perturbations either experience quantum decoherence (for light environments $m < 3H/2$) or recoherence (for heavy environments $m \geq 3H/2$), see Fig. 3 of [154]. This behaviour can be traced back to the mode function dynamics of massive scalar fields in de Sitter. In Figs. 4.2 and 4.3, we complement this analysis by presenting the massive environment dynamics in terms of its squeezing parameters. It can be seen that, indeed, light and heavy environments have a different behaviour in terms of these parameters: heavy fields experience less squeezing (*Left* panel of Fig. 4.2) which is directed in an opposite direction (*Right* panel of Fig. 4.2) compared to light environments. Late-time analytical behaviour can be readily obtained by expecting the power spectra in Eqs. (4.6) and (4.7) in powers of $k \ll aH$ and $m \gg H$ (note that for the lightest case, we here considered a massless environment instead of

$m = H$ which is used in Fig. 3 of [154]). The leading order is controlled by[1]

$$r_k \simeq \begin{cases} \ln \frac{aH}{k} \\ \frac{1}{2} \ln \frac{aH}{k} + \ln\left(\ln \frac{aH}{k}\right) \\ \frac{1}{2} \ln \frac{am}{k} \end{cases} \quad \text{and} \quad \varphi_k \simeq \begin{cases} -\frac{k}{qH} & \text{for } m = 0H \\ \frac{2}{3}\frac{k}{aH} & \text{for } m = 3H/2 \\ \frac{3}{2}\frac{H^2}{m^2}\frac{k}{aH} & \text{for } m = 2H \end{cases} \tag{4.10}$$

Lastly, squeezed states being Gaussian states, their Wigner function can be represented in the phase space in terms of ellipses which are the σ contours of the multivariate Gaussian [302]. In Fig. 4.3, it can be seen that light and heavy fields tend to be anti-correlated due to their opposite sign in φ_k.

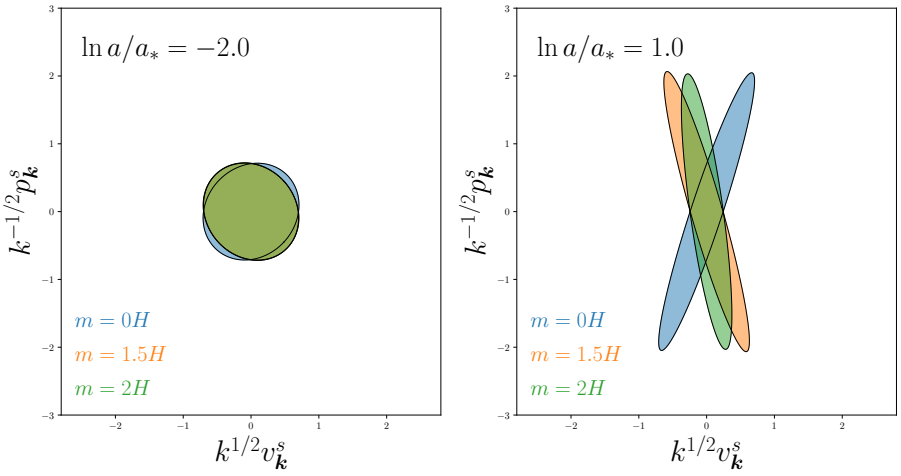

Figure 4.3: Phase-space representation of the state (1σ contour) two efolds before Hubble crossing (*Left*) and one efold after Hubble crossing (*Right*). Squeezed states being Gaussian, they can be represented as ellipses in the phase space [302]. Light ($m < 3H/2$) and heavy ($m \geq 3H/2$) environments tend to be anti-correlated due to their opposite sign in φ_k. Courtesy of A. Micheli for friendly sharing plotting code used in [226].

This limited study hopefully highlights some of the differences between light and heavy environments expressed in terms of their squeezing parameters. Further investigations would be necessary in order to fully account for the observations of [154] in the language of [251]. In particular, it would be interesting to understand when the regime presented in Eq. (4.4) is entered in terms of the microphysical parameters of the problem. We leave it for future work.

[1] For $m = 3H/2$, the exact expressions are

$$r_k = \frac{1}{2} \ln \left[\frac{\left|6\left(\gamma_{\mathrm{E}} + \ln \frac{z}{2}\right) + 4 - 3i\pi\right|^2}{8\pi z} + \mathcal{O}(z) \right] \tag{4.8}$$

$$\varphi_k = \frac{2z\left[3\pi^2 + 8\left(\gamma_{\mathrm{E}} + \ln \frac{z}{2}\right) + 12\left(\gamma_{\mathrm{E}} + \ln \frac{z}{2}\right)^2\right]}{\left|6\left(\gamma_{\mathrm{E}} + \ln \frac{z}{2}\right) + 4 - 3i\pi\right|^2} + \mathcal{O}(z^2) \tag{4.9}$$

where $z \equiv k/aH$. Simplified expressions are given in Eq. (4.10) to improve the comparison.

Four-mode squeezed states: two-field quantum systems and the symplectic group $\mathrm{Sp}(4,\mathbb{R})$

Thomas Colas,[a,b] **Julien Grain,**[a] **Vincent Vennin**[b]

[a]Université Paris-Saclay, CNRS, Institut d'Astrophysique Spatiale, 91405, Orsay, France
[b]Laboratoire Astroparticule et Cosmologie, Université Denis Diderot Paris 7, 10 rue Alice Domon et Léonie Duquet, 75013 Paris, France

E-mail: thomas.colas@universite-paris-saclay.fr, julien.grain@universite-paris-saclay.fr, vincent.vennin@apc.in2p3.fr

Abstract. We construct the four-mode squeezed states and study their physical properties. These states describe two linearly-coupled quantum scalar fields, which makes them physically relevant in various contexts such as cosmology. They are shown to generalise the usual two-mode squeezed states of single-field systems, with additional transfers of quanta between the fields. To build them in the Fock space, we use the symplectic structure of the phase space. For this reason, we first present a pedagogical analysis of the symplectic group $\mathrm{Sp}(4,\mathbb{R})$ and its Lie algebra, from which we construct the four-mode squeezed states and discuss their structure. We also study the reduced single-field system obtained by tracing out one of the two fields. This procedure being easier in the phase space, it motivates the use of the Wigner function which we introduce as an alternative description of the state. It allows us to discuss environmental effects in the case of linear interactions. In particular, we find that there is always a range of interaction coupling for which decoherence occurs without substantially affecting the power spectra (hence the observables) of the system.

Contents

1 Introduction

Two-mode squeezed states [1–3] have been widely studied in the past for the important role they play in quantum optics (see *e.g.* Refs. [4, 5] for reviews), but also in the cosmological context where they describe primordial density perturbations, amplified by gravitational instability from the vacuum quantum fluctuations [6–12]. In general, they characterise the quantum state of linear single-field systems, where each pair of Fourier modes is placed in a two-mode squeezed state [13].

When more degrees of freedom are present however, two-mode squeezed state are insufficient and the squeezing formalism needs to be generalised to higher numbers of modes.

This is why, in this work, we construct the four-mode squeezed states, which describe two linearly-coupled quantum scalar fields. The motivation behind this analysis is twofold. First, there are a number of situations where two-field systems are directly relevant, for instance during the inflationary phase our primordial universe underwent. Even if current cosmological data is consistent with single-field setups [14], from a theoretical point of view, inflation takes place in a regime that is far beyond the reach of accelerators, and most physical setups that have been proposed to embed inflation contain extra scalar fields, for instance in the string-theoretic context [15–19]. Those additional degrees of freedom are usually associated to entropic perturbations. Four-mode squeezed states would then naturally appear in two-field inflation models, and provide insight about multi-field cosmology in general. Second, this setup provides a way to investigate environmental effects in the case of linear interactions, by tracing over one of the two fields. More precisely, when the system of observational relevance couples to unobserved degrees of freedom (referred to as the "environment"), quantum entanglement builds up between the system and the environment. This affects observational predictions and also leads to the quantum decoherence of the observable sector [20–22]. This phenomenon is usually investigated by the means of effective methods that only provide results that are perturbative in the interaction strength and that rely on additional assumptions, see *e.g.* Ref. [23]. By considering that one of the two fields represents the observed system and the other field stands for the environment, the formalism we develop will allow us to go beyond those methods and present exact results.

Let us stress that the explicit construction of the squeezed quantum states, especially in the Fock's space, is not only of formal interest. As we will explain, it provides important insight into the physical mechanisms at play in the dynamics of those states and in the emergence of peculiar properties such as quantum entanglement. Furthermore, it is required in a number of concrete computations (see for instance Refs. [24–28]).

Although we are inspired by problems formulated in the context of cosmology, it is worth mentioning that the formalism we develop here is generic and broad in applicability. It does not require prior knowledge of the concepts and tools relevant in cosmology (which will only be mentioned in our concluding remarks for illustrative purpose), to which we plan to apply our results in separate publications.

Let us now describe how this article is organised, and highlight its main results. In Sec. 2, we introduce the physical setup describing two free scalar fields, both at the classical and quantum levels, and we highlight the symplectic structure that underlies its phase space. This leads us to introducing the symplectic group in four dimensions, $\mathrm{Sp}(4,\mathbb{R})$, which we formally describe in Sec. 3. This section reviews material that may also be found in other references on the same topic (apart from the fully factorised form of group elements, Eq. (3.22), which, up to our knowledge, is a new result), see *e.g.* Refs. [29–33]. As a consequence, it may be skipped by those readers already familiar with the use of symplectic groups in quantum mechanics. Otherwise, it provides a self-contained presentation of the techniques employed in the rest of the paper. The Hamiltonians leading to the four-mode squeezed states are then built in Sec. 4, where we also construct the evolution operator using theses results. In particular, we comment on the physical interpretation of the generators of the Lie algebra, when acting in the Hamiltonian. As an example, we also briefly apply our formalism to describe two massless fields in a cosmological background. Finally, we use the previous results to write a tractable expression for the evolution operator from which four-mode squeezed states can be obtained. Sec. 5 is devoted to the explicit construction of the four-mode squeezed states in the Fock basis, see Eqs. (5.6) and (5.7), which constitute one of the main results of this

paper. An expansion around the limit where the two fields are uncoupled further allows us to discuss the physical interpretation of these formulas, to interpret the four-mode squeezed states in terms of particle transfer and to link their structure to the relevant microphysical parameters. We also derive the Wigner function of the system, which provides an alternative description of the state in the phase space. Although equivalent to the Fock-space description, its simple Gaussian form, built out of the power spectra of the configuration fields, makes some calculations simpler. Finally, in Sec. 6, we investigate environmental effects by tracing out one of the two fields and studying how the reduced quantum state of the first field is affected. This is done both at the level of the density matrix and of the Wigner function. Two independent calculations of the purity are thus performed, and then expanded in the small-coupling limit where they are shown to lead to the same result. Sec. 7 presents our conclusions, and the paper ends by four appendices to which various technical aspects of the calculations presented in the main text are deferred.

2 Quantum phase space of two free fields

2.1 Two scalar fields in a homogeneous and isotropic background

Let us consider two real-valued scalar fields $\phi_1(t,\vec{x})$ and $\phi_2(t,\vec{x})$, with conjugate momenta $\pi_1(t,\vec{x})$ and $\pi_2(t,\vec{x})$. These phase-space coordinates can be arranged into the four-dimensional vector $\boldsymbol{z}(\vec{x}) = (\phi_1(\vec{x}), \phi_2(\vec{x}), \pi_1(\vec{x}), \pi_2(\vec{x}))^{\mathrm{T}}$ where "T" stands for the transpose and explicit time dependence is dropped for notational convenience. In this work, for simplicity, we focus on the case of free fields, for which the Hamiltonian H is a local quadratic form,

$$H = \frac{1}{2}\int \mathrm{d}^3\vec{x}\boldsymbol{z}^{\mathrm{T}}(\vec{x})\boldsymbol{H}(t)\boldsymbol{z}(\vec{x})\,. \tag{2.1}$$

In the cosmological context, one may view ϕ_1 and ϕ_2 as two test fields (*i.e.* they do not backreact on the background geometry), or as the perturbations of some cosmological fields where cosmological perturbation theory is carried out at leading order. In Eq. (2.1), $\boldsymbol{H}(t)$ is a four-by-four real symmetric matrix, which we assume does not depend on the spatial coordinate $\vec{x}$, so the background on which the fields evolve is homogeneous. Note that $\boldsymbol{H}(t)$ may however involve the gradient operator $\partial/\partial\vec{x}$ (though to positive powers only, to be compatible with the locality assumption).

Phase space is equipped with the Poisson bracket

$$\{F,G\} = \int \mathrm{d}^3\vec{x}\left[\frac{\delta F}{\delta\phi_1(\vec{x})}\frac{\delta G}{\delta\pi_1(\vec{x})} - \frac{\delta F}{\delta\pi_1(\vec{x})}\frac{\delta G}{\delta\phi_1(\vec{x})} + \frac{\delta F}{\delta\phi_2(\vec{x})}\frac{\delta G}{\delta\pi_2(\vec{x})} - \frac{\delta F}{\delta\pi_2(\vec{x})}\frac{\delta G}{\delta\phi_2(\vec{x})}\right], \tag{2.2}$$

which can be written in matricial form for the phase-space coordinates as

$$\{\boldsymbol{z}(\vec{x}), \boldsymbol{z}^T(\vec{y})\} = \boldsymbol{\Omega}\delta^3(\vec{x}-\vec{y})\,. \tag{2.3}$$

In this expression, δ is the Dirac distribution, the matrix $\boldsymbol{\Omega}$ is given by

$$\boldsymbol{\Omega} = \begin{pmatrix} 0 & \boldsymbol{I}_2 \\ -\boldsymbol{I}_2 & 0 \end{pmatrix}, \tag{2.4}$$

where $\boldsymbol{I}_n$ is the $n \times n$ identity matrix, and the notation in Eq. (2.3) has to be understood as $\{\boldsymbol{z}_\mu(\vec{x}), \boldsymbol{z}_\nu(\vec{y})\} = \boldsymbol{\Omega}_{\mu\nu}\delta^3(\vec{x}-\vec{y})$ with $\mu, \nu = 1 \cdots 4$. The time evolution of any function F of the phase-space field variables is given by

$$\dot{F}(\boldsymbol{z}) = \{F(\boldsymbol{z}), H\}\,, \tag{2.5}$$

where a dot means differentiating with respect to the time variable.

Fourier space

Since the background is homogeneous, it is useful to work in Fourier space and to introduce

$$\boldsymbol{z}_{\vec{k}} = \begin{pmatrix} \phi_{1,\vec{k}} \\ \phi_{2,\vec{k}} \\ \pi_{1,\vec{k}} \\ \pi_{2,\vec{k}} \end{pmatrix} = \int \frac{\mathrm{d}^3\vec{x}}{(2\pi)^{3/2}} \boldsymbol{z}(\vec{x}) e^{-i\vec{k}.\vec{x}}. \tag{2.6}$$

The condition for the fields to be real-valued, $\boldsymbol{z}(\vec{x}) = \boldsymbol{z}^*(\vec{x})$, translates into $\boldsymbol{z}^*_{\vec{k}} = \boldsymbol{z}_{-\vec{k}}$. This means that half of the Fourier modes are enough to parametrise the entire (now complex) phase space. In practice, any integral over $k \in \mathbb{R}^3$ can be split into an integral over $\mathbb{R}^{3+} \equiv \mathbb{R}^2 \times \mathbb{R}^+$ and $\mathbb{R}^{3-} \equiv \mathbb{R}^2 \times \mathbb{R}^-$, where the latter can be related to the former by a simple change of integration variable $\vec{k} \to -\vec{k}$ and using the relation $\boldsymbol{z}^*_{\vec{k}} = \boldsymbol{z}_{-\vec{k}}$. For the Hamiltonian (2.1), this leads to

$$H = \int_{\mathbb{R}^{3+}} \mathrm{d}^3\vec{k}\, \boldsymbol{z}^\dagger_{\vec{k}} \boldsymbol{H}_k(t) \boldsymbol{z}_{\vec{k}}\,, \tag{2.7}$$

which avoids double counting the degrees of freedom of the theory. In Eq. (2.7), $\boldsymbol{H}_k(t)$ corresponds to $\boldsymbol{H}(t)$ where the spatial gradient $\partial/\partial\vec{x}$ is replaced with $i\vec{k}$. If we further assume the background to be isotropic, $\boldsymbol{H}_k(t)$ only depends on the norm $k = |\vec{k}|$ of $\vec{k}$, hence the notation.

Plugging Eq. (2.6) into Eq. (2.2), one can compute

$$\{\boldsymbol{z}_{\vec{k}}, \boldsymbol{z}^\dagger_{\vec{q}}\} = \boldsymbol{\Omega}\delta^3(\vec{k}-\vec{q})\,, \tag{2.8}$$

which is of the same form as Eq. (2.3). This shows that the Poisson brackets are preserved when going to Fourier space (in the language that will be introduced in Sec. 2.2, the Fourier transform is a "symplectic transformation"), so phase space can be equivalently parametrised with the Fourier coordinates, and the Poisson bracket (2.2) can also be written as

$$\{F, G\} = \int_{\mathbb{R}^3} \mathrm{d}^3\vec{k} \left(\frac{\delta F}{\delta\phi_{1,\vec{k}}} \frac{\delta G}{\delta\pi^*_{1,\vec{k}}} - \frac{\delta F}{\delta\pi_{1,\vec{k}}} \frac{\delta G}{\delta\phi^*_{1,\vec{k}}} + \frac{\delta F}{\delta\phi_{2,\vec{k}}} \frac{\delta G}{\delta\pi^*_{2,\vec{k}}} - \frac{\delta F}{\delta\pi_{2,\vec{k}}} \frac{\delta G}{\delta\phi^*_{2,\vec{k}}} \right). \tag{2.9}$$

Finally, applying the equation of motion (2.5) to the Fourier phase-space coordinates yields

$$\dot{\boldsymbol{z}}_{\vec{k}} = (\boldsymbol{\Omega}\boldsymbol{H}_k)\, \boldsymbol{z}_{\vec{k}}\,, \tag{2.10}$$

where the explicit time dependence of $\boldsymbol{H}_k$ has been dropped for notational convenience. This equation shows that, for free fields in a homogeneous and isotropic background, Fourier modes decouple and evolve independently. This implies that each Fourier sector can be studied separately, which greatly simplifies the analysis. From now on, we therefore focus on a single Fourier sector, *i.e.* $\vec{k}$ in $\mathbb{R}^{3+}$ is fixed hereafter.

Quantisation

So far, linear Hamiltonian systems have been described at the classical level. We now follow the canonical quantisation prescriptions and promote the phase-space coordinates to quantum operators acting on a Hilbert space, $\widehat{\boldsymbol{z}}_{\vec{k}} := (\widehat{\phi}_{1,\vec{k}}, \widehat{\phi}_{2,\vec{k}}, \widehat{\pi}_{1,\vec{k}}, \widehat{\pi}_{2,\vec{k}})^{\mathrm{T}}$ (where, from now on, hats denote quantum operators). These operators satisfy the canonical commutation relations

$$\left[\widehat{\boldsymbol{z}}_{\vec{k}}, \widehat{\boldsymbol{z}}^{\dagger}_{\vec{q}}\right] = i\boldsymbol{\Omega}\delta^3(\vec{k}-\vec{q})\,, \tag{2.11}$$

which is the quantum analogue of Eq. (2.8) and where, hereafter, we work with $\hbar = 1$. The Hamiltonian operator reads $\widehat{H} = \int_{\mathbb{R}^{3+}} \mathrm{d}^3\vec{k}\,\widehat{\boldsymbol{z}}^{\dagger}_{\vec{k}}\boldsymbol{H}_k\widehat{\boldsymbol{z}}_{\vec{k}}$, and the dynamics of any function of the quantum phase-space variables is given by the Heisenberg equation $\dot{F}(\widehat{\boldsymbol{z}}_{\vec{k}}) = -i[F(\widehat{\boldsymbol{z}}_{\vec{k}}), \widehat{H}]$. In particular, for the field variables themselves, this gives rise to $\dot{\widehat{\boldsymbol{z}}}_{\vec{k}} = (\boldsymbol{\Omega}\boldsymbol{H}_k)\widehat{\boldsymbol{z}}_{\vec{k}}$, which directly transposes Eq. (2.10).

Creation and annihilation operators are defined in the usual way, *i.e.*

$$\widehat{a}_{j,\vec{k}} = \frac{1}{\sqrt{2}}\left(\sqrt{k}\widehat{\phi}_{j,\vec{k}} + \frac{i}{\sqrt{k}}\widehat{\pi}_{j,\vec{k}}\right) \quad \text{for} \quad j = 1, 2\,, \tag{2.12}$$

where the prefactors $\sqrt{k}$ and $1/\sqrt{k}$ are introduced for dimensional reasons. This can be written in matricial form as

$$\widehat{\boldsymbol{a}}_{\vec{k}} = \begin{pmatrix} \widehat{a}_{1,\vec{k}} \\ \widehat{a}_{2,\vec{k}} \\ \widehat{a}^{\dagger}_{1,-\vec{k}} \\ \widehat{a}^{\dagger}_{2,-\vec{k}} \end{pmatrix} = \boldsymbol{U}\boldsymbol{D}_k\widehat{\boldsymbol{z}}_{\vec{k}}\,, \tag{2.13}$$

where "†" stands for the conjugate transpose, and the matrices $\boldsymbol{U}$ and $\boldsymbol{D}_k$ are defined as

$$\boldsymbol{U} = \frac{1}{\sqrt{2}}\begin{pmatrix} \boldsymbol{I}_2 & i\boldsymbol{I}_2 \\ \boldsymbol{I}_2 & -i\boldsymbol{I}_2 \end{pmatrix} \quad \text{and} \quad \boldsymbol{D}_k = \begin{pmatrix} \sqrt{k}\boldsymbol{I}_2 & 0 \\ 0 & \boldsymbol{I}_2/\sqrt{k} \end{pmatrix}. \tag{2.14}$$

One can check that $\boldsymbol{U}$ is a unitary matrix, *i.e.* $\boldsymbol{U}\boldsymbol{U}^{\dagger} = \boldsymbol{U}^{\dagger}\boldsymbol{U} = \boldsymbol{I}_4$. In principle, $\boldsymbol{D}_k$ may be replaced with $\boldsymbol{M}_k\boldsymbol{D}_k$, where $\boldsymbol{M}_k$ is any (dimensionless) symplectic matrix (formally defined below in Sec. 2.2). It only leads to a different definition of the vacuum state (*i.e.* the state that is annihilated by the annihilation operators) [13]. Let us note that the ordering in $\widehat{\boldsymbol{a}}_{\vec{k}}$ is different than in $\widehat{\boldsymbol{z}}_{\vec{k}}$, since in $\widehat{\boldsymbol{a}}_{\vec{k}}$ the first two entries concern the $\vec{k}$ sector and the last two entries the $-\vec{k}$ sector.[1]

The dynamics of the creation and annihilation operators is generated by the quadratic Hamiltonian $\widehat{\mathcal{H}} = \int_{\mathbb{R}^{3+}} \mathrm{d}^3\vec{k}\,\widehat{\boldsymbol{a}}^{\dagger}_{\vec{k}}\boldsymbol{\mathcal{H}}_k\widehat{\boldsymbol{a}}_{\vec{k}}$, where $\boldsymbol{\mathcal{H}}_k$ reads [13]

$$\boldsymbol{\mathcal{H}}_k = \boldsymbol{U}\left[(\boldsymbol{D}_k^{-1})^{\mathrm{T}}\boldsymbol{H}_k\boldsymbol{D}_k^{-1} + (\boldsymbol{D}_k^{-1})^{\mathrm{T}}\boldsymbol{\Omega}\dot{\boldsymbol{D}}_k^{-1}\right]\boldsymbol{U}^{\dagger}\,. \tag{2.15}$$

[1] This is because the classical version of Eq. (2.13) gives $\boldsymbol{z}_{-\vec{k}} = \boldsymbol{D}_k^{-1}\boldsymbol{U}^{\dagger}\boldsymbol{a}_{-\vec{k}}$ and $\boldsymbol{z}^*_{\vec{k}} = \boldsymbol{D}_k^{-1}\boldsymbol{U}^{\mathrm{T}}\boldsymbol{a}^*_{\vec{k}}$. The reality condition $\boldsymbol{z}^*_{\vec{k}} = \boldsymbol{z}_{-\vec{k}}$ thus entails $\boldsymbol{a}_{-\vec{k}} = \boldsymbol{U}\boldsymbol{U}^{\mathrm{T}}\boldsymbol{a}^*_{\vec{k}}$, where $\boldsymbol{U}\boldsymbol{U}^{\mathrm{T}} = \begin{pmatrix} 0 & \boldsymbol{I}_2 \\ \boldsymbol{I}_2 & 0 \end{pmatrix}$, explaining the structure of the $\widehat{\boldsymbol{a}}_{\vec{k}}$ vector.

The canonical commutation relations are given by

$$\left[\widehat{\boldsymbol{a}}_{\vec{k}}, \widehat{\boldsymbol{a}}_{\vec{q}}^{\dagger}\right] = i\boldsymbol{\mathcal{J}}\delta^3(\vec{k}-\vec{q}) \quad \text{where} \quad \boldsymbol{\mathcal{J}} = \boldsymbol{U}\boldsymbol{\Omega}\boldsymbol{U}^{\dagger} = -i\begin{pmatrix}\boldsymbol{I}_2 & 0\\ 0 & -\boldsymbol{I}_2\end{pmatrix}, \tag{2.16}$$

and any function of the creation and annihilation operators evolves according to $\dot{F}(\widehat{\boldsymbol{a}}_{\vec{k}}) = \left[F(\widehat{\boldsymbol{a}}_{\vec{k}}), \widehat{\mathcal{H}}\right]$. In particular, for the creation and annihilation operators themselves, one obtains

$$\dot{\widehat{\boldsymbol{a}}}_{\vec{k}} = (\boldsymbol{\mathcal{J}}\boldsymbol{\mathcal{H}}_k)\,\widehat{\boldsymbol{a}}_{\vec{k}}. \tag{2.17}$$

2.2 Symplectic structure of the phase space

In Sec. 2.1, we saw that the Fourier transform preserves the Poisson brackets of the phase-space variables. Another example of a transformation that preserves the Poisson brackets is provided by the Hamiltonian evolution itself. Indeed, the equation of motion (2.10) can be solved as

$$\boldsymbol{z}_{\vec{k}}(t) = \boldsymbol{G}_k(t, t_{\rm in})\boldsymbol{z}_{\vec{k}}(t_{\rm in}), \tag{2.18}$$

where $\boldsymbol{G}_k$ is a (4×4)-real matrix called the Green's matrix and that satisfies $\dot{\boldsymbol{G}}_k = \boldsymbol{\Omega}\boldsymbol{H}_k\boldsymbol{G}_k + \boldsymbol{I}_4\delta(t-t_{\rm in})$, with initial condition $\boldsymbol{G}_k(t_{\rm in}, t_{\rm in}) = \boldsymbol{I}_4$. Note that, as $\boldsymbol{H}_k$, $\boldsymbol{G}_k$ only depends on the wavenumber k. One can also check that $\boldsymbol{G}_k$ satisfies

$$\boldsymbol{G}_k^{\rm T}\boldsymbol{\Omega}\boldsymbol{G}_k = \boldsymbol{\Omega}. \tag{2.19}$$

This is indeed obviously the case at initial time, and by plugging the equation of motion for $\boldsymbol{G}_k$ in the time derivative of the left-hand-side of Eq. (2.19), one obtains a vanishing result after using that $\boldsymbol{H}_k$ is symmetric and that $\boldsymbol{\Omega}^{\rm T}\boldsymbol{\Omega} = -\boldsymbol{\Omega}^2 = \boldsymbol{I}_4$.

In general, real matrices satisfying Eq. (2.19) are called symplectic, and they form the symplectic group $\mathrm{Sp}(4,\mathbb{R})$. They describe all possible reparametrisations of phase space through linear canonical transformations, *i.e.* transformations that preserve the Poisson brackets. Indeed, consider two phase-space coordinates $\boldsymbol{z}_{\vec{k}}$ and $\widetilde{\boldsymbol{z}}_{\vec{k}}$, related through a linear transformation

$$\widetilde{\boldsymbol{z}}_{\vec{k}} = \boldsymbol{M}_k\boldsymbol{z}_{\vec{k}}. \tag{2.20}$$

One can check that the Poisson brackets are preserved, *i.e.* $\{\widetilde{\boldsymbol{z}}_{\vec{k}}, \widetilde{\boldsymbol{z}}_{\vec{k}}^{\dagger}\} = \{\boldsymbol{z}_{\vec{k}}, \boldsymbol{z}_{\vec{q}}^{\dagger}\} = \boldsymbol{\Omega}$, if and only if $\boldsymbol{M}_k \in \mathrm{Sp}(4,\mathbb{R})$ [*i.e.* $\boldsymbol{M}_k$ satisfies Eq. (2.19)]. This ensures that the Poisson bracket between two arbitrary phase-space functions is the same when calculated with the $\boldsymbol{z}_{\vec{k}}$-variables or with the $\widetilde{\boldsymbol{z}}_{\vec{k}}$-variables. One can check that the equations of motion for the new set of canonical variables $\widetilde{\boldsymbol{z}}_{\vec{k}}$ are then given by Hamilton equations with the new Hamiltonian kernel

$$\widetilde{\boldsymbol{H}}_k = (\boldsymbol{M}_k^{-1})^{\rm T}\boldsymbol{H}_k\boldsymbol{M}_k^{-1} + (\boldsymbol{M}_k^{-1})^{\rm T}\boldsymbol{\Omega}\dot{\boldsymbol{M}}_k^{-1}, \tag{2.21}$$

and the dynamics is solved by $\widetilde{\boldsymbol{z}}_{\vec{k}}(t) = \widetilde{\boldsymbol{G}}_k(t, t_{\rm in})\widetilde{\boldsymbol{z}}_{\vec{k}}(t_{\rm in})$ where $\widetilde{\boldsymbol{G}}_k(t, t_{\rm in}) = \boldsymbol{M}_k(t)\boldsymbol{G}_k(t, t_{\rm in})\boldsymbol{M}_k^{-1}(t_{\rm in})$. Symplectic transformations thus constitute a fundamental symmetry of the Hamiltonian phase space, and this is why the symplectic group for linear scalar-field systems is the main topic of the present work.

Let us note that in this framework, the dynamical evolution is nothing but a particular symplectic transformation since, as stressed above, the Green's matrix is symplectic. One can also check that for the transformation that goes from $\boldsymbol{z}_{\vec{k}}(t)$ to $\boldsymbol{z}_{\vec{k}}(t_{\rm in})$, generated by the matrix $\boldsymbol{G}_k^{-1}(t,t_{\rm in})$, the new Hamiltonian vanishes, as can be shown by plugging the equation of motion for $\boldsymbol{G}_k$ into Eq. (2.21). This is consistent with the fact that the $\boldsymbol{z}_{\vec{k}}(t_{\rm in})$ variables are indeed time independent, and in that case the dynamics is entirely contained in the canonical transformation that relates them with the primary variables $\boldsymbol{z}_{\vec{k}}(t)$.

Finally, when one works with the creation and annihilation operators introduced in Sec. 2.1, a similar description applies. The equation of motion given in Eq. (2.17) can be solved in terms of the Green's matrix,

$$\widehat{\boldsymbol{a}}_{\vec{k}}(t) = \boldsymbol{\mathcal{G}}_k(t,t_{\rm in})\widehat{\boldsymbol{a}}_{\vec{k}}(t_{\rm in})\,, \tag{2.22}$$

where $\boldsymbol{\mathcal{G}}_k(t,t_{\rm in}) = \boldsymbol{U}\boldsymbol{D}_k\boldsymbol{G}_k(t,t_{\rm in})\boldsymbol{D}_k^{-1}\boldsymbol{U}^\dagger$ such that $\boldsymbol{\mathcal{G}}_k^\dagger\boldsymbol{\mathcal{J}}\boldsymbol{\mathcal{G}}_k = \boldsymbol{\mathcal{J}}$ and $\det(\boldsymbol{\mathcal{G}}_k) = 1$. Similarly, one can check that any generic canonical transformation $\widehat{\boldsymbol{z}}_{\vec{k}} \to \boldsymbol{M}_k\widehat{\boldsymbol{z}}_{\vec{k}}$ gives rise to $\widehat{\boldsymbol{a}}_{\vec{k}} \to \boldsymbol{\mathcal{M}}_k\widehat{\boldsymbol{a}}_{\vec{k}}$, where $\boldsymbol{\mathcal{M}}_k = \boldsymbol{U}\boldsymbol{D}_k\boldsymbol{M}_k\boldsymbol{D}_k^{-1}\boldsymbol{U}^\dagger$ satisfies $\boldsymbol{\mathcal{M}}_k^\dagger\boldsymbol{\mathcal{J}}\boldsymbol{\mathcal{M}}_k = \boldsymbol{\mathcal{J}}$ and $\det(\boldsymbol{\mathcal{M}}_k) = 1$.

3 Sp(4, ℝ) toolkit

In the previous section, we have seen how symplectic transformations naturally arise in the phase-space description of linear Hamiltonian systems, both as a fundamental reparametrisation symmetry and as a way to generate the dynamics. This is why in this section, we further study the mathematical structure of the symplectic group in four dimensions, which is relevant to discuss the physics of two scalar fields. Readers already familiar with the use of symplectic groups in quantum mechanics can easily skip this section, which mostly consists in a review of the mathematical tools employed in the rest of the paper. It may otherwise serve as a pedagogical introduction to the techniques employed in the subsequent calculations, and set out our main notations.

3.1 Generators and Lie algebra

As explained around Eq. (2.19), the group of symplectic (4×4)-matrices, denoted $\mathrm{Sp}(4,\mathbb{R})$, is defined as

$$\mathrm{Sp}(4,\mathbb{R}) = \{\boldsymbol{M}\in\mathcal{M}_4(\mathbb{R}) : \boldsymbol{M}^{\rm T}\boldsymbol{\Omega}\boldsymbol{M} = \boldsymbol{\Omega}\}\,, \tag{3.1}$$

where $\mathcal{M}_n(\mathbb{R})$ is the set of $(n\times n)$-real matrices. Since $\boldsymbol{\Omega}^{\rm T}\boldsymbol{\Omega} = -\boldsymbol{\Omega}^2 = \boldsymbol{I}_4$, one can show that, if $\boldsymbol{M}\in\mathrm{Sp}(4,\mathbb{R})$, then $\boldsymbol{M}^{\rm T}\in\mathrm{Sp}(4,\mathbb{R})$ (this is because Eq. (3.1) leads to $\boldsymbol{M}^{\rm T} = -\boldsymbol{\Omega}\boldsymbol{M}^{-1}\boldsymbol{\Omega}$, which implies that $\boldsymbol{M}\boldsymbol{\Omega}\boldsymbol{M}^{\rm T} = \boldsymbol{\Omega}$). One can also readily check that $\mathrm{Sp}(4,\mathbb{R})$ is indeed a group, and it follows from Eq. (3.1) that all symplectic matrices have unit determinant [34].

$\mathrm{Sp}(4,\mathbb{R})$ is a Lie group, that is a continuous group whose multiplication and inversion operations are differentiable, so one can investigate global properties of the group by looking at its local or linearised version, given in terms of its so-called Lie algebra. The Lie algebra is a vector space under the bracket operation $[\boldsymbol{X},\boldsymbol{Y}] = \boldsymbol{X}\boldsymbol{Y} - \boldsymbol{Y}\boldsymbol{X}$ that completely captures the local structure of the group. When analysing Lie groups, finding a basis of this vector space, *i.e.* a set of so-called "generators", and deriving their commutators, is of paramount importance. The number of generators specifies both the dimension of the Lie group and its associated Lie algebra. In what follows, the Lie algebra of $\mathrm{Sp}(4,\mathbb{R})$ is denoted $\mathfrak{sp}(4,\mathbb{R})$.

The exponential map allows us to connect the Lie algebra to its corresponding Lie group. For any $\boldsymbol{X} \in \mathfrak{sp}(4,\mathbb{R})$, $\boldsymbol{M} = \exp(\boldsymbol{X})$ is an element of $\mathrm{Sp}(4,\mathbb{R})$ (see Ref. [33] for a recent complete characterisation of the exponential map of $\mathrm{Sp}(4,\mathbb{R})$). Note that the exponential map is not surjective, meaning that there exist elements of $\mathrm{Sp}(4,\mathbb{R})$ that cannot be written as $\exp(\boldsymbol{X})$. By plugging $\boldsymbol{M} = \exp(\boldsymbol{X})$ into Eq. (3.1), and upon writing the obtained formula as an expansion in $\boldsymbol{X}$, one finds that the Lie algebra is defined according to

$$\mathfrak{sp}(4,\mathbb{R}) = \{\boldsymbol{X} \in \mathcal{M}_4(\mathbb{R}) : \boldsymbol{\Omega}\boldsymbol{X} + \boldsymbol{X}^{\mathrm{T}}\boldsymbol{\Omega} = 0\}. \tag{3.2}$$

This allows one to write a generic element of the Lie algebra as

$$\boldsymbol{X} = \begin{pmatrix} \boldsymbol{A} & \boldsymbol{B} \\ \boldsymbol{C} & -\boldsymbol{A}^{\mathrm{T}} \end{pmatrix} \tag{3.3}$$

where $\boldsymbol{A}$, $\boldsymbol{B}$ and $\boldsymbol{C}$ are three (2×2) real matrices, $\boldsymbol{B}$ and $\boldsymbol{C}$ being symmetric. This implies that $\mathfrak{sp}(4,\mathbb{R})$ is a ten-dimensional vector space, since $\boldsymbol{A}$ contains four degrees of freedom while $\boldsymbol{B}$ and $\boldsymbol{C}$ being symmetric, they contain three degrees of freedom each. Denoting by $\boldsymbol{K}_i$, $i = 1\cdots 10$, a basis of 10 generators, a generic element of the Lie algebra can be decomposed as

$$\boldsymbol{X} = \sum_{i=1}^{10} \alpha_i \boldsymbol{K}_i, \qquad \alpha_i \in \mathbb{R}. \tag{3.4}$$

Our next step is to exhibit such a basis.

To that end, we first introduce the Kronecker product. For two (2×2)-matrices

$$\boldsymbol{A} = \begin{pmatrix} a_{11} & a_{12} \\ a_{21} & a_{22} \end{pmatrix} \quad \text{and} \quad \boldsymbol{B} = \begin{pmatrix} b_{11} & b_{12} \\ b_{21} & b_{22} \end{pmatrix}, \tag{3.5}$$

the Kronecker product $\boldsymbol{A}\otimes\boldsymbol{B}$ is a (4×4)-matrix defined as

$$\boldsymbol{A}\otimes\boldsymbol{B} = \begin{pmatrix} a_{11}\boldsymbol{B} & a_{12}\boldsymbol{B} \\ a_{21}\boldsymbol{B} & a_{22}\boldsymbol{B} \end{pmatrix} = \left(\begin{array}{cc|cc} a_{11}b_{11} & a_{11}b_{12} & a_{12}b_{11} & a_{12}b_{12} \\ a_{11}b_{21} & a_{11}b_{22} & a_{12}b_{21} & a_{12}b_{22} \\ \hline a_{21}b_{11} & a_{21}b_{12} & a_{22}b_{11} & a_{22}b_{12} \\ a_{21}b_{21} & a_{21}b_{22} & a_{22}b_{21} & a_{22}b_{22} \end{array}\right). \tag{3.6}$$

The reason why this construction is useful is because, within the two-field system at hand, each field is individually described by an $\mathfrak{sp}(2,\mathbb{R})$ algebra. It is therefore natural for expect that $\mathfrak{sp}(4,\mathbb{R})$ contains products of elements of $\mathfrak{sp}(2,\mathbb{R})$ with themselves. The generators of $\mathfrak{sp}(2,\mathbb{R})$ can be simply written in terms of the Pauli matrices [13],

$$\mathfrak{sp}(2,\mathbb{R}) = \mathrm{Span}\{\boldsymbol{\sigma}_x, i\boldsymbol{\sigma}_y, \boldsymbol{\sigma}_z\}, \tag{3.7}$$

with

$$\boldsymbol{\sigma}_x = \begin{pmatrix} 0 & 1 \\ 1 & 0 \end{pmatrix}, \qquad \boldsymbol{\sigma}_y = \begin{pmatrix} 0 & -i \\ i & 0 \end{pmatrix}, \qquad \boldsymbol{\sigma}_z = \begin{pmatrix} 1 & 0 \\ 0 & -1 \end{pmatrix}, \tag{3.8}$$

so $\mathfrak{sp}(2,\mathbb{R})$ is of dimension 3. This implies that over the 10 generators of $\mathfrak{sp}(4,\mathbb{R})$, 6 provide two copies of $\mathfrak{sp}(2,\mathbb{R})$ and describe the two sectors separately, and 4 are related to the coupling between the two sectors. For $\boldsymbol{\sigma}_a, \boldsymbol{\sigma}_b \in \{\boldsymbol{I}_2, \boldsymbol{\sigma}_x, i\boldsymbol{\sigma}_y, \boldsymbol{\sigma}_z\}$, there are 16 combinations

$\boldsymbol{\sigma}_a \otimes \boldsymbol{\sigma}_b$ for $a, b \in \{0, \cdots, 3\}$, namely $\boldsymbol{I}_4$ and the 15 Dirac matrices [29]. Among them, only 10 are of the form (3.3),[2] which are listed in Table 1, where they are organised in three subsets. The so-called squeezing generators are diagonal. Through the exponential map, they give rise to group elements of the form $\exp(d_1 \boldsymbol{K}_1) = \mathrm{diag}(e^{d_1}, e^{-d_1}, e^{-d_1}, e^{d_1})$ and $\exp(d_2 \boldsymbol{K}_2) = \mathrm{diag}(e^{d_2}, e^{d_2}, e^{-d_2}, e^{-d_2})$ with d_1 and d_2 two real parameters. Therefore, they elongate one phase-space direction while contracting the other, hence their name. The two other kinds of generators are called rotations and boosts. When squared, rotations give $-\boldsymbol{I}_4$ and boosts give $\boldsymbol{I}_4$. Therefore, once exponentiated, rotations generate group elements of the form $\exp(\theta_i \boldsymbol{K}_i) = \cos\theta_i \boldsymbol{I}_4 + \sin\theta_i \boldsymbol{K}_i$ for $i \in \{3, 4, 5, 6\}$ with $\theta_i \in \mathbb{R}$, while boosts generate $\exp(\alpha_i \boldsymbol{K}_i) = \cosh\alpha_i \boldsymbol{I}_4 + \sinh\alpha_i \boldsymbol{K}_i$ for $i \in \{7, 8, 9, 10\}$ with $\alpha_i \in \mathbb{R}$, hence their name.

Squeezing	Rotation	Boost
$\boldsymbol{K}_1 = \boldsymbol{\sigma}_z \otimes \boldsymbol{\sigma}_z = \begin{pmatrix} 1 & 0 & 0 & 0 \\ 0 & -1 & 0 & 0 \\ 0 & 0 & -1 & 0 \\ 0 & 0 & 0 & 1 \end{pmatrix}$	$\boldsymbol{K}_3 = i\boldsymbol{\sigma}_y \otimes \boldsymbol{I}_2 = \begin{pmatrix} 0 & 0 & 1 & 0 \\ 0 & 0 & 0 & 1 \\ -1 & 0 & 0 & 0 \\ 0 & -1 & 0 & 0 \end{pmatrix}$	$\boldsymbol{K}_7 = \boldsymbol{\sigma}_x \otimes \boldsymbol{I}_2 = \begin{pmatrix} 0 & 0 & 1 & 0 \\ 0 & 0 & 0 & 1 \\ 1 & 0 & 0 & 0 \\ 0 & 1 & 0 & 0 \end{pmatrix}$
$\boldsymbol{K}_2 = \boldsymbol{\sigma}_z \otimes \boldsymbol{I}_2 = \begin{pmatrix} 1 & 0 & 0 & 0 \\ 0 & 1 & 0 & 0 \\ 0 & 0 & -1 & 0 \\ 0 & 0 & 0 & -1 \end{pmatrix}$	$\boldsymbol{K}_4 = i\boldsymbol{\sigma}_y \otimes \boldsymbol{\sigma}_z = \begin{pmatrix} 0 & 0 & 1 & 0 \\ 0 & 0 & 0 & -1 \\ -1 & 0 & 0 & 0 \\ 0 & 1 & 0 & 0 \end{pmatrix}$	$\boldsymbol{K}_8 = \boldsymbol{\sigma}_x \otimes \boldsymbol{\sigma}_z = \begin{pmatrix} 0 & 0 & 1 & 0 \\ 0 & 0 & 0 & -1 \\ 1 & 0 & 0 & 0 \\ 0 & -1 & 0 & 0 \end{pmatrix}$
	$\boldsymbol{K}_5 = \boldsymbol{I}_2 \otimes i\boldsymbol{\sigma}_y = \begin{pmatrix} 0 & 1 & 0 & 0 \\ -1 & 0 & 0 & 0 \\ 0 & 0 & 0 & 1 \\ 0 & 0 & -1 & 0 \end{pmatrix}$	$\boldsymbol{K}_9 = \boldsymbol{\sigma}_z \otimes \boldsymbol{\sigma}_x = \begin{pmatrix} 0 & 1 & 0 & 0 \\ 1 & 0 & 0 & 0 \\ 0 & 0 & 0 & -1 \\ 0 & 0 & -1 & 0 \end{pmatrix}$
	$\boldsymbol{K}_6 = i\boldsymbol{\sigma}_y \otimes \boldsymbol{\sigma}_x = \begin{pmatrix} 0 & 0 & 0 & 1 \\ 0 & 0 & 1 & 0 \\ 0 & -1 & 0 & 0 \\ -1 & 0 & 0 & 0 \end{pmatrix}$	$\boldsymbol{K}_{10} = \boldsymbol{\sigma}_x \otimes \boldsymbol{\sigma}_x = \begin{pmatrix} 0 & 0 & 0 & 1 \\ 0 & 0 & 1 & 0 \\ 0 & 1 & 0 & 0 \\ 1 & 0 & 0 & 0 \end{pmatrix}$

Table 1. Generators of $\mathfrak{sp}(4, \mathbb{R})$ in the fundamental representation.

Now that we have explicitly obtained the generators of the Lie algebra, let us identify their respective role. The two $\mathfrak{sp}(2, \mathbb{R})$ algebras are given by $\{(\boldsymbol{K}_1 + \boldsymbol{K}_2)/2, (\boldsymbol{K}_3 + \boldsymbol{K}_4)/2, (\boldsymbol{K}_7 + \boldsymbol{K}_8)/2\}$ and $\{(\boldsymbol{K}_1 - \boldsymbol{K}_2)/2, (\boldsymbol{K}_3 - \boldsymbol{K}_4)/2, (\boldsymbol{K}_7 - \boldsymbol{K}_8)/2\}$, each of them being composed of a squeezing, a rotation and a boost. They act on each sector separately and would be enough to describe two non-interacting degrees of freedom. Formally, they generate the $\mathrm{Sp}(2, \mathbb{R}) \times \mathrm{Sp}(2, \mathbb{R})$ subgroup of $\mathrm{Sp}(4, \mathbb{R})$. The 4 remaining generators are associated with the coupling between the two sectors. They correspond to the rotations $\boldsymbol{K}_5$ and $\boldsymbol{K}_6$ and the boosts $\boldsymbol{K}_9$ and $\boldsymbol{K}_{10}$, which entangle the two sectors, as will be made clear in Sec. 3.4. One can indeed check that these 4 generators (and only them) have non-vanishing off-diagonal elements within the (2×2) blocks, which, from the ordering of the phase-space variables in

[2] Formally, the 15 Dirac matrices form the $\mathfrak{o}(3, 3)$ algebra. $\mathfrak{sp}(4, \mathbb{R})$ is isomorphic to $\mathfrak{o}(3, 2)$, which is a subalgebra of $\mathfrak{o}(3, 3)$ [29].

Eq. (2.6), implies that they mix the two fields. This is why, hereafter, they will be referred to as the coupling generators.

To complete our description of the Lie algebra, let us finally provide the commutators between its generators. They can be obtained from the multiplication rule of the Kronecker product for square matrices,[3]

$$(\boldsymbol{A}\otimes\boldsymbol{B})\,(\boldsymbol{C}\otimes\boldsymbol{D}) = (\boldsymbol{AC})\otimes(\boldsymbol{BD})\,, \tag{3.9}$$

together with the formula

$$\boldsymbol{\sigma}_i\boldsymbol{\sigma}_j = \delta_{ij}\boldsymbol{I}_2 + i\varepsilon_{ijk}\boldsymbol{\sigma}_k \quad \text{for} \quad \{i,j,k\}\in\{x,y,z\}\,, \tag{3.10}$$

where δ_{ab} is the Kronecker symbol and ε_{abc} is the Levi-Civita symbol. For instance, one has $[\boldsymbol{K}_6,\boldsymbol{K}_4] = [i\boldsymbol{\sigma}_y\otimes\boldsymbol{\sigma}_x, i\boldsymbol{\sigma}_y\otimes\boldsymbol{\sigma}_z] = (i\boldsymbol{\sigma}_y)^2\otimes\boldsymbol{\sigma}_x\boldsymbol{\sigma}_z - (i\boldsymbol{\sigma}_y)^2\otimes\boldsymbol{\sigma}_z\boldsymbol{\sigma}_x = -\boldsymbol{I}_2\otimes(-i\boldsymbol{\sigma}_y) + \boldsymbol{I}_2\otimes(i\boldsymbol{\sigma}_y) = 2\boldsymbol{K}_5$. All other commutators are presented in Appendix A, where we also derive the various subalgebras. We do not reproduce these formulas here for display convenience, and will simply refer to Appendix A when needed.

3.2 Bloch-Messiah decomposition

The explicit derivation of the 10 generators of the Lie algebra allows one to decompose any element of the group (within the exponential map) onto these generators, upon exponentiating Eq. (3.4). This parametrisation of the exponential map is performed in Ref. [33] (see also Refs. [31, 32]). When all 10 parameters are non vanishing, it however leads to expressions that may be cumbersome to manipulate, and which, as mentioned above, do not reach all the elements of the group. This is why, in this section, we turn our attention to an alternative decomposition, the so-called Bloch-Messiah decomposition (also sometimes called Euler decomposition) [35], which allows one to write any symplectic matrix as

$$\boldsymbol{M}(\boldsymbol{\theta},\boldsymbol{d},\boldsymbol{\varphi}) = \boldsymbol{R}(\boldsymbol{\theta})\boldsymbol{Z}(\boldsymbol{d})\boldsymbol{R}(\boldsymbol{\varphi})\,. \tag{3.11}$$

Here, $\boldsymbol{R}(\boldsymbol{\theta}),\boldsymbol{R}(\boldsymbol{\varphi})\in\mathrm{Sp}(4,\mathbb{R})\cap\mathrm{SO}(4)$ are constructed from the four rotation generators and $\boldsymbol{Z}(\boldsymbol{d})$ from the two squeezing generators, *i.e.*

$$\boldsymbol{R}(\boldsymbol{\theta}) = \exp(\theta_3\boldsymbol{K}_3 + \theta_4\boldsymbol{K}_4 + \theta_5\boldsymbol{K}_5 + \theta_6\boldsymbol{K}_6) \tag{3.12}$$

and a similar expression for $\boldsymbol{R}(\boldsymbol{\varphi})$ with $\boldsymbol{\varphi} = (\varphi_1,\varphi_2,\varphi_3,\varphi_4)$, and

$$\boldsymbol{Z}(\boldsymbol{d}) = \exp(d_1\boldsymbol{K}_1 + d_2\boldsymbol{K}_2). \tag{3.13}$$

The 8 parameters contained in $\boldsymbol{\theta}$ and $\boldsymbol{\varphi}$ are called the rotation parameters, while $\boldsymbol{d}$ contains the so-called squeezing parameters. Note that the parameters associated with the coupling generators are θ_5, φ_5, θ_6 and φ_6, which thus control the mixing between the two sectors.

One may note that only 6 out of the 10 generators of $\mathfrak{sp}(4,\mathbb{R})$ are involved in the Bloch-Messiah decomposition. It therefore provides a factorised expression of the group elements that is slightly more convenient to manipulate. Moreover, the three blocks of the

[3] Other properties of the Kronecker product that will be used in the following are that it is bilinear and associative, and that for square matrices, $(\boldsymbol{A}\otimes\boldsymbol{B})^{-1} = \boldsymbol{A}^{-1}\otimes\boldsymbol{B}^{-1}$, $(\boldsymbol{A}\otimes\boldsymbol{B})^{*} = \boldsymbol{A}^{*}\otimes\boldsymbol{B}^{*}$ and $(\boldsymbol{A}\otimes\boldsymbol{B})^{T} = \boldsymbol{A}^{T}\otimes\boldsymbol{B}^{T}$.

decomposition can be further factorised down. Indeed, in Appendix A, it is shown that $\boldsymbol{K}_1$ and $\boldsymbol{K}_2$ commute, so

$$\boldsymbol{Z}(\boldsymbol{d}) = \exp(d_1\boldsymbol{K}_1)\cdot\exp(d_2\boldsymbol{K}_2). \tag{3.14}$$

Regarding the rotation operators, still in Appendix A, it is shown that $\boldsymbol{K}_3$ commutes with the other three rotation generators, namely $\boldsymbol{K}_4$, $\boldsymbol{K}_5$ and $\boldsymbol{K}_6$ [see Eq. (A.2)], so $\boldsymbol{K}_3$ generates a separate U(1) Lie group; while $\boldsymbol{K}_4$, $\boldsymbol{K}_5$ and $\boldsymbol{K}_6$ generate a SU(2) Lie group [see Eq. (A.20)]. As a consequence, the four rotation generators form[4]

$$\mathrm{Sp}(4,\mathbb{R})\cap\mathrm{SO}(4)\cong\mathrm{U}(2)\cong\mathrm{SU}(2)\times\mathrm{U}(1)\,, \tag{3.15}$$

where " $\cong$ " indicates group isomorphisms. This leads to factorising

$$\boldsymbol{R}(\boldsymbol{\theta}) = \exp(\theta_3\boldsymbol{K}_3)\cdot\exp(\theta_4\boldsymbol{K}_4+\theta_5\boldsymbol{K}_5+\theta_6\boldsymbol{K}_6)\,, \tag{3.16}$$

and a similar expression for $\boldsymbol{R}(\boldsymbol{\varphi})$. Finally, one can use the Baker-Campbell-Haussdorf formula [36–39] to further factorise the remaining SU(2) part. This can be done by first introducing the complexified Lie algebra

$$\boldsymbol{S}_z = \frac{1}{2i}\boldsymbol{K}_4, \qquad \boldsymbol{S}_+ = \frac{1}{2i}\left(\boldsymbol{K}_5 - i\boldsymbol{K}_6\right), \qquad \boldsymbol{S}_- = \frac{1}{2i}\left(\boldsymbol{K}_5 + i\boldsymbol{K}_6\right), \tag{3.17}$$

where the notation is purposely reminiscent of spin physics. One can check that $\boldsymbol{S}_z^\dagger = \boldsymbol{S}_z$ and $\boldsymbol{S}_+^\dagger = \boldsymbol{S}_-$, and from the SU(2) commutation relations derived in Eq. (A.20), one has

$$[\boldsymbol{S}_z,\boldsymbol{S}_+] = \boldsymbol{S}_+, \qquad [\boldsymbol{S}_z,\boldsymbol{S}_-] = -\boldsymbol{S}_-, \qquad [\boldsymbol{S}_+,\boldsymbol{S}_-] = 2\boldsymbol{S}_z\,. \tag{3.18}$$

Expanding $\theta_4\boldsymbol{K}_4+\theta_5\boldsymbol{K}_5+\theta_6\boldsymbol{K}_6$ onto $\boldsymbol{S}_z$, $\boldsymbol{S}_+$ and $\boldsymbol{S}_-$, the Baker-Campbell-Haussdorf formula thus leads to [39]

$$\exp(\theta_4\boldsymbol{K}_4+\theta_5\boldsymbol{K}_5+\theta_6\boldsymbol{K}_6) = \exp(p_+\boldsymbol{S}_+)\exp(p_z\boldsymbol{S}_z)\exp(p_-\boldsymbol{S}_-)\,, \tag{3.19}$$

where

$$p_z = -2\ln\left(\cos\theta - i\frac{\theta_4}{\theta}\sin\theta\right), \qquad p_- = \frac{-\tau^*\sin\theta}{\theta\cos\theta - i\theta_4\sin\theta}, \qquad p_+ = \frac{\tau\sin\theta}{\theta\cos\theta - i\theta_4\sin\theta}, \tag{3.20}$$

and where we have introduced

$$\tau = -\theta_6 + i\theta_5 \qquad \text{and} \qquad \theta = \sqrt{\theta_4^2+\theta_5^2+\theta_6^2}\,. \tag{3.21}$$

[4]The role played by the 4 rotation generators can be further understood as follows. As explained in Sec. 3.1, $(\boldsymbol{K}_3+\boldsymbol{K}_4)/2$ and $(\boldsymbol{K}_3-\boldsymbol{K}_4)/2$ generate separate rotations in the first and second sectors respectively. Thus $\boldsymbol{K}_3$ induces the same rotation in both sectors and θ_3 can be thought of as a "coherent phase" (which is why $\boldsymbol{K}_3$ decouples from the other generators), while $\boldsymbol{K}_4$ generates opposite rotations in the two sectors and θ_4 can be thought of as a "phase shift". For the two coupling generators, $\boldsymbol{K}_5$ operates the same rotation in the position plane and in the momentum plane, so it can be understood as a field redefinition; while $\boldsymbol{K}_6$ operates a rotation that mixes positions and momenta of the two sectors.

A similar expression can be found for $\boldsymbol{R}(\boldsymbol{\varphi})$, where q_z, q_-, q_+ denote the parameters analogue to p_z, p_-, p_+. Combining the above results, any element of $\mathrm{Sp}(4,\mathbb{R})$ can be decomposed according to

$$\begin{aligned}\boldsymbol{M} = &\overbrace{[\exp(p_+\boldsymbol{S}_+)\cdot\exp(p_z\boldsymbol{S}_z)\cdot\exp(p_-\boldsymbol{S}_-)\cdot\exp(\theta_3\boldsymbol{K}_3)]}^{\boldsymbol{R}(\boldsymbol{\theta})}\cdot\overbrace{[\exp(d_1\boldsymbol{K}_1)\cdot\exp(d_2\boldsymbol{K}_2)]}^{\boldsymbol{Z}(\boldsymbol{d})}\\ &\cdot\overbrace{[\exp(q_+\boldsymbol{S}_+)\cdot\exp(q_z\boldsymbol{S}_z)\cdot\exp(q_-\boldsymbol{S}_-)\cdot\exp(\varphi_3\boldsymbol{K}_3)]}^{\boldsymbol{R}(\boldsymbol{\varphi})}\,.\end{aligned} \tag{3.22}$$

This fully factorised form will be of particular convenience when it comes to characterising the quantum states of the system in Sec. 5.

3.3 Helicity basis

In Sec. 2.1, the creation and annihilation operators have been introduced as an equivalent parametrisation of phase space, called the helicity basis. In the quantum mechanical context, it leads to the convenient occupation-number representation, which is why we now translate the above considerations into that basis.

We recall that when applying a canonical transformation, the helicity variables transform via matrices of the form $\boldsymbol{\mathcal{M}}_k = \boldsymbol{U}\boldsymbol{M}_k\boldsymbol{U}^\dagger$ for $\boldsymbol{M}_k \in \mathrm{Sp}(4,\mathbb{R})$, which satisfy $\boldsymbol{\mathcal{M}}_k^\dagger\boldsymbol{\mathcal{J}}\boldsymbol{\mathcal{M}}_k = \boldsymbol{\mathcal{J}}$ and $\det(\boldsymbol{\mathcal{M}}_k) = 1$, see the discussion below Eq. (2.22). In particular, this is the case for the Green matrix $\boldsymbol{\mathcal{G}}_k(t,t_{\mathrm{in}})$. Those two conditions define the $\mathrm{SU}(2,2)$ group, but given that $\mathrm{SU}(2,2)$ is a fifteen dimensional Lie group, $\mathrm{Sp}(4,\mathbb{R})$ cannot be isomorphic to the whole group and instead constitutes a ten dimensional subgroup, which we denote $\mathscr{Sp}(4,\mathbb{R})$. More precisely, decomposing a generic matrix $\boldsymbol{M}_k \in \mathcal{M}_4(\mathbb{R})$ into blocks according to

$$\boldsymbol{M}_k = \begin{pmatrix}\boldsymbol{A} & \boldsymbol{B}\\ \boldsymbol{C} & \boldsymbol{D}\end{pmatrix} \tag{3.23}$$

with $\boldsymbol{A},\boldsymbol{B},\boldsymbol{C},\boldsymbol{D} \in \mathcal{M}_2(\mathbb{R})$, the condition $\boldsymbol{\mathcal{M}}_k = \boldsymbol{U}\boldsymbol{M}_k(t)\boldsymbol{U}^\dagger$ can be written as

$$\boldsymbol{\mathcal{M}}_k = \begin{pmatrix}\boldsymbol{\mathcal{A}} & \boldsymbol{\mathcal{B}}\\ \boldsymbol{\mathcal{B}}^* & \boldsymbol{\mathcal{A}}^*\end{pmatrix}, \tag{3.24}$$

where $\boldsymbol{\mathcal{A}} = (1/2)[(\boldsymbol{A}+\boldsymbol{D}) + i(\boldsymbol{C}-\boldsymbol{B})]$ and $\boldsymbol{\mathcal{B}} = (1/2)[(\boldsymbol{A}-\boldsymbol{D}) + i(\boldsymbol{C}+\boldsymbol{B})]$. As explained below Eq. (3.1), if $\boldsymbol{M}_k \in \mathrm{Sp}(4,\mathbb{R})$ then $\boldsymbol{M}_k^{\mathrm{T}} \in \mathrm{Sp}(4,\mathbb{R})$, which implies that $\boldsymbol{\mathcal{M}}_k^\dagger$ is also symplectic, hence $\boldsymbol{\mathcal{M}}_k\boldsymbol{\mathcal{J}}\boldsymbol{\mathcal{M}}_k^\dagger = \boldsymbol{\mathcal{J}}$. This leads to the two conditions

$$\boldsymbol{\mathcal{A}}\boldsymbol{\mathcal{A}}^\dagger - \boldsymbol{\mathcal{B}}\boldsymbol{\mathcal{B}}^\dagger = \boldsymbol{I}_2 \quad \text{and} \quad \boldsymbol{\mathcal{A}}\boldsymbol{\mathcal{B}}^{\mathrm{T}} - \boldsymbol{\mathcal{B}}\boldsymbol{\mathcal{A}}^{\mathrm{T}} = 0\,. \tag{3.25}$$

Upon expanding the matrices $\boldsymbol{\mathcal{A}}$ and $\boldsymbol{\mathcal{B}}$ in terms of the so-called Bogolyubov coefficients,

$$\boldsymbol{\mathcal{A}} = \begin{pmatrix}\alpha_{11} & \alpha_{12}\\ \alpha_{21} & \alpha_{22}\end{pmatrix} \qquad \text{and} \qquad \boldsymbol{\mathcal{B}} = \begin{pmatrix}\beta_{11} & \beta_{12}\\ \beta_{21} & \beta_{22}\end{pmatrix}, \tag{3.26}$$

Eq. (3.25) leads to the four conditions

$$|\alpha_{11}|^2 + |\alpha_{12}|^2 - |\beta_{11}|^2 - |\beta_{12}|^2 = 1\,, \tag{3.27}$$

$$|\alpha_{21}|^2 + |\alpha_{22}|^2 - |\beta_{21}|^2 - |\beta_{22}|^2 = 1\,, \tag{3.28}$$

$$\alpha_{11}\alpha_{21}^* + \alpha_{12}\alpha_{22}^* - \beta_{11}\beta_{21}^* - \beta_{12}\beta_{22}^* = 0\,, \tag{3.29}$$

$$\alpha_{11}\beta_{21} + \alpha_{12}\beta_{22} - \alpha_{21}\beta_{11} - \alpha_{22}\beta_{12} = 0\,. \tag{3.30}$$

This fixes 2 real and 2 complex combinations out of the 8 complex Bogolyubov coefficients, that is 6 out of the 16 real parameters, and one recovers the 10 degrees of freedom of $\mathrm{Sp}(4,\mathbb{R})$.

One may note that the Green matrix $\boldsymbol{\mathcal{G}}_k(t,t_{\rm in})$ being an element of $\mathscr{S}p(4,\mathbb{R})$, it can also be written in terms of Bogolyubov coefficients according to Eqs. (3.24) and (3.26). In that case, the relations (3.27)-(3.30) translate the fact that the Poisson brackets (or their quantum analogue, the commutation relations) are preserved by the dynamical evolution. Moreover, when applying $\widehat{\boldsymbol{a}}_{\vec{k}}(t) = \boldsymbol{\mathcal{G}}_k(t,t_{\rm in})\widehat{\boldsymbol{a}}_{\vec{k}}(t_{\rm in})$, one notices that $\boldsymbol{\mathcal{A}}$ and $\boldsymbol{\mathcal{A}}^*$ transform annihilation into annihilation operators, and creation into creation operators, respectively. Therefore, they maintain the overall excitation number while reshuffling the excitations between the different sectors. On the contrary, $\boldsymbol{\mathcal{B}}$ and $\boldsymbol{\mathcal{B}}^*$ convert annihilation into creation operators and conversely, so they create or annihilate new excitations. We finally note that $\alpha_{11},\alpha_{22},\beta_{11}$ and β_{22} act on each sector separately while $\alpha_{12},\alpha_{21},\beta_{12}$ and β_{21} mix the two sectors. As a consistency check, one can verify that when these mixing Bogolyubov coefficients vanish, Eqs. (3.27)-(3.30) reduce to the $\mathrm{Sp}(2,\mathbb{R})$-constraint on the Bogolyubov coefficients [13], namely $|\alpha_{11}|^2 - |\beta_{11}|^2 = |\alpha_{22}|^2 - |\beta_{22}|^2 = 1$.

Let us now study the infinitesimal properties of $\mathscr{S}p(4,\mathbb{R})$, as we did for $\mathrm{Sp}(4,\mathbb{R})$ in Sec. 3.1. We observe that the ten generators of $\mathscr{S}p(4,\mathbb{R})$ can be found by simple correspondence with the ten generators of $\mathrm{Sp}(4,\mathbb{R})$, upon introducing $\exp(\alpha_i \boldsymbol{L}_i) \equiv \boldsymbol{U}\exp(\alpha_i \boldsymbol{K}_i)\boldsymbol{U}^\dagger = \exp(\alpha_i \boldsymbol{U}\boldsymbol{K}_i\boldsymbol{U}^\dagger)$, where $i = 1\cdots 10$ and where we have used the fact that $\boldsymbol{U}$ is unitary. Writing $K_i = \boldsymbol{\sigma}_{a_i}\otimes\boldsymbol{\sigma}_{b_i}$ and $\boldsymbol{U} = u\otimes\boldsymbol{I}_2$ with

$$u = \frac{1}{\sqrt{2}}\begin{pmatrix} 1 & i \\ 1 & -i \end{pmatrix}, \tag{3.31}$$

the generators of $\mathscr{S}p(4,\mathbb{R})$ can be calculated by means of Eq. (3.9) and one has $\boldsymbol{L}_i = \boldsymbol{U}\boldsymbol{K}_i\boldsymbol{U}^\dagger = (\boldsymbol{u}\otimes\boldsymbol{I}_2)(\boldsymbol{\sigma}_{a_i}\otimes\boldsymbol{\sigma}_{b_i})(\boldsymbol{u}^\dagger\otimes\boldsymbol{I}_2) = \boldsymbol{u}\boldsymbol{\sigma}_{a_i}\boldsymbol{u}^\dagger\otimes\boldsymbol{\sigma}_{b_i}$. Given that $\boldsymbol{u}\boldsymbol{\sigma}_x\boldsymbol{u}^\dagger = -\boldsymbol{\sigma}_y$, $\boldsymbol{u}\boldsymbol{\sigma}_y\boldsymbol{u}^\dagger = -\boldsymbol{\sigma}_z$ and $\boldsymbol{u}\boldsymbol{\sigma}_z\boldsymbol{u}^\dagger = \boldsymbol{\sigma}_x$, one concludes that the generators of $\mathscr{S}p(4,\mathbb{R})$ are merely a reshuffling of those of $\mathrm{Sp}(4,\mathbb{R})$, where the detailed correspondence is given in Table 2. In particular, one observes that rotations in the helicity basis are block diagonal (which generalises the $\mathrm{Sp}(2,\mathbb{R})$ result where rotations in the helicity basis are (2×2) diagonal matrices [13]). Note that the commutation relations between the $\boldsymbol{L}_i$ operators directly follow from those between the $\boldsymbol{K}_i$ operators given in Appendix A.

Squeezing	Rotation	Boost
$\boldsymbol{L}_1 = \boldsymbol{K}_8$	$\boldsymbol{L}_3 = -i\boldsymbol{K}_2$	$\boldsymbol{L}_7 = i\boldsymbol{K}_3$
$\boldsymbol{L}_2 = \boldsymbol{K}_7$	$\boldsymbol{L}_4 = -i\boldsymbol{K}_1$	$\boldsymbol{L}_8 = i\boldsymbol{K}_4$
	$\boldsymbol{L}_5 = \boldsymbol{K}_5$	$\boldsymbol{L}_9 = \boldsymbol{K}_{10}$
	$\boldsymbol{L}_6 = -i\boldsymbol{K}_9$	$\boldsymbol{L}_{10} = i\boldsymbol{K}_6$

Table 2. Generators of the helicity basis $\mathscr{S}p(4,\mathbb{R})$ in the fundamental representation, $\boldsymbol{L}_i = \boldsymbol{U}\boldsymbol{K}_i\boldsymbol{U}^\dagger$, where the $\boldsymbol{K}_i$ generators are given in Table 1.

The Bloch-Messiah decomposition (3.11) can also be performed in the helicity basis,

$$\boldsymbol{\mathcal{M}}(\boldsymbol{\theta},\boldsymbol{d},\boldsymbol{\varphi}) = \boldsymbol{\mathcal{R}}(\boldsymbol{\theta})\boldsymbol{\mathcal{Z}}(\boldsymbol{d})\boldsymbol{\mathcal{R}}(\boldsymbol{\varphi})\,, \tag{3.32}$$

where $\boldsymbol{\mathcal{Z}} = \boldsymbol{U}\boldsymbol{Z}\boldsymbol{U}^\dagger$ and $\boldsymbol{\mathcal{R}} = \boldsymbol{U}\boldsymbol{R}\boldsymbol{U}^\dagger$ are the squeezing matrix and the rotation matrix in the helicity basis. This expression allows us to connect the Bogolyubov coefficients with the squeezing and rotation parameters. Using the above results, an explicit calculation yields

$$\begin{aligned}
\alpha_{11} =& e^{-i(\theta_3+\varphi_3)}\left(\cos\theta - i\frac{\theta_4}{\theta}\sin\theta\right)\left(\cos\varphi - i\frac{\varphi_4}{\varphi}\sin\varphi\right)\cosh r_1 \\
&- e^{-i(\theta_3+\varphi_3)}\left[(\theta_5 - i\theta_6)\frac{\sin\theta}{\theta}\right]\left[(\varphi_5 + i\varphi_6)\frac{\sin\varphi}{\varphi}\right]\cosh r_2\,, \qquad (3.33)\\
\alpha_{12} =& e^{-i(\theta_3+\varphi_3)}\left(\cos\theta - i\frac{\theta_4}{\theta}\sin\theta\right)\left[(\varphi_5 - i\varphi_6)\frac{\sin\varphi}{\varphi}\right]\cosh r_1 \\
&+ e^{-i(\theta_3+\varphi_3)}\left[(\theta_5 - i\theta_6)\frac{\sin\theta}{\theta}\right]\left(\cos\varphi + i\frac{\varphi_4}{\varphi}\sin\varphi\right)\cosh r_2\,, \qquad (3.34)\\
\alpha_{21} =& - e^{-i(\theta_3+\varphi_3)}\left[(\theta_5 + i\theta_6)\frac{\sin\theta}{\theta}\right]\left(\cos\varphi - i\frac{\varphi_4}{\varphi}\sin\varphi\right)\cosh r_1 \\
&- e^{-i(\theta_3+\varphi_3)}\left(\cos\theta + i\frac{\theta_4}{\theta}\sin\theta\right)\left[(\varphi_5 + i\varphi_6)\frac{\sin\varphi}{\varphi}\right]\cosh r_2\,, \qquad (3.35)\\
\alpha_{22} =& - e^{-i(\theta_3+\varphi_3)}\left[(\theta_5 + i\theta_6)\frac{\sin\theta}{\theta}\right]\left[(\varphi_5 - i\varphi_6)\frac{\sin\varphi}{\varphi}\right]\cosh r_1 \\
&+ e^{-i(\theta_3+\varphi_3)}\left(\cos\theta + i\frac{\theta_4}{\theta}\sin\theta\right)\left(\cos\varphi + i\frac{\varphi_4}{\varphi}\sin\varphi\right)\cosh r_2\,, \qquad (3.36)
\end{aligned}$$

and

$$\begin{aligned}
\beta_{11} =& e^{-i(\theta_3-\varphi_3)}\left(\cos\theta - i\frac{\theta_4}{\theta}\sin\theta\right)\left(\cos\varphi + i\frac{\varphi_4}{\varphi}\sin\varphi\right)\sinh r_1 \\
&- e^{-i(\theta_3-\varphi_3)}\left[(\theta_5 - i\theta_6)\frac{\sin\theta}{\theta}\right]\left[(\varphi_5 - i\varphi_6)\frac{\sin\varphi}{\varphi}\right]\sinh r_2\,, \qquad (3.37)\\
\beta_{12} =& e^{-i(\theta_3-\varphi_3)}\left(\cos\theta - i\frac{\theta_4}{\theta}\sin\theta\right)\left[(\varphi_5 + i\varphi_6)\frac{\sin\varphi}{\varphi}\right]\sinh r_1 \\
&+ e^{-i(\theta_3-\varphi_3)}\left[(\theta_5 - i\theta_6)\frac{\sin\theta}{\theta}\right]\left(\cos\varphi - i\frac{\varphi_4}{\varphi}\sin\varphi\right)\sinh r_2\,, \qquad (3.38)\\
\beta_{21} =& - e^{-i(\theta_3-\varphi_3)}\left[(\theta_5 + i\theta_6)\frac{\sin\theta}{\theta}\right]\left(\cos\varphi + i\frac{\varphi_4}{\varphi}\sin\varphi\right)\sinh r_1 \\
&- e^{-i(\theta_3-\varphi_3)}\left(\cos\theta + i\frac{\theta_4}{\theta}\sin\theta\right)\left[(\varphi_5 - i\varphi_6)\frac{\sin\varphi}{\varphi}\right]\sinh r_2\,, \qquad (3.39)\\
\beta_{22} =& - e^{-i(\theta_3-\varphi_3)}\left[(\theta_5 + i\theta_6)\frac{\sin\theta}{\theta}\right]\left[(\varphi_5 + i\varphi_6)\frac{\sin\varphi}{\varphi}\right]\sinh r_1 \\
&+ e^{-i(\theta_3-\varphi_3)}\left(\cos\theta + i\frac{\theta_4}{\theta}\sin\theta\right)\left(\cos\varphi - i\frac{\varphi_4}{\varphi}\sin\varphi\right)\sinh r_2\,, \qquad (3.40)
\end{aligned}$$

where $\theta = \sqrt{\theta_4^2 + \theta_5^2 + \theta_6^2}$ and $\varphi = \sqrt{\varphi_4^2 + \varphi_5^2 + \varphi_6^2}$ have already been defined in Eq. (3.21), and where we have introduced

$$r_1 = d_1 + d_2 \quad \text{and} \quad r_2 = d_2 - d_1\,. \qquad (3.41)$$

One can check that if the rotation parameters associated with the coupling generators vanish, *i.e.* if $\theta_5 = \theta_6 = \varphi_5 = \varphi_6 = 0$, then the mixing Bogolyubov coefficients vanish too, *i.e.* $\alpha_{12} =$

$\alpha_{21} = \beta_{12} = \beta_{21} = 0$, and the link between the Bogolyubov coefficients and the squeezing and rotation parameters reduces to the one obtained in $\mathrm{Sp}(2,\mathbb{R})$ [13].

Finally, a fully factorised form for the elements of $\mathscr{S}p(4,\mathbb{R})$ can be obtained from transposing Eq. (3.22), which gives rise to

$$\begin{aligned}\boldsymbol{\mathcal{M}} = &\overbrace{\left[\exp(p_+\boldsymbol{L}_+)\cdot\exp(p_z\boldsymbol{L}_z)\cdot\exp(p_-\boldsymbol{L}_-)\cdot\exp(\theta_3\boldsymbol{L}_3)\right]}^{\boldsymbol{\mathcal{R}}(\boldsymbol{\theta})}\cdot\overbrace{\left[\exp(d_1\boldsymbol{L}_1)\cdot\exp(d_2\boldsymbol{L}_2)\right]}^{\boldsymbol{\mathcal{Z}}(\boldsymbol{d})}\\ &\cdot\overbrace{\left[\exp(q_+\boldsymbol{L}_+)\cdot\exp(q_z\boldsymbol{L}_z)\cdot\exp(q_-\boldsymbol{L}_-)\cdot\exp(\varphi_3\boldsymbol{L}_3)\right]}^{\boldsymbol{\mathcal{R}}(\boldsymbol{\varphi})},\end{aligned} \tag{3.42}$$

where $\boldsymbol{L}_z = \boldsymbol{U}\boldsymbol{S}_z\boldsymbol{U}^\dagger = \boldsymbol{L}_4/(2i)$, $\boldsymbol{L}_+ = \boldsymbol{U}\boldsymbol{S}_+\boldsymbol{U}^\dagger = (\boldsymbol{L}_5 - i\boldsymbol{L}_6)/(2i)$ and $\boldsymbol{L}_- = \boldsymbol{U}\boldsymbol{S}_-\boldsymbol{U}^\dagger = (\boldsymbol{L}_5 + i\boldsymbol{L}_6)/(2i)$.

3.4 Quantum representation

Since the Green's matrix is an element of the symplectic group, in order to describe the dynamics in the occupation-number representation, one first needs to derive the quantum representation of the elements of $\mathscr{S}p(4,\mathbb{R})$. This can be done by following the procedure outlined in Refs. [40–42] and presented in details in Appendix B of Ref. [13]. It consists in first linearising the elements of the $\mathscr{S}p(4,\mathbb{R})$ Lie group,

$$\boldsymbol{\mathcal{M}}_k \simeq \boldsymbol{I}_4 + \sum_{a=1}^{10}\varepsilon_k^a\boldsymbol{L}_a, \tag{3.43}$$

where ε_k^a are (small) real parameters. This generates a canonical transformation on the helicity variables, given by

$$\widehat{\boldsymbol{a}}'_{\vec{k}} \simeq \widehat{\boldsymbol{a}}_{\vec{k}} + \sum_{a=1}^{10}\varepsilon_k^a\boldsymbol{L}_a\widehat{\boldsymbol{a}}_{\vec{k}}\,. \tag{3.44}$$

Our goal is to find a set of operators $\widehat{L}_a^{\vec{k}}$ such that this can be written as a unitary transformation $\widehat{\boldsymbol{a}}'_{\vec{k}} = \widehat{\mathcal{M}}^\dagger\widehat{\boldsymbol{a}}_{\vec{k}}\widehat{\mathcal{M}}$, with

$$\widehat{\mathcal{M}} \simeq \widehat{\mathbb{I}} + \int_{\mathbb{R}^3}\mathrm{d}^3\vec{q}\sum_{a=1}^{10}\varepsilon_{\vec{q}}^a\widehat{L}_a^{\vec{q}}\,. \tag{3.45}$$

Note that $\widehat{L}_a^{\vec{q}}$ has to be anti-hermitian for $\widehat{\mathcal{M}}$ to be unitary. By expanding this transformation in $\epsilon_{\vec{q}}^a$, one obtains $\widehat{\boldsymbol{a}}'_{\vec{k}} \simeq \widehat{\boldsymbol{a}}_{\vec{k}} + \left[\widehat{\boldsymbol{a}}_{\vec{k}}, \int_{\mathbb{R}^3}\mathrm{d}^3q\sum_{a=1}^{10}\varepsilon_q^a\widehat{L}_a^{\vec{q}}\right]$ (where the commutator is performed on each entry of $\widehat{\boldsymbol{a}}_{\vec{k}}$). Since this formula should match Eq. (3.44), and given the commutation relations (2.16), this suggests to look for $\widehat{L}_a^{\vec{q}}$ operators that are quadratic in the creation and annihilation operators,

$$\widehat{L}_a^{\vec{q}} = \widehat{\boldsymbol{a}}_{\vec{q}}^\dagger\boldsymbol{\mathcal{Q}}^a\widehat{\boldsymbol{a}}_{\vec{q}}, \tag{3.46}$$

where $\boldsymbol{\mathcal{Q}}^a$ is anti-hermitian since $\widehat{L}_a^{\vec{q}}$ is. Making use of Eq. (2.16), this leads to $\left[\widehat{\boldsymbol{a}}_{\vec{k}}, \int_{\mathbb{R}^3}\mathrm{d}^3q\sum_{a=1}^{10}\varepsilon_q^a\widehat{L}_a^{\vec{q}}\right] = i\boldsymbol{\mathcal{J}}\sum_{a=1}^{10}\varepsilon_k^a\boldsymbol{\mathcal{Q}}^a\widehat{\boldsymbol{a}}_{\vec{k}}$. By identification with Eq. (3.44), this gives $\boldsymbol{L}_a = i\boldsymbol{\mathcal{J}}\boldsymbol{\mathcal{Q}}^a$, which can be inverted as

$$\boldsymbol{\mathcal{Q}}^a = i\boldsymbol{\mathcal{J}}\boldsymbol{L}_a\,. \tag{3.47}$$

Squeezing	$\widehat{L}_1^{\vec{k}} = \left(\widehat{a}^\dagger_{1,\vec{k}}\widehat{a}^\dagger_{1,-\vec{k}} - \widehat{a}_{1,\vec{k}}\widehat{a}_{1,-\vec{k}}\right) - \left(\widehat{a}^\dagger_{2,\vec{k}}\widehat{a}^\dagger_{2,-\vec{k}} - \widehat{a}_{2,\vec{k}}\widehat{a}_{2,-\vec{k}}\right)$ $\widehat{L}_2^{\vec{k}} = \left(\widehat{a}^\dagger_{1,\vec{k}}\widehat{a}^\dagger_{1,-\vec{k}} - \widehat{a}_{1,\vec{k}}\widehat{a}_{1,-\vec{k}}\right) + \left(\widehat{a}^\dagger_{2,\vec{k}}\widehat{a}^\dagger_{2,-\vec{k}} - \widehat{a}_{2,\vec{k}}\widehat{a}_{2,-\vec{k}}\right)$
Rotation	$\widehat{L}_3^{\vec{k}} = -i\left(\widehat{a}^\dagger_{1,\vec{k}}\widehat{a}_{1,\vec{k}} + \widehat{a}^\dagger_{1,-\vec{k}}\widehat{a}_{1,-\vec{k}} + 1\right) - i\left(\widehat{a}^\dagger_{2,\vec{k}}\widehat{a}_{2,\vec{k}} + \widehat{a}^\dagger_{2,-\vec{k}}\widehat{a}_{2,-\vec{k}} + 1\right)$ $\widehat{L}_4^{\vec{k}} = -i\left(\widehat{a}^\dagger_{1,\vec{k}}\widehat{a}_{1,\vec{k}} + \widehat{a}^\dagger_{1,-\vec{k}}\widehat{a}_{1,-\vec{k}} + 1\right) + i\left(\widehat{a}^\dagger_{2,\vec{k}}\widehat{a}_{2,\vec{k}} + \widehat{a}^\dagger_{2,-\vec{k}}\widehat{a}_{2,-\vec{k}} + 1\right)$ $\widehat{L}_5^{\vec{k}} = \left(\widehat{a}^\dagger_{1,\vec{k}}\widehat{a}_{2,\vec{k}} + \widehat{a}^\dagger_{1,-\vec{k}}\widehat{a}_{2,-\vec{k}}\right) - \left(\widehat{a}^\dagger_{2,\vec{k}}\widehat{a}_{1,\vec{k}} + \widehat{a}^\dagger_{2,-\vec{k}}\widehat{a}_{1,-\vec{k}}\right)$ $\widehat{L}_6^{\vec{k}} = -i\left(\widehat{a}^\dagger_{1,\vec{k}}\widehat{a}_{2,\vec{k}} + \widehat{a}^\dagger_{1,-\vec{k}}\widehat{a}_{2,-\vec{k}}\right) - i\left(\widehat{a}^\dagger_{2,\vec{k}}\widehat{a}_{1,\vec{k}} + \widehat{a}^\dagger_{2,-\vec{k}}\widehat{a}_{1,-\vec{k}}\right)$
Boost	$\widehat{L}_7^{\vec{k}} = i\left(\widehat{a}^\dagger_{1,\vec{k}}\widehat{a}^\dagger_{1,-\vec{k}} + \widehat{a}_{1,\vec{k}}\widehat{a}_{1,-\vec{k}}\right) + i\left(\widehat{a}^\dagger_{2,\vec{k}}\widehat{a}^\dagger_{2,-\vec{k}} + \widehat{a}_{2,\vec{k}}\widehat{a}_{2,-\vec{k}}\right)$ $\widehat{L}_8^{\vec{k}} = i\left(\widehat{a}^\dagger_{1,\vec{k}}\widehat{a}^\dagger_{1,-\vec{k}} + \widehat{a}_{1,\vec{k}}\widehat{a}_{1,-\vec{k}}\right) - i\left(\widehat{a}^\dagger_{2,\vec{k}}\widehat{a}^\dagger_{2,-\vec{k}} + \widehat{a}_{2,\vec{k}}\widehat{a}_{2,-\vec{k}}\right)$ $\widehat{L}_9^{\vec{k}} = \left(\widehat{a}^\dagger_{1,\vec{k}}\widehat{a}^\dagger_{2,-\vec{k}} + \widehat{a}^\dagger_{2,\vec{k}}\widehat{a}^\dagger_{1,-\vec{k}}\right) - \left(\widehat{a}_{1,\vec{k}}\widehat{a}_{2,-\vec{k}} + \widehat{a}_{2,\vec{k}}\widehat{a}_{1,-\vec{k}}\right)$ $\widehat{L}_{10}^{\vec{k}} = i\left(\widehat{a}^\dagger_{1,\vec{k}}\widehat{a}^\dagger_{2,-\vec{k}} + \widehat{a}^\dagger_{2,\vec{k}}\widehat{a}^\dagger_{1,-\vec{k}}\right) + i\left(\widehat{a}_{1,\vec{k}}\widehat{a}_{2,-\vec{k}} + \widehat{a}_{2,\vec{k}}\widehat{a}_{1,-\vec{k}}\right)$

Table 3. Quantum representation of the generators of $\mathscr{S}p(4,\mathbb{R})$.

This yields the generators $\widehat{L}_a^{\vec{q}}$ of the quantum representation listed in Table 3.

Another set of generators that is obtained from straightforward linear combinations of the $\widehat{L}_a^{\vec{k}}$ operators is given by

$$\widehat{a}^\dagger_{i,\vec{k}}\widehat{a}^\dagger_{i,-\vec{k}}\,, \qquad \widehat{a}_{i,\vec{k}}\widehat{a}_{i,-\vec{k}}\,, \qquad \widehat{a}^\dagger_{i,\vec{k}}\widehat{a}_{i,\vec{k}} + \widehat{a}^\dagger_{i,-\vec{k}}\widehat{a}_{i,-\vec{k}} + 1 \qquad \text{with} \quad i = 1,2\,, \tag{3.48}$$

which correspond to the two $\mathfrak{sp}(2,\mathbb{R})$ subalgebra identified below Eq. (3.8), and

$$\widehat{a}^\dagger_{i,\vec{k}}\widehat{a}^\dagger_{j,-\vec{k}} + \widehat{a}^\dagger_{j,\vec{k}}\widehat{a}^\dagger_{i,-\vec{k}}\,, \quad \widehat{a}_{i,\vec{k}}\widehat{a}_{j,-\vec{k}} + \widehat{a}_{j,\vec{k}}\widehat{a}_{i,-\vec{k}}\,, \quad \widehat{a}^\dagger_{i,\vec{k}}\widehat{a}_{j,\vec{k}} + \widehat{a}^\dagger_{i,-\vec{k}}\widehat{a}_{j,-\vec{k}} \quad \text{with} \quad i,j = 1,2\,, \tag{3.49}$$

which correspond to the coupling generators. The operators in Eqs. (3.48) generate two-mode creation, two-mode annihilation and a number counting operation respectively, acting on each sector separately. The first and second mixing generators in Eq. (3.49) originate from the two mixing boosts ($\widehat{L}_9^{\vec{k}}$ and $\widehat{L}_{10}^{\vec{k}}$). They correspond to the creation and annihilation of entangled pairs of particles with opposite momenta in the two sectors. The third mixing generator in Eq. (3.49) originates from the two mixing rotations ($\widehat{L}_5^{\vec{k}}$ and $\widehat{L}_6^{\vec{k}}$). It does not lead to net particle creation, but rather transfer excitations from one sector to the other. One can check that all these operations preserve momentum conservation.

4 Quantum dynamics

In Sec. 2, we explained how the symplectic group $\mathrm{Sp}(4,\mathbb{R})$ naturally appears in the description of physical systems made of two free fields. Having then studied its mathematical structure in Sec. 3, we now want to apply these tools to describe the dynamics of two-field systems. To this end, we explore the structure of the system's Hamiltonian in Sec. 4.1, before applying our findings to an explicit example. Then, we provide in Sec. 4.2 a tractable expression of the evolution operator.

4.1 Hamiltonian structure

In this section, we express the Hamiltonian in the occupation-number representation, to see which interactions are allowed in the theory on generic grounds. The only constraint we have on the Hamiltonian is that it stems from a real symmetric kernel, *i.e.* $\boldsymbol{H}_k$ is a real symmetric matrix. From Eq. (2.15), $\boldsymbol{\mathcal{H}}_k$ can thus be written as $\boldsymbol{\mathcal{H}}_k = \boldsymbol{U}\boldsymbol{N}_k\boldsymbol{U}^\dagger$, where $\boldsymbol{N}_k = (\boldsymbol{D}_k^{-1})^{\mathrm{T}}\boldsymbol{H}_k\boldsymbol{D}_k^{-1} + (\boldsymbol{D}_k^{-1})^{\mathrm{T}}\boldsymbol{\Omega}\dot{\boldsymbol{D}}_k^{-1}$ is a real symmetric matrix (the first term is obviously symmetric, while for the second term, this can be shown by differentiating with respect to time the symplectic relation (2.19) satisfied by $\boldsymbol{D}_k^{-1}$, and by using that $\boldsymbol{\Omega}^{\mathrm{T}} = -\boldsymbol{\Omega}$), which we parametrise as

$$\boldsymbol{N}_k = \begin{pmatrix} \boldsymbol{A} & \boldsymbol{C} \\ \boldsymbol{C}^{\mathrm{T}} & \boldsymbol{B} \end{pmatrix}, \tag{4.1}$$

with $\boldsymbol{A}, \boldsymbol{B}, \boldsymbol{C} \in \mathcal{M}_2(\mathbb{R})$ and $\boldsymbol{A}^{\mathrm{T}} = \boldsymbol{A}$, $\boldsymbol{B}^{\mathrm{T}} = \boldsymbol{B}$. This leads to

$$\boldsymbol{\mathcal{H}}_k = \begin{pmatrix} \mathfrak{a} & \mathfrak{b} \\ \mathfrak{b}^* & \mathfrak{a}^* \end{pmatrix} \tag{4.2}$$

with $\mathfrak{a} = (\boldsymbol{A} + \boldsymbol{B}) + i(\boldsymbol{C}^{\mathrm{T}} - \boldsymbol{C})$ and $\mathfrak{b} = (\boldsymbol{A} - \boldsymbol{B}) + i(\boldsymbol{C}^{\mathrm{T}} + \boldsymbol{C})$. Inverting those formulas, one obtains that $\mathfrak{a} + \mathfrak{a}^* = 2(A + B)$ and $\mathfrak{a} - \mathfrak{a}^* = 2i(C^{\mathrm{T}} - C)$, so the real part of $\mathfrak{a}$ should be symmetric while its imaginary part should be antisymmetric; and $\mathfrak{b} + \mathfrak{b}^* = 2(A - B)$ and $\mathfrak{b} - \mathfrak{b}^* = 2i(C^{\mathrm{T}} + C)$, so both the real and imaginary parts of $\mathfrak{b}$ should be symmetric. This imposes that $\mathfrak{a}$ and $\mathfrak{b}$ are of the form

$$\mathfrak{a} = \begin{pmatrix} F_{1,k} & F_{1\leftrightarrow 2,k}e^{i\varphi_k} \\ F_{1\leftrightarrow 2,k}e^{-i\varphi_k} & F_{2,k} \end{pmatrix}, \quad \mathfrak{b} = \begin{pmatrix} R_{1,k}e^{i\Theta_{1,k}} & R_{1\leftrightarrow 2,k}e^{i\xi_k} \\ R_{1\leftrightarrow 2,k}e^{i\xi_k} & R_{2,k}e^{i\Theta_{2,k}} \end{pmatrix}, \tag{4.3}$$

where $F_{1,k}$, $F_{1\leftrightarrow 2,k}$, $F_{2,k}$, φ_k, $R_{1,k}$, $R_{1\leftrightarrow 2,k}$, $R_{2,k}$, $\Theta_{1,k}$, $\Theta_{2,k}$ and ξ_k are ten real parameters, that in general depend on time, and which indeed saturate the ten degrees of freedom contained in $\boldsymbol{N}_k$. In fact, since the Green matrix is generated from the (integrated) Hamiltonian, those ten parameters fully determine the squeezing and rotation parameters, or equivalently the Bogolyubov coefficients, that characterise the dynamics.

The Hamiltonian $\widehat{\mathcal{H}} = \int_{\mathbb{R}^{3+}} \mathrm{d}^3\vec{k}\,\hat{\boldsymbol{a}}_{\vec{k}}^\dagger \boldsymbol{\mathcal{H}}_k \hat{\boldsymbol{a}}_{\vec{k}}$ thus contain three terms,

$$\widehat{\mathcal{H}} = \int_{\mathbb{R}^{3+}} \mathrm{d}^3\vec{k} \left(\widehat{\mathcal{H}}_{1,\vec{k}} + \widehat{\mathcal{H}}_{2,\vec{k}} + \widehat{\mathcal{H}}_{1\leftrightarrow 2,\vec{k}} \right), \tag{4.4}$$

with

$$\widehat{\mathcal{H}}_{i,\vec{k}} = F_{i,k}\left(\hat{a}_{i,\vec{k}}^\dagger \hat{a}_{i,\vec{k}} + \hat{a}_{i,-\vec{k}}^\dagger \hat{a}_{i,-\vec{k}} + 1\right) + R_{i,k}\left(e^{i\Theta_{i,k}}\hat{a}_{i,\vec{k}}^\dagger \hat{a}_{i,-\vec{k}}^\dagger + \mathrm{h.c.}\right) \quad \text{for} \quad i = 1, 2\,, \tag{4.5}$$

$$\widehat{\mathcal{H}}_{1\leftrightarrow 2,\vec{k}} = F_{1\leftrightarrow 2,k}e^{i\varphi_k}\left(\hat{a}_{1,\vec{k}}^\dagger \hat{a}_{2,\vec{k}} + \hat{a}_{1,-\vec{k}}^\dagger \hat{a}_{2,-\vec{k}}\right) + R_{1\leftrightarrow 2,k}e^{i\xi_k}\left(\hat{a}_{1,\vec{k}}^\dagger \hat{a}_{2,-\vec{k}}^\dagger + \hat{a}_{2,\vec{k}}^\dagger \hat{a}_{1,-\vec{k}}^\dagger\right) + \mathrm{h.c.}\,. \tag{4.6}$$

The Hamiltonian can thus be decomposed onto the quantum generators listed in Table 3 (this is because $\boldsymbol{\mathcal{J}}\boldsymbol{\mathcal{H}}_k$ is an element of the Lie algebra), hence we can benefit from their physical interpretation discussed in Sec. 3.4. The components $\widehat{\mathcal{H}}_1$ and $\widehat{\mathcal{H}}_2$ drive each sector separately and are made of two terms: a harmonic part controlled by $F_{i,k}$ that does not induce particle creation, and a parametric part controlled by $R_{i,k}$ that changes the particle

content. Physically, this parametric amplification is related to the presence of an external field (the electric field for the Schwinger effect [43], the gravitational field for the Hawking effect, space-time curvature for the physics of cosmological perturbations, *etc.*). The component $\widehat{\mathcal{H}}_{1\leftrightarrow 2}$ is an interaction term between the two sectors, and also contains two contributions: a "transferring" part, controlled by $F_{1\leftrightarrow 2,k}(t)$ and built from the two mixing rotation operators, that transfers particles from one sector to the other; and an "entangling" part, controlled by $R_{1\leftrightarrow 2,k}$ and built from the two mixing boost operators, that creates or annihilates joint pairs of particles in the two sectors.

Let us note that even when the entangling part is absent, *i.e.* when $R_{1\leftrightarrow 2,k} = 0$, entanglement between the two sectors can still indirectly arise from first creating particles in the two sectors separately with the parametric terms, and then transferring those particles between sectors by means of the transferring term.

Example of two massless fields in a cosmological background

Let us illustrate the formalism introduced above with a simple example. We consider two massless scalar fields ϕ and χ on a Friedmann-Lemaître-Robertson-Walker spatially flat geometry,

$$\mathrm{d}s^2 = a^2(\eta)\left(-\mathrm{d}\eta^2 + \delta^{ij}\mathrm{d}x_i\mathrm{d}x_j\right) , \tag{4.7}$$

where a is the scale factor and η is the conformal time. The Ricci scalar R of this metric is given by $R = 6a''/a^3$, where a prime denotes derivation with respect to conformal time. The action is given by

$$S = -\int \mathrm{d}^4x\sqrt{-\det g}\left(\frac{1}{2}g^{\mu\nu}\partial_\mu\phi\partial_\nu\phi + \frac{R}{2}\zeta\phi^2 + \frac{1}{2}g^{\mu\nu}\partial_\mu\chi\partial_\nu\chi + \frac{R}{2}\zeta\chi^2 + \lambda^2\phi\chi\right) , \tag{4.8}$$

where ζ is the conformal coupling constant and λ is a coupling parameter that has dimension of a mass. Expanding the scalar fields into Fourier modes as in Eq. (2.6) and making use of the reality prescription $\phi^*_{\vec{k}} = \phi_{-\vec{k}}$ and $\chi^*_{\vec{k}} = \chi_{-\vec{k}}$, with the the metric (4.7) the action reads

$$\begin{aligned} S \equiv \int \mathrm{d}\eta L = -\int \mathrm{d}\eta \int_{\mathbb{R}^{3+}} \mathrm{d}^3\vec{k}\Big[&a^2\phi'_{-\vec{k}}\phi'_{\vec{k}} + \left(k^2a^2 + R\zeta a^4\right)\phi_{-\vec{k}}\phi_{\vec{k}} \\ &+a^2\chi'_{-\vec{k}}\chi'_{\vec{k}} + \left(k^2a^2 + R\zeta a^4\right)\chi_{-\vec{k}}\chi_{\vec{k}} + \lambda^2a^4\left(\phi_{-\vec{k}}\chi_{\vec{k}} + \chi_{-\vec{k}}\phi_{\vec{k}}\right)\Big] , \end{aligned} \tag{4.9}$$

which also defines the Lagrangian density L. The conjugate momenta can be identified as $p^\phi_{\vec{k}} = a^2\phi'_{-\vec{k}}$ and $p^\chi_{\vec{k}} = a^2\chi'_{-\vec{k}}$, and upon performing a Legendre transform, one obtains a Hamiltonian of the form (2.7), with

$$\boldsymbol{H}_k = \begin{pmatrix} k^2a^2 + R\zeta a^4 & \lambda^2a^4 & 0 & 0 \\ \lambda^2a^4 & k^2a^2 + R\zeta a^4 & 0 & 0 \\ 0 & 0 & 1/a^2 & 0 \\ 0 & 0 & 0 & 1/a^2 \end{pmatrix} \qquad \text{and} \qquad \boldsymbol{z}_{\vec{k}} = \begin{pmatrix} \phi_{\vec{k}} \\ \chi_{\vec{k}} \\ p^\phi_{\vec{k}} \\ p^\chi_{\vec{k}} \end{pmatrix} . \tag{4.10}$$

The momentum sector of the Hamiltonian (*i.e.* the bottom-right block) can be simplified by performing a canonical transformation of the form (2.20), $\widetilde{\boldsymbol{z}}_{\vec{k}} = \boldsymbol{M}_k\boldsymbol{z}_{\vec{k}}$, with

$$\boldsymbol{M}_k = \begin{pmatrix} a & 0 & 0 & 0 \\ 0 & a & 0 & 0 \\ a' & 0 & 1/a & 0 \\ 0 & a' & 0 & 1/a \end{pmatrix} . \tag{4.11}$$

One can check that $\boldsymbol{M}_k$ satisfies the symplectic relation (2.19), and that the new Hamiltonian kernel, given by Eq. (2.21), reads

$$\widetilde{\boldsymbol{H}}_k = \begin{pmatrix} k^2 + R\zeta a^2 - a''/a & \lambda^2 a^2 & 0 & 0 \\ \lambda^2 a^2 & k^2 + R\zeta a^2 - a''/a & 0 & 0 \\ 0 & 0 & 1 & 0 \\ 0 & 0 & 0 & 1 \end{pmatrix} . \tag{4.12}$$

The $\tilde{\boldsymbol{z}}_{\vec{k}}$ variables are usually referred to as the Mukhanov-Sasaki variables, and in the helicity basis, Eq. (2.15) gives rise to a Hamiltonian kernel of the form (4.2), with

$$kR_{i,k} = \frac{a^2}{2} R\zeta - \frac{a''}{2a} , \qquad kF_{i,k} = k^2 + kR_{i,k} , \qquad F_{1\leftrightarrow 2,k} = R_{1\leftrightarrow 2,k} = \frac{\lambda^2 a^2}{2k} , \tag{4.13}$$

and where all the phases vanish, *i.e.* $\varphi_k = \Theta_{1,k} = \Theta_{2,k} = \xi_k = 0$. This allows one to relate the four Hamiltonian contributions identified in Sec. 4.1, namely the harmonic, parametric, transferring and entangling terms, to the microphysical parameters of the problem. In particular, one can see that the parametric term is generated by the external "field" $a(t)$ (since when the scale factor is a constant, $R_{i,k} = 0$), and that the transferring and entangling terms are controlled by the coupling parameter λ, in agreement with the discussion in Sec. 4.1.

Since $R = 6a''/a^3$, the parametric term is given by $kR_{i,k} = (3\zeta - 1/2)a''/a$. Therefore, if one sets $\zeta = 1/6$, the parametric term vanishes, and the harmonic term simply becomes $F_{i,k} = k$, as in flat space time. This is because, in that case, the fields are conformally coupled to the metric, which removes the effect of space-time expansion that otherwise generates parametric amplification. This implies that, in the absence of direct coupling (*i.e.* if $\lambda = 0$), there is no particle creation, and the above system is made of uncoupled harmonic oscillators. However, in the presence of direct coupling, both the transferring and the entangling terms become non vanishing, which guarantees that entangled pairs of particles are created and exchanged between the two fields. This is because the interaction term breaks conformal invariance, as noticed in Ref. [44].

4.2 Evolution operator

We now investigate the integrated dynamics. As explained in Sec. 3.3, the Green's matrix in the helicity basis, $\boldsymbol{\mathcal{G}}_k(t, t_{\rm in})$, belongs to $\mathscr{S}p(4, \mathbb{R})$. Its quantum analogue, the so-called evolution operator $\widehat{\mathcal{U}}_{\vec{k}}(t, t_{\rm in})$, thus lies in the quantum representation of $\mathscr{S}p(4, \mathbb{R})$, which was studied in Sec. 3.4. In this section, we make use of the formal results derived above to derive a tractable expression for the evolution operator.

Since the Green matrix is separable in Fourier space for free fields, the evolution operator is also factorisable as

$$\widehat{\mathcal{U}}(t, t_{\rm in}) = \prod_{\vec{k}\in\mathbb{R}^{3+}} \widehat{\mathcal{U}}_{\vec{k}}(t, t_{\rm in}) , \tag{4.14}$$

where $\widehat{\mathcal{U}}_{\vec{k}}(t, t_{\rm in}) \in \mathscr{S}p(4, \mathbb{R})$. Making use of the Bloch-Messiah decomposition presented in Secs. 3.2 and 3.3, one can write

$$\widehat{\mathcal{U}}_{\vec{k}}(t, t_{\rm in}) = \widehat{\mathcal{R}}_{\vec{k}}(\boldsymbol{\theta}_k) \cdot \widehat{\mathcal{Z}}_{\vec{k}}(\boldsymbol{d}_k) \cdot \widehat{\mathcal{R}}_{\vec{k}}(\boldsymbol{\varphi}_k) , \tag{4.15}$$

see Eq. (3.32), where the squeezing and rotation parameters depend only on the norm of the wavevector, since this is also the case for the Green's matrix. Further factorisation can be

obtained by the procedure outlined in Sec. 3.3 and leading to Eq. (3.42), and replacing the generators in Eq. (3.42) by their expression in the quantum representation given in Table 3, one finds that the evolution operator involves three types of operation only, namely

$$\widehat{\mathcal{R}}_{i,\vec{k}}(\theta_k) \equiv \exp\left[-i\theta_k\left(\widehat{a}^\dagger_{i,\vec{k}}\widehat{a}_{i,\vec{k}} + \widehat{a}^\dagger_{i,-\vec{k}}\widehat{a}_{i,-\vec{k}} + 1\right)\right] , \tag{4.16}$$

$$\widehat{\mathcal{Z}}_{i,\vec{k}}(r_k) \equiv \exp\left[r_k\left(\widehat{a}^\dagger_{i,\vec{k}}\widehat{a}^\dagger_{i,-\vec{k}} - \widehat{a}_{i,\vec{k}}\widehat{a}_{i,-\vec{k}}\right)\right] , \tag{4.17}$$

$$\widehat{\mathcal{R}}_{i\to j,\vec{k}}(p_k) \equiv \exp\left[ip_k\left(\widehat{a}^\dagger_{j,\vec{k}}\widehat{a}_{i,\vec{k}} + \widehat{a}^\dagger_{j,-\vec{k}}\widehat{a}_{i,-\vec{k}}\right)\right] . \tag{4.18}$$

The operators $\widehat{\mathcal{R}}_{i,\vec{k}}(\theta_k)$ are constructed from the rotation generators and induce global phase shifts in sector i, without changing the particle content. The squeezing operators $\widehat{\mathcal{Z}}_{i,\vec{k}}(r_k)$ create pairs of entangled particles in each sector separately, and $\widehat{\mathcal{R}}_{i\to j,\vec{k}}(p_k)$ transfers particles from one sector to the other without changing their overall number. In order to express the operators $\widehat{\mathcal{R}}_{\vec{k}}(\boldsymbol{\theta}_k), \widehat{\mathcal{R}}_{\vec{k}}(\boldsymbol{\varphi}_k)$ and $\widehat{\mathcal{Z}}_{\vec{k}}(\boldsymbol{d}_k)$ that appear in Eq. (4.15) in terms of $\widehat{\mathcal{R}}_{i,\vec{k}}, \widehat{\mathcal{R}}_{i\to j,\vec{k}}$ and $\widehat{\mathcal{Z}}_{i,\vec{k}}$, we adopt a diagrammatic representation analogous to quantum circuits:

$\widehat{\mathcal{R}}_{\vec{k}}(\boldsymbol{\varphi}_k)$:

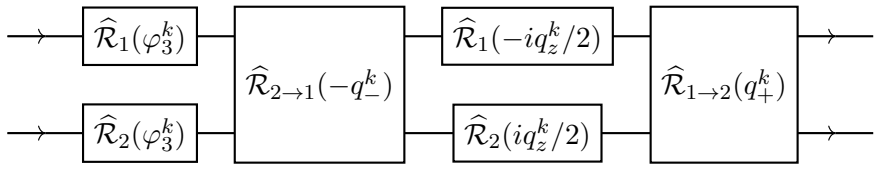

$\widehat{\mathcal{Z}}_{\vec{k}}(\boldsymbol{d}_k)$:

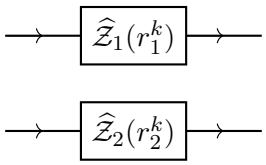

$\widehat{\mathcal{R}}_{\vec{k}}(\boldsymbol{\theta}_k)$:

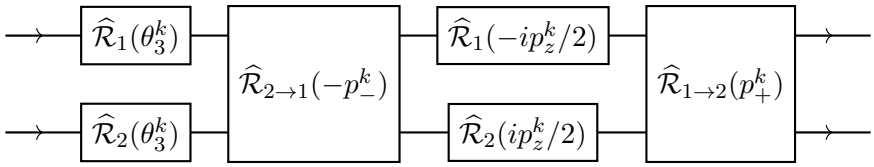

In those graphical representations, the top line stands for operations performed on the first sector, the bottom line on the second sector, and entangling operations are displayed with joint boxes. To run a "circuit", one successively applies the operations from the left to right (along the direction shown with the arrows). The parameters entering the circuits were introduced in Sec. 3.2. The squeezing parameters $r_1^k = d_1^k + d_2^k$ and $r_2^k = d_2^k - d_1^k$ control the two-mode creation in each sector, while the mixing parameters p_z^k, p_-^k, p_+^k and q_z^k, q_-^k, q_+^k control the entanglement between the two sectors. This shows that dynamical evolution can be seen as successive applications of phase rotations within each sector, creations of particles with opposite momenta in each subspace, and particle transfers between the two sectors.

5 Quantum state

We are now in a position to write down the quantum state of the system in the occupation-number basis. To that hand, we first need to equip our Hilbert space with a Fock-space structure. In practice, we impose that the creation and annihilation operators are ladder operators for the Hamiltonian at initial time $t_{\rm in}$, *i.e.*

$$\left[\widehat{\mathcal{H}}, \widehat{a}^\dagger_{i,\pm\vec{k}}\right] = c_{i,k}\widehat{a}^\dagger_{i,\pm\vec{k}} \qquad \text{and} \qquad \left[\widehat{\mathcal{H}}, \widehat{a}_{i,\pm\vec{k}}\right] = -c_{i,k}\widehat{a}_{i,\pm\vec{k}} \tag{5.1}$$

at $t_{\rm in}$, for $i = 1, 2$ and where $c_{i,k}$ are real parameters. Among the various terms (4.5) and (4.6) that the Hamiltonian may contain, only number counting operators, $\widehat{N}_{i,\pm\vec{k}} \equiv \widehat{a}^\dagger_{i,\pm\vec{k}}\widehat{a}_{i,\pm\vec{k}}$, give commutators of the form (5.1). This imposes that only the harmonic terms, *i.e.* those controlled by $F_{i,k}$, can be present at initial time, leading to $c_{i,k} = F_{i,k}(t_{\rm in})$; while one must have $R_{i,k}(t_{\rm in}) = R_{1\leftrightarrow 2,k}(t_{\rm in}) = F_{1\leftrightarrow 2,k}(t_{\rm in}) = 0$. This is for instance the case in the example discussed in Sec. 4.1 if the expansion is initially accelerating, since one can check that, then, in the asymptotic past (*i.e.* in the limit $a \to 0$), only $F_{i,k} \simeq k$ survives in Eq. (4.13). More generally, this is true in inflating backgrounds where Fourier modes get blue-shifted below the Hubble scale at early time, and hereafter we will assume that this condition is indeed satisfied.

We then build the Fock basis of the initial Hilbert space,

$$\mathcal{E}(t_{\rm in}) = \prod_{\vec{k}\in\mathbb{R}^{3+}} \mathcal{E}^{(1)}_{\vec{k}}(t_{\rm in}) \otimes \mathcal{E}^{(1)}_{-\vec{k}}(t_{\rm in}) \otimes \mathcal{E}^{(2)}_{\vec{k}}(t_{\rm in}) \otimes \mathcal{E}^{(2)}_{-\vec{k}}(t_{\rm in}), \tag{5.2}$$

which is a quadripartite system. The four-mode vacuum state is the one annihilated by all four annihilation operators, denoted by

$$|\emptyset(t_{\rm in})\rangle = \prod_{\vec{k}\in\mathbb{R}^{3+}} |0^{(1)}_{\vec{k}},\, 0^{(1)}_{-\vec{k}},\, 0^{(2)}_{\vec{k}},\, 0^{(2)}_{-\vec{k}}\rangle\,(t_{\rm in})\,, \tag{5.3}$$

and the rest of the Fock space can be built by successive applications of creation operators, which leads to the Fock states

$$|m^{(1)}_{\vec{k}}, n^{(1)}_{-\vec{k}}, s^{(2)}_{\vec{k}}, t^{(2)}_{-\vec{k}}\rangle\,(t_{\rm in}) = \frac{\left(\widehat{a}^\dagger_{1,\vec{k}}\right)^m}{m!}\frac{\left(\widehat{a}^\dagger_{1,-\vec{k}}\right)^n}{n!}\frac{\left(\widehat{a}^\dagger_{2,\vec{k}}\right)^s}{s!}\frac{\left(\widehat{a}^\dagger_{2,-\vec{k}}\right)^t}{t!}|0^{(1)}_{\vec{k}}, 0^{(1)}_{-\vec{k}}, 0^{(2)}_{\vec{k}}, 0^{(2)}_{-\vec{k}}\rangle\,(t_{\rm in}). \tag{5.4}$$

From now on, we drop the argument $t_{\rm in}$ to make the notation lighter.

5.1 Four-mode squeezed state

The evolved vacuum is obtained by application of the evolution operator on the initial vacuum[5]

$$|\emptyset(t)\rangle = \widehat{\mathcal{U}}(t, t_{\rm in})\,|\emptyset(t_{\rm in})\rangle\,. \tag{5.5}$$

[5]Note that, in place of the initial vacuum, one may consider an initial state of the form $|\Psi(t_{\rm in})\rangle = \prod_{\vec{k}}\widehat{\mathcal{A}}_{\vec{k}}(t_{\rm in})\,|\emptyset(t_{\rm in})\rangle$, where $\widehat{\mathcal{A}}_{\vec{k}}(t_{\rm in}) \in \mathscr{S}p(4,\mathbb{R})$. Such states are often referred to as "alpha vacua" [45] (where further restrictions on $\widehat{\mathcal{A}}_{\vec{k}}(t_{\rm in})$ sometimes apply). Since the product of two elements of $\mathscr{S}p(4,\mathbb{R})$ still lies in $\mathscr{S}p(4,\mathbb{R})$, the evolved alpha vacua are still of the form (5.5), so our discussion encompasses this possibility.

In this section, we present its explicit expression in the Fock space, where we derive the most generic form of a four-mode squeezed state.

In Appendix B, we apply the operators appearing in the circuits sketched in Sec. 4.2 onto the vacuum state (5.3) one after the other, and derive the following expression for the evolved vacuum state $|\emptyset(t)\rangle = \prod_{\vec{k}\in\mathbb{R}^{3+}} |\emptyset_{\vec{k}}(t)\rangle$,

$$|\emptyset_{\vec{k}}(t)\rangle = \sum_{n,m=0}^{\infty} \sum_{s,t=-n}^{m} c_k(n,m,s,t)\, |(n+s)^{(1)}_{\vec{k}}, (n+t)^{(1)}_{-\vec{k}}, (m-s)^{(2)}_{\vec{k}}, (m-t)^{(2)}_{-\vec{k}}\rangle\,, \tag{5.6}$$

with

$$\begin{aligned} c_k(n,m,s,t) = {} & \frac{e^{-2i\left[\theta_3^k(n+m+1)+\varphi_3^k\right]}}{\cosh r_1^k \cosh r_2^k} (-1)^{n+m} e^{p_z^k(m-n)} \tanh^n(r_1^k) \tanh^m(r_2^k) (ip_+^k)^{-s-t} \frac{m!}{n!} \\ & \sqrt{\frac{(m-s)!(m-t)!}{(n+s)!(n+t)!}} \sum_{i=\max(0,s)}^{m} \frac{\left(p_-^k p_+^k e^{-p_z^k}\right)^i (n+i)!}{i!(i-s)!(m-i)!} \sum_{j=\max(0,t)}^{m} \frac{\left(p_-^k p_+^k e^{-p_z^k}\right)^j (n+j)!}{j!(j-t)!(m-j)!} \end{aligned} \tag{5.7}$$

(and where the summation index t should not be confused with the time parameter). This generic expression of four-mode squeezed states expanded in the Fock basis is one of the main results of this paper. It features an infinite tower of entangled states, characterised by non-trivial numbers of excitations. More precisely, there are 6 indices being summed over, which can be interpreted as follows. The indices i and j are internal and can be resumed within each Fock state separately, their physical interpretation will be made clearer below.[6] The indices n and m are related to the creation of entangled pairs of excitations with opposite wavevector inside each sector separately, and arise from the squeezing operation (4.17). The indices s and t are related to the transfer of excitations between the two sectors, with wavevector $\vec{k}$ and $-\vec{k}$ respectively. They arise from the transferring operation (4.18) and entangle the two sectors. They are negative when excitations go from the first sector to the second sector, positive otherwise, and their bounds guarantee that the number of excitations remains non negative. One should also note that $c_k(m,n,s,t)$ is invariant when swapping n,m and s,t, *i.e.* $\vec{k}$ and $-\vec{k}$, which is a consequence of statistical isotropy. The form of the expansion (5.6) is therefore a direct consequence of the symmetries of the problem, although the precise expression of $c_k(m,n,s,t)$ given in Eq. (5.7) required a non-trivial calculation.

Let us stress that only seven out of the ten $\mathrm{Sp}(4,\mathbb{R})$ squeezing and rotation parameters enter Eq. (5.7). This is because, as explained in Appendix B, the rotation $\widehat{\mathcal{R}}_{\vec{k}}(\boldsymbol{\varphi}_k)$ only adds a global phase to the initial vacuum state, since it is invariant under rotations (in practice, this global phase is irrelevant, which reduces the number of effective parameters down to

[6] The internal indices i and j can be resumed in terms of the hypergeometric function ${}_2F_1$, leading to

$$\begin{aligned} c_k(n,m,s,t) = {} & \frac{e^{-2i\left[\varphi_3^k+\theta_3^k(n+m+1)\right]}}{\cosh r_1^k \cosh r_2^k} (-1)^{n+m} e^{p_z^k(m-n)} \tanh^n\left(r_1^k\right) \tanh^m\left(r_2^k\right) \left(p_-^k p_+^k e^{-p_z^k}\right)^{\max(0,s)+\max(0,t)} \\ & (ip_+^k)^{-s-t} \frac{m!}{n!} \sqrt{\frac{(m-s)!(m-t)!}{(n+s)!(n+t)!}} \frac{1}{|s|!|t|!} \frac{[n+\max(0,s)]![n+\max(0,t)]!}{[m-\max(0,s)]![m-\max(0,t)]!} \\ & {}_2F_1\left[-m+\max(0,s), 1+n+\max(0,s), 1-s+2\max(0,s), -p_-^k p_+^k e^{-p_z^k}\right] \\ & {}_2F_1\left[-m+\max(0,t), 1+n+\max(0,t), 1-t+2\max(0,t), -p_-^k p_+^k e^{-p_z^k}\right]. \end{aligned} \tag{5.8}$$

six). As a consequence, q_-^k, q_+^k and q_z^k are ineffective (had we started from a different initial state, those parameters would have entered the final result, see footnote 5). In practice, once the Hamiltonian of the system is specified, the dynamics can be integrated, which yields the seven relevant squeezing and rotation parameters, r_1^k, r_2^k, φ_3^k, θ_3^k, p_-^k, p_+^k and p_z^k, and thus fully determines the quantum state of the system at any time.

As a consistency check, one may verify that in the decoupled limit, the product of two two-mode squeezed states is recovered. Setting the two mixing parameters θ_5^k and θ_6^k to zero, Eq. (3.21) leads to $\theta^k = |\theta_4^k|$ and $\tau_k = 0$, so Eq. (3.20) gives $p_-^k = p_+^k = 0$ and $p_z^k = 2i\theta_4^k$. In Eq. (5.7), the overall factor $(p_-^k)^{i+j}$ is therefore non vanishing only when $i+j=0$, *i.e.* $i=j=0$ since i and j are non negative. Then, the overall factor $(p_+^k)^{i+j-s-t}$ is non vanishing only when $s+t=0$, but since $s \leq i = 0$ and $t \leq j = 0$, this implies that $s=t=0$, so only one term remains. This gives rise to

$$\begin{aligned} |\emptyset_{\vec{k}}(t)\rangle \;=\; e^{-2i(\theta_3^k+\varphi_3^k)} \sum_{n=0}^{\infty} \overbrace{\frac{(-1)^n e^{-2in(\theta_3^k+\theta_4^k)}}{\cosh r_1^k} \tanh^n(r_1^k)}^{c_{1,k}(n)} \left| n_{\vec{k}}^{(1)}, n_{-\vec{k}}^{(1)} \right\rangle \\ \times \sum_{m=0}^{\infty} \underbrace{\frac{(-1)^m e^{-2im(\theta_3^k-\theta_4^k)}}{\cosh r_2^k} \tanh^m(r_2^k)}_{c_{2,k}(m)} \left| m_{\vec{k}}^{(2)}, m_{-\vec{k}}^{(2)} \right\rangle , \end{aligned} \tag{5.9}$$

which defines the two-mode squeezed states coefficients $c_{i,k}(n)$. Up to a global irrelevant phase, this is indeed the product of two, uncoupled and disentangled, two-mode squeezed states [13].

Expansion around the uncoupled limit

In order to gain some physical insight into the structure of the four-mode squeezed states, and having in mind possible comparisons with perturbative techniques that expand in the amplitude of the interaction Hamiltonian (*i.e.* in the terms in the Hamiltonian that mix the two sectors), let us now expand the evolved vacuum state (5.7) around the uncoupled limit (5.9). From Eq. (3.21), one can see that the coupling parameters, *i.e.* θ_5^k, φ_5^k, θ_6^k and φ_6^k, only appear through the combination $\tau_k = -(\theta_6^k - i\theta_5^k) = |\tau_k| e^{i \arg(\tau_k)}$, since $\theta^k = \sqrt{(\theta_4^k)^2 + |\tau_k|^2}$, and given that φ_5^k and φ_6^k are irrelevant, as explained above. As a consequence, an expansion around the uncoupled limit is an expansion in $|\tau_k|$. Upon expanding Eq. (5.7) up to quadratic order in $|\tau_k|$, one obtains

$$\begin{aligned} |\emptyset_{\vec{k}}(t)\rangle = \sum_{n,m=0}^{\infty} c_{1,k}(n) c_{2,k}(m) \Bigg\{ & \left| n_{\vec{k}}^{(1)}, n_{-\vec{k}}^{(1)}, m_{\vec{k}}^{(2)}, m_{-\vec{k}}^{(2)} \right\rangle \\ & + |\tau_k| \left[\mathcal{F}_k(n, m+1) \left| 1_{1\to 2} \right\rangle - \mathcal{F}_k^*(n+1, m) \left| 1_{2\to 1} \right\rangle \right] \\ & + \frac{|\tau_k|^2}{2} \Big[\mathcal{F}_k(n, m+2) \mathcal{F}_k(n-1, m+1) \left| 2_{1\to 2} \right\rangle + \mathcal{F}_k^*(n+2, m) \mathcal{F}_k^*(n+1, m-1) \left| 2_{2\to 1} \right\rangle \\ & + 2\mathcal{F}_k^2(n, m+1) \left| 1\text{-}1_{1\to 2} \right\rangle + 2(\mathcal{F}_k^*)^2(n+1, m) \left| 1\text{-}1_{2\to 1} \right\rangle \\ & - 2\mathcal{F}_k(n, m) \mathcal{F}_k^*(n+1, m+1) \left| 2_{1\leftrightarrow 2} \right\rangle + 2\mathcal{G}_k(n, m) \left| n_{\vec{k}}^{(1)}, n_{-\vec{k}}^{(1)}, m_{\vec{k}}^{(2)}, m_{-\vec{k}}^{(2)} \right\rangle \Big] \Bigg\}, \end{aligned} \tag{5.10}$$

where the Fock states that appear in this expansion are labeled by the number of particles being transferred from one sector to the other (while respecting statistical isotropy), and are given by

$$
\begin{aligned}
|1_{1\to2}\rangle &\simeq \left|(n-1)^{(1)}_{\vec{k}}, n^{(1)}_{-\vec{k}}, (m+1)^{(2)}_{\vec{k}}, m^{(2)}_{-\vec{k}}\right\rangle + \left|n^{(1)}_{\vec{k}}, (n-1)^{(1)}_{-\vec{k}}, m^{(2)}_{\vec{k}}, (m+1)^{(2)}_{-\vec{k}}\right\rangle \\
|1_{2\to1}\rangle &= \left|(n+1)^{(1)}_{\vec{k}}, n^{(1)}_{-\vec{k}}, (m-1)^{(2)}_{\vec{k}}, m^{(2)}_{-\vec{k}}\right\rangle + \left|n^{(1)}_{\vec{k}}, (n+1)^{(1)}_{-\vec{k}}, m^{(2)}_{\vec{k}}, (m-1)^{(2)}_{-\vec{k}}\right\rangle \\
|2_{1\to2}\rangle &= \left|(n-2)^{(1)}_{\vec{k}}, n^{(1)}_{-\vec{k}}, (m+2)^{(2)}_{\vec{k}}, m^{(2)}_{-\vec{k}}\right\rangle + \left|n^{(1)}_{\vec{k}}, (n-2)^{(1)}_{-\vec{k}}, m^{(2)}_{\vec{k}}, (m+2)^{(2)}_{-\vec{k}}\right\rangle \\
|2_{2\to1}\rangle &= \left|(n+2)^{(1)}_{\vec{k}}, n^{(1)}_{-\vec{k}}, (m-2)^{(2)}_{\vec{k}}, m^{(2)}_{-\vec{k}}\right\rangle + \left|n^{(1)}_{\vec{k}}, (n+2)^{(1)}_{-\vec{k}}, m^{(2)}_{\vec{k}}, (m-2)^{(2)}_{-\vec{k}}\right\rangle \\
|2_{1\leftrightarrow2}\rangle &= \left|(n+1)^{(1)}_{\vec{k}}, (n-1)^{(1)}_{-\vec{k}}, (m-1)^{(2)}_{\vec{k}}, (m+1)^{(2)}_{-\vec{k}}\right\rangle \\
&\quad + \left|(n-1)^{(1)}_{\vec{k}}, (n+1)^{(1)}_{-\vec{k}}, (m+1)^{(2)}_{\vec{k}}, (m-1)^{(2)}_{-\vec{k}}\right\rangle \\
|1\text{-}1_{1\to2}\rangle &= \left|(n-1)^{(1)}_{\vec{k}}, (n-1)^{(1)}_{-\vec{k}}, (m+1)^{(2)}_{\vec{k}}, (m+1)^{(2)}_{-\vec{k}}\right\rangle \\
|1\text{-}1_{2\to1}\rangle &= \left|(n+1)^{(1)}_{\vec{k}}, (n+1)^{(1)}_{-\vec{k}}, (m-1)^{(2)}_{\vec{k}}, (m-1)^{(2)}_{-\vec{k}}\right\rangle
\end{aligned}
\tag{5.11}
$$

with the weighting functions

$$
\mathcal{F}_k(n,m) = i\frac{\sin\theta_4^k}{\theta_4^k} e^{i[\theta_4^k + \arg(\tau_k)]}\sqrt{nm}\,, \tag{5.12}
$$

$$
\mathcal{G}_k(n,m) = -2\mathcal{F}_k(n+1,m)\mathcal{F}_k^*(n+1,m) - i(n-m)\frac{\theta_4^k - e^{i\theta_4^k}\sin\theta_4^k}{(\theta_4^k)^2}. \tag{5.13}
$$

These expressions can be interpreted as follows. At linear order in τ, the only effect of the interaction is to add contributions from states where one particle has been exchanged between the two sectors [those are displayed in the second line of Eq. (5.10)]. The amplitude of these additional states is controlled by $\mathcal{F}_k$, which thus measures the rate at which particles transfer. It involves the phase θ_4^k through a function of order one, and the product of the numbers of particles in the two sectors, which mostly determines its amplitude. At quadratic order in τ, the new states that appear in the expansion are obtained by exchanging two particles: either two particles with the same wavevector transfer from one sector to the other [third line of Eq. (5.10)], or two particles with opposite wavevector transfer from one sector to the other [fourth line of Eq. (5.10)], or two particles with opposite wavevector and from opposite sectors change sector [first term in the fifth line of Eq. (5.10)], or, finally, one particle changes sector and then moves back to its original sector [last term in the fifth line of Eq. (5.10)]. The amplitude of those states are now controlled by squared powers of $\mathcal{F}_k$, the only exception being the last state, controlled by $\mathcal{G}_k$, which also involves the second term in Eq. (5.13). This can be interpreted as follows. When a particle transiently visits the opposite sector and is then reinstated, its journey to the other side modifies its state if the two sectors evolve differently. This is the case if $n \neq m$, which is why the second term in Eq. (5.13) is controlled by $n - m$.

One concludes that an expansion in the amplitude of the interaction, around the uncoupled limit, is essentially an expansion in the number of particles being exchanged: at order $|\tau_k|^p$, p particles are transferred, which allows one to predict the form of the new

states that appear in the expansion (*e.g.* $|p_{1\to2}\rangle = \left|(n-p)^{(1)}_{\vec{k}}, n^{(1)}_{-\vec{k}}, (m+p)^{(2)}_{\vec{k}}, m^{(2)}_{-\vec{k}}\right\rangle + \left|n^{(1)}_{\vec{k}}, (n-p)^{(1)}_{-\vec{k}}, m^{(2)}_{\vec{k}}, (m+p)^{(2)}_{-\vec{k}}\right\rangle$, *etc.*). In particular, one can see that the diagonal elements, *i.e.* the amplitudes associated to the states of the form $\left|n^{(1)}_{\vec{k}}, n^{(1)}_{-\vec{k}}, m^{(2)}_{\vec{k}}, m^{(2)}_{-\vec{k}}\right\rangle$, where, within each sector, there are the same number of excitations in each wavevector, receive contributions from even powers of $|\tau_k|$ only. More generally, one can show that $c_k(n,m,s,t) = \mathcal{O}(|\tau|^{|s|+|t|})$, and that $c_k(n,m,s,t)$ only receives contributions of order $|\tau|^{|s|+|t|+2q}$, where q is a positive integer number counting the number of particles being sent away and then sent back to their original sector. This is described by the sums over i and j in Eq. (5.7), where i counts the number of quanta travelling from sector 1 to sector 2 and travelling back, and j counts the number of quanta travelling along the opposite journey. This completes the physical interpretation of all six summation indices appearing in Eq. (5.7).

5.2 Phase-space representation

Although the quantum state derived in the Fock basis in Sec. 5.1 is enough to fully characterise the system, and in spite of the clear physical interpretation it yields, the seemingly complicated structure of Eq. (5.7) may call for alternative, simpler representations of the state. In this section, we provide such an alternative description by means of the Wigner function [40, 41, 46].

Gaussian state

As we will see, the reason why the Wigner function is a convenient tool is that, the dynamics being linear, the evolved vacuum state is a Gaussian state, which is fully characterised by its two-point function

$$\boldsymbol{\Sigma}_{\vec{k},\vec{q}}(t) = \langle\emptyset|\, \widehat{\boldsymbol{z}}_{\vec{k}}(t)\widehat{\boldsymbol{z}}^{\dagger}_{\vec{q}}(t)\,|\emptyset\rangle \ , \tag{5.14}$$

which here is expressed in the Heisenberg picture. Using the statistical isotropy and homogeneity we have already invoked, different Fourier modes are uncoupled and one has

$$\boldsymbol{\Sigma}_{\vec{k},\vec{q}}(t) = \boldsymbol{\Sigma}_k(t)\delta^3(\vec{k}-\vec{q})\,. \tag{5.15}$$

Our first goal is to relate $\boldsymbol{\Sigma}_k$ to the Bogolyubov coefficients introduced in Sec. 3.3, since those describe the dynamical evolution of the system. In the helicity basis (2.13), Eq. (5.14) gives rise to

$$\boldsymbol{\Sigma}_k(t) = \boldsymbol{D}_k^{-1}\boldsymbol{U}^{\dagger}\,\langle\emptyset_{\vec{k}}|\,\widehat{\boldsymbol{a}}_{\vec{k}}(t)\widehat{\boldsymbol{a}}^{\dagger}_{\vec{k}}(t)\,|\emptyset_{\vec{k}}\rangle\,\boldsymbol{U}\boldsymbol{D}_k^{-1}\,, \tag{5.16}$$

where the ladder operators evolve according to Eq. (2.22),[7] *i.e.* by means of the Green matrix $\boldsymbol{\mathcal{G}}_k(t,t_{\rm in})$. Since the Green matrix is an element of $\mathscr{Sp}(4,\mathbb{R})$, it can be written down in terms

[7] In the quantum representation constructed in Sec. 3.4, the evolution of the ladder operators is rather given by $\widehat{\boldsymbol{a}}_{\vec{k}}(t) = \widehat{\mathcal{U}}^{\dagger}_{\vec{k}}(t,t_{\rm in})\widehat{\boldsymbol{a}}_{\vec{k}}(t_{\rm in})\widehat{\mathcal{U}}_{\vec{k}}(t,t_{\rm in})$, but one can show that this is strictly equivalent to Eq. (2.22). Indeed, upon writing the evolution operator $\widehat{\mathcal{U}}_{\vec{k}}$ in the fully factorised form derived in Sec. 4.2, computing the commutators between the ten elementary operations and the $\widehat{\boldsymbol{a}}_{\vec{k}}(t_{\rm in})$ operators, and relating the Bogolyubov coefficients to the squeezing and rotation parameters using Eqs. (3.33)-(3.40), one can check that the same result (5.19)-(5.21) is obtained.

of Bogolyubov coefficients as in Eqs. (3.24) and (3.26). Moreover, the ordering of the ladder operators in Eq. (2.13) is such that

$$\langle \emptyset |\, \widehat{\boldsymbol{a}}_{\vec{k}}(t_{\rm in}) \widehat{\boldsymbol{a}}^{\dagger}_{\vec{k}}(t_{\rm in})\, |\emptyset\rangle = \begin{pmatrix} 1 & 0 \\ 0 & 0 \end{pmatrix} \otimes \boldsymbol{I}_2\,, \tag{5.17}$$

so one obtains

$$\boldsymbol{\Sigma}_k(t) = \underbrace{\begin{pmatrix} \mathbf{Cov}_k^{(\phi\phi)} & \mathbf{Cov}_k^{(\phi\pi)} \\ \mathbf{Cov}_k^{(\phi\pi)\rm T} & \mathbf{Cov}_k^{(\pi\pi)} \end{pmatrix}}_{\mathbf{Cov}_k(t)} + \frac{i}{2}\boldsymbol{\Omega}, \tag{5.18}$$

where the second term, $i\boldsymbol{\Omega}/2$, stems from the quantum commutator (2.11), and which defines the covariance matrix $\mathbf{Cov}_k(t)$. It is a real, symmetric, positive and semi-definite 4×4 matrix, where $\mathbf{Cov}_k^{(\phi\phi)}$, $\mathbf{Cov}_k^{(\pi\pi)}$ and $\mathbf{Cov}_k^{(\phi\pi)}$ are 2×2 matrices containing the position-position spectra, momentum-momentum spectra and position-momentum spectra, reading

$$\mathbf{Cov}_k^{(\phi\phi)} = \frac{1}{k}\begin{pmatrix} \frac{1}{2}\left(|\alpha_{11}+\beta_{11}^*|^2+|\alpha_{12}+\beta_{12}^*|^2\right) & \mathrm{Re}\left[\beta_{11}\left(\beta_{21}^*+\alpha_{21}\right)+\beta_{12}\left(\beta_{22}^*+\alpha_{22}\right)\right] \\ \mathrm{Re}\left[\beta_{11}\left(\beta_{21}^*+\alpha_{21}\right)+\beta_{12}\left(\beta_{22}^*+\alpha_{22}\right)\right] & \frac{1}{2}\left(|\alpha_{21}+\beta_{21}^*|^2+|\alpha_{22}+\beta_{12}^*|^2\right) \end{pmatrix} \tag{5.19}$$

$$\mathbf{Cov}_k^{(\pi\pi)} = k\begin{pmatrix} \frac{1}{2}\left(|\alpha_{11}-\beta_{11}^*|^2+|\alpha_{12}-\beta_{12}^*|^2\right) & \mathrm{Re}\left[\beta_{11}\left(\beta_{21}^*-\alpha_{21}\right)+\beta_{12}\left(\beta_{22}^*-\alpha_{22}\right)\right] \\ \mathrm{Re}\left[\beta_{11}\left(\beta_{21}^*-\alpha_{21}\right)+\beta_{12}\left(\beta_{22}^*-\alpha_{22}\right)\right] & \frac{1}{2}\left(|\alpha_{21}-\beta_{21}^*|^2+|\alpha_{22}-\beta_{12}^*|^2\right) \end{pmatrix} \tag{5.20}$$

$$\mathbf{Cov}_k^{(\phi\pi)} = \begin{pmatrix} \mathrm{Im}\left(\alpha_{11}\beta_{11}+\alpha_{12}\beta_{12}\right) & -\mathrm{Im}\left[\beta_{11}\left(\beta_{21}^*-\alpha_{21}\right)+\beta_{12}\left(\beta_{22}^*-\alpha_{22}\right)\right] \\ \mathrm{Im}\left[\beta_{11}\left(\beta_{21}^*+\alpha_{21}\right)+\beta_{12}\left(\beta_{22}^*+\alpha_{22}\right)\right] & \mathrm{Im}\left(\alpha_{21}\beta_{21}+\alpha_{22}\beta_{22}\right) \end{pmatrix}. \tag{5.21}$$

An expression of $\mathbf{Cov}_k(t)$ in terms of the squeezing and rotation parameters can also be obtained from the Bloch-Messiah decomposition of $\boldsymbol{\mathcal{G}}_k(t,t_{\rm in})$ given in Eq. (3.32), where one notes that the squeezing and rotation parameters entering that decomposition are the same as those appearing in the evolution operator $\widehat{\mathcal{U}}_{\vec{k}}(t,t_{\rm in})$ given in Eq. (4.15), see footnote 7. In order to write the result in a compact form, we introduce the complex parameter

$$\widetilde{\tau}_k \equiv e^{-\frac{p_z}{2}} = \cos(\theta^k) + i\theta_4^k \mathrm{sinc}(\theta^k), \tag{5.22}$$

in terms of which the position-position power spectra read

$$\begin{aligned} \mathrm{Cov}_{11,k}^{(\phi\phi)} =& \frac{1}{2k}\Bigg\{ |\widetilde{\tau}_k|^2 \left[\cosh(2r_1^k) + \cos(2\theta_3^k + 2\mathrm{arg}\widetilde{\tau}_k)\sinh(2r_1^k)\right] \\ &+ \mathrm{sinc}^2(\theta^k)\,|\tau_k|^2 \left[\cosh(2r_2^k) - \cos(2\theta_3^k + 2\mathrm{arg}\tau_k)\sinh(2r_2^k)\right]\Bigg\}, \end{aligned} \tag{5.23}$$

$$\begin{aligned} \mathrm{Cov}_{22,k}^{(\phi\phi)} =& \frac{1}{2k}\Bigg\{ |\widetilde{\tau}_k|^2 \left[\cosh(2r_2^k) + \cos(2\theta_3^k - 2\mathrm{arg}\widetilde{\tau}_k)\sinh(2r_2^k)\right] \\ &+ \mathrm{sinc}^2(\theta^k)\,|\tau_k|^2 \left[\cosh(2r_1^k) - \cos(2\theta_3^k - 2\mathrm{arg}\tau_k)\sinh(2r_1^k)\right]\Bigg\}, \end{aligned} \tag{5.24}$$

$$\mathrm{Cov}^{(\phi\phi)}_{12,k} = \frac{1}{2k}\mathrm{sinc}(\theta^k)\,|\widetilde{\tau}_k|\,|\tau_k|\Bigg\{\sin(\arg\tau_k + \arg\widetilde{\tau}_k)\left[\cosh(2r_2^k) - \cosh(2r_1^k)\right] + \sin(2\theta_3^k - \arg\tau_k + \arg\widetilde{\tau}_k)\sinh(2r_1^k) + \sin(2\theta_3^k + \arg\tau_k - \arg\widetilde{\tau}_k)\sinh(2r_2^k)\Bigg\}. \tag{5.25}$$

The momentum-momentum power spectra are given by

$$\mathrm{Cov}^{(\pi\pi)}_{11,k} = \frac{k}{2}\Bigg\{|\widetilde{\tau}_k|^2\left[\cosh(2r_1^k) - \cos(2\theta_3^k + 2\arg\widetilde{\tau}_k)\sinh(2r_1^k)\right] + \mathrm{sinc}^2(\theta^k)\,|\tau_k|^2\left[\cosh(2r_2^k) + \cos(2\theta_3^k + 2\arg\tau_k)\sinh(2r_2^k)\right]\Bigg\}, \tag{5.26}$$

$$\mathrm{Cov}^{(\pi\pi)}_{22,k} = \frac{k}{2}\Bigg\{|\widetilde{\tau}_k|^2\left[\cosh(2r_2^k) - \cos(2\theta_3^k - 2\arg\widetilde{\tau}_k)\sinh(2r_2^k)\right] + \mathrm{sinc}^2(\theta^k)\,|\tau_k|^2\left[\cosh(2r_1^k) + \cos(2\theta_3^k - 2\arg\tau_k)\sinh(2r_1^k)\right]\Bigg\}, \tag{5.27}$$

$$\mathrm{Cov}^{(\pi\pi)}_{12,k} = \frac{k}{2}\mathrm{sinc}(\theta^k)\,|\widetilde{\tau}_k|\,|\tau_k|\Bigg\{\sin(\arg\tau_k + \arg\widetilde{\tau}_k)\left[\cosh(2r_2^k) - \cosh(2r_1^k)\right] - \sin(2\theta_3^k - \arg\tau_k + \arg\widetilde{\tau}_k)\sinh(2r_1^k) - \sin(2\theta_3^k + \arg\tau_k - \arg\widetilde{\tau}_k)\sinh(2r_2^k)\Bigg\}, \tag{5.28}$$

and the position-momentum power spectra by

$$\mathrm{Cov}^{(\phi\pi)}_{11,k} = \frac{1}{2}\Bigg[-|\widetilde{\tau}_k|^2\sin(2\theta_3^k + 2\arg\widetilde{\tau}_k)\sinh(2r_1^k) + \mathrm{sinc}^2(\theta^k)\,|\tau_k|^2\sin(2\theta_3^k + 2\arg\tau_k)\sinh(2r_2^k)\Bigg], \tag{5.29}$$

$$\mathrm{Cov}^{(\phi\pi)}_{22,k} = \frac{1}{2}\Bigg[-|\widetilde{\tau}_k|^2\sin(2\theta_3^k - 2\arg\widetilde{\tau}_k)\sinh(2r_2^k) + \mathrm{sinc}^2(\theta^k)\,|\tau_k|^2\sin(2\theta_3^k - 2\arg\tau_k)\sinh(2r_1^k)\Bigg], \tag{5.30}$$

$$\mathrm{Cov}^{(\phi\pi)}_{12,k} = \frac{1}{2}\mathrm{sinc}(\theta^k)\,|\widetilde{\tau}_k|\,|\tau_k|\Bigg\{\cos(\arg\tau_k + \arg\widetilde{\tau}_k)\left[\cosh(2r_1^k) - \cosh(2r_2^k)\right] + \cos(2\theta_3^k - \arg\tau_k + \arg\widetilde{\tau}_k)\sinh(2r_1^k) + \cos(2\theta_3^k + \arg\tau_k - \arg\widetilde{\tau}_k)\sinh(2r_2^k)\Bigg\}, \tag{5.31}$$

$$\mathrm{Cov}^{(\phi\pi)}_{21,k} = \frac{1}{2}\mathrm{sinc}(\theta^k)\,|\widetilde{\tau}_k|\,|\tau_k|\Bigg\{\cos(\arg\tau_k + \arg\widetilde{\tau}_k)\left[\cosh(2r_2^k) - \cosh(2r_1^k)\right]$$

$$+\cos(2\theta_3^k-\arg\tau_k+\arg\widetilde{\tau}_k)\sinh(2r_1^k)+\cos(2\theta_3^k+\arg\tau_k-\arg\widetilde{\tau}_k)\sinh(2r_2^k)\Big\}, \tag{5.32}$$

where the remaining spectra are obtained from the symmetry of $\mathbf{Cov}_k(t)$. We stress that, contrary to what was done around Eq. (5.10), there is no expansion in τ_k in these expressions. In practice, solving the dynamics of the system yields the Bogolyubov coefficients, or equivalently the squeezing and rotation parameters, from which the covariance matrix can be obtained from the above expressions. Finally, let us note that in the absence of interaction, $\widetilde{\tau}_k = e^{i\theta_4^k}$ and $\tau_k = 0$, and Eqs. (5.23), (5.26) and (5.29) reduce to the power spectra describing a two-mode squeezed state (see *e.g.* Eqs. (6.18), (6.19) and (6.20) of Ref. [13]). This allows us to highlight the great similarity in the structure of the power spectra obtained from the two-mode and the four-mode squeezed states. For instance, in the expression of the diagonal elements of $\mathbf{Cov}_k^{(\phi\phi)}$, $\mathbf{Cov}_k^{(\pi\pi)}$ and $\mathbf{Cov}_k^{(\phi\pi)}$, the first line is given by $|\tilde{\tau}_k|^2$ multiplied the power spectrum of a two-mode squeezed state in the sector of interest (position-position, momentum-momentum and position-momentum respectively). Since $|\tilde{\tau}_k|^2 \leq 1$, this parameter can be interpreted as describing a loss of power in a given sector induced by its couplings to the other sector. On the contrary, the second line in these expressions is given by $|\tau_k|^2$ multiplied by the power spectrum of a two-mode squeezed state in the other sector, and thus corresponds to an increase of power in a given sector coming from the opposite sector.

Wigner function

Let us now introduce the Wigner function. By inverting Eq. (2.12), one can see that the field position and momentum operators, $\widehat{\phi}_{i,\vec{k}}$ and $\widehat{\pi}_{i,\vec{k}}$, involve creation and annihilation operators with opposite wavevectors. For convenience, it is useful to treat the two sectors $\vec{k}$ and $-\vec{k}$ separately, and to introduce the new position and momentum variables [12]

$$\widehat{\mathfrak{q}}_{i,\vec{k}} = \frac{1}{\sqrt{2k}}\left(\widehat{a}_{i,\vec{k}} + \widehat{a}^{\dagger}_{i,\vec{k}}\right), \tag{5.33}$$

$$\widehat{\mathfrak{p}}_{i,\vec{k}} = -i\sqrt{\frac{k}{2}}\left(\widehat{a}_{i,\vec{k}} - \widehat{a}^{\dagger}_{i,\vec{k}}\right), \tag{5.34}$$

with $i = 1, 2$, which do not mix opposite Fourier modes. When going from $\widehat{\phi}_{i,\vec{k}}$ and $\widehat{\pi}_{i,\vec{k}}$ to $\widehat{\mathfrak{q}}_{i,\vec{k}}$ and $\widehat{\mathfrak{p}}_{i,\vec{k}}$, one simply decomposes the four complex field variables, $\boldsymbol{z}_{\vec{k}} = (\phi_{1,\vec{k}}, \phi_{2,\vec{k}}, \pi_{1,\vec{k}}, \pi_{2,\vec{k}})^{\mathrm{T}}$ into eight real field variables, $\boldsymbol{\mathfrak{q}}_{\vec{k}} \equiv (\mathfrak{q}_{1,\vec{k}}, \mathfrak{q}_{1,-\vec{k}}, \mathfrak{q}_{2,\vec{k}}, \mathfrak{q}_{2,-\vec{k}}, \mathfrak{p}_{1,\vec{k}}, \mathfrak{p}_{1,-\vec{k}}, \mathfrak{p}_{2,\vec{k}}, \mathfrak{p}_{2,-\vec{k}})^{\mathrm{T}}$, according to

$$\phi_{i,\vec{k}} = \frac{1}{2}\left[\left(\mathfrak{q}_{i,\vec{k}} + \mathfrak{q}_{i,-\vec{k}}\right) + \frac{i}{k}\left(\mathfrak{p}_{i,\vec{k}} - \mathfrak{p}_{i,-\vec{k}}\right)\right], \tag{5.35}$$

$$\pi_{i,\vec{k}} = \frac{1}{2i}\left[k\left(\mathfrak{q}_{i,\vec{k}} - \mathfrak{q}_{i,-\vec{k}}\right) + i\left(\mathfrak{p}_{i,\vec{k}} + \mathfrak{p}_{i,-\vec{k}}\right)\right]. \tag{5.36}$$

This transformation can be readily inverted, and is canonical.[8] The helicity basis can be described by the eight-dimensional version of Eq. (2.13), *i.e.* $\widehat{\boldsymbol{\mathfrak{a}}}_{\vec{k}} \equiv (\widehat{a}_{1,\vec{k}}, \widehat{a}_{1,-\vec{k}}, \widehat{a}_{2,\vec{k}}, \widehat{a}_{2,-\vec{k}},$

[8] This can be seen by introducing $\widehat{\phi}^{\mathrm{R}}_{i,\vec{k}} = (\widehat{\phi}_{i,\vec{k}} + \widehat{\phi}^{\dagger}_{i,\vec{k}})/\sqrt{2}$, $\widehat{\phi}^{\mathrm{I}}_{i,\vec{k}} = (\widehat{\phi}_{i,\vec{k}} - \widehat{\phi}^{\dagger}_{i,\vec{k}})/(\sqrt{2}i)$ and similarly for $\widehat{\pi}^{\mathrm{R}}_{i,\vec{k}}$ and $\widehat{\pi}^{\mathrm{I}}_{i,\vec{k}}$, and by showing that the 8×8 matrix that relates those variables to $\boldsymbol{\mathfrak{q}}_{\vec{k}}$ satisfies the symplectic relation (2.19) in 8 dimensions.

$\widehat{a}^\dagger_{1,\vec{k}}$, $\widehat{a}^\dagger_{1,-\vec{k}}$, $\widehat{a}^\dagger_{2,\vec{k}}$, $\widehat{a}^\dagger_{2,-\vec{k}})^{\mathrm{T}}$, which is related to the vector $\widehat{\mathfrak{q}}_{\vec{k}}$ via

$$\widehat{\mathfrak{a}}_{\vec{k}} = [(\boldsymbol{U}\boldsymbol{D}_k) \otimes \boldsymbol{I}_2]\, \widehat{\mathfrak{q}}_{\vec{k}}\,, \tag{5.37}$$

and whose commutators are given by

$$\left[\widehat{\mathfrak{a}}_{\vec{k}}, \widehat{\mathfrak{a}}^\dagger_{\vec{q}}\right] = i(\boldsymbol{\mathcal{J}} \otimes \boldsymbol{I}_2)\delta^3(\vec{k} - \vec{q}). \tag{5.38}$$

The real variables $\mathfrak{q}_{\vec{k}}$ can be used to introduce the Wigner-Weyl transform [47–49], which allows one to connect quantum operators $\widehat{O}_{\vec{k}}$ to classical functions in the phase space $\widetilde{\mathcal{O}}_{\vec{k}}(\mathfrak{q}_{\vec{k}})$, according to

$$\widetilde{\mathcal{O}}_{\vec{k}}(\mathfrak{q}_{\vec{k}}) = \frac{1}{(2\pi)^4}\int_{\mathbb{R}^4} \mathrm{d}x_1\mathrm{d}x_2\mathrm{d}y_1\mathrm{d}y_2 e^{-i\mathfrak{p}_{1,\vec{k}}x_1 - i\mathfrak{p}_{2,\vec{k}}x_2 - i\mathfrak{p}_{1,-\vec{k}}y_1 - i\mathfrak{p}_{2,-\vec{k}}y_2}$$
$$\left\langle \mathfrak{q}_{1,\vec{k}} + \frac{x_1}{2}, \mathfrak{q}_{2,\vec{k}} + \frac{x_2}{2}, \mathfrak{q}_{1,-\vec{k}} + \frac{y_1}{2}, \mathfrak{q}_{2,-\vec{k}} + \frac{y_2}{2}\right| \widehat{O}_{\vec{k}} \left|\mathfrak{q}_{1,\vec{k}} - \frac{x_1}{2}, \mathfrak{q}_{2,\vec{k}} - \frac{x_2}{2}, \mathfrak{q}_{1,-\vec{k}} - \frac{y_1}{2}, \mathfrak{q}_{2,-\vec{k}} - \frac{y_2}{2}\right\rangle. \tag{5.39}$$

In general, the quantum state of a system can be equivalently described in terms of its density matrix $\widehat{\rho}(t) = |\emptyset(t)\rangle\langle\emptyset(t)| = \prod_{\vec{k}\in\mathbb{R}^{3+}} \widehat{\rho}_{\vec{k}}(t)$, or in terms of its Wigner function $W(t) = \prod_{\vec{k}\in\mathbb{R}^{3+}} W_{\vec{k}}(\mathfrak{q}_{\vec{k}}, t)$, which is the Wigner-Weyl transform of the density matrix [50, 51].

The inverse Wigner-Weyl transform, which allows one to go from the Wigner function to the density matrix, is given in Appendix D, see Eq. (D.1). The Wigner functions $W_{\vec{k}}(\mathfrak{q}_{\vec{k}}, t)$ can be interpreted as *quasi* distribution functions in the sense that expectation values of quantum operators can be expressed as

$$\langle\emptyset_{\vec{k}}(t)|\, \widehat{\mathcal{O}}_{\vec{k}}\, |\emptyset_{\vec{k}}(t)\rangle = \mathrm{Tr}\left[\widehat{\rho}_{\vec{k}}(t)\widehat{\mathcal{O}}_{\vec{k}}\right] = (2\pi)^4 \int \mathrm{d}\mathfrak{q}_{\vec{k}}\; \widetilde{\mathcal{O}}_{\vec{k}}(\mathfrak{q}_{\vec{k}}) W_{\vec{k}}(\mathfrak{q}_{\vec{k}}, t), \tag{5.40}$$

where the $(2\pi)^4$ prefactor can be absorbed in the normalisation of the Wigner function if needed. For Gaussian states, as shown *e.g.* in Appendix G of Ref. [12], the Wigner functions are Gaussian functions (hence the statement that the state is "Gaussian") and read

$$W_{\vec{k}}(\mathfrak{q}_{\vec{k}}, t) = \frac{1}{(2\pi)^4\sqrt{\det \mathbf{Cov}_{8\times8,k}}} e^{-\frac{1}{2}\mathfrak{q}^{\mathrm{T}}_{\vec{k}}\mathbf{Cov}^{-1}_{8\times8,k}\mathfrak{q}_{\vec{k}}}\,, \tag{5.41}$$

where $\mathbf{Cov}_{8\times8,k}$ is the 8×8 covariance matrix in the field basis $\mathfrak{q}_{\vec{k}}$, defined through

$$\langle\emptyset|\, \widehat{\mathfrak{q}}_{\vec{k}}(t)\widehat{\mathfrak{q}}^\dagger_{\vec{k}}(t)\, |\emptyset\rangle = \mathbf{Cov}_{8\times8,k}(t) + \frac{i}{2}\boldsymbol{\Omega} \otimes \boldsymbol{I}_2\,. \tag{5.42}$$

It can be computed in a similar way as what was done around Eq. (5.16), and Eq. (5.37) gives rise to

$$\mathbf{Cov}_{8\times8,k}(t) = \mathbf{Cov}_k(t) \otimes \boldsymbol{I}_2\,, \tag{5.43}$$

where the inverse is simply given by $\mathbf{Cov}^{-1}_{8\times8,k} = \mathbf{Cov}^{-1}_k \otimes \boldsymbol{I}_2$, see footnote 3.

The advantage of working with the Wigner functions $W_{\vec{k}}(\mathfrak{q}_{\vec{k}}, t)$ rather than the quantum state or the density matrix in the Fock basis, lies in the simplicity of the Gaussian function (5.41). It describes entirely the quantum state of the system from the knowledge of its two-point correlation functions, and can therefore greatly simplify some calculations, as will be made explicit in the next section. The drawback of this approach is that the entangled structure, otherwise easily interpretable from Eq. (5.7), is now hidden in the details of the power spectra of the system.

6 Decoherence

Having determined in Sec. 5 the quantum state of a linear two-field system, both in the Fock basis where one obtains direct products of four-mode squeezed states and at the level of the Wigner function, we now consider the case where one of the two fields is unobservable and can be traced over. This corresponds to situations where measurements can only be performed on the first field, dubbed the "system", while the second field, dubbed the "environment", cannot be directly accessed. When the two fields become entangled, this leads to the concept of quantum decoherence [22], and we choose to illustrate the usefulness of the various tools introduced above by studying this notion for the systems at hand.

6.1 Reduced density matrix

Let $\widehat{O} = \widehat{O}_1 \otimes \widehat{\mathbb{I}}_2$ be a quantum operator describing an observable of the first field only, where $\widehat{\mathbb{I}}_2$ denotes the identity acting in the second-field sector (*i.e.* the environment). Its expectation value is given by $\mathrm{Tr}(\widehat{\rho}\widehat{O}) = \mathrm{Tr}_1\mathrm{Tr}_2[\widehat{\rho}(\widehat{O}_1 \otimes \widehat{\mathbb{I}}_2)] = \mathrm{Tr}_1[\mathrm{Tr}_2(\widehat{\rho})\widehat{O}_1]$, see Eq. (5.40), where Tr_i denotes the trace over the degrees of freedom contained in the field i. The expectation value of $\widehat{O}$ can therefore be obtained from the reduced density matrices

$$\widehat{\rho}_{\vec{k},\mathrm{red}} = \mathrm{Tr}_2(\widehat{\rho}_{\vec{k}}) = \sum_{n,m=0}^{\infty} \left[\boldsymbol{I}_2^{(1)} \otimes \langle n_{\vec{k}}^{(2)}, m_{-\vec{k}}^{(2)}|\right] \widehat{\rho}_{\vec{k}} \left[\boldsymbol{I}_2^{(1)} \otimes |n_{\vec{k}}^{(2)}, m_{-\vec{k}}^{(2)}\rangle\right] \tag{6.1}$$

by tracing over in the first-field sector (*i.e.* the system). In Eq. (6.1), for explicitness, the trace over the environmental degrees of freedom has been expanded in the Fock basis. The reduced density matrix thus contains all accessible information about the system.

If the two fields are entangled, the reduced density matrix follows non-unitary evolution, and describes a mixed (as opposed to pure) state. This can be described by the so-called purity

$$\gamma_{\vec{k}} = \mathrm{Tr}(\widehat{\rho}_{\vec{k},\mathrm{red}}^2)\,. \tag{6.2}$$

For a pure state, $\rho^2 = \rho$ and $\gamma = 1$, while mixed states have $1/d \leq \gamma \leq 1$ in general, where d is the dimension of the Fock space of the system (which is infinite in the present case) and the limit $\gamma \to 1/d$ corresponds to a maximally decohered state. Therefore, purity provides a measure of the information loss into the environment, hence of decoherence. Note that it is simply related to the linear entropy $S_{\vec{k},\mathrm{lin}} = 1 - \gamma_{\vec{k}}$, which itself provides a lower bound to the entanglement entropy $S_{\vec{k},\mathrm{ent}} = -\mathrm{Tr}(\rho \ln \rho)$, and which, as the entanglement entropy, characterises one's ignorance about the state of a system.

For the system at hand, one can check that if the two fields are uncoupled, then the reduced density matrix is pure. Indeed, if the quantum state is given by Eq. (5.9), the reduced density matrix reads

$$\begin{aligned}\widehat{\rho}_{\vec{k},\mathrm{red}} =& \mathrm{Tr}_2\left(\sum_{n,m,\bar{n},\bar{m}=0}^{\infty} c_{1,k}(n)c_{1,k}^*(\bar{n})c_{2,k}(m)c_{2,k}^*(\bar{m}) \left|n_{\vec{k}}^{(1)}, n_{-\vec{k}}^{(1)} m_{\vec{k}}^{(2)}, m_{-\vec{k}}^{(2)}\right\rangle \left\langle \bar{n}_{\vec{k}}^{(1)}, \bar{n}_{-\vec{k}}^{(1)} \bar{m}_{\vec{k}}^{(2)}, \bar{m}_{-\vec{k}}^{(2)}\right|\right) \\ =& \sum_{m=0}^{\infty} |c_{2,k}(m)|^2 \sum_{n,\bar{n}=0}^{\infty} c_{1,k}(n)c_{1,k}^*(\bar{n}) \left|n_{\vec{k}}^{(1)}, n_{-\vec{k}}^{(1)}\right\rangle \left\langle \bar{n}_{\vec{k}}^{(1)}, \bar{n}_{-\vec{k}}^{(1)}\right|\,,\end{aligned} \tag{6.3}$$

where we have performed the trace in the Fock basis as in Eq. (6.1). From the expression of the $c_{i,k}(n)$ coefficients given in Eq. (5.9), one can easily check that $\sum_n |c_{i,k}(n)|^2 = 1$, hence the reduced density matrix is the one of a (pure) two-mode squeezed state, and using again the identity $\sum_n |c_{i,k}(n)|^2 = 1$, it has purity $\gamma_{\vec{k}} = 1$.

In general, for the evolved vacuum state given in Eq. (5.6), the density matrix $\widehat{\rho}_{\vec{k}}(t) = |\emptyset_{\vec{k}}(t)\rangle \langle \emptyset_{\vec{k}}(t)|$ is written down explicitly in Appendix C, where it is shown that the tracing-out procedure of Eq. (6.1) gives rise to

$$\widehat{\rho}_{\vec{k},\mathrm{red}} = \sum_{n=0}^{\infty} \sum_{n'=-\infty}^{\infty} \sum_{s,t=-\min(n,n')}^{\infty} \Xi_k(n,n',s,t) \, |(n+s)^{(1)}_{\vec{k}}, (n+t)^{(1)}_{-\vec{k}}\rangle \, \langle (n'+s)^{(1)}_{\vec{k}}, (n'+t)^{(1)}_{-\vec{k}}| \tag{6.4}$$

with

$$\Xi_k(n,n',s,t) = \sum_{m=\max(0,s,t)}^{\infty} \sum_{m'=-m}^{n'} c_k(n,m,s,t) c_k^*(n'-m', m+m', s+m', t+m') \, . \tag{6.5}$$

This expression differs from the uncoupled case (6.3) due to the presence of the s and t indices, related to the transfer of excitations from one sector to the other. One can check that the invariance of the c_k coefficients under exchanging s and t, which was noted below Eq. (5.7) as a manifestation of the statistical isotropy of the state, guarantees that the Ξ_k coefficients are also invariant under swapping s and t, hence the reduced state is also statistically isotropic.

Let us also recall that if one performs a perturbative expansion in the interaction Hamiltonian, that is, as argued in Sec. 5.1, an expansion in τ_k, then the corrections to $c_k(n,m,s,t)$ are of order $\mathcal{O}(|\tau_k|^{|s|+|t|+2q})$, where q is a non-negative integer number that stands for the number of particles that change sectors and then change back. As a consequence, the corrections to $\Xi_k(n,n',s,t)$ are of order $\mathcal{O}[|\tau_k|^{2(|s|+|t|+Q)}]$, where $Q = m' + q + q'$, where q and q' are associated with the two c_k coefficients appearing in Eq. (6.5). This implies that, while we saw that the diagonal elements of the full quantum state received even corrections in $|\tau_k|$ only, see the discussion at the very end of Sec. 5.1, we have now showed that all the entries of the reduced density matrix receive even corrections in $|\tau_k|$ only. As a consequence, the leading correction to observables performed on the system is always quadratic in the coupling constants, in agreement with the results of Ref. [23].

From Eq. (6.4), the purity (6.2) can also be obtained, and in Appendix C it is shown that

$$\gamma_{\vec{k}}(t) = \sum_{n=0}^{\infty} \sum_{n',u=-\infty}^{\infty} \sum_{s,t=-\min(n,n')}^{\infty} \Xi_k(n,n',s,t) \Xi_k(n'-u, n-u, s+u, t+u). \tag{6.6}$$

Let us stress that the above formulas are not perturbative and allow one to compute the reduced density matrix and its purity up to arbitrary order in the interaction terms.

Small-coupling limit

In order to gain more insight, one can however derive the leading-order result in the interaction parameter $|\tau_k|$. After a lengthy though straightforward calculation, the reduced density matrix derived from the perturbed evolved vacuum state (5.10) is given by

$$\widehat{\rho}_{\vec{k},\mathrm{red}}(t) = \sum_{n,n'=0}^{\infty} c_{1,k}(n) c_{1,k}^*(n') \left| n^{(1)}_{\vec{k}}, n^{(1)}_{-\vec{k}} \right\rangle \left\langle n'^{(1)}_{\vec{k}}, n'^{(1)}_{-\vec{k}} \right| + |\tau_k|^2 \sum_{n,n',m=0}^{\infty} c_{1,k}(n) c_{1,k}^*(n')$$

$$
\begin{aligned}
&\Big\{|c_{2,k}(m)|^2\mathcal{F}_k(n,m+1)\mathcal{F}_k^*(n',m+1)\\
&\qquad\times\left[\left|(n-1)^{(1)}_{\vec{k}},n^{(1)}_{-\vec{k}}\right\rangle\left\langle(n'-1)^{(1)}_{\vec{k}},n'^{(1)}_{-\vec{k}}\right|+\left|n^{(1)}_{\vec{k}},(n-1)^{(1)}_{-\vec{k}}\right\rangle\left\langle n'^{(1)}_{\vec{k}},(n'-1)^{(1)}_{-\vec{k}}\right|\right]\\
&+|c_{2,k}(m)|^2\mathcal{F}_k^*(n+1,m)\mathcal{F}_k(n'+1,m)\\
&\qquad\times\left[\left|(n+1)^{(1)}_{\vec{k}},n^{(1)}_{-\vec{k}}\right\rangle\left\langle(n'+1)^{(1)}_{\vec{k}},n'^{(1)}_{-\vec{k}}\right|+\left|n^{(1)}_{\vec{k}},(n+1)^{(1)}_{-\vec{k}}\right\rangle\left\langle n'^{(1)}_{\vec{k}},(n'+1)^{(1)}_{-\vec{k}}\right|\right]\\
&-c_{2,k}(m)c_{2,k}^*(m+1)\mathcal{F}_k(n,m+1)\mathcal{F}_k(n'+1,m+1)\\
&\qquad\times\left[\left|(n-1)^{(1)}_{\vec{k}},n^{(1)}_{-\vec{k}}\right\rangle\left\langle n'^{(1)}_{\vec{k}},(n'+1)^{(1)}_{-\vec{k}}\right|+\left|n^{(1)}_{\vec{k}},(n-1)^{(1)}_{-\vec{k}}\right\rangle\left\langle(n'+1)^{(1)}_{\vec{k}},n'^{(1)}_{-\vec{k}}\right|\right]\\
&-c_{2,k}(m)c_{2,k}^*(m-1)\mathcal{F}_k^*(n+1,m)\mathcal{F}_k^*(n',m)\\
&\qquad\times\left[\left|(n+1)^{(1)}_{\vec{k}},n^{(1)}_{-\vec{k}}\right\rangle\left\langle n'^{(1)}_{\vec{k}},(n'-1)^{(1)}_{-\vec{k}}\right|+\left|n^{(1)}_{\vec{k}},(n+1)^{(1)}_{-\vec{k}}\right\rangle\left\langle(n'-1)^{(1)}_{\vec{k}},n'^{(1)}_{-\vec{k}}\right|\right]\\
&+c_{2,k}(m)c_{2,k}^*(m-1)\left[\mathcal{F}_k^*(n',m)\right]^2\left|n^{(1)}_{\vec{k}},n^{(1)}_{-\vec{k}}\right\rangle\left\langle(n'-1)^{(1)}_{\vec{k}},(n'-1)^{(1)}_{-\vec{k}}\right|\\
&+c_{2,k}(m)c_{2,k}^*(m+1)\left[\mathcal{F}_k(n,m+1)\right]^2\left|(n-1)^{(1)}_{\vec{k}},(n-1)^{(1)}_{-\vec{k}}\right\rangle\left\langle n'^{(1)}_{\vec{k}},n'^{(1)}_{-\vec{k}}\right|\\
&+c_{2,k}(m)c_{2,k}^*(m+1)\left[\mathcal{F}_k(n'+1,m+1)\right]^2\left|n^{(1)}_{\vec{k}},n^{(1)}_{-\vec{k}}\right\rangle\left\langle(n'+1)^{(1)}_{\vec{k}},(n'+1)^{(1)}_{-\vec{k}}\right|\\
&+c_{2,k}(m)c_{2,k}^*(m-1)\left[\mathcal{F}_k^*(n+1,m)\right]^2\left|(n+1)^{(1)}_{\vec{k}},(n+1)^{(1)}_{-\vec{k}}\right\rangle\left\langle n'^{(1)}_{\vec{k}},n'^{(1)}_{-\vec{k}}\right|\\
&+|c_{2,k}(m)|^2\left[\mathcal{G}_k^*(n',m)+\mathcal{G}_k(n,m)\right]\left|n^{(1)}_{\vec{k}},n^{(1)}_{-\vec{k}}\right\rangle\left\langle n'^{(1)}_{\vec{k}},n'^{(1)}_{-\vec{k}}\right|\Big\}.
\end{aligned}
\tag{6.7}
$$

One can see that the leading correction in $|\tau_k|$ is indeed of quadratic order [despite the full state (5.10) having linear contributions], in agreement with the above discussion. This expression allows one to evaluate the purity (6.2) and one obtains

$$
\begin{aligned}
\gamma_{\vec{k}}(t)=&1+4\left|\tau_k\right|^2\sum_{n,m=0}^{\infty}\Re\mathrm{e}\Big\{|c_{1,k}(n)|^2|c_{2,k}(m)|^2\mathcal{G}_k(n,m)\\
&+2c_{1,k}(n+1)c_{1,k}^*(n)c_{2,k}(m)c_{2,k}^*(m+1)\left[\mathcal{F}_k(n+1,m+1)\right]^2\Big\},
\end{aligned}
\tag{6.8}
$$

where the relation $\sum_n|c_{i,k}(n)|^2=1$ has been used. Making use of Eqs. (5.12) and (5.13), the sums appearing in the expression can be carried out explicitly, and in terms of the squeezing and rotation parameters, one obtains

$$
\gamma_{\vec{k}}=1-4\left|\tau_k\right|^2\mathrm{sinc}^2\left(\theta_4^k\right)\left[\sinh^2\left(r_1^k-r_2^k\right)+\cos^2\left(\theta_4^k-\arg\tau_k\right)\sinh\left(2r_1^k\right)\sinh\left(2r_2^k\right)\right].
\tag{6.9}
$$

One can check that, as $|\tau_k|$ increases away from 0, $\gamma_{\vec{k}}$ decreases away from 1, since the term inside the squared braces in Eq. (6.9) is always positive. One can also see that larger squeezing amplitudes r_1^k and r_2^k lead to more efficient decoherence, as usually encountered [11]. It is finally worth pointing out that in the specific configuration where $r_1^k=r_2^k$ and $\theta_4^k=\arg\tau_k\pm\pi$, the leading-order correction to the purity vanishes.

6.2 Reduced Wigner function

As argued in Sec. 5.2, a complementary (and sometimes simpler from a computational standpoint) tool to analyse the four-mode squeezed state is provided by the Wigner function.

Let us first establish how the Wigner function of the reduced system can be obtained from the one of the full two-field setup.

We consider again an operator of the form $\widehat{O}_{\vec{k}} = \widehat{O}_{1,\vec{k}} \otimes \widehat{\mathbb{I}}_2$. From Eq. (5.39), its Wigner-Weyl transform is simply given by $\widetilde{O}_{\vec{k}} = \widetilde{O}_{1,\vec{k}}/(2\pi)^2$, where $\widetilde{O}_{1,\vec{k}}$ is the Wigner-Weyl transform of $\widehat{O}_{1,\vec{k}}$ within the first-field sector,

$$\widetilde{\mathcal{O}}_{1,\vec{k}}(\mathfrak{q}_{1,\vec{k}}) = \int_{\mathbb{R}^2} \frac{\mathrm{d}x_1 \mathrm{d}y_1}{(2\pi)^2} e^{-i\mathfrak{p}_{1,\vec{k}}x_1 - i\mathfrak{p}_{1,-\vec{k}}y_1} \left\langle \mathfrak{q}_{1,\vec{k}} + \frac{x_1}{2}, \mathfrak{q}_{1,-\vec{k}} + \frac{y_1}{2} \right| \widehat{O}_{1,\vec{k}} \left| \mathfrak{q}_{1,\vec{k}} - \frac{x_1}{2}, \mathfrak{q}_{1,-\vec{k}} - \frac{y_1}{2} \right\rangle, \tag{6.10}$$

with $\mathfrak{q}_{1,\vec{k}} \equiv (\mathfrak{q}_{1,\vec{k}}, \mathfrak{q}_{1,-\vec{k}}, \mathfrak{p}_{1,\vec{k}}, \mathfrak{p}_{1,-\vec{k}})^{\mathrm{T}}$. Plugging this result into Eq. (5.40), the expectation value of $\widehat{O}_{\vec{k}}$ is given by

$$\langle \emptyset_{\vec{k}}(t)| \widehat{\mathcal{O}}_{\vec{k}} |\emptyset_{\vec{k}}(t)\rangle = (2\pi)^2 \int \mathrm{d}\mathfrak{q}_{1,\vec{k}}\, \widetilde{\mathcal{O}}_{1,\vec{k}}(\mathfrak{q}_{1,\vec{k}}) W_{\vec{k},\mathrm{red}}(\mathfrak{q}_{1,\vec{k}}, t), \tag{6.11}$$

where we have defined the reduced Wigner function

$$W_{\vec{k},\mathrm{red}}(\mathfrak{q}_{1,\vec{k}}, t) = \int_{\mathbb{R}^4} \mathrm{d}^4\mathfrak{q}_{2,\vec{k}}\, W_{\vec{k}}(\mathfrak{q}_{1,\vec{k}}, \mathfrak{q}_{2,\vec{k}}, t). \tag{6.12}$$

Comparing Eq. (6.11) with Eq. (5.40), one can see that $W_{\vec{k},\mathrm{red}}$ can be used to compute quantum expectation values of observables in the first-field space. Therefore, it corresponds to the Wigner function in the reduced phase space (where the different powers of 2π come from the different dimensions of the phase spaces). In other words, $W_{\vec{k},\mathrm{red}}$ is the Wigner-Weyl transform of $\widehat{\rho}_{\vec{k},\mathrm{red}}(t)$, which is shown explicitly in Appendix D. This is why partial trace in the Hilbert space is equivalent to partial integration in the phase space.

If the Wigner function is Gaussian, this partial integration can be easily done, and marginalisation over a phase-space variable simply corresponds to removing the associated lines and columns in the covariance matrix. From Eq. (5.41), this implies that

$$W_{\vec{k},\mathrm{red}}(\mathfrak{q}_{1,\vec{k}}, t) = \frac{1}{(2\pi)^2\sqrt{\det \mathbf{Cov}_{\vec{k},\mathrm{red}}}} e^{-\frac{1}{2}\mathfrak{q}_{1,\vec{k}}^{\mathrm{T}} \mathbf{Cov}_{\vec{k},\mathrm{red}}^{-1} \mathfrak{q}_{1,\vec{k}}}, \tag{6.13}$$

where $\mathbf{Cov}_{\vec{k},\mathrm{red}}$ is obtained from Eq. (5.43) by removing the lines and columns related to the second sector (*i.e.* the third, the fourth, the seventh and the eighth lines and columns).

The purity of the reduced system can then be computed from the reduced Wigner function, by using the property of the Wigner-Weyl transform [46]

$$\mathrm{Tr}\left(\widehat{A}\widehat{B}\right) = (2\pi)^2 \int_{\mathbb{R}^4} \mathrm{d}^4\mathfrak{q}_{1,\vec{k}} \widetilde{A}\widetilde{B}\,, \tag{6.14}$$

where $\widehat{A}$ and $\widehat{B}$ are two quantum operators acting on the first-field system and $\widetilde{A}$ and $\widetilde{B}$ are their Wigner-Weyl transforms. With $\widehat{A} = \widehat{B} = \widehat{\rho}_{\vec{k},\mathrm{red}}$, Eq. (6.14) gives rise to the following expression for the purity (6.2),

$$\gamma_{\vec{k}}(t) = (2\pi)^2 \int_{\mathbb{R}^4} \mathrm{d}^4\mathfrak{q}_{1,\vec{k}} W^2_{\vec{k},\mathrm{red}}(\mathfrak{q}_{1,\vec{k}}, t). \tag{6.15}$$

Plugging Eq. (6.13) into that formula, one obtains

$$\gamma_{\vec{k}}(t) = \left(16\,\det\mathbf{Cov}_{\vec{k},\mathrm{red}}\right)^{-1/2} = \frac{1}{4}\left[\mathrm{Cov}_{11,k}^{(\phi\phi)}\mathrm{Cov}_{11,k}^{(\pi\pi)} - \left(\mathrm{Cov}_{11,k}^{(\phi\pi)}\right)^2\right]^{-1}. \tag{6.16}$$

As a consequence, for a Gaussian state, the purity of the system can be directly evaluated from the knowledge of the power spectra in the observable sector [52]. More precisely, the power spectra appear through a specific combination, *i.e.* the determinant of the (reduced) covariance matrix, which makes the purity invariant under canonical transformations [13]. Let us indeed recall that in a two-dimensional (*i.e.* single-field) system, there is a single symplectic invariant [52, 53], the so-called symplectic eigenvalue $\sigma_{\vec{k}}(t)$, which is such that the eigenvalues of $\mathbf{Cov}_{\vec{k},\mathrm{red}}\mathbf{\Omega}$ are given by $\pm i\sigma_{\vec{k}}(t)$. This leads to $\sigma_{\vec{k}} = 1/(2\sqrt{\gamma_{\vec{k}}})$, and the condition $\gamma_{\vec{k}} < 1$ is equivalent to $\sigma_{\vec{k}} > 1/2$. In passing, let us note that, for Gaussian states, the entanglement entropy introduced below Eq. (6.2) is related to the symplectic eigenvalue by [54] $S_{\vec{k},\mathrm{ent}} = (\sigma_{\vec{k}} + 1/2)\log_2(\sigma_{\vec{k}} + 1/2) - (\sigma_{\vec{k}} - 1/2)\log_2(\sigma_{\vec{k}} - 1/2)$. This allows one to relate the linear and entanglement entropies, and check the above statement that the former provides a lower bound to the latter.

If the two fields are uncoupled, the reduced system is in a pure state and one has [13] $\mathrm{Cov}_{11,k}^{(\phi\phi)}\mathrm{Cov}_{11,k}^{(\pi\pi)} - \left(\mathrm{Cov}_{11,k}^{(\phi\pi)}\right)^2 = 1/4$. This implies that $\gamma_{\vec{k}}(t) = 1$, $\sigma_{\vec{k}}(t) = 1/2$ and $S_{\vec{k},\mathrm{lin}}(t) = S_{\vec{k},\mathrm{ent}}(t) = 0$. Otherwise, $\gamma_{\vec{k}} < 1$ signals the presence of decoherence. An obvious, yet crucial consequence of Eq. (6.16) is that decoherence, *i.e.* the reduction of $\gamma_{\vec{k}}$ away from unity, cannot be achieved without modifying the power spectra. In other words, for any system that undergoes decoherence, the observational predictions are necessarily altered, and an important question that will be addressed below is whether or not decoherence can proceed while keeping this alteration negligible [23, 55].

Let us finally stress that unlike the approach presented in Sec. 6.1, which relies on a detailed analysis of the mathematical structure of $\mathrm{Sp}(4,\mathbb{R})$ and leads to a formula, Eq. (6.6), that involves nine infinite sums; the Wigner function formalism only makes use of Gaussian integrals. It can therefore be straightforwardly generalised to higher-dimension systems (*i.e.* containing more fields), while the approach of Sec. 6.1 would require further analyses of the groups $\mathrm{Sp}(2n,\mathbb{R})$. By plugging Eqs. (5.23), (5.26) and (5.29) into Eq. (6.16), one can finally obtain a fully non-perturbative expression for the purity in terms of the squeezing parameters

$$\begin{aligned}\gamma_{\vec{k}}(t) = &\Bigg\{ |\widetilde{\tau}_k|^4 + \mathrm{sinc}^4(\theta^k)\,|\tau_k|^4 + 2\mathrm{sinc}^2(\theta^k)\,|\tau_k|^2\,|\widetilde{\tau}_k|^2 \times \\ &\left[\cosh(2r_1^k)\cosh(2r_2^k) + \cos\left(2\mathrm{arg}\widetilde{\tau}_k - 2\mathrm{arg}\tau_k\right)\sinh(2r_1^k)\sinh(2r_2^k)\right]\Bigg\}^{-1}, \end{aligned} \tag{6.17}$$

where we recall that $\widetilde{\tau}_k$ is defined in Eq. (5.22), and τ_k and θ^k in Eq. (3.21).

Small-coupling limit

Similarly to what was done at the end of Sec. 6.1, let us now further expand the purity in the limit where the system and the environment fields are weakly coupled. The power spectra in the observable sector are given by Eqs. (5.23), (5.26) and (5.29). Expanding these

expressions up to second order in the interaction parameter $|\tau_k|$ [recalling that $(\theta_6^k - i\theta_5^k) = |\tau_k| e^{i\mathrm{arg}\tau_k}$ and $\theta^k = \sqrt{(\theta_4^k)^2 + |\tau_k|^2}$], one obtains

$$\begin{aligned}
\mathrm{Cov}_{11,k}^{(\phi\phi)} =& \frac{1}{2k}\Bigg(\Big[\cosh(2r_1^k) + \cos(2\theta_3^k + 2\theta_4^k)\sinh(2r_1^k)\Big] + |\tau_k|^2\Bigg\{-\frac{\sin^2\theta_4^k}{\theta_4^k}\cosh(2r_1^k) \\
&+ \frac{1}{2(\theta_4^k)^2}\Big[\cos(2\theta_3^k) - \cos(2\theta_3^k + 2\theta_4^k) - 2\theta_4^k\sin(2\theta_3^k + 2\theta_4^k)\Big]\sinh(2r_1^k) \\
&+ \frac{\sin^2\theta_4^k}{(\theta_4^k)^2}\Big[\cosh(2r_2^k) - \cos(2\theta_3^k + 2\mathrm{arg}\tau_k)\sinh(2r_2^k)\Big]\Bigg\}\Bigg) \qquad (6.18) \\
\mathrm{Cov}_{11,k}^{(\pi\pi)} =& \frac{k}{2}\Bigg(\Big[\cosh(2r_1^k) - \cos(2\theta_3^k + 2\theta_4^k)\sinh(2r_1^k)\Big] + |\tau_k|^2\Bigg\{-\frac{\sin^2\theta_4^k}{\theta_4^k}\cosh(2r_1^k) \\
&- \frac{1}{2(\theta_4^k)^2}\Big[\cos(2\theta_3^k) - \cos(2\theta_3^k + 2\theta_4^k) - 2\theta_4^k\sin(2\theta_3^k + 2\theta_4^k)\Big]\sinh(2r_1^k) \\
&+ \frac{\sin^2\theta_4^k}{(\theta_4^k)^2}\Big[\cosh(2r_2^k) + \cos(2\theta_3^k + 2\mathrm{arg}\tau_k)\sinh(2r_2^k)\Big]\Bigg\}\Bigg) \qquad (6.19) \\
\mathrm{Cov}_{11,k}^{(\phi\pi)} =& \frac{1}{2}\Bigg(-\sin(2\theta_3^k + 2\theta_4^k)\sinh(2r_1^k) + |\tau_k|^2\Bigg\{\frac{\sin^2\theta_4^k}{(\theta_4^k)^2}\sin(2\theta_3^k + 2\mathrm{arg}\tau_k)\sinh(2r_2^k) \\
&+ \frac{1}{2(\theta_4^k)^2}\Big[-\sin(2\theta_3^k) + \sin(2\theta_3^k + 2\theta_4^k) - 2\theta_4^k\cos(2\theta_3^k + 2\theta_4^k)\Big]\sinh(2r_1^k)\Bigg\}\Bigg). \qquad (6.20)
\end{aligned}$$

In the limit where the two fields are uncoupled, $\tau_k = 0$, one recovers the result obtained for two-mode squeezed states in Ref. [13]. One can also check that in agreement with the discussion of Sec. 6.1, the leading correction to the power spectra is of quadratic order in $|\tau_k|$. Let us stress that those corrections involve parameters that describe the environment sector, such as r_2^k, hence observations carried out on the system alone can a priori lead to indirect information about the microphysical evolution of the traced over field(s). One should also note that, through the dynamical evolution, the presence of the interaction modifies all Bogolyubov coefficients, hence all squeezing and rotation parameters. This is why formally, in the above expressions, the leading terms (*i.e.* the ones before $|\tau_k|^2$) need also be expanded.

By plugging Eqs. (6.18), (6.19) and (6.20) into Eq. (6.16), one can finally derive an expression for the purity expanded at quadratic order in $|\tau_k|^2$, and by doing so one exactly recovers Eq. (6.9). This is an important consistency check as the two methods employed to derive this result are completely independent (and, as already argued, the approach based on the Wigner function is computationally less heavy).

This calculation also makes explicit that as one increases the interaction strength, one decreases the purity and hence makes decoherence more efficient, but one also induces larger corrections to the observable power spectra. This allows one to answer the question asked above, namely whether or not decoherence can proceed without affecting too much the power spectra. As noticed below Eq. (6.9), decoherence becomes more efficient as quantum squeezing increases, and in the large-squeezing limit, the correction to $\gamma_{\vec{k}} = 1$ is controlled by $|\tau_k|^2 e^{2r}$. However, from Eqs. (6.18), (6.19) and (6.20), one can see that the relative correction to the power spectra is rather controlled by $|\tau_k|^2$ in that limit. As a consequence, if the

interaction strength is such that

$$e^{-r} \ll |\tau_k| \ll 1\,, \tag{6.21}$$

decoherence takes place while keeping corrections to observable predictions tiny.

7 Conclusion

In this work, we have performed a detailed study of the quantum dynamics of two scalar fields, quadratically coupled, and embedded in a homogeneous and isotropic background. Their dynamics is generated by a quadratic Hamiltonian with time-dependent coefficients. Evolution of such systems (either classical or quantum) is obtained by applying elements of the symplectic group $\mathrm{Sp}(4,\mathbb{R})$ to the initial configuration, so we have first investigated the mathematical structure of this group by presenting various descriptions of it. In particular, using the Bloch-Messiah decomposition that we further developed using the commutation relations of the Lie algebra, we have derived fully factorised expressions for the group elements of $\mathrm{Sp}(4,\mathbb{R})$. The ten parameters entering these expressions are dubbed the squeezing and rotation parameters, as per the three parameters entering the decomposition of $\mathrm{Sp}(2,\mathbb{R})$. Alternatively, this group is described by Bogolyubov coefficients, which we explicitly related to the squeezing and rotation parameters.

We then provided the quantum representation of the Lie algebra of $\mathrm{Sp}(4,\mathbb{R})$, from which the quantum Hamiltonian can be easily expressed and interpreted. Couplings between the two fields manifest themselves through exchanges of quanta from one sector to the other (hence preserving the total number of quanta), and through direct productions of pairs in which each quantum belongs to a different sector. The latter provides a direct way to entangle the two sectors and those particles add up to the direct pair production occurring within each sector separately. The former also leads to entanglement but in an indirect way by transferring quanta which have been previously created in a given sector. Using this group-theoretic approach, we then showed that the evolution operator can be interpreted as the successive application of three blocks of quantum operations on the initial state. This sequence of operations schematically consists in first exchanging quanta between the two sectors, then creating pairs within each sector separately, and finally mixing again these newly-created quanta between the two sectors.

Applying the evolution operator to the vacuum state allowed us to derive the most general expression for the four-mode squeezed states, see Eqs. (5.6) and (5.7), which, to our knowledge, has not been presented in the literature so far. It can be viewed as the copy of two two-mode squeezed states, one for each sector, which then exchange quanta according to their couplings. Its mathematical structure exhibits a power expansion in the coupling between the two fields, in which the power at each order gives the number of transfers between the two sectors. As an example, we provided explicit formulas for an expansion truncated at second order, *i.e.* including up to two exchanges of particles between the two fields. We finally described the four-mode squeezed states in terms of their Wigner functions, which were shown to be Gaussian. Their covariance is built from all the cross-spectra and we expressed them using either the Bogolyubov coefficients or the ten squeezing and rotation parameters.

In cases where one of the two sectors is unobserved (say the second sector, which we referred to as the "environment"), entanglement between the two fields leads to quantum decoherence in the first sector (dubbed the "system"), as well as modifications of its observable

predictions. We studied this mechanism by first computing the reduced density matrix starting from the four-mode squeezed state. We showed that the environment induces corrections to observables that are necessarily of even power in the coupling strength. This is because, in order to preserve statistical isotropy, any particle transfer between the two sectors must be compensated by the inverse transfer of a particle with the same wavenumber, or by the transfer of a particle with opposite wavenumber, so the number of transfers is even. The purity of the system, $\gamma_{\vec{k}}$, was also calculated from the reduced density matrix. We then investigated decoherence using the Wigner function and found that it substantially simplifies calculations. Indeed, we showed that tracing out the environment is readily obtained in the phase-space representation by marginalising the Wigner function over the phase-space of the environment. Since the Wigner function of a four-mode squeezed state is Gaussian, this operation is trivial. This allowed us to obtain a non-perturbative expression of the purity in terms of the power spectra of the system. We have finally expanded the result at second-order in the coupling parameters in both approaches (where we have checked that the same result is obtained).

The fact that the purity can be expressed in terms of the power spectra of the system entails that decoherence, *i.e.* the decrease of the purity, cannot proceed without affecting the observable power spectra. However, we have shown that in the large squeezing limit, there exists a regime, given by Eq. (6.21), where the interaction strength is large enough to make the system decohere but small enough to keep the observables mostly unchanged, shedding some light on the results of Refs. [23, 55]. This also confirmed that squeezed states are more easily subject to decoherence [11].

Though limited to quadratic coupling, let us stress that our approach to decoherence does not rely on any approximation scheme, since the full quantum state of the joint system-plus-environment setup is first derived exactly, before tracing out the environment. It thus provides an ideal case study to frame the range of applicability of approximate approaches to decoherence, such as the Lindblad formalism (at least in the simple situation of quadratic couplings). One may indeed compare the exact results obtained in this work with the ones derived from those effective methods, and this is the topic of a future work.

As mentioned in Sec. 1, our results are directly relevant for cosmology, in order to describe scalar fields in flat and non-flat Friedmann-Lemaître-Robertson-Walker geometries, quantum fields in curved spaces possibly with derivative couplings, and in the context of primordial cosmology, adiabatic and isocurvature perturbations in multiple-field inflation scenarios. But more generally, our results are relevant for any time-dependent, quadratic Hamiltonian that couples two degrees of freedom, regardless of the origin of these degrees of freedom. They thus offer a wide range of applications. In particular, the phase-space approach can be readily extended to cases where the environment is made of more than one scalar field. Suppose indeed that N scalar fields, initially in their vacuum state, compose the environment. The Wigner function of the system-plus-environment setup is described by an $(N+1)$-dimensional Gaussian. Tracing out (*i.e.*, in phase space, marginalising) over N scalar fields is thus as trivial as tracing out over one single field. This may be used to understand how isocurvature modes can lead to the decoherence of the adiabatic sector, and should be compared with effective-field theory approaches for such systems [56].

Finally, since squeezed states feature quantum entanglement, they are an interesting playground to discuss possible setups for Bell and Leggett-Garg inequality violations in continuous systems, see Refs. [25, 27, 57, 58]. These analyses have been carried out for two-mode squeezed states, where only one type of entanglement can be harvested, namely the one be-

tween modes $\vec{k}$ and $-\vec{k}$ of the same field. Since the two subsystems $\vec{k}$ and $-\vec{k}$ are not locally distinct in real space, this necessarily restricts the analysis to those Bell inequalities where locality is not part of the assumptions being tested (such as, for instance, the Leggett-Garg or the temporal-Bell inequalities). The situation is however different for multiple-field systems, where one may chose to measure a field ϕ_1 at position $\vec{x}_1$ and another field ϕ_2 at position $\vec{x}_2$. This is because, on top of the entanglement between modes $\vec{k}$ and $-\vec{k}$ of the same field, one now has entanglement between quanta in different fields. This thus opens up the possibility to test for a wider class of Bell inequalities. Let us also mention that the present work would additionally allow one to assess how decoherence affects the ability to test Bell inequalities with squeezed states.

A Commutation relations in the Lie algebra $\mathfrak{sp}(4,\mathbb{R})$

Following the procedure exemplified at the end of Sec. 3.1, which relies on combining the multiplication rule of the Kronecker product, Eq. (3.9), with the commutation relations between the Pauli matrices, Eq. (3.10), the commutators between the generators of $\mathfrak{sp}(4,\mathbb{R})$, as listed in Table 1, are given by

$$\text{Sq./Sq. :} \quad [\boldsymbol{K}_1,\boldsymbol{K}_2]=0; \tag{A.1}$$

$$\text{Rot./Rot. :} \quad [\boldsymbol{K}_3,\boldsymbol{K}_5]=0, \quad [\boldsymbol{K}_3,\boldsymbol{K}_6]=0, \quad [\boldsymbol{K}_3,\boldsymbol{K}_4]=0, \tag{A.2}$$

$$[\boldsymbol{K}_5,\boldsymbol{K}_6]=2\boldsymbol{K}_4, \quad [\boldsymbol{K}_6,\boldsymbol{K}_4]=2\boldsymbol{K}_5, \quad [\boldsymbol{K}_4,\boldsymbol{K}_5]=2\boldsymbol{K}_6; \tag{A.3}$$

$$\text{Boost/Boost :} \quad [\boldsymbol{K}_7,\boldsymbol{K}_8]=0, \quad [\boldsymbol{K}_7,\boldsymbol{K}_{10}]=0, \quad [\boldsymbol{K}_9,\boldsymbol{K}_8]=0, \tag{A.4}$$

$$[\boldsymbol{K}_9,\boldsymbol{K}_7]=2\boldsymbol{K}_6, \quad [\boldsymbol{K}_8,\boldsymbol{K}_{10}]=2\boldsymbol{K}_5, \quad [\boldsymbol{K}_9,\boldsymbol{K}_{10}]=2\boldsymbol{K}_3; \tag{A.5}$$

$$\text{Sq./Rot. :} \quad [\boldsymbol{K}_1,\boldsymbol{K}_6]=0, \quad [\boldsymbol{K}_2,\boldsymbol{K}_5]=0, \tag{A.6}$$

$$[\boldsymbol{K}_1,\boldsymbol{K}_3]=2\boldsymbol{K}_8, \quad [\boldsymbol{K}_1,\boldsymbol{K}_4]=2\boldsymbol{K}_7, \quad [\boldsymbol{K}_1,\boldsymbol{K}_5]=2\boldsymbol{K}_9, \tag{A.7}$$

$$[\boldsymbol{K}_2,\boldsymbol{K}_3]=2\boldsymbol{K}_7, \quad [\boldsymbol{K}_2,\boldsymbol{K}_4]=2\boldsymbol{K}_8, \quad [\boldsymbol{K}_2,\boldsymbol{K}_6]=2\boldsymbol{K}_{10}; \tag{A.8}$$

$$\text{Sq./Boost :} \quad [\boldsymbol{K}_1,\boldsymbol{K}_{10}]=0, \quad [\boldsymbol{K}_2,\boldsymbol{K}_9]=0, \tag{A.9}$$

$$[\boldsymbol{K}_1,\boldsymbol{K}_7]=2\boldsymbol{K}_4, \quad [\boldsymbol{K}_1,\boldsymbol{K}_8]=2\boldsymbol{K}_3, \quad [\boldsymbol{K}_1,\boldsymbol{K}_9]=2\boldsymbol{K}_5, \tag{A.10}$$

$$[\boldsymbol{K}_2,\boldsymbol{K}_7]=2\boldsymbol{K}_3, \quad [\boldsymbol{K}_2,\boldsymbol{K}_8]=2\boldsymbol{K}_4, \quad [\boldsymbol{K}_2,\boldsymbol{K}_{10}]=2\boldsymbol{K}_6; \tag{A.11}$$

$$\text{Rot./Boost :} \quad [\boldsymbol{K}_4,\boldsymbol{K}_9]=0, \quad [\boldsymbol{K}_4,\boldsymbol{K}_{10}]=0, \tag{A.12}$$

$$[\boldsymbol{K}_5,\boldsymbol{K}_7]=0, \quad [\boldsymbol{K}_6,\boldsymbol{K}_8]=0, \tag{A.13}$$

$$[\boldsymbol{K}_3,\boldsymbol{K}_7]=2\boldsymbol{K}_2, \quad [\boldsymbol{K}_3,\boldsymbol{K}_8]=2\boldsymbol{K}_1, \tag{A.14}$$

$$[\boldsymbol{K}_4,\boldsymbol{K}_7]=2\boldsymbol{K}_1, \quad [\boldsymbol{K}_4,\boldsymbol{K}_8]=2\boldsymbol{K}_2, \tag{A.15}$$

$$[\boldsymbol{K}_5,\boldsymbol{K}_9]=2\boldsymbol{K}_1, \quad [\boldsymbol{K}_6,\boldsymbol{K}_{10}]=2\boldsymbol{K}_2, \tag{A.16}$$

$$[\boldsymbol{K}_3,\boldsymbol{K}_{10}]=2\boldsymbol{K}_9, \quad [\boldsymbol{K}_9,\boldsymbol{K}_3]=2\boldsymbol{K}_{10}, \tag{A.17}$$

$$[\boldsymbol{K}_5,\boldsymbol{K}_{10}]=2\boldsymbol{K}_8, \quad [\boldsymbol{K}_8,\boldsymbol{K}_5]=2\boldsymbol{K}_{10}, \tag{A.18}$$

$$[\boldsymbol{K}_6,\boldsymbol{K}_7]=2\boldsymbol{K}_9, \quad [\boldsymbol{K}_9,\boldsymbol{K}_6]=2\boldsymbol{K}_7. \tag{A.19}$$

One can identify various subalgebras, which is particularly useful when it comes to factorising down elements of the group. Since all subalgebras are three dimensional, we can use Bianchi classification to sort them. In the following equation, each line corresponds to a subalgebra, *i.e.* a set of closed generators by the adjoint operation:

$$\text{Type IX}: \quad [\boldsymbol{K}_5,\boldsymbol{K}_6]=2\boldsymbol{K}_4, \quad [\boldsymbol{K}_6,\boldsymbol{K}_4]=2\boldsymbol{K}_5, \quad [\boldsymbol{K}_4,\boldsymbol{K}_5]=2\boldsymbol{K}_6; \tag{A.20}$$

$$\text{Type VIII}: \quad [\boldsymbol{K}_1,\boldsymbol{K}_3]=2\boldsymbol{K}_8, \quad [\boldsymbol{K}_3,\boldsymbol{K}_8]=2\boldsymbol{K}_1, \quad [\boldsymbol{K}_8,\boldsymbol{K}_1]=-2\boldsymbol{K}_3\,; \tag{A.21}$$

$$[\boldsymbol{K}_1,\boldsymbol{K}_4]=2\boldsymbol{K}_7, \quad [\boldsymbol{K}_4,\boldsymbol{K}_7]=2\boldsymbol{K}_1, \quad [\boldsymbol{K}_7,\boldsymbol{K}_1]=-2\boldsymbol{K}_4\,; \tag{A.22}$$

$$[\boldsymbol{K}_1,\boldsymbol{K}_5]=2\boldsymbol{K}_9, \quad [\boldsymbol{K}_5,\boldsymbol{K}_9]=2\boldsymbol{K}_1, \quad [\boldsymbol{K}_9,\boldsymbol{K}_1]=-2\boldsymbol{K}_5\,; \tag{A.23}$$

$$[\boldsymbol{K}_2,\boldsymbol{K}_3]=2\boldsymbol{K}_7, \quad [\boldsymbol{K}_3,\boldsymbol{K}_7]=2\boldsymbol{K}_2, \quad [\boldsymbol{K}_7,\boldsymbol{K}_2]=-2\boldsymbol{K}_3\,; \tag{A.24}$$

$$[\boldsymbol{K}_2,\boldsymbol{K}_4]=2\boldsymbol{K}_8, \quad [\boldsymbol{K}_4,\boldsymbol{K}_8]=2\boldsymbol{K}_2, \quad [\boldsymbol{K}_8,\boldsymbol{K}_2]=-2\boldsymbol{K}_4\,; \tag{A.25}$$

$$[\boldsymbol{K}_2,\boldsymbol{K}_6]=2\boldsymbol{K}_{10}, \quad [\boldsymbol{K}_6,\boldsymbol{K}_{10}]=2\boldsymbol{K}_2, \quad [\boldsymbol{K}_{10},\boldsymbol{K}_2]=-2\boldsymbol{K}_6\,; \tag{A.26}$$

$$[\boldsymbol{K}_9,\boldsymbol{K}_6]=2\boldsymbol{K}_7, \quad [\boldsymbol{K}_6,\boldsymbol{K}_7]=2\boldsymbol{K}_9, \quad [\boldsymbol{K}_7,\boldsymbol{K}_9]=-2\boldsymbol{K}_6\,; \tag{A.27}$$

$$[\boldsymbol{K}_8,\boldsymbol{K}_5]=2\boldsymbol{K}_{10}, \quad [\boldsymbol{K}_5,\boldsymbol{K}_{10}]=2\boldsymbol{K}_8, \quad [\boldsymbol{K}_{10},\boldsymbol{K}_8]=-2\boldsymbol{K}_5\,; \tag{A.28}$$

$$[\boldsymbol{K}_9,\boldsymbol{K}_3]=2\boldsymbol{K}_{10}, \quad [\boldsymbol{K}_3,\boldsymbol{K}_{10}]=2\boldsymbol{K}_9, \quad [\boldsymbol{K}_{10},\boldsymbol{K}_9]=-2\boldsymbol{K}_3\,. \tag{A.29}$$

The type IX Bianchi algebra is related to a $\mathfrak{su}(2)$ subalgebra that contains three rotation generators while the type VIII Bianchi algebra is isomorphic to $\mathfrak{sl}(2,\mathbb{R})$ subalgebras. The first six type-VIII subalgebras contain a rotation, a squeezing and a boost generator, so they can be related to $\mathfrak{sp}(2,\mathbb{R}) \cong \mathfrak{sl}(2,\mathbb{R})$, the last three type-VIII subalgebras are made of a rotation and two boost generators, making their interpretation less obvious.

B Evolved vacuum state

This appendix presents the computation that leads to the expression of the evolved vacuum state in the occupation-number representation given in Eqs. (5.6) and (5.7). Starting from the initial vacuum state (5.3), we follow the different operations displayed in the quantum circuits of Sec. 4.2. Let us first consider $\widehat{\mathcal{R}}_{\vec{k}}(\boldsymbol{\varphi}_k)$, which for convenience we reproduce here:

$\widehat{\mathcal{R}}_{\vec{k}}(\boldsymbol{\varphi}_k)$:

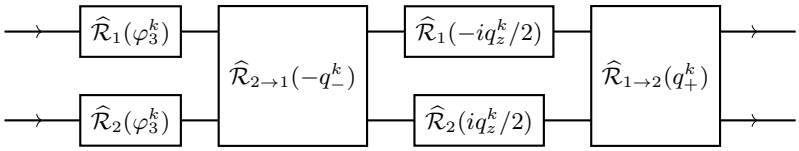

Since the operators contained in $\widehat{\mathcal{R}}_{\vec{k}}(\boldsymbol{\varphi}_k)$ do not create particles, the components $\widehat{\mathcal{R}}_{2\to1}$ and $\widehat{\mathcal{R}}_{1\to2}$ leave the initial vacuum state unchanged. Moreover, the operator $\widehat{\mathcal{R}}_1(-iq_z^k/2)$ generates an overall factor $e^{-q_z^k/2}$, which is exactly compensated by the operator $\widehat{\mathcal{R}}_2(iq_z^k/2)$ that generates an overall factor $e^{q_z^k/2}$. As a consequence, only the overall phase shift controlled by φ_3^k remains, and the evolved vacuum state can be obtained as

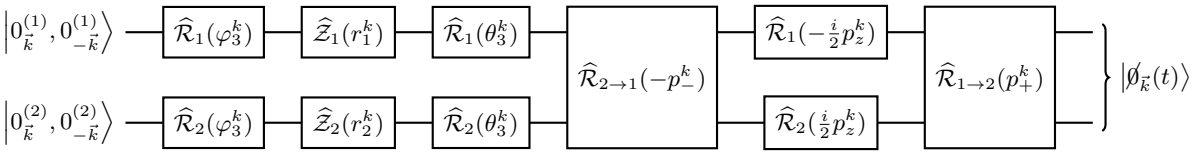

where we recall that $\widehat{\mathcal{R}}_i$, $\widehat{\mathcal{Z}}_i$ and $\widehat{\mathcal{R}}_{i\to j}$ with $i,j=1,2$ are defined in Eqs. (4.16), (4.17) and (4.18). Let us see how these operators act one after the other.

The operators $\widehat{\mathcal{R}}_1(\varphi_3^k)$ and $\widehat{\mathcal{R}}_2(\varphi_3^k)$ simply add a global phase factor $e^{-2i\varphi_3^k}$, so the initial vacuum state is first transformed according to

$$e^{-2i\varphi_3^k}\,|0^{(1)}_{\vec{k}},\ 0^{(1)}_{-\vec{k}},\ 0^{(2)}_{\vec{k}},\ 0^{(2)}_{-\vec{k}}\rangle\ . \tag{B.1}$$

To derive the action of the squeezing operators $\widehat{\mathcal{Z}}_i$, we recall that the two squeezing generators commute, and that they act on each sector separately. As a consequence, we can use the result for two-mode squeezed states in $\mathrm{Sp}(2,\mathbb{R})$, as derived *e.g.* in Ref. [13], and write

$$\widehat{\mathcal{Z}}_1(r_1^k)\left[|0^{(1)}_{\vec{k}},\ 0^{(1)}_{-\vec{k}}\rangle\otimes\chi^{(2)}_{\vec{k}}\right] = \frac{1}{\cosh r_1^k}\sum_{n=0}^{\infty}(-1)^n\tanh^n r_1^k\,|n^{(1)}_{\vec{k}},\ n^{(1)}_{-\vec{k}}\rangle\otimes\chi^{(2)}_{\vec{k}}\,, \tag{B.2}$$

$$\widehat{\mathcal{Z}}_2(r_2^k)\left[\chi^{(1)}_{\vec{k}}\otimes|0^{(2)}_{\vec{k}},\ 0^{(2)}_{-\vec{k}}\rangle\right] = \chi^{(1)}_{\vec{k}}\otimes\frac{1}{\cosh r_2^k}\sum_{m=0}^{\infty}(-1)^m\tanh^m r_2^k\,|m^{(2)}_{\vec{k}},\ m^{(2)}_{-\vec{k}}\rangle\,, \tag{B.3}$$

where $\chi^{(i)}_{\vec{k}}$ is any vector belonging to $\mathcal{E}^{(i)}_{\vec{k}}\otimes\mathcal{E}^{(i)}_{-\vec{k}}$ for $i=1,2$ and the squeezing parameters r_1^k and r_2^k control the two-mode creation in each sector. At this stage the state is thus given by

$$\frac{e^{-2i\varphi_3^k}}{\cosh r_1^k\cosh r_2^k}\sum_{n,m=0}^{\infty}(-1)^{n+m}\tanh^n r_1^k\tanh^m r_2^k\,|n^{(1)}_{\vec{k}},n^{(1)}_{-\vec{k}},m^{(2)}_{\vec{k}},m^{(2)}_{-\vec{k}}\rangle\ . \tag{B.4}$$

Then comes the contribution from $\widehat{\mathcal{R}}_i(\theta_3^k)$, which simply involves number counting operators, see Eq. (4.16), so the state becomes

$$\frac{e^{-2i(\varphi_3^k+\theta_3^k)}}{\cosh r_1^k\cosh r_2^k}\sum_{n,m=0}^{\infty}(-1)^{n+m}e^{-2i\theta_3^k(n+m)}\tanh^n r_1^k\tanh^m r_2^k\,|n^{(1)}_{\vec{k}},n^{(1)}_{-\vec{k}},m^{(2)}_{\vec{k}},m^{(2)}_{-\vec{k}}\rangle\ . \tag{B.5}$$

The action of $\widehat{\mathcal{R}}_{2\to1}$ is more involved since it transfers excitations from one sector to the other. We first note that, in $\widehat{\mathcal{R}}_{2\to1}$ and $\widehat{\mathcal{R}}_{1\to2}$, the domains $\vec{k}$ and $-\vec{k}$ can be factorised out since $\left[\widehat{a}^\dagger_{1,\vec{k}}\widehat{a}_{2,\vec{k}},\widehat{a}^\dagger_{1,-\vec{k}}\widehat{a}_{2,-\vec{k}}\right]=\left[\widehat{a}^\dagger_{2,\vec{k}}\widehat{a}_{1,\vec{k}},\widehat{a}^\dagger_{2,-\vec{k}}\widehat{a}_{1,-\vec{k}}\right]=0$. This implies that

$$\widehat{\mathcal{R}}_{2\to1}(-p_-^k) = \exp\left[-ip_-^k\left(\widehat{a}^\dagger_{1,\vec{k}}\widehat{a}_{2,\vec{k}}\right)\right]\exp\left[-ip_-^k\left(\widehat{a}^\dagger_{1,-\vec{k}}\widehat{a}_{2,-\vec{k}}\right)\right] \tag{B.6}$$

$$= \left[\sum_{i=0}^{\infty}\frac{(-ip_-^k)^i}{i!}\left(\widehat{a}^\dagger_{1,\vec{k}}\widehat{a}_{2,\vec{k}}\right)^i\right]\left[\sum_{j=0}^{\infty}\frac{(-ip_-^k)^j}{j!}\left(\widehat{a}^\dagger_{1,-\vec{k}}\widehat{a}_{2,-\vec{k}}\right)^j\right], \tag{B.7}$$

where the exponentials have been Taylor expanded, and a similar expression for $\widehat{\mathcal{R}}_{1\to2}(p_+^k)$ can be written down for future use, namely

$$\widehat{\mathcal{R}}_{1\to2}(p_+^k) = \left[\sum_{k=0}^{\infty}\frac{(ip_+^k)^k}{k!}\left(\widehat{a}^\dagger_{2,\vec{k}}\widehat{a}_{1,\vec{k}}\right)^k\right]\left[\sum_{\ell=0}^{\infty}\frac{(ip_+^k)^\ell}{\ell!}\left(\widehat{a}^\dagger_{2,-\vec{k}}\widehat{a}_{1,-\vec{k}}\right)^\ell\right]. \tag{B.8}$$

The action of $\widehat{a}^\dagger_{i,\pm\vec{k}}\widehat{a}_{j_{\pm\vec{k}}}$ is to transfer an excitation from sector j to sector i, so upon applying Eq. (B.7) onto Eq. (B.5), with the schematic normalisation $\widehat{a}\,|n\rangle = \sqrt{n}\,|n-1\rangle$ and $\widehat{a}^\dagger\,|n\rangle = \sqrt{n+1}\,|n+1\rangle$, the state becomes

$$\frac{e^{-2i(\varphi_3^k+\theta_3^k)}}{\cosh r_1^k \cosh r_2^k}\sum_{n,m=0}^{\infty}(-1)^{n+m}e^{-2i\theta_3^k(n+m)}\tanh^n r_1^k \tanh^m r_2^k \sum_{i=0}^{m}\frac{(-ip_-^k)^i}{i!}\sum_{j=0}^{m}\frac{(-ip_-^k)^j}{j!}$$
$$\sqrt{\frac{m!}{(m-i)!}}\sqrt{\frac{m!}{(m-j)!}}\sqrt{\frac{(n+i)!}{n!}}\sqrt{\frac{(n+j)!}{n!}}\,|(n+i)^{(1)}_{\vec{k}},(n+j)^{(1)}_{-\vec{k}},(m-i)^{(2)}_{\vec{k}},(m-j)^{(2)}_{-\vec{k}}\rangle\ . \tag{B.9}$$

The next step is to apply $\widehat{\mathcal{R}}_1(-\frac{i}{2}p_z^k)$ and $\widehat{\mathcal{R}}_2(\frac{i}{2}p_z^k)$, which add imaginary phases (*i.e.* exponential modulation) to each term that depend on their number of particles, and the state (B.9) becomes

$$\frac{e^{-2i(\varphi_3^k+\theta_3^k)}}{\cosh r_1^k \cosh r_2^k}\sum_{n,m=0}^{\infty}(-1)^{n+m}e^{-2i\theta_3^k(n+m)}\tanh^n r_1^k \tanh^m r_2^k \sum_{i=0}^{m}\frac{(-ip_-^k)^i}{i!}\sum_{j=0}^{m}\frac{(-ip_-^k)^j}{j!}$$
$$\sqrt{\frac{m!}{(m-i)!}}\sqrt{\frac{m!}{(m-j)!}}\sqrt{\frac{(n+i)!}{n!}}\sqrt{\frac{(n+j)!}{n!}}e^{-\frac{p_z^k}{2}(2n+i+j)}e^{\frac{p_z^k}{2}(2m-i-j)}$$
$$|(n+i)^{(1)}_{\vec{k}},(n+j)^{(1)}_{-\vec{k}},(m-i)^{(2)}_{\vec{k}},(m-j)^{(2)}_{-\vec{k}}\rangle\ . \tag{B.10}$$

Finally, the application of $\widehat{\mathcal{R}}_{1\to2}(p_+^k)$ can be done using Eq. (B.8), and one obtains

$$\frac{e^{-2i(\varphi_3^k+\theta_3^k)}}{\cosh r_1^k \cosh r_2^k}\sum_{n,m=0}^{\infty}(-1)^{n+m}e^{-2i\theta_3^k(n+m)}\tanh^n r_1^k \tanh^m r_2^k \sum_{i=0}^{m}\frac{(-ip_-^k)^i}{i!}\sum_{j=0}^{m}\frac{(-ip_-^k)^j}{j!}$$
$$\sqrt{\frac{m!}{(m-i)!}}\sqrt{\frac{m!}{(m-j)!}}\sqrt{\frac{(n+i)!}{n!}}\sqrt{\frac{(n+j)!}{n!}}e^{-\frac{p_z^k}{2}(2n+i+j)}e^{\frac{p_z^k}{2}(2m-i-j)}$$
$$\sum_{k=0}^{n+i}\frac{(ip_+^k)^k}{k!}\sum_{\ell=0}^{n+j}\frac{(ip_+^k)^\ell}{\ell!}\sqrt{\frac{(n+i)!}{(n+i-k)!}}\sqrt{\frac{(n+j)!}{(n+j-\ell)!}}\sqrt{\frac{(m-i+k)!}{(m-i)!}}\sqrt{\frac{(m-j+\ell)!}{(m-j)!}}$$
$$|(n+i-k)^{(1)}_{\vec{k}},(n+j-\ell)^{(1)}_{-\vec{k}},(m-i+k)^{(2)}_{\vec{k}},(m-j+\ell)^{(2)}_{-\vec{k}}\rangle\ . \tag{B.11}$$

This expression can be slightly simplified by replacing the sum over k and ℓ with a sum over $s \equiv i-k$ and $t = j-\ell$, and one obtains

$$|\emptyset_{\vec{k}}(t)\rangle = \frac{e^{-2i(\varphi_3^k+\theta_3^k)}}{\cosh r_1^k \cosh r_2^k}\sum_{n,m=0}^{\infty}(-1)^{n+m}e^{-2i\theta_3^k(n+m)}e^{p_z^k(m-n)}\tanh^n r_1^k \tanh^m r_2^k$$
$$\sum_{i,j=0}^{m}\frac{(-ip_-^k e^{-p_z^k})^{i+j}}{i!j!}\frac{(n+i)!(n+j)!m!}{(m-i)!(m-j)!n!}\sum_{s=-n}^{i}\sum_{t=-n}^{j}\frac{(ip_+^k)^{i+j-s-t}}{(i-s)!(j-t)!}\sqrt{\frac{(m-s)!(m-t)!}{(n+s)!(n+t)!}}$$
$$|(n+s)^{(1)}_{\vec{k}},(n+t)^{(1)}_{-\vec{k}},(m-s)^{(2)}_{\vec{k}},(m-t)^{(2)}_{-\vec{k}}\rangle\ .$$

(B.12)

In order to first sum over the indices appearing in the number of particle eigenstates, one can flip the ordering of the sums over i, j and s, t, using that $\sum_{i=0}^{m}\sum_{s=-n}^{i} = \sum_{s=-n}^{m}\sum_{i=\max(s,0)}^{m}$ and $\sum_{j=0}^{m}\sum_{t=-n}^{j} = \sum_{t=-n}^{m}\sum_{j=\max(t,0)}^{m}$, leading to

$$
\begin{aligned}
|\emptyset_{\vec{k}}(t)\rangle \;=\; & \frac{e^{-2i(\varphi_3^k+\theta_3^k)}}{\cosh r_1^k \cosh r_2^k} \sum_{n,m=0}^{\infty} (-1)^{n+m} e^{-2i\theta_3^k(n+m)} e^{p_z^k(m-n)} \tanh^n r_1^k \tanh^m r_2^k \frac{m!}{n!} \\
& \sum_{s,t=-n}^{m} \sqrt{\frac{(m-s)!(m-t)!}{(n+s)!(n+t)!}} (ip_+^k)^{-s-t} \sum_{i=\max(s,0)}^{m} \sum_{j=\max(t,0)}^{m} \frac{(p_-^k p_+^k e^{-p_z^k})^{i+j}}{i!j!(i-s)!(j-t)!} \\
& \frac{(n+i)!(n+j)!}{(m-i)!(m-j)!} \left|(n+s)_{\vec{k}}^{(1)}, (n+t)_{-\vec{k}}^{(1)}, (m-s)_{\vec{k}}^{(2)}, (m-t)_{-\vec{k}}^{(2)}\right\rangle .
\end{aligned}
\tag{B.13}
$$

This is the result presented in Eqs. (5.6) and (5.7) in the main text.

C Reduced density matrix

In this appendix, we explicitly trace out the environmental degrees of freedom in Fock space as discussed in Sec. 6.1, leading to the expression for the reduced density matrix and the purity given in Eqs. (6.4) and (6.6). For the evolved vacuum state given in Eq. (5.6), the density matrix $\widehat{\rho}_{\vec{k}}(t) = |\emptyset_{\vec{k}}(t)\rangle \langle\emptyset_{\vec{k}}(t)|$ reads

$$
\begin{aligned}
\widehat{\rho}_{\vec{k}} = & \sum_{n,m=0}^{\infty} \sum_{s,t=-n}^{m} \sum_{n',m'=0}^{\infty} \sum_{s',t'=-n'}^{m'} c_k(n,m,s,t) c_k^*(n',m',s',t') \\
& \left|(n+s)_{\vec{k}}^{(1)}, (n+t)_{-\vec{k}}^{(1)}, (m-s)_{\vec{k}}^{(2)}, (m-t)_{-\vec{k}}^{(2)}\right\rangle \left\langle (n'+s')_{\vec{k}}^{(1)}, (n'+t')_{-\vec{k}}^{(1)}, (m'-s')_{\vec{k}}^{(2)}, (m'-t')_{-\vec{k}}^{(2)}\right| .
\end{aligned}
\tag{C.1}
$$

Following Eq. (6.1), one can trace out the environmental degrees of freedom in the Fock basis. When doing so, the only non-vanishing terms are such that $m - s = m' - s'$ and $m - t = m' - t'$. This allows one to fix s' and t', and since the conditions $-n' \leq s', t' \leq m'$ imposed by the sum boundaries in Eq. (C.1) imply that $m - m' - n' \leq s, t \leq m$, the reduced density matrix reads

$$
\begin{aligned}
\widehat{\rho}_{\vec{k},\mathrm{red}}(t) = & \sum_{n,m,n',m'=0}^{\infty} \sum_{s,t=\max(-n,m-m'-n')}^{m} c_k(n,m,s,t) c_k^*(n',m',s+m'-m,t+m'-m) \\
& \left|(n+s)_{\vec{k}}^{(1)}, (n+t)_{-\vec{k}}^{(1)}\right\rangle \left\langle (n'+s+m'-m)_{\vec{k}}^{(1)}, (n'+t+m'-m)_{-\vec{k}}^{(1)}\right| .
\end{aligned}
\tag{C.2}
$$

Let us now replace n' and m' by the new indices $N = n' + m' - m$ and $M = m' - m$. This gives rise to

$$
\begin{aligned}
\widehat{\rho}_{\vec{k},\mathrm{red}}(t) = & \sum_{n,m=0}^{\infty} \sum_{M=-m}^{\infty} \sum_{N=M}^{\infty} \sum_{s,t=\max(-n,-N)}^{m} c_k(n,m,s,t) c_k^*(N-M,m+M,s+M,t+M) \\
& \left|(n+s)_{\vec{k}}^{(1)}, (n+t)_{-\vec{k}}^{(1)}\right\rangle \left\langle (N+s)_{\vec{k}}^{(1)}, (N+t)_{-\vec{k}}^{(1)}\right| .
\end{aligned}
\tag{C.3}
$$

One can note that the indices m and M do not appear explicitly in the elements of the Fock basis, which is the reason why we have performed the above change of indices. In order to rewrite the sums over m and M as internal sums, similarly to what was done between Eqs. (B.12) and (B.13), one can re-order the various indices and write

$$\begin{aligned}\widehat{\rho}_{\vec{k},\mathrm{red}}(t) = &\sum_{n=0}^{\infty}\sum_{N=-\infty}^{\infty}\sum_{s,t=-\min(n,N)}^{\infty} |(n+s)^{(1)}_{\vec{k}},(n+t)^{(1)}_{-\vec{k}}\rangle\langle(N+s)^{(1)}_{\vec{k}},(N+t)^{(1)}_{-\vec{k}}| \\ &\underbrace{\sum_{m=\max(0,s,t)}^{\infty}\sum_{M=-m}^{N} c_k(n,m,s,t)c_k^*(N-M,m+M,s+M,t+M)}_{\Xi_k(n,N,s,t)},\end{aligned} \tag{C.4}$$

which defines the coefficients Ξ_k, and which matches Eqs. (6.4) and (6.5) given in the main text (where the indices have been renamed for notational convenience).

From this expression, the purity of the system can also be computed. Squaring Eq. (C.4), one obtains

$$\begin{aligned}\widehat{\rho}^2_{\vec{k},\mathrm{red}} = &\sum_{n,n'=0}^{\infty}\sum_{N,N'=-\infty}^{\infty}\sum_{s,t=-\min(n,N)}^{\infty} \Xi_k(n,N,s,t)\Xi_k(n',N',s+N-n',t+N-n') \\ &|(n+s)^{(1)}_{\vec{k}},(n+t)^{(1)}_{-\vec{k}}\rangle\langle(N'+N-n'+s)^{(1)}_{\vec{k}},(N'+N-n'+t)^{(1)}_{-\vec{k}}|,\end{aligned} \tag{C.5}$$

from which the purity (6.2) can be expressed as

$$\gamma_{\vec{k}}(t) = \sum_{n=0}^{\infty}\sum_{N,N'=-\infty}^{\infty}\sum_{s,t=-\min(n,N)}^{\infty} \Xi_k(n,N,s,t)\Xi_k(N+N'-n,N',s+n-N',t+n-N'). \tag{C.6}$$

This expression can be slightly simplified by replacing the sum over N' by a sum over $u \equiv n - N'$, and one obtains

$$\gamma_{\vec{k}}(t) = \sum_{n=0}^{\infty}\sum_{N,u=-\infty}^{\infty}\sum_{s,t=-\min(n,N)}^{\infty} \Xi_k(n,N,s,t)\Xi_k(N-u,n-u,s+u,t+u). \tag{C.7}$$

This matches Eq. (6.6) given in the main text, where the indices have been slightly renamed for notational convenience.

D Equivalence between tracing out in Hilbert space and marginalisation in the phase space

In Sec. 6.2, we have shown that a partial trace of the density matrix in Hilbert space is associated to a partial integration over the corresponding degrees of freedom of the Wigner function in phase space. This proof was however indirect, and relied on the equivalence between different ways of computing the expectation value of quantum operators. In this appendix, for completeness, we provide a direct proof that the reduced Wigner function is nothing but the Wigner-Weyl transform of the reduced density matrix.

For Hermitian operators, the Wigner-Weyl transform introduced in Eq. (5.39) can be inverted, and the classical phase-space function $\widetilde{\mathcal{O}}_{\vec{k}}(\mathbf{q}_{\vec{k}})$ gives rise to the quantum operator $\widehat{O}_{\vec{k}}$ through

$$\widehat{O}_{\vec{k}} = \frac{1}{(2\pi)^4}\int_{\mathbb{R}^8} \mathrm{d}^8\boldsymbol{\zeta}_{\vec{k}}\, \widehat{D}(\boldsymbol{\zeta}_{\vec{k}}) \int_{\mathbb{R}^8} \mathrm{d}^8\mathbf{q}_{\vec{k}}\, \exp\left(i\boldsymbol{\zeta}_{\vec{k}}\cdot\mathbf{q}_{\vec{k}}\right)\widetilde{\mathcal{O}}_{\vec{k}}(\mathbf{q}_{\vec{k}})\,. \tag{D.1}$$

It is obtained by integrating the four-mode displacement operator $\widehat{D}(\boldsymbol{\zeta}_{\vec{k}})$ against the Fourier transform of $\widetilde{\mathcal{O}}_{\vec{k}}(\mathbf{q}_{\vec{k}})$, where $\boldsymbol{\zeta}_{\vec{k}}$ is the conjugate vector to $\mathbf{q}_{\vec{k}}$, expanded as

$$\boldsymbol{\zeta}_{\vec{k}} \equiv \left(\zeta_{1,\vec{k}}, \zeta_{1,-\vec{k}}, \zeta_{2,\vec{k}}, \zeta_{2,-\vec{k}}, \kappa_{1,\vec{k}}, \kappa_{1,-\vec{k}}, \kappa_{2,\vec{k}}, \kappa_{2,-\vec{k}}\right)^{\mathrm{T}}, \tag{D.2}$$

and the displacement operator $\widehat{D}(\boldsymbol{\zeta}_{\vec{k}})$ is defined as

$$\widehat{D}(\boldsymbol{\zeta}_{\vec{k}}) = \widehat{D}_{1,\vec{k}}(\boldsymbol{\zeta}_{\vec{k}})\widehat{D}_{1,-\vec{k}}(\boldsymbol{\zeta}_{\vec{k}})\widehat{D}_{2,\vec{k}}(\boldsymbol{\zeta}_{\vec{k}})\widehat{D}_{2,-\vec{k}}(\boldsymbol{\zeta}_{\vec{k}})\,, \tag{D.3}$$

where $\widehat{D}_{i,\pm\vec{k}}(\boldsymbol{\zeta}_{\vec{k}})$ are the one-mode displacement operators

$$\widehat{D}_{i,\pm\vec{k}}(\boldsymbol{\zeta}_{\vec{k}}) = \exp\left(\gamma_{i,\pm\vec{k}}\widehat{a}^{\dagger}_{i,\pm\vec{k}} - \gamma^{*}_{i,\pm\vec{k}}\widehat{a}_{i,\pm\vec{k}}\right) \tag{D.4}$$

for $i = 1, 2$ and

$$\gamma_{i,\pm\vec{k}} = -\frac{1}{\sqrt{2}}\left(\kappa_{i,\pm\vec{k}} + i\zeta_{i,\pm\vec{k}}\right). \tag{D.5}$$

The reason why $\widehat{D}(\boldsymbol{\zeta}_{\vec{k}})$ can be factorised in the form (D.3) is because the creation and annihilation operators commute across the four modes.

Since the Wigner function $W_{\vec{k}}(\mathbf{q}_{\vec{k}}, t)$ is the Wigner-Weyl transform of the density matrix $\widehat{\rho}_{\vec{k}}(t)$, one can use Eq. (D.1) to extract the density matrix from the Wigner function,

$$\widehat{\rho}_{\vec{k}}(t) = \frac{1}{(2\pi)^4}\int_{\mathbb{R}^8} \mathrm{d}^8\boldsymbol{\zeta}_{\vec{k}}\, \widehat{D}(\boldsymbol{\zeta}_{\vec{k}}) \int_{\mathbb{R}^8} \mathrm{d}^8\mathbf{q}_{\vec{k}}\, \exp\left(i\boldsymbol{\zeta}_{\vec{k}}\cdot\mathbf{q}_{\vec{k}}\right) W_{\vec{k}}(\mathbf{q}_{\vec{k}}, t)\,. \tag{D.6}$$

Similarly, the reduced density matrix must be connected to the reduced Wigner function (that we here aim at determining) through a relation of the form

$$\widehat{\rho}_{\vec{k},\mathrm{red}}(t) = \frac{1}{(2\pi)^2}\int_{\mathbb{R}^4} \mathrm{d}^4\boldsymbol{\zeta}_{1,\vec{k}}\, \widehat{D}_1(\boldsymbol{\zeta}_{1,\vec{k}}) \int_{\mathbb{R}^4} \mathrm{d}^4\mathbf{q}_{1,\vec{k}}\, \exp\left(i\mathbf{q}_{1,\vec{k}}.\boldsymbol{\zeta}_{1,\vec{k}}\right) W_{\vec{k},\mathrm{red}}(\mathbf{q}_{1,\vec{k}}, t), \tag{D.7}$$

where $\widehat{D}_1(\boldsymbol{\zeta}_{1,\vec{k}}) = \widehat{D}_{1,\vec{k}}(\boldsymbol{\zeta}_{1,\vec{k}})\widehat{D}_{1,-\vec{k}}(\boldsymbol{\zeta}_{1,\vec{k}})$ is the first-sector displacement operator. Let us recall that $\widehat{\rho}_{\vec{k},\mathrm{red}}$ is defined in Eq. (6.1) as the partial trace of the density matrix $\widehat{\rho}_{\vec{k}}$ over the environmental degrees of freedom. By plugging Eq. (D.6) into Eq. (6.1), and expanding $\widehat{D}(\boldsymbol{\zeta}_{\vec{k}})$ as in Eq. (D.3), one finds

$$\begin{aligned}\widehat{\rho}_{\vec{k},\mathrm{red}}(t) =& \frac{1}{(2\pi)^2}\int_{\mathbb{R}^4} \mathrm{d}^4\boldsymbol{\zeta}_{1,\vec{k}}\, \widehat{D}_1(\boldsymbol{\zeta}_{1,\vec{k}}) \int_{\mathbb{R}^4} \mathrm{d}^4\mathbf{q}_{1,\vec{k}} \exp\left(i\mathbf{q}_{1,\vec{k}}.\boldsymbol{\zeta}_{1,\vec{k}}\right) \\ & \left[\frac{1}{(2\pi)^2}\int_{\mathbb{R}^4} \mathrm{d}^4\boldsymbol{\zeta}_{2,\vec{k}} \sum_{u,v=0}^{\infty} \langle u^{(2)}_{\vec{k}}, v^{(2)}_{-\vec{k}}(t)|\, \widehat{D}_2(\boldsymbol{\zeta}_{2,\vec{k}})\, |u^{(2)}_{\vec{k}}, v^{(2)}_{-\vec{k}}(t)\rangle\right.\end{aligned}$$

$$\int_{\mathbb{R}^4} \mathrm{d}^4\mathbf{q}_{2,\vec{k}}\ \exp\left(i\mathbf{q}_{2,\vec{k}}.\boldsymbol{\zeta}_{2,\vec{k}}\right) W_{\vec{k}}(\mathbf{q}_{1,\vec{k}},\mathbf{q}_{2,\vec{k}},t)\Bigg]\,. \tag{D.8}$$

By comparing this expression with Eq. (D.7), one can read off

$$W_{\vec{k},\mathrm{red}}(\mathbf{q}_{1,\vec{k}},t) = \frac{1}{(2\pi)^2}\int_{\mathbb{R}^4} \mathrm{d}^4\mathbf{q}_{2,\vec{k}}\ W_{\vec{k}}(\mathbf{q}_{1,\vec{k}},\mathbf{q}_{2,\vec{k}},t)\mathcal{N}(\mathbf{q}_{2,\vec{k}})\,, \tag{D.9}$$

where

$$\mathcal{N}(\mathbf{q}_{2,\vec{k}}) = \int_{\mathbb{R}^4} \mathrm{d}^4\boldsymbol{\zeta}_{2,\vec{k}}\ \exp\left(i\mathbf{q}_{2,\vec{k}}.\boldsymbol{\zeta}_{2,\vec{k}}\right) \sum_{u,v=0}^{\infty} \langle u^{(2)}_{\vec{k}},\ v^{(2)}_{-\vec{k}}(t)|\ \widehat{D}_2(\boldsymbol{\zeta}_{2,\vec{k}})\,|u^{(2)}_{\vec{k}},\ v^{(2)}_{-\vec{k}}(t)\rangle\,. \tag{D.10}$$

To evaluate $\mathcal{N}(\mathbf{q}_{2,\vec{k}})$, we first use the factorisation (D.3) and compute

$$\begin{aligned}\sum_{u,v=0}^{\infty} \langle u^{(2)}_{\vec{k}},\ v^{(2)}_{-\vec{k}}(t)|\ \widehat{D}_2(\boldsymbol{\zeta}_{2,\vec{k}})\,|u^{(2)}_{\vec{k}},\ v^{(2)}_{-\vec{k}}(t)\rangle = \\ \left[\sum_{u=0}^{\infty} \langle u^{(2)}_{\vec{k}}|\ \widehat{D}_{2,\vec{k}}(\boldsymbol{\zeta}_{2,\vec{k}})\,|u^{(2)}_{\vec{k}}\rangle\right]\cdot\left[\sum_{v=0}^{\infty} \langle v^{(2)}_{-\vec{k}}|\ \widehat{D}_{2,-\vec{k}}(\boldsymbol{\zeta}_{2,\vec{k}})\,|v^{(2)}_{-\vec{k}}\rangle\right].\end{aligned} \tag{D.11}$$

Using the Baker–Campbell–Hausdorff formula, and recalling that $[\widehat{a}_{i,\pm\vec{k}}, \widehat{a}^{\dagger}_{i,\pm\vec{k}}] = 1$, the one-mode displacement operator (D.4) can be written as

$$\widehat{D}_{i,\pm\vec{k}}(\boldsymbol{\zeta}_{i,\vec{k}}) = e^{-\frac{1}{2}\left|\gamma_{i,\pm\vec{k}}\right|^2}\cdot\exp\left(\gamma_{i,\pm\vec{k}}\widehat{a}^{\dagger}_{i,\pm\vec{k}}\right)\cdot\exp\left(-\gamma^*_{i,\pm\vec{k}}\widehat{a}_{i,\pm\vec{k}}\right), \tag{D.12}$$

where $\gamma_{i,\pm\vec{k}}$ is given in Eq. (D.5). This means that, when evaluating $\langle u^{(i)}_{\pm\vec{k}}|\ \widehat{D}_{i,\pm\vec{k}}(\boldsymbol{\zeta}_{i,\pm\vec{k}})\,|u^{(i)}_{\pm\vec{k}}\rangle$, one first has to compute

$$\exp\left(-\gamma^*_{i,\pm\vec{k}}\widehat{a}_{i,\pm\vec{k}}\right)|u^{(i)}_{\pm\vec{k}}\rangle = \sum_{n=0}^{u}\frac{1}{n!}\left(-\gamma^*_{i,\pm\vec{k}}\right)^n\sqrt{u(u-1)\cdots(u-n+1)}\left|(u-n)^{(i)}_{\pm\vec{k}}\right\rangle \tag{D.13}$$

where we have simply Taylor expanded the exponential function, and then

$$\begin{aligned}\exp\left(\gamma_{i,\pm\vec{k}}\widehat{a}^{\dagger}_{i,\pm\vec{k}}\right)|(u-n)^{(i)}_{\pm\vec{k}}\rangle = \\ \sum_{m=0}^{\infty}\frac{1}{n!}\left(\gamma_{i,\pm\vec{k}}\right)^m\sqrt{(u-n+1)(u-n+2)\cdots(u-n+m)}\left|(u-n+m)^{(i)}_{\pm\vec{k}}\right\rangle.\end{aligned} \tag{D.14}$$

This leads to

$$\langle u^{(i)}_{\pm\vec{k}}|\ \widehat{D}_{i,\pm\vec{k}}(\boldsymbol{\zeta}_{i,\pm\vec{k}})\,|u^{(i)}_{\pm\vec{k}}\rangle = e^{-\frac{1}{2}\left|\gamma_{i,\pm\vec{k}}\right|^2}\sum_{n=0}^{u}\frac{1}{n!}\left(-\left|\gamma_{i,\pm\vec{k}}\right|^2\right)^n\frac{u(u-1)\cdots(u-n+1)}{n!}\,. \tag{D.15}$$

The remaining sum over n can be performed by means of the Laguerre polynomials $L_u(z)$, see Eq. (18.5.12) of Ref. [59],

$$\langle u^{(i)}_{\pm\vec{k}}|\ \widehat{D}_{i,\pm\vec{k}}(\boldsymbol{\zeta}_{i,\pm\vec{k}})\,|u^{(i)}_{\pm\vec{k}}\rangle = e^{-\frac{1}{2}\left|\gamma_{i,\pm\vec{k}}\right|^2}L_u\left(\left|\gamma_{i,\pm\vec{k}}\right|^2\right). \tag{D.16}$$

Plugging this formula into Eq. (D.11), one obtains

$$\sum_{u,v=0}^{\infty} \langle u^{(2)}_{\vec{k}},\ v^{(2)}_{-\vec{k}}(t)|\, \widehat{D}_2(\boldsymbol{\zeta}_{2,\vec{k}})\, |u^{(2)}_{\vec{k}},\ v^{(2)}_{-\vec{k}}(t)\rangle = \\ e^{-\frac{1}{2}\left(\left|\gamma_{2,\vec{k}}\right|^2+\left|\gamma_{2,-\vec{k}}\right|^2\right)} \sum_{u=0}^{\infty} L_u\left(\left|\gamma_{2,\vec{k}}\right|^2\right) \sum_{v=0}^{\infty} L_v\left(\left|\gamma_{2,-\vec{k}}\right|^2\right). \tag{D.17}$$

According to Eq. (D.10), we now need to evaluate the Fourier transform of the above expression with respect to $\boldsymbol{\zeta}_{2,\vec{k}}$, in order to compute $\mathcal{N}(\mathbf{q}_{2,\vec{k}})$. To this end, we introduce the generating function of the Laguerre polynomials [see Eq. (18.12.13) of Ref. [59]],

$$G_z(t) = \sum_{n=0}^{\infty} t^n L_n(z) = \frac{1}{1-t} \exp\left(-\frac{zt}{1-t}\right). \tag{D.18}$$

Evaluating this formula with $t = 1-\varepsilon$ in the limit $\varepsilon \to 0$, one obtains

$$\sum_{u=0}^{\infty} L_u\left(\left|\gamma_{2,\pm\vec{k}}\right|^2\right) = \lim_{\varepsilon_{\pm\vec{k}}\to 0}\left[G_{\left|\gamma_{2,\pm\vec{k}}\right|^2}(1-\varepsilon_{\pm\vec{k}})\right], \tag{D.19}$$

where we introduce $\varepsilon_{\pm\vec{k}}$ for each sector, $\vec{k}$ and $-\vec{k}$. This allows one to write $\mathcal{N}(\mathbf{q}_{2,\vec{k}})$ as the product of two limits of the Fourier transform of a Gaussian, *i.e.*

$$\mathcal{N}(\mathbf{q}_{2,\vec{k}}) = \prod_{s=+/-} \lim_{\varepsilon_{s\vec{k}}\to 0}\left[\frac{1}{\varepsilon_{s\vec{k}}}\int_{\mathbb{R}^2} \mathrm{d}^2\boldsymbol{\zeta}_{2,s\vec{k}}\ \exp\left(i\mathbf{q}_{2,s\vec{k}}.\boldsymbol{\zeta}_{2,s\vec{k}}\right)\exp\left(-\frac{2-\varepsilon_{s\vec{k}}}{4\varepsilon_{s\vec{k}}}\boldsymbol{\zeta}^2_{2,s\vec{k}}\right)\right], \tag{D.20}$$

where we have used the fact that $|\gamma_{2,\pm\vec{k}}|^2 = (\zeta^2_{2,\pm\vec{k}} + \kappa^2_{2,\pm\vec{k}})/2 = \boldsymbol{\zeta}^2_{2,\pm\vec{k}}/2$. The Fourier transform of a Gaussian is also a Gaussian and we have

$$\mathcal{N}(\mathbf{q}_{2,\vec{k}}) = \prod_{s=+/-} \lim_{\varepsilon_{s\vec{k}}\to 0}\left[\left(\frac{4\pi}{2-\varepsilon_{s\vec{k}}}\right)\exp\left(-\frac{\varepsilon_{s\vec{k}}}{2-\varepsilon_{s\vec{k}}}\mathbf{q}^2_{2,s\vec{k}}\right)\right] = (2\pi)^2. \tag{D.21}$$

We conclude that $\mathcal{N}(\mathbf{q}_{2,\vec{k}})$ simply corresponds to a global phase-space volume, with no dependence on the phase-space location.

The reduced Wigner function is finally given by Eq. (D.9), which leads to

$$W_{\vec{k},\mathrm{red}}(\mathbf{q}_{1,\vec{k}}, t) = \int_{\mathbb{R}^4} \mathrm{d}^4\mathbf{q}_{2,\vec{k}}\ W_{\vec{k}}(\mathbf{q}_{1,\vec{k}}, \mathbf{q}_{2,\vec{k}}, t), \tag{D.22}$$

i.e. it is simply obtained by marginalising the full Wigner function over the environmental degrees of freedom in phase-space. This matches Eq. (6.12) given in the main text. Let us stress that the above result is fully generic and does not assume any specific shape for the Wigner function. It can be easily generalised to an arbitrary number of degrees of freedom both in the system and in the environment sectors, since the Wigner-Weyl transform is generated by a kernel that can be written in a fully factorisable form. Non-factorisability due to entanglement is entirely contained in the Wigner function. Therefore, the reduced Wigner function is always obtained from the full Wigner function by simply integrating over the phase-space variables describing the environmental sector. In a sense, marginalisation in phase space is the Wigner-Weyl representation of the partial trace.

References

[1] S.M. Barnett and P.M. Radmore, *Methods in Theoretical Quantum Optics*, Clarendon Press Publication, Oxford (1997).

[2] C.M. Caves and B.L. Schumaker, *New formalism for two-photon quantum optics. 1. Quadrature phases and squeezed states*, *Phys. Rev.* **A31** (1985) 3068.

[3] B.L. Schumaker and C.M. Caves, *New formalism for two-photon quantum optics. 2. Mathematical foundation and compact notation*, *Phys. Rev.* **A31** (1985) 3093.

[4] V.V. Dodonov, *'Nonclassical' states in quantum optics: a 'squeezed' review of the first 75 years*, *J. Opt. B* **4** (2002) R1.

[5] R. Schnabel, *Squeezed states of light and their applications in laser interferometers*, *Phys. Rept.* **684** (2017) 1 [1611.03986].

[6] L. Grishchuk and Y. Sidorov, *Squeezed quantum states of relic gravitons and primordial density fluctuations*, *Phys. Rev.* **D42** (1990) 3413.

[7] L. Grishchuk, H. Haus and K. Bergman, *Generation of squeezed radiation from vacuum in the cosmos and the laboratory*, *Phys. Rev.* **D46** (1992) 1440.

[8] A. Albrecht, P. Ferreira, M. Joyce and T. Prokopec, *Inflation and squeezed quantum states*, *Phys. Rev. D* **50** (1994) 4807 [astro-ph/9303001].

[9] D. Polarski and A.A. Starobinsky, *Semiclassicality and decoherence of cosmological perturbations*, *Class. Quant. Grav.* **13** (1996) 377 [gr-qc/9504030].

[10] J. Lesgourgues, D. Polarski and A.A. Starobinsky, *Quantum to classical transition of cosmological perturbations for nonvacuum initial states*, *Nucl. Phys.* **B497** (1997) 479 [gr-qc/9611019].

[11] C. Kiefer, D. Polarski and A.A. Starobinsky, *Quantum to classical transition for fluctuations in the early universe*, *Int. J. Mod. Phys.* **D7** (1998) 455 [gr-qc/9802003].

[12] J. Martin and V. Vennin, *Quantum Discord of Cosmic Inflation: Can we Show that CMB Anisotropies are of Quantum-Mechanical Origin?*, *Phys. Rev.* **D93** (2016) 023505 [1510.04038].

[13] J. Grain and V. Vennin, *Squeezing formalism and canonical transformations in cosmology*, *JCAP* **2002** (2020) 022 [1910.01916].

[14] Planck collaboration, *Planck 2018 results. I. Overview and the cosmological legacy of Planck*, *Astron. Astrophys.* **641** (2020) A1 [1807.06205].

[15] N. Turok, *String Driven Inflation*, *Phys. Rev. Lett.* **60** (1988) 549.

[16] T. Damour and A. Vilenkin, *String theory and inflation*, *Phys. Rev. D* **53** (1996) 2981 [hep-th/9503149].

[17] S. Kachru, R. Kallosh, A.D. Linde, J.M. Maldacena, L.P. McAllister and S.P. Trivedi, *Towards inflation in string theory*, *JCAP* **10** (2003) 013 [hep-th/0308055].

[18] A. Krause and E. Pajer, *Chasing brane inflation in string-theory*, *JCAP* **07** (2008) 023 [0705.4682].

[19] D. Baumann and L. McAllister, *Inflation and String Theory*, Cambridge Monographs on Mathematical Physics, Cambridge University Press (5, 2015), 10.1017/CBO9781316105733, [1404.2601].

[20] W.H. Zurek, *Pointer basis of quantum apparatus: Into what mixture does the wave packet collapse?*, *Phys. Rev. D* **24** (1981) 1516.

[21] W.H. Zurek, *Environment-induced superselection rules*, *Phys. Rev. D* **26** (1982) 1862.

[22] E. Joos and H. Zeh, *The Emergence of classical properties through interaction with the environment*, *Z. Phys. B* **59** (1985) 223.

[23] J. Martin and V. Vennin, *Observational constraints on quantum decoherence during inflation*, *JCAP* **05** (2018) 063 [1801.09949].

[24] E. Oudot, P. Sekatski, F. Fröwis, N. Gisin and N. Sangouard, *Two-mode squeezed states as Schrödinger cat-like states*, *Journal of the Optical Society of America B Optical Physics* **32** (2015) 2190 [1410.8421].

[25] J. Martin and V. Vennin, *Leggett-Garg Inequalities for Squeezed States*, *Phys. Rev. A* **94** (2016) 052135 [1611.01785].

[26] S. Choudhury and S. Panda, *Quantum entanglement in de Sitter space from stringy axion: An analysis using α vacua*, *Nucl. Phys. B* **943** (2019) 114606 [1712.08299].

[27] K. Ando and V. Vennin, *Bipartite temporal Bell inequalities for two-mode squeezed states*, *Phys. Rev. A* **102** (2020) 052213 [2007.00458].

[28] S. Kanno, J. Soda and J. Tokuda, *Indirect detection of gravitons through quantum entanglement*, 2103.17053.

[29] Y.S. Kim and M.E. Noz, *Dirac Matrices and Feynman's Rest of the Universe*, *Symmetry* **4** (2012) 626 [1210.6251].

[30] K. Hasebe, *$Sp(4;\mathbb{R})$ Squeezing for Bloch Four-Hyperboloid via The Non-Compact Hopf Map*, *J. Phys. A* **53** (2020) 055303 [1904.12259].

[31] A. Garcia-Chung, *Symplectic group in polymer quantum mechanics*, *Phys. Rev. D* **101** (2020) 106004 [2003.00388].

[32] A. Garcia-Chung, *Squeeze operator: a classical view*, 2003.04257.

[33] G. Chacón-Acosta and A. García-Chung, *The relation between the symplectic group $Sp(4,\mathbb{R})$ and its Lie algebra: its application in polymer quantum mechanics*, 2102.12049.

[34] H. Goldstein, C. Poole and J. Safko, *Classical Mechanics*, Addison Wesley (2002).

[35] C. Bloch and A. Messiah, *The Canonical form of an antisymmetric tensor and its application to the theory of superconductivity*, *Nucl. Phys.* **39** (1962) 95.

[36] R. Puri, T. Asakura, K. Brenner, T. Hansch, F. Krausz, H. Weber et al., *Mathematical Methods of Quantum Optics*, Physics and astronomy online library, Springer (2001).

[37] A. Perelomov, *Generalized Coherent States and Their Applications*, Modern Methods of Plant Analysis, Springer-Verlag (1986).

[38] S. Barnett and P. Radmore, *Methods in Theoretical Quantum Optics*, Oxford Series in Optical and Imaging Sciences, Clarendon Press (2002).

[39] D. Truax, *Baker-campbell-hausdorff Relations and Unitarity of SU(2) and SU(1,1) Squeeze Operators*, *Phys. Rev. D* **31** (1985) 1988.

[40] R. Simon, E.C.G. Sudarshan and N. Mukunda, *Gaussian-wigner distributions in quantum mechanics and optics*, *Phys. Rev. A* **36** (1987) 3868.

[41] R. Simon, E. Sudarshan and N. Mukunda, *Gaussian wigner distributions: A complete characterization*, *Physics Letters A* **124** (1987) 223 .

[42] Arvind, B. Dutta, N. Mukunda and R. Simon, *The Real symplectic groups in quantum mechanics and optics*, *Pramana* **45** (1995) 471 [quant-ph/9509002].

[43] J. Martin, *Inflationary perturbations: The Cosmological Schwinger effect*, *Lect. Notes Phys.* **738** (2008) 193 [0704.3540].

[44] A. Matacz, *The Emergence of classical behavior in the quantum fluctuations of a scalar field in an expanding universe*, *Class. Quant. Grav.* **10** (1993) 509.

[45] M.B. Einhorn and F. Larsen, *Squeezed states in the de Sitter vacuum*, *Phys. Rev.* **D68** (2003) 064002 [hep-th/0305056].

[46] W.B. Case, *Wigner functions and weyl transforms for pedestrians*, *American Journal of Physics* **76** (2008) 937 [https://doi.org/10.1119/1.2957889].

[47] H. Weyl, *Quantenmechanik und Gruppentheorie*, *Zeitschrift fur Physik* **46** (1927) 1.

[48] H.J. Groenewold, *On the principles of elementary quantum mechanics*, *Physica* **12** (1946) 405.

[49] J.E. Moyal and M.S. Bartlett, *Quantum mechanics as a statistical theory*, *Proceedings of the Cambridge Philosophical Society* **45** (1949) 99.

[50] W.B. Case, *Wigner functions and Weyl transforms for pedestrians*, *American Journal of Physics* **76** (2008) 937.

[51] U. Seyfarth, A.B. Klimov, H. de Guise, G. Leuchs and L.L. Sanchez-Soto, *Wigner function for SU(1,1)*, *Quantum* **4** (2020) 317 [1911.11703].

[52] A. Serafini, F. Illuminati and S. De Siena, *Von Neumann entropy, mutual information and total correlations of Gaussian states*, *J. Phys. B* **37** (2004) L21 [quant-ph/0307073].

[53] T.F. Demarie, *Pedagogical introduction to the entropy of entanglement for Gaussian states*, *arXiv e-prints* (2012) arXiv:1209.2748 [1209.2748].

[54] J. Eisert, M. Cramer and M.B. Plenio, *Area laws for the entanglement entropy - a review*, *Rev. Mod. Phys.* **82** (2010) 277 [0808.3773].

[55] J. Martin and V. Vennin, *Non Gaussianities from Quantum Decoherence during Inflation*, *JCAP* **06** (2018) 037 [1805.05609].

[56] L. Pinol, *Multifield inflation beyond $N_{field} = 2$: non-Gaussianities and single-field effective theory*, 2011.05930.

[57] J. Martin and V. Vennin, *Bell inequalities for continuous-variable systems in generic squeezed states*, *Phys. Rev.* **A93** (2016) 062117 [1605.02944].

[58] J. Martin and V. Vennin, *Obstructions to Bell CMB Experiments*, *Phys. Rev.* **D96** (2017) 063501 [1706.05001].

[59] "*NIST Digital Library of Mathematical Functions*." http://dlmf.nist.gov/, Release 1.1.1 of 2021-03-15.

Chapter 5

Benchmarking the cosmological master equations

Preface

In this article, we use an exactly solvable model to confront Open EFT techniques against exact results. The goal is to assess the regime of validity of the master equation program, in particular regarding its ability to implement non-perturbative resummation. By comparing the precision reached by the master equation in computing standard observables such as the power spectra and quantum information properties such as the purity, we evaluate how the resummation improves the results compared to standard perturbation theory.

We first review the diversity of approximation schemes leading to the derivation of master equations along the line of Sec. 3.3.1 and highlight the generality of non-Markovian dynamics in time-dependent backgrounds. We also illustrate how non-Markovian master equations relate to standard perturbation theory.

Focusing on the comparison between exact and effective open dynamics, we derive the exact transport equations and compare them with the one obtained from the master equation. It allows us to account for a set of terms dubbed as spurious, harmless in the perturbative limit where they cancel against each other but whose presence ruin the resummation, as described in Sec. 3.4.1. Without benchmarking the cosmological master equations against an exactly solvable model, we would have missed this crucial ingredient necessary to implement non-perturbative resummation in non-Markovian settings.

Once the spurious terms are removed by hand, the resummation performs remarkably well. It strongly improves the results at the level of the standard observables and the quantum information properties compared to standard perturbation theory. In particular, in the presence of secular corrections, the relative error scales as $\ln^2 a$ in standard perturbation theory and as $\ln a$ in the resummed version of the master equation. It illustrates the late-time resummation performed by the master equation.

The article [244] can be found online at:

- https://link.springer.com/article/10.1140/epjc (published version);
- https://arxiv.org/abs/2209.01929 (arXiv version).

Benchmarking the cosmological master equations

Thomas Colas,[a,b,c] **Julien Grain,**[a,b] **Vincent Vennin**[c,b]

[a]Université Paris-Saclay, CNRS, Institut d'Astrophysique Spatiale, 91405, Orsay, France
[b]Laboratoire Astroparticule et Cosmologie, CNRS Université Paris Cité, 10 rue Alice Domon et Léonie Duquet, 75013 Paris, France
[c]Laboratoire de Physique de l'École Normale Supérieure, ENS, Université PSL, CNRS, Sorbonne Université, Université Paris Cité, F-75005 Paris, France

E-mail: thomas.colas@universite-paris-saclay.fr, julien.grain@universite-paris-saclay.fr, vincent.vennin@ens.fr

Abstract. Master equations are commonly employed in cosmology to model the effect of additional degrees of freedom, treated as an "environment", onto a given "system". However, they rely on assumptions that are not necessarily satisfied in cosmology, where the environment may be out of equilibrium and the background is dynamical. In this work, we apply the master-equation program to a model that is exactly solvable, and which consists of two linearly coupled scalar fields evolving on a cosmological background. The light field plays the role of the system and the heavy field is the environment. By comparing the exact solution to the output of the master equation, we can critically assess its performance. We find that the master equation exhibits a set of "spurious" terms that explicitly depend on the initial conditions, and which arise as a consequence of working on a dynamical background. Although they cancel out in the perturbative limit of the theory (*i.e.* at leading orders in the interaction strength), they spoil resummation. However, when those terms are removed, the master equation performs impressively well to reproduce the power spectra and the amount of the decoherence of the light field, even in the strongly decohered regime. We conclude that master equations are able to perform late-time resummation, even though the system is far from the Markovian limit, provided spurious contributions are suppressed.

Keywords: physics of the early universe, inflation, quantum field theory on curved space

Contents

1 Introduction

According to the standard model of cosmology, all structures in our universe emerge from the gravitational amplification of vacuum quantum fluctuations at early times. This idea is supported by the data, *e.g.* the measurements of the cosmic microwave background anisotropies [1], which reveal that primordial fluctuations are almost scale invariant, quasi Gaussian and adiabatic. Those observations are consistent with a phase of primordial inflation, driven by a single scalar field along a smooth potential.

However, most physical setups that have been proposed to embed inflation contain a large number of additional degrees of freedom [2]. Even if they provide negligible contributions to the dynamics of the universe expansion, they may affect the emergence of cosmic structures in various ways. For instance, they could lead to entropic fluctuations, or to deviations from Gaussian statistics, that future cosmological surveys might be able to detect [3, 4]. They may also contribute to processes occurring after inflation (such as the production of curvature perturbations [5], dark matter [6], or dark energy [7, 8]) but that crucially depend on the way those extra fields are excited during inflation. At the more fundamental level, additional degrees of freedom may also alter the quantum state in which primordial density fluctuations are placed, in particular through the mechanism of decoherence [9–18]. Decoherence [19–21] is usually associated with the erasure of genuine quantum signatures so this may affect our ability to prove or disprove that cosmic structures are of quantum-mechanical origin [22, 23].

For those reasons, it has become of increasing importance to design reliable tools to model the presence of additional degrees of freedom in the early universe [24–40]. One such approach is the so-called master equation program (see for instance Refs. [41, 42]), where an effective equation of motion is obtained for the reduced density matrix of a "system" of interest, once the degrees of freedom contained in the "environment" have been traced out. One of its appealing advantages is its ability to resum late-time secular effects [43–49], hence to go beyond standard perturbation theory and implement non-perturbative resummations in cosmology.

However, master equations were primarily developed in the context of quantum optics, so they rely on assumptions (*e.g.* that the environment comprises a large reservoir in thermal equilibrium) that are not necessarily satisfied in cosmology. There, since the background is dynamical, the Hamiltonian is time-dependent [50] and the environment is generally out-of-equilibrium [51]. This is why, in this work, we want to understand under which conditions the master-equation program can be employed in cosmology, and what physical insight one shall expect to get out of it.

We address this issue by considering a toy model that is exactly solvable, such that the output of master equations can be compared to the exact result and examined in a critical way. This allows us to benchmark master equations. In practice, we consider two linearly coupled scalar field evolving on a homogeneous and isotropic universe. The model has been solved exactly in Refs. [52, 53], where it has been shown that each Fourier sector is placed in a four-mode squeezed state, which is a Gaussian state. By tracing over the heaviest field, one obtains the reduced state of the lightest field, which follows a non-unitary evolution, and which can be compared with the predictions of different approaches, such as master equations or standard perturbative techniques. In this model, the environment does not reach thermal equilibrium, and as we will show the Markovian limit [54] is not attained either. This is why it is a priori challenging for conventional master-equation approaches to properly describe its dynamics.

The rest of this article is organised as follows. In Sec. 2, we introduce the master-equation formalism, and clarify the levels at which the different approximations enter the calculation. In Sec. 3, we introduce the cosmological model mentioned above, and show how it can be solved exactly. We then apply the master-equation program to this setting, and find that it exhibits a set of terms that we dub "spurious". These terms do not exist in the perturbative limit of the theory, and they prevent resummation due to their dependence on the initial conditions. In Sec. 4 we then analyse the ability of the master equation to reproduce the power spectra of the model, as well as to predict the amount of quantum decoherence, when spurious terms are removed "by hand". We find that master equations are impressively efficient in that case, even in the strongly decohered regime, and that they perform much better than standard perturbative

methods (such as *e.g.* the in-in formalism). This also leads us to draw a few conclusions as to whether a heavy scalar field can efficiently decohere cosmological fluctuations. In Sec. 5, we summarise our main findings and further discuss the status of the spurious terms. The paper ends by a few technical appendices, to which we defer the derivation of some of the results given in the main text.

2 The master-equation bestiary

The master-equation program proposes to describe the quantum state of a system when it weakly couples to an environment. In practice, one considers a Hamiltonian of the form

$$\widehat{\mathcal{H}} = \widehat{\mathcal{H}}_{\rm S} + \widehat{\mathcal{H}}_{\rm E} + g\widehat{\mathcal{H}}_{\rm int}\,, \tag{2.1}$$

where $\widehat{\mathcal{H}}_{\rm S}$ and $\widehat{\mathcal{H}}_{\rm E}$ respectively denote the Hamiltonians for the system and the environment in the absence of interactions, and $g\widehat{\mathcal{H}}_{\rm int}$ is the interaction term, controlled by the coupling constant g. The system alone is described by the reduced density matrix, which is obtained from the full density matrix by tracing over the environmental degrees of freedom,

$$\widehat{\rho}_{\rm red} = {\rm Tr}_{\rm E}(\widehat{\rho})\,. \tag{2.2}$$

An evolution equation for $\widehat{\rho}_{\rm red}$ can be derived with different levels of approximation, corresponding to as many different master equations. In this section, we review the most common master equations, see Ref. [41] for further details (readers already familiar with the master-equation basic tools may want to skip this section and jump to Sec. 3).

2.1 An exact master equation: the Nakajima-Zwanzig equation

Our first step is to derive an exact, formal master equation, before applying an approximation scheme. Hereafter we work in the interaction picture, where quantum states evolve with the interaction Hamiltonian $g\widehat{\mathcal{H}}_{\rm int}$ and operators evolve with the free Hamiltonian, *i.e.* the Hamiltonian in the absence of interactions $\widehat{\mathcal{H}}_0 \equiv \widehat{\mathcal{H}}_{\rm S} + \widehat{\mathcal{H}}_{\rm E}$. Operators in the interaction picture are denoted with an overall tilde, in order to make the distinction with the Schrödinger and Heisenberg pictures where they carry an overall hat. The link between the Schrödinger and the interaction picture is given by

$$\widetilde{\rho}(\eta) = \widehat{\mathcal{U}}_0^\dagger(\eta)\widehat{\rho}(\eta)\widehat{\mathcal{U}}_0(\eta) \quad \text{and} \quad \widetilde{\mathcal{H}}_{\rm int}(\eta) = \widehat{\mathcal{U}}_0^\dagger(\eta)\widehat{\mathcal{H}}_{\rm int}(\eta)\widehat{\mathcal{U}}_0(\eta)\,, \tag{2.3}$$

where η denotes time and where we have introduced the free evolution operator

$$\widehat{\mathcal{U}}_0(\eta) = \mathcal{T}\exp\left[-i\int_{\eta_0}^{\eta}\widehat{\mathcal{H}}_0(\eta'){\rm d}\eta'\right] = \mathcal{T}\exp\left[-i\int_{\eta_0}^{\eta}\widehat{\mathcal{H}}_{\rm S}(\eta'){\rm d}\eta'\right]\otimes\mathcal{T}\exp\left[-i\int_{\eta_0}^{\eta}\widehat{\mathcal{H}}_{\rm E}(\eta'){\rm d}\eta'\right], \tag{2.4}$$

with $\mathcal{T}$ indicating time ordering (time arguments increase from right to left). In this work we employ natural units where $\hbar = c = 1$. As mentioned above, in the interaction picture the total density matrix evolves with the interaction Hamiltonian,

$$\frac{{\rm d}\widetilde{\rho}}{{\rm d}\eta} = -ig\left[\widetilde{\mathcal{H}}_{\rm int}(\eta), \widetilde{\rho}(\eta)\right] \equiv g\mathcal{L}(\eta)\widetilde{\rho}(\eta)\,, \tag{2.5}$$

which defines the Liouville–Von-Neumann super-operator[1] $\mathcal{L}$.

[1] In this work, following Ref. [41], "super-operator" denotes an operation which maps positive operators to positive operators.

Let us now introduce the projection super-operator $\mathcal{P}$, defined as

$$\mathcal{P}\widetilde{\rho} = \mathrm{Tr}_{\mathrm{E}}\left(\widetilde{\rho}\right) \otimes \widetilde{\rho}_{\mathrm{E}}\,, \tag{2.6}$$

where $\widetilde{\rho}_{\mathrm{E}}$ is a fixed reference state in the environment. In practice, it is taken as the state of the environment in the absence of interactions with the system, which is indeed constant in the interaction picture. One can check that $\mathcal{P}$ is a projector, *i.e.* $\mathcal{P}^2 = \mathcal{P}$, and that $\mathcal{P}\widetilde{\rho}$ contains the relevant information to reconstruct the reduced state (2.2) of the system. Upon applying the super-projector $\mathcal{P}$ and its complementary projector $\mathcal{Q} = \mathrm{Id} - \mathcal{P}$ to Eq. (2.5), one obtains

$$\frac{\partial}{\partial\eta}\mathcal{P}\widetilde{\rho}(\eta) = g\mathcal{P}\mathcal{L}(\eta)\widetilde{\rho}(\eta), \tag{2.7}$$

$$\frac{\partial}{\partial\eta}\mathcal{Q}\widetilde{\rho}(\eta) = g\mathcal{Q}\mathcal{L}(\eta)\widetilde{\rho}(\eta). \tag{2.8}$$

Here we have used that since the reference state $\widetilde{\rho}_{\mathrm{E}}$ is independent of time, $\mathcal{P}$ and $\mathcal{Q}$ commute with $\partial/\partial\eta$. Inserting the identity $\mathrm{Id} = \mathcal{P} + \mathcal{Q}$ between the Liouville operator and the density matrix, one obtains

$$\frac{\partial}{\partial\eta}\mathcal{P}\widetilde{\rho}(\eta) = g\mathcal{P}\mathcal{L}(\eta)\mathcal{P}\widetilde{\rho}(\eta) + g\mathcal{P}\mathcal{L}(\eta)\mathcal{Q}\widetilde{\rho}(\eta), \tag{2.9}$$

$$\frac{\partial}{\partial\eta}\mathcal{Q}\widetilde{\rho}(\eta) = g\mathcal{Q}\mathcal{L}(\eta)\mathcal{P}\widetilde{\rho}(\eta) + g\mathcal{Q}\mathcal{L}(\eta)\mathcal{Q}\widetilde{\rho}(\eta). \tag{2.10}$$

A formal solution of Eq. (2.10) is given by

$$\mathcal{Q}\widetilde{\rho}(\eta) = \mathcal{G}_{\mathcal{Q}}(\eta,\eta_0)\mathcal{Q}\widetilde{\rho}(\eta_0) + g\int_{\eta_0}^{\eta}\mathrm{d}\eta'\mathcal{G}_{\mathcal{Q}}(\eta,\eta')\mathcal{Q}\mathcal{L}(\eta')\mathcal{P}\widetilde{\rho}(\eta'), \tag{2.11}$$

where η_0 is some initial time and $\mathcal{G}_{\mathcal{Q}}(\eta,\eta')$ is the propagator defined as

$$\mathcal{G}_{\mathcal{Q}}(\eta,\eta') \equiv \mathcal{T}\exp\left[g\int_{\eta'}^{\eta}\mathrm{d}\eta''\mathcal{Q}\mathcal{L}(\eta'')\right]. \tag{2.12}$$

Plugging Eq. (2.11) into Eq. (2.9), one then obtains a closed equation for the time evolution of the projected density matrix $\mathcal{P}\widetilde{\rho}$, namely

$$\frac{\partial}{\partial\eta}\mathcal{P}\widetilde{\rho}(\eta) = g\mathcal{P}\mathcal{L}(\eta)\mathcal{G}_{\mathcal{Q}}(\eta,\eta_0)\mathcal{Q}\widetilde{\rho}(\eta_0) + g\mathcal{P}\mathcal{L}(\eta)\mathcal{P}\widetilde{\rho}(\eta) + g^2\int_{\eta_0}^{\eta}\mathrm{d}\eta'\mathcal{P}\mathcal{L}(\eta)\mathcal{G}_{\mathcal{Q}}(\eta,\eta')\mathcal{Q}\mathcal{L}(\eta')\mathcal{P}\widetilde{\rho}(\eta'). \tag{2.13}$$

This is the Nakajima-Zwanzig equation. Although formal, it provides an exact master equation for the reduced state of the system. It can be further simplified by assuming that the initial state does not contain correlations between the system and the environment, *i.e.* $\widetilde{\rho}(\eta_0) = \mathrm{Tr}_{\mathrm{E}}(\widetilde{\rho}) \otimes \mathrm{Tr}_{\mathrm{S}}(\widetilde{\rho}) = \mathrm{Tr}_{\mathrm{E}}(\widetilde{\rho}) \otimes \widetilde{\rho}_{\mathrm{E}}$, hence $\mathcal{Q}\widetilde{\rho}(\eta_0) = 0$. Moreover, without loss of generality one can assume that the expectation value of the interaction Hamiltonian vanishes in the reference state, *i.e.* $\mathrm{Tr}_{\mathrm{E}}(\widetilde{\mathcal{H}}_{\mathrm{int}}\widetilde{\rho}_{\mathrm{E}}) = 0$ [if this is not satisfied, one simply redefines $\widetilde{\mathcal{H}}_{\mathrm{S}}$ by adding $g\mathrm{Tr}_{\mathrm{E}}(\widetilde{\mathcal{H}}_{\mathrm{int}}\widetilde{\rho}_{\mathrm{E}}) \otimes \mathrm{Id}_{\mathrm{E}}$ to it]. This leads to $\mathcal{P}\mathcal{L}(\eta)\mathcal{P} = 0$,[2] so the Nakajima-Zwanzig

[2]This can be shown by computing

$$\mathcal{P}\mathcal{L}\mathcal{P}\widetilde{\rho} = -i\mathcal{P}\left[\widetilde{\mathcal{H}}_{\mathrm{int}}, \mathcal{P}\widetilde{\rho}\right] = -i\mathcal{P}\left[\widetilde{\mathcal{H}}_{\mathrm{int}}, \mathrm{Tr}_{\mathrm{E}}(\widetilde{\rho}) \otimes \widetilde{\rho}_{\mathrm{E}}\right] = -i\left[\mathrm{Tr}_{\mathrm{E}}\left(\widetilde{\mathcal{H}}_{\mathrm{int}}\widetilde{\rho}_{\mathrm{E}}\right), \mathrm{Tr}_{\mathrm{E}}\left(\widetilde{\rho}\right)\right] \otimes \widetilde{\rho}_{\mathrm{E}} = 0\,. \tag{2.14}$$

equation reduces to

$$\frac{\partial}{\partial\eta}\mathcal{P}\widetilde{\rho}(\eta) = g^2\int_{\eta_0}^{\eta}\mathrm{d}\eta'\mathcal{K}(\eta,\eta')\mathcal{P}\widetilde{\rho}(\eta'), \tag{2.15}$$

where we have introduced the memory kernel $\mathcal{K}(\eta,\eta')$ defined as

$$\mathcal{K}(\eta,\eta') = \mathcal{P}\mathcal{L}(\eta)\mathcal{G}_{\mathcal{Q}}(\eta,\eta')\mathcal{Q}\mathcal{L}(\eta')\mathcal{P}. \tag{2.16}$$

In this form, the master equation is as difficult to solve as the Liouville equation (2.5) of the full setup. However, it allows efficient approximation schemes to be designed, as we shall now see. The first approximation relies on the assumption of weak coupling between the system and the environment and is discussed in Sec. 2.2, the second approximation concerns properties of the environment itself and is developed in Sec. 2.3.

2.2 Born approximation: the time-convolutionless cumulant expansion

An effective description of the system alone is in general possible only when it weakly couples to its environment. This naturally provides a small parameter, namely the interaction strength, in which to perform an expansion. This is the so-called Born approximation, which also addresses one of the difficulties inherent to the Nakajima-Zwanzig equation (2.15), namely the fact that it is non-local in time, *i.e.* the time derivative of $\mathcal{P}\widetilde{\rho}(\eta)$ depends on its past history $\mathcal{P}\widetilde{\rho}(\eta')$ for $\eta' < \eta$. The Time-ConvolutionLess projection operator method (TCL in the following) consists in expanding the dynamics of the system in powers of the coupling constant g, rendering the equation local in time (while preserving its non-Markovian nature[3]). One thus obtains an equation of the form

$$\frac{\partial}{\partial\eta}\mathcal{P}\widetilde{\rho}(\eta) = \sum_{n=2}^{\infty} g^n\mathcal{K}_n(\eta)\mathcal{P}\widetilde{\rho}(\eta)\,, \tag{2.17}$$

where the $\mathcal{K}_n$ operators are called the TCL_n operators and can be computed iteratively. This can be done by expanding Eq. (2.12) in g, and by using Eq. (2.17) to express $\mathcal{P}\widetilde{\rho}(\eta')$ in terms of $\mathcal{P}\widetilde{\rho}(\eta)$ in the right-hand side of Eq. (2.15), at the required order. For instance, at leading order in g, $\mathcal{G}_{\mathcal{Q}}(\eta,\eta') = \mathrm{Id}$, see Eq. (2.12), so Eq. (2.16) leads to $\mathcal{K}(\eta,\eta') = \mathcal{P}\mathcal{L}(\eta)\mathcal{Q}\mathcal{L}(\eta')\mathcal{P} = \mathcal{P}\mathcal{L}(\eta)\mathcal{L}(\eta')\mathcal{P}$, where we have used that $\mathcal{Q} = 1-\mathcal{P}$ and that $\mathcal{P}\mathcal{L}\mathcal{P} = 0$, see footnote 2. At that order, Eq. (2.15) also indicates that $\mathcal{P}\widetilde{\rho}$ is constant hence

$$\mathcal{K}_2(\eta) = \int_{\eta_0}^{\eta}\mathrm{d}\eta'\mathcal{P}\mathcal{L}(\eta)\mathcal{L}(\eta')\mathcal{P}\,, \tag{2.18}$$

and truncating Eq. (2.17) at order $n = 2$ leads to the TCL_2 master equation

$$\frac{\mathrm{d}\widetilde{\rho}_{\mathrm{red}}}{\mathrm{d}\eta} = -g^2\int_{\eta_0}^{\eta}\mathrm{d}\eta'\mathrm{Tr}_{\mathrm{E}}\left[\widetilde{\mathcal{H}}_{\mathrm{int}}(\eta),\left[\widetilde{\mathcal{H}}_{\mathrm{int}}(\eta'),\widetilde{\rho}_{\mathrm{red}}(\eta)\otimes\widetilde{\rho}_{\mathrm{E}}\right]\right]. \tag{2.19}$$

This expansion can be carried on. At order $n = 3$, one needs to expand the memory kernel $\mathcal{K}(\eta,\eta')$ at order g and keep $\mathcal{P}\widetilde{\rho}(\eta') \simeq \mathcal{P}\widetilde{\rho}(\eta)$ in the right-hand side of

[3] In this work, following Ref. [41], the dynamical map $\widetilde{\rho}(\eta) \to \widetilde{\rho}(\eta') = \mathcal{M}_{\eta\to\eta'}\widetilde{\rho}(\eta)$ is said to be Markovian if its generators form a semi-group, *i.e.* $\mathcal{M}_{\eta\to\eta'} = \mathcal{M}_{\eta''\to\eta'}\mathcal{M}_{\eta\to\eta''}$. Note that a Markovian master equation is necessarily local in time, but the reverse is not necessarily true.

Eq. (2.15), given that $\mathcal{P}\widetilde{\rho}(\eta') - \mathcal{P}\widetilde{\rho}(\eta) = \mathcal{O}\big(g^2\big)$ as shown above. One obtains $\mathcal{K}_3(\eta) = \int_{\eta_0}^{\eta} \mathrm{d}\eta' \int_{\eta'}^{\eta} \mathrm{d}\eta'' \mathcal{P}\mathcal{L}(\eta)\mathcal{Q}\mathcal{L}(\eta'')\mathcal{Q}\mathcal{L}(\eta')\mathcal{P}$, so

$$\mathcal{K}_3(\eta) = \int_{\eta_0}^{\eta} \mathrm{d}\eta' \int_{\eta'}^{\eta} \mathrm{d}\eta'' \mathcal{P}\mathcal{L}(\eta)\mathcal{L}(\eta'')\mathcal{L}(\eta')\mathcal{P} \tag{2.20}$$

where we have used again that $\mathcal{Q} = 1 - \mathcal{P}$ and that $\mathcal{P}\mathcal{L}\mathcal{P} = 0$. Note that, if the odd moments of the interaction Hamiltonian vanish in the environment (as will be the case for the model studied in the rest of this work), *i.e.* $\mathrm{Tr}_{\mathrm{E}}[\mathcal{H}_{\mathrm{int}}(\eta_1)\cdots\mathcal{H}_{\mathrm{int}}(\eta_{2p+1})\widetilde{\rho}_{\mathrm{E}}] = 0$, a similar calculation as the one performed in footnote 2 for $p = 1$ then shows that $\mathcal{P}\mathcal{L}(\eta_1)\cdots\mathcal{L}(\eta_{p+1})\mathcal{P} = 0$. This implies that $\mathcal{K}_3$ vanishes, as well as all odd TCL_n generators.

In that case, the leading correction comes from TCL_4, which receives two contributions. The first one comes from the term of order g^2 in the memory kernel $\mathcal{K}(\eta, \eta')$ while keeping $\mathcal{P}\widetilde{\rho}(\eta') \simeq \mathcal{P}\widetilde{\rho}(\eta)$ in the right-hand side of Eq. (2.15). The second contribution comes from keeping the memory kernel at leading order but expand $\mathcal{P}\widetilde{\rho}(\eta')$ at order g^2. The latter can be formally obtained from the TCL_2 equation, the solution of which reads $\mathcal{P}\widetilde{\rho}(\eta') = \mathcal{P}\widetilde{\rho}(\eta_0) + g^2 \int_{\eta_0}^{\eta'} \mathcal{K}_2(\eta'')\mathcal{P}\widetilde{\rho}(\eta'')\mathrm{d}\eta''$. Together with Eq. (2.18), this leads to

$$\begin{aligned}\mathcal{K}_4(\eta) = \int_{\eta_0}^{\eta} \mathrm{d}\eta_1 \int_{\eta_0}^{\eta_1} \mathrm{d}\eta_2 \int_{\eta_0}^{\eta_2} \mathrm{d}\eta_3 \Big[&\mathcal{P}\mathcal{L}(\eta)\mathcal{L}(\eta_1)\mathcal{L}(\eta_2)\mathcal{L}(\eta_3)\mathcal{P} - \mathcal{P}\mathcal{L}(\eta)\mathcal{L}(\eta_1)\mathcal{P}\mathcal{L}(\eta_2)\mathcal{L}(\eta_3)\mathcal{P} \\ &- \mathcal{P}\mathcal{L}(\eta)\mathcal{L}(\eta_2)\mathcal{P}\mathcal{L}(\eta_1)\mathcal{L}(\eta_3)\mathcal{P} - \mathcal{P}\mathcal{L}(\eta)\mathcal{L}(\eta_3)\mathcal{P}\mathcal{L}(\eta_1)\mathcal{L}(\eta_2)\mathcal{P}\Big].\end{aligned} \tag{2.21}$$

This expansion can be carried on to the required level of accuracy, which allows one to work out Eq. (2.17) when truncated at the corresponding order TCL_n. Note that, even if the TCL_2 order may be sufficient for practical purposes, the derivation of the fourth-order generator is useful to control the validity of the cumulant expansion, by evaluating the error estimate $g^2||\mathcal{K}_4||/||\mathcal{K}_2||$ and checking that it is indeed small.

2.3 Markovian approximation: the Lindblad equation

The TCL_2 master equation (2.19) is in general not Markovian in the sense given in footnote 3, since it involves a convolution over the past history through the integral over η'. However, a further approximation can be performed that renders the dynamics Markovian. This leads to the so-called Gorini–Kossakowski–Sudarshan–Lindblad equation, in short Lindblad equation in what follows. It can be obtained by first decomposing the interaction Hamiltonian as

$$\widehat{\mathcal{H}}_{\mathrm{int}}(\eta) = \sum_i \widehat{\boldsymbol{O}}_i^{(\mathrm{S})}(\eta) \otimes \widehat{\boldsymbol{O}}_i^{(\mathrm{E})}(\eta)\,, \tag{2.22}$$

where $\widehat{\boldsymbol{O}}_i^{(\mathrm{S})}$ and $\widehat{\boldsymbol{O}}_i^{(\mathrm{E})}$ form a basis of operators acting on the system and the environment respectively. Plugging this decomposition into Eq. (2.19), the TCL_2 master equation reads

$$\begin{aligned}\frac{\mathrm{d}\widetilde{\rho}_{\mathrm{red}}}{\mathrm{d}\eta} = -\sum_{i,j} g^2 \int_{\eta_0}^{\eta} \mathrm{d}\eta' \Bigg\{ &\Re\mathrm{e}\left[\boldsymbol{\mathcal{K}}_{ij}^{>}(\eta,\eta')\right]\left[\widetilde{\boldsymbol{O}}_i^{(\mathrm{S})}(\eta), \left[\widetilde{\boldsymbol{O}}_j^{(\mathrm{S})\dagger}(\eta'), \widetilde{\rho}_{\mathrm{red}}(\eta)\right]\right] \\ &+ i\Im\mathrm{m}\left[\boldsymbol{\mathcal{K}}_{ij}^{>}(\eta,\eta')\right]\left[\widetilde{\boldsymbol{O}}_i^{(\mathrm{S})}(\eta), \left\{\widetilde{\boldsymbol{O}}_j^{(\mathrm{S})\dagger}(\eta'), \widetilde{\rho}_{\mathrm{red}}(\eta)\right\}\right]\Bigg\},\end{aligned} \tag{2.23}$$

where $\{A, B\} \equiv AB + BA$ denotes the anticommutator and the memory kernel $\boldsymbol{\mathcal{K}}^{>}_{ij}(\eta, \eta')$ is defined as

$$\boldsymbol{\mathcal{K}}^{>}_{ij}(\eta, \eta') = \mathrm{Tr}_{\mathrm{E}}\left[\widehat{\boldsymbol{O}}^{(\mathrm{E})}_{i}(\eta)\widehat{\boldsymbol{O}}^{(\mathrm{E})\dagger}_{j}(\eta')\widehat{\rho}_{\mathrm{E}}\right]. \tag{2.24}$$

This expression is given in the Heisenberg picture. It involves the two-point correlation functions of the $\widehat{\boldsymbol{O}}^{(\mathrm{E})}_{i}$ operators in the environment, and thus depends on the environment properties.

Typical environments contain a large number of degrees of freedom, hence they behave as reservoirs in which these correlation functions quickly decay with $|\eta - \eta'|$. More precisely, if the relaxation time of the environment is small compared to the typical time scales over which the system evolves, one may coarse-grain the evolution of the system on scales larger than the environment relaxation time. The memory kernel is then sharply peaked, such that the integral over η' only receives contributions close to its upper bound η. In this limit, the past history ($\eta' < \eta$) is not involved in the dynamics anymore, which therefore becomes Markovian.

Formally, if $\boldsymbol{\mathcal{K}}^{>}_{ij}(\eta, \eta') \propto \delta(\eta - \eta')$, in the Schrödinger picture Eq. (2.23) takes the form

$$\frac{\mathrm{d}\widehat{\rho}_{\mathrm{red}}}{\mathrm{d}\eta} = -i\left[\widehat{\mathcal{H}}_{\mathrm{S}}(\eta), \widehat{\rho}_{\mathrm{red}}(\eta)\right] + \sum_{i,j}\boldsymbol{\mathcal{D}}_{ij}\left[\widehat{\boldsymbol{O}}^{(\mathrm{S})}_{i}\widehat{\rho}_{\mathrm{red}}(\eta)\widehat{\boldsymbol{O}}^{\dagger(\mathrm{S})}_{j} - \frac{1}{2}\left\{\widehat{\boldsymbol{O}}^{\dagger(\mathrm{S})}_{j}\widehat{\boldsymbol{O}}^{(\mathrm{S})}_{i}, \widehat{\rho}_{\mathrm{red}}(\eta)\right\}\right], \tag{2.25}$$

where the dissipator matrix $\boldsymbol{\mathcal{D}}_{ij}$ is a positive semi-definite matrix. This entails that it can be diagonalised by a unitary transformation (due to the hermiticity implied by the positive semi-definiteness), and in this basis Eq. (2.25) becomes[4]

$$\frac{\mathrm{d}\widehat{\rho}_{\mathrm{red}}}{\mathrm{d}\eta} = -i\left[\widehat{\mathcal{H}}_{\mathrm{S}}(\eta), \widehat{\rho}_{\mathrm{red}}(\eta)\right] + \sum_{k}\gamma_{k}\left[\widehat{\boldsymbol{L}}_{k}\widehat{\rho}_{\mathrm{red}}(\eta)\widehat{\boldsymbol{L}}^{\dagger}_{k} - \frac{1}{2}\left\{\widehat{\boldsymbol{L}}^{\dagger}_{k}\widehat{\boldsymbol{L}}_{k}, \widehat{\rho}_{\mathrm{red}}(\eta)\right\}\right] \tag{2.26}$$

where $\widehat{\boldsymbol{L}}_{k}$ are the so-called jump operators and γ_{k} are the positive eigenvalues of the dissipator matrix. This is called a Lindblad equation and is the most generic form of a Markovian dynamical equation that preserves trace, Hermiticity and positivity of the density matrix [54]. This is why Lindblad equations play a key role when studying environmental effects. However, they rely on strong hypotheses regarding the decay rate of the memory kernel in the environment, which may or may not be always satisfied. Indeed, in the cosmological context, fields evolve on a dynamical background, which implies that the environment does not necessarily reach a stationary state in which fluctuations swiftly decay. One of the goals of this article is to check the reliability of the master-equation approach for cosmological systems.

2.4 Link with perturbative methods

Later on in this work, we will investigate the extent to which TCL master equations go beyond perturbative effects and enable some non-perturbative resummation. At this stage however, it is important to stress that, when solved perturbatively, they reduce to standard perturbative results. This is because, when deriving the TCL_{n} equation, no contribution of order lower than g^{n} has been dropped.

[4] Another approximation known as the rotating-wave approximation is sometimes performed to obtain the Lindblad equation. Since the evolution of the system is coarse-grained over time scales larger than those describing the dynamics of the environment, this approximation consists in removing the quickly oscillating terms appearing in the master equation, for consistency. The implementation of this approach is however challenging in cosmology, where the dynamical background prevents the existence of a natural frequency basis [55].

More explicitly, the Liouville–Von-Neumann equation (2.5) can be formally solved as

$$\widetilde{\rho}(\eta) = |\emptyset\rangle\langle\emptyset| - ig\int_{-\infty}^{\eta} \mathrm{d}\eta' \left[\widetilde{\mathcal{H}}_{\rm int}(\eta'), \widetilde{\rho}(\eta')\right], \tag{2.27}$$

where $|\emptyset\rangle$ denotes the initial state of the combined system-environment setup. By recursively evaluating $\widetilde{\rho}$ in the right-hand side with Eq. (2.27) itself, one obtains

$$\widetilde{\rho}(\eta) = \sum_{n=0}^{\infty}(-ig)^n \int_{-\infty}^{\eta} \mathrm{d}\eta_1 \int_{-\infty}^{\eta_1} \mathrm{d}\eta_2 \cdots \int_{-\infty}^{\eta_{n-1}} \mathrm{d}\eta_n \left[\widetilde{\mathcal{H}}_{\rm int}(\eta_1), \left[\widetilde{\mathcal{H}}_{\rm int}(\eta_2), \cdots \left[\widetilde{\mathcal{H}}_{\rm int}(\eta_n), |\emptyset\rangle\langle\emptyset|\right]\cdots\right]\right], \tag{2.28}$$

which displays all contributions to the quantum state order-by-order in g. In turn, this allows one to compute corrections to the observables at all orders, as in the in-in formalism.[5]

Let us see how this compares with a perturbative solution of TCL_n. For TCL_2, since the right-hand side of Eq. (2.19) is proportional to g^2, one has $\widetilde{\rho}_{\rm red}(\eta)\otimes\widetilde{\rho}_{\rm E} = \widetilde{\rho}_{\rm red}(\eta_0)\otimes\widetilde{\rho}_{\rm E} + \mathcal{O}\big(g^2\big) = |\emptyset\rangle\langle\emptyset| + \mathcal{O}\big(g^2\big)$, and Eq. (2.19) leads to

$$\widetilde{\rho}_{\rm red}(\eta) = |\emptyset\rangle\langle\emptyset| - g^2\int_{\eta_0}^{\eta} \mathrm{d}\eta' \mathrm{Tr}_{\rm E}\left[\widetilde{\mathcal{H}}_{\rm int}(\eta), \left[\widetilde{\mathcal{H}}_{\rm int}(\eta'), |\emptyset\rangle\langle\emptyset|\right]\right] + \mathcal{O}\big(g^4\big)\,. \tag{2.31}$$

Assuming that $\mathrm{Tr}_{\rm E}(\widetilde{\mathcal{H}}_{\rm int}\widetilde{\rho}_{\rm E}) = 0$ as done above Eq. (2.15), this reduces to Eq. (2.28) when traced over the environmental degrees of freedom and truncated at order g^2. This shows that solving TCL_2 at order g^2 is equivalent to Standard Perturbation Theory (SPT hereafter) at that same order. Likewise, one can show that solving TCL_n perturbatively at order g^n is equivalent to SPT_n. Therefore, TCL_n contains *all* terms of order g^n, and *some* terms of order $g^{m>n}$.[6]

This is why TCL is at least as good as SPT, and one of our goals is to determine how much better it is when employed in a cosmological context. In other words, when master equations are used as *bona fide* dynamical maps (*i.e.* when they are taken *per se* and solved without further perturbative expansion), we want to investigate their ability to resum late-time secular effects in situations of cosmological interest [44, 46, 59].

3 Curved-space Caldeira-Leggett model

Let us now apply the master-equation program to two massive test fields φ and χ in a Friedmann-Lemaître-Robertson-Walker geometry, described by the metric

$$\mathrm{d}s^2 = a^2(\eta)\left(-\mathrm{d}\eta^2 + \mathrm{d}\vec{x}^2\right), \tag{3.1}$$

[5] This can also be shown in the in-in formalism, where the expectation value of an operator $\widehat{O}$ at time η reads

$$\langle\widehat{O}\rangle(\eta) = \langle\emptyset|\,\overline{\mathcal{T}}\left[e^{ig\int_{-\infty}^{\eta}\mathrm{d}\eta'\widetilde{\mathcal{H}}_{\rm int}(\eta')}\right]\widetilde{O}(\eta)\mathcal{T}\left[e^{-ig\int_{-\infty}^{\eta}\mathrm{d}\eta''\widetilde{\mathcal{H}}_{\rm int}(\eta'')}\right]|\emptyset\rangle\,, \tag{2.29}$$

where $\overline{\mathcal{T}}$ denotes anti time-ordering. By Taylor expanding the exponential functions, one obtains

$$\langle\widehat{O}\rangle(\eta) = \sum_{n=0}^{\infty}(ig)^n \int_{-\infty}^{\eta} \mathrm{d}\eta_1 \int_{-\infty}^{\eta_1} \mathrm{d}\eta_2 \cdots \int_{-\infty}^{\eta_{n-1}} \mathrm{d}\eta_n \,\langle\emptyset|\left[\widetilde{\mathcal{H}}_{\rm int}(\eta_n), \left[\widetilde{\mathcal{H}}_{\rm int}(\eta_{n-1}), \cdots \left[\widetilde{\mathcal{H}}_{\rm int}(\eta_1), \widetilde{O}(\eta)\right]\cdots\right]\right]|\emptyset\rangle\,. \tag{2.30}$$

Using that $\langle\widehat{O}\rangle(\eta) = \mathrm{Tr}[\widetilde{O}(\eta)\widetilde{\rho}(\eta)]$, together with $\mathrm{Tr}[\widetilde{O}(\eta)[\widetilde{\mathcal{H}}_{\rm int}(\eta_i), |\emptyset\rangle\langle\emptyset|]] = -\langle\emptyset|[\widetilde{\mathcal{H}}_{\rm int}(\eta_i), \widetilde{O}(\eta)]|\emptyset\rangle$, this is indeed consistent with Eq. (2.28).

[6] Let us stress that since the TCL expansion is organised differently from the one of SPT, it does not admit a straightforward diagrammatic representation. In this sense it is more comparable to the Dynamical Renormalisation Group (DRG) resummation [56–58] where diagrams are partially resummed.

where a is the scale factor and η is conformal time. For convenience we restrict the analysis to a de-Sitter background for which $a(\eta) \equiv -1/(H\eta)$, where H is the constant Hubble parameter and η varies between $-\infty$ and 0. We consider the case where the fields are minimally coupled to gravity and where their self-interaction is quadratic, so the action is of the form

$$S = -\int \mathrm{d}^4x\sqrt{-\det g}\left[\left(\frac{1}{2}g^{\mu\nu}\partial_\mu\varphi\partial_\nu\varphi + \frac{1}{2}m^2\varphi^2\right) + \left(\frac{1}{2}g^{\mu\nu}\partial_\mu\chi\partial_\nu\chi + \frac{1}{2}M^2\chi^2\right) + \lambda^2\varphi\chi\right]. \quad (3.2)$$

In this expression, m and M are the masses of the two fields and we assume that they satisfy $m < 3H/2 < M$. So φ and χ can be respectively considered as light and heavy, in the cosmological sense. Having in mind possible applications to cosmological perturbations, where the adiabatic degree of freedom is light, in what follows they will respectively play the role of the system and of the environment. The parameter λ, which also has dimension of a mass, controls their interaction. If those fields were to describe cosmological perturbations, higher-order interaction terms would be parametrically suppressed, and this setting would correspond to the leading order in cosmological perturbation theory. This model, refereed to as the curved-space Caldeira-Leggett model [53, 60–62], is therefore of physical interest, and as we shall now see it has the advantage to be exactly solvable.

The quantum state of the fields φ and χ was studied in details in Refs. [52, 63], where it was shown that each Fourier sector is placed in a four-mode squeezed state. On super-Hubble scales, the dynamical background leads to the creation of pairs of particles with opposite wave-momenta in each field, and the interaction then entangles these particles, leading to correlations between the two fields. Four-mode squeezed states are Gaussian states, and since the action (3.2) is quadratic Gaussianity is indeed preserved throughout the evolution. Such states are fully described by their covariance matrix (*i.e.* their quantum two-point expectation values). This is why our goal is now to compute the covariance matrix of the system.

3.1 Exact description

The action (3.2) being quadratic, different Fourier modes decouple on a homogeneous background, which makes it useful to introduce

$$v_\varphi(\eta,\boldsymbol{k}) \equiv a(\eta)\int_{\mathbb{R}^3}\frac{\mathrm{d}^3\boldsymbol{x}}{(2\pi)^{3/2}}\varphi(\boldsymbol{x})e^{-i\boldsymbol{k}.\boldsymbol{x}} \quad \text{and} \quad v_\chi(\eta,\boldsymbol{k}) \equiv a(\eta)\int_{\mathbb{R}^3}\frac{\mathrm{d}^3\boldsymbol{x}}{(2\pi)^{3/2}}\chi(\boldsymbol{x})e^{-i\boldsymbol{k}.\boldsymbol{x}}. \quad (3.3)$$

An additional prefactor a is introduced in these expressions for later convenience. The conjugate momenta can be obtained from Eq. (3.2) and read

$$p_\varphi = v_\varphi' - \frac{a'}{a}v_\varphi \quad \text{and} \quad p_\chi = v_\chi' - \frac{a'}{a}v_\chi\,, \quad (3.4)$$

where hereafter a prime denotes derivation with respect to the conformal time η. A Legendre transform gives the Hamiltonian

$$H = \int_{\mathbb{R}^{3+}}\mathrm{d}^3\boldsymbol{k}\boldsymbol{z}^\dagger\boldsymbol{H}(\eta)\boldsymbol{z}\,, \quad (3.5)$$

where the phase-space variables have been arranged into the vector $\boldsymbol{z} \equiv (v_\varphi, p_\varphi, v_\chi, p_\chi)^{\mathrm{T}}$, and where $\boldsymbol{H}$ is a four-by-four matrix given by

$$\boldsymbol{H}(\eta) = \begin{pmatrix} \boldsymbol{H}^{(\varphi)} & \boldsymbol{V} \\ \boldsymbol{V} & \boldsymbol{H}^{(\chi)} \end{pmatrix}, \quad (3.6)$$

with

$$\boldsymbol{H}^{(\varphi)}(\eta) = \begin{pmatrix} k^2 + m^2 a^2 & \frac{a'}{a} \\ \frac{a'}{a} & 1 \end{pmatrix}, \quad \boldsymbol{H}^{(\chi)}(\eta) = \begin{pmatrix} k^2 + M^2 a^2 & \frac{a'}{a} \\ \frac{a'}{a} & 1 \end{pmatrix}, \quad \boldsymbol{V}(\eta) \equiv \begin{pmatrix} \lambda^2 a^2 & 0 \\ 0 & 0 \end{pmatrix}. \tag{3.7}$$

Note that, since φ and χ are real fields, one has $\boldsymbol{z}^*(\eta, \boldsymbol{k}) = \boldsymbol{z}(\eta, -\boldsymbol{k})$. This explains why, in order to avoid double counting, the integral in Eq. (3.5) is performed over $\mathbb{R}^{3+} \equiv \mathbb{R}^2 \times \mathbb{R}^+$.

Following the canonical quantisation prescription, field variables are promoted to quantum operators. In order to work with hermitian operators, we split the fields into real and imaginary components, that is

$$\widehat{\boldsymbol{z}} = \frac{1}{\sqrt{2}} \left(\widehat{\boldsymbol{z}}^{\mathrm{R}} + i \widehat{\boldsymbol{z}}^{\mathrm{I}} \right), \tag{3.8}$$

such that $\widehat{\boldsymbol{z}}^s$ is Hermitian for $s = \mathrm{R}, \mathrm{I}$. These variables are canonical since $[\widehat{v}_i^s(\boldsymbol{k}), \widehat{p}_j^{s'}(\boldsymbol{q})] = i\delta^3(\boldsymbol{k} - \boldsymbol{q})\delta_{i,j}\delta_{s,s'}$ where $i, j = \varphi, \chi$. In this basis, the Hamiltonian takes the same form as in Eq. (3.5), *i.e.*

$$\widehat{H} = \frac{1}{2} \sum_{s=\mathrm{R},\mathrm{I}} \int_{\mathbb{R}^{3+}} \mathrm{d}^3\boldsymbol{k} \, (\widehat{\boldsymbol{z}}^s)^{\mathrm{T}} \, \boldsymbol{H}(\eta) \widehat{\boldsymbol{z}}^s \, . \tag{3.9}$$

Being separable, there is no mode coupling nor interactions between the R and I sectors and the state is factorisable in this decomposition. Hence, from now on, we focus on a given wavenumber $\boldsymbol{k}$ and a given s-sector, and to make notations lighter we leave the $\boldsymbol{k}$ and s dependence implicit.

A further factorisation can be performed under the field-space rotation

$$\widehat{\boldsymbol{z}} = \underbrace{\begin{pmatrix} \cos\theta & 0 & -\sin\theta & 0 \\ 0 & \cos\theta & 0 & -\sin\theta \\ \sin\theta & 0 & \cos\theta & 0 \\ 0 & \sin\theta & 0 & \cos\theta \end{pmatrix}}_{\boldsymbol{P}} \widehat{\boldsymbol{z}}_{\ell-\mathrm{h}} \, , \quad \text{where} \quad \theta = \frac{1}{2} \arctan\left(\frac{2\lambda^2}{m^2 - M^2} \right), \tag{3.10}$$

where ℓ and h stand for "light" and "heavy" respectively. In this basis the two fields decouple, and their masses are given by

$$m_\ell^2 = \frac{1}{2} \left[m^2 + M^2 - \left(M^2 - m^2\right) \sqrt{1 + \left(\frac{2\lambda^2}{M^2 - m^2} \right)^2} \right], \tag{3.11}$$

$$m_{\mathrm{h}}^2 = \frac{1}{2} \left[m^2 + M^2 + \left(M^2 - m^2\right) \sqrt{1 + \left(\frac{2\lambda^2}{M^2 - m^2} \right)^2} \right]. \tag{3.12}$$

These expressions imply that $m_\ell^2 < m^2 < M^2 < m_{\mathrm{h}}^2$ so after the field-space rotation it remains true that $m_\ell^2 < 9H^2/4 < m_{\mathrm{h}}^2$, hence the notation.

In this basis, the problem reduces to the dynamics of two uncoupled free fields evolving in a de-Sitter background. In the Heisenberg picture, this can be cast in terms of the mode-function decomposition

$$\widehat{v}_i(\eta) = v_i(\eta)\widehat{a}_i + v_i^*(\eta)\widehat{a}_i^\dagger \tag{3.13}$$

for $i = \ell, \mathrm{h}$ and where $\widehat{a}_i$ and $\widehat{a}_i^\dagger$ are the creation and annihilation operators of the uncoupled fields. Heisenberg's equation yield the classical equation of motion for the mode functions, *i.e.*

$$v_\ell'' + \left(k^2 - \frac{\nu_\ell^2 - \frac{1}{4}}{\eta^2}\right) v_\ell = 0 \quad \text{and} \quad v_\mathrm{h}'' + \left(k^2 - \frac{\nu_\mathrm{h}^2 - \frac{1}{4}}{\eta^2}\right) v_\mathrm{h} = 0\,. \tag{3.14}$$

In these expressions, $\nu_\ell = \frac{3}{2}\sqrt{1 - \left(\frac{2m_\ell}{3H}\right)^2}$ and $\nu_\mathrm{h} = \frac{3}{2}\sqrt{1 - \left(\frac{2m_\mathrm{h}}{3H}\right)^2} \equiv i\mu_\mathrm{h}$. By normalising the mode functions to the Bunch-Davies vacuum [64] in the asymptotic, sub-Hubble past, one obtains[7]

$$v_\ell(\eta) = \frac{1}{2}\sqrt{\frac{\pi z}{k}} e^{i\frac{\pi}{2}\left(\nu_\ell + \frac{1}{2}\right)} H_{\nu_\ell}^{(1)}(z) \quad \text{and} \quad v_\mathrm{h}(\eta) = \frac{1}{2}\sqrt{\frac{\pi z}{k}} e^{-\frac{\pi}{2}\mu_\mathrm{h} + i\frac{\pi}{4}} H_{i\mu_\mathrm{h}}^{(1)}(z)\,. \tag{3.15}$$

In these expressions, $z \equiv -k\eta$ and $H_\nu^{(1)}$ is the Hankel function of the first kind and of order ν. The mode functions of the momenta operators can be obtained by using Eq. (3.4), which still applies in the $\ell - \mathrm{h}$ basis, and one finds

$$p_\ell(\eta) = -\frac{1}{2}\sqrt{\frac{k\pi}{z}} e^{i\frac{\pi}{2}\left(\nu_\ell + \frac{1}{2}\right)} \left[\left(\nu_\ell + \frac{3}{2}\right) H_{\nu_\ell}^{(1)}(z) - z H_{\nu_\ell + 1}^{(1)}(z)\right], \tag{3.16}$$

$$p_\mathrm{h}(\eta) = -\frac{1}{2}\sqrt{\frac{k\pi}{z}} e^{-\frac{\pi}{2}\mu_\mathrm{h} + i\frac{\pi}{4}} \left[\left(i\mu_\mathrm{h} + \frac{3}{2}\right) H_{i\mu_\mathrm{h}}^{(1)}(z) - z H_{i\mu_\mathrm{h} + 1}^{(1)}(z)\right]. \tag{3.17}$$

As mentioned above, the state being Gaussian, it is fully characterised by the covariance matrix

$$\boldsymbol{\Sigma}(\eta) = \frac{1}{2}\mathrm{Tr}\left[\left\{\widehat{\boldsymbol{z}}(\eta), \widehat{\boldsymbol{z}}^\mathrm{T}(\eta)\right\}\widehat{\rho}_0\right], \tag{3.18}$$

where $\widehat{\rho}_0$ is the Schrödinger state at initial time, $\widehat{\rho}_0 = \widehat{\rho}(\eta_0)$. In the uncoupled basis, this leads to a block-diagonal covariance matrix of the form

$$\boldsymbol{\Sigma}_{\ell-\mathrm{h}}(\eta) = \begin{pmatrix} \boldsymbol{\Sigma}_\ell(\eta) & \boldsymbol{0} \\ \boldsymbol{0} & \boldsymbol{\Sigma}_\mathrm{h}(\eta) \end{pmatrix} \quad \text{where} \quad \boldsymbol{\Sigma}_i(\eta) = \begin{pmatrix} |v_i(\eta)|^2 & \Re\mathrm{e}\left[v_i(\eta)p_i^*(\eta)\right] \\ \Re\mathrm{e}\left[v_i(\eta)p_i^*(\eta)\right] & |p_i(\eta)|^2 \end{pmatrix} \tag{3.19}$$

for $i = \ell, \mathrm{h}$. In the $\varphi - \chi$ basis, the covariance matrix can be readily obtained by performing the rotation

$$\boldsymbol{\Sigma}(\eta) = \boldsymbol{P}\cdot\boldsymbol{\Sigma}_{\ell-\mathrm{h}}(\eta)\cdot\boldsymbol{P}^\mathrm{T} \equiv \begin{pmatrix} \boldsymbol{\Sigma}_{\varphi\varphi}(\eta) & \boldsymbol{\Sigma}_{\varphi\chi}(\eta) \\ \boldsymbol{\Sigma}_{\varphi\chi}(\eta) & \boldsymbol{\Sigma}_{\chi\chi}(\eta) \end{pmatrix}, \tag{3.20}$$

with

$$\boldsymbol{\Sigma}_{\varphi\varphi}(\eta) = \cos^2(\theta)\boldsymbol{\Sigma}_\ell(\eta) + \sin^2(\theta)\boldsymbol{\Sigma}_\mathrm{h}(\eta), \tag{3.21}$$

$$\boldsymbol{\Sigma}_{\varphi\chi}(\eta) = \cos(\theta)\sin(\theta)\left[\boldsymbol{\Sigma}_\ell(\eta) - \boldsymbol{\Sigma}_\mathrm{h}(\eta)\right], \tag{3.22}$$

$$\boldsymbol{\Sigma}_{\chi\chi}(\eta) = \cos^2(\theta)\boldsymbol{\Sigma}_\mathrm{h}(\eta) + \sin^2(\theta)\boldsymbol{\Sigma}_\ell(\eta). \tag{3.23}$$

Finally, the reduced state of the system φ is obtained by tracing out the χ field, see Eq. (2.2). It is still a Gaussian state, with covariance matrix given by $\boldsymbol{\Sigma}_{\varphi\varphi}$ [52]. We have

[7] Note that, since all mass parameters (including λ) are negligible compared to k/a in the asymptotic past, the Bunch-Davies vacuum can be set both in the $\varphi - \chi$ and in the $\ell - \mathrm{h}$ basis [65]. The vacuum state being invariant under rotations (see Ref. [52]), those two prescriptions are identical.

thus found an exact solution to the problem at hand (namely compute the reduced state of the system), to which we will now compare effective methods in order to test their robustness.

As explained in Sec. 1, one of the main physical effects driven by the interaction with an environment is decoherence, namely the transition from a pure quantum state into a statistical mixture. The loss of quantum coherence can be measured with the so-called purity parameter $\gamma(\eta) \equiv \mathrm{Tr}\left(\widehat{\rho}_{\mathrm{red}}^2\right)$ which measures the amount of quantum entanglement between the system and the environment. Pure states correspond to $\gamma = 1$, and mixed states have $\gamma < 1$ (with $\gamma = 0$ corresponding to a maximally mixed state). The amount by which χ decoheres φ is given by

$$\gamma(\eta) = \frac{1}{4}\det\left[\boldsymbol{\Sigma}_{\varphi\varphi}(\eta)\right]^{-1}\,, \tag{3.24}$$

the expression being valid for any Gaussian state [52]. In the absence of interactions between the system and the environment, $\det\boldsymbol{\Sigma}_{\varphi\varphi} = 1/4$ so $\gamma = 1$. Otherwise, the system is said to have decohered when $\gamma \ll 1$.

3.2 Effective description: the TCL_2 master equation

We now turn our attention to the TCL_2 master equation (2.23). We remind that it is formulated in the interaction picture, where the interaction Hamiltonian reads $\widetilde{\mathcal{H}}_{\mathrm{int}}(\eta) = a^2(\eta)\widetilde{v}_\varphi(\eta)\widetilde{v}_\chi(\eta)$. The TCL_2 master equation (2.19) thus takes the form

$$\frac{\mathrm{d}\widetilde{\rho}_{\mathrm{red}}}{\mathrm{d}\eta} = -\lambda^4 a^2(\eta)\int_{\eta_0}^{\eta}\mathrm{d}\eta' a^2(\eta')\Big\{\Re\mathrm{e}\left[\mathcal{K}^{>}(\eta,\eta')\right]\left[\widetilde{v}_\varphi(\eta),\left[\widetilde{v}_\varphi(\eta'),\widetilde{\rho}_{\mathrm{red}}(\eta)\right]\right] + i\Im\mathrm{m}\left[\mathcal{K}^{>}(\eta,\eta')\right]\left[\widetilde{v}_\varphi(\eta),\left\{\widetilde{v}_\varphi(\eta'),\widetilde{\rho}_{\mathrm{red}}(\eta)\right\}\right]\Big\}, \tag{3.25}$$

where the memory kernel is given by

$$\mathcal{K}^{>}(\eta,\eta') \equiv \mathrm{Tr}_{\mathrm{E}}\left[\widehat{v}_\chi(\eta)\widehat{v}_\chi(\eta')\widehat{\rho}_{\mathrm{E}}\right] \tag{3.26}$$

and we recall that $\widehat{\rho}_{\mathrm{E}}$ corresponds to the state of the environment in the absence of interactions with the system [a derivation of Eq. (3.25) following microphysical considerations is also presented in Appendix A]. Since $\widehat{v}_\chi(\eta)\widehat{v}_\chi(\eta')$ is not hermitian for $\eta \neq \eta'$, the kernel $\mathcal{K}^{>}(\eta,\eta')$ is complex and can be evaluated as follows. In the interaction picture, operators evolve with the free Hamiltonian, so one can use the results obtained in Sec. 3.1 in the uncoupled basis. More precisely, a similar mode-function decomposition as in Eq. (3.13) can be introduced,

$$\widetilde{v}_i(\eta) = v_i(\eta)\widehat{a}_i + v_i^*(\eta)\widehat{a}_i^\dagger \tag{3.27}$$

where $i = \varphi, \chi$, and an analogous expression for $\widetilde{p}_i(\eta)$. The mode functions are still given by Eqs. (3.15)-(3.17), where m_ℓ and m_{h} are simply replaced with m and M. This leads to

$$\mathcal{K}^{>}(\eta,\eta') = v_\chi(\eta)v_\chi^*(\eta'). \tag{3.28}$$

Interpretating the master equation

While the above form (3.25) of the cosmological master equation is compact, it makes the connection with quantum Brownian motion [62, 66–69] less apparent. A form that is easier to interpret can be obtained by expressing all operators at the same time. This can be achieved by

inverting the mode-function expansion to yield $\widehat{a}_\varphi$ and $\widehat{a}^\dagger_\varphi$ in terms of $\widetilde{v}_\varphi(\eta)$ and $\widetilde{p}_\varphi(\eta)$. Inserting those expressions in Eq. (3.27) evaluated at time η' leads to

$$\widetilde{v}_\varphi(\eta') = -2\Im\mathrm{m}\left[p_\varphi(\eta)v^*_\varphi(\eta')\right]\widetilde{v}_\varphi(\eta) + 2\Im\mathrm{m}\left[v_\varphi(\eta)v^*_\varphi(\eta')\right]\widetilde{p}_\varphi(\eta)\,. \tag{3.29}$$

Here we have used that $\Im\mathrm{m}\left[v_\varphi(\eta)p^*_\varphi(\eta)\right] = -1/2$, which comes from the canonical commutation relation $[\widetilde{v}_\varphi(\eta), \widetilde{p}_\varphi(\eta)] = 1$. Plugging Eq. (3.29) into Eq. (3.25), one finds

$$\begin{aligned}\frac{\mathrm{d}\widetilde{\rho}_{\mathrm{red}}}{\mathrm{d}\eta} =& -i\Big[\overbrace{\frac{1}{2}\widetilde{\boldsymbol{z}}_i(\eta)\boldsymbol{\Delta}_{ij}(\eta)\widetilde{\boldsymbol{z}}_j(\eta)}^{\widetilde{H}^{(\mathrm{LS})}(\eta)}, \widetilde{\rho}_{\mathrm{red}}(\eta)\Big] - \frac{1}{2}\sum_{i,j}\boldsymbol{D}_{ij}(\eta)\left[\widetilde{\boldsymbol{z}}_i(\eta), [\widetilde{\boldsymbol{z}}_j(\eta), \widetilde{\rho}_{\mathrm{red}}(\eta)]\right] \\ & - \frac{i}{2}\boldsymbol{\Delta}_{12}(\eta)\sum_{i,j}\boldsymbol{\omega}_{ij}\left[\widetilde{\boldsymbol{z}}_i(\eta), \{\widetilde{\boldsymbol{z}}_j(\eta), \widetilde{\rho}_{\mathrm{red}}(\eta)\}\right],\end{aligned} \tag{3.30}$$

which defines the "Lamb-shift" Hamiltonian $\widetilde{H}^{(\mathrm{LS})}$ (see below), where $\boldsymbol{\omega} = \begin{pmatrix} 0 & 1 \\ -1 & 0 \end{pmatrix}$, and where we have used the canonical commutation relation again. In this expression, $\widetilde{\boldsymbol{z}}(\eta) \equiv (\widetilde{v}_\varphi(\eta), \widetilde{p}_\varphi(\eta))^{\mathrm{T}}$ and the two-by-two matrices $\boldsymbol{D}$ and $\boldsymbol{\Delta}$ are given by

$$\boldsymbol{D}_{11}(\eta) = -4\lambda^4 a^2(\eta)\int_{\eta_0}^{\eta}\mathrm{d}\eta' a^2(\eta')\Im\mathrm{m}\left[p_\varphi(\eta)v^*_\varphi(\eta')\right]\Re\mathrm{e}\left[v_\chi(\eta)v^*_\chi(\eta')\right], \tag{3.31}$$

$$\boldsymbol{D}_{12}(\eta) = \boldsymbol{D}_{21}(\eta) = 2\lambda^4 a^2(\eta)\int_{\eta_0}^{\eta}\mathrm{d}\eta' a^2(\eta')\Im\mathrm{m}\left[v_\varphi(\eta)v^*_\varphi(\eta')\right]\Re\mathrm{e}\left[v_\chi(\eta)v^*_\chi(\eta')\right], \tag{3.32}$$

$$\boldsymbol{D}_{22}(\eta) = 0, \tag{3.33}$$

and

$$\boldsymbol{\Delta}_{11}(\eta) = -4\lambda^4 a^2(\eta)\int_{\eta_0}^{\eta}\mathrm{d}\eta' a^2(\eta')\Im\mathrm{m}\left[p_\varphi(\eta)v^*_\varphi(\eta')\right]\Im\mathrm{m}\left[v_\chi(\eta)v^*_\chi(\eta')\right], \tag{3.34}$$

$$\boldsymbol{\Delta}_{12}(\eta) = \boldsymbol{\Delta}_{21}(\eta) = 2\lambda^4 a^2(\eta)\int_{\eta_0}^{\eta}\mathrm{d}\eta' a^2(\eta')\Im\mathrm{m}\left[v_\varphi(\eta)v^*_\varphi(\eta')\right]\Im\mathrm{m}\left[v_\chi(\eta)v^*_\chi(\eta')\right], \tag{3.35}$$

$$\boldsymbol{\Delta}_{22}(\eta) = 0\,. \tag{3.36}$$

The corresponding equation in the Schrödinger picture can be obtained using the fact that operators are mapped between the two pictures with the free Hamiltonian of the system, see Eq. (2.3), and one finds[8]

$$\frac{\mathrm{d}\widehat{\rho}_{\mathrm{red}}}{\mathrm{d}\eta} = -i\left[\widehat{H}^{(\varphi)}(\eta) + \widehat{H}^{(\mathrm{LS})}(\eta), \widehat{\rho}_{\mathrm{red}}(\eta)\right] + \sum_{i,j}\boldsymbol{\mathcal{D}}_{ij}(\eta)\left[\widehat{\boldsymbol{z}}_i\widehat{\rho}_{\mathrm{red}}(\eta)\widehat{\boldsymbol{z}}_j - \frac{1}{2}\{\widehat{\boldsymbol{z}}_j\widehat{\boldsymbol{z}}_i, \widehat{\rho}_{\mathrm{red}}(\eta)\}\right]. \tag{3.38}$$

[8]Here we use that since $\boldsymbol{D}$ is symmetric, $\boldsymbol{\omega}$ is anti-symmetric given the canonical commutation relations between phase-space variables $[\widehat{\boldsymbol{z}}_i, \widehat{\boldsymbol{z}}_j] = \boldsymbol{w}_{ij}$, one has

$$\begin{aligned}\boldsymbol{D}_{ij}\left[\widehat{\boldsymbol{z}}_i, [\widehat{\boldsymbol{z}}_j, \widehat{\rho}_{\mathrm{red}}]\right] &= \boldsymbol{D}_{ij}\left(-2\widehat{\boldsymbol{z}}_i\widehat{\rho}_{\mathrm{red}}\widehat{\boldsymbol{z}}_j + \{\widehat{\boldsymbol{z}}_j\widehat{\boldsymbol{z}}_i, \widehat{\rho}_{\mathrm{red}}\}\right), \\ \boldsymbol{\omega}_{ij}\left[\widehat{\boldsymbol{z}}_i, \{\widehat{\boldsymbol{z}}_j, \widehat{\rho}_{\mathrm{red}}\}\right] &= \boldsymbol{\omega}_{ij}\left(2\widehat{\boldsymbol{z}}_i\widehat{\rho}_{\mathrm{red}}\widehat{\boldsymbol{z}}_j - \{\widehat{\boldsymbol{z}}_j\widehat{\boldsymbol{z}}_i, \widehat{\rho}_{\mathrm{red}}\}\right).\end{aligned} \tag{3.37}$$

In this expression, the dissipator matrix is defined as

$$\boldsymbol{\mathcal{D}}(\eta) \equiv \boldsymbol{D}(\eta) - i\boldsymbol{\Delta}_{12}(\eta)\boldsymbol{\omega} = \begin{pmatrix} \boldsymbol{D}_{11}(\eta) & \boldsymbol{D}_{12}(\eta) - i\boldsymbol{\Delta}_{12}(\eta) \\ \boldsymbol{D}_{12}(\eta) + i\boldsymbol{\Delta}_{12}(\eta) & 0 \end{pmatrix}. \tag{3.39}$$

One can see that Eq. (3.38) has the same form as the Lindblad equation (2.25), with the crucial difference that the dissipator matrix $\boldsymbol{\mathcal{D}}(\eta)$ is not positive semi-definite in the present case.[9] It is also worth stressing that Eq. (3.30) has the same form as the master equation obtained by Hu, Paz and Zhang in their seminal paper [67] and that describes quantum Brownian motion. The first term in the right-hand side of Eq. (3.30) provides a unitary contribution, which renormalises the energy levels of the system due to the interaction with the environment [41, 79, 80]. This is why it is often referred to as the Lamb–shift Hamiltonian. In our case, it reads

$$\widehat{H}^{(\varphi)}(\eta) + \widehat{H}^{(\mathrm{LS})}(\eta) = \frac{1}{2}\left[\widehat{p}_\varphi\widehat{p}_\varphi + \left(k^2 + m^2a^2 + \boldsymbol{\Delta}_{11}\right)\widehat{v}_\varphi\widehat{v}_\varphi + \left(\frac{a'}{a} + \boldsymbol{\Delta}_{12}\right)\{\widehat{v}_\varphi, \widehat{p}_\varphi\}\right]. \tag{3.40}$$

One can thus see that $\boldsymbol{\Delta}_{11}$ renormalises the mass of the field φ, while $\boldsymbol{\Delta}_{12}$ renormalises the comoving Hubble parameter. Note that, in the context of effective-field theoretic calculations, these contributions are usually re-absorbed in an effective speed of sound c_{S}^2 [27, 81, 82]. The second and the third terms in Eq. (3.30) are of a different nature, since they capture the non-unitary evolution of the system and thus cannot be described by an effectively local Lagrangian. This is due to dissipation and decoherence, which respectively correspond to the imaginary and the real part of the dissipator matrix in Eq. (3.38).[10]

Finally, in phase space, the TCL_2 master equation takes the form of a Fokker-Planck equation for the reduced Wigner function W_{red}. The latter is defined by the Wigner-Weyl transform of the reduced density matrix [96], and provides a quantum analogue of a phase-space quasi probability distribution. In Appendix B, we derive general results on the phase-space representation of the TCL_2 master equation. In particular, we find that performing the Wigner-Weyl transform of Eq. (3.30) leads to

$$\frac{\mathrm{d}W_{\mathrm{red}}}{\mathrm{d}\eta} = \left\{\widetilde{H}^{(\varphi)} + \widetilde{H}^{(\mathrm{LS})}, W_{\mathrm{red}}\right\} + \boldsymbol{\Delta}_{12}\sum_i \frac{\partial}{\partial \boldsymbol{z}_i}\left(\boldsymbol{z}_i W_{\mathrm{red}}\right) - \frac{1}{2}\sum_{i,j}\left[\boldsymbol{\omega}\boldsymbol{D}\boldsymbol{\omega}\right]_{ij}\frac{\partial^2 W_{\mathrm{red}}}{\partial \boldsymbol{z}_i \partial \boldsymbol{z}_j}, \tag{3.41}$$

where brackets correspond to Poisson brackets (not to be confused with the anti-commutator). Only the term involving $\widetilde{H}^{(\varphi)} + \widetilde{H}^{(\mathrm{LS})}$ is unitary, as mentioned above. The second term, proportional to $\boldsymbol{\Delta}_{12}$, is dissipative: it is a drift (or friction) term that accounts for the energy transfer from the system into the environment [22]. Finally, the term proportional to $\boldsymbol{\omega}\boldsymbol{D}\boldsymbol{\omega}$ corresponds to diffusion and leads to decoherence. One can show that this equation admits Gaussian solutions, hence the reduced state of the system is still Gaussian in TCL.

[9] If the dynamical map generated by Eq. (3.38) were Markovian in the sense introduced in footnote 3, *i.e.* if it described a semi-group evolution, then according to Lindblad theorem [54] the fact that its dissipator is not semi-definite positive would imply that it is not Completely Positive and Trace Preserving (CPTP). However, Eq. (3.38) belongs to the class of so-called "Gaussian master equations", which were shown to be CPTP in Refs. [70, 71] (and thus map a quantum state to another proper quantum state). The contrapositive of Lindblad's theorem thus imposes that our master equation is non-Markovian [32, 41, 72–78].

[10] The fact that the real and the imaginary part of the memory kernel lead to distinct physical effects is also encountered in the influence-functional approach [45, 66, 83–92], of which the master equation is the dynamical generator [93, 94]. Indeed, in the influence functional description, $\Im\mathrm{m}\left[\mathcal{K}^{>}(\eta,\eta')\right]$ is related to the retarded and advanced Green's function of the environment and can be interpreted as a dissipation kernel, while $\Re\mathrm{e}\left[\mathcal{K}^{>}(\eta,\eta')\right]$ is related to the Keldysh-Green's function [42, 95] and can be interpreted as a noise kernel [51].

3.3 Transport equations

As mentioned above, the state being Gaussian, it is fully characterised by its covariance matrix. Since the initial covariance matrix is the same in all approaches (TCL_2, exact, SPT) a first strategy to benchmark the cosmological master equation consists in comparing the equation of motion for the covariance of the system, usually refereed to as the transport equations.

TCL_2 transport equation

In the TCL approach, the transport equations can be obtained by differentiating Eq. (3.18) with respect to time in the Schrödinger picture, and using Eq. (3.38) to evaluate $\mathrm{d}\widehat{\rho}_{\mathrm{red}}/\mathrm{d}\eta$. This gives

$$\frac{\mathrm{d}\boldsymbol{\Sigma}_{\mathrm{TCL}}}{\mathrm{d}\eta} = \boldsymbol{\omega}\left(\boldsymbol{H}^{(\varphi)} + \boldsymbol{\Delta}\right)\boldsymbol{\Sigma}_{\mathrm{TCL}} - \boldsymbol{\Sigma}_{\mathrm{TCL}}\left(\boldsymbol{H}^{(\varphi)} + \boldsymbol{\Delta}\right)\boldsymbol{\omega} - \boldsymbol{\omega}\boldsymbol{D}\boldsymbol{\omega} - 2\boldsymbol{\Delta}_{12}\boldsymbol{\Sigma}_{\mathrm{TCL}}\,, \tag{3.42}$$

where $\boldsymbol{D}$ and $\boldsymbol{\Delta}$ were introduced in Eqs. (3.31)-(3.36). The first two terms correspond to the unitary evolution, which as stressed above receives an additional contribution from the Lamb-shift Hamiltonian. The last two terms respectively correspond to the diffusion (a source term proportional to $\boldsymbol{D}$) and the dissipation (a damping term proportional to $\boldsymbol{\Delta}_{12}$).

Exact transport equation

In the exact approach presented in Sec. 3.1, the transport equations for the full system-plus-environment setup can be obtained by differentiating Eq. (3.18) with respect to time in the Heisenberg picture, and using the Heisenberg equations to evaluate $\mathrm{d}\widehat{\boldsymbol{z}}/\mathrm{d}\eta$. The Hamiltonian (3.9) being quadratic, one finds

$$\frac{\mathrm{d}\boldsymbol{\Sigma}}{\mathrm{d}\eta} = \boldsymbol{\Omega}\boldsymbol{H}\boldsymbol{\Sigma} - \boldsymbol{\Sigma}\boldsymbol{H}\boldsymbol{\Omega}, \tag{3.43}$$

where $\boldsymbol{H}$ was defined in Eq. (3.6) and $\boldsymbol{\Omega}$ is a four-by-four block-diagonal matrix where each 2×2 block on the diagonal is $\boldsymbol{\omega}$.

Using blockwise multiplication we can split the above into a set of coupled differential equations for the covariance of the system ($\boldsymbol{\Sigma}_{\varphi\varphi}$), of the environment ($\boldsymbol{\Sigma}_{\chi\chi}$), and for their cross-covariance ($\boldsymbol{\Sigma}_{\varphi\chi}$). Using Eqs. (3.7), it reads

$$\frac{\mathrm{d}\boldsymbol{\Sigma}_{\varphi\varphi}}{\mathrm{d}\eta} = \boldsymbol{\omega}\boldsymbol{H}^{(\varphi)}\boldsymbol{\Sigma}_{\varphi\varphi} - \boldsymbol{\Sigma}_{\varphi\varphi}\boldsymbol{H}^{(\varphi)}\boldsymbol{\omega} + \boldsymbol{\omega}\boldsymbol{V}\boldsymbol{\Sigma}_{\varphi\chi}^{\mathrm{T}} - \boldsymbol{\Sigma}_{\varphi\chi}\boldsymbol{V}\boldsymbol{\omega}, \tag{3.44}$$

$$\frac{\mathrm{d}\boldsymbol{\Sigma}_{\chi\chi}}{\mathrm{d}\eta} = \boldsymbol{\omega}\boldsymbol{H}^{(\chi)}\boldsymbol{\Sigma}_{\chi\chi} - \boldsymbol{\Sigma}_{\chi\chi}\boldsymbol{H}^{(\chi)}\boldsymbol{\omega} + \boldsymbol{\omega}\boldsymbol{V}^{\mathrm{T}}\boldsymbol{\Sigma}_{\varphi\chi} - \boldsymbol{\Sigma}_{\varphi\chi}^{\mathrm{T}}\boldsymbol{V}\boldsymbol{\omega}, \tag{3.45}$$

$$\frac{\mathrm{d}\boldsymbol{\Sigma}_{\varphi\chi}}{\mathrm{d}\eta} = \boldsymbol{\omega}\boldsymbol{H}^{(\varphi)}\boldsymbol{\Sigma}_{\varphi\chi} - \boldsymbol{\Sigma}_{\varphi\chi}\boldsymbol{H}^{(\chi)}\boldsymbol{\omega} + \boldsymbol{\omega}\boldsymbol{V}\boldsymbol{\Sigma}_{\chi\chi} - \boldsymbol{\Sigma}_{\varphi\varphi}\boldsymbol{V}\boldsymbol{\omega}. \tag{3.46}$$

Note that these transport equations can also be obtained in the phase-space representation (*i.e.* using Wigner functions), as explained in Appendix B. In the present case, a first integral of the above system can be easily constructed, since we know that, in spite of having three covariance matrices ($\boldsymbol{\Sigma}_{\varphi\varphi}$, $\boldsymbol{\Sigma}_{\chi\chi}$ and $\boldsymbol{\Sigma}_{\varphi\chi}$), only two combinations are independent (namely $\boldsymbol{\Sigma}_{\ell}$ and $\boldsymbol{\Sigma}_{\mathrm{h}}$). More precisely, from Eq. (3.21) one can show that $\boldsymbol{\Sigma}_{\varphi\chi} = \boldsymbol{\Sigma}_{\varphi\chi}^{\mathrm{T}} = \tan(2\theta)(\boldsymbol{\Sigma}_{\varphi\varphi} - \boldsymbol{\Sigma}_{\chi\chi})/2$. Focusing on the dynamics of the reduced system, Eq. (3.44) can thus be written as

$$\frac{\mathrm{d}\boldsymbol{\Sigma}_{\varphi\varphi}}{\mathrm{d}\eta} = \boldsymbol{\omega}\left(\boldsymbol{H}^{(\varphi)} + \boldsymbol{\Delta}_{\mathrm{ex}}\right)\boldsymbol{\Sigma}_{\varphi\varphi} - \boldsymbol{\Sigma}_{\varphi\varphi}\left(\boldsymbol{H}^{(\varphi)} + \boldsymbol{\Delta}_{\mathrm{ex}}\right)\boldsymbol{\omega} - \boldsymbol{\omega}\boldsymbol{D}_{\mathrm{ex}}\boldsymbol{\omega}\,, \tag{3.47}$$

where

$$\boldsymbol{\Delta}_{\rm ex} \equiv -\frac{\lambda^2}{M^2-m^2}\boldsymbol{V} \quad \text{and} \quad \boldsymbol{D}_{\rm ex} \equiv -\frac{\lambda^2}{M^2-m^2}\left(\boldsymbol{\omega}\boldsymbol{\Sigma}_{\chi\chi}\boldsymbol{V} - \boldsymbol{V}\boldsymbol{\Sigma}_{\chi\chi}\boldsymbol{\omega}\right). \tag{3.48}$$

The reason why we write the exact transport equation in this form is to allow for an easy comparison with its TCL_2 counterpart (3.42). This suggests to interpret $\boldsymbol{\Delta}_{\rm ex}$ as a Lamb-shift contribution in the exact approach, and $\boldsymbol{D}_{\rm ex}$ as a diffusion matrix. From Eq. (3.48), the only non-vanishing entries of those matrices are given by

$$\boldsymbol{\Delta}_{\rm ex,11} = -\frac{\lambda^4 a^2}{M^2-m^2}, \tag{3.49}$$

$$\boldsymbol{D}_{\rm ex,11} = -2\frac{\lambda^4 a^2}{M^2-m^2}\boldsymbol{\Sigma}_{\chi\chi,12}, \qquad \boldsymbol{D}_{\rm ex,12} = \frac{\lambda^4 a^2}{M^2-m^2}\boldsymbol{\Sigma}_{\chi\chi,11}. \tag{3.50}$$

Note that, in the asymptotic past, when $a \to 0$, the above coefficients vanish, which confirms that the two fields become effectively uncoupled and that Bunch-Davies initial conditions can be safely set, see footnote 7.

SPT transport equation

In the perturbative approach introduced in Sec. 2.4, at leading order, the transport equation is simply given by the exact transport equation, Eq. (3.47), where the right-hand side is truncated at order λ^4:

$$\frac{\mathrm{d}\boldsymbol{\Sigma}_{\rm SPT}}{\mathrm{d}\eta} = \boldsymbol{\omega}\boldsymbol{H}^{(\varphi)}\boldsymbol{\Sigma}_{\rm SPT} - \boldsymbol{\Sigma}_{\rm SPT}\boldsymbol{H}^{(\varphi)}\boldsymbol{\omega} + \boldsymbol{\omega}\boldsymbol{\Delta}_{\rm ex}\boldsymbol{\Sigma}^{\rm free}_{\varphi\varphi} - \boldsymbol{\Sigma}^{\rm free}_{\varphi\varphi}\boldsymbol{\Delta}_{\rm ex}\boldsymbol{\omega} - \boldsymbol{\omega}\boldsymbol{D}_{\rm SPT}\boldsymbol{\omega}. \tag{3.51}$$

Here, $\boldsymbol{\Sigma}^{\rm free}_{\varphi\varphi}$ corresponds to $\boldsymbol{\Sigma}_{\varphi\varphi}$ evaluated in the free theory and is given by the second part of Eq. (3.19) with the mode functions v_φ and p_φ. Similarly, $\boldsymbol{D}_{\rm SPT}$ is given by Eq. (3.50) where $\boldsymbol{\Sigma}_{\chi\chi}$ is replaced with $\boldsymbol{\Sigma}^{\rm free}_{\chi\chi}$, which is given by the second part of Eq. (3.19) with the mode functions v_χ and p_χ. Note that $\boldsymbol{\Delta}_{\rm ex}$ does not need to be expanded since it is already of order λ^4, see Eq. (3.49).

Even though the covariance matrix in SPT can be obtained by integrating the above transport equation, in the present situation an exact solution to the full theory is known, so it can also be obtained by expanding Eq. (3.21) in λ. Here, not only $\theta^2 = \lambda^4/(m^2-M^2)^2 + \mathcal{O}(\lambda^8)$ needs to be expanded, see Eq. (3.10), but also $m_\ell^2 = m^2 - \lambda^4/(M^2-m^2) + \mathcal{O}(\lambda^8)$ and $m_{\rm h}^2 = M^2 + \lambda^4/(M^2-m^2) + \mathcal{O}(\lambda^8)$ in $\boldsymbol{\Sigma}_{\rm h}$ and $\boldsymbol{\Sigma}_\ell$, see Eqs. (3.11)-(3.12). On the numerical results presented below, we have checked that these two approaches coincide.

3.4 Spurious terms

The TCL_2 coefficients are expressed as integrals between η_0 and η, see Eqs. (3.31)-(3.36), where $\eta_0 \to -\infty$ if Bunch-Davies initial conditions are chosen. Formally, they can be written as

$$\boldsymbol{D}_{11} = F_{\boldsymbol{D}_{11}}(\eta,\eta) - F_{\boldsymbol{D}_{11}}(\eta,\eta_0), \tag{3.52}$$

where $F_{\boldsymbol{D}_{11}}(\eta,\cdot)$ is the primitive of the integrand appearing in Eq. (3.31), which itself depends on η, and with similar notations for the other TCL_2 coefficients. The F functions are derived explicitly in Appendix C, where it is shown that the integrals (3.31)-(3.36) can be performed analytically and involve products of four Hankel functions. The second term in Eq. (3.52), the

one of the form $F(\eta,\eta_0)$, features several properties that we now describe and that will lead us to dub it "spurious".

First, the spurious terms involve the initial time η_0, which implies that they carry explicit dependence on the initial conditions. If the environment memory kernel (3.26) is sufficiently peaked around $\eta'=\eta$, that is if the integrands in Eqs. (3.31)-(3.36) are much smaller around $\eta'=\eta_0$ than around $\eta'=\eta$, then this contribution should be suppressed compared to the non-spurious one. This is similar to the Lindbladian limit discussed in Sec. 2.3. Whether or not this is the case can be verified explicitly in the super-Hubble regime (*i.e.* at late time, $-k\eta \ll 1$) where the F functions take simple forms. The expansion in the limit $-k\eta \ll 1$ is performed in Appendix C.3, where it is shown that the spurious terms dominate for all coefficients. More precisely, $F_{\boldsymbol{D}_{11}}(\eta,\eta) \propto (-k\eta)^{-2}$ while $F_{\boldsymbol{D}_{11}}(\eta,\eta_0) \propto (-k\eta)^{-7/2}$, $F_{\boldsymbol{D}_{12}}(\eta,\eta) \propto (-k\eta)^{-1}$ while $F_{\boldsymbol{D}_{11}}(\eta,\eta_0) \propto (-k\eta)^{-5/2}$, $F_{\boldsymbol{\Delta}_{11}}(\eta,\eta) \propto (-k\eta)^{-2}$ while $F_{\boldsymbol{\Delta}_{11}}(\eta,\eta_0) \propto (-k\eta)^{-7/2}$, and $F_{\boldsymbol{\Delta}_{12}}(\eta,\eta)$ vanishes while $F_{\boldsymbol{\Delta}_{12}}(\eta,\eta_0) \propto (-k\eta)^{-5/2}$. Let us stress that the late-time domination of the spurious terms is strongly related to having a dynamical background. This is the first indication we encounter that applying the master-equation program to cosmology may not be as straightforward as in other situations.

Second, in Appendix C.1, we notice that, using various identities satisfied by the Hankel functions, the expressions for the non-spurious contributions can be vastly simplified. More precisely, after a lengthy though straightforward calculation we find that

$$\begin{aligned} F_{\boldsymbol{D}_{11}}(\eta,\eta) =& \boldsymbol{D}_{\mathrm{SPT},11}(\eta)\,, \quad & F_{\boldsymbol{D}_{12}}(\eta,\eta) = \boldsymbol{D}_{\mathrm{SPT},12}(\eta)\,, \\ F_{\boldsymbol{\Delta}_{11}}(\eta,\eta) =& \boldsymbol{\Delta}_{\mathrm{ex},11}(\eta)\,, & F_{\boldsymbol{\Delta}_{12}}(\eta,\eta) = 0\,. \end{aligned} \tag{3.53}$$

Let us now recall the result obtained in Sec. 2.4, namely the fact that the perturbative version of TCL is strictly equivalent to SPT. This implies that $\boldsymbol{\Sigma}_{\mathrm{TCL}} = \boldsymbol{\Sigma}_{\mathrm{SPT}} + \mathcal{O}(\lambda^8)$, where $\boldsymbol{\Sigma}_{\mathrm{SPT}}$ only contains terms of order λ^0 (namely $\boldsymbol{\Sigma}^{\mathrm{free}}_{\varphi\varphi}$) and λ^4. As a consequence, the right-hand sides of Eqs. (3.42) and (3.51) coincide at order λ^4. The terms of order λ^0 are trivially identical, and for the terms of order λ^4 one obtains (recalling that both $\boldsymbol{D}$ and $\boldsymbol{\Delta}$ are of order λ^4)

$$\boldsymbol{\omega}\boldsymbol{\Delta}\boldsymbol{\Sigma}^{\mathrm{free}}_{\varphi\varphi} - \boldsymbol{\Sigma}^{\mathrm{free}}_{\varphi\varphi}\boldsymbol{\Delta}\boldsymbol{\omega} - \boldsymbol{\omega}\boldsymbol{D}\boldsymbol{\omega} - 2\boldsymbol{\Delta}_{12}\boldsymbol{\Sigma}_{\mathrm{SPT}} = \boldsymbol{\omega}\boldsymbol{\Delta}_{\mathrm{ex}}\boldsymbol{\Sigma}^{\mathrm{free}}_{\varphi\varphi} - \boldsymbol{\Sigma}^{\mathrm{free}}_{\varphi\varphi}\boldsymbol{\Delta}_{\mathrm{ex}}\boldsymbol{\omega} - \boldsymbol{\omega}\boldsymbol{D}_{\mathrm{SPT}}\boldsymbol{\omega}\,. \tag{3.54}$$

Each term in the left-hand side can be decomposed into a non-spurious part and a spurious part, see Eq. (3.52). An important remark is that, thanks to Eq. (3.53), the non-spurious part exactly coincides with the right-hand side, hence the spurious contributions cancel out. We have therefore proven that the spurious terms are absent from the perturbative limit of TCL and only arise at higher order. This is obviously consistent with the fact that, at leading order, TCL coincides with the exact theory, which is not plagued by any spurious contribution.

Third, we have checked that if one includes the spurious terms when solving the TCL transport equation (3.42), then the result quickly blows up. This is due to the late-time divergences of the spurious contributions mentioned above. On the contrary, as we will see below, if one removes them, then the result is remarkably well-behaved.

To summarise, spurious terms cancel out at leading order in the interaction strength, and at higher order, the fact that they carry an explicit dependence on the initial time, combined with their late-time divergent behaviour, indicates that they cannot be resummed. This leads us to conclude that, for the simple model we have considered here, resummation cannot be efficiently performed with the standard master-equation program.

However, this may be due to the over-simplicity of that particular model, which contains a single degree of freedom in the environment. As we further argue in Sec. 5, if "larger"

environment are considered, initial-time dependent terms may be parametrically suppressed. In order to gain insight on such situations, in what follows we analyse the consequences of removing the spurious terms "by hand".

If spurious contributions are removed, Eq. (3.53) indicates that $\boldsymbol{D} = \boldsymbol{D}_{\rm SPT}$ and that $\boldsymbol{\Delta} = \boldsymbol{\Delta}_{\rm ex}$. The $\boldsymbol{\Delta}$ matrix is perfectly captured by TCL since $\boldsymbol{\Delta}_{\rm ex}$ only contains contributions proportional to λ^4, see Eq. (3.48). In particular, there is no damping term, *i.e.* $\boldsymbol{\Delta}_{12} = 0$ (note however that this is due to the specifics of the interaction we consider, which is such that $\boldsymbol{V}_{12} = 0$). The diffusive part, *i.e.* the one driven by $\boldsymbol{D}$, is however only partly contained in TCL, where $\boldsymbol{D} = \boldsymbol{D}_{\rm SPT}$, whereas $\boldsymbol{D}_{\rm ex}$ contains terms of higher-order in λ. We therefore expect spurious-free TCL to lie somewhere between SPT and the exact theory, which we now further investigate.

4 Non-perturbative resummation

In Sec. 2.4, we have shown that the TCL master equation reduces to standard perturbation theory when solved at leading order in the interaction strength. In Appendix D this equivalence is shown explicitly for the toy model introduced in Sec. 3. However, the TCL master equation can also be treated as a *bona fide* dynamical map for the quantum state of the system, and solved as it is. In that case, its ability to resum secular effects has been investigated in various contexts [22, 43, 44, 46, 59], and we now want to study how late-time resummation proceeds in the (spurious-free) cosmological Caldeira-Leggett model.

4.1 Power spectra

As mentioned above, both in the exact and TCL descriptions, the state of the system remains Gaussian, hence it is fully characterised by its covariance matrix, *i.e.* by its power spectra. This is why we first compare these setups at the level of their power spectra. If the cosmological Caldeira-Leggett model were to describe cosmological perturbations, note that the configuration-configuration power spectrum would be directly related to cosmological observables, such as the CMB temperature anisotropies.

The power spectra in the exact theory are given by Eq. (3.21), and as explained above, by expanding these formulas at first order in λ^4 one obtains their SPT counterpart. In the TCL setup, the power spectra can be obtained by solving the transport equation (3.42). In the model under consideration, there is no damping term, $\boldsymbol{\Delta}_{12} = 0$, but in general it can be absorbed by introducing

$$\boldsymbol{\sigma}_{\rm TCL} \equiv e^{\Gamma(\eta,\eta_0)}\boldsymbol{\Sigma}_{\rm TCL} \qquad \text{with} \qquad \Gamma(\eta,\eta_0) \equiv 2\int_{\eta_0}^{\eta} \mathrm{d}\eta' \boldsymbol{\Delta}_{12}(\eta')\,, \tag{4.1}$$

which is solution of a damping-free transport equation, namely

$$\frac{\mathrm{d}\boldsymbol{\sigma}_{\rm TCL}}{\mathrm{d}\eta} = \boldsymbol{\omega}\left(\boldsymbol{H}^{(\varphi)} + \boldsymbol{\Delta}\right)\boldsymbol{\sigma}_{\rm TCL} - \boldsymbol{\sigma}_{\rm TCL}\left(\boldsymbol{H}^{(\varphi)} + \boldsymbol{\Delta}\right)\boldsymbol{\omega} - e^{\Gamma(\eta,\eta_0)}\boldsymbol{\omega}\boldsymbol{D}\boldsymbol{\omega}\,. \tag{4.2}$$

This equation can be seen as a homogeneous part, describing unitary evolution, and a source term, describing diffusion. The homogeneous part is generated by the Hamiltonian $H^{(\varphi)}+H^{(\rm LS)}$, and by denoting $\boldsymbol{g}_{\rm LS}(\eta,\eta_0)$ the associated Green's matrix, the solution of Eq. (4.2) reads

$$\boldsymbol{\sigma}_{\rm TCL}(\eta) = \boldsymbol{g}_{\rm LS}(\eta,\eta_0)\boldsymbol{\sigma}_{\rm TCL}(\eta_0)\boldsymbol{g}^{\rm T}_{\rm LS}(\eta,\eta_0) - \int_{\eta_0}^{\eta}\mathrm{d}\eta' e^{\Gamma(\eta',\eta_0)}\boldsymbol{g}_{\rm LS}(\eta,\eta')\left[\boldsymbol{\omega}\boldsymbol{D}(\eta')\boldsymbol{\omega}\right]\boldsymbol{g}^{\rm T}_{\rm LS}(\eta,\eta'). \tag{4.3}$$

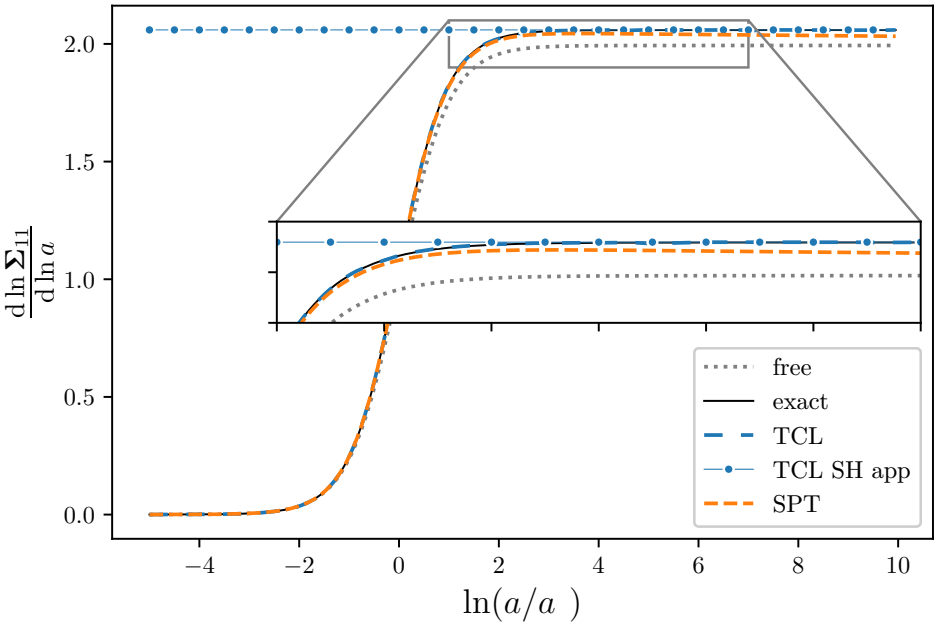

Figure 1. Growth rate of the configuration-configuration power spectrum as a function of time, labeled with the scale factor ($a_* = k/H$ corresponds to the time of Hubble exit, *i.e.* when $\eta_* = -1/k$). The result is displayed in the free (grey), exact (black), TCL_2 (blue) and SPT (orange) theories. The blue dotted line corresponds to the super-Hubble expansion for TCL, see Eq. (4.6), which leads to the growth rate $\mathrm{d}\ln \boldsymbol{\Sigma}_{\mathrm{TCL},11}/\mathrm{d}\ln a = 2\nu_{\mathrm{LS}} - 1$. The parameters are set to $\lambda = H$, $m = H/10$ and $M = \sqrt{10}H$.

Note that $\boldsymbol{g}_{\mathrm{LS}}$ is obtained from the Lamb-shift corrected mode functions

$$\boldsymbol{g}_{\mathrm{LS}}(\eta,\eta') = 2\begin{pmatrix} \Im\mathrm{m}\,[v_{\mathrm{LS}}(\eta)p^*_{\mathrm{LS}}(\eta')] & -\Im\mathrm{m}\,[v_{\mathrm{LS}}(\eta)v^*_{\mathrm{LS}}(\eta')] \\ \Im\mathrm{m}\,[p_{\mathrm{LS}}(\eta)p^*_{\mathrm{LS}}(\eta')] & -\Im\mathrm{m}\,[p_{\mathrm{LS}}(\eta)v^*_{\mathrm{LS}}(\eta')] \end{pmatrix}, \tag{4.4}$$

where v_{LS} is the solution of $v''_{\mathrm{LS}} + \omega^2_{\mathrm{LS}} v_{\mathrm{LS}} = 0$ where $\omega^2_{\mathrm{LS}} = k^2 + m^2a^2 + \boldsymbol{\Delta}_{11} - \boldsymbol{\Delta}'_{12} + \boldsymbol{\Delta}^2_{12} - 2\boldsymbol{\Delta}_{12}a'/a$, see Eq. (3.40), with Bunch-Davies initial conditions, and $p_{\mathrm{LS}} = v'_{\mathrm{LS}} - (a'/a)v_{\mathrm{LS}}$ as in Eq. (3.4).[11] This leads to

$$\begin{aligned} \boldsymbol{\Sigma}_{\mathrm{TCL}}(\eta) =& e^{-\Gamma(\eta,\eta_0)}\boldsymbol{g}_{\mathrm{LS}}(\eta,\eta_0)\boldsymbol{\Sigma}_{\mathrm{TCL}}(\eta_0)\boldsymbol{g}^{\mathrm{T}}_{\mathrm{LS}}(\eta,\eta_0) \\ &- \int_{\eta_0}^{\eta} \mathrm{d}\eta' e^{-\Gamma(\eta,\eta')}\boldsymbol{g}_{\mathrm{LS}}(\eta,\eta')\left[\boldsymbol{\omega}\boldsymbol{D}(\eta')\boldsymbol{\omega}\right]\boldsymbol{g}^{\mathrm{T}}_{\mathrm{LS}}(\eta,\eta'). \end{aligned} \tag{4.5}$$

In practice, this integral is computed numerically from a large negative value of η_0 (sufficiently large that we check the result does not depend on η_0).

Growth rate

First we compare in Fig. 1 the growth rate of the configuration-configuration power spectrum, $\mathrm{d}\ln \boldsymbol{\Sigma}_{11}/\mathrm{d}\ln a$. The result is given in the free theory (*i.e.* setting $\lambda = 0$, grey line), in the exact

[11] In the present case, since $\boldsymbol{\Delta}_{12} = 0$ and $\boldsymbol{\Delta}_{11} = \boldsymbol{\Delta}_{\mathrm{ex},11}$, where $\boldsymbol{\Delta}_{\mathrm{ex},11}$ is given in Eq. (3.49), one has $\omega^2_{\mathrm{LS}} = k^2 + [m^2 - \lambda^4/(M^2 - m^2)]a^2$. This implies that v_{LS} and p_{LS} can be expressed in terms of Hankel functions as in Eqs. (3.15) and (3.16), with ν replaced by $\nu_{\mathrm{LS}} = \frac{3}{2}\sqrt{1 - \left(\frac{2m_{\mathrm{LS}}}{3H}\right)^2}$ where $m^2_{\mathrm{LS}} = m^2 - \lambda^4/(M^2 - m^2)$. This is consistent with effective-field theoretic approaches where the masses of light scalar fields are renormalised by heavy fields with contributions $\mathcal{O}(\lambda^4/M^2)$ [97].

theory (black line), in TCL (blue line) and in SPT (orange line). The difference between these different setups becomes more pronounced at late time, on which the inset zooms in. One can see that TCL provides an excellent approximation, better than SPT, which itself is closer to the exact result than the free theory.

The behaviour of the TCL covariance matrix can be further understood by investigating the super-Hubble (*i.e.* late time, $-k\eta \ll 1$) limit of the transport equation (3.42). In this regime, an expansion of the coefficients can be found in Appendix C.3. By inserting power-law ansatz for the entries of the covariance matrix, one finds that the diffusion term becomes negligible at large scales, and that

$$\boldsymbol{\Sigma}_{\mathrm{TCL},11} \propto a^{2\nu_{\mathrm{LS}}-1}\,, \quad \boldsymbol{\Sigma}_{\mathrm{TCL},12} \propto a^{2\nu_{\mathrm{LS}}}\,, \quad \boldsymbol{\Sigma}_{\mathrm{TCL},22} \propto a^{2\nu_{\mathrm{LS}}+1}\,, \tag{4.6}$$

where ν_{LS} was introduced in footnote 11. The corresponding growth rate, $2\nu_{\mathrm{LS}}-1$, is displayed in Fig. 1 with the dotted blue line, and one can check that it asymptotes the TCL result at late time indeed.

In the exact theory, the term involving $\boldsymbol{\Sigma}_\ell$ dominates over the one involving $\boldsymbol{\Sigma}_{\mathrm{h}}$ in Eq. (3.21), so the growth rate is given by $2\nu_\ell - 1$, where ν_ℓ is given below Eq. (3.14). It is worth stressing that by expanding ν_ℓ at leading order in λ^4, one recovers ν_{LS} [namely $m_\ell^2 = m_{\mathrm{LS}}^2 + \mathcal{O}(\lambda^8)$]. As a consequence, TCL correctly reproduces the growth rate at first order in λ^4.

Although this may seem as a perturbative result, let us stress that the resummed non-perturbative feature lies in Eq. (4.6). Indeed, in SPT, expanding $\boldsymbol{\Sigma}_{\varphi\varphi}$ at leading order in λ^4 leads to

$$\boldsymbol{\Sigma}_{\mathrm{SPT},11} \propto a^{2\nu_\varphi-1}\left[1 + \frac{\lambda^4}{H^2\nu_\varphi\left(M^2-m^2\right)}\ln a\right] \tag{4.7}$$

at late time, where $\nu_\varphi = \frac{3}{2}\sqrt{1-\left(\frac{2m}{3H}\right)^2}$. This matches Eq. (4.6) at leading order in λ^4, but Eq. (4.6) contains all higher-order terms in λ^4 that allow the logs to be resumed. In particular, Eq. (4.7) implies that at late time, the growth rate in SPT approaches the one of the free theory, $2\nu_\varphi - 1$, while as stated above the growth rate of TCL incorporates the first correction in λ^4.

Relative deviation to the exact result

The performance reached by TCL or SPT is given by the relative deviation of their covariance matrices to the exact result. This is displayed in Fig. 2 for $m^2 = 10^{-4}H^2$ and $\lambda^2 = H^2$, which purposely corresponds to a large coupling. One can check that TCL is always more accurate than SPT, and that the difference in accuracy becomes more pronounced at larger M. This can be understood as follows. In the super-Hubble regime, TCL behaves according to Eq. (4.6), which is super-imposed in Fig. 2 and indeed provides a good fit. It leads to

$$\frac{\left|\boldsymbol{\Sigma}_{\mathrm{TCL},11} - \boldsymbol{\Sigma}_{\varphi\varphi,11}\right|}{\boldsymbol{\Sigma}_{\varphi\varphi,11}} \simeq a^{2(\nu_{\mathrm{LS}}-\nu_\ell)} - 1 = \frac{\lambda^8\ln(a)}{\nu_\varphi H^2\left(M^2-m^2\right)^3} + \mathcal{O}\left(\lambda^{12}\right)\,. \tag{4.8}$$

The last result is expanded at leading order in λ (hence in $\ln a$), which provides a good approximation as long as the relative error is much smaller than one, as in Fig. 2. In SPT, Eq. (4.7) gives rise to

$$\frac{\left|\boldsymbol{\Sigma}_{\mathrm{SPT},11} - \boldsymbol{\Sigma}_{\varphi\varphi,11}\right|}{\boldsymbol{\Sigma}_{\varphi\varphi,11}} \simeq \frac{\lambda^8\ln^2(a)}{2\left(M^2-m^2\right)^2H^4\nu_\varphi^2} + \mathcal{O}\left(\lambda^{12}\right) \tag{4.9}$$

at late time. There are two main differences between Eqs. (4.8) and (4.9). First, when the environment is heavy, $M \gg H$, the relative error in TCL decays as λ^8/M^6 while it is suppressed

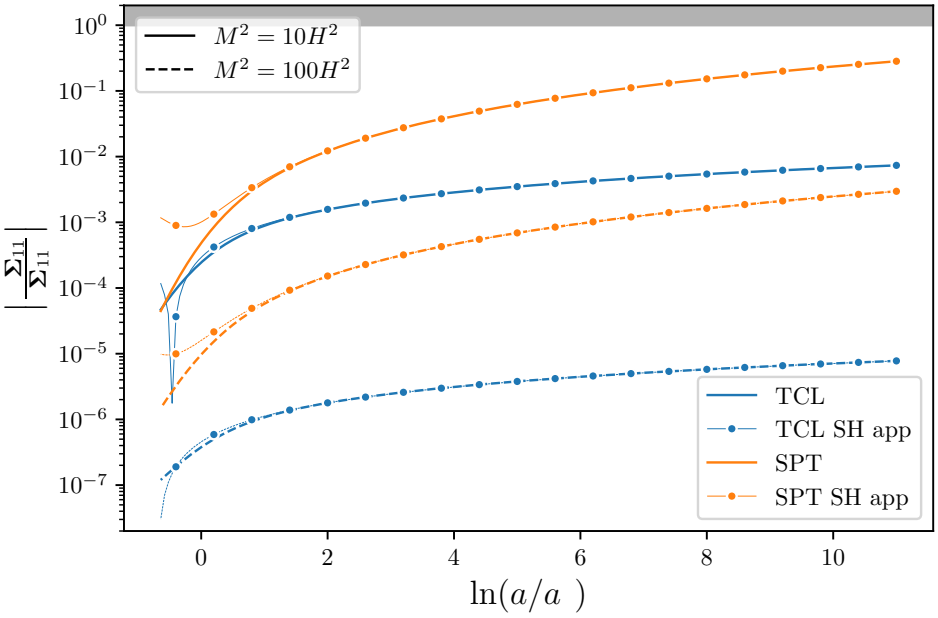

Figure 2. Relative error in the configuration-configuration power spectrum in TCL_2 ($|\mathbf{\Sigma}_{\mathrm{TCL},11} - \mathbf{\Sigma}_{\varphi\varphi,11}|/\mathbf{\Sigma}_{\varphi\varphi,11}$, blue lines) and SPT ($|\mathbf{\Sigma}_{\mathrm{SPT},11} - \mathbf{\Sigma}_{\varphi\varphi,11}|/\mathbf{\Sigma}_{\varphi\varphi,11}$, orange lines). The result is displayed as a function of time, labeled with the scale factor, and for $M^2 = 10H^2$ (solid lines) and $M^2 = 100H^2$ (dashed lines). The dotted lines correspond to the super-Hubble formula (4.6), which indeed provide a good fit at late time. The parameters are taken as $m^2 = 10^{-4}H^2$ and $\lambda^2 = H^2$. The grey-shaded area is where the error is larger than 100%.

by λ^8/M^4 in SPT. This explains why, when going from $M^2 = 10H^2$ to $M^2 = 100H^2$ in Fig. 2, the relative error decreases by a factor 10^3 in TCL and by a factor 10^2 in SPT. This indicates that, although both results become more accurate as the environment is heavier, the gain in accuracy is much stronger for TCL. Second, the relative error in SPT increases as $\ln^2(a)$ at late time, while it only increases as $\ln(a)$ in TCL. This is why in Fig. 2, the difference in accuracy between these two approaches becomes even larger as time proceeds.

Finally, in Fig. 3 we display the relative error for all power spectra (*i.e.* all entries of the covariance matrix), as a function of the interaction strength λ. When λ is small, the relative error scales as λ^8 for both SPT and TCL, in agreement with the fact that both methods match the exact result at order λ^4 [see Sec. 2.4, see also Eqs. (4.8) and (4.9)]. One can also see that both in TCL and in SPT, the reconstruction of the configuration-configuration power spectrum is better than for the configuration-momentum power spectrum, which is itself better than the momentum-momentum power spectrum. In TCL, all power spectra are accurately computed up to large values of λ. For instance, even when $\lambda/H = 1$, the relative error is smaller than 10^{-4} for all power spectra. In SPT however, the momentum-momentum power spectrum is already out of control for such values of λ. Indeed, the correlators involving the momentum are given with less precision in SPT, and the perturbative expansion breaks down for the momentum-momentum power spectrum much sooner than for the configuration-configuration power spectrum. This will be of prime importance below, since those correlators play an essential role in the process of decoherence.

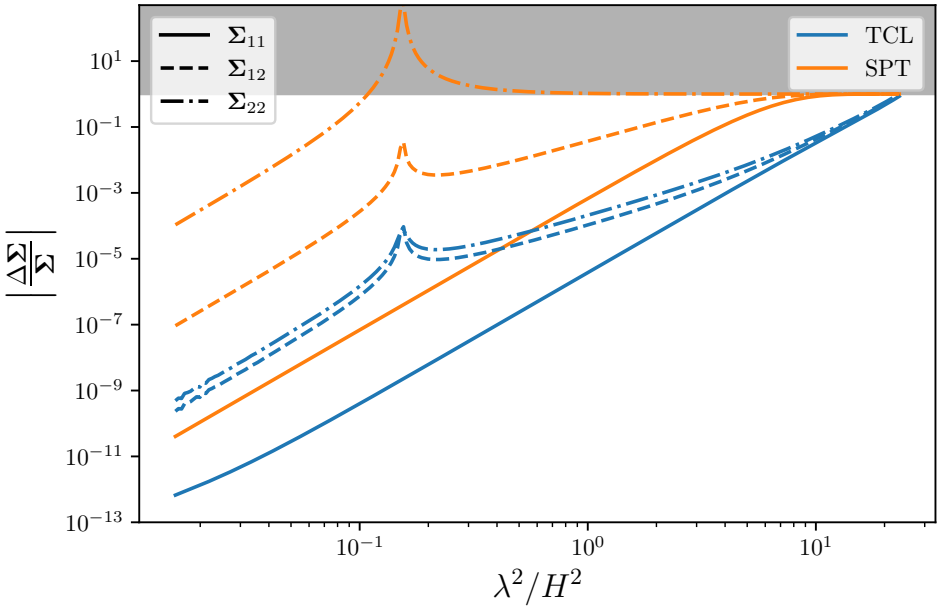

Figure 3. Relative error in all entries of the covariance matrix of the system. The blue lines correspond to the TCL_2 result $|\boldsymbol{\Sigma}_{\mathrm{TCL},ij} - \boldsymbol{\Sigma}_{\varphi\varphi,ij}|/|\boldsymbol{\Sigma}_{\varphi\varphi,ij}|$, while the orange lines correspond to standard perturbation theory (SPT) $|\boldsymbol{\Sigma}^{(2)}_{\varphi\varphi,ij} - \boldsymbol{\Sigma}_{\varphi\varphi,ij}|/|\boldsymbol{\Sigma}_{\varphi\varphi,ij}|$. Different line styles correspond to different entries of the covariance matrix, and the parameters of the model are chosen as $m^2 = 10^{-4}H^2$, $M^2 = 10^2 H^2$ and $a/a_* = e^5$. The grey-shaded area is where the error is larger than 100%. The peaky features correspond to where the exact power spectrum $\boldsymbol{\Sigma}_{\varphi\varphi,12}$ vanishes and $\boldsymbol{\Sigma}_{\varphi\varphi,22}$ goes through a local minimum.

4.2 Decoherence

We turn our attention to decoherence that we measure using the purity whose expression for Gaussian states is given by Eq. (3.24). The result is displayed in Fig. 4. As time proceeds, the system entangles with its environment, decoherence occurs (*i.e.* γ decreases away from 1), and the system becomes maximally mixed soon after Hubble-crossing for the parameters used in the figure.

The lower panel displays the error relative to the exact result. One can see that, when time proceeds, the SPT result quickly diverges. So perturbation theory is only able to describe quasi pure states, for which $1 - \gamma \ll 1$, and breaks down when decoherence proceeds. The reason for the weak performance of SPT is that the purity parameter is driven by the so-called cosmological decaying mode, which is encoded in the power spectra involving the momentum. Around Fig. 3 we saw that those are precisely the correlators that SPT predicts with the least accuracy. On the contrary, TCL_2 remarkably describes the full decoherence process, and is able to approximate the full quantum state even in the strongly decohered regime. The relative error freezes to a tiny value at large scales (here of the order 10^{-6}), which is a manifestation of the resummation occurring in TCL.

The simplest way to access the late-time behaviour of the purity is to derive an equation of motion for $\det(\boldsymbol{\Sigma}_{\mathrm{TCL}})$ from the transport equation (3.42), namely

$$\frac{\mathrm{d}\det(\boldsymbol{\Sigma}_{\mathrm{TCL}})}{\mathrm{d}\eta} = \boldsymbol{D}_{11}\boldsymbol{\Sigma}_{\mathrm{TCL},11} + 2\boldsymbol{D}_{12}\boldsymbol{\Sigma}_{\mathrm{TCL},12} - 4\boldsymbol{\Delta}_{12}\det(\boldsymbol{\Sigma}_{\mathrm{TCL}}). \tag{4.10}$$

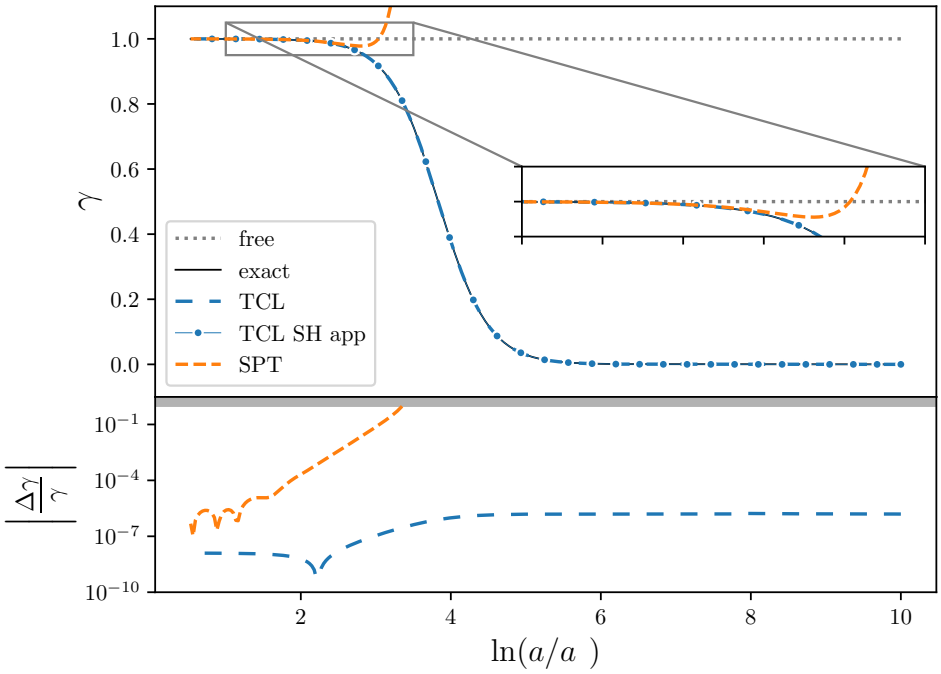

Figure 4. Purity parameter (3.24) in the free (grey), exact (black), TCL_2 (blue), and SPT (orange) approaches as a function of time. The dotted line corresponds to the super-Hubble expansion of the TCL result, see Eq. (4.11). The lower panel shows the error of TCL_2 and SPT relative to the exact result. The parameters are set to $m^2 = 10^{-4}H^2$ and $M^2 = 10^2H^2$ with $\lambda^2 = 10^{-1}H^2$. The perturbative result rapidly diverges, while TCL_2 accurately predicts the amount of decoherence even in the fully decohered regime.

All unitary contributions (*i.e.* those involving $\boldsymbol{H}^{(\varphi)}$ and $\boldsymbol{\Delta}_{11}$) have cancelled out (indeed, only non-unitary contributions can change the purity). This implies that diffusion, controlled by $\boldsymbol{D}$, is crucial in the process of decoherence (since $\boldsymbol{\Delta}_{12} = 0$ in the present case). It contrasts with Sec. 4.1 where we had found that $\boldsymbol{D}$ gives negligible corrections to the power spectra on large scales – those negligible corrections are precisely the ones driving decoherence. The results of Appendix C.3 together with Eq. (4.6) indicate that the two first terms of Eq. (4.10) are of the same order $a^{2\nu_{\mathrm{LS}}-1}$ at late time. In this limit Eq. (4.10) can be integrated, and one obtains

$$\det(\boldsymbol{\Sigma}_{\mathrm{TCL}}) \simeq \frac{1}{4} + \frac{2^{2\nu_{\mathrm{LS}}-3}}{\pi}\Gamma^2\left(\nu_{\mathrm{LS}}\right)\left(\frac{\lambda}{H}\right)^4\left(\frac{H}{M}\right)^3\left(\frac{a}{a_*}\right)^{2\nu_{\mathrm{LS}}}, \tag{4.11}$$

where the prefactors in Eq. (4.6) have been set by neglecting diffusion (alternatively, they can be set by asymptotic matching at Hubble crossing and this gives a very similar result) and we have neglected contributions exponentially suppressed by M/H to reach a concise expression (they be easily kept but do not bring any particular insight). The purity $\gamma_{\mathrm{TCL}} = 1/(4\det\boldsymbol{\Sigma}_{\mathrm{TCL}})$ obtained from this expression is displayed in Fig. 4 with the dotted line. One can check that it provides an excellent approximation to the full TCL result, hence to the exact result too.

The above formula (4.11) also allows us to study under which conditions decoherence occurs for the model at hand. It is non perturbative in λ since one should recall that ν_{LS} depends on λ, see footnote 11, although the rate of decoherence is mostly proportional to $(\lambda/H)^4$. Similarly, although ν_{LS} depends on M, decoherence occurs at a rate mostly proportional to $(H/M)^3$, so

it is slower for heavier environments. Finally, it is very efficient on super-Hubble scales, since it scales as $a^{2\nu_{\rm LS}} \sim a^3$, so roughly as the spatial volume, as often encountered [14, 17]. For instance, for scales of astrophysical interest today that are such that $a/a_* \sim e^{50}$ at the end of inflation, for $M/H = 100$ and $m/H = 10^{-2}$, one finds that decoherence proceeds during inflation as soon as $\lambda/H > 10^{-15}$, a very small value indeed.

5 Conclusion

Let us now summarise our main results and open up a few prospects. In this work, we have investigated how the master-equation program can be implemented in cosmology. To this end, we have used a toy model where two scalar fields are linearly coupled and evolve on a de-Sitter background. It has the advantage of being exactly solvable, an "integrable system", in which the performance of effective methods can be assessed and compared with more traditional, perturbative techniques.

We have derived the second-order Time-ConvolutionLess (TCL) equation in this setup, which is a master equation for the reduced density matrix of the system (here the lighter field), and which features the memory kernel of the environment (here the heavier field). It possesses three contributions: a unitary "Lamb-shift" term (renormalisation of the bare Hamiltonian), a dissipation term (energy exchange with the environment) and a diffusive term (driving the quantum decoherence process). They can all be expressed in terms of integrals ranging from the initial time to the time at which the master equation is written.

Usually, the memory kernel is sufficiently peaked around the coincident configuration that these integrals are dominated by their upper bound, hence they carry negligible dependence on the initial time. This is the case if the relaxation time of the environment around its stationary configuration is small compared to the time scale over which the evolution of the system is tracked. This is the so-called Markovian, or Lindbladian limit. In the present case however, due to the presence of a dynamical background, there is no such thing as a stationary configuration for the environment, which strongly departs from being a thermal bath. In practice we find that these integrals carry a non-negligible dependence on the initial time, through a set of terms that we have dubbed "spurious".

We have then shown that these spurious terms cancel out when the TCL equation is solved perturbatively in the coupling constant, *i.e.* they are absent from the perturbative version of the theory. This is consistent with the fact that the perturbative solution to the TCL equation is strictly equivalent to standard perturbation theory (such as the in-in formalism for instance). When solving the TCL equation non-perturbatively however, they lead to unphysical diverging behaviours, which clearly signals their problematic nature.

However, if one removes them "by hand" (which does not necessarily makes the dynamics Markovian, see footnote 9), one finds that the TCL equation provides an excellent approximation to the full theory: it successfully reproduces all power spectra up to large values of the interaction strength, and it tracks the amount of decoherence very accurately, including at late time when the system is in a strongly mixed state. This is due to an explicit resummation of logarithmic terms (*i.e.* of powers of $\ln a$, where a is the scale factor of the universe), and in Appendix E we show that this resummation is more efficient than the late-time resummation technique proposed in Ref. [44]. The incorporation of these late-time secular effects makes TCL vastly superior to perturbative methods. Although we have found that it does not require particularly heavy environment, the advantage of TCL compared to perturbative methods is even more

pronounced when the mass M of the environmental field is larger than the Hubble scale H, since the relative error of the former scales as $(H/M)^6$ while it scales as $(H/M)^4$ for the latter.

To summarise, we have found that the master-equation program can be successfully applied in cosmological backgrounds, *provided spurious terms are suppressed.*

The presence of the spurious terms may be related to the simplicity of our toy model, where only one field is contained in the environment, which can therefore not be considered as a proper reservoir. If multiple fields were present indeed, all with different masses, thus oscillating at different frequencies, the memory kernel would be suppressed away from the coincident limit through the accumulation of random phases [41, 73] (technically, the memory kernel would involve some Fourier transform of the mass distribution of the environmental fields, which may be peaked if that distribution is sufficiently broad). This mechanism was studied *e.g.* in the context of black-hole physics in Ref. [98]. Another possibility would be to consider non-linear interactions between the two fields, which would imply that one Fourier mode in the system couples to all Fourier modes in the environment, hence making the number of environmental degrees of freedom to which the system couples infinite. One could also consider situations in which non-linearities only arise within the environmental sector,[12] as in quasi-single field models [28, 99]. The same mechanism of random phase addition would presumably occur in those cases, which would also lead to a suppression of the spurious terms. Whether or not that suppression is enough should be the subject of further investigations. Another, maybe more adventurous question, is whether or not one can design an improved master equation, where the removal of spurious contributions is automatically taken care of. Indeed, our results show that master equations free from spurious terms are extremely powerful at deriving reliable predictions for cosmology, and perform much better than perturbative methods. We plan to address these issues in future works.

6 Acknowledgments

It is a pleasure to thank Suddhasattwa Brahma, Cliff Burgess, Denis Comelli, Jaime Calderón-Figueroa, Bei-Lok Hu, Christian Käding, Greg Kaplanek and Amaury Micheli for interesting discussions.

A Microphysical derivation of the TCL_2 master equation

In this appendix, we present an alternative derivation of the TCL_2 master equation (3.25) in the curved-space Caldeira-Leggett model, which does not rely on the cumulant expansion of the Nakajima-Zwanzig equation. We start from the Liouville–Von-Neumann equation in the interaction picture (2.5), namely

$$\frac{\mathrm{d}\widetilde{\rho}}{\mathrm{d}\eta} = -i\lambda^2 \left[\widetilde{\mathcal{H}}_{\mathrm{int}}(\eta), \widetilde{\rho}(\eta)\right] . \tag{A.1}$$

As noted in Eq. (2.27), it can be solved formally as

$$\widetilde{\rho}(\eta) = \widetilde{\rho}(\eta_0) - i\lambda^2 \int_{\eta_0}^{\eta} \mathrm{d}\eta' \left[\widetilde{\mathcal{H}}_{\mathrm{int}}(\eta'), \widetilde{\rho}(\eta')\right] . \tag{A.2}$$

[12] Let us note that the presence of non-linearities, even if confined to the environmental sector, would leave an imprint on the non-Gaussian statistics of the system [28, 30].

Inserting this expression into Eq. (A.1), one obtains

$$\frac{\mathrm{d}\widetilde{\rho}}{\mathrm{d}\eta} = -i\lambda^2\left[\widetilde{\mathcal{H}}_{\rm int}(\eta),\widetilde{\rho}(\eta_0)\right] - \lambda^4\int_{\eta_0}^{\eta}\mathrm{d}\eta'\left[\widetilde{\mathcal{H}}_{\rm int}(\eta),\left[\widetilde{\mathcal{H}}_{\rm int}(\eta'),\widetilde{\rho}(\eta')\right]\right] + \mathcal{O}(\lambda^6)\,. \tag{A.3}$$

This procedure could be iterated to obtain higher-order nested commutators, controlled by higher powers of the interaction strength. If the coupling constant λ is small (Born approximation), one may stop at order $\mathcal{O}(\lambda^4)$ where the first non-unitary effects appear.

Our next task is to turn Eq. (A.3) into an ordinary differential equation that is local in time for the reduced density matrix $\widetilde{\rho}_{\rm red}(\eta)$. By tracing Eq. (A.3) over the environmental degrees of freedom, one finds

$$\frac{\mathrm{d}\widetilde{\rho}_{\rm red}}{\mathrm{d}\eta} \simeq -i\lambda^2{\rm Tr}_{\rm E}\left[\widetilde{\mathcal{H}}_{\rm int}(\eta),\widetilde{\rho}(\eta_0)\right] - \lambda^4\int_{\eta_0}^{\eta}\mathrm{d}\eta'{\rm Tr}_{\rm E}\left[\widetilde{\mathcal{H}}_{\rm int}(\eta),\left[\widetilde{\mathcal{H}}_{\rm int}(\eta'),\widetilde{\rho}(\eta')\right]\right]. \tag{A.4}$$

In the interaction picture, the deviation of $\widetilde{\rho}$ from its initial configuration is necessarily controlled by some positive power p of the interaction strength,

$$\widetilde{\rho}(\eta) = \widetilde{\rho}_{\rm red}(\eta_0)\otimes\widetilde{\rho}_{\rm E}(\eta_0) + \lambda^p\widetilde{\rho}_{\rm correl}(\eta) \tag{A.5}$$

where ${\rm Tr}_{\rm E}(\widetilde{\rho}_{\rm correl}) = {\rm Tr}_{\rm S}(\widetilde{\rho}_{\rm correl}) = 0$. Consequently,

$$\begin{aligned}\frac{\mathrm{d}\widetilde{\rho}_{\rm red}}{\mathrm{d}\eta} =& -i\lambda^2{\rm Tr}_{\rm E}\left[\widetilde{\mathcal{H}}_{\rm int}(\eta),\widetilde{\rho}_{\rm red}(\eta_0)\otimes\widetilde{\rho}_{\rm E}(\eta_0)\right]\\ &- i\lambda^{p+2}{\rm Tr}_{\rm E}\left[\widetilde{\mathcal{H}}_{\rm int}(\eta),\widetilde{\rho}_{\rm correl}(\eta_0)\right]\\ &- \lambda^4\int_{\eta_0}^{\eta}\mathrm{d}\eta'{\rm Tr}_{\rm E}\left[\widetilde{\mathcal{H}}_{\rm int}(\eta),\left[\widetilde{\mathcal{H}}_{\rm int}(\eta'),\widetilde{\rho}_{\rm red}(\eta')\otimes\widetilde{\rho}_{\rm E}(\eta')\right]\right]\\ &- \lambda^{p+4}\int_{\eta_0}^{\eta}\mathrm{d}\eta'{\rm Tr}_{\rm E}\left[\widetilde{\mathcal{H}}_{\rm int}(\eta),\left[\widetilde{\mathcal{H}}_{\rm int}(\eta'),\widetilde{\rho}_{\rm correl}(\eta')\right]\right].\end{aligned} \tag{A.6}$$

Which term dominates depends on the value of p, which can be determined as follows. Let us first recall that $\widetilde{\mathcal{H}}_{\rm int}(\eta)$ was given above Eq. (3.25) and reads

$$\widetilde{\mathcal{H}}_{\rm int}(\eta) = a^2(\eta)\widetilde{v}_{\varphi}(\eta)\widetilde{v}_{\chi}(\eta)\,, \tag{A.7}$$

which leads to

$${\rm Tr}_{\rm E}\left[\widetilde{\mathcal{H}}_{\rm int}(\eta),\widetilde{\rho}_{\rm red}(\eta_0)\otimes\widetilde{\rho}_{\rm E}(\eta_0)\right] = a^2(\eta)\left[\widetilde{v}_{\varphi}(\eta),\widetilde{\rho}_{\rm red}(\eta_0)\right]{\rm Tr}_{\rm E}\left[\widetilde{v}_{\chi}(\eta)\widetilde{\rho}_{\rm E}(\eta_0)\right]. \tag{A.8}$$

Note that

$${\rm Tr}_{\rm E}\left[\widetilde{v}_{\chi}(\eta)\widetilde{\rho}_{\rm E}(\eta_0)\right] = \left\langle\widetilde{v}_{\chi}(\eta-\eta_0)\right\rangle \tag{A.9}$$

which is the mean value of the environment field operator. Such a mean value can always be absorbed in a redefinition of the field, such that the first term in the right-hand side of Eq. (A.6) vanishes. From Eq. (A.5), $\mathrm{d}\widetilde{\rho}_{\rm red}/\mathrm{d}\eta$ necessarily contains a term of order $\mathcal{O}\left(\lambda^p\right)$, so the only possibility is that $p = 4$. As a consequence, the terms of order $\mathcal{O}\left(\lambda^{p+2}\right)$ and $\mathcal{O}\left(\lambda^{p+4}\right)$ can be neglected, and one finds

$$\frac{\mathrm{d}\widetilde{\rho}_{\rm red}}{\mathrm{d}\eta} = -\lambda^4\int_{\eta_0}^{\eta}\mathrm{d}\eta'{\rm Tr}_{\rm E}\left[\widetilde{\mathcal{H}}_{\rm int}(\eta),\left[\widetilde{\mathcal{H}}_{\rm int}(\eta'),\widetilde{\rho}_{\rm red}(\eta')\otimes\widetilde{\rho}_{\rm E}(\eta')\right]\right]. \tag{A.10}$$

At leading order in λ, one can safely replace $\widetilde{\rho}_{\rm red}(\eta')$ by $\widetilde{\rho}_{\rm red}(\eta)$ and $\widetilde{\rho}_{\rm E}(\eta')$ by $\widehat{\rho}_{\rm E}$ in Eq. (A.10). This leads to a manifestly time-local equation, namely

$$\frac{\mathrm{d}\widetilde{\rho}_{\rm red}}{\mathrm{d}\eta} = -\lambda^4 \int_{\eta_0}^{\eta} \mathrm{d}\eta' \mathrm{Tr}_{\rm E}\left[\widetilde{\mathcal{H}}_{\rm int}(\eta), \left[\widetilde{\mathcal{H}}_{\rm int}(\eta'), \widetilde{\rho}_{\rm red}(\eta)\otimes\widehat{\rho}_{\rm E}\right]\right] \tag{A.11}$$

which is consistent with Eq. (2.19). Replacing $\mathcal{H}_{\rm int}$ by Eq. (A.7) and expanding the commutators yields the result

$$\begin{aligned}\frac{\mathrm{d}\widetilde{\rho}_{\rm red}}{\mathrm{d}\eta} =& -\lambda^4 a^2(\eta)\int_{\eta_0}^{\eta}\mathrm{d}\eta' a^2(\eta') \\ &\Big\{\left[\widetilde{v}_\varphi(\eta)\widetilde{v}_\varphi(\eta')\widetilde{\rho}_{\rm red}(\eta) - \widetilde{v}_\varphi(\eta')\widetilde{\rho}_{\rm red}(\eta)\widetilde{v}_\varphi(\eta)\right]\mathcal{K}^{>}(\eta,\eta') \\ &-\left[\widetilde{v}_\varphi(\eta)\widetilde{\rho}_{\rm red}(\eta)\widetilde{v}_\varphi(\eta') - \widetilde{\rho}_{\rm red}(\eta)\widetilde{v}_\varphi(\eta')\widetilde{v}_\varphi(\eta)\right]\mathcal{K}^{<}(\eta,\eta')\Big\},\end{aligned} \tag{A.12}$$

where the memory kernels are defined as in Eq. (3.26), namely

$$\mathcal{K}^{>}(\eta,\eta') \equiv \mathrm{Tr}_{\rm E}\left[\widehat{v}_\chi(\eta)\widehat{v}_\chi(\eta')\widehat{\rho}_{\rm E}\right], \tag{A.13}$$

$$\mathcal{K}^{<}(\eta,\eta') \equiv \mathrm{Tr}_{\rm E}\left[\widehat{v}_\chi(\eta')\widehat{v}_\chi(\eta)\widehat{\rho}_{\rm E}\right]. \tag{A.14}$$

As in Eq. (3.28), they can be expressed in terms of the mode functions

$$\mathcal{K}^{>}(\eta,\eta') = v_\chi(\eta)v_\chi^*(\eta') \tag{A.15}$$

$$\mathcal{K}^{<}(\eta,\eta') = v_\chi^*(\eta)v_\chi(\eta') = \mathcal{K}^{>*}(\eta,\eta'), \tag{A.16}$$

and the master equation reads

$$\begin{aligned}\frac{\mathrm{d}\widetilde{\rho}_{\rm red}}{\mathrm{d}\eta} =& -\lambda^4 a^2(\eta)\int_{\eta_0}^{\eta}\mathrm{d}\eta' a^2(\eta') \\ &\Big\{\left[\widetilde{v}_\varphi(\eta)\widetilde{v}_\varphi(\eta')\widetilde{\rho}_{\rm red}(\eta) - \widetilde{v}_\varphi(\eta')\widetilde{\rho}_{\rm red}(\eta)\widetilde{v}_\varphi(\eta)\right]\mathcal{K}^{>}(\eta,\eta') \\ &-\left[\widetilde{v}_\varphi(\eta)\widetilde{\rho}_{\rm red}(\eta)\widetilde{v}_\varphi(\eta') - \widetilde{\rho}_{\rm red}(\eta)\widetilde{v}_\varphi(\eta')\widetilde{v}_\varphi(\eta)\right]\mathcal{K}^{>*}(\eta,\eta')\Big\}.\end{aligned} \tag{A.17}$$

Expanding $\mathcal{K}^{>}$ into its real and imaginary part, one recovers Eq. (3.25).

B Phase-space representation of the TCL$_2$ master equation

An alternative representation of the quantum state is given in the phase-space by the Wigner function (see Ref. [96] for a brief introduction). For Gaussian states, the Wigner function takes the simple form of a multivariate Gaussian [100], which makes it particularly convenient to work with.

The Wigner function is defined as the inverse Weyl transform of the density matrix. For a generic quantum operator $\widehat{O}$, the inverse Wigner-Weyl transform reads

$$W_{\widehat{O}}(v_\varphi, p_\varphi) = 2\int_{-\infty}^{\infty}\mathrm{d}y e^{-2ip_\varphi y}\left\langle v_\varphi + y\right|\widehat{O}\left|v_\varphi - y\right\rangle \tag{B.1}$$

and is a function of the phase-space variables v_φ and p_φ. The above formula is written in the configuration representation, it can also be written in the momentum representation,

$$W_{\widehat{O}}(v_\varphi, p_\varphi) = 2\int_{-\infty}^{\infty} \mathrm{d}k e^{2ikv_\varphi} \langle p_\varphi + k| \widehat{O} |p_\varphi - k\rangle \,. \tag{B.2}$$

In this way, commutators of quantum operators are mapped to the Poisson brackets of their phase-space representations. Indeed, using the above formulas, one finds

$$W_{[\widehat{v}_\varphi,\widehat{O}]} = i\frac{\partial}{\partial p_\varphi} W_O \quad \text{and} \quad W_{[\widehat{p}_\varphi,\widehat{O}]} = -i\frac{\partial}{\partial v_\varphi} W_O \,, \tag{B.3}$$

$$W_{\{\widehat{v}_\varphi,\widehat{O}\}} = 2v_\varphi W_O \quad \text{and} \quad W_{\{\widehat{p}_\varphi,\widehat{O}\}} = 2p_\varphi W_O \,. \tag{B.4}$$

This leads to

$$i\boldsymbol{\omega}_{ij} W_{[\widehat{\boldsymbol{z}}_j,\widehat{O}]} = \frac{\partial W_O}{\partial \boldsymbol{z}_i} \,, \tag{B.5}$$

$$\frac{1}{2} W_{\{\widehat{\boldsymbol{z}}_i,\widehat{O}\}} = \boldsymbol{z}_i W_O \,, \tag{B.6}$$

where we have introduced the phase-space vector $\boldsymbol{z} = (v_\varphi, p_\varphi)^{\mathrm{T}}$.

These relations can be used to compute the inverse Weyl transform of the TCL_2 master equation (3.30). Using that $\boldsymbol{\omega}$ is antisymmetric, one finds

$$\frac{\mathrm{d}W_{\mathrm{red}}}{\mathrm{d}\eta} = \left\{\widetilde{H}_0 + \widetilde{H}^{(\mathrm{LS})}, W_{\mathrm{red}}\right\} + \boldsymbol{\Delta}_{12} \sum_i \frac{\partial}{\partial \boldsymbol{z}_i} (\boldsymbol{z}_i W_{\mathrm{red}}) - \frac{1}{2}\sum_{i,j} [\boldsymbol{\omega}\boldsymbol{D}\boldsymbol{\omega}]_{ij} \frac{\partial^2 W_{\mathrm{red}}}{\partial \boldsymbol{z}_i \partial \boldsymbol{z}_j} \,, \tag{B.7}$$

where $W_{\mathrm{red}} = W_{\widehat{\rho}_{\mathrm{red}}}$ is the reduced Wigner function, *i.e.* the inverse Wigner-Weyl transform of the reduced density matrix $\widehat{\rho}_{\mathrm{red}}$. The curly brackets now represent Poisson's brackets, not to be confused with the anticommutators for quantum operators. This coincides with Eq. (3.41).

The first term in Eq. (B.7) corresponds to the free evolution dressed by the Lamb-shift Hamiltonian. This part of the equation only captures unitary/time-reversible evolution. The second term is a damping term reading as a total derivative and the last term is a diffusion term. These last two terms can be combined into a single second-order differential operator involving the dissipator matrix defined in Eq. (3.39), and they induce a non-unitary evolution.

Let us finally mention that the TCL_2 transport equation can be simply obtained from Eq. (B.7) using the Gaussianity of the state. Indeed, the state being Gaussian, the reduced Wigner function is given by

$$W_{\mathrm{red}} = \sqrt{\frac{1}{4\pi^2 \det \boldsymbol{\Sigma}_{\mathrm{TCL}}}} \exp\left[-\frac{1}{2}\sum_{i,j} \boldsymbol{z}_i \left(\boldsymbol{\Sigma}_{\mathrm{TCL}}\right)^{-1}_{ij} \boldsymbol{z}_j\right] , \tag{B.8}$$

where $\boldsymbol{\Sigma}_{\mathrm{TCL}}$ is the covariance of the reduced system. Upon inserting Eq. (B.8) into Eq. (B.7), one obtains

$$\frac{\mathrm{d}\boldsymbol{\Sigma}_{\mathrm{TCL}}}{\mathrm{d}\eta} = \boldsymbol{\omega}\left(\boldsymbol{H}^{(\varphi)} + \boldsymbol{\Delta}\right)\boldsymbol{\Sigma}_{\mathrm{TCL}} - \boldsymbol{\Sigma}_{\mathrm{TCL}}\left(\boldsymbol{H}^{(\varphi)} + \boldsymbol{\Delta}\right)\boldsymbol{\omega} - \boldsymbol{\omega}\boldsymbol{D}\boldsymbol{\omega} - 2\boldsymbol{\Delta}_{12}\boldsymbol{\Sigma}_{\mathrm{TCL}} \,, \tag{B.9}$$

which indeed coincides with Eq. (3.42).

C Coefficients of the transport equation for TCL_2

In this appendix, we work out the coefficients of the transport equation for TCL_2, defined in Eqs. (3.31), (3.32), (3.34) and (3.35). They involve the scale factor, which in a de-Sitter universe is given by $a = k/(Hz)$, as well as the mode functions

$$v_\varphi(\eta) = \frac{1}{2}\sqrt{\frac{\pi z}{k}} e^{i\frac{\pi}{2}\left(\nu_\varphi+\frac{1}{2}\right)} H^{(1)}_{\nu_\varphi}(z)\,, \tag{C.1}$$

$$p_\varphi(\eta) = -\frac{1}{2}\sqrt{\frac{k\pi}{z}} e^{i\frac{\pi}{2}\left(\nu_\varphi+\frac{1}{2}\right)} \left[\left(\nu_\varphi+\frac{3}{2}\right) H^{(1)}_{\nu_\varphi}(z) - z H^{(1)}_{\nu_\varphi+1}(z)\right]\,, \tag{C.2}$$

$$v_\chi(\eta) = \frac{1}{2}\sqrt{\frac{\pi z}{k}} e^{-\frac{\pi}{2}\mu_\chi+i\frac{\pi}{4}} H^{(1)}_{i\mu_\chi}(z)\,, \tag{C.3}$$

$$p_\chi(\eta) = -\frac{1}{2}\sqrt{\frac{k\pi}{z}} e^{-\frac{\pi}{2}\mu_\chi+i\frac{\pi}{4}} \left[\left(i\mu_\chi+\frac{3}{2}\right) H^{(1)}_{i\mu_\chi}(z) - z H^{(1)}_{i\mu_\chi+1}(z)\right]\,. \tag{C.4}$$

Here, we recall that $z = -k\eta$, $H^{(1)}_\nu$ is the Hankel function of the first kind and of order ν and

$$\nu_\varphi = \frac{3}{2}\sqrt{1-\left(\frac{2m}{3H}\right)^2} \quad \text{and} \quad \mu_\chi = \frac{3}{2}\sqrt{\left(\frac{2M}{3H}\right)^2-1}\,. \tag{C.5}$$

C.1 Exact results

In order to perform the integrals involved in Eqs. (3.31)-(3.35), we will make use of the formula

$$\int \mathcal{C}_{\nu_1}(Az)\mathcal{D}_{\nu_2}(Az)\frac{\mathrm{d}z}{z} = \frac{\mathcal{C}_{\nu_1}(Az)\mathcal{D}_{\nu_2}(Az)}{\nu_1+\nu_2} + \frac{Az}{{\nu_1}^2-\nu_2^2}\left[\mathcal{C}_{\nu_1}(Az)\mathcal{D}_{\nu_2+1}(Az) - \mathcal{C}_{\nu_1+1}(Az)\mathcal{D}_{\nu_2}(Az)\right]\,, \tag{C.6}$$

see Eq. (10.22.6) of Ref. [101], where $\mathcal{C}_{\nu_1}$ and $\mathcal{D}_{\nu_2}$ are any of the Bessel functions, and A is a fixed arbitrary parameter. Anticipating the computation, let us finally define

$$F_{\nu,\mu}(z) \equiv \frac{H^{(2)}_\nu(z)H^{(1)}_{i\mu}(z)}{\nu+i\mu} + \frac{z}{\nu^2+\mu^2}\left[H^{(2)}_\nu(z)H^{(1)}_{i\mu+1}(z) - H^{(2)}_{\nu+1}(z)H^{(1)}_{i\mu}(z)\right]\,, \tag{C.7}$$

$$G_{\nu,\mu}(z) \equiv \frac{H^{(2)}_\nu(z)H^{(2)}_{-i\mu}(z)}{\nu-i\mu} + \frac{z}{\nu^2+\mu^2}\left[H^{(2)}_\nu(z)H^{(2)}_{-i\mu+1}(z) - H^{(2)}_{\nu+1}(z)H^{(2)}_{-i\mu}(z)\right]\,, \tag{C.8}$$

in terms of which it will be convenient to express our results.

$\boldsymbol{D}_{11}$ coefficient

We start with $\boldsymbol{D}_{11}$ defined in Eq. (3.31), namely

$$\boldsymbol{D}_{11}(\eta) = -4\lambda^4 a^2(\eta)\int_{\eta_0}^{\eta}\mathrm{d}\eta' a^2(\eta')\Im\mathrm{m}\left[p_\varphi(\eta)v^*_\varphi(\eta')\right]\Re\mathrm{e}\left[v_\chi(\eta)v^*_\chi(\eta')\right]\,. \tag{C.9}$$

Expanding the real and the imaginary parts, and replacing $a = k/(Hz)$, it is given by

$$\boldsymbol{D}_{11}(z) = i\frac{k^3}{z^2}\frac{\lambda^4}{H^4}\int_z^{z_0}\frac{\mathrm{d}z'}{(z')^2}\left[p_\varphi(z)v^*_\varphi(z') - p^*_\varphi(z)v_\varphi(z')\right]\left[v_\chi(z)v^*_\chi(z') + v^*_\chi(z)v_\chi(z')\right]\,. \tag{C.10}$$

We thus have four terms,

$$\begin{aligned}\boldsymbol{D}_{11}(z) =& i\frac{k^3}{z^2}\frac{\lambda^4}{H^4}p_\varphi(z)v_\chi(z)\int_z^{z_0}\frac{\mathrm{d}z'}{(z')^2}v_\varphi^*(z')v_\chi^*(z')\\ &+ i\frac{k^3}{z^2}\frac{\lambda^4}{H^4}p_\varphi(z)v_\chi^*(z)\int_z^{z_0}\frac{\mathrm{d}z'}{(z')^2}v_\varphi^*(z')v_\chi(z')\\ &- i\frac{k^3}{z^2}\frac{\lambda^4}{H^4}p_\varphi^*(z)v_\chi(z)\int_z^{z_0}\frac{\mathrm{d}z'}{(z')^2}v_\varphi(z')v_\chi^*(z')\\ &- i\frac{k^3}{z^2}\frac{\lambda^4}{H^4}p_\varphi^*(z)v_\chi^*(z)\int_z^{z_0}\frac{\mathrm{d}z'}{(z')^2}v_\varphi(z')v_\chi(z')\,,\end{aligned} \tag{C.11}$$

which can be re-organised as

$$\boldsymbol{D}_{11}(z) = 2\frac{k^3}{z^2}\frac{\lambda^4}{H^4}\Im\mathrm{m}\left[p_\varphi(z)v_\chi(z)\int_{z_0}^{z}\frac{\mathrm{d}z'}{(z')^2}v_\varphi^*(z')v_\chi^*(z') + p_\varphi(z)v_\chi^*(z)\int_{z_0}^{z}\frac{\mathrm{d}z'}{(z')^2}v_\varphi^*(z')v_\chi(z')\right]. \tag{C.12}$$

Therefore, we have two integrals to compute. Making use of Eq. (C.6), they are given by

$$\begin{aligned}\int_{z_0}^{z}\frac{\mathrm{d}z'}{(z')^2}v_\varphi^*(z')v_\chi^*(z') =& -i\frac{\pi}{4k}e^{-\frac{\pi}{2}\mu_\chi - i\frac{\pi}{2}\nu_\varphi}\left[G_{\nu_\varphi,\mu_\chi}(z) - G_{\nu_\varphi,\mu_\chi}(z_0)\right],\\ \int_{z_0}^{z}\frac{\mathrm{d}z'}{(z')^2}v_\varphi^*(z')v_\chi(z') =& \frac{\pi}{4k}e^{-\frac{\pi}{2}\mu_\chi - i\frac{\pi}{2}\nu_\varphi}\left[F_{\nu_\varphi,\mu_\chi}(z) - F_{\nu_\varphi,\mu_\chi}(z_0)\right].\end{aligned} \tag{C.13}$$

We conclude that $\boldsymbol{D}_{11}$ can be written as

$$\boldsymbol{D}_{11}(z) = F_{\boldsymbol{D}_{11}}(z,z) - F_{\boldsymbol{D}_{11}}(z,z_0)\,, \tag{C.14}$$

where

$$\begin{aligned}F_{\boldsymbol{D}_{11}}(z_1,z_2) =& \frac{\pi}{2}\frac{k^2}{z^2}\frac{\lambda^4}{H^4}e^{-\frac{\pi}{2}\mu_\chi}\Im\mathrm{m}\Big[-ip_\varphi(z_1)v_\chi(z_1)G_{\nu_\varphi,\mu_\chi}(z_2)e^{-i\frac{\pi}{2}\nu_\varphi}\\ &+ p_\varphi(z_1)v_\chi^*(z_1)F_{\nu_\varphi,\mu_\chi}(z_2)e^{-i\frac{\pi}{2}\nu_\varphi}\Big].\end{aligned} \tag{C.15}$$

It is worth noting that in the case where $z_1 = z_2$, this function can be further simplified by making repeated use of the Wronskian identity (see Eq. (10.5.5) of Ref. [101]), namely

$$H_{\nu+1}^{(1)}(z)H_\nu^{(2)}(z) - H_\nu^{(1)}(z)H_{\nu+1}^{(2)}(z) = -\frac{4i}{\pi z}\,. \tag{C.16}$$

Recalling that $[H_\nu^{(1)}(z)]^* = H_{\nu^*}^{(2)}(z)$ and $[H_\nu^{(2)}(z)]^* = H_{\nu^*}^{(1)}(z)$, after a tedious but straightforward calculation it leads to

$$F_{\boldsymbol{D}_{11}}(z,z) = -\frac{2}{\nu_\varphi^2+\mu_\chi^2}\left(\frac{k}{z}\right)\left(\frac{\lambda}{H}\right)^4\Re\mathrm{e}\left[v_\chi(z)p_\chi^*(z)\right]\,. \tag{C.17}$$

Given that Eq. (C.5) leads to $\nu_\varphi^2+\mu_\chi^2 = (M^2-m^2)/H^2$, and since $\boldsymbol{\Sigma}^{\text{free}}_{\chi\chi,12}(z) = \Re\mathrm{e}\,[v_\chi(z)p_\chi^*(z)]$, this can be rewritten as

$$F_{\boldsymbol{D}_{11}}(z,z) = -2\frac{\lambda^4a^2}{M^2-m^2}\boldsymbol{\Sigma}^{\text{free}}_{\chi\chi,12}(z)\,, \tag{C.18}$$

where we have also used that $a = -k/(Hz)$ in a de-Sitter universe. This corresponds to $\boldsymbol{D}_{11}$ in the exact theory when evaluated at leading order in the interaction strength, see Eq. (3.50). In other words, we have shown that

$$F_{\boldsymbol{D}_{11}}(z,z) = \boldsymbol{D}_{\text{SPT},11}(z)\,. \tag{C.19}$$

$\boldsymbol{D_{12}}$ coefficient

The other coefficients can be computed similarly. For $\boldsymbol{D}_{12}$ defined in Eqs. (3.32), one has

$$\begin{aligned}\boldsymbol{D}_{12}(\eta) =& 2\lambda^4 a^2(\eta)\int_{\eta_0}^{\eta} \mathrm{d}\eta' a^2(\eta')\Im\mathrm{m}\left[v_\varphi(\eta)v_\varphi^*(\eta')\right]\Re\mathrm{e}\left[v_\chi(\eta)v_\chi^*(\eta')\right]\\ =& \frac{i}{2}\frac{k^3}{z^2}\frac{\lambda^4}{H^4}\int_{z_0}^{z}\frac{\mathrm{d}z'}{(z')^2}\left[v_\varphi(z)v_\varphi^*(z') - v_\varphi^*(z)v_\varphi(z')\right]\left[v_\chi(z)v_\chi^*(z') + v_\chi^*(z)v_\chi(z')\right].\end{aligned} \tag{C.20}$$

This leads to

$$\boldsymbol{D}_{12}(z) = F_{\boldsymbol{D}_{12}}(z,z) - F_{\boldsymbol{D}_{12}}(z,z_0), \tag{C.21}$$

where

$$\begin{aligned}F_{\boldsymbol{D}_{12}}(z_1,z_2) = -\frac{\pi}{4}\frac{k^2}{z^2}\frac{\lambda^4}{H^4}e^{-\frac{\pi}{2}\mu_\chi}\Im\mathrm{m}\Big[& -iv_\varphi(z_1)v_\chi(z_1)G_{\nu_\varphi,\mu_\chi}(z_2)e^{-i\frac{\pi}{2}\nu_\varphi}\\ & +v_\varphi(z_1)v_\chi^*(z_1)F_{\nu_\varphi,\mu_\chi}(z_2)e^{-i\frac{\pi}{2}\nu_\varphi}\Big].\end{aligned} \tag{C.22}$$

As for $F_{\boldsymbol{D}_{11}}$, this expression can be simplified in the coincident configuration $z_1 = z_2$ by repeatedly using the Wronskian identity (C.16), and one finds

$$F_{\boldsymbol{D}_{12}}(z,z) = \left(\frac{k}{z}\right)^2\left(\frac{\lambda}{H}\right)^4\frac{|v_\chi(z)|^2}{\mu_\chi^2+\nu_\varphi^2}. \tag{C.23}$$

Using again that $\nu_\varphi^2+\mu_\chi^2 = (M^2-m^2)/H^2$, this can be written as

$$F_{\boldsymbol{D}_{12}}(z,z) = \frac{\lambda^4 a^2}{M^2-m^2}\boldsymbol{\Sigma}^{\mathrm{free}}_{\chi\chi,11}(z) = \boldsymbol{D}_{\mathrm{SPT},12}(z), \tag{C.24}$$

where we recognise the leading-order contribution in $\boldsymbol{D}_{\mathrm{ex},12}$, see Eq. (3.50).

$\boldsymbol{\Delta_{11}}$ coefficient

For $\boldsymbol{\Delta}_{11}$ defined in Eqs. (3.34), one has

$$\begin{aligned}\boldsymbol{\Delta}_{11}(\eta) =& -4\lambda^4 a^2(\eta)\int_{\eta_0}^{\eta}\mathrm{d}\eta' a^2(\eta')\Im\mathrm{m}\left[p_\varphi(\eta)v_\varphi^*(\eta')\right]\Im\mathrm{m}\left[v_\chi(\eta)v_\chi^*(\eta')\right]\\ =& -\frac{k^3}{z^2}\frac{\lambda^4}{H^4}\int_{z_0}^{z}\frac{\mathrm{d}z'}{(z')^2}\left[p_\varphi(z)v_\varphi^*(z') - p_\varphi^*(z)v_\varphi(z')\right]\left[v_\chi(z)v_\chi^*(z') - v_\chi^*(z)v_\chi(z')\right].\end{aligned} \tag{C.25}$$

This leads to

$$\boldsymbol{\Delta}_{11}(z) = F_{\boldsymbol{\Delta}_{11}}(z,z) - F_{\boldsymbol{\Delta}_{11}}(z,z_0), \tag{C.26}$$

where

$$\begin{aligned}F_{\boldsymbol{\Delta}_{11}}(z_1,z_2) = -\frac{\pi}{2}\frac{k^2}{z^2}\frac{\lambda^4}{H^4}e^{-\frac{\pi}{2}\mu_\chi}\Re\mathrm{e}\Big[& -ip_\varphi(z_1)v_\chi(z_1)G_{\nu_\varphi,\mu_\chi}(z_2)e^{-i\frac{\pi}{2}\nu_\varphi}\\ & -p_\varphi(z_1)v_\chi^*(z_1)F_{\nu_\varphi,\mu_\chi}(z_2)e^{-i\frac{\pi}{2}\nu_\varphi}\Big].\end{aligned} \tag{C.27}$$

This expression can be simplified when $z_1 = z_2$ using the Wronskian identity (C.16), if one further uses two additional properties of the Hankel functions. The first one is the recurrence relation (see Eq. (10.6.1) of Ref. [101])

$$H^{(2)}_{\nu-1}(z) + H^{(2)}_{\nu+1}(z) = \frac{2\nu}{z} H^{(2)}_{\nu}\,, \tag{C.28}$$

and the second one is the inversion formula

$$H^{(1)}_{-\nu}(z) = e^{i\pi\nu} H^{(1)}_{\nu}(z)\,, \qquad H^{(2)}_{-\nu}(z) = e^{-i\pi\nu} H^{(2)}_{\nu}(z)\,. \tag{C.29}$$

After a tedious but straightforward calculation, this leads to

$$F_{\boldsymbol{\Delta}_{11}}(z,z) = -\left(\frac{k}{z}\right)^2 \left(\frac{\lambda}{H}\right)^4 \frac{1}{\nu_\varphi^2 + \mu_\chi^2} = \boldsymbol{\Delta}_{\rm ex,11}\,, \tag{C.30}$$

where we have recognised $\boldsymbol{\Delta}_{\rm ex,11}$, see Eq. (3.49), using again that $\nu_\varphi^2 + \mu_\chi^2 = (M^2 - m^2)/H^2$. Note that, here, the agreement between $F_{\boldsymbol{\Delta}_{11}}(z,z)$ and $\boldsymbol{\Delta}_{\rm ex,11}$ is valid at all orders, given that $\boldsymbol{\Delta}_{\rm ex,11}$ only contains terms of order λ^4.

$\boldsymbol{\Delta}_{12}$ coefficient

Finally, for $\boldsymbol{\Delta}_{12}$ defined in Eqs. (3.35), one has

$$\begin{aligned}\boldsymbol{\Delta}_{12}(\eta) =& 2\lambda^4 a^2(\eta) \int_{\eta_0}^{\eta} \mathrm{d}\eta' a^2(\eta') \Im\mathrm{m}\left[v_\varphi(\eta) v_\varphi^*(\eta')\right] \Im\mathrm{m}\left[v_\chi(\eta) v_\chi^*(\eta')\right] \\ =& \frac{1}{2}\frac{k^3}{z^2}\frac{\lambda^4}{H^4} \int_{z_0}^{z} \frac{\mathrm{d}z'}{(z')^2} \left[v_\varphi(z) v_\varphi^*(z') - v_\varphi^*(z) v_\varphi(z')\right] \left[v_\chi(z) v_\chi^*(z') - v_\chi^*(z) v_\chi(z')\right],\end{aligned} \tag{C.31}$$

and this leads to

$$\boldsymbol{\Delta}_{12}(z) = F_{\boldsymbol{\Delta}_{12}}(z,z) - F_{\boldsymbol{\Delta}_{12}}(z,z_0)\,, \tag{C.32}$$

where

$$\begin{aligned}F_{\boldsymbol{\Delta}_{12}}(z_1,z_2) = \frac{\pi}{4}\frac{k^2}{z^2}\frac{\lambda^4}{H^4} e^{-\frac{\pi}{2}\mu_\chi} \Re\mathrm{e}\Big[&- i v_\varphi(z_1) v_\chi(z_1) G_{\nu_\varphi,\mu_\chi}(z_2) e^{-i\frac{\pi}{2}\nu_\varphi} \\ &- v_\varphi(z_1) v_\chi^*(z_1) F_{\nu_\varphi,\mu_\chi}(z_2) e^{-i\frac{\pi}{2}\nu_\varphi}\Big].\end{aligned} \tag{C.33}$$

This expression can be simplified when $z_1 = z_2$ using the Wronskian identity (C.16), and we find that it vanishes,

$$F_{\boldsymbol{\Delta}_{12}}(z,z) = 0\,. \tag{C.34}$$

In particular, it implies that $F_{\boldsymbol{\Delta}_{12}}(z,z) = \boldsymbol{\Delta}_{\rm ex,12}(z)$ and that, as for $F_{\boldsymbol{\Delta}_{11}}(z,z)$, this is valid at all orders in λ^4 given that both quantities identically vanish.

C.2 Sub-Hubble limit

In order to gain analytic insight, let us expand the coefficients derived above in the sub-Hubble ($z \gg 1$) and super-Hubble ($z \ll 1$) limits. In the sub-Hubble limit, one can use the asymptotic expansion

$$H^{(1)}_{\nu}(z) = \sqrt{\frac{2}{\pi z}} e^{-iz - i\frac{\pi}{2}\nu - i\frac{\pi}{4}} \sum_{k=0}^{\infty} a_k(\nu) \left(\frac{i}{z}\right)^k\,, \tag{C.35}$$

$$H_\nu^{(2)}(z) = \sqrt{\frac{2}{\pi z}} e^{iz + i\frac{\pi}{2}\nu + i\frac{\pi}{4}} \sum_{k=0}^{\infty} a_k(\nu) \left(\frac{-i}{z}\right)^k , \tag{C.36}$$

see Eq. (10.17.5) of Ref. [101], with

$$a_k(\nu) = \frac{\left(\frac{1}{2} - \nu\right)_k \left(\frac{1}{2} + \nu\right)_k}{(-2)^k k!} \tag{C.37}$$

where the parenthesis with lower index indicate the Pochhammer's symbol, *i.e.* $(x)_k = \Gamma(x + k)/\Gamma(x)$. Inserting these formulas into Eqs. (C.7) and (C.8), one obtains

$$F_{\nu,\mu}(z) = -\frac{e^{\frac{\pi}{2}(\mu + i\nu)}}{\pi} \left(\frac{4i}{\nu^2 + \mu^2} + \frac{2}{z} - i\frac{\nu^2 + \mu^2}{2z^2}\right) + \mathcal{O}(z^{-3}) , \tag{C.38}$$

$$G_{\nu,\mu}(z) = -\frac{e^{\frac{\pi}{2}(\mu + i\nu)}}{\pi} \frac{e^{-2iz}}{z^2} + \mathcal{O}(z^{-3}) . \tag{C.39}$$

Note that $F_{\nu,\mu}(z)$ is non vanishing in the sub-Hubble regime. Let us now expand Eqs. (C.15), (C.22), (C.27) and (C.33) in the limit $z_1, z_2 \gg 1$. At leading order, one obtains

$$F_{\boldsymbol{D}_{11}}(z_1, z_2) \simeq \frac{k^2\lambda^4}{2H^4 z_1^3} \left(\frac{2}{\nu_\varphi^2 + \mu_\chi^2} - 1 + \frac{z_1}{z_2}\right) , \tag{C.40}$$

$$F_{\boldsymbol{D}_{12}}(z_1, z_2) \simeq \frac{k\lambda^4}{2H^4 \left(\nu_\varphi^2 + \mu_\chi^2\right) z_1^2} , \tag{C.41}$$

$$F_{\boldsymbol{\Delta}_{11}}(z_1, z_2) \simeq -\frac{k^2\lambda^4}{H^4 \left(\nu_\varphi^2 + \mu_\chi^2\right) z_1^2} , \tag{C.42}$$

$$F_{\boldsymbol{\Delta}_{12}}(z_1, z_2) \simeq \frac{k\lambda^4 (z_1 - z_2)}{4H^4 z_1^3 z_2} . \tag{C.43}$$

C.3 Super-Hubble limit

To organise the super-Hubble expansion, we introduce the quantities

$$\alpha_\nu(z) \equiv \frac{1 + i\cot\pi\nu}{\Gamma(1 + \nu)} \left(\frac{z}{2}\right)^{\nu - \frac{3}{2}} , \qquad \beta_\nu(z) \equiv \frac{-i}{\sin\pi\nu} \frac{1}{\Gamma(1 - \nu)} \left(\frac{z}{2}\right)^{\frac{3}{2} - \nu} , \tag{C.44}$$

$$\gamma_\mu(z) \equiv \frac{1 + \coth\pi\mu}{\Gamma(1 + i\mu)} \left(\frac{z}{2}\right)^{i\mu} , \qquad \delta_\mu(z) \equiv \frac{-1}{\sinh\pi\mu} \frac{1}{\Gamma(1 - i\mu)} \left(\frac{z}{2}\right)^{-i\mu} , \tag{C.45}$$

together with the function

$$f_x(z) \equiv \sum_{k=0}^{\infty} \frac{(-1)^k \left(\frac{z}{2}\right)^{2k}}{k!\,(x + 1)_k} \tag{C.46}$$

$$= 1 - \frac{\left(\frac{z}{2}\right)^2}{x + 1} + \frac{\left(\frac{z}{2}\right)^4}{2(x + 1)(x + 2)} + \mathcal{O}(z^6) \tag{C.47}$$

such that

$$H_\nu^{(1)}(z) = \alpha_\nu(z) f_\nu(z) \left(\frac{z}{2}\right)^{\frac{3}{2}} + \beta_\nu(z) f_{-\nu}(z) \left(\frac{z}{2}\right)^{-\frac{3}{2}} , \tag{C.48}$$

$$H_{i\mu}^{(1)}(z) = \gamma_\mu(z) f_{i\mu}(z) + \delta_\mu(z) f_{-i\mu}(z) , \tag{C.49}$$

and

$$H^{(1)}_{\nu+1}(z) = \frac{\alpha_\nu(z)}{\nu+1} f_{\nu+1}(z) \left(\frac{z}{2}\right)^{\frac{5}{2}} + \nu\beta_\nu(z) f_{-\nu-1}(z) \left(\frac{z}{2}\right)^{-\frac{5}{2}}, \tag{C.50}$$

$$H^{(1)}_{i\mu+1}(z) = \frac{\gamma_\mu(z)}{i\mu+1} f_{i\mu+1}(z) \frac{z}{2} + i\mu\delta_\mu(z) f_{-i\mu-1}(z) \left(\frac{z}{2}\right)^{-1}, \tag{C.51}$$

see Eqs. (10.2.2), (10.4.7) and (10.4.8) of Ref. [101]. This allows one to expand Eqs. (C.7) and (C.8), and one finds

$$\begin{aligned} F_{\nu,\mu}(z) =& -2\sqrt{2} z^{-3/2} \beta^*_\nu \left[\frac{(\nu+i\mu)\gamma_\mu + (\nu-i\mu)\delta_\mu}{\nu^2+\mu^2}\right] + \frac{z^{1/2}}{\sqrt{2}} \beta^*_\nu \left[\frac{(1-i\mu)\gamma_\mu + (1+i\mu)\delta_\mu}{(1+\mu^2)(\nu-1)}\right] \\ &+ \frac{z^{3/2}}{2\sqrt{2}} \alpha^*_\nu \left[\frac{(\nu-i\mu)\gamma_\mu + (\nu+i\mu)\delta_\mu}{\nu^2+\mu^2}\right] + \mathcal{O}(z^{5/2}). \end{aligned} \tag{C.52}$$

and

$$\begin{aligned} G_{\nu,\mu}(z) =& -2\sqrt{2} z^{-3/2} \beta^*_\nu \left[\frac{(\nu-i\mu)\gamma^*_\mu + (\nu+i\mu)\delta^*_\mu}{\nu^2+\mu^2}\right] + \frac{z^{1/2}}{\sqrt{2}} \beta^*_\nu \left[\frac{(1+i\mu)\gamma^*_\mu + (1-i\mu)\delta^*_\mu}{(1+\mu^2)(\nu-1)}\right] \\ &+ \frac{z^{3/2}}{2\sqrt{2}} \alpha^*_\nu \left[\frac{(\nu+i\mu)\gamma^*_\mu + (\nu-i\mu)\delta^*_\mu}{\nu^2+\mu^2}\right] + \mathcal{O}(z^{5/2}). \end{aligned} \tag{C.53}$$

Hereafter, to lighten the notation, we have dropped the explicit z-dependence of α_ν, β_ν, γ_μ and δ_μ. This is because, since ν_φ is close to $3/2$ in practice, see Eq. (C.5), this does not affect the power counting in z, see Eqs. (C.44)-(C.45).

It is worth noting that the terms of orders $z^{-3/2}$ and $z^{1/2}$ cancel out in $F^*_{\nu,\mu}(z) + G_{\nu,\mu}(z)$ since β_ν is pure imaginary, see Eq. (C.45). One indeed has

$$F^*_{\nu,\mu}(z) + G_{\nu,\mu}(z) = \frac{1}{\nu^2+\mu^2} \frac{z^{3/2}}{\sqrt{2}} \Re\mathrm{e}\,(\alpha_\nu) \left[(\nu+i\mu)\gamma^*_\mu + (\nu-i\mu)\delta^*_\mu\right] + \mathcal{O}(z^{5/2}). \tag{C.54}$$

Let us now expand the coefficients of the transport equation in the super-Hubble limit, *i.e.* when $z \ll 1$ (but keeping z_0 arbitrary).

$\boldsymbol{D_{11}}$ coefficient

For $\boldsymbol{D}_{11}$, one finds

$$\begin{aligned} \boldsymbol{D}_{11} =& z^{-7/2} S^{(-7/2)}_{\boldsymbol{D}_{11}}(z, z_0) + \frac{\pi}{2} \frac{e^{-\pi\mu_\chi}}{\nu_\varphi^2 + \mu_\chi^2} \frac{\lambda^4}{H^4} \left[\frac{3}{2} \left|\gamma_{\mu_\chi} + \delta_{\mu_\chi}\right|^2 + 2\mu_\chi \Im\mathrm{m}\left(\gamma^*_{\mu_\chi} \delta_{\mu_\chi}\right)\right] \frac{k^2}{z^2} \\ &+ z^{-3/2} S^{(-3/2)}_{\boldsymbol{D}_{11}}(z, z_0), \end{aligned} \tag{C.55}$$

where

$$S^{(-7/2)}_{\boldsymbol{D}_{11}}(z, z_0) = -\frac{\pi^2 k^2}{2\sqrt{2}} \left(\nu_\varphi - \frac{3}{2}\right) \frac{\lambda^4}{H^4} \Im\mathrm{m} \left\{\beta_{\nu_\varphi} \left[F^*_{\nu_\varphi,\mu_\chi}(z_0) + G_{\nu_\varphi,\mu_\chi}(z_0)\right] \left(\gamma_{\mu_\chi} + \delta_{\mu_\chi}\right)\right\} e^{-\pi\mu_\chi} \tag{C.56}$$

and

$$S^{(-3/2)}_{\boldsymbol{D}_{11}}(z, z_0) = -\frac{\pi^2}{16\sqrt{2}} \frac{1}{(1+\mu_\chi^2)(\nu_\varphi - 1)} \frac{\lambda^4}{H^4} k^2 \Im\mathrm{m} \left[\beta_{\nu_\varphi} \left[F^*_{\nu_\varphi,\mu_\chi}(z_0) + G_{\nu_\varphi,\mu_\chi}(z_0)\right]\right.$$

$$\Big(\gamma_{\mu_\chi}(\mu_\chi+i)\left\{\mu_\chi(-7+2\nu_\varphi)+i\left[10+\nu_\varphi(-7+2\nu_\varphi)\right]\right\} \tag{C.57}$$
$$+\delta_{\mu_\chi}(\mu_\chi-i)\left\{\mu_\chi(-7+2\nu_\varphi)-i\left[10+\nu_\varphi(-7+2\nu_\varphi)\right]\right\}\Big)\Big]e^{-\pi\mu_\chi}$$
$$+\frac{\pi^2}{16\sqrt{2}}\left(\frac{3}{2}+\nu_\varphi\right)\frac{\lambda^4}{H^4}\frac{k^2}{z^{1/2}}\Im\mathrm{m}\left\{\left[-\alpha^*_{\nu_\varphi}F^*_{\nu_\varphi,\mu_\chi}(z_0)+\alpha_{\nu_\varphi}G_{\nu_\varphi,\mu_\chi}(z_0)\right]\right.$$
$$\left.\left(\gamma_{\mu_\chi}+\delta_{\mu_\chi}\right)\right\}e^{-\pi\mu_\chi}+\mathcal{O}(z^{1/2})$$

are spurious contributions, *i.e.* they arise from the term $F_{\boldsymbol{D}_{11}}(z,z_0)$ in Eq. (C.14).

$\boldsymbol{D_{12}}$ coefficient

One finds

$$\boldsymbol{D}_{12}=z^{-5/2}S^{(-5/2)}_{\boldsymbol{D}_{12}}(z,z_0)+\frac{\pi}{4}\frac{\left|\gamma_{\mu_\chi}+\delta_{\mu_\chi}\right|^2}{\nu_\varphi^2+\mu_\chi^2}\frac{\lambda^4}{H^4}e^{-\pi\mu_\chi}\frac{k}{z}+z^{-1/2}S^{(-1/2)}_{\boldsymbol{D}_{12}}(z,z_0)\,, \tag{C.58}$$

where

$$S^{(-5/2)}_{\boldsymbol{D}_{12}}(z,z_0)=\frac{\pi^2}{4\sqrt{2}}\frac{\lambda^4}{H^4}k\Im\mathrm{m}\left\{\beta_{\nu_\varphi}\left[F^*_{\nu_\varphi,\mu_\chi}(z_0)+G_{\nu_\varphi,\mu_\chi}(z_0)\right]\left(\gamma_{\mu_\chi}+\delta_{\mu_\chi}\right)\right\}e^{-\pi\mu_\chi} \tag{C.59}$$

and

$$S^{(-1/2)}_{\boldsymbol{D}_{12}}(z,z_0)=\frac{\pi^2 k}{16\sqrt{2}}\frac{e^{-\pi\mu_\chi}}{(1+\mu_\chi^2)(\nu_\varphi-1)}\frac{\lambda^4}{H^4}\Im\mathrm{m}\left\{\beta_{\nu_\varphi}\left[F^*_{\nu_\varphi,\mu_\chi}(z_0)+G_{\nu_\varphi,\mu_\chi}(z_0)\right]\right.$$
$$\left.\left[(1+\mu_\chi^2)\left(\gamma_{\mu_\chi}+\delta_{\mu_\chi}\right)+(1-i\mu_\chi)(1-\nu_\varphi)\gamma_{\mu_\chi}+(1+i\mu_\chi)(1-\nu_\varphi)\delta_{\mu_\chi}\right]\right\} \tag{C.60}$$

are again spurious contributions.

$\boldsymbol{\Delta_{11}}$ coefficient

For $\boldsymbol{\Delta}_{11}$, we have

$$\boldsymbol{\Delta}_{11}=z^{-7/2}S^{(-7/2)}_{\boldsymbol{\Delta}_{11}}(z,z_0)-\frac{\pi}{2}\frac{\mu_\chi e^{-\pi\mu_\chi}}{\nu_\varphi^2+\mu_\chi^2}\frac{\lambda^4}{H^4}\left(\left|\gamma_{\mu_\chi}\right|^2-\left|\delta_{\mu_\chi}\right|^2\right)\frac{k^2}{z^2}+z^{-3/2}S^{(-3/2)}_{\boldsymbol{\Delta}_{11}}(z,z_0)\,, \tag{C.61}$$

where

$$S^{(-7/2)}_{\boldsymbol{\Delta}_{11}}(z,z_0)=\frac{\pi^2k^2}{2\sqrt{2}}\left(\nu_\varphi-\frac{3}{2}\right)\frac{\lambda^4}{H^4}\Re\mathrm{e}\left\{\beta_{\nu_\varphi}\left[F^*_{\nu_\varphi,\mu_\chi}(z_0)+G_{\nu_\varphi,\mu_\chi}(z_0)\right]\left(\gamma_{\mu_\chi}+\delta_{\mu_\chi}\right)\right\}e^{-\pi\mu_\chi} \tag{C.62}$$

and

$$
\begin{aligned}
S^{(-3/2)}_{\mathbf{\Delta}_{11}}(z,z_0) =& \frac{\pi^2 k^2}{16\sqrt{2}} \frac{1}{(1+\mu_\chi^2)(\nu_\varphi-1)} \frac{\lambda^4}{H^4} \Re\mathrm{e} \Bigg[\beta_{\nu_\varphi} \left[F^*_{\nu_\varphi,\mu_\chi}(z_0) + G_{\nu_\varphi,\mu_\chi}(z_0) \right] \\
& \Big(\gamma_{\mu_\chi}(\mu_\chi + i) \left\{ \mu_\chi(-7+2\nu_\varphi) + i\left[10+\nu_\varphi(-7+2\nu_\varphi)\right] \right\} \\
& + \delta_{\mu_\chi}(\mu_\chi - i) \left\{ \mu_\chi(-7+2\nu_\varphi) - i\left[10+\nu_\varphi(-7+2\nu_\varphi)\right] \right\} \Big) \Bigg] e^{-\pi\mu_\chi} \\
& - \frac{\pi^2}{16\sqrt{2}} \left(\frac{3}{2}+\nu_\varphi\right) \frac{\lambda^4}{H^4} \frac{k^2}{z^{1/2}} \Re\mathrm{e} \Big\{ \left[-\alpha^*_{\nu_\varphi} F^*_{\nu_\varphi,\mu_\chi}(z_0) + \alpha_{\nu_\varphi} G_{\nu_\varphi,\mu_\chi}(z_0) \right] \\
& \left(\gamma_{\mu_\chi} + \delta_{\mu_\chi}\right) \Big\} e^{-\pi\mu_\chi}
\end{aligned}
\tag{C.63}
$$

are spurious contributions. It is also worth noting that, in Eq. (C.61), one can simplify

$$
|\gamma_{\mu_\chi}|^2 - |\delta_{\mu_\chi}|^2 = 2\frac{e^{\pi\mu}}{\pi\mu} \,. \tag{C.64}
$$

$\mathbf{\Delta_{12}}$ coefficient

Finally, for $\mathbf{\Delta}_{12}$, one obtains

$$
\mathbf{\Delta}_{12}(z) = z^{-5/2} S^{(-5/2)}_{\mathbf{\Delta}_{12}}(z,z_0) + z^{-1/2} S^{(-1/2)}_{\mathbf{\Delta}_{12}}(z,z_0) \tag{C.65}
$$

which only contains spurious terms as shown in Eq. (C.34), given by

$$
S^{(-5/2)}_{\mathbf{\Delta}_{12}}(z,z_0) = -\frac{\pi^2 k}{4\sqrt{2}} \frac{\lambda^4}{H^4} \Re\mathrm{e} \left\{ \beta_{\nu_\varphi} \left[F^*_{\nu_\varphi,\mu_\chi}(z_0) + G_{\nu_\varphi,\mu_\chi}(z_0) \right] \left(\gamma_{\mu_\chi} + \delta_{\mu_\chi}\right) \right\} e^{-\pi\mu_\chi} \tag{C.66}
$$

and

$$
\begin{aligned}
S^{(-1/2)}_{\mathbf{\Delta}_{12}}(z,z_0) = -\frac{\pi^2 k}{16\sqrt{2}} \frac{e^{-\pi\mu_\chi}}{(1+\mu_\chi^2)(\nu_\varphi-1)} \frac{\lambda^4}{H^4} \Re\mathrm{e} \Big\{ & \beta_{\nu_\varphi} \left[F^*_{\nu_\varphi,\mu_\chi}(z_0) + G_{\nu_\varphi,\mu_\chi}(z_0) \right] \\
& \left[(1+\mu_\chi^2)\left(\gamma_{\mu_\chi} + \delta_{\mu_\chi}\right) + (1-i\mu_\chi)(1-\nu_\varphi)\gamma_{\mu_\chi} + (1+i\mu_\chi)(1-\nu_\varphi)\delta_{\mu_\chi} \right] \Big\} \,.
\end{aligned}
\tag{C.67}
$$

D Comparison between TCL and perturbation theory in the curved-space Caldeira-Leggett model

In this appendix, we compare Standard Perturbation Theory (SPT) to the perturbative solutions of the TCL master equation, in the context of the curved-space Caldeira-Leggett model introduced in Sec. 3. This will allow us to exhibit a concrete manifestation of the generic statement proven in Sec. 2.4, that TCL_n solved perturbatively at order n coincides with SPT_n.

D.1 Perturbation theory

The two-field system detailed in Sec. 3.1 being linear, the field operators admit a decomposition of the form

$$
\widehat{v}_\varphi(\eta) = v_{\varphi\varphi}(\eta)\widehat{a}_\varphi + v^*_{\varphi\varphi}(\eta)\widehat{a}^\dagger_\varphi + v_{\varphi\chi}(\eta)\widehat{a}_\chi + v^*_{\varphi\chi}(\eta)\widehat{a}^\dagger_\chi \,, \tag{D.1}
$$

$$\widehat{v}_\chi(\eta) = v_{\chi\varphi}(\eta)\widehat{a}_\varphi + v^*_{\chi\varphi}(\eta)\widehat{a}^\dagger_\varphi + v_{\chi\chi}(\eta)\widehat{a}_\chi + v^*_{\chi\chi}(\eta)\widehat{a}^\dagger_\chi\,, \tag{D.2}$$

where $(\widehat{a}_\varphi;\widehat{a}^\dagger_\varphi)$ and $(\widehat{a}_\chi;\widehat{a}^\dagger_\chi)$ are the creation and annihilation operators of the φ and χ quanta respectively. This generalises the decomposition (3.13) to the case where fields interact and exchange quanta. A similar decomposition can be introduced for the momenta operators $\widehat{p}_\varphi$ and $\widehat{p}_\chi$, where the Hamiltonian (3.6)-(3.7) gives the mode functions

$$p_{ij}(\eta) = v'_{ij}(\eta) - \frac{a'}{a}v_{ij}(\eta) \tag{D.3}$$

for $i,j \in \{\varphi,\chi\}$. Using Heisenberg's equations, one finds that the mode functions evolve according to

$$v''_{ij} + \omega_i^2(\eta)v_{ij} = -\lambda^2 a^2(\eta)v_{\bar{i}j}\,, \tag{D.4}$$

where we have introduced $\omega^2_\varphi(\eta) \equiv k^2 + m^2a^2(\eta) - a''/a$ and $\omega^2_\chi(\eta) \equiv k^2 + M^2a^2(\eta) - a''/a$, and where $\bar{i} = \chi$ when $i = \varphi$ and $\bar{i} = \varphi$ when $i = \chi$. This constitutes a set of coupled differential equations, where the coupling is mediated by λ^2. It can thus be solved perturbatively in λ.

- **Zeroth order**: The right-hand side of Eq. (D.4) vanishes, hence the uncoupled dynamics is recovered, namely $v^{(0)}_{ii}(\eta) = v_i(\eta)$ and $v^{(0)}_{i\bar{i}}(\eta) = 0$, where v_φ and v_χ are the free-field mode functions [*i.e.* they are given by Eq. (3.15) if one replaces ν_ℓ by ν_φ and μ_h by μ_χ]. One also has $p^{(0)}_{ii}(\eta) = p_i(\eta)$ and $p^{(0)}_{i\bar{i}}(\eta) = 0$.

- **First order**: At first order, the right-hand side of Eq. (D.4) needs to be replaced with the zeroth-order solution. This does not change the diagonal mode functions $v^{(1)}_{ii}(\eta) = v^{(0)}_{ii}(\eta)$ and $p^{(1)}_{ii}(\eta) = p^{(0)}_{ii}(\eta)$, while the cross mode functions now obey $v^{(1)\prime\prime}_{i\bar{i}} + \omega_i^2 v^{(1)}_{i\bar{i}} = \lambda^2a^2v_{\bar{i}}$. Using the Green's functions of the homogeneous (hence uncoupled) system of differential equation, $g_i(\eta,\eta') = 2\Im\mathrm{m}\left[v_i(\eta)v_i^*(\eta')\right]$, this gives rise to

$$v^{(1)}_{i\bar{i}}(\eta) = -2\lambda^2\int_{\eta_0}^{\eta}\mathrm{d}\eta_1 a^2(\eta_1)\Im\mathrm{m}\left[v_i(\eta)v_i^*(\eta_1)\right]v_{\bar{i}}(\eta_1). \tag{D.5}$$

  Using Eq. (D.3), this leads to

$$p^{(1)}_{i\bar{i}}(\eta) = -2\lambda^2\int_{\eta_0}^{\eta}\mathrm{d}\eta_1 a^2(\eta_1)\Im\mathrm{m}\left[p_i(\eta)v_i^*(\eta_1)\right]v_{\bar{i}}(\eta_1). \tag{D.6}$$

- **Second order**: At second order, Eq. (D.4) is sourced by the first-order solution, so the diagonal mode functions obey $v^{(2)\prime\prime}_{ii} + \omega_i^2 v^{(2)}_{ii} = -\lambda^2a^2v^{(1)}_{\bar{i}i}$. Using again the homogeneous Green functions, together with Eq. (D.5), this gives rise to

$$v^{(2)}_{ii}(\eta) = v_i(\eta) + 4\lambda^4\int_{\eta_0}^{\eta}\mathrm{d}\eta_1 a^2(\eta_1)\int_{\eta_0}^{\eta_1}\mathrm{d}\eta_2 a^2(\eta_2)\Im\mathrm{m}\left[v_i(\eta)v_i^*(\eta_1)\right]\Im\mathrm{m}\left[v_{\bar{i}}(\eta_1)v_{\bar{i}}^*(\eta_2)\right]v_i(\eta_2). \tag{D.7}$$

  Using Eq. (D.3), this leads to

$$p^{(2)}_{ii}(\eta) = p_i(\eta) + 4\lambda^4\int_{\eta_0}^{\eta}\mathrm{d}\eta_1 a^2(\eta_1)\int_{\eta_0}^{\eta_1}\mathrm{d}\eta_2 a^2(\eta_2)\Im\mathrm{m}\left[p_i(\eta)v_i^*(\eta_1)\right]\Im\mathrm{m}\left[v_{\bar{i}}(\eta_1)v_{\bar{i}}^*(\eta_2)\right]v_i(\eta_2). \tag{D.8}$$

  One may also compute the cross mode functions, and carry on the expansion, but that would lead to subdominant corrections to the power spectra.

The covariance matrix can be computed using Eq. (3.18), and one finds

$$\boldsymbol{\Sigma}_{\varphi\varphi}(\eta) = \begin{pmatrix} |v_{\varphi\varphi}(\eta)|^2 + |v_{\varphi\chi}(\eta)|^2 & \Re\mathrm{e}\left[v_{\varphi\varphi}(\eta)p^*_{\varphi\varphi}(\eta)\right] + \Re\mathrm{e}\left[v_{\varphi\chi}(\eta)p^*_{\varphi\chi}(\eta)\right] \\ \Re\mathrm{e}\left[v_{\varphi\varphi}(\eta)p^*_{\varphi\varphi}(\eta)\right] + \Re\mathrm{e}\left[v_{\varphi\chi}(\eta)p^*_{\varphi\chi}(\eta)\right] & |p_{\varphi\varphi}(\eta)|^2 + |p_{\varphi\chi}(\eta)|^2 \end{pmatrix}, \tag{D.9}$$

$$\boldsymbol{\Sigma}_{\chi\chi}(\eta) = \begin{pmatrix} |v_{\chi\chi}(\eta)|^2 + |v_{\chi\varphi}(\eta)|^2 & \Re\mathrm{e}\left[v_{\chi\chi}(\eta)p^*_{\chi\chi}(\eta)\right] + \Re\mathrm{e}\left[v_{\chi\varphi}(\eta)p^*_{\chi\varphi}(\eta)\right] \\ \Re\mathrm{e}\left[v_{\chi\chi}(\eta)p^*_{\chi\chi}(\eta)\right] + \Re\mathrm{e}\left[v_{\chi\varphi}(\eta)p^*_{\chi\varphi}(\eta)\right] & |p_{\chi\chi}(\eta)|^2 + |p_{\chi\varphi}(\eta)|^2 \end{pmatrix}, \tag{D.10}$$

$$\boldsymbol{\Sigma}_{\varphi\chi}(\eta) = \begin{pmatrix} \Re\mathrm{e}\left[v_{\varphi\varphi}(\eta)v^*_{\chi\varphi}(\eta)\right] + \Re\mathrm{e}\left[v_{\chi\chi}(\eta)v^*_{\varphi\chi}(\eta)\right] & \Re\mathrm{e}\left[v_{\varphi\varphi}(\eta)p^*_{\chi\varphi}(\eta)\right] + \Re\mathrm{e}\left[p_{\chi\chi}(\eta)v^*_{\varphi\chi}(\eta)\right] \\ \Re\mathrm{e}\left[p_{\varphi\varphi}(\eta)v^*_{\chi\varphi}(\eta)\right] + \Re\mathrm{e}\left[v_{\chi\chi}(\eta)p^*_{\varphi\chi}(\eta)\right] & \Re\mathrm{e}\left[p_{\varphi\varphi}(\eta)p^*_{\chi\varphi}(\eta)\right] + \Re\mathrm{e}\left[p_{\chi\chi}(\eta)p^*_{\varphi\chi}(\eta)\right] \end{pmatrix}. \tag{D.11}$$

By inserting the mode functions obtained above into these expressions, one obtains the first perturbative corrections to the power spectra. For the configuration-configuration power spectrum of the φ field, one finds

$$\boldsymbol{\Sigma}^{(2)}_{\varphi\varphi,11}(\eta) = \left|v^{(0)}_{\varphi\varphi}(\eta)\right|^2 + \left|v^{(1)}_{\varphi\chi}(\eta)\right|^2 + 2\Re\mathrm{e}\left[v^{(2-0)}_{\varphi\varphi}(\eta)v^{(0)*}_{\varphi\varphi}(\eta)\right], \tag{D.12}$$

where we have introduced the short-hand notation $v^{(2-0)}_{\varphi\varphi}(\eta) = v^{(2)}_{\varphi\varphi}(\eta) - v^{(0)}_{\varphi\varphi}(\eta)$, which selects the terms of order λ^2 in $v^{(2)}_{\varphi\varphi}(\eta)$. This gives rise to

$$\begin{aligned}\boldsymbol{\Sigma}^{(2)}_{\varphi\varphi,11}(\eta) =& |v_\varphi(\eta)|^2 + 4\lambda^4\left|\int_{\eta_0}^{\eta}\mathrm{d}\eta_1 a^2(\eta_1)\Im\mathrm{m}\left[v_\varphi(\eta)v^*_\varphi(\eta_1)\right]v_\chi(\eta_1)\right|^2 \\ &+8\lambda^4\Re\mathrm{e}\left\{v_\varphi(\eta)\int_{\eta_0}^{\eta}\mathrm{d}\eta_1 a^2(\eta_1)\int_{\eta_0}^{\eta_1}\mathrm{d}\eta_2 a^2(\eta_2)\Im\mathrm{m}\left[v_\varphi(\eta)v^*_\varphi(\eta_1)\right]\Im\mathrm{m}\left[v_\chi(\eta_1)v^*_\chi(\eta_2)\right]v^*_\varphi(\eta_2)\right\}.\end{aligned} \tag{D.13}$$

For the configuration-momentum power spectrum, one obtains

$$\boldsymbol{\Sigma}^{(2)}_{\varphi\varphi,12}(\eta) = \Re\mathrm{e}\left[v^{(0)}_{\varphi\varphi}(\eta)p^{(0)*}_{\varphi\varphi}(\eta)\right] + \Re\mathrm{e}\left[v^{(1)}_{\varphi\chi}(\eta)p^{(1)*}_{\varphi\chi}(\eta)\right] + \Re\mathrm{e}\left[v^{(0)}_{\varphi\varphi}(\eta)p^{(2-0)*}_{\varphi\varphi}(\eta) + v^{(2-0)}_{\varphi\varphi}(\eta)p^{(0)*}_{\varphi\varphi}(\eta)\right], \tag{D.14}$$

namely

$$\begin{aligned}\boldsymbol{\Sigma}^{(2)}_{\varphi\varphi,12}(\eta) =& \Re\mathrm{e}\left[v_\varphi(\eta)p^*_\varphi(\eta)\right] \\ &+4\lambda^4\int_{\eta_0}^{\eta}\mathrm{d}\eta' a^2(\eta')\Im\mathrm{m}\left[v_\varphi(\eta)v^*_\varphi(\eta')\right]v_\chi(\eta')\int_{\eta_0}^{\eta}\mathrm{d}\eta'' a^2(\eta'')\Im\mathrm{m}\left[p_\varphi(\eta)v^*_\varphi(\eta'')\right]v_\chi(\eta'') \\ &+4\lambda^4\Re\mathrm{e}\left\{v_\varphi(\eta)\int_{\eta_0}^{\eta}\mathrm{d}\eta_1 a^2(\eta_1)\int_{\eta_0}^{\eta_1}\mathrm{d}\eta_2 a^2(\eta_2)\Im\mathrm{m}\left[p_\varphi(\eta)v^*_\varphi(\eta_1)\right]\Im\mathrm{m}\left[v_\chi(\eta_1)v^*_\chi(\eta_2)\right]v^*_\varphi(\eta_2)\right\} \\ &+4\lambda^4\Re\mathrm{e}\left\{p_\varphi(\eta)\int_{\eta_0}^{\eta}\mathrm{d}\eta_1 a^2(\eta_1)\int_{\eta_0}^{\eta_1}\mathrm{d}\eta_2 a^2(\eta_2)\Im\mathrm{m}\left[v_\varphi(\eta)v^*_\varphi(\eta_1)\right]\Im\mathrm{m}\left[v_\chi(\eta_1)v^*_\chi(\eta_2)\right]v^*_\varphi(\eta_2)\right\}.\end{aligned} \tag{D.15}$$

Finally, for the momentum-momentum power spectrum, one has

$$\boldsymbol{\Sigma}^{(2)}_{\varphi\varphi,22}(\eta) = \left|p^{(0)}_{\varphi\varphi}(\eta)\right|^2 + \left|p^{(1)}_{\varphi\chi}(\eta)\right|^2 + 2\Re\mathrm{e}\left[p^{(2-0)}_{\varphi\varphi}(\eta)p^{(0)*}_{\varphi\varphi}(\eta)\right], \tag{D.16}$$

which leads to

$$\boldsymbol{\Sigma}^{(2)}_{\varphi\varphi,22}(\eta) = |p_\varphi(\eta)|^2 + 4\lambda^4 \left| \int_{\eta_0}^{\eta} \mathrm{d}\eta_1 a^2(\eta_1) \Im\mathrm{m}\, \left[p_\varphi(\eta) v^*_\varphi(\eta_1)\right] v_\chi(\eta_1) \right|^2 + 8\lambda^4 \Re\mathrm{e} \left\{ p_\varphi(\eta) \int_{\eta_0}^{\eta} \mathrm{d}\eta_1 a^2(\eta_1) \int_{\eta_0}^{\eta_1} \mathrm{d}\eta_2 a^2(\eta_2) \Im\mathrm{m}\, \left[p_\varphi(\eta) v^*_\varphi(\eta_1)\right] \Im\mathrm{m}\, \left[v_\chi(\eta_1) v^*_\chi(\eta_2)\right] v^*_\varphi(\eta_2) \right\}. \tag{D.17}$$

D.2 Perturbative solution of TCL

Let us start with the TCL_2 master equation written in the form

$$\begin{aligned} \frac{\mathrm{d}\widetilde{\rho}_{\mathrm{red}}}{\mathrm{d}\eta} =& -\lambda^4 a^2(\eta) \int_{\eta_0}^{\eta} \mathrm{d}\eta' a^2(\eta') \\ & \Big\{ \left[\widetilde{v}_\varphi(\eta)\widetilde{v}_\varphi(\eta')\widetilde{\rho}_{\mathrm{red}}(\eta) - \widetilde{v}_\varphi(\eta')\widetilde{\rho}_{\mathrm{red}}(\eta)\widetilde{v}_\varphi(\eta)\right] \mathcal{K}^{>}(\eta,\eta') \\ & - \left[\widetilde{v}_\varphi(\eta)\widetilde{\rho}_{\mathrm{red}}(\eta)\widetilde{v}_\varphi(\eta') - \widetilde{\rho}_{\mathrm{red}}(\eta)\widetilde{v}_\varphi(\eta')\widetilde{v}_\varphi(\eta)\right] \mathcal{K}^{>*}(\eta,\eta') \Big\}. \end{aligned} \tag{D.18}$$

This equation was obtained in Eq. (A.17) from microphysical considerations and is just a convenient rewriting of Eq. (3.25). We want to solve it at order λ^4, *i.e.* drop all contributions of higher order. Since the right-hand side is already proportional to λ^4, this implies that it can be evaluated in the free theory, where $\widetilde{\rho}_{\mathrm{red}}(\eta) \simeq \widetilde{\rho}_{\mathrm{red}}(\eta_0)$. One can thus integrate Eq. (D.18), which leads to

$$\begin{aligned} \widetilde{\rho}^{(2)}_{\mathrm{red}}(\eta) =& \widetilde{\rho}_{\mathrm{red}}(\eta_0) - \lambda^4 \int_{\eta_0}^{\eta} \mathrm{d}\eta' a^2(\eta') \int_{\eta_0}^{\eta'} \mathrm{d}\eta'' a^2(\eta'') \\ & \Big\{ \left[\widetilde{v}_\varphi(\eta')\widetilde{v}_\varphi(\eta'')\widetilde{\rho}_{\mathrm{red}}(\eta_0) - \widetilde{v}_\varphi(\eta'')\widetilde{\rho}_{\mathrm{red}}(\eta_0)\widetilde{v}_\varphi(\eta')\right] v_\chi(\eta') v^*_\chi(\eta'') \\ & - \left[\widetilde{v}_\varphi(\eta')\widetilde{\rho}_{\mathrm{red}}(\eta_0)\widetilde{v}_\varphi(\eta'') - \widetilde{\rho}_{\mathrm{red}}(\eta_0)\widetilde{v}_\varphi(\eta'')\widetilde{v}_\varphi(\eta')\right] v^*_\chi(\eta') v_\chi(\eta'') \Big\}, \end{aligned} \tag{D.19}$$

where we have used that the memory kernels are related to the free mode functions via Eq. (A.15).

Let us now compute the entries of the covariance matrix using this expression for $\widetilde{\rho}^{(2)}_{\mathrm{red}}$. The configuration-configuration power spectrum reads

$$\boldsymbol{\Sigma}^{(2)}_{\mathrm{TCL},11}(\eta) = \mathrm{Tr}\left[\widetilde{v}_\varphi(\eta)\widetilde{v}_\varphi(\eta)\widetilde{\rho}^{(2)}_{\mathrm{red}}(\eta)\right], \tag{D.20}$$

that is

$$\begin{aligned} \boldsymbol{\Sigma}^{(2)}_{\mathrm{TCL},11}(\eta) =& \mathrm{Tr}\left[\widetilde{v}_\varphi(\eta)\widetilde{v}_\varphi(\eta)\widetilde{\rho}_{\mathrm{red}}(\eta_0)\right] \\ & - \lambda^4 \int_{\eta_0}^{\eta} \mathrm{d}\eta' a^2(\eta') v_\chi(\eta') \int_{\eta_0}^{\eta'} \mathrm{d}\eta'' a^2(\eta'') v^*_\chi(\eta'') \\ & \left\{ \mathrm{Tr}\left[\widetilde{v}_\varphi(\eta)\widetilde{v}_\varphi(\eta)\widetilde{v}_\varphi(\eta')\widetilde{v}_\varphi(\eta'')\widetilde{\rho}_{\mathrm{red}}(\eta_0)\right] - \mathrm{Tr}\left[\widetilde{v}_\varphi(\eta)\widetilde{v}_\varphi(\eta)\widetilde{v}_\varphi(\eta'')\widetilde{\rho}_{\mathrm{red}}(\eta_0)\widetilde{v}_\varphi(\eta')\right] \right\} \\ & + \lambda^4 \int_{\eta_0}^{\eta} \mathrm{d}\eta' a^2(\eta') v^*_\chi(\eta') \int_{\eta_0}^{\eta'} \mathrm{d}\eta'' a^2(\eta'') v_\chi(\eta'') \\ & \left\{ \mathrm{Tr}\left[\widetilde{v}_\varphi(\eta)\widetilde{v}_\varphi(\eta)\widetilde{v}_\varphi(\eta')\widetilde{\rho}_{\mathrm{red}}(\eta_0)\widetilde{v}_\varphi(\eta'')\right] - \mathrm{Tr}\left[\widetilde{v}_\varphi(\eta)\widetilde{v}_\varphi(\eta)\widetilde{\rho}_{\mathrm{red}}(\eta_0)\widetilde{v}_\varphi(\eta'')\widetilde{v}_\varphi(\eta')\right] \right\}. \end{aligned} \tag{D.21}$$

Since the initial state is the Bunch-Davies vacuum, $\widetilde{\rho}_{\rm red}(\eta_0) = |\emptyset\rangle\langle\emptyset|$, using the mode-function decomposition (3.27) one obtains

$$\begin{aligned}\boldsymbol{\Sigma}^{(2)}_{\rm TCL,11}(\eta) =& |v_\varphi(\eta)|^2 \\ &- 4\lambda^4 \Re\mathrm{e}\left[v_\varphi^2(\eta)\int_{\eta_0}^{\eta}\mathrm{d}\eta' a^2(\eta')v_\varphi^*(\eta')v_\chi(\eta')\int_{\eta_0}^{\eta'}\mathrm{d}\eta'' a^2(\eta'')v_\varphi^*(\eta'')v_\chi^*(\eta'')\right. \\ &\left.- |v_\varphi(\eta)|^2\int_{\eta_0}^{\eta}\mathrm{d}\eta' a^2(\eta')v_\varphi(\eta')v_\chi(\eta')\int_{\eta_0}^{\eta'}\mathrm{d}\eta'' a^2(\eta'')v_\varphi^*(\eta'')v_\chi^*(\eta'')\right].\end{aligned} \tag{D.22}$$

This expression matches Eq. (D.13), as can be shown by expanding the real and imaginary parts and relabeling the integration domain. Following the same method, one finds

$$\begin{aligned}\boldsymbol{\Sigma}^{(2)}_{\rm TCL,12}(\eta) =& \Re\mathrm{e}\left[v_\varphi(\eta)p_\varphi^*(\eta)\right] \\ &- 4\lambda^4\Re\mathrm{e}\left\{v_\varphi(\eta)p_\varphi(\eta)\int_{\eta_0}^{\eta}\mathrm{d}\eta' a^2(\eta')v_\varphi^*(\eta')v_\chi(\eta')\int_{\eta_0}^{\eta'}\mathrm{d}\eta'' a^2(\eta'')v_\varphi^*(\eta'')v_\chi^*\left(\eta''\right)\right. \\ &\left.- \Re\mathrm{e}\left[v_\varphi(\eta)p_\varphi^*(\eta)\right]\int_{\eta_0}^{\eta}\mathrm{d}\eta' a^2(\eta')v_\varphi(\eta')v_\chi(\eta')\int_{\eta_0}^{\eta'}\mathrm{d}\eta'' a^2(\eta'')v_\varphi^*(\eta'')v_\chi^*(\eta'')\right\},\end{aligned} \tag{D.23}$$

which can be shown to match Eq. (D.15), and

$$\begin{aligned}\boldsymbol{\Sigma}^{(2)}_{\rm TCL,22}(\eta) =& |p_\varphi(\eta)|^2 \\ &- 4\lambda^4 \Re\mathrm{e}\left[p_\varphi^2(\eta)\int_{\eta_0}^{\eta}\mathrm{d}\eta' a^2(\eta')v_\varphi^*(\eta')v_\chi(\eta')\int_{\eta_0}^{\eta'}\mathrm{d}\eta'' a^2(\eta'')v_\varphi^*(\eta'')v_\chi^*(\eta'')\right. \\ &\left.- |p_\varphi(\eta)|^2\int_{\eta_0}^{\eta}\mathrm{d}\eta' a^2(\eta')v_\varphi(\eta')v_\chi(\eta')\int_{\eta_0}^{\eta'}\mathrm{d}\eta'' a^2(\eta'')v_\varphi^*(\eta'')v_\chi^*(\eta'')\right],\end{aligned} \tag{D.24}$$

which can be shown to match Eq. (D.17).

E Comparison with other late-time resummation techniques

In this section, we compare TCL with the late-time resummation technique proposed in Ref. [44] and also studied in Ref. [59]. The idea is to keep track of the growing mode only, in order to simplify the analysis in the late-time limit. As we will make clear, the method also implicitly performs an additional layer of approximation compared to TCL, which makes it less efficient.

The starting point is to rewrite the free mode function

$$v_\varphi(z) = \frac{1}{2}\sqrt{\frac{\pi z}{k}}e^{i\frac{\pi}{2}\left(\nu_\varphi+\frac{1}{2}\right)}H^{(1)}_{\nu_\varphi}(z), \tag{E.1}$$

where we recall that $z = -k\eta$, as (see Eq. (10.4.3) of Ref. [101])

$$v_\varphi(z) = e^{i\frac{\pi}{2}\left(\nu_\varphi+\frac{1}{2}\right)}\frac{v_-(z)+iv_+(z)}{\sqrt{2}} \tag{E.2}$$

where

$$v_+(z) = \sqrt{\frac{\pi z}{2k}}Y_{\nu_\varphi}(z) \quad \text{and} \quad v_-(z) = \sqrt{\frac{\pi z}{2k}}J_{\nu_\varphi}(z) \tag{E.3}$$

are real functions. Here, J_ν and Y_ν are the Bessel functions of the first and second kind respectively, and of order ν. The reason why this decomposition is convenient is that v_- corresponds to the cosmological "decaying mode" [*i.e.* $v_-(\eta)$ decreases on super-Hubble scales], while v_+ stands for the growing mode. Let us recall that the heavy-field mode function cannot be divided into a growing mode and a decaying mode, since both modes oscillate with similar amplitude on super-Hubble scales.

In the interaction picture, where operators evolve as in the free theory, the mode-function expansion (3.27) of the field operators can then be written as

$$\widetilde{v}_\varphi(\eta) = v_\varphi(\eta)\widehat{a}_\varphi + v_\varphi^*(\eta)\widehat{a}_\varphi^\dagger \tag{E.4}$$

$$= v_-(\eta)\widehat{P}_\varphi + v_+(\eta)\widehat{Q}_\varphi\,, \tag{E.5}$$

where

$$\widehat{P}_\varphi = \frac{1}{\sqrt{2}}\left[e^{i\frac{\pi}{2}\left(\nu_\varphi+\frac{1}{2}\right)}\widehat{a}_\varphi + e^{-i\frac{\pi}{2}\left(\nu_\varphi+\frac{1}{2}\right)}\widehat{a}_\varphi^\dagger\right], \tag{E.6}$$

$$\widehat{Q}_\varphi = \frac{i}{\sqrt{2}}\left[e^{i\frac{\pi}{2}\left(\nu_\varphi+\frac{1}{2}\right)}\widehat{a}_\varphi - e^{-i\frac{\pi}{2}\left(\nu_\varphi+\frac{1}{2}\right)}\widehat{a}_\varphi^\dagger\right]. \tag{E.7}$$

One can check that they constitute a set of canonical variables since $\left[\widehat{Q}_\varphi, \widehat{P}_\varphi\right] = i$.

The idea proposed in Refs. [44, 59] is to insert the decomposition (E.5) into the TCL_2 master equation (3.25) in order to identify the leading late-time contribution. One finds

$$\begin{aligned}
\frac{\mathrm{d}\widetilde{\rho}_{\mathrm{red}}^{\mathrm{IR}}}{\mathrm{d}\eta} = -\lambda^4 a^2(\eta)\Big\{ & v_-(\eta)X_-^*(\eta)v_\chi(\eta)\left[\widehat{P}_\varphi^2\widetilde{\rho}_{\mathrm{red}}(\eta) - \widehat{P}_\varphi\widetilde{\rho}_{\mathrm{red}}(\eta)\widehat{P}_\varphi\right] \\
& + v_-(\eta)X_-(\eta)v_\chi^*(\eta)\left[\widetilde{\rho}_{\mathrm{red}}(\eta)\widehat{P}_\varphi^2 - \widehat{P}_\varphi\widetilde{\rho}_{\mathrm{red}}(\eta)\widehat{P}_\varphi\right] \\
& + v_+(\eta)X_-^*(\eta)v_\chi(\eta)\left[\widehat{Q}_\varphi\widehat{P}_\varphi\widetilde{\rho}_{\mathrm{red}}(\eta) - \widehat{P}_\varphi\widetilde{\rho}_{\mathrm{red}}(\eta)\widehat{Q}_\varphi\right] \\
& + v_+(\eta)X_-(\eta)v_\chi^*(\eta)\left[\widetilde{\rho}_{\mathrm{red}}(\eta)\widehat{P}_\varphi\widehat{Q}_\varphi - \widehat{Q}_\varphi\widetilde{\rho}_{\mathrm{red}}(\eta)\widehat{P}_\varphi\right] \\
& + v_-(\eta)X_+^*(\eta)v_\chi(\eta)\left[\widehat{P}_\varphi\widehat{Q}_\varphi\widetilde{\rho}_{\mathrm{red}}(\eta) - \widehat{Q}_\varphi\widetilde{\rho}_{\mathrm{red}}(\eta)\widehat{P}_\varphi\right] \\
& + v_-(\eta)X_+(\eta)v_\chi^*(\eta)\left[\widetilde{\rho}_{\mathrm{red}}(\eta)\widehat{Q}_\varphi\widehat{P}_\varphi - \widehat{P}_\varphi\widetilde{\rho}_{\mathrm{red}}(\eta)\widehat{Q}_\varphi\right] \\
& + v_+(\eta)X_+^*(\eta)v_\chi(\eta)\left[\widehat{Q}_\varphi^2\widetilde{\rho}_{\mathrm{red}}(\eta) - \widehat{Q}_\varphi\widetilde{\rho}_{\mathrm{red}}(\eta)\widehat{Q}_\varphi\right] \\
& + v_+(\eta)X_+(\eta)v_\chi^*(\eta)\left[\widetilde{\rho}_{\mathrm{red}}(\eta)\widehat{Q}_\varphi^2 - \widehat{Q}_\varphi\widetilde{\rho}_{\mathrm{red}}(\eta)\widehat{Q}_\varphi\right]\Big\},
\end{aligned} \tag{E.8}$$

where

$$X_+(\eta) \equiv \int_{\eta_0}^{\eta} \mathrm{d}\eta' a^2(\eta')v_+(\eta')v_\chi(\eta'), \tag{E.9}$$

$$X_-(\eta) \equiv \int_{\eta_0}^{\eta} \mathrm{d}\eta' a^2(\eta')v_-(\eta')v_\chi(\eta'). \tag{E.10}$$

The authors of Refs. [44, 59] argue that dropping the decaying-mode contributions constitutes a valid approximation in the infrared (IR) limit, and for this reason hereafter we label the quantities computed in this scheme with the superscript "IR".

In the interaction picture, the configuration-configuration power spectrum reads

$$\begin{aligned}\langle\widetilde{v}_\varphi(\eta)\widetilde{v}_\varphi(\eta)\rangle =& v_-(\eta)v_-(\eta)\left\langle\widehat{P}_\varphi^2\right\rangle + v_-(\eta)v_+(\eta)\left\langle\widehat{Q}_\varphi\widehat{P}_\varphi+\widehat{P}_\varphi\widehat{Q}_\varphi\right\rangle + v_+(\eta)v_+(\eta)\left\langle\widehat{Q}_\varphi^2\right\rangle \\ \simeq& v_+(\eta)v_+(\eta)\left\langle\widehat{Q}_\varphi^2\right\rangle,\end{aligned} \tag{E.11}$$

where in the second line we have neglected the decaying mode contribution. The next step is to compute $\left\langle\widehat{Q}_\varphi^2\right\rangle(\eta) = \mathrm{Tr}\left[\widehat{Q}_\varphi^2\widetilde{\rho}_{\rm red}(\eta)\right]$ with the IR master equation (E.8). Upon differentiating this expression with respect to time, one obtains

$$\frac{\mathrm{d}\left\langle\widehat{Q}_\varphi^2\right\rangle}{\mathrm{d}\eta} = \Gamma(\eta)\left\langle\widehat{Q}_\varphi^2\right\rangle \tag{E.12}$$

where

$$\Gamma(\eta) = 4\lambda^4 a^2(\eta)v_-(\eta)\Im\mathrm{m}\left[v_\chi(\eta)X_+^*(\eta)\right], \tag{E.13}$$

which gives rise to

$$\left\langle\widehat{Q}_\varphi^2\right\rangle(\eta) = e^{\int_{\eta_*}^{\eta}\mathrm{d}\eta'\Gamma(\eta')}\left\langle\widehat{Q}_\varphi^2\right\rangle(\eta_*). \tag{E.14}$$

Since we are interested in the late-time behaviour of the power spectra, we can assume $-k\eta \ll 1$ and let η_* denote the Hubble crossing time, $\eta_* \equiv -1/k$, if the above integral is dominated by its upper bound (hence does not depend much on the choice of the lower bound). If the effect of the interaction with the environment is small in sub-Hubble scales, as argued in Ref. [44] one can evaluate $\langle\widehat{Q}_\varphi^2\rangle(\eta_*)$ in the free theory, which simply yields

$$\left\langle\widehat{Q}_\varphi^2\right\rangle(\eta_*) \simeq 1\,. \tag{E.15}$$

In the super-Hubble limit, using the results derived in Appendix C.3, one can also approximate

$$X_+^*(z) \simeq \frac{\pi}{H^2}\frac{(-1)^{3/4}}{\nu_\varphi^2+\mu_\chi^2}\frac{z^{-\nu_\varphi}}{\sin(\pi\nu_\varphi)\Gamma(1-\nu_\varphi)}\left[\nu_\varphi\left(\gamma_{\mu_\chi}^*+\delta_{\mu_\chi}^*\right) - i\mu_\chi\left(\gamma_{\mu_\chi}^*-\delta_{\mu_\chi^*}\right)\right]e^{-\pi\mu_\chi}, \tag{E.16}$$

where γ_μ and δ_μ were defined in Eq. (C.45). This leads to

$$\Gamma(z) = \frac{\pi}{2\nu_\varphi}\frac{1}{\nu_\varphi^2+\mu_\chi^2}\frac{\lambda^4}{H^4}\frac{k}{z}\mu_\chi\left(\left|\gamma_{\mu_\chi}\right|^2-\left|\delta_{\mu_\chi}\right|^2\right)e^{-\pi\mu_\chi}, \tag{E.17}$$

where $|\gamma_{\mu_\chi}|^2 - |\delta_{\mu_\chi}|^2 = 2e^{\pi\mu_\chi}/(\pi\mu_\chi)$. One thus has

$$\int_{\eta_*}^{\eta}\mathrm{d}\eta'\Gamma(\eta') \simeq -\frac{1}{\nu_\varphi}\frac{1}{\nu_\varphi^2+\mu_\chi^2}\frac{\lambda^4}{H^4}\ln(-k\eta), \tag{E.18}$$

which one can check does not depend on the detailed choice of η_* as announced above. Combining the above results, one obtains

$$\boldsymbol{\Sigma}_{\mathrm{IR},11}(\eta) = e^{-\frac{1}{\nu_\varphi}\frac{1}{\nu_\varphi^2+\mu_\chi^2}\frac{\lambda^4}{H^4}\ln(-k\eta)}|v_\varphi(\eta)|^2. \tag{E.19}$$

The configuration-momentum and momentum-momentum power spectra can be computed along similar lines. Starting from

$$\widetilde{p}_\varphi(\eta) = p_+(\eta)\widehat{Q}_\varphi + p_-(\eta)\widehat{P}_\varphi \tag{E.20}$$

and using the fact that $p_+ = v'_+ - (a'/a)v_+$ and $p_- = v'_- - (a'/a)v_-$ are still growing and decaying respectively, one has

$$\langle \widetilde{v}_\varphi(\eta)\widetilde{p}_\varphi(\eta)\rangle \simeq v_+(\eta)p_+(\eta)\left\langle \widehat{Q}^2_\varphi\right\rangle , \tag{E.21}$$

$$\langle \widetilde{p}_\varphi(\eta)\widetilde{p}_\varphi(\eta)\rangle \simeq p_+(\eta)p_+(\eta)\left\langle \widehat{Q}^2_\varphi\right\rangle . \tag{E.22}$$

This implies that the same correction is obtained for all power spectra, *i.e.*

$$\boldsymbol{\Sigma}_{\mathrm{IR},11}(\eta) = e^{-\frac{1}{\nu_\varphi}\frac{1}{\nu_\varphi^2+\mu_\chi^2}\frac{\lambda^4}{H^4}\ln(-k\eta)}|v_\varphi(\eta)|^2, \tag{E.23}$$

$$\boldsymbol{\Sigma}_{\mathrm{IR},12}(\eta) = e^{-\frac{1}{\nu_\varphi}\frac{1}{\nu_\varphi^2+\mu_\chi^2}\frac{\lambda^4}{H^4}\ln(-k\eta)}\Re\mathrm{e}\left[v_\varphi(\eta)p^*_\varphi(\eta)\right], \tag{E.24}$$

$$\boldsymbol{\Sigma}_{\mathrm{IR},22}(\eta) = e^{-\frac{1}{\nu_\varphi}\frac{1}{\nu_\varphi^2+\mu_\chi^2}\frac{\lambda^4}{H^4}\ln(-k\eta)}|p_\varphi(\eta)|^2. \tag{E.25}$$

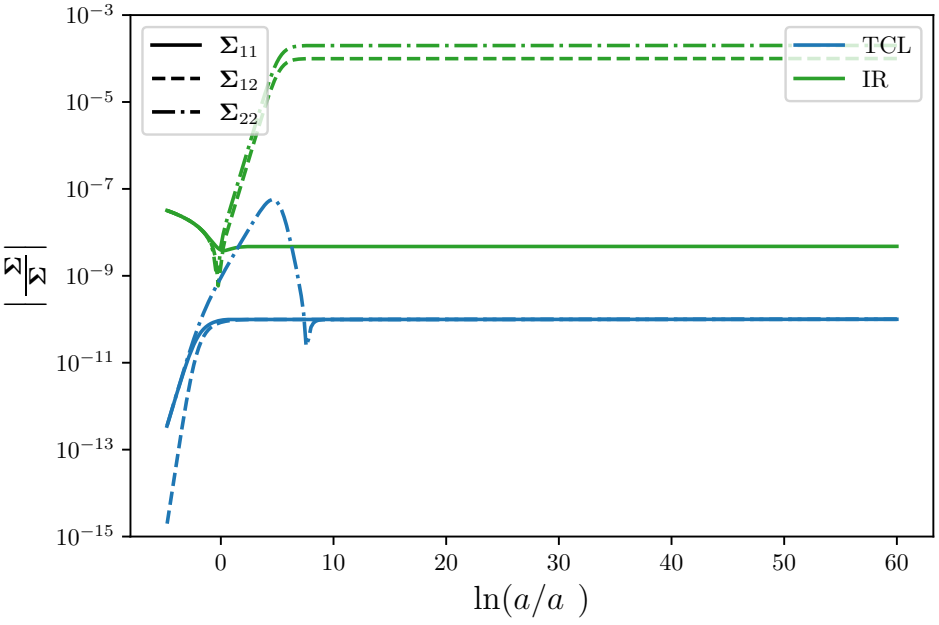

Figure 5. Relative error in the three power spectra for TCL_2 (blue curves) and the IR resummation method presented in Appendix E (green curves). The parameters are taken as $m^2 = 10^{-4}H^2$, $M^2 = 10^3H^2$ and $\lambda^2 = 10^{-3}H^2$.

These expressions feature manifest resummations over powers of $\ln(a)$, which we now compare with the resummation performed by the TCL_2 master equation. The relative difference between the three power spectra and their exact counterpart is displayed in Fig. 5, both for TCL_2 (blue curves)[13] and IR (green curves).

[13]Let us note that at late time, the relative error in TCL asymptotes a constant in Fig. 5, hence it is not described by Eq. (4.8). The reason is that Eq. (4.8) captures the error in the growth rate, while for the parameters displayed in Fig. 5 the error in the overall amplitude provides the dominant contribution.

Let us first note that the growth rate of the power spectra is correctly captured in the IR approach, even at strong coupling where the perturbative result usually breaks down. This can be further understood by noting that Eqs. (E.23)-(E.25) take the same form as Eq. (4.6) with

$$\nu_{\rm IR} = \frac{1}{2\nu_\varphi}\frac{1}{\nu_\varphi^2+\mu_\chi^2}\left(\frac{\lambda}{H}\right)^4 + \nu_\varphi\,, \tag{E.26}$$

while according to footnote 11, in TCL_2 one has

$$\nu_{\rm LS} = \frac{3}{2}\sqrt{1-\left(\frac{2m_{\rm LS}}{3H}\right)^2} \quad \text{where} \quad m_{\rm LS}^2 = m^2 - \frac{\lambda^4}{M^2-m^2} \tag{E.27}$$

and we recall that in the exact theory

$$\nu_\ell = \frac{3}{2}\sqrt{1-\left(\frac{2m_\ell}{3H}\right)^2} \quad \text{where} \quad m_\ell^2 = \frac{1}{2}\left[m^2+M^2-\left(M^2-m^2\right)\sqrt{1+\left(\frac{2\lambda^2}{M^2-m^2}\right)^2}\right]. \tag{E.28}$$

Since Eqs. (E.26), (E.27) and (E.28) coincide when expanded at first order in λ^4, one concludes that, at the level of the growth rate, the Lamb-shift renormalisation of the mass is correctly accounted for in the IR approach [44] as for TCL, at least at leading order in the coupling constant. This is similar to the dynamical renormalisation group (DRG) treatment of late-time secular divergences in de Sitter performed in Refs. [56–58], as pointed out in Refs. [44, 46, 59].

The IR approach however fails to reproduce the overall amplitude of the power spectra beyond the perturbative level, which explains why it does not perform as well as TCL. Let us also note that another disadvantage of the IR method is that it does not allow one to track decoherence, which as explained in Sec. 4.2 is not driven by the growing modes.

References

[1] Planck collaboration, *Planck 2018 results. X. Constraints on inflation*, *Astron. Astrophys.* **641** (2020) A10 [1807.06211].

[2] J. Martin, C. Ringeval and V. Vennin, *Encyclopædia Inflationaris*, *Phys. Dark Univ.* **5-6** (2014) 75 [1303.3787].

[3] L. Amendola et al., *Cosmology and fundamental physics with the Euclid satellite*, *Living Rev. Rel.* **21** (2018) 2 [1606.00180].

[4] SKA Cosmology SWG collaboration, *Overview of Cosmology with the SKA*, *PoS* **AASKA14** (2015) 016 [1501.04076].

[5] D.H. Lyth and D. Wands, *Generating the curvature perturbation without an inflaton*, *Phys. Lett.* **B524** (2002) 5 [hep-ph/0110002].

[6] K. Enqvist, R.J. Hardwick, T. Tenkanen, V. Vennin and D. Wands, *A novel way to determine the scale of inflation*, *JCAP* **02** (2018) 006 [1711.07344].

[7] C. Ringeval, T. Suyama, T. Takahashi, M. Yamaguchi and S. Yokoyama, *Dark energy from primordial inflationary quantum fluctuations*, *Phys. Rev. Lett.* **105** (2010) 121301 [1006.0368].

[8] C. Kiefer, F. Queisser and A.A. Starobinsky, *Cosmological Constant from Decoherence*, *Class. Quant. Grav.* **28** (2011) 125022 [1010.5331].

[9] R.H. Brandenberger, V.F. Mukhanov and T. Prokopec, *Entropy of a classical stochastic field and cosmological perturbations*, *Phys. Rev. Lett.* **69** (1992) 3606 [astro-ph/9206005].

[10] A.O. Barvinsky, A.Y. Kamenshchik, C. Kiefer and I.V. Mishakov, *Decoherence in quantum cosmology at the onset of inflation*, *Nucl. Phys. B* **551** (1999) 374 [gr-qc/9812043].

[11] F.C. Lombardo and D. Lopez Nacir, *Decoherence during inflation: The Generation of classical inhomogeneities*, *Phys. Rev. D* **72** (2005) 063506 [gr-qc/0506051].

[12] C. Kiefer, I. Lohmar, D. Polarski and A.A. Starobinsky, *Pointer states for primordial fluctuations in inflationary cosmology*, *Class. Quant. Grav.* **24** (2007) 1699 [astro-ph/0610700].

[13] P. Martineau, *On the decoherence of primordial fluctuations during inflation*, *Class. Quant. Grav.* **24** (2007) 5817 [astro-ph/0601134].

[14] C.P. Burgess, R. Holman and D. Hoover, *Decoherence of inflationary primordial fluctuations*, *Phys. Rev. D* **77** (2008) 063534 [astro-ph/0601646].

[15] T. Prokopec and G.I. Rigopoulos, *Decoherence from Isocurvature perturbations in Inflation*, *JCAP* **11** (2007) 029 [astro-ph/0612067].

[16] E. Nelson, *Quantum Decoherence During Inflation from Gravitational Nonlinearities*, *JCAP* **03** (2016) 022 [1601.03734].

[17] J. Martin and V. Vennin, *Observational constraints on quantum decoherence during inflation*, *JCAP* **05** (2018) 063 [1801.09949].

[18] J. Martin and V. Vennin, *Non Gaussianities from Quantum Decoherence during Inflation*, *JCAP* **06** (2018) 037 [1805.05609].

[19] W.H. Zurek, *Pointer Basis of Quantum Apparatus: Into What Mixture Does the Wave Packet Collapse?*, *Phys. Rev. D* **24** (1981) 1516.

[20] W.H. Zurek, *Environment induced superselection rules*, *Phys. Rev. D* **26** (1982) 1862.

[21] E. Joos and H. Zeh, *The Emergence of classical properties through interaction with the environment*, *Z. Phys. B* **59** (1985) 223.

[22] T.J. Hollowood and J.I. McDonald, *Decoherence, discord and the quantum master equation for cosmological perturbations*, *Phys. Rev. D* **95** (2017) 103521 [1701.02235].

[23] J. Martin, A. Micheli and V. Vennin, *Discord and decoherence*, *JCAP* **04** (2022) 051 [2112.05037].

[24] D. Koks, A. Matacz and B. Hu, *Entropy and uncertainty of squeezed quantum open systems*, *Phys. Rev. D* **55** (1997) 5917 [quant-ph/9612016].

[25] C. Anastopoulos and B.L. Hu, *A Master Equation for Gravitational Decoherence: Probing the Textures of Spacetime*, *Class. Quant. Grav.* **30** (2013) 165007 [1305.5231].

[26] M. Fukuma, Y. Sakatani and S. Sugishita, *Master equation for the Unruh-DeWitt detector and the universal relaxation time in de Sitter space*, *Phys. Rev. D* **89** (2014) 064024 [1305.0256].

[27] C. Cheung, P. Creminelli, A.L. Fitzpatrick, J. Kaplan and L. Senatore, *The Effective Field Theory of Inflation*, *JHEP* **03** (2008) 014 [0709.0293].

[28] X. Chen and Y. Wang, *Quasi-Single Field Inflation and Non-Gaussianities*, *JCAP* **04** (2010) 027 [0911.3380].

[29] L. Senatore and M. Zaldarriaga, *The Effective Field Theory of Multifield Inflation*, *JHEP* **04** (2012) 024 [1009.2093].

[30] V. Assassi, D. Baumann, D. Green and L. McAllister, *Planck-Suppressed Operators*, *JCAP* **01** (2014) 033 [1304.5226].

[31] N. Arkani-Hamed and J. Maldacena, *Cosmological Collider Physics*, 1503.08043.

[32] S. Shandera, N. Agarwal and A. Kamal, *Open quantum cosmological system*, *Phys. Rev. D* **98** (2018) 083535 [1708.00493].

[33] S. Akhtar, S. Choudhury, S. Chowdhury, D. Goswami, S. Panda and A. Swain, *Open Quantum Entanglement: A study of two atomic system in static patch of de Sitter space*, *Eur. Phys. J. C* **80** (2020) 748 [1908.09929].

[34] C.P. Burgess, *Introduction to Effective Field Theory*, Cambridge University Press (12, 2020), 10.1017/9781139048040.

[35] S. Banerjee, S. Choudhury, S. Chowdhury, R.N. Das, N. Gupta, S. Panda et al., *Indirect detection of Cosmological Constant from interacting open quantum system*, *Annals Phys.* **443** (2022) 168941 [2004.13058].

[36] L. Pinol, S. Aoki, S. Renaux-Petel and M. Yamaguchi, *Inflationary flavor oscillations and the cosmic spectroscopy*, 2112.05710.

[37] J. Oppenheim, C. Sparaciari, B. Šoda and Z. Weller-Davies, *Gravitationally induced decoherence vs space-time diffusion: testing the quantum nature of gravity*, 2203.01982.

[38] G.L. Pimentel and D.-G. Wang, *Boostless Cosmological Collider Bootstrap*, 2205.00013.

[39] S. Jazayeri and S. Renaux-Petel, *Cosmological Bootstrap in Slow Motion*, 2205.10340.

[40] S. Brahma, A. Berera and J. Calderón-Figueroa, *Quantum corrections to the primordial tensor spectrum: Open EFTs & Markovian decoupling of UV modes*, 2206.05797.

[41] H.P. Breuer and F. Petruccione, *The theory of open quantum systems*, Oxford University Press (2002), 10.1093/acprof:oso/9780199213900.001.0001.

[42] E.A. Calzetta and B.-L.B. Hu, *Nonequilibrium Quantum Field Theory*, Cambridge Monographs on Mathematical Physics, Cambridge University Press (9, 2008), 10.1017/CBO9780511535123.

[43] C.P. Burgess, R. Holman, G. Tasinato and M. Williams, *EFT Beyond the Horizon: Stochastic Inflation and How Primordial Quantum Fluctuations Go Classical*, *JHEP* **03** (2015) 090 [1408.5002].

[44] D. Boyanovsky, *Effective field theory during inflation: Reduced density matrix and its quantum master equation*, *Phys. Rev.* **D92** (2015) 023527 [1506.07395].

[45] D. Boyanovsky, *Effective field theory during inflation. II. Stochastic dynamics and power spectrum suppression*, *Phys. Rev. D* **93** (2016) 043501 [1511.06649].

[46] C. Burgess, R. Holman and G. Tasinato, *Open EFTs, IR effects & late-time resummations: systematic corrections in stochastic inflation*, *JHEP* **01** (2016) 153 [1512.00169].

[47] G. Kaplanek, C.P. Burgess and R. Holman, *Qubit heating near a hotspot*, *JHEP* **08** (2021) 132 [2106.10803].

[48] S. Chaykov, N. Agarwal, S. Bahrami and R. Holman, *Loop corrections in Minkowski spacetime away from equilibrium 1: Late-time resummations*, 2206.11288.

[49] S. Chaykov, N. Agarwal, S. Bahrami and R. Holman, *Loop corrections in Minkowski spacetime away from equilibrium 2: Finite-time results*, 2206.11289.

[50] J. Martin, *Inflationary perturbations: The Cosmological Schwinger effect*, *Lect. Notes Phys.* **738** (2008) 193 [0704.3540].

[51] J.-T. Hsiang and B.-L. Hu, *Fluctuation-Dissipation Relation for a Quantum Brownian Oscillator in a Parametrically Squeezed Thermal Field*, 2107.13343.

[52] T. Colas, J. Grain and V. Vennin, *Four-mode squeezed states: two-field quantum systems and the symplectic group* $\mathrm{Sp}(4,\mathbb{R})$, *Eur. Phys. J. C* **82** (2022) 6 [2104.14942].

[53] S. Banerjee, S. Choudhury, S. Chowdhury, J. Knaute, S. Panda and K. Shirish, *Thermalization Phenomena in Quenched Quantum Brownian Motion in De Sitter Space*, 2104.10692.

[54] G. Lindblad, *On the Generators of Quantum Dynamical Semigroups*, *Commun. Math. Phys.* **48** (1976) 119.

[55] G. Kaplanek and E. Tjoa, *Mapping Markov: On effective master equations for two accelerated qubits*, 2207.13750.

[56] D. Boyanovsky, H.J. de Vega, R. Holman and M. Simionato, *Dynamical renormalization group resummation of finite temperature infrared divergences*, *Phys. Rev. D* **60** (1999) 065003 [hep-ph/9809346].

[57] C.P. Burgess, L. Leblond, R. Holman and S. Shandera, *Super-Hubble de Sitter Fluctuations and the Dynamical RG*, *JCAP* **03** (2010) 033 [0912.1608].

[58] D. Green and A. Premkumar, *Dynamical RG and Critical Phenomena in de Sitter Space*, *JHEP* **04** (2020) 064 [2001.05974].

[59] S. Brahma, A. Berera and J. Calderón-Figueroa, *Universal signature of quantum entanglement across cosmological distances*, 2107.06910.

[60] A.O. Caldeira and A.J. Leggett, *Influence of dissipation on quantum tunneling in macroscopic systems*, *Phys. Rev. Lett.* **46** (1981) 211.

[61] A.O. Caldeira and A.J. Leggett, *Quantum tunneling in a dissipative system*, *Annals Phys.* **149** (1983) 374.

[62] A.O. Caldeira and A.J. Leggett, *Path integral approach to quantum Brownian motion*, *Physica A* **121** (1983) 587.

[63] S. Choudhury, S. Panda, N. Pandey and A. Roy, *Four-mode squeezed states in de Sitter space: A study with two field interacting quantum system*, 2203.15815.

[64] T.S. Bunch and P.C.W. Davies, *Quantum Field Theory in de Sitter Space: Renormalization by Point Splitting*, *Proc. Roy. Soc. Lond.* **A360** (1978) 117.

[65] J. Grain and V. Vennin, *Squeezing formalism and canonical transformations in cosmology*, *JCAP* **2002** (2020) 022 [1910.01916].

[66] B.L. Hu and A. Matacz, *Quantum Brownian motion in a bath of parametric oscillators: A Model for system - field interactions*, *Phys. Rev. D* **49** (1994) 6612 [gr-qc/9312035].

[67] B.L. Hu, J.P. Paz and Y. Zhang, *Quantum brownian motion in a general environment: Exact master equation with nonlocal dissipation and colored noise*, *Phys. Rev. D* **45** (1992) 2843.

[68] J.J. Halliwell and T. Yu, *Alternative derivation of the hu-paz-zhang master equation of quantum brownian motion*, *Phys. Rev. D* **53** (1996) 2012.

[69] Y.-W. Huang and W.-M. Zhang, *Exact Master Equation for Quantum Brownian Motion with Generalization to Momentum-Dependent System-Environment Couplings*, 2204.09965.

[70] L. Ferialdi, *Exact closed master equation for gaussian non-markovian dynamics*, *Physical Review Letters* **116** (2016) .

[71] L. Diósi and L. Ferialdi, *General non-markovian structure of gaussian master and stochastic schrödinger equations*, *Physical Review Letters* **113** (2014) .

[72] R.S. Whitney, *Staying positive: going beyond Lindblad with perturbative master equations*, *Journal of Physics A Mathematical General* **41** (2008) 175304 [0711.0074].

[73] H.-P. Breuer, E.-M. Laine, J. Piilo and B. Vacchini, *Colloquium: Non-markovian dynamics in open quantum systems*, *Rev. Mod. Phys.* **88** (2016) 021002.

[74] D. Moustos and C. Anastopoulos, *Non-Markovian time evolution of an accelerated qubit*, *Phys. Rev. D* **95** (2017) 025020 [1611.02477].

[75] F. Nicacio and R.N.P. Maia, *Gauge Quantum Thermodynamics of Time-local non-Markovian Evolutions*, 2204.02966.

[76] S. Prudhoe and S. Shandera, *Classifying the non-Markovian, non-time-local, and entangling dynamics of an open quantum system*, 2201.07080.

[77] G. Spaventa and P. Verrucchi, *Nature and origin of the operators entering the master equation of an open quantum system*, 2209.14209.

[78] D. Chruściński, *Dynamical maps beyond Markovian regime*, 2209.14902.

[79] C.A. Brasil, F.F. Fanchini and R.d.J. Napolitano, *A simple derivation of the lindblad equation*, *Revista Brasileira de Ensino de Física* **35** (2013) 01–09.

[80] D. Manzano, *A short introduction to the lindblad master equation*, *AIP Advances* **10** (2020) 025106.

[81] D. Baumann and D. Green, *Equilateral Non-Gaussianity and New Physics on the Horizon*, *JCAP* **09** (2011) 014 [1102.5343].

[82] S. Garcia-Saenz and S. Renaux-Petel, *Flattened non-Gaussianities from the effective field theory of inflation with imaginary speed of sound*, *JCAP* **11** (2018) 005 [1805.12563].

[83] F.C. Lombardo, *Influence functional approach to decoherence during inflation*, *Braz. J. Phys.* **35** (2005) 391 [gr-qc/0412069].

[84] M.G. Jackson and K. Schalm, *Model Independent Signatures of New Physics in the Inflationary Power Spectrum*, *Phys. Rev. Lett.* **108** (2012) 111301 [1007.0185].

[85] M.G. Jackson, *Integrating out Heavy Fields in Inflation*, 1203.3895.

[86] D. Boyanovsky, *Information loss in effective field theory: entanglement and thermal entropies*, *Phys. Rev. D* **97** (2018) 065008 [1801.06840].

[87] D. Boyanovsky, *Imprint of entanglement entropy in the power spectrum of inflationary fluctuations*, *Phys. Rev. D* **98** (2018) 023515 [1804.07967].

[88] C. Burrage, C. Käding, P. Millington and J. Minář, *Open quantum dynamics induced by light scalar fields*, *Phys. Rev. D* **100** (2019) 076003 [1812.08760].

[89] C. Burrage, C. Käding, P. Millington and J. Minář, *Influence functionals, decoherence and conformally coupled scalars*, *J. Phys. Conf. Ser.* **1275** (2019) 012041 [1902.09607].

[90] L. Pinol, S. Renaux-Petel and Y. Tada, *A manifestly covariant theory of multifield stochastic inflation in phase space: solving the discretisation ambiguity in stochastic inflation*, *JCAP* **04** (2021) 048 [2008.07497].

[91] S. Choudhury, S. Dey, R.M. Gharat, S. Mandal and N. Pandey, *Schwinger-Keldysh path integral formalism for a Quenched Quantum Inverted Oscillator*, 2210.01134.

[92] C. Käding and M. Pitschmann, *A new method for directly computing reduced density matrices*, 2204.08829.

[93] H.-P. Breuer, A. Ma and F. Petruccione, *Time-local master equations: influence functional and cumulant expansion*, *arXiv e-prints* (2002) quant [quant-ph/0209153].

[94] D. Boyanovsky, *Effective Field Theory out of Equilibrium: Brownian quantum fields*, *New J. Phys.* **17** (2015) 063017 [1503.00156].

[95] A. Kamenev and A. Levchenko, *Keldysh technique and non-linear sigma model: basic principles and applications*, *Advances in Physics* **58** (2009) 197–319.

[96] W.B. Case, *Wigner functions and weyl transforms for pedestrians*, *American Journal of Physics* **76** (2008) 937 [https://doi.org/10.1119/1.2957889].

[97] C.P. Burgess, *Introduction to Effective Field Theory*, *Ann. Rev. Nucl. Part. Sci.* **57** (2007) 329 [hep-th/0701053].

[98] C.P. Burgess, R. Holman and G. Kaplanek, *Quantum Hotspots: Mean Fields, Open EFTs, Nonlocality and Decoherence Near Black Holes*, *Fortsch. Phys.* **2022** (2021) 2200019 [2106.10804].

[99] S. Pi and M. Sasaki, *Curvature Perturbation Spectrum in Two-field Inflation with a Turning Trajectory*, *JCAP* **10** (2012) 051 [1205.0161].

[100] R. Simon, E.C.G. Sudarshan and N. Mukunda, *Gaussian-wigner distributions in quantum mechanics and optics*, *Phys. Rev. A* **36** (1987) 3868.

[101] "*NIST Digital Library of Mathematical Functions*." http://dlmf.nist.gov/, Release 1.1.6 of 2022-06-30.

Chapter 6

Quantum recoherence in the early universe

Preface

In this Letter, we answer the question of knowing if entropic perturbations lead to quantum decoherence of the curvature perturbations. Depending on the mass of the entropic perturbations, one can either observe quantum decoherence for light environments $m < 3H/2$ or quantum recoherence for heavy environments $m > 3H/2$.

The model we consider is generic in the sense it encompasses all multifield models of inflation, written in adiabatic and entropic basis, focusing on the linear coupling between the curvature perturbations and the first entropic sector as discussed along Eq. (2.102). When $\mathcal{F}$ is heavy, the field is stabilised at the bottom of its potential and becomes proportional to $\dot{\zeta}$ on super-Hubble scales. It this case, the coupling proportional to $\dot{\zeta}\mathcal{F}$ becomes inefficient, the heavy field decouples from the dynamics of the adiabatic sector and quantum recoherence occurs. On the contrary, when the field is light, it acquires a growing mode such that the coupling keeps generating entangled pairs of quanta between the adiabatic and entropic sectors on super-Hubble scale, driving an effective phase of decoherence.

On the top of solving this model numerically using the exact transport equations, we also derive an Open EFT for the adiabatic sector. The unitary part reduces to the standard WEFT on super-Hubble scales where the effects of the heavy field is captured by an effective speed of sound for the adiabatic sector. In this case, there is no secular correction to resum and, despite working remarkably well at the perturbative level, the master equation resummation introduces small errors which lead to a positivity violation at late-time.

Finally, we stress that both recoherence and decoherence are equally surprising compared to the flat-space expectation that the only way to reach a form of irreversibility is to increase the size of the environment up to a thermodynamical limit where the Poincaré recurrence time is infinite. In cosmology, the lack of volume conservation allow us to evade Poincaré theorem. Due to the presence of a dynamical background, cosmological OQS rather compare to driven OQS than standard OQS.

The article [154] can be found online at:

- https://iopscience.iop.org/article/10.1209/0295-5075/acdd94 (published version);
- https://arxiv.org/abs/2212.09486 (arXiv version).

Quantum recoherence in the early universe

Thomas Colas,[1,2] Julien Grain,[1] and Vincent Vennin[3,2]

[1] *Université Paris-Saclay, CNRS, Institut d'Astrophysique Spatiale, 91405, Orsay, France*
[2] *Laboratoire Astroparticule et Cosmologie, Université Denis Diderot Paris 7, 10 rue Alice Domon et Léonie Duquet, 75013 Paris, France*
[3] *Laboratoire de Physique de l'Ecole Normale Supérieure, ENS, CNRS, Université PSL, Sorbonne Université, Université Paris Cité, F-75005 Paris, France*

Despite being created through a fundamentally quantum-mechanical process, cosmological structures have not yet revealed any sign of genuine quantum correlations. Among the obstructions to the direct detection of quantum signatures in cosmology, environmental-induced decoherence is arguably one of the most inevitable. Yet, we discover a mechanism of quantum recoherence for the adiabatic perturbations when they couple to an entropic sector. After a transient phase of decoherence, a turning point is reached, recoherence proceeds and adiabatic perturbations exhibit a large amount of self-coherence at late-time. This result is also understood by means of a non-Markovian master equation, which reduces to Wilsonian effective-field theory in the unitary limit. This allows us to critically assess the validity of open-quantum-system methods in cosmology and to highlight that re(de)coherence from linear interactions has no flat-space analogue.

Our current understanding of cosmology traces back the origin of structures to quantum fluctuations in the primordial vacuum. Not only inflation, the leading scenario [1–13], but also most alternatives [14–17] rely on this mechanism. However, whether or not one can prove (or disprove) the quantum origin of cosmological inhomogeneities remains an open issue [18–29]. Independently of the observational challenge it may constitute, it is generally argued [30–46] that any genuine quantum signature is likely to be erased by the quantum decoherence [47–49] induced by environmental degrees of freedom. This is why studying decoherence channels [50–61] has become of primary importance to assess the severity of this potential obstruction. Recent progresses in the cosmological open-quantum-system program provide this line of investigation with a robust toolbox, which nonetheless needs to be adapted and benchmarked since cosmology tends to break some of the assumptions it otherwise rests on [62–64]. In this Letter, we investigate the decoherence process in arguably one of the most generic extensions to single-field slow-roll inflation [65–72]. Contrary to common wisdom, we discover that, after a transient phase of decoherence, *recoherence* takes place and the final state exhibits large levels of self-coherence. Notably, this result has no flat-space analogue.

Heavy fields are ubiquitous when inflation is embedded in high-energy constructions, both from a model-building perspective [70–81] and from an effective-field-theory (EFT) approach [65–69, 82]. From a bottom-up viewpoint, the dynamics of the fluctuations in the adiabatic direction ζ and the entropic direction $\mathcal{F}$ is given at linear order by [68]

$$\begin{aligned}\mathcal{L} =& a^2\epsilon M_{\rm Pl}^2\zeta'^2 - a^2\epsilon M_{\rm Pl}^2\left(\partial_i\zeta\right)^2 + \frac{1}{2}a^2\mathcal{F}'^2 \\ &- \frac{1}{2}a^2\left(\partial_i\mathcal{F}\right)^2 - \frac{1}{2}m^2a^4\mathcal{F}^2 - \rho a^3\sqrt{2\epsilon}M_{\rm Pl}\zeta'\mathcal{F}.\end{aligned} \tag{1}$$

The Lagrangian density $\mathcal{L}$ is expressed in conformal time η, primes denote derivative with respect to η and $\left(\partial_i\zeta\right)^2 \equiv \delta_{ij}\partial_i\zeta\partial_j\zeta$. Finally, a is the scale factor, ϵ the first slow-roll parameter and $M_{\rm Pl}$ the Planck mass. The massless degree of freedom ζ is the curvature perturbation and is directly observed in the cosmic microwave background (CMB) [83, 84] and the large-scale structure of the universe [85–88]. The coupling ρ corresponds to the rate of turn in field space and mixes the adiabatic and entropic directions. It is constant at leading order in slow roll [77–80], and when a specific model is considered, it can be related to its microphysical parameters [65–67]. From an EFT perspective, $\zeta'\mathcal{F}$ is the only operator compatible with the shift symmetry of the Goldstone mode and with spatial homogeneity of the background [68], hence Eq. (1) captures the leading effect in the derivative expansion of generic multiple-field models [71].

This setting has mostly been studied from a phenomenological perspective, *i.e.* focusing on calculations of the observable power spectrum using the in-in formalism [77–80] or by means of single-field Wilsonian EFTs [65–69]. The latter approaches incorporate unitary effects only, hence they cannot describe decoherence [89]. In this Letter, we make this possible by treating Eq. (1) within the open-quantum-system framework and by extracting quantum-information-theoretic properties of the curvature perturbations. This leads us to the phenomenon of quantum recoherence. We solve the problem both exactly and using an effective approach, allowing us to better assess the performance of such methods in a cosmological context.

Quantum recoherence. From an open-quantum-system perspective, our goal is to describe the dynamics of the adiabatic sector (the *system*) once the heavy entropic direction (the *environment*) has been integrated out. Eq. (1) being quadratic, different Fourier modes decouple on a homogeneous background, which allows us to focus on a given mode $\boldsymbol{k}$. In the asymptotic past, this mode is placed in the Bunch-Davies vacuum state [90], described by

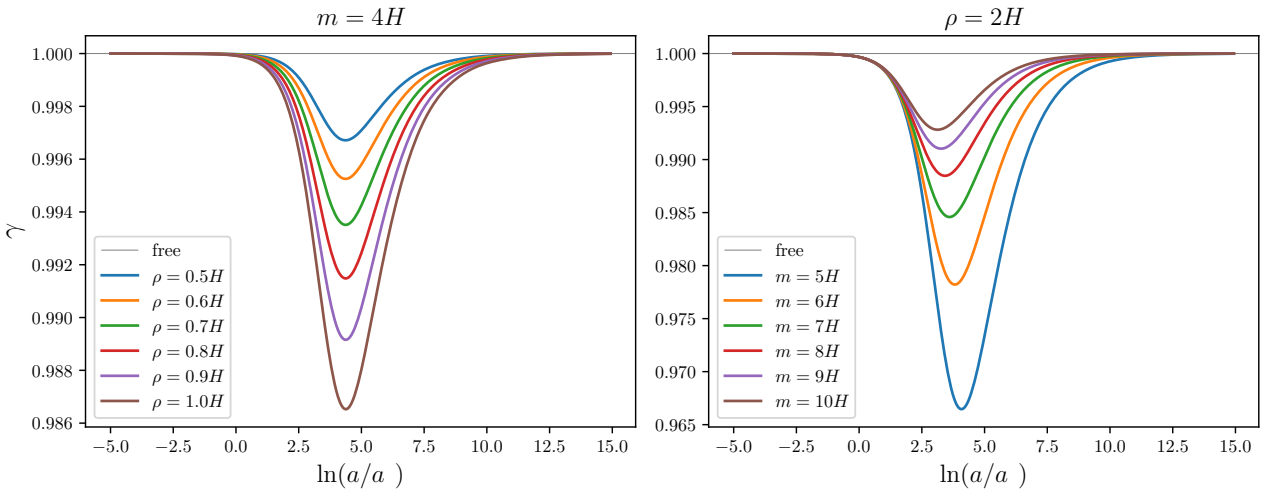

FIG. 1. State purity γ as a function of the number of efolds $\ln(a/a_*)$ since Hubble exit of the scale $k = a_*H$, for a few values of the coupling parameter ρ (left panel) and of the entropic mass m (right panel). After a transient phase of decoherence, the purity reaches a minimum and increases again. This recoherence phenomenon yields high levels of self-coherence at late-time. In practice, Eqs. (S10) and (S11) of the SM are integrated with Bunch-Davies initial conditions from $\ln(a/a_*) = -15$ to $\ln(a/a_*) = 15$ and for constant H.

the Gaussian density matrix $\widehat{\rho}_0$, and the linearity of the dynamics preserves the Gaussianity of the state [91–93]. Hence, the state of the system is entirely characterised by the covariance $\mathbf{\Sigma}_{ij}(\eta) \equiv \frac{1}{2}\mathrm{Tr}\left\{[\widehat{\boldsymbol{z}}_{\zeta,i}(\eta)\widehat{\boldsymbol{z}}_{\zeta,j}(\eta) + \widehat{\boldsymbol{z}}_{\zeta,j}(\eta)\widehat{\boldsymbol{z}}_{\zeta,i}(\eta)]\widehat{\rho}_0\right\}$ where $\widehat{\boldsymbol{z}}_\zeta \equiv (\widehat{v}_\zeta, \widehat{p}_\zeta)^{\mathrm{T}}$ contains the configuration and momentum operators of the Mukhanov-Sasaki variable $v_\zeta \equiv -a\sqrt{2\epsilon}M_{\mathrm{Pl}}\zeta$. In the Supplemental Material (SM), from Eq. (1) we derive an exact equation of motion for $\mathbf{\Sigma}_{ij}(\eta)$, known as a transport equation [94–96]. When integrated numerically, the power spectra one obtains are well reproduced by standard EFT results [66, 79, 80] in the regime $m \gg H$, as is shown in the SM. In particular, we recover that the main effect from the heavy field is a simple rescaling, proportional to ρ^2/m^2, of the amplitude of the scale-invariant power spectrum of ζ. This rescaling is however degenerate with other single-field effects such as a reduced speed of sound [77, 97, 98], so it cannot be used to reveal the existence of an environment.

The state being Gaussian, the covariance $\mathbf{\Sigma}(\eta)$ not only contains all observables of the adiabatic sector but also fully specifies its quantum state, *i.e.* the reduced density matrix $\widehat{\rho}_{\mathrm{red}} \equiv \mathrm{Tr}_{\mathcal{F}}(\widehat{\rho})$ where the entropic degrees of freedom are traced over. This allows us to study quantum properties of $\widehat{\rho}_{\mathrm{red}}$, in particular the transition from a pure quantum state into a statistical mixture due to the interaction with an environment [47–49]. This transition is assessed by the so-called purity parameter [99, 100] $\gamma \equiv \mathrm{Tr}\left(\widehat{\rho}^2_{\mathrm{red}}\right)$, which equals one if the state is pure and is smaller than one otherwise. The system is said to have decohered when $\gamma \ll 1$, with $\gamma = 0$ corresponding to a maximally mixed state. The link between the numerical value of γ and the erasure of explicit quantum signatures (such as Bell inequality violations) has been investigated in Ref. [101] for the class of states considered in this work. Note that γ remains invariant under reparametrisation of the canonical variables [102], and for a Gaussian state one simply has $\gamma(\eta) = \frac{1}{4}\det\left[\mathbf{\Sigma}(\eta)\right]^{-1}$ [103, 104].

In Fig. 1, we display the purity parameter γ as a function of the number of efolds $\ln(a/a_*)$ since Hubble exit of the scale $k = a_*H$ under consideration, where at leading order in slow roll H is constant. After a transient phase of decoherence, a turning point occurs and recoherence (*i.e.* growing γ) takes place, with large levels of self-coherence at late time. For heavy masses $m \gg H$, the turning point occurs in the sub-Hubble regime, when the scale k crosses the Compton wavelength of the entropic field $1/m$, as shown in Fig. 2. The departure from a pure state increases with ρ and decreases with m, in agreement with the EFT intuition that heavier environments leave a smaller imprint on light degrees of freedom. At late time, one can expand the transport equations in the super-Hubble limit and in the SM we find that, at leading order in ρ^2,

$$\gamma = \gamma_\infty - \frac{\rho^2}{m^2}\frac{k}{am}\,. \tag{2}$$

This confirms that the purity does increase at late time for all super-Hubble scales, at a rate controlled by the ratio between the Compton wavelength and the mode wavelength. Thus it quickly reaches the asymptotic value $\gamma_\infty < 1$, since for the scales probed in the CMB, $k/(am)$ is typically of order $e^{-50}H/m$.

The occurrence of recoherence might seem surprising in the light of previous works on decoherence in this model [37, 105] and in other cosmological scenarios [37, 50, 53–61, 64]. One may indeed expect that, once information about the system has "leaked" into the environment, it cannot "come back". Yet we argue that there is no contradiction with the existing literature. This is due to the small effective size of the environment here: the system couples to a single Fourier mode of the environment. This implies that,

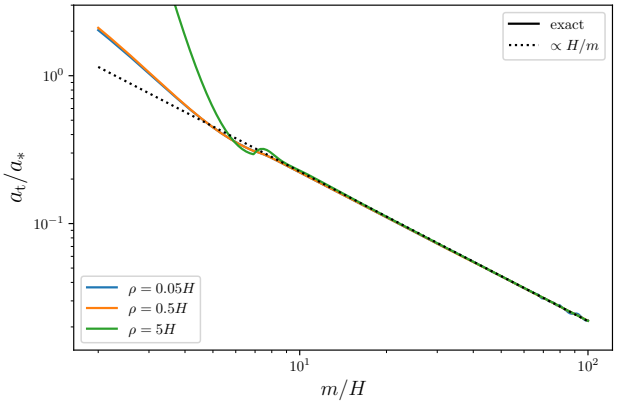

FIG. 2. Turning point for the purity: value of the scale factor a_t at which the purity starts increasing, as a function of m and for a few values of ρ. When $m \gg H$, $a_t \simeq 2.3k/m$, which corresponds to the Compton wavelength of the entropic field.

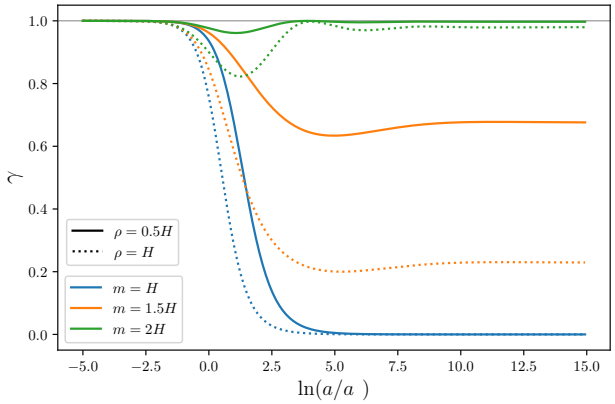

FIG. 3. Same as in Fig. 1 for lighter environments. At late time, one either observes recoherence ($m > 3H/2$), purity freezing ($m \simeq 3H/2$, with an asymptotic value that strongly depends on ρ) or decoherence ($m < 3H/2$).

contrary to the open quantum systems usually considered, the environment does not behave as a thermal bath [89].

To gain further insight into the finite-environment effects to be expected in this model, one may consider its analogue in Minkowski spacetime. When the background is static, linear interactions can only induce mixing between the light and heavy sectors so that the purity exhibits oscillations at frequencies given by the characteristic timescales of the system and the environment, as checked explicitly in the SM. If the coupling is quenched off, oscillations stop and the purity freezes at the time of the quench. In de-Sitter spacetime, this is precisely what happens, since the non-trivial background dynamics makes the coupling effectively time dependent.

This can be seen in Fig. 3 where small entropic masses are used to better highlight the following stages in the evolution of purity. When $k \gg am$, the mode functions of both fields oscillate at the same frequency k/a, in their vacuum state. Then $am \gg k \gg aH$ and the two frequencies differ: the system oscillates at frequency k/a while the environment oscillates at frequency m, hence the purity oscillates as in flat space. Finally, when $k \ll aH$, two behaviours can be observed, depending on m/H. If $m > \frac{3}{2}H$, entropic perturbations are heavy hence they oscillate and quickly decay [66]. Since ζ' also decays as $1/a^2$ on super-Hubble scales [106] (this is the so-called "decaying mode"), the coupling between adiabatic and entropic perturbations is effectively turned off. This is why the value of the purity freezes (see the cases $m = 1.5H$ and $m = 2H$ in Fig. 3). When the environment is lighter, $\mathcal{F}$ acquires a growing mode that keeps the interaction term $\zeta'\mathcal{F}$ active in spite of the decay of ζ'. This leads to decoherence (see the case $m = H$ in Fig. 3), driven by the dynamics of the expansion. This is similar to the setup studied in Ref. [37], where an additional $\zeta\mathcal{F}$ interaction term is considered that is not suppressed by the decaying mode ζ' on large scales, and to the cosmological two-field model investigated in Ref. [64]. In all these cases, the system is driven into a mixed state by the dynamical generation of entangled pairs of quanta between ζ and $\mathcal{F}$, which explains why decoherence takes place in spite of the environment being effectively made of one single degree of freedom.

In the present setting, the entropic direction is typically expected to be heavy, but it is interesting to see that, formally, by varying m, one interpolates between these three possible outcomes: recoherence, purity freezing and decoherence. Note that the intermediate mass $m \simeq \frac{3}{2}H$ is also of phenomenological interest in the context of quasi-single field inflation [68, 77–80], and that the fate of the purity in that case is particularly sensitive to ρ, see Fig. 3.

A master-equation treatment. The model (1) being linear, it can be solved exactly but this is in general not possible. This is why open quantum systems are usually approached with effective methods known as master equations. We now apply such methods to the present setup, in order to check their validity, and to shed additional light on the imprint left by $\mathcal{F}$ on ζ.

Master equations are commonly employed in cosmology to model the effect of additional degrees of freedom, treated as an environment, onto a given system [40, 46, 53, 58, 61–64, 107–118]. One of their appealing advantages is their ability to re-sum late-time secular effects [64, 113, 114, 119–123], hence to go beyond standard perturbation theory and implement non-perturbative resummations in cosmology. Note that the recoherence phenomenon being a manifestly non-Markovian feature, it cannot be modelled by an irreversible dynamical-map such as the Lindblad equation [124]. It requires the use of more sophisticated non-Markovian master equations such as the time-convolutionless (TCL) master equation discussed in Refs. [64, 89, 125–127],

$$\frac{\mathrm{d}\widehat{\rho}_{\rm red}}{\mathrm{d}\eta} = -i\left[\widehat{H}_0^{\mathcal{S}}(\eta) + \widehat{H}^{(\rm LS)}(\eta), \widehat{\rho}_{\rm red}(\eta)\right] \qquad (3)$$
$$+\boldsymbol{\mathcal{D}}_{ij}(\eta)\left[\widehat{\boldsymbol{z}}_{\zeta,i}\widehat{\rho}_{\rm red}(\eta)\widehat{\boldsymbol{z}}_{\zeta,j} - \frac{1}{2}\left\{\widehat{\boldsymbol{z}}_{\zeta,j}\widehat{\boldsymbol{z}}_{\zeta,i}, \widehat{\rho}_{\rm red}(\eta)\right\}\right].$$

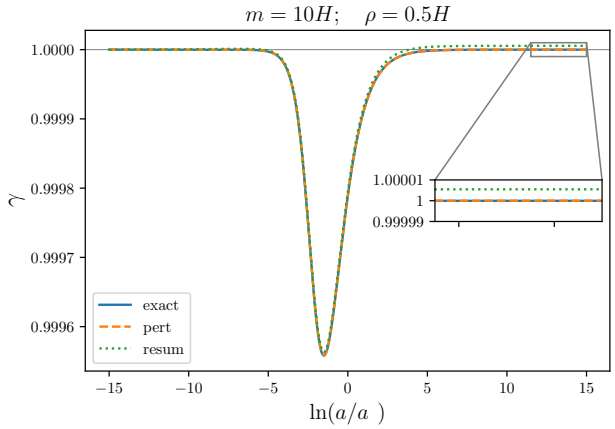

FIG. 4. Same as in Fig. 1, where the solution of the master equation (3) is also shown (green line), together with its perturbative limit (orange line). The agreement is excellent, and becomes even better when decreasing ρ or when increasing m. At late time, the full master equation does not perform better than the perturbative theory, and even leads to slight violations of the positivity of the dynamical map (see the inset where $\gamma > 1$).

Here, $\widehat{H}_0^{\mathcal{S}}$ is the free Hamiltonian of the system, and the effect of the environment is encoded into the "Lamb-shift" Hamiltonian $\widehat{H}^{(\mathrm{LS})}$ and the dissipator matrix $\boldsymbol{\mathcal{D}}$. These objects are constructed out of the two-point functions of the environment and formally rely on convolutions from initial time to final time of the free mode functions of the system and the environment. Their detailed expression is obtained following the procedure of Ref. [64] in the SM, where the master equation (3) is derived explicitly. The Lamb-shift term captures the renormalisation of the free Hamiltonian due to the interactions with the environment. At late-time where $k \ll aH$, it yields an effective speed of sound $c_{\mathrm{s}}^2 = 1 - \rho^2/m^2 + \mathcal{O}[k/(aH), H^4/m^4]$, which rescales the kinetic term by $\widehat{p}_\zeta^2 \to c_{\mathrm{s}}^2 \widehat{p}_\zeta^2$. This effect is also found in Wilsonian EFT treatments of the model [65–67, 78, 80]. Although non-perturbative, it only leads to a slight rescaling of the power spectra as mentioned above. This correction is however unitary, hence it cannot account for de(re)coherence [89], which is instead driven by the second line of Eq. (3).

From Eq. (3), one can derive effective transport equations for $\boldsymbol{\Sigma}(\eta)$ [64], given in the SM. This leads to the purity shown in Fig. 4, where "resum" stands for the full solution of Eq. (3), in which partial resummation is supposed to take place; and "pert" corresponds to the solution at leading order in ρ^2 [since $\boldsymbol{\mathcal{D}} = \mathcal{O}(\rho^2)$ this amounts to evaluating $\widehat{\rho}_{\mathrm{red}}$ in the free theory in the second line of Eq. (3)]. In Ref. [64], this was shown to coincide with the result of the in-in formalism [128–131]. In practice, in the SM it also allows us to unambiguously identify and remove the so-called "spurious terms", which cancel out at leading order but otherwise spoil the resummation [64]. In Fig. 4 one can see that the master equation provides an excellent fit to the full result, both in its perturbative limit and when solved entirely. In particular, it accurately captures the turning point of the purity. This is remarkable, since the highly non-Markovian nature of the recoherence phenomenon may have cast some doubts on the existence of an effective single-field description that would be under control.

One also notices that the non-perturbative resummation performed by the master equation does not significantly improve the perturbative treatment. The reason is that, as stressed above, the coupling between the adiabatic and entropic sector is effectively switched off at late time. There is therefore no secular effects to be resummed, and the perturbative and non-perturbative results only differ by overall constant factors in the power spectra, as checked explicitly in the SM. Therefore, the only non-perturbative effect is unitary. It consists in the rescaling of c_{s} mentioned above, which only advances horizon crossing. This contrasts with the situation studied in Ref. [64], where an effective mass is generated for the light degree of freedom. This dresses the anomalous dimension of the light field, generating a secular growth at the perturbative level which is then resummed by the master equation (or other methods such as the dynamical renormalisation group [132–134]).

Finally, let us note that the master equation leads to a tiny violation of positivity at late time, see the inset in Fig. 4 where the purity slightly overshoots one, implying that $\det[\boldsymbol{\Sigma}(\eta)] < 1/4$ (hence violating Heisenberg inequality [89]). This signals a small breakdown of the effective theory, and determining under which conditions this class of non-Markovian Gaussian dynamical maps remains completely positive and trace preserving (CPTP) would deserve further investigations [63, 135–138].

Conclusions. In this Letter, we have shown that heavy entropic degrees of freedom do *not* lead to quantum decoherence of adiabatic fluctuations in the early universe, at least through their dominant interaction term. More precisely, we found that after a transient phase of decoherence, the adiabatic fluctuations recohere once the mode under consideration crosses out the Compton wavelength of the entropic field. This is because, at late time, the interaction is effectively quenched off as a result of spacetime expansion. This makes the state purity freeze to a value close to unity. Therefore, heavy entropic fields leave a small imprint not only on cosmological observables, but also on quantum-information properties of the quantum state.

We also found that an effective master equation derived from open-quantum-system methods performs remarkably well when compared to the full theory. Wilsonian EFTs have also been used to describe the model, but they do not capture non-unitary effects, hence they cannot describe decoherence. The master equation treatment has allowed us to check that non-unitary effects are negligible in the observables of the system (hence Wilsonian EFTs can safely be used in that respect), although they are crucial as far as decoherence is concerned. Let us stress that, since recoherence is inherently a non-Markovian process, the

master equation needs to be kept non-Markovian too, *i.e.* beyond the Lindblad limit. We noted that, due to the effective decoupling between adiabatic and entropic modes at late time, there is no secular growth that the master equation would otherwise resum. This even leads to a slight violation of positivity by the effective dynamical map, which questions its ability to account for non-perturbative effects in the absence of secular divergences (when secular terms are present, non-perturbative resummation was found to be successful in Ref. [64]).

These results do not preclude other decoherence channels (such as higher-order coupling between adiabatic and entropic fluctuations, single-field gravitational decoherence [46], etc.) to effectively decohere cosmological perturbations, but it suggests that decoherence in the early universe may not be as ubiquitous as common wisdom suggests. This is crucial to determine whether or not genuine quantum signals can be detected in cosmological structures [18, 22, 25, 43, 44, 101, 139, 140]. Natural prospects of our work include the investigation of models with sharp turns [66, 96], the impact of multiple entropic directions [71] on the emergence of Markovianity [138], as well as non-linear interactions [72, 141, 142]. In this latter case, mode coupling is expected to enlarge the size of the effective environment, but also to induce non-Gaussianities [42], which are tightly constrained [143–146]. One may also study how our results vary when changing the initial quantum state [147–151].

Let us end by stressing that, when the system is coupled to a single mode as in the present setting (and as in the two-field model of Ref. [64]), decoherence or recoherence are possible only because we work in a dynamical background. In flat spacetime indeed, as explained above finite-size environments and time-independent Hamiltonians can only lead to oscillations in the purity. This is a consequence of Poincaré recurrence-time theorem [152], which relies on volume conservation. In cosmology however, the large-scale dynamics either amplifies or extinguishes the effective coupling, which yields decoherence or recoherence respectively. Those phenomena have therefore no flat-space analogue. Since most open-quantum-system methods are developed in the context of laboratory experiments, hence in flat spacetimes, their use in cosmology requires a critical analysis of their applicability, to which this work hopefully contributes.

Acknowledgements. It is a pleasure to thank Cliff Burgess, Richard Holman, Greg Kaplanek, Ancel Larzul, Jérôme Martin, Amaury Micheli, Sébastien Renaux-Petel, Marco Schiró, Mattia Walschaers and Denis Werth for interesting discussions.

[1] A. A. Starobinsky, JETP Lett. **30**, 682 (1979), [Pisma Zh. Eksp. Teor. Fiz.30,719(1979)].
[2] A. H. Guth, Phys. Rev. **D23**, 347 (1981).
[3] A. A. Starobinsky, Phys. Lett. **B91**, 99 (1980).
[4] K. Sato, Mon. Not. Roy. Astron. Soc. **195**, 467 (1981).
[5] A. D. Linde, *Second Seminar on Quantum Gravity Moscow, USSR, October 13-15, 1981*, Phys. Lett. **B108**, 389 (1982).
[6] V. F. Mukhanov and G. V. Chibisov, JETP Lett. **33**, 532 (1981), [Pisma Zh. Eksp. Teor. Fiz.33,549(1981)].
[7] A. H. Guth and S. Y. Pi, Phys. Rev. Lett. **49**, 1110 (1982).
[8] A. Albrecht and P. J. Steinhardt, Phys. Rev. Lett. **48**, 1220 (1982).
[9] A. A. Starobinsky, Phys. Lett. **B117**, 175 (1982).
[10] S. W. Hawking, Phys. Lett. **B115**, 295 (1982).
[11] A. D. Linde, Phys. Lett. **B129**, 177 (1983).
[12] J. M. Bardeen, P. J. Steinhardt, and M. S. Turner, Phys. Rev. **D28**, 679 (1983).
[13] V. F. Mukhanov, Sov.Phys.JETP **67**, 1297 (1988).
[14] J. Khoury, B. A. Ovrut, P. J. Steinhardt, and N. Turok, Phys. Rev. D **64**, 123522 (2001), arXiv:hep-th/0103239.
[15] R. Brandenberger and P. Peter, Found. Phys. **47**, 797 (2017), arXiv:1603.05834 [hep-th].
[16] I. Agullo and P. Singh, arXiv e-prints , arXiv:1612.01236 (2016), arXiv:1612.01236 [gr-qc].
[17] A. Barrau, T. Cailleteau, J. Grain, and J. Mielczarek, Class. Quant. Grav. **31**, 053001 (2014), arXiv:1309.6896 [gr-qc].
[18] D. Campo and R. Parentani, Phys. Rev. D **74**, 025001 (2006), arXiv:astro-ph/0505376.
[19] J. Martin and V. Vennin, Phys. Rev. **D93**, 023505 (2016), arXiv:1510.04038 [astro-ph.CO].
[20] J. Maldacena, Fortsch. Phys. **64**, 10 (2016), arXiv:1508.01082 [hep-th].
[21] J. Martin and V. Vennin, Phys. Rev. **A93**, 062117 (2016), arXiv:1605.02944 [quant-ph].
[22] J. Martin and V. Vennin, Phys. Rev. **A94**, 052135 (2016), arXiv:1611.01785 [quant-ph].
[23] S. Kanno, J. P. Shock, and J. Soda, Phys. Rev. D **94**, 125014 (2016), arXiv:1608.02853 [hep-th].
[24] S. Choudhury, S. Panda, and R. Singh, Eur. Phys. J. C **77**, 60 (2017), arXiv:1607.00237 [hep-th].
[25] J. Martin and V. Vennin, Phys. Rev. **D96**, 063501 (2017), arXiv:1706.05001 [astro-ph.CO].
[26] D. Green and R. A. Porto, Phys. Rev. Lett. **124**, 251302 (2020), arXiv:2001.09149 [hep-th].
[27] K. Ando and V. Vennin, Phys. Rev. A **102**, 052213 (2020), arXiv:2007.00458 [quant-ph].
[28] L. Espinosa-Portalés and V. Vennin, JCAP **07** (07), 037, arXiv:2203.03505 [quant-ph].
[29] A. Micheli and P. Peter, (2022), arXiv:2211.00182 [gr-qc].
[30] R. H. Brandenberger, R. Laflamme, and M. Mijic, Mod. Phys. Lett. A **5**, 2311 (1990).
[31] R. H. Brandenberger, V. F. Mukhanov, and T. Prokopec, Phys. Rev. Lett. **69**, 3606 (1992), arXiv:astro-ph/9206005.
[32] A. O. Barvinsky, A. Y. Kamenshchik, C. Kiefer, and I. V. Mishakov, Nucl. Phys. B **551**, 374 (1999),

arXiv:gr-qc/9812043.
[33] F. C. Lombardo and D. Lopez Nacir, Phys. Rev. D **72**, 063506 (2005), arXiv:gr-qc/0506051.
[34] C. Kiefer, I. Lohmar, D. Polarski, and A. A. Starobinsky, Class. Quant. Grav. **24**, 1699 (2007), arXiv:astro-ph/0610700.
[35] P. Martineau, Class. Quant. Grav. **24**, 5817 (2007), arXiv:astro-ph/0601134.
[36] C. P. Burgess, R. Holman, and D. Hoover, Phys. Rev. D **77**, 063534 (2008), arXiv:astro-ph/0601646.
[37] T. Prokopec and G. I. Rigopoulos, JCAP **11**, 029, arXiv:astro-ph/0612067.
[38] C. Kiefer and D. Polarski, Adv. Sci. Lett. **2**, 164 (2009), arXiv:0810.0087 [astro-ph].
[39] E. Nelson, JCAP **03**, 022, arXiv:1601.03734 [gr-qc].
[40] T. J. Hollowood and J. I. McDonald, Phys. Rev. D **95**, 103521 (2017), arXiv:1701.02235 [gr-qc].
[41] J. Martin and V. Vennin, JCAP **05**, 063, arXiv:1801.09949 [astro-ph.CO].
[42] J. Martin and V. Vennin, JCAP **06**, 037, arXiv:1805.05609 [astro-ph.CO].
[43] S. Kanno, J. Soda, and J. Tokuda, Phys. Rev. D **103**, 044017 (2021), arXiv:2007.09838 [hep-th].
[44] J. Martin, A. Micheli, and V. Vennin, JCAP **04** (04), 051, arXiv:2112.05037 [quant-ph].
[45] A. Daddi Hammou and N. Bartolo, (2022), arXiv:2211.07598 [astro-ph.CO].
[46] C. P. Burgess, R. Holman, G. Kaplanek, J. Martin, and V. Vennin, (2022), arXiv:2211.11046 [hep-th].
[47] W. H. Zurek, Phys. Rev. D **24**, 1516 (1981).
[48] W. H. Zurek, Phys. Rev. D **26**, 1862 (1982).
[49] E. Joos and H. Zeh, Z. Phys. B **59**, 223 (1985).
[50] D. Koks, A. Matacz, and B. Hu, Phys. Rev. D **55**, 5917 (1997), [Erratum: Phys.Rev.D 56, 5281 (1997)], arXiv:quant-ph/9612016.
[51] D. Campo and R. Parentani, Phys. Rev. D **78**, 065044 (2008), arXiv:0805.0548 [hep-th].
[52] D. Campo and R. Parentani, Phys. Rev. D **78**, 065045 (2008), arXiv:0805.0424 [hep-th].
[53] C. Anastopoulos and B. L. Hu, Class. Quant. Grav. **30**, 165007 (2013), arXiv:1305.5231 [gr-qc].
[54] M. Fukuma, Y. Sakatani, and S. Sugishita, Phys. Rev. D **89**, 064024 (2014), arXiv:1305.0256 [hep-th].
[55] S. Akhtar, S. Choudhury, S. Chowdhury, D. Goswami, S. Panda, and A. Swain, Eur. Phys. J. C **80**, 748 (2020), arXiv:1908.09929 [hep-th].
[56] G. Kaplanek and C. P. Burgess, JHEP **01**, 098, arXiv:2007.05984 [hep-th].
[57] G. Kaplanek and C. P. Burgess, Journal of High Energy Physics **2020**, 8 (2020), arXiv:1912.12951 [hep-th].
[58] S. Brahma, A. Berera, and J. Calderón-Figueroa, Class. Quant. Grav. **39**, 245002 (2022), arXiv:2107.06910 [hep-th].
[59] C. P. Burgess, R. Holman, and G. Kaplanek, Fortsch. Phys. **2022**, 2200019 (2021), arXiv:2106.10804 [hep-th].
[60] J. Oppenheim, C. Sparaciari, B. Šoda, and Z. Weller-Davies, (2022), arXiv:2203.01982 [quant-ph].
[61] S. Brahma, A. Berera, and J. Calderón-Figueroa, JHEP **08**, 225, arXiv:2206.05797 [hep-th].
[62] S. Shandera, N. Agarwal, and A. Kamal, Phys. Rev. D **98**, 083535 (2018), arXiv:1708.00493 [hep-th].
[63] G. Kaplanek and E. Tjoa, (2022), arXiv:2207.13750 [quant-ph].
[64] T. Colas, J. Grain, and V. Vennin, Eur. Phys. J. C **82**, 1085 (2022), arXiv:2209.01929 [hep-th].
[65] A. Achucarro, J.-O. Gong, S. Hardeman, G. A. Palma, and S. P. Patil, JCAP **01**, 030, arXiv:1010.3693 [hep-ph].
[66] S. Cespedes, V. Atal, and G. A. Palma, JCAP **05**, 008, arXiv:1201.4848 [hep-th].
[67] A. Achucarro, J.-O. Gong, S. Hardeman, G. A. Palma, and S. P. Patil, JHEP **05**, 066, arXiv:1201.6342 [hep-th].
[68] V. Assassi, D. Baumann, D. Green, and L. McAllister, JCAP **01**, 033, arXiv:1304.5226 [hep-th].
[69] X. Tong, Y. Wang, and S. Zhou, JCAP **11**, 045, arXiv:1708.01709 [astro-ph.CO].
[70] L. Pinol, JCAP **04**, 002, arXiv:2011.05930 [astro-ph.CO].
[71] L. Pinol, S. Aoki, S. Renaux-Petel, and M. Yamaguchi, (2021), arXiv:2112.05710 [hep-th].
[72] S. Jazayeri and S. Renaux-Petel, (2022), arXiv:2205.10340 [hep-th].
[73] N. Turok, Phys. Rev. Lett. **60**, 549 (1988).
[74] T. Damour and A. Vilenkin, Phys. Rev. D **53**, 2981 (1996), arXiv:hep-th/9503149.
[75] S. Kachru, R. Kallosh, A. D. Linde, J. M. Maldacena, L. P. McAllister, and S. P. Trivedi, JCAP **10**, 013, arXiv:hep-th/0308055.
[76] A. Krause and E. Pajer, JCAP **07**, 023, arXiv:0705.4682 [hep-th].
[77] X. Chen and Y. Wang, JCAP **04**, 027, arXiv:0911.3380 [hep-th].
[78] A. J. Tolley and M. Wyman, Phys. Rev. D **81**, 043502 (2010), arXiv:0910.1853 [hep-th].
[79] X. Chen and Y. Wang, JCAP **09**, 021, arXiv:1205.0160 [hep-th].
[80] S. Pi and M. Sasaki, JCAP **10**, 051, arXiv:1205.0161 [hep-th].
[81] D. Baumann and L. McAllister, *Inflation and String Theory*, Cambridge Monographs on Mathematical Physics (Cambridge University Press, 2015) arXiv:1404.2601 [hep-th].
[82] G. Shiu and J. Xu, Phys. Rev. D **84**, 103509 (2011), arXiv:1108.0981 [hep-th].
[83] N. Aghanim *et al.* (Planck), Astron. Astrophys. **641**, A6 (2020), arXiv:1807.06209 [astro-ph.CO].
[84] Y. Akrami *et al.* (Planck), Astron. Astrophys. **641**, A10 (2020), arXiv:1807.06211 [astro-ph.CO].
[85] D. J. Eisenstein *et al.* (SDSS), Astrophys. J. **633**, 560 (2005), arXiv:astro-ph/0501171.
[86] T. Delubac *et al.* (BOSS), Astron. Astrophys. **574**, A59 (2015), arXiv:1404.1801 [astro-ph.CO].
[87] T. Colas, G. D'amico, L. Senatore, P. Zhang, and F. Beutler, JCAP **06**, 001, arXiv:1909.07951 [astro-ph.CO].
[88] C. Doux *et al.* (DES), Mon. Not. Roy. Astron. Soc. **515**, 1942 (2022), arXiv:2203.07128 [astro-ph.CO].
[89] H. P. Breuer and F. Petruccione, *The theory of open quantum systems* (Oxford University Press, 2002).
[90] T. S. Bunch and P. C. W. Davies, Proc. Roy. Soc. Lond. **A360**, 117 (1978).
[91] R. Simon, E. C. G. Sudarshan, and N. Mukunda, Phys. Rev. A **36**, 3868 (1987).
[92] R. Simon, E. Sudarshan, and N. Mukunda, Physics Letters A **124**, 223 (1987).
[93] T. Colas, J. Grain, and V. Vennin, Eur. Phys. J. C **82**, 6 (2022), arXiv:2104.14942 [quant-ph].
[94] P. Ehrenfest, Zeitschrift für Physik **45**, 455 (1927).
[95] D. Werth, L. Pinol, and S. Renaux-Petel, (2023), arXiv:2302.00655 [hep-th].
[96] R. N. Raveendran and S. Chakraborty, (2023),

arXiv:2302.02584 [astro-ph.CO].
[97] E. Pajer, F. Schmidt, and M. Zaldarriaga, Phys. Rev. **D88**, 083502 (2013), arXiv:1305.0824 [astro-ph.CO].
[98] Z. Kenton and D. J. Mulryne, JCAP **1510** (10), 018, arXiv:1507.08629 [astro-ph.CO].
[99] A. Serafini, F. Illuminati, and S. De Siena, J. Phys. B **37**, L21 (2004), arXiv:quant-ph/0307073.
[100] M. Walschaers, PRX Quantum **2**, 030204 (2021), arXiv:2104.12596 [quant-ph].
[101] J. Martin, A. Micheli, and V. Vennin, (2022), arXiv:2211.10114 [quant-ph].
[102] Single-mode Gaussian systems are fully characterised by a unique symplectic invariant (*i.e.* independent of the choice of canonical variables used to parametrise phase space). Any (symplectic-invariant) decoherence tracer, such as the entanglement entropy, thus follows the same trend as purity.
[103] M. G. Paris, F. Illuminati, A. Serafini, and S. de Siena, Phys. Rev. A **68**, 012314 (2003), arXiv:quant-ph/0304059 [quant-ph].
[104] G. Adesso, S. Ragy, and A. R. Lee, arXiv e-prints , arXiv:1401.4679 (2014), arXiv:1401.4679 [quant-ph].
[105] R. N. Raveendran, K. Parattu, and L. Sriramkumar, Gen. Rel. Grav. **54**, 91 (2022), arXiv:2206.05760 [astro-ph.CO].
[106] D. H. Lyth, K. A. Malik, and M. Sasaki, JCAP **0505**, 004, arXiv:astro-ph/0411220 [astro-ph].
[107] R. Feynman and F. Vernon, Annals of Physics **24**, 118 (1963).
[108] A. Caldeira and A. Leggett, Physica A: Statistical Mechanics and its Applications **121**, 587 (1983).
[109] B. L. Hu, J. P. Paz, and Y. Zhang, Phys. Rev. D **45**, 2843 (1992).
[110] B. L. Hu and A. Matacz, Phys. Rev. D **49**, 6612 (1994), arXiv:gr-qc/9312035.
[111] J. Eisert and M. B. Plenio, Phys. Rev. Lett. **89**, 137902 (2002), arXiv:quant-ph/0111016.
[112] C. P. Burgess, Ann. Rev. Nucl. Part. Sci. **57**, 329 (2007), arXiv:hep-th/0701053.
[113] D. Boyanovsky, Phys. Rev. **D92**, 023527 (2015), arXiv:1506.07395 [astro-ph.CO].
[114] D. Boyanovsky, Phys. Rev. D **93**, 043501 (2016), arXiv:1511.06649 [astro-ph.CO].
[115] D. Boyanovsky, Phys. Rev. D **98**, 023515 (2018), arXiv:1804.07967 [astro-ph.CO].
[116] S. Banerjee, S. Choudhury, S. Chowdhury, J. Knaute, S. Panda, and K. Shirish, (2021), arXiv:2104.10692 [hep-th].
[117] S. Prudhoe and S. Shandera, (2022), arXiv:2201.07080 [quant-ph].
[118] S. Cao and D. Boyanovsky, (2022), arXiv:2212.05161 [astro-ph.CO].
[119] C. P. Burgess, R. Holman, G. Tasinato, and M. Williams, JHEP **03**, 090, arXiv:1408.5002 [hep-th].
[120] C. Burgess, R. Holman, and G. Tasinato, JHEP **01**, 153, arXiv:1512.00169 [gr-qc].
[121] G. Kaplanek, C. P. Burgess, and R. Holman, JHEP **08**, 132, arXiv:2106.10803 [hep-th].
[122] S. Chaykov, N. Agarwal, S. Bahrami, and R. Holman, (2022), arXiv:2206.11288 [hep-th].
[123] S. Chaykov, N. Agarwal, S. Bahrami, and R. Holman, (2022), arXiv:2206.11289 [hep-th].
[124] G. Lindblad, Commun. Math. Phys. **48**, 119 (1976).
[125] N. G. Van Kampen, Physica **74**, 215 (1974).
[126] N. G. Van Kampen, Physica **74**, 239 (1974).
[127] H.-P. Breuer, A. Ma, and F. Petruccione, arXiv e-prints , quant-ph/0209153 (2002), arXiv:quant-ph/0209153 [quant-ph].
[128] S. Weinberg, Phys. Rev. D **74**, 023508 (2006), arXiv:hep-th/0605244.
[129] P. Adshead, R. Easther, and E. A. Lim, Phys. Rev. D **80**, 083521 (2009), arXiv:0904.4207 [hep-th].
[130] X. Chen, Y. Wang, and Z.-Z. Xianyu, JCAP **12**, 006, arXiv:1703.10166 [hep-th].
[131] E. Dimastrogiovanni, M. Fasiello, and L. Pinol, JCAP **09**, 031, arXiv:2203.17192 [astro-ph.CO].
[132] D. Boyanovsky, H. J. de Vega, R. Holman, and M. Simionato, Phys. Rev. D **60**, 065003 (1999), arXiv:hep-ph/9809346.
[133] C. P. Burgess, L. Leblond, R. Holman, and S. Shandera, JCAP **03**, 033, arXiv:0912.1608 [hep-th].
[134] D. Green and A. Premkumar, JHEP **04**, 064, arXiv:2001.05974 [hep-th].
[135] R. S. Whitney, Journal of Physics A Mathematical General **41**, 175304 (2008), arXiv:0711.0074 [quant-ph].
[136] L. Diósi and L. Ferialdi, Physical Review Letters **113**, 10.1103/physrevlett.113.200403 (2014).
[137] L. Ferialdi, Physical Review Letters **116**, 10.1103/physrevlett.116.120402 (2016).
[138] H.-P. Breuer, E.-M. Laine, J. Piilo, and B. Vacchini, Rev. Mod. Phys. **88**, 021002 (2016).
[139] A. Berera, S. Brahma, R. Brandenberger, J. Calderón-Figueroa, and A. Heavens, Phys. Rev. D **104**, 063519 (2021), arXiv:2107.06914 [hep-ph].
[140] A. Berera and J. Calderón-Figueroa, Phys. Rev. D **105**, 123033 (2022), arXiv:2205.11816 [quant-ph].
[141] G. L. Pimentel and D.-G. Wang, (2022), arXiv:2205.00013 [hep-th].
[142] D.-G. Wang, G. L. Pimentel, and A. Achúcarro, (2022), arXiv:2212.14035 [astro-ph.CO].
[143] Y. Akrami *et al.* (Planck), Astron. Astrophys. **641**, A9 (2020), arXiv:1905.05697 [astro-ph.CO].
[144] G. D'Amico, M. Lewandowski, L. Senatore, and P. Zhang, (2022), arXiv:2201.11518 [astro-ph.CO].
[145] G. Cabass, M. M. Ivanov, O. H. E. Philcox, M. Simonović, and M. Zaldarriaga, Phys. Rev. Lett. **129**, 021301 (2022), arXiv:2201.07238 [astro-ph.CO].
[146] W. Riquelme *et al.*, (2022), arXiv:2209.07187 [astro-ph.CO].
[147] J. Lesgourgues, D. Polarski, and A. A. Starobinsky, Nucl. Phys. **B497**, 479 (1997), arXiv:gr-qc/9611019 [gr-qc].
[148] R. Baunach, N. Bolis, R. Holman, S. Moltner, and B. J. Richard, JCAP **07**, 050, arXiv:2104.13410 [hep-th].
[149] S. Wenderoth, H.-P. Breuer, and M. Thoss, (2022), arXiv:2211.17149 [quant-ph].
[150] M. I. Letey, Z. Shumaylov, F. J. Agocs, W. J. Handley, M. P. Hobson, and A. N. Lasenby, (2022), arXiv:2211.17248 [gr-qc].
[151] D. Ghosh, A. H. Singh, and F. Ullah, (2022), arXiv:2207.06430 [hep-th].
[152] H. Poincaré, Acta Mathematica **13**, 1 (1890).

SUPPLEMENTAL MATERIAL
"Quantum recoherence in the early universe"

Thomas Colas, Julien Grain, and Vincent Vennin

This supplemental material contains some technical details of the calculations presented in the main text. In Sec. I, we derive the transport equations whose solutions are given in the main text. In Sec. II, we show that purity exhibits oscillation when our setting is considered in flat spacetime. In Sec. III, we derive and solve the master equation associated to our problem, closely following Ref. [64].

I. EXACT SOLUTION

A. Hamiltonian formulation

Starting from the Lagrangian density

$$\mathcal{L} = a^2\epsilon M_{\rm Pl}^2\zeta'^2 - a^2\epsilon M_{\rm Pl}^2\left(\partial_i\zeta\right)^2 + \frac{1}{2}a^2\mathcal{F}'^2 - \frac{1}{2}a^2\left(\partial_i\mathcal{F}\right)^2 - \frac{1}{2}m^2a^4\mathcal{F}^2 - \rho a^3\sqrt{2\epsilon}M_{\rm Pl}\zeta'\mathcal{F}, \tag{S1}$$

we first introduce the rescaled Mukhanov-Sasaki like variables $v_\zeta(\eta,\boldsymbol{x}) \equiv -a(\eta)\sqrt{2\epsilon}M_{\rm Pl}\zeta(\eta,\boldsymbol{x})$ and $v_\mathcal{F}(\eta,\boldsymbol{x}) \equiv a(\eta)\mathcal{F}(\eta,\boldsymbol{x})$. One can then Fourier transform the fields

$$v_\alpha(\eta,\boldsymbol{k}) \equiv \int_{\mathbb{R}^3}\frac{{\rm d}^3\boldsymbol{x}}{(2\pi)^{3/2}}v_\alpha(\eta,\boldsymbol{x})e^{-i\boldsymbol{k}.\boldsymbol{x}}, \tag{S2}$$

for $\alpha = \zeta,\mathcal{F}$. The conjugate momenta are obtained from Eq. (1) and read

$$p_\zeta = v_\zeta' - \frac{a'}{a}v_\zeta + \rho a v_\mathcal{F} \quad \text{and} \quad p_\mathcal{F} = v_\mathcal{F}' - \frac{a'}{a}v_\mathcal{F}\,. \tag{S3}$$

A Legendre transform gives the Hamiltonian

$$H = \int_{\mathbb{R}^{3+}}{\rm d}^3\boldsymbol{k}\boldsymbol{z}^\dagger\boldsymbol{H}(\eta)\boldsymbol{z}\,, \tag{S4}$$

where the phase-space variables have been arranged into the vector $\boldsymbol{z} \equiv (v_\zeta, p_\zeta, v_\mathcal{F}, p_\mathcal{F})^{\rm T}$ and $\boldsymbol{H}$ is a four-by-four matrix given by

$$\boldsymbol{H}(\eta) = \begin{pmatrix} \boldsymbol{H}^{(\mathcal{S})} & \boldsymbol{V} \\ \boldsymbol{V}^{\rm T} & \boldsymbol{H}^{(\mathcal{E})} \end{pmatrix}, \tag{S5}$$

with

$$\boldsymbol{H}^{(\mathcal{S})}(\eta) = \begin{pmatrix} k^2 & \frac{a'}{a} \\ \frac{a'}{a} & 1 \end{pmatrix}, \quad \boldsymbol{H}^{(\mathcal{E})}(\eta) = \begin{pmatrix} k^2 + \left(m^2+\rho^2\right)a^2 & \frac{a'}{a} \\ \frac{a'}{a} & 1 \end{pmatrix}, \quad \boldsymbol{V}(\eta) \equiv \begin{pmatrix} 0 & 0 \\ -\rho a & 0 \end{pmatrix}. \tag{S6}$$

Note that, since ζ and $\mathcal{F}$ are real fields, one has the constrain $\boldsymbol{z}^*(\eta,\boldsymbol{k}) = \boldsymbol{z}(\eta,-\boldsymbol{k})$. This explains why, in order to avoid double counting, the integral in Eq. (S4) is performed over $\mathbb{R}^{3+} \equiv \mathbb{R}^2\times\mathbb{R}^+$. Remarkably, the linear mixing ρ enters the definition of the entropic mass $m^2+\rho^2$ when the problem is described in terms of canonical variables. From now on, we thus redefine $m^2 \to m^2+\rho^2$.

Following the canonical quantisation prescription, field variables are promoted to quantum operators. In order to work with hermitian operators, we split the fields into real and imaginary components, that is

$$\widehat{\boldsymbol{z}} = \frac{1}{\sqrt{2}}\left(\widehat{\boldsymbol{z}}^{\rm R} + i\widehat{\boldsymbol{z}}^{\rm I}\right), \tag{S7}$$

such that $\widehat{\boldsymbol{z}}^s$ is Hermitian for $s = {\rm R},{\rm I}$. These variables are canonical since $[\widehat{v}_\alpha^s(\boldsymbol{k}), \widehat{p}_{\alpha'}^{s'}(\boldsymbol{q})] = i\delta^3(\boldsymbol{k}-\boldsymbol{q})\delta_{\alpha,\alpha'}\delta_{s,s'}$. In this basis, the Hamiltonian takes the same form as in Eq. (S4), *i.e.*

$$\widehat{H}(\eta) = \frac{1}{2}\sum_{s={\rm R},{\rm I}}\int_{\mathbb{R}^{3+}}{\rm d}^3\boldsymbol{k}\left(\widehat{\boldsymbol{z}}^s\right)^{\rm T}\boldsymbol{H}(\eta)\widehat{\boldsymbol{z}}^s\,. \tag{S8}$$

Being separable, there is no mode coupling nor interactions between the R and I sectors and the state is factorisable in this decomposition. Hence, from now on, we focus on a given wavenumber $\boldsymbol{k}$ and a given s-sector, and to make notations lighter we leave the $\boldsymbol{k}$ and s dependence implicit.

B. Transport equations

The transport equations for the full system-plus-environment setup can be obtained by differentiating

$$\boldsymbol{\Sigma}_{ij}^{(\mathcal{S}+\mathcal{E})}(\eta) \equiv \frac{1}{2}\mathrm{Tr}\left\{[\widehat{\boldsymbol{z}}_i(\eta)\widehat{\boldsymbol{z}}_j(\eta) + \widehat{\boldsymbol{z}}_j(\eta)\widehat{\boldsymbol{z}}_i(\eta)]\widehat{\rho}_0\right\} \tag{S9}$$

with respect to time in the Heisenberg picture, and using the Heisenberg equations to evaluate $\mathrm{d}\widehat{\boldsymbol{z}}/\mathrm{d}\eta$. The density matrix $\widehat{\rho}_0$ specifies the initial Bunch-Davies vacuum in which the adiabatic and entropic directions both start. The Hamiltonian (S8) being quadratic, one finds

$$\frac{\mathrm{d}\boldsymbol{\Sigma}^{(\mathcal{S}+\mathcal{E})}}{\mathrm{d}\eta} = \boldsymbol{\Omega}\boldsymbol{H}\boldsymbol{\Sigma}^{(\mathcal{S}+\mathcal{E})} - \boldsymbol{\Sigma}^{(\mathcal{S}+\mathcal{E})}\boldsymbol{H}\boldsymbol{\Omega}, \tag{S10}$$

where $\boldsymbol{H}$ was defined in Eq. (S5) and $\boldsymbol{\Omega}$ is a four-by-four block-diagonal matrix where each 2×2 block on the diagonal is the symplectic matrix $\boldsymbol{\omega} = \begin{pmatrix} 0 & 1 \\ -1 & 0 \end{pmatrix}$. Once Eq. (S10) is known, one can derive an exact equation for $\det\boldsymbol{\Sigma}$

$$\frac{\mathrm{d}\det\boldsymbol{\Sigma}}{\mathrm{d}\eta} = \boldsymbol{\Sigma}_{11}^{(\mathcal{S}+\mathcal{E})}\frac{\mathrm{d}\boldsymbol{\Sigma}_{22}^{(\mathcal{S}+\mathcal{E})}}{\mathrm{d}\eta} + \boldsymbol{\Sigma}_{22}^{(\mathcal{S}+\mathcal{E})}\frac{\mathrm{d}\boldsymbol{\Sigma}_{11}^{(\mathcal{S}+\mathcal{E})}}{\mathrm{d}\eta} - 2\boldsymbol{\Sigma}_{12}^{(\mathcal{S}+\mathcal{E})}\frac{\mathrm{d}\boldsymbol{\Sigma}_{12}^{(\mathcal{S}+\mathcal{E})}}{\mathrm{d}\eta} \tag{S11}$$

where $\boldsymbol{\Sigma}$ is the system's covariance. Eqs. (S10) and (S11) provide a set of eleven coupled ordinary differential equations that we numerically integrate from $\log(-k\eta_{\mathrm{ini}}) = 15$ to $\log(-k\eta_{\mathrm{fin}}) = -15$. Note that Eq. (S11) is redundant with Eqs. (S10), but since it arises from cancellations between quantities that diverge at late time, to compute the purity it is numerically more efficient to treat it as independent. Initial conditions are computed in the Bunch-Davies vacuum where $\boldsymbol{\Sigma}_{11}^{(\mathcal{S}+\mathcal{E})} = \boldsymbol{\Sigma}_{33}^{(\mathcal{S}+\mathcal{E})} = 1/(2k)$, $\boldsymbol{\Sigma}_{22}^{(\mathcal{S}+\mathcal{E})} = \boldsymbol{\Sigma}_{44}^{(\mathcal{S}+\mathcal{E})} = k/2$ and all other correlations initially vanish. The entries of $\boldsymbol{\Sigma}$ are shown in Fig. S1 where we observe that, at late-time, the effect of the heavy environment is to simply rescale the amplitude of the power spectra by approximately $\rho^2/(2m^2)$, in agreement with the results derived in the past literature with effective methods, see e.g. Refs. [79, 80] for the in-in treatment and Refs. [65, 66] for the Wilsonian EFT approach.

C. Mode functions

In the interaction picture, operators evolve according to the free Hamiltonian $\widehat{H}_0(\eta) = \widehat{H}_0^{\mathcal{S}}(\eta)\otimes\widehat{H}_0^{\mathcal{E}}(\eta)$ where

$$\widehat{H}_0^{\mathcal{S}}(\eta) = \frac{1}{2}\left(\widehat{p}_\zeta\widehat{p}_\zeta + k^2\widehat{v}_\zeta\widehat{v}_\zeta + \frac{a'}{a}\{\widehat{v}_\zeta,\widehat{p}_\zeta\}\right) \tag{S12}$$

$$\widehat{H}_0^{\mathcal{E}}(\eta) = \frac{1}{2}\left[\widehat{p}_\mathcal{F}\widehat{p}_\mathcal{F} + \left(k^2 + m^2a^2\right)\widehat{v}_\mathcal{F}\widehat{v}_\mathcal{F} + \frac{a'}{a}\{\widehat{v}_\mathcal{F},\widehat{p}_\mathcal{F}\}\right] \tag{S13}$$

with $\{A,B\} = AB + BA$ the anticommutator, while states and density matrices evolve according to the interaction Hamiltonian

$$\widehat{H}_{\mathrm{int}}(\eta) = -\rho a(\eta)\widehat{p}_\zeta\widehat{v}_\mathcal{F} \tag{S14}$$

where we used the fact that the ζ and $\mathcal{F}$ sectors commute. In this picture, the field operators admit a simple mode-function decomposition

$$\widetilde{v}_\alpha(\eta) = v_\alpha(\eta)\widehat{a}_\alpha + v_\alpha^*(\eta)\widehat{a}_\alpha^\dagger \tag{S15}$$

where $\widehat{a}_\alpha$ and $\widehat{a}_\alpha^\dagger$ are the creation and annihilation operators of the uncoupled fields. From now on, tildas denote operators in the interaction picture. Heisenberg's equations yield the classical equations of motion for the mode

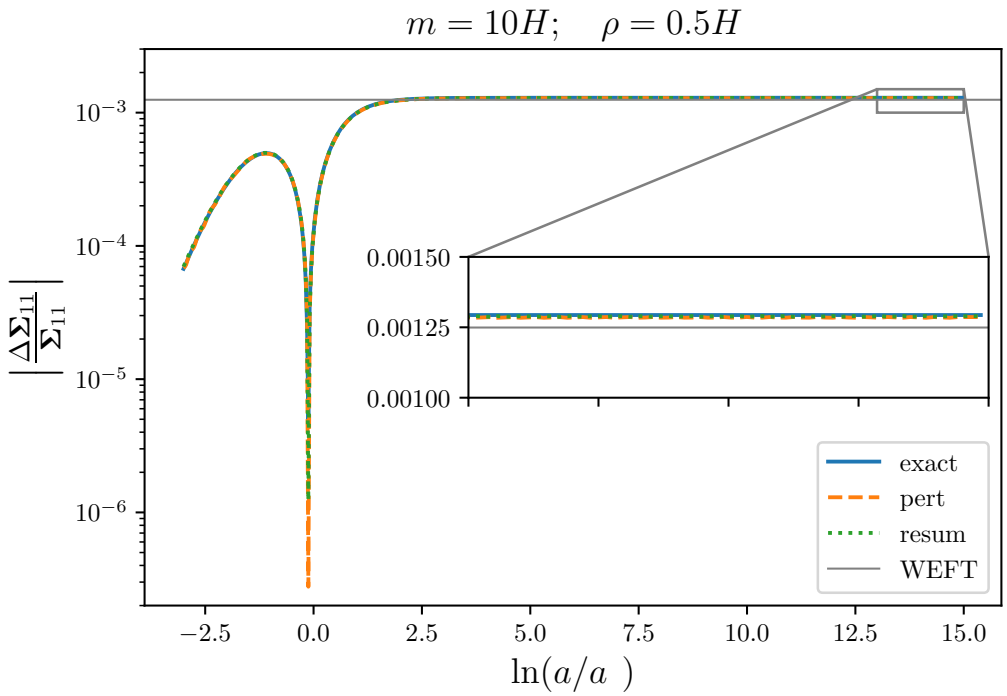

FIG. S1. Relative correction to the free configuration-configuration power spectrum $|\mathbf{\Sigma}_{11} - \mathbf{\Sigma}_{11}^{(0)}|/\mathbf{\Sigma}_{11}^{(0)}$, as a function of time labeled by the number of e-folds $\ln(a/a_*)$ since Hubble crossing, for $m = 10H$ and $\rho = 0.5H$. The blue curve is obtained from integrating the exact transport equations (S10) between $\ln(a/a_*) = -15$ to $\ln(a/a_*) = 15$. The green curve corresponds to the master transport equation (S64), and the orange curve to its perturbative limit (S66). The grey curve stands for the late-time result from Wilsonian EFT [65, 66], which reduces to the in-in formalism [79, 80] in the perturbative limit. The slight deviation from the orange curve is due to the additional expansion in H/m usually performed in WEFT. Similar behaviours are observed for the other two power spectra, namely $\mathbf{\Sigma}_{12}$ and $\mathbf{\Sigma}_{22}$.

functions, *i.e.*

$$v_\zeta'' + \left(k^2 - \frac{2}{\eta^2}\right) v_\zeta = 0 \quad \text{and} \quad v_\mathcal{F}'' + \left(k^2 - \frac{\nu_\mathcal{F}^2 - \frac{1}{4}}{\eta^2}\right) v_\mathcal{F} = 0\,. \tag{S16}$$

In these expressions, $\nu_\mathcal{F} = \frac{3}{2}\sqrt{1 - \frac{4}{9}\frac{m^2}{H^2}} \equiv i\mu_\mathcal{F}$ if $m^2 > \frac{9}{4}H^2$, which we will assume to be the case in the following, except explicitly stated otherwise. By normalising the mode functions to the Bunch-Davies vacuum in the asymptotic, sub-Hubble past, one obtains

$$v_\zeta(\eta) = -\frac{1}{2}\sqrt{\frac{\pi z}{k}} H_{3/2}^{(1)}(z) = \left(1 + \frac{i}{z}\right)\frac{e^{iz}}{\sqrt{2k}}, \tag{S17}$$

$$v_\mathcal{F}(\eta) = \frac{1}{2}\sqrt{\frac{\pi z}{k}} e^{-\frac{\pi}{2}\mu_\mathcal{F} + i\frac{\pi}{4}} H_{i\mu_\mathcal{F}}^{(1)}(z)\,. \tag{S18}$$

In these expressions, $z \equiv -k\eta$ and $H_\nu^{(1)}$ is the Hankel function of the first kind and of order ν. The mode functions of the momentum operators read

$$p_\zeta(\eta) = \frac{1}{2}\sqrt{k\pi z} H_{1/2}^{(1)}(z) = -i\sqrt{\frac{k}{2}} e^{iz}, \tag{S19}$$

$$p_\mathcal{F}(\eta) = -\frac{1}{2}\sqrt{\frac{k\pi}{z}} e^{-\frac{\pi}{2}\mu_\mathcal{F} + i\frac{\pi}{4}} \left[\left(i\mu_\mathcal{F} + \frac{3}{2}\right) H_{i\mu_\mathcal{F}}^{(1)}(z) - z H_{i\mu_\mathcal{F}+1}^{(1)}(z)\right], \tag{S20}$$

where one can check that the mode functions are normalised in a way that the field operators obey their canonical commutation relations.

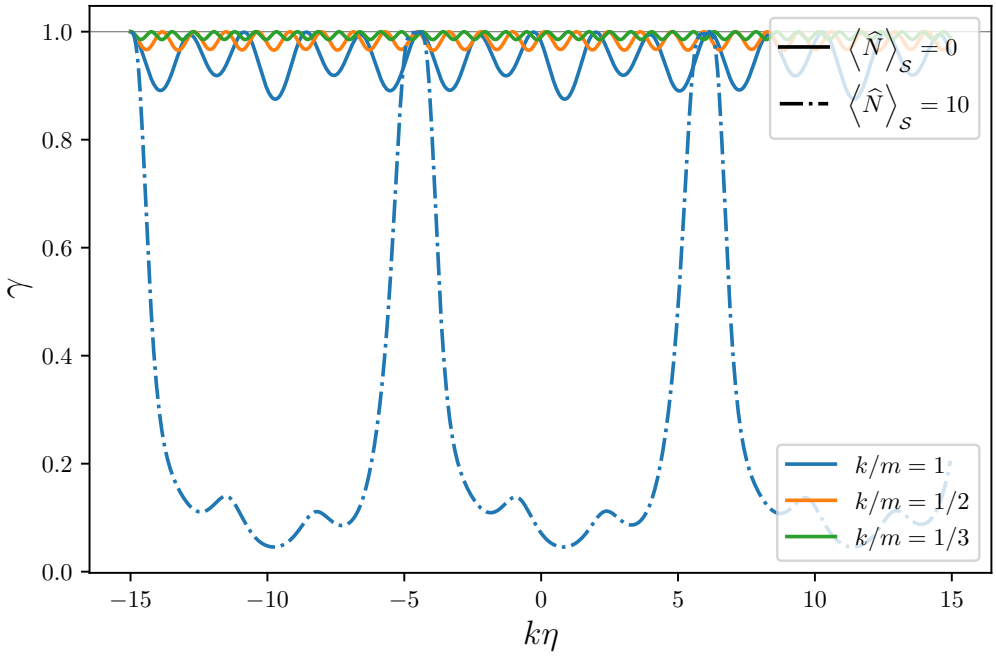

FIG. S2. Purity in flat spacetime, as a function of time, for a few values of the ratio between the Compton wavelength and the physical wavelength k/m. Oscillations take place at frequencies $2\omega_{\mathcal{S}}$, $2\omega_{\mathcal{E}}$, $\omega_{\mathcal{S}} + \omega_{\mathcal{E}}$ and $\omega_{\mathcal{S}} - \omega_{\mathcal{E}}$; where $\omega_{\mathcal{S}} \equiv k$ and $\omega_{\mathcal{E}} \equiv \sqrt{k^2 + m^2}$. In the sub-Compton regime, $k/m > 1$, the slowest frequency is $\omega_{\mathcal{E}} - \omega_{\mathcal{S}}$, which decreases with k/m (this is why oscillations are more rapid for smaller values of k/m in the figure). One can see that the amplitude of the oscillations also decreases as k/m becomes smaller, in agreement with the fact that heavier environments yield weaker perturbations of the system. Different initial states specified by $|\emptyset\rangle_{\mathcal{S}} \otimes |\emptyset\rangle_{\mathcal{E}}$ (solid curves) and $|2\text{MSS}\rangle_{\mathcal{S}} \otimes |\emptyset\rangle_{\mathcal{E}}$ (dash-dotted curve) show that initial conditions also affect the system-environment entanglement but do not alter the recurrence phenomenon (*i.e.* the fact that purity goes back to one, periodically), which is unavoidable.

II. PURITY OSCILLATIONS IN MINKOWSKI SPACETIME

The flat-space analogue of the model studied in this work is obtained by taking the limit where $a = 1$ and $a' = 0$ in Eq. (S6). This leads to Fig. S2 where we consider two sets of initial conditions. The first set consists in a vacuum state $|\emptyset\rangle_{\mathcal{S}} \otimes |\emptyset\rangle_{\mathcal{E}}$. For the initial covariance matrix, it gives the same prescription as above, $\mathbf{\Sigma}_{11}^{(\mathcal{S}+\mathcal{E})} = \mathbf{\Sigma}_{33}^{(\mathcal{S}+\mathcal{E})} = 1/(2k)$, $\mathbf{\Sigma}_{22}^{(\mathcal{S}+\mathcal{E})} = \mathbf{\Sigma}_{44}^{(\mathcal{S}+\mathcal{E})} = k/2$ where all other correlations initially vanish. The second set consists in a Gaussian state $|2\text{MSS}\rangle_{\mathcal{S}} \otimes |\emptyset\rangle_{\mathcal{E}}$ with $|2\text{MSS}\rangle_{\mathcal{S}}$ being a two-mode squeezed state chosen so that the initial occupation number of the system is

$$\left\langle \widehat{N} \right\rangle_{\mathcal{S}} \equiv {}_{\mathcal{S}}\langle 2\text{MSS}|\widehat{a}_{\zeta}^{\dagger}\widehat{a}_{\zeta}\,|2\text{MSS}\rangle_{\mathcal{S}} = 10. \tag{S21}$$

It amounts to picking a set of squeezing parameters [93] (r, φ) such that $\cosh r = 2\left\langle \widehat{N} \right\rangle_{\mathcal{S}} + 1$ and φ is arbitrary, e.g. taken to zero, which fixes the initial correlations at

$$\mathbf{\Sigma}_{11}^{(\mathcal{S}+\mathcal{E})} = \frac{1}{2k}\left(\cosh 2r + \sinh 2r \cos 2\varphi\right) \tag{S22}$$

$$\mathbf{\Sigma}_{22}^{(\mathcal{S}+\mathcal{E})} = \frac{k}{2}\left(\cosh 2r - \sinh 2r \cos 2\varphi\right) \tag{S23}$$

$$\mathbf{\Sigma}_{12}^{(\mathcal{S}+\mathcal{E})} = \frac{1}{2}\sinh 2r \sin 2\varphi \tag{S24}$$

while keeping $\mathbf{\Sigma}_{33}^{(\mathcal{S}+\mathcal{E})} = 1/(2k)$, $\mathbf{\Sigma}_{44}^{(\mathcal{S}+\mathcal{E})} = k/2$ and all other correlations vanish. The evolution of the purity for both types of initial conditions in shown in Fig. S2, where we observe a recurrence phenomenon [152] at a frequency depending on the ratio between the Compton wavelength and the physical wavelength, k/m. Having a larger occupation number at initial time increases and fastens the system-environment entanglement but recurrence invariably occurs.

III. MASTER EQUATION

In this section we review the approach developed in Ref. [64] and perform its direct application to the model considered in this work.

A. Second-order master equation for a generic linear two-field systems

Let us consider two scalar fields ζ (the "system") and $\mathcal{F}$ (the "environment"), linearly coupled in a homogeneous and isotropic background. The coupling is assumed to be weak, which allows us to work within the Born-approximation regime. When expanding the dynamics of the system in powers of the coupling, at second order one obtains the time-convolutionless$_2$ (TCL$_2$) master equation for the reduced density matrix of the system $\widetilde{\rho}_{\rm red}$, which in the interaction picture reads

$$\frac{\mathrm{d}\widetilde{\rho}_{\rm red}}{\mathrm{d}\eta} = -\int_{\eta_0}^{\eta}\mathrm{d}\eta'\mathrm{Tr}_{\mathcal{E}}\left[\widetilde{H}_{\rm int}(\eta),\left[\widetilde{H}_{\rm int}(\eta'),\widetilde{\rho}_{\rm red}(\eta)\otimes\widetilde{\rho}_{\mathcal{E}}\right]\right]. \tag{S25}$$

Here, the quadratic interaction Hamiltonian can be expressed as

$$\widetilde{H}_{\rm int}(\eta) = \widetilde{\boldsymbol{z}}_{\zeta}^{\rm T}(\eta)\boldsymbol{V}(\eta)\widetilde{\boldsymbol{z}}_{\mathcal{F}}(\eta). \tag{S26}$$

$\boldsymbol{V}(\eta)$ is an arbitrary 2×2 matrix containing the linear couplings between the two fields and $\widetilde{\boldsymbol{z}}_{\alpha} = (\widetilde{v}_{\alpha},\widetilde{p}_{\alpha})^{\rm T}$, $\alpha=\zeta,\mathcal{F}$ gathers the configuration and momentum operators of the system and the environment. In order to write Eq. (S25) in the Schrödinger picture, we need to recast it in terms of local-in-time operators for the system. We use the fact that in the interaction picture, operators evolve with the free Hamiltonian $\widehat{\mathcal{H}}_0(\eta)$ so that

$$\widetilde{\boldsymbol{z}}_{\zeta}(\eta') = \bar{\mathcal{T}}\exp\left[i\int_{\eta}^{\eta'}\widehat{\mathcal{H}}_0(\eta'')\mathrm{d}\eta''\right]\widetilde{\boldsymbol{z}}_{\zeta}(\eta)\mathcal{T}\exp\left[-i\int_{\eta}^{\eta'}\widehat{\mathcal{H}}_0(\eta'')\mathrm{d}\eta''\right] \tag{S27}$$

$$= \boldsymbol{G}^{(\mathcal{S})}(\eta',\eta)\widetilde{\boldsymbol{z}}_{\zeta}(\eta) \tag{S28}$$

where $\boldsymbol{G}^{(\mathcal{S})}(\eta',\eta) \equiv \mathrm{Tr}\left\{\left[\widehat{\boldsymbol{z}}_{\zeta}^{\rm T}(\eta'),\widetilde{\boldsymbol{z}}_{\zeta}(\eta)\right]\widehat{\rho}_{\mathcal{S}}\right\}$ is the Green's matrix of the free system, with $\widehat{\rho}_{\mathcal{S}}$ the initial state of the system. Developing Eq. (S25) and expressing it in terms of equal-time operators using Eq. (S28), one finds

$$\begin{aligned}\frac{\mathrm{d}\widetilde{\rho}_{\rm red}}{\mathrm{d}\eta} = -\int_{\eta_0}^{\eta}\mathrm{d}\eta'\Big\{&\left[\widetilde{\boldsymbol{z}}_{\zeta,i}(\eta)\widetilde{\boldsymbol{z}}_{\zeta,j}(\eta)\widetilde{\rho}_{\rm red}(\eta) - \widetilde{\boldsymbol{z}}_{\zeta,j}(\eta)\widetilde{\rho}_{\rm red}(\eta)\widetilde{\boldsymbol{z}}_{\zeta,i}(\eta)\right]\boldsymbol{\mathcal{D}}_{ij}^{>}(\eta,\eta')\\ &-\left[\widetilde{\boldsymbol{z}}_{\zeta,i}(\eta)\widetilde{\rho}_{\rm red}(\eta)\widetilde{\boldsymbol{z}}_{\zeta,j}(\eta) - \widetilde{\rho}_{\rm red}(\eta)\widetilde{\boldsymbol{z}}_{\zeta,j}(\eta)\widetilde{\boldsymbol{z}}_{\zeta,i}(\eta)\right]\boldsymbol{\mathcal{D}}_{ij}^{>*}(\eta,\eta')\Big\},\end{aligned} \tag{S29}$$

where implicit summation over repeated indices apply. The memory kernel $\boldsymbol{\mathcal{D}}^{>}(\eta,\eta')$ is defined by

$$\boldsymbol{\mathcal{D}}^{>}(\eta,\eta') \equiv \boldsymbol{V}(\eta)\boldsymbol{\mathcal{K}}^{>}(\eta,\eta')\boldsymbol{V}^{\rm T}(\eta')\boldsymbol{G}^{(\mathcal{S})}(\eta',\eta) \tag{S30}$$

where $\boldsymbol{\mathcal{K}}^{>}(\eta,\eta') \equiv \mathrm{Tr}\left[\widehat{\boldsymbol{z}}_{\mathcal{F}}^{\rm T}(\eta)\widetilde{\boldsymbol{z}}_{\mathcal{F}}(\eta')\widehat{\rho}_{\mathcal{E}}\right]$ is the Wightman function of the free environment with $\widetilde{\rho}_{\mathcal{E}}$ the initial state of the environment. One can finally decompose the memory kernel in real and imaginary parts $\boldsymbol{\mathcal{D}}^{>}(\eta,\eta') \equiv \boldsymbol{\mathcal{D}}^{\rm Re}(\eta,\eta') + i\boldsymbol{\mathcal{D}}^{\rm Im}(\eta,\eta')$. After some straightforward manipulations, one obtains the TCL$_2$ master equation in the Schrödinger picture

$$\frac{\mathrm{d}\widehat{\rho}_{\rm red}}{\mathrm{d}\eta} = -i\left[\widehat{H}^{(\mathcal{S})}(\eta) + \widehat{H}^{(\rm LS)}(\eta),\widehat{\rho}_{\rm red}(\eta)\right] + \left[\boldsymbol{D}_{ij}(\eta) - i\Delta_{-}(\eta)\boldsymbol{\omega}_{ij}\right]\left[\widehat{\boldsymbol{z}}_{\zeta,i}\widehat{\rho}_{\rm red}(\eta)\widehat{\boldsymbol{z}}_{\zeta,j} - \frac{1}{2}\left\{\widehat{\boldsymbol{z}}_{\zeta,j}\widehat{\boldsymbol{z}}_{\zeta,i},\widehat{\rho}_{\rm red}(\eta)\right\}\right]. \tag{S31}$$

The Lamb-shift Hamiltonian is a quadratic form $\widehat{H}^{(\rm LS)}(\eta) = \frac{1}{2}\widehat{\boldsymbol{z}}_{\zeta}^{\rm T}\boldsymbol{\Delta}(\eta)\widehat{\boldsymbol{z}}_{\zeta}$ where

$$\boldsymbol{\Delta}_{ij}(\eta) = 2\int_{\eta_0}^{\eta}\mathrm{d}\eta'\boldsymbol{\mathcal{D}}_{(ij)}^{\rm Im}(\eta,\eta'). \tag{S32}$$

The noise and dissipation kernels are respectively defined as

$$\boldsymbol{D}_{ij}(\eta) = 2\int_{\eta_0}^{\eta} \mathrm{d}\eta' \boldsymbol{\mathcal{D}}^{\mathrm{Re}}_{(ij)}(\eta,\eta') \tag{S33}$$

$$\Delta_{-}(\eta) = 2\int_{\eta_0}^{\eta} \mathrm{d}\eta' \boldsymbol{\mathcal{D}}^{\mathrm{Im}}_{-}(\eta,\eta') \tag{S34}$$

where we used the symmetric and antisymmetric decomposition of 2×2 matrices $\boldsymbol{A}_{ij} = \boldsymbol{A}_{(ij)} + A_{-}\boldsymbol{\omega}_{ij}$ where $\boldsymbol{A}_{(ji)} = \boldsymbol{A}_{(ij)}$. For the specific model discussed in this article, the definition of $\boldsymbol{V}(\eta)$ is given in Eq. (S6).

B. Cosmological master equation

Using the mode-function decomposition of the fields obtained in Sec. I C, we derive the Wightman function of the environment

$$\boldsymbol{\mathcal{K}}^{>}(\eta,\eta') = \begin{pmatrix} v_{\mathcal{F}}(\eta)v^{*}_{\mathcal{F}}(\eta') & p_{\mathcal{F}}(\eta)v^{*}_{\mathcal{F}}(\eta') \\ v_{\mathcal{F}}(\eta)p^{*}_{\mathcal{F}}(\eta') & p_{\mathcal{F}}(\eta)p^{*}_{\mathcal{F}}(\eta') \end{pmatrix}, \tag{S35}$$

and the Green's matrix of the system

$$\boldsymbol{G}^{(\mathcal{S})}(\eta',\eta) = 2\begin{pmatrix} -\Im\mathrm{m}\left[p_{\zeta}(\eta)v^{*}_{\zeta}(\eta')\right] & \Im\mathrm{m}\left[v_{\zeta}(\eta)v^{*}_{\zeta}(\eta')\right] \\ -\Im\mathrm{m}\left[p_{\zeta}(\eta)p^{*}_{\zeta}(\eta')\right] & \Im\mathrm{m}\left[v_{\zeta}(\eta)p^{*}_{\zeta}(\eta')\right] \end{pmatrix}, \tag{S36}$$

where we used the Bunch-Davies initial vacuum prescription. Inserting Eqs. (S35) and (S36) into the expression of the memory kernel given in Eq. (S30), we obtain the master equation presented in the main text which we rewrite here for convenience

$$\frac{\mathrm{d}\widehat{\rho}_{\mathrm{red}}}{\mathrm{d}\eta} = -i\left[\widehat{H}^{\mathcal{S}}_{0}(\eta) + \widehat{H}^{(\mathrm{LS})}(\eta), \widehat{\rho}_{\mathrm{red}}(\eta)\right] + \boldsymbol{\mathcal{D}}_{ij}(\eta)\left[\widehat{\boldsymbol{z}}_{\zeta,i}\widehat{\rho}_{\mathrm{red}}(\eta)\widehat{\boldsymbol{z}}_{\zeta,j} - \frac{1}{2}\left\{\widehat{\boldsymbol{z}}_{\zeta,j}\widehat{\boldsymbol{z}}_{\zeta,i}, \widehat{\rho}_{\mathrm{red}}(\eta)\right\}\right], \tag{S37}$$

where $\widehat{H}^{(\mathrm{LS})}(\eta) = \frac{1}{2}\widehat{\boldsymbol{z}}^{\mathrm{T}}_{\zeta}\boldsymbol{\Delta}(\eta)\widehat{\boldsymbol{z}}_{\zeta}$ and $\boldsymbol{\mathcal{D}} \equiv \boldsymbol{D}(\eta) + i\Delta_{12}(\eta)\boldsymbol{\omega}$. The entries of the $\boldsymbol{\Delta}$ and $\boldsymbol{D}$ matrices are given by the so-called master-equation coefficients defined as

$$\boldsymbol{\Delta}_{11}(\eta) = 0 \tag{S38}$$

$$\boldsymbol{\Delta}_{12}(\eta) = \boldsymbol{\Delta}_{21}(\eta) = -2\rho^2 a(\eta)\int_{\eta_0}^{\eta}\mathrm{d}\eta' a(\eta')\Im\mathrm{m}\left[p_{\zeta}(\eta)p^{*}_{\zeta}(\eta')\right]\Im\mathrm{m}\left[v_{\mathcal{F}}(\eta)v^{*}_{\mathcal{F}}(\eta')\right] \tag{S39}$$

$$\boldsymbol{\Delta}_{22}(\eta) = 4\rho^2 a(\eta)\int_{\eta_0}^{\eta}\mathrm{d}\eta' a(\eta')\Im\mathrm{m}\left[v_{\zeta}(\eta)p^{*}_{\zeta}(\eta')\right]\Im\mathrm{m}\left[v_{\mathcal{F}}(\eta)v^{*}_{\mathcal{F}}(\eta')\right], \tag{S40}$$

and

$$\boldsymbol{D}_{11}(\eta) = 0 \tag{S41}$$

$$\boldsymbol{D}_{12}(\eta) = \boldsymbol{D}_{21}(\eta) = -2\rho^2 a(\eta)\int_{\eta_0}^{\eta}\mathrm{d}\eta' a(\eta')\Im\mathrm{m}\left[p_{\zeta}(\eta)p^{*}_{\zeta}(\eta')\right]\Re\mathrm{e}\left[v_{\mathcal{F}}(\eta)v^{*}_{\mathcal{F}}(\eta')\right] \tag{S42}$$

$$\boldsymbol{D}_{22}(\eta) = 4\rho^2 a(\eta)\int_{\eta_0}^{\eta}\mathrm{d}\eta' a(\eta')\Im\mathrm{m}\left[v_{\zeta}(\eta)p^{*}_{\zeta}(\eta')\right]\Re\mathrm{e}\left[v_{\mathcal{F}}(\eta)v^{*}_{\mathcal{F}}(\eta')\right]. \tag{S43}$$

C. Master-equation coefficients

A simple manipulation of Eqs. (S39), (S40), (S42) and (S43) leads to

$$\boldsymbol{\Delta}_{12}(\eta) = -\frac{\rho^2}{H^2}\frac{k}{z}\Re\mathrm{e}\left[p_{\zeta}(z)v_{\mathcal{F}}(z)\int_{z_0}^{z}\frac{\mathrm{d}z'}{z'}p^{*}_{\zeta}(z')v^{*}_{\mathcal{F}}(z') - p_{\zeta}(z)v^{*}_{\mathcal{F}}(z)\int_{z_0}^{z}\frac{\mathrm{d}z'}{z'}p^{*}_{\zeta}(z')v_{\mathcal{F}}(z')\right] \tag{S44}$$

$$\boldsymbol{\Delta}_{22}(z) = 2\frac{\rho^2}{H^2}\frac{k}{z}\Re\mathrm{e}\left[v_{\zeta}(z)v_{\mathcal{F}}(z)\int_{z_0}^{z}\frac{\mathrm{d}z'}{z'}p^{*}_{\zeta}(z')v^{*}_{\mathcal{F}}(z') - v_{\zeta}(z)v^{*}_{\mathcal{F}}(z)\int_{z_0}^{z}\frac{\mathrm{d}z'}{z'}p^{*}_{\zeta}(z')v_{\mathcal{F}}(z')\right], \tag{S45}$$

and

$$\boldsymbol{D}_{12}(\eta) = \frac{\rho^2}{H^2}\frac{k}{z}\Im\mathrm{m}\left[p_\zeta(z)v_\mathcal{F}(z)\int_{z_0}^{z}\frac{\mathrm{d}z'}{z'}p_\zeta^*(z')v_\mathcal{F}^*(z') + p_\zeta(z)v_\mathcal{F}^*(z)\int_{z_0}^{z}\frac{\mathrm{d}z'}{z'}p_\zeta^*(z')v_\mathcal{F}(z')\right] \tag{S46}$$

$$\boldsymbol{D}_{22}(\eta) = -2\frac{\rho^2}{H^2}\frac{k}{z}\Im\mathrm{m}\left[v_\zeta(z)v_\mathcal{F}(z)\int_{z_0}^{z}\frac{\mathrm{d}z'}{z'}p_\zeta^*(z')v_\mathcal{F}^*(z') + v_\zeta(z)v_\mathcal{F}^*(z)\int_{z_0}^{z}\frac{\mathrm{d}z'}{z'}p_\zeta^*(z')v_\mathcal{F}(z')\right], \tag{S47}$$

where we defined the variable $z \equiv -k\eta$. To obtain analytical expressions for the master-equation coefficients, we have to compute two integrals. The first one is

$$I_1(z,z_0) = \int_{z_0}^{z}\frac{\mathrm{d}z'}{z'}p_\zeta^*(z')v_\mathcal{F}^*(z'). \tag{S48}$$

Inserting the mode function expressions given in Eqs. (S17), (S18), (S19) and (S20), we obtain

$$I_1(z,z_0) = \frac{i}{2}\sqrt{\frac{\pi}{2}}e^{-\frac{\pi}{2}\mu_\mathcal{F}}e^{-i\frac{\pi}{4}}\int_{z_0}^{z}\frac{\mathrm{d}z'}{\sqrt{z'}}e^{-iz'}H^{(2)}_{-i\mu_\mathcal{F}}(z') \equiv F_{I_1}(z) - F_{I_1}(z_0) \tag{S49}$$

with

$$F_{I_1}(z) = i\sqrt{\frac{\pi}{2}}e^{-\frac{\pi}{2}\mu_\mathcal{F}}e^{-i\frac{\pi}{4}}\sqrt{z}\left[\gamma^*_{\mu_\mathcal{F}}(z)g_{\mu_\mathcal{F}}(z) + \delta^*_{\mu_\mathcal{F}}(z)g_{-\mu_\mathcal{F}}(z)\right] \tag{S50}$$

where we have introduced for later convenience the notations

$$\gamma_{\mu_\mathcal{F}}(z) \equiv \frac{1+\coth\pi\mu_\mathcal{F}}{\Gamma(1+i\mu_\mathcal{F})}\left(\frac{z}{2}\right)^{i\mu_\mathcal{F}}, \qquad \delta_{\mu_\mathcal{F}}(z) \equiv \frac{-1}{\sinh\pi\mu_\mathcal{F}}\frac{1}{\Gamma(1-i\mu_\mathcal{F})}\left(\frac{z}{2}\right)^{-i\mu_\mathcal{F}} \tag{S51}$$

and

$$g_{\mu_\mathcal{F}}(z) = \frac{1}{1-2i\mu_\mathcal{F}}{}_2F_2{}^{\frac{1}{2}-i\mu_\mathcal{F},\frac{1}{2}-i\mu_\mathcal{F}}_{\frac{3}{2}-i\mu_\mathcal{F},1-2i\mu_\mathcal{F}}(-2iz), \tag{S52}$$

${}_2F_2$ being the $(2,2)$ generalized hypergeometric function. Note that $g^*_{\mu_\mathcal{F}}(z) = g_{-\mu_\mathcal{F}}(-z)$. The second integral is

$$I_2(z,z_0) = \int_{z_0}^{z}\frac{\mathrm{d}z'}{z'}p_\zeta^*(z')v_\mathcal{F}(z') \tag{S53}$$

and following the same procedure, one finds

$$I_2(z,z_0) = \frac{i}{2}\sqrt{-\frac{\pi}{2}}e^{-\frac{\pi}{2}\mu_\mathcal{F}}e^{i\frac{\pi}{4}}\int_{z_0}^{z}\frac{\mathrm{d}z'}{\sqrt{z'}}e^{-iz'}H^{(1)}_{i\mu_\mathcal{F}}(z') \equiv F_{I_2}(z) - F_{I_2}(z_0) \tag{S54}$$

with

$$F_{I_2}(z) = i\sqrt{\frac{\pi}{2}}e^{-\frac{\pi}{2}\mu_\mathcal{F}}e^{i\frac{\pi}{4}}\sqrt{z}\left[\delta_{\mu_\mathcal{F}}(z)g_{\mu_\mathcal{F}}(z) + \gamma_{\mu_\mathcal{F}}(z)g_{-\mu_\mathcal{F}}(z)\right]. \tag{S55}$$

Inserting Eqs. (S49) and (S54) into the expression of the master equation coefficients (S44), (S45), (S46) and (S47) and using the functions $F_{I_1}(z)$ and $F_{I_2}(z)$, we obtain analytic expressions for the TCL_2 coefficients.

1. *Spurious terms*

In Ref. [64], it has been shown that some terms dubbed "spurious" appear in the master-equation coefficients, that cancel out in the perturbative limit but ruin the resummation otherwise. More precisely, the master-equation coefficients are expressed as integrals between η_0 and η, see Eqs. (S44)-(S47), i.e.

$$\boldsymbol{\Delta}_{12} = F_{\boldsymbol{\Delta}_{12}}(\eta,\eta) - F_{\boldsymbol{\Delta}_{12}}(\eta,\eta_0), \tag{S56}$$

where $F_{\boldsymbol{\Delta}_{12}}(\eta,\cdot)$ is the primitive of the integrand appearing in Eq. (S44), which itself depends on η, and with similar notations for the other coefficients. The second term in Eq. (S56), the one that depends on the initial time η_0, is the "spurious" one. In the exact solution of Sec. I, there is no such initial-time dependent term in the

dynamical equations, and indeed one can show that it cancels out at all orders in perturbation theory [64]. At leading order in the interaction strength, the master equation reduces to standard perturbation theory, hence again one can show that the spurious contribution vanishes [64]. At higher order however, the master equation stops being exact, since it only performs resummation of the leading-order interaction. This is why the spurious term alters the result. However, since we know that it should vanish at all orders, one can simply remove it by hand, and thus restore the ability of the master equation to perform efficient resummation [64]. One may be worried that, from Eq. (S56), the spurious terms are only defined up to an additive constant. However, since they are known to vanish at all (and in particular at leading) orders, they can be determined without ambiguity by comparison with the perturbative theory. In the following we thus remove spurious terms, which amounts to discarding all $F_{I_1}(z_0)$ and $F_{I_2}(z_0)$ terms in the above expressions.

2. *Super-Hubble limit*

We now exhibit the late-time super-Hubble limit of the master equation coefficients where we perform a systematic expansion in powers of $z \ll 1$. Expanding the mode functions and various elements appearing in Eqs. (S44), (S45), (S46) and (S47) in the super-Hubble regime, we obtain

$$\boldsymbol{\Delta}_{12}(z) = \frac{\rho^2}{H^2}\frac{16k^2}{9+40\mu_{\mathcal{F}}^2+16\mu_{\mathcal{F}}^4}\frac{z}{k} + \mathcal{O}(z^3) \tag{S57}$$

$$\boldsymbol{\Delta}_{22}(z) = -\frac{\rho^2}{H^2}\frac{1}{\frac{9}{4}+\mu_{\mathcal{F}}^2} + \mathcal{O}(z^2), \tag{S58}$$

and

$$\boldsymbol{D}_{12}(z) = -\frac{\rho^2}{H^2}\frac{1}{\mu_{\mathcal{F}}}\frac{(-6+8\mu_{\mathcal{F}}^2)k^2}{9+40\mu_{\mathcal{F}}^2+16\mu_{\mathcal{F}}^4}\frac{z}{k} + \mathcal{O}(z^3) \tag{S59}$$

$$\boldsymbol{D}_{22}(z) = -\frac{3}{2}\frac{\rho^2}{H^2}\frac{1}{\mu_{\mathcal{F}}}\frac{1}{\frac{9}{4}+\mu_{\mathcal{F}}^2} + \mathcal{O}(z^2). \tag{S60}$$

Note that, in the heavy case where $\mu_{\mathcal{F}} \simeq m/H \gg 1$, Eqs. (S57) and (S58) lead to $\boldsymbol{\Delta}_{12} \ll a'/a$ and $\boldsymbol{\Delta}_{22} \to -\rho^2/m^2$, from which we deduce that the Lamb-shift Hamiltonian renormalises the free dynamics as

$$\widehat{H}_0^{\mathcal{S}}(\eta) + \widehat{H}^{(\mathrm{LS})}(\eta) \simeq \frac{1}{2}\left[\left(1-\frac{\rho^2}{m^2}\right)\widehat{p}_\zeta\widehat{p}_\zeta + k^2\widehat{v}_\zeta\widehat{v}_\zeta + \frac{a'}{a}\left\{\widehat{v}_\zeta,\widehat{p}_\zeta\right\}\right]. \tag{S61}$$

One can thus see that $\boldsymbol{\Delta}_{22}$ renormalises the kinetical term, generating an effective speed of sound

$$c_{\mathrm{S}}^2 = 1 - \frac{\rho^2}{m^2} + \mathcal{O}\left(\frac{k}{aH}, \frac{H^4}{m^4}\right) \tag{S62}$$

as stated in the main text.

D. Effective transport equations

1. *Transport equations derivation*

The covariance matrix of the system expressed in the Schrödinger picture reads

$$\boldsymbol{\Sigma}_{ij}(\eta) \equiv \frac{1}{2}\mathrm{Tr}\left[\left\{\widehat{\boldsymbol{z}}_{\zeta,i}, \widehat{\boldsymbol{z}}_{\zeta,j}\right\}\widehat{\rho}_{\mathrm{red}}(\eta)\right]. \tag{S63}$$

By differentiating Eq. (S63) with respect to time and inserting Eq. (3) in the right-hand side, we obtain the effective transport equations for the covariance matrix,

$$\frac{\mathrm{d}\boldsymbol{\Sigma}}{\mathrm{d}\eta} = \boldsymbol{\omega}\left(\boldsymbol{H}^{(\mathcal{S})}+\boldsymbol{\Delta}\right)\boldsymbol{\Sigma} - \boldsymbol{\Sigma}\left(\boldsymbol{H}^{(\mathcal{S})}+\boldsymbol{\Delta}\right)\boldsymbol{\omega} - \boldsymbol{\omega}\boldsymbol{D}\boldsymbol{\omega} + 2\boldsymbol{\Delta}_{12}\boldsymbol{\Sigma}. \tag{S64}$$

As mentioned above, a numerically efficient way to access the late-time behaviour of the purity is to derive an equation of motion for $\det \boldsymbol{\Sigma}$ from the transport equation of the covariance, leading to

$$\frac{\mathrm{d}\det\boldsymbol{\Sigma}}{\mathrm{d}\eta} = \mathrm{Tr}\left(\boldsymbol{\Sigma}\boldsymbol{D}\right) + 4\boldsymbol{\Delta}_{12}\det\boldsymbol{\Sigma}. \tag{S65}$$

2. *Perturbative treatment*

In the main text, the numerical solution of Eqs. (S64)-(S65) (labeled "resum" in Fig. 4 of the main text) is compared with a perturbative solution (labeled "pert"), where the solution is derived at leading order in ρ^2. Since $\boldsymbol{\Delta}$ and $\boldsymbol{D}$ are of order ρ^2, this amounts to replacing $\boldsymbol{\Sigma}$ by its free-theory counterpart $\boldsymbol{\Sigma}^{(0)}$ when multiplied by $\boldsymbol{\Delta}$ or $\boldsymbol{D}$ in the right-hand side of Eqs. (S64)-(S65),

$$\frac{\mathrm{d}\boldsymbol{\Sigma}^{(2)}}{\mathrm{d}\eta} = \boldsymbol{\omega}\boldsymbol{H}^{(\mathcal{S})}\boldsymbol{\Sigma}^{(2)} - \boldsymbol{\Sigma}^{(2)}\boldsymbol{H}^{(\mathcal{S})}\boldsymbol{\omega} + \boldsymbol{\omega}\boldsymbol{\Delta}\boldsymbol{\Sigma}^{(0)} - \boldsymbol{\Sigma}^{(0)}\boldsymbol{\Delta}\boldsymbol{\omega} - \boldsymbol{\omega}\boldsymbol{D}\boldsymbol{\omega} + 2\boldsymbol{\Delta}_{12}\boldsymbol{\Sigma}^{(0)}. \tag{S66}$$

and

$$\frac{\mathrm{d}\det(\boldsymbol{\Sigma}^{(2)})}{\mathrm{d}\eta} = \mathrm{Tr}\left(\boldsymbol{\Sigma}^{(0)}\boldsymbol{D}\right) + \boldsymbol{\Delta}_{12}, \tag{S67}$$

where the superscript indicates the order at which a given observable is computed and we used the fact that $\det(\boldsymbol{\Sigma}^{(0)}) = 1/4$. In this limit, the environmental effects just play the role of source terms. In Fig. S1, the non-perturbative solution of Eq. (S64) and its perturbative limit (S66) are compared to the exact result. As explained in the main text, since the interaction is effectively switched off at late time, there is no substantial resummation in the current setting (contrary to the situation investigated in Ref. [64]). This is why the non-perturbative solution shows no sign of improvement at late time.

3. *Super-Hubble expansion*

Inserting the super-Hubble expansion of the master equation coefficients obtained in Sec. III C 2 into the transport equations (S64), and working order-by-order in z, one finds

$$\boldsymbol{\Sigma}_{11}(z) = A_{-2}^{\boldsymbol{\Sigma}_{11}} z^{-2} + f_1\left(A_{-2}^{\boldsymbol{\Sigma}_{11}}\right) + f_2\left(A_0^{\boldsymbol{\Sigma}_{12}}\right) z\,, \tag{S68}$$

$$\boldsymbol{\Sigma}_{12}(z) = -k A_{-2}^{\boldsymbol{\Sigma}_{11}} z^{-1} + A_0^{\boldsymbol{\Sigma}_{12}} + f_3\left(A_0^{\boldsymbol{\Sigma}_{12}}\right) z^2\,, \tag{S69}$$

$$\boldsymbol{\Sigma}_{22}(z) = k^2 A_{-2}^{\boldsymbol{\Sigma}_{11}} - 2k A_0^{\boldsymbol{\Sigma}_{12}} z + A_2^{\boldsymbol{\Sigma}_{22}} z^2 + 2k f_3\left(A_0^{\boldsymbol{\Sigma}_{12}}\right) z^3\,. \tag{S70}$$

Here, $A_{-2}^{\boldsymbol{\Sigma}_{11}}, A_0^{\boldsymbol{\Sigma}_{12}}$ and $A_2^{\boldsymbol{\Sigma}_{22}}$ are three constants that cannot be determined by a mere super-Hubble expansion, since they result from the full integrated dynamics (they can however be set by numerical matching to the full solution). In the free theory, they are given by $A_{-2}^{\boldsymbol{\Sigma}_{11}(0)} = 1/(2k), A_0^{\boldsymbol{\Sigma}_{12}(0)} = 0$ and $A_2^{\boldsymbol{\Sigma}_{22}(0)} = 0$ but otherwise receive $\mathcal{O}(\rho^2)$ corrections. We have also defined

$$f_1\left(A_{-2}^{\boldsymbol{\Sigma}_{11}}\right) \equiv \left(1 - \frac{\rho^2}{H^2}\frac{1}{\frac{1}{4}+\mu_{\mathcal{F}}^2}\right) A_{-2}^{\boldsymbol{\Sigma}_{11}} \tag{S71}$$

$$f_2\left(A_0^{\boldsymbol{\Sigma}_{12}}\right) \equiv -\frac{2}{3k}\left(1 - \frac{\rho^2}{H^2}\frac{1}{\frac{9}{4}+\mu_{\mathcal{F}}^2}\right) A_0^{\boldsymbol{\Sigma}_{12}} + \frac{1}{2k}\frac{\rho^2}{H^2}\frac{1}{\mu_{\mathcal{F}}}\frac{1}{\frac{9}{4}+\mu_{\mathcal{F}}^2} \tag{S72}$$

$$f_3\left(A_0^{\boldsymbol{\Sigma}_{12}}\right) \equiv \frac{2}{3}\left[1 - \frac{\rho^2}{H^2}\left(\frac{1}{9+4\mu_{\mathcal{F}}^2} + \frac{3}{1+4\mu_{\mathcal{F}}^2}\right)\right] A_0^{\boldsymbol{\Sigma}_{12}} + \frac{\rho^2}{H^2}\frac{4}{9+40\mu_{\mathcal{F}}^2+16\mu_{\mathcal{F}}^4}. \tag{S73}$$

This shows that the presence of the environment does not change the dominant scaling in z, but simply modifies the coefficients of the expansion by $\mathcal{O}(\rho^2)$-suppressed corrections. This is again evidence that no secular growth needs to be resummed, and the main effect is perturbative.

One can also use these results to extract the super-Hubble behaviour of the purity parameter. Using

Eqs. (S68)-(S70), and expanding in ρ^2, one finds

$$\det \mathbf{\Sigma} = \underbrace{\frac{1}{4} + \frac{A_2^{\mathbf{\Sigma}_{22}}}{2k} + k\left(A_{-2}^{\mathbf{\Sigma}_{11}} - \frac{1}{2k}\right) - \frac{\rho^2}{1+4\mu^2}}_{\det \mathbf{\Sigma}_\infty} + \frac{1+8\mu_{\mathcal{F}}+4\mu_{\mathcal{F}}^2}{9\mu_{\mathcal{F}}+40\mu_{\mathcal{F}}^3+16\mu_{\mathcal{F}}^5}\frac{\rho^2}{H^2}z + \mathcal{O}\big(\rho^4, z^2\big)\ . \tag{S74}$$

The asymptotic value $\det \mathbf{\Sigma}_\infty$ cannot be determined without numerical matching, since it depends on the two ρ^2-suppressed constants $A_2^{\mathbf{\Sigma}_{22}}$ and $A_{-2}^{\mathbf{\Sigma}_{11}} - 1/(2k)$. The rate at which purity grows is however fully determined by the above relation, and recalling that $\gamma = 1/(4\det \mathbf{\Sigma})$, one finds

$$\begin{aligned}\gamma &= \gamma_\infty - \frac{1+8\mu_{\mathcal{F}}+4\mu_{\mathcal{F}}^2}{\frac{9}{4}\mu_{\mathcal{F}}+10\mu_{\mathcal{F}}^3+4\mu_{\mathcal{F}}^5}\frac{\rho^2}{H^2}z \\ &\simeq \gamma_\infty - \frac{\rho^2}{H^2}\frac{1}{\mu_{\mathcal{F}}^3}z \simeq \gamma_\infty - \frac{\rho^2}{m^2}\frac{H}{m}z\end{aligned} \tag{S75}$$

where in the second line we have taken the limit $m \gg H$. This coincides with Eq. (2) in the main text.

Conclusions

Summary: *The first apples*

In this manuscript, we have presented our contribution to the development of Open EFTs in cosmology. A lot of work remains to be done, yet a few observations can be gathered as guidelines for future investigations.

Driven Cosmological Open Quantum Systems

The most remarkable difference between flat and curved-space OQS is the presence of a dynamical background in the latter. It renders all the parameters in the action time dependent. In particular, the coupling between the system and its surrounding environment now becomes dynamical. As we saw in Chapter 5 with the study of quantum decoherence and in Chapter 6 with the study of recoherence, the role of the expanding background is crucial for understanding the quantum information properties of the system. Indeed, neither decoherence nor recoherence could occur for time-independent Hamiltonians and finite number of dynamical degrees of freedom [188]. While Poincaré recurrence theorem [303] prevents the emergence of irreversibility unless a thermodynamic limit is reached, cosmology evades this principle by breaking volume conservation.

As a consequence, the flat space intuition must be considered with caution if the driven nature of the OQS is not carefully accounted for. It urges the need to reconstruct an understanding of quantum information for cosmology and black hole physics. Accounting for the presence of a dynamical background may be modelled through techniques originating from the study of driven OQS such as Floquet theory [304, 305]. It may also help us to construct better analogues for the physics of the early universe [306–308].

Non-Markovian cosmological environments

The presence of a dynamical background also plays a crucial role in preventing the system and its environment to reach some form of stationarity. The squeezing mechanism studied in Chapter 4 invariably affects all massless and light degrees of freedom in the early universe. The thermal properties of squeezed states have been studied in [309] where the authors demonstrated that a squeezed field cannot reach equilibration. It constitutes a first difficulty to treat environments experiencing squeezing as late-time stationarity is never reached in cosmology.

It renders non-Markovian dynamics ubiquitous in the context of dynamical backgrounds. The coefficient of the master equations considered in Chapter 5 are in general time dependent and the semi-group property is not fulfilled. It renders crucial to develop understanding of this class of dynamics, as raised by the authors of [269], as it leads to non-trivial phenomena such as quantum recoherence we accounted for in Chapter 6. Quantum recoherence cannot be captured by an irreversible dynamical map such as the one generated from a Linbladian, hence the importance of Time-ConvolutionLess (TCL) and other non-Markovian techniques to effectively capture this effect.

On the need of non-unitary extensions

Before pursuing further this research program, we have to assess the benefits it may provide. Among them, accessing the non-unitary dynamics seems an interesting feature in the context of cosmology. Indeed, the lack of energy conservation renders the implementation of Wilsonian EFTs less obvious in cosmology than in the context of scattering amplitudes, if not impossible in the absence of symmetry [22]. We may also need to incorporate non-unitary effects such as dissipation if we want to correctly account for the low-energy EFT in the presence of generic environments.

Throughout this manuscript, we illustrated in simple examples how Open EFTs may encompass the Wilsonian EFT results at late-time, for instance through the effective mass observed in Chapter 5 or through the effective speed of sound in Chapter 6. We also illustrated how the renormalization of the unitary evolution due to the interactions with the surrounding environment (the Lamb-shift) relates with the non-unitary evolution that cannot be captured in the standard Wilsonian EFT language (dissipation and decoherence). The lack of energy conservation being one of the most stringent differences between cosmology and particle physics, the understanding of the non-unitary nature of the cosmological dynamics it implies may allow us to bypass the difficulties of importing tools from one field to the other (for e.g. positivity bounds [310]) or to understand the impossibility for doing so.

A partial understanding of the phenomenology

Even if a complete phenomenology of decoherence during inflation is still lacking, the content of this manuscript already provides some broad picture for the case of linear interactions. Comparing the results obtained in Chapter 5 and Chapter 6, it seems that whenever we are in presence of "growing modes" (in terms of the rescaled Mukhanov-Sasaki like variables) in the coupling, we observe complete decoherence by the end of inflation for the modes of interest in the CMB.

Let us illustrate this statement based on the framework proposed in Chapter 6. When entropic perturbations are heavy, they oscillate at super-Hubble scales and do not acquire a growing mode. Hence, if they couple to $\dot{\zeta}$ which is not growing either at late time, we do not observe decoherence but rather quantum recoherence (Fig. 1 of [154]). If we instead couple the heavy entropic perturbations to ζ, the presence of a growing mode prevents the coupling to decay away and we rather observe complete decoherence (Fig. 4 of [244]). Now, if instead we consider a light environment for which $m < 3H/2$, the entropic perturbations acquire a growing mode. When coupled to $\dot{\zeta}$, the presence of the growing mode is sufficient to drive decoherence instead of recoherence (blue curve of Fig. 3 in [154]). Finally, if we couple this light environment with ζ instead of $\dot{\zeta}$, obviously we observe decoherence due to the presence of growing modes.

Beyond linear interactions, the intuition that the decoherence rate is driven by the presence of growing modes at super-Hubble scales can be found not only in recent articles [228, 229, 311] but also in old results [221, 232] reinterpreted in terms of the enlarged phenomenology today accessible. The presence of light degrees of freedom experiencing quantum squeezing due to the pair creation process induced by the dynamical background seems crucial in this regard.

Towards non-perturbative resummation in cosmology

Among the promises of Open EFTs, implementing non-perturbative resummations in cosmology is certainly one of the most remarkable. In order to avoid playing with smoke and mirrors, we need to specify what to expect from these resummations. Studied in the context of secular divergences, they capture the cumulative effect of perturbative corrections. In this sense, they still rely on a sense of perturbativity which holds at the level of the master equation derivation. If they improve the late-time behaviour of the system observables as seen in Chapter 5, they should not allow us to access the strong coupling regime.

The implementation of the Open EFT resummation for Gaussian systems can be made at the level of the transport equations which form a closed system. In the case of non-Markovian dynamics, extra care must apply due to the the appearance of a set of terms dubbed as spurious which cancel against each other in the perturbative limit yet ruin the resummation, as first noticed in Chapter 5. As developed in Chapter 6, we can identify these terms by comparing the Open EFT results with the ones obtained from standard techniques at the perturbative level where they should match.

Clearly, the understanding of non-perturbative resummations in cosmology is far from reaching an end. Resumming non-linear interactions in the master equation framework remains an open question. Beyond Open EFTs, we still need to understand the relations with the other techniques existing on the market such as the Dynamical Renormalization Group [289–291], diagrammatic resummations [292, 295, 296, 312] and stochastic inflation [90, 174, 293, 313].

Future directions

Decoherence from non-linearities during inflation

The complete agreement of the current cosmological data with adiabatic and Gaussian primordial perturbations observed in the CMB [75] and the LSS [76–78] put constraints on the level of non-linear interactions one can expect. Despite their smallness, single-field slow-roll self-interactions may already be enough to generate complete decoherence of the curvature perturbations for the scales of interest in standard scenarios [228]. Yet, non-Gaussian signatures being slow-roll suppressed in this class of model [49], a direct evidence of this decoherence channel in the higher-order statistics remains inaccessible.

At the same time, it is a known fact that hidden sectors may enhance the non-Gaussian signal from primordial cosmology [105, 147, 155, 156, 314–316]. By doing so, they open new decoherence channels directly related to observational signatures such as the non-Gaussian parameter $f_{\rm NL}$. Examplified in the case of quasi-single field models and the cosmological collider signal, the environment imprints its signature by generating distinctive shapes of primordial non-Gaussianities such as the well-known mass dependence of the squeezed limit of the curvature perturbation bispectrum [147, 317, 318]. Future work aims at connecting this smoking gun for multifield inflation to the quantum information aspects of the inflationary model, such as the decoherence of the curvature perturbations.

This study opens the door for an enlarged exploration of the non-linear phe-

nomenology of quantum information properties of inflationary models. Understanding the higher-spin exchanges through Yukawa types of interactions for fermions [319], Chern-Simons for gauge vectors [320] and GR non-linearities for gravitons [49] would allow us to assess what are the most efficient decoherence channels and their observational signatures. In the future, the exploration of the phenomenology may also include the role played by the symmetries, the initial state or the impact of soft modes on the quantum information properties of the adiabatic sector.

Understanding Markovianity in cosmology

Despite the lack of stationarity and the ubiquity of non-Markovian environments in cosmology, the peculiar super-Hubble dynamics often takes over at late time in the presence of light degrees of freedom, leading to an effective phase of decoherence. In this case, the positive eigenvalue of the dissipator grows in time while the negative eigenvalue decreases or saturates. It suggests that a meaningful Markovian limit, after appropriate coarse-graining in time, could emerge. Still, a systematic method to reach this limit and a complete understanding of the physical prerequisite it requires are missing.

In OQS theory, Markovian environments are large and stationary so they form a bath [188]. They possess efficient scrambling properties and dissipate information about the initial conditions in timescales shorter than the system can resolve. In this sense, they naturally relate to some form of thermodynamic limit. In cosmology, where the dynamical background plays a crucial role, how would Markovianity emerge when a large N limit is gradually taken, N being the number of environmental degrees of freedom? In particular, are the statistical distributions (the spectral densities) of Markovian environments similar to their flat space analogues? Studies along this line have been conducted in the context of black holes [239] and future works aim at clarifying this point in primordial cosmology to enable the design of Markovian cosmological environments.

Finally, the bottom-up construction of Markovian dynamical map [273] is one of the cornerstones of OQS theory. Yet, the implications it poses on the construction of generic dynamical map in the context of cosmology has not been developed so far to our knowledge. It might help us in constraining the landscape of non-unitary dynamics accessible in cosmology. We conclude that the emergence of Markovianity is a subtle and promising topic which deserves further investigation in the context of QFT in curved-spacetimes.

Bottom-up constructions of Open EFTs

Throughout this manuscript, despite our desire to constrain model-independent extensions to single-field slow-roll inflation, we only cherry-picked models of phenomenological interest from which we derived single-field Open EFT in order to study non-unitary effects such as quantum decoherence during inflation. Given the wealth of possible cosmological environments and range of possible interactions with the adiabatic sector, model-agnostic approaches would be valuable.

In order to develop a bottom-up construction of cosmological Open EFTs, a first step would be to precisely connect the unitary part of the dynamics with the one obtained from Wilsonian EFT approaches. The systematic construction of Wilsonian

EFT unitary dynamics [1,6] may provide guidelines on the way we should approach non-unitary sector. Quantifying deviations from unitarity by accounting for whether or not it is a resolvable effect from the IR standpoint also matters for constructions that rely on the unitarity of the IR description. Finally, recent developments around the cosmological bootstrap [247, 314–316, 321–323] greatly clarify how fundamental physical requirements are encoded on the cosmological correlators of the theory. The extension of these works to constrain non-unitary extensions may be a promising avenue.

Lastly, non-equilibrium EFTs [8, 9, 324, 325] provide an unified framework for hydrodynamical systems in which non-unitary dissipative effects are systematically captured from a bottom-up perspective. Based on the Schwinger-Keldysh formalism, Open and non-equilibrium EFTs share the same language and it might be possible to adapt these techniques to the context of cosmology.

Conclusion

The early universe promise is the one of exploring so far unknown territories. To achieve this task, there is a need to understand how fundamental descriptions materialise themselves in a given regime. Open EFTs provide a set of tools to help us understanding the evolution of observable degrees of freedom in the absence of energy conservation. It gives rise to interesting out-of-equilibrium phenomena such as dissipation and decoherence. Throughout this manuscript, we developed the implementation of Open EFT techniques in primordial cosmology. We hope this work improves the understanding of these tools in curved space-time and provides a preliminary exploration of the rich phenomenology offered by inflation. Surely there is still much to be learned at the interface of quantum optics, condensed matter and high-energy physics.

Compte-rendu en français

Ce compte-rendu contient une description succincte en langue française des principaux résultats obtenus durant cette thèse.

Inflation et nouvelle physique

Partie intégrante du modèle standard de la cosmologie, la phase inflationnaire prédit la génération d'inhomogénéités cosmologiques par amplification de fluctuations quantiques dans l'univers primordial. A l'origine des grandes structures de l'univers (galaxies, filaments, vides, etc.), ces fluctuations sont ainsi contraintes par les observations cosmologiques. Si l'étude du Fond Diffus Cosmologique [27] a confirmé à un très grand degré de précision l'existence de fluctuations invariantes d'échelles, quasi-Gaussienne et adiatiques consistantes avec le scénario d'inflation à un champ, l'absence de détection d'ondes gravitationnelles primordiales laisse une incertitude sur l'échelle d'énergie $\rho^{1/4}$ à laquelle l'inflation se produit [73]

$$1 \text{ MeV} \ll \rho^{1/4} < 10^{16} \text{ GeV}. \tag{6.1}$$

Pouvant se produire à des énergies bien supérieures à celles des accélérateurs de particules (de l'ordre de 10^3 GeV), la phase inflationnaire peut offrir un accès privilégié à la physique des hautes énergies, au-delà du Modèle Standard de la physique des particules. Il s'agit également d'un terrain de jeu idéal pour tester la nature quantique ou classique des perturbations de la métrique, explorant ainsi la limite semi-classique des théories de gravitation quantique. Ainsi, de nouvelles campagnes cosmologiques telles que *EUCLID* [99], *Vera Rubin* [100], *LiteBIRD* [96] ou encore *LISA* [104] visent, entre autres objectifs scientifiques, la caractérisation de la phase inflationnaire. Si la collecte de nouvelles données est essentielle à l'exploration de la physique au-delà des modèles standards, cette dernière doit également s'accompagner par le développement d'outils capables d'organiser l'extraction d'information des données cosmologiques.

Théorie effectives des champs

Une théorie physique s'exprime souvent de manière différente suivant l'échelle à laquelle elle est considérée. En hydrodynamique, la description microscopique du système nécessite la modélisation d'un large nombre de molécules en intéractions. Cependant, l'étude des vagues océaniques ne requiert que la compréhension de la dynamique d'un fluide parfait [18]. L'approche effective cherche à organiser ce dialogue entre échelles. Il s'agit de comprendre comme une théorie fondamentale exprimée aux petites échelles (l'UV) s'exprime aux grandes échelles (l'IR) où sont collectées les données expérimentales.

- *De l'UV vers l'IR*: l'approche effective cherche à identifier les degrés de liberté pertinents dans l'IR ainsi que l'existence de symétries et de hiérarchies d'échelles permettant une simplification de la physique aux grandes échelles.

- *De l'IR vers l'UV* : l'approche effective cherche à caractériser l'information sur la théorie fondamentale récupérable par l'étude des données expérimentales de l'IR.

En particulier, en présence d'incertitudes sur la théorie UV sous-jacente, l'approche effective construit une étude systématique de caractérisation de cette incertitude.

Parmi le large panel de questions auxquelles on se doit de répondre pour construire une théorie effective aux grandes échelles, ce manuscrit s'est particulièrement intéressé à celle de l'unitarité. Il s'agit de comprendre si l'information contenu dans le secteur IR est stable dans le temps ou s'il peut se produire un effet de perte par dilution dans des degrés de liberté inaccessible aux grandes échelles. Pour reprendre l'exemple de l'hydrodynamique, il est possible de dériver une théorie locale et unitaire décrivant un fluide parfait, notamment adapté à la modélisation de vagues océaniques dans le régime d'eau profonde [4]. Cependant, l'hydrodynamique fournit nombre d'exemples tels que le phénomène de couche limite ou la turbulence où les imperfections d'un fluide, notamment sa viscosité, joue un rôle majeur [18]. Pour décrire de tels effets, il est nécessaire d'aller au-delà de la dynamique unitaire [8]. Qu'en est-il de la cosmologie ? Est-il pertinent d'inclure de tels effets dans notre description de l'univers primordial ? S'il est difficile de répondre de manière univoque à ces questions, il est pour autant certain que la dynamique inflationnaire, de par l'expansion des distances physiques qu'elle engendre, tend à prévenir l'émergence de secteurs UV et IR clairement ségrégués. Ainsi, ce manuscrit vise à l'inclusion d'effets diffusifs et non-unitaires dans notre description effective de l'univers primordial.

Systèmes Quantiques Ouverts cosmologiques

Notre approche se fonde sur la théorie des Systèmes Quantiques Ouverts (SQO) [188] appliquée à la Théorie Quantique des Champs en espace-temps courbe [326]. En premier lieu, il s'agit de distinguer le système, constitué des degrés de liberté expérimentalement accessible, de l'environnement qui l'entoure, cette collection de degrés de liberté expérimentalement inaccessibles. L'impact de l'environnement sur le système est ensuite modélisé de manière effective à l'aide de la théorie des SQO. Trois effets physiques sont capturés de cette manière :

- Le décalage de Lamb : une renormalization des niveaux d'énergie du système dû à la présence de son environnement;
- La dissipation : un échange d'énergie et d'entropie entre l'environnement et le système qui tend à briser l'invariance par translation temporelle de l'IR;
- La diffusion : un effet de bruit généré par l'environnement qui a tendance à élargir la fonction d'onde du système.

Il s'agit d'implémenter cette méthode en cosmologie primordiale. Le système consiste alors dans les degrés de liberté observables dans le Fond Diffus Cosmologique [51] et les grandes structures de l'univers [37]. Dans le contexte inflationnaire, il s'agit souvent d'un unique champs scalaire, ce composant adiabatique connu sous le nom de perturbation de courbure, aux échelles sondées par le Fond Diffus Cosmologique, d'une dizaine à quelques milliers de mégaparsecs (Mpc). L'environnement

est alors constitué des degrés de liberté ayant pu être présents dans l'univers primordial qui n'ont pas encore été détectés de manière significative. Il peut s'agir par exemple d'une nouvelle physique à haute énergie, d'extensions multichamps ou simplement des petites échelles couplées au système par les non-linéarités de la relativité générale.

L'intérêt d'une modélisation en SQO est triple. En premier lieu, il y a un intérêt *technique* car l'approche en SQO permet l'implémentation d'une re-sommation non-perturbative, ouvrant la voix à un dépassement des résultats perturbatifs en cosmologie [173, 174, 261]. Il y a ensuite une motivation *conceptuelle* car en présence d'un environnement, un système quantique a tendance à perdre après un temps très court ses propriétés quantiques suite au mécanisme de décohérence. Permettant de modéliser ce phénomène, les SQO offrent une opportunité de comprendre pourquoi, malgré son origine quantique, notre univers semble par tant d'aspects classique [106, 117, 189]. Enfin, il y a un intérêt *phénoménologique* car les effets non-unitaires laissent une empreinte sur les observables cosmologiques [298, 299, 327]. En l'absence d'études systématiques de ces effets, il y a un risque d'interpréter de manière erronée le signal cosmologique.

Pour ces raisons, l'approche en SQO offre une possibilité d'interpréter par le biais d'outils nouveaux la physique en jeu dans l'univers primordial.

Etats comprimés à quatre modes

La dynamique inflationnaire est le plus souvent modélisée par la présence d'un unique champ scalaire, l'inflaton, évoluant dans un potentiel plat. Cette modélisation connue sous le nom d'inflation à roulement lent à un champ, prédit non seulement l'émergence d'une phase inflationnaire mais également l'émergence d'inhomogénéités cosmologiques dûes aux fluctuations quantiques de l'inflaton. L'extraction de ces inhomogénéités du vide primordial procède d'un phénomène de création de paires de quanta en présence d'une trame d'espace-temps dynamique [114, 116, 328]. L'état quantique décrivant ces perturbations cosmologiques à l'ordre linéaire est connu comme étant un état comprimé à deux modes [121]. L'étude de cet état a révélé que, suite à la production de paires de quanta, les corrélations engendrées ne peuvent être entièrement capturées par une théorie classique [120]. La nature quantique des corrélations peut même être exhibée par une violation des inégalités de Bell [106, 110]. Ainsi, ces observations soulèvent l'espoir d'une possible démonstration expérimentale de l'origine quantique des inhomogénéités cosmologiques.

Cet espoir doit être tempéré de par les nombreuses obstructions techniques et conceptuelles limitant la réalisation pratique d'une telle expérience. Parmi ces obstructions, ce manuscrit se penche sur la question de la décohérence [191–193]. En présence d'un environnement, un système a tendance à perdre ses propriétés quantiques après une durée d'interaction d'autant plus courte que le système est grand. Ce mécanisme explique (partiellement) l'émergence d'un monde classique aux échelles macroscopiques. En présence de décohérence, l'observation directe des signatures quantiques de l'inflation est grandement menacée. Ainsi, nous avons cherché à inclure l'impact de la décohérence sur la dynamique des perturbations cosmologiques.

Dans le premier article de cette thèse [251], nous nous sommes penchés sur l'extension du formalisme des états comprimés afin d'inclure, au-delà du mécanisme

de création de paires de quanta du système, le phénomène de décohérence quantique par couplage à un environnement. Dans cette étude, nous avons considéré deux champs scalaires linéairement couplés. Le premier degré de liberté représente le système et le second l'environnement. La dynamique peut être comprise comme la création de deux états comprimés à deux modes, un pour le système et un pour l'environnement, autour desquels des quanta peuvent être échangés entre les deux secteurs. L'état final est un état comprimé à quatre modes. Son étude révèle qu'il existe un régime de paramètres où la décohérence est effective sans pour autant que les observables du systèmes ne soient affectées de manière significative. Ainsi, il est possible de rester dans la fenêtre observationnelle de l'inflation à roulement lent à un champ tout en perdant la possibilité d'observer les propriétés quantiques de l'inflation de par la décohérence.

Cette étude offre une compréhension aux échelles microphysiques du mécanisme de décohérence durant l'inflation. Pour autant, son implémentation dans des modèles concrets se révèle difficile en raison de la nécessité de modéliser la dynamique couplée d'un grand nombre de paramètres. Pour cette raison, dans la suite de cette thèse, nous avons cherché à modéliser de manière effective le phénomène de décohérence.

Etude comparée des SQO cosmologiques

Par l'étude de la dynamique non-unitaire, les SQO permettent une modélisation effective du phénomène de décohérence. Pour se faire, il est nécessaire de supposer un certain nombre d'hypothèses sur la nature de l'environnement et sa manière de se coupler au système. Dans le deuxième article de cette thèse [244], nous avons remarqué que certaines des hypothèses régulièrement utilisées en optique quantique ne s'appliquent pas en cosmologie. En effet, la plupart des expériences en laboratoire impliquent des environnements proches de bains thermiques (par exemple, la pièce dans laquelle une table optique est installée). Ces environnements sont constitués d'un grand nombre de degrés de liberté en interaction, dissipent l'information rapidement et obéissent à une statistique thermique. En cosmologie, ces hypothèses doivent être réévaluées car la présence d'un fond dynamique génère une perte de stationnarité. L'environnement varie en fonction du temps, ce qui implique de travailler hors-équilibre. En examinant les différents régimes d'approximations exploitables dans la simplification des équations maîtresses [188], nous avons observé que le théorème de Lindblad [273] n'est pas nécessairement valide en cosmologie. Il est donc parfois nécessaire de s'appuyer sur des équations maîtresses non-Markovienne pour l'étude de l'évolution des propriétés quantiques de l'inflation.

L'étude de la dynamique non-Markovienne des SQO étant un sujet actif de recherche contemporaine [279], il est nécessaire d'évaluer l'implémentation de ces techniques pour la description de la physique de l'univers primordial. Notre article [244] propose une étude comparative visant la caractérisation des SQO cosmologiques. L'idée directrice est de travailler avec un modèle suffisamment simple pour que ce dernier soit exactement soluble, afin de comparer les résultats exacts à ceux effectifs obtenus par l'usage des équations maîtresses. En se restreignant à des interactions linéaires, la dynamique du système reste alors Gaussienne, simplifiant grandement le traitement analytique du problème.

En premier lieu, cette étude a confirmé que la restriction des équations maîtresses à l'approximation de Born, c'est-à-dire l'expansion systématique des générateurs

dynamiques en puissance de la constante de couplage système-environnement, permet de retrouver intégralement les résultats de l'approche perturbative utilisée en cosmologie. Dans cette limite, les équations maîtresses sont utiles pour organiser l'expansion, identifier les termes unitaires et non-unitaires ou encore accéder à certaines propriétés quantiques mais ne présentent pas d'avantage calculatoire. Ce résultat peut cependant être dépassé par l'implémentation d'une re-sommation non-perturbative. Cette re-sommation a d'abord été considérée dans le cadre de l'étude des divergences séculières de l'inflation, cet effet cumulatif de petites corrections s'amplifiant dans le temps [173,174,261]. Notre modèle intégrable fournit un terrain de jeu idéal pour clairement établir la portée de la re-sommation. Nous avons montré que son implémentation repose sur la résolution non-perturbative des équations de transport effectives obtenues par l'équation maîtresse. Nous avons également identifié un ensemble de termes fallacieux s'annulant entre eux dans la limite perturbative mais générant une erreur incontrôlée lorsqu'ils sont inclus dans la re-sommation. L'origine de ces termes se trouve dans la nature non-Markovienne de la carte dynamique ainsi que dans caractère non-diagrammatique de la re-sommation. En effet, si ces termes s'annulent entre eux ordre par ordre en théorie des perturbations, la re-sommation partielle tend à briser cette relation. Il est possible d'identifier sans équivoque ces termes en utilisant la limite perturbative de l'équation maîtresse, cette dernière se devant d'être équivalente à la théorie des perturbations usuelle. Une fois identifiés et retirés, l'équation maîtresse devient alors capable d'implémenter une re-sommation non-perturbative physique.

Nous avons enfin caractérisé l'ampleur de la re-sommation par comparaison aux résultats perturbatifs. Au niveau des observables du système, on observe un écart à la théorie exacte réduit du fait de la re-sommation. La convergence en fonction des paramètres du problème est grandement améliorée et l'erreur moins divergente sur le temps long. Ainsi, le régime de contrôle analytique est étendu grâce à la re-sommation. Au niveau des propriétés quantiques, le calcul perturbatif devient rapidement inexact à mesure que l'on sort du régime de faible décohérence alors même que la re-sommation permet d'évaluer avec précision la pureté du système au temps long où la perte de cohérence est manifeste. Ainsi, cette étude nous a permis de caractériser l'implémentation des SQO en cosmologie, en particulier leur capacité à aller au-delà du régime perturbatif.

Recohérence quantique dans l'univers primordial

Ayant acquis une meilleure compréhension de l'implémentation des SQO en cosmologie, nous nous sommes penchés dans la dernière publication de ce manuscrit à l'utilisation de ces outils dans l'étude de l'évolution des inhomogénéités cosmologiques. Dans [154], nous avons considéré un système constitué des perturbations de courbure, ce degré de liberté adiabatique dont les fluctuations quantiques génèrent les anisotropies de température du Fond Diffus Cosmologiques [50]. Ce degré de liberté est modélisé par la Théorie Effective des Champs de l'Inflation [2], une approche englobant la phénoménologie de l'inflation à roulement lent à un champ. Nous avons ensuite considéré pour environnement un second champ scalaire pouvant provenir d'une extension de la théorie à haute énergie ou d'une construction multichamps [155]. Ce degré de liberté entropique est moins contraint que le degré adiabatique et peut notamment avoir une masse. Le couplage entre les deux

secteurs est déterminé par les symétries du problème, sous la forme d'une expansion systématique [314]. Si un modèle précis est considéré, il est possible de relier les paramètres microphysiques du modèle aux constantes de couplage de cette approche effective.

La limite linéaire de cette construction est un problème bien connu de l'inflation multichamps : le mélange linéaire des degrés entropiques et adiabatiques [144–153]. Notre étude [154] vise à comprendre si la présence de degrés entropiques génère à l'ordre linéaire la décohérence des perturbations adiabatiques. Nous avons montré que la réponse à cette question dépend de la masse du secteur entropique. Alors qu'un secteur entropique léger ($m < 3H/2$, où m est la masse entropique et H le paramètre de Hubble) génère la décohérence du système, un secteur entropique lourd $m \geq 3H/2$ entraîne un phénomène de recohérence où la pureté du système atteint une valeur asymptotique stable et proche de sa valeur initiale au temps long. Ce phénomène s'explique par la dynamique des champs scalaires dans l'espace de de Sitter. Alors que les champs légers subissent l'extraction de paires dûe à la présence du fond dynamique, les champs lourds ne sont pas amplifiés. Par conséquent, alors que le mélange adiabatique-entropique est efficace dans le cas d'un environnement léger, la présence d'un champ lourd rend l'interaction système-environnement inefficace au temps long.

Cette observation illustre comment le mécanisme de décohérence quantique pourrait ne pas être si commun que les études préliminaires le suggèrent. Afin de comprendre la dynamique des propriétés quantiques inflationnaires, il est nécessaire de modéliser avec soin l'impact du fond dynamique sur les champs quantiques de l'inflation, par exemple par l'usage des techniques des SQO non-Markoviens.

Conclusion et perspectives

Ces études ouvrent la voie à une exploration étendue de la phénoménologie des propriétés quantiques de l'inflation. Il s'agit désormais d'étendre ces résultats au régime non-linéaire. Par ailleurs, l'évaluation de l'impact des effets non-unitaires sur les observables cosmologiques reste un sujet ouvert.

Au-delà de ces chantiers engagés, la compréhension de l'émergence de la Markovianité dans les SQO cosmologiques reste partielle. A l'avenir, une étude élargie de ce concept pourrait simplifier l'implémentation des SQO en cosmologie. La définition de critères de décohérence pourrait également permettre d'établir des résultats généraux, par exemple l'absence de décohérence dans le vide en espace-temps plat. Enfin, la compréhension des états quantiques non-Gaussien pourrait-être améliorée par l'utilisation d'outils de l'optique quantique et de la Théorie de l'Information Quantique [205].

L'ensemble de ces travaux ouvre la voie vers une inclusion systématique des effets non-unitaires dans la dynamique inflationnaire, caractérisant ainsi une des principales différences entre la Théorie Quantique des Champs en espace-temps plat et courbe. Derrière une compréhension élargie de la physique de l'univers primordial se cache alors peut-être l'espoir de s'élever vers l'UV par la cosmologie.

Bibliography

[1] C.P. Burgess, *Introduction to Effective Field Theory*, Cambridge University Press (Dec., 2020), 10.1017/9781139048040.

[2] C. Cheung, P. Creminelli, A.L. Fitzpatrick, J. Kaplan and L. Senatore, *The Effective Field Theory of Inflation*, *JHEP* **03** (2008) 014.

[3] D. Baumann, A. Nicolis, L. Senatore and M. Zaldarriaga, *Cosmological Non-Linearities as an Effective Fluid*, *JCAP* **07** (2012) 051 [1004.2488].

[4] S. Dubovsky, L. Hui, A. Nicolis and D.T. Son, *Effective field theory for hydrodynamics: thermodynamics, and the derivative expansion*, *Phys. Rev. D* **85** (2012) 085029 [1107.0731].

[5] J.J.M. Carrasco, M.P. Hertzberg and L. Senatore, *The Effective Field Theory of Cosmological Large Scale Structures*, *JHEP* **09** (2012) 082 [1206.2926].

[6] L. Senatore, *Lectures on Inflation*, in *Theoretical Advanced Study Institute in Elementary Particle Physics: New Frontiers in Fields and Strings*, pp. 447–543, 2017, DOI [1609.00716].

[7] A. Nicolis, *Lectures on Effective Field Theory for phases of matter*, in *Rethinking Beyond Standard Model Physics: Cargese Summer School*, 2022.

[8] H. Liu and P. Glorioso, *Lectures on non-equilibrium effective field theories and fluctuating hydrodynamics*, *PoS* **TASI2017** (2018) 008 [1805.09331].

[9] M. Hongo, S. Kim, T. Noumi and A. Ota, *Effective field theory of time-translational symmetry breaking in nonequilibrium open system*, *JHEP* **02** (2019) 131 [1805.06240].

[10] G. Kaplanek, *Some Applications of Open Effective Field Theories to Gravitating Quantum Systems*, Ph.D. thesis, McMaster U., 2022.

[11] W.D. Goldberger, *Effective Field Theory for Compact Binary Dynamics*, 2212.06677.

[12] C. de Rham, *Massive Gravity*, *Living Rev. Rel.* **17** (2014) 7 [1401.4173].

[13] E.A. Calzetta and B.-L.B. Hu, *Nonequilibrium Quantum Field Theory*, Cambridge Monographs on Mathematical Physics, Cambridge University Press (Sept., 2008), 10.1017/CBO9780511535123.

[14] A.V. Manohar, *Introduction to Effective Field Theories*, 1804.05863.

[15] J.F. Donoghue, *Introduction to the effective field theory description of gravity*, in *Advanced School on Effective Theories*, 6, 1995 [gr-qc/9512024].

[16] S. Weinberg, *Effective Field Theory for Inflation*, *Phys. Rev. D* **77** (2008) 123541 [0804.4291].

[17] S. Endlich, A. Nicolis and J. Wang, *Solid Inflation*, *JCAP* **10** (2013) 011 [1210.0569].

[18] E. Guyon, J. Hulin, L. Petit and C. Mitescu, *Physical Hydrodynamics*, Oxford University Press (2015).

[19] R. Brown, *A brief account of microscopical observations made in the months of June, July and August 1827, on the particles contained in the pollen of plants; and on the general existence of active molecules in organic and inorganic bodies*, *The Philosophical Magazine* **4** (1828) 161 [https://doi.org/10.1080/14786442808674769].

[20] A. Einstein, *Investigations on the Theory of the Brownian Movement*, Dover Books on Physics Series, Dover Publications (1956).

[21] J. Perrin, *Les atomes*, *Revue de Métaphysique et de Morale* **21** (1913) 4.

[22] C.P. Burgess and G. Kaplanek, *Gravity, Horizons and Open EFTs*, 2212.09157.

[23] S. Dodelson, *Modern Cosmology*, Academic Press, Amsterdam (2003).

[24] D. Baumann, *Inflation*, in *Theoretical Advanced Study Institute in Elementary Particle Physics: Physics of the Large and the Small*, pp. 523–686, 2011, DOI.

[25] L. Pinol, *Multifield aspects in the early Universe : Inflation and Reheating*, Ph.D. thesis, Sorbonne Université, Paris, Inst. Astrophys., 2021.

[26] A.G. Riess et al., *A Comprehensive Measurement of the Local Value of the Hubble Constant with 1 km/s/Mpc Uncertainty from the Hubble Space Telescope and the SH0ES Team*, *Astrophys. J. Lett.* **934** (2022) L7 [2112.04510].

[27] Planck collaboration, *Planck 2018 results. I. Overview and the cosmological legacy of Planck*, *Astron. Astrophys.* **641** (2020) A1 [1807.06205].

[28] A.A. Hakobyan, V.Z. Adibekyan, L.S. Aramyan, A.R. Petrosian, J.M. Gomes, G.A. Mamon et al., *Supernovae and their host galaxies. I. The SDSS DR8 database and statistics*, *Astronomy & Astrophysics* **544** (2012) A81 [1206.5016].

[29] B. Reid, S. Ho, N. Padmanabhan, W.J. Percival, J. Tinker, R. Tojeiro et al., *SDSS-III Baryon Oscillation Spectroscopic Survey Data Release 12: galaxy target selection and large-scale structure catalogues*, *Monthly Notices of the Royal Astronomical Society* **455** (2016) 1553 [1509.06529].

[30] N. Aghanim and others, *Planck 2018 results. VI. Cosmological parameters*, *Astron. Astrophys.* **641** (2020) A6.

[31] R.T. Cox, *Probability, Frequency and Reasonable Expectation*, *American Journal of Physics* **14** (1946) 1.

[32] H. Jeffreys, *Theory of Probability*, Clarendon Press, Oxford, England (1939).

[33] B. de Finetti, *Theory of Probability: A Critical Introductory Treatment*, Wiley (1979).

[34] R. Trotta, *Bayes in the sky: Bayesian inference and model selection in cosmology*, *Contemp. Phys.* **49** (2008) 71 [0803.4089].

[35] S. Renaux-Petel, K. Turzyński and V. Vennin, *Geometrical destabilization, premature end of inflation and Bayesian model selection*, *JCAP* **11** (2017) 006 [1706.01835].

[36] R. Trotta, *Applications of Bayesian model selection to cosmological parameters*, *Mon. Not. Roy. Astron. Soc.* **378** (2007) 72 [astro-ph/0504022].

[37] T. Colas, G. D'amico, L. Senatore, P. Zhang and F. Beutler, *Efficient Cosmological Analysis of the SDSS/BOSS data from the Effective Field Theory of Large-Scale Structure*, *JCAP* **06** (2020) 001.

[38] E. Di Valentino, O. Mena, S. Pan, L. Visinelli, W. Yang, A. Melchiorri et al., *In the realm of the Hubble tension—a review of solutions*, *Class. Quant. Grav.* **38** (2021) 153001 [2103.01183].

[39] M. Douspis, L. Salvati and N. Aghanim, *On the Tension between Large Scale Structures and Cosmic Microwave Background*, *PoS* **EDSU2018** (2018) 037 [1901.05289].

[40] P. Coles and F. Lucchin, *Cosmology: The Origin and evolution of cosmic structure*, John Wiley & Sons (1995).

[41] C.M. Will, *The Confrontation between General Relativity and Experiment*, *Living Rev. Rel.* **17** (2014) 4 [1403.7377].

[42] N.V. Krishnendu and F. Ohme, *Testing General Relativity with Gravitational Waves: An Overview*, *Universe* **7** (2021) 497 [2201.05418].

[43] P. Foka and M.A. Janik, *An overview of experimental results from ultra-relativistic heavy-ion collisions at the CERN LHC: Hard probes*, *Rev. Phys.* **1** (2016) 172 [1702.07231].

[44] A. Fienga and O. Minazzoli, *Testing GR and alternative theories with planetary ephemerides*, 2303.01821.

[45] S. Dodelson, *Coherent phase argument for inflation*, *AIP Conf. Proc.* **689** (2003) 184 [hep-ph/0309057].

[46] WMAP collaboration, *First year Wilkinson Microwave Anisotropy Probe (WMAP) observations: Implications for inflation*, *Astrophys. J. Suppl.* **148** (2003) 213 [astro-ph/0302225].

[47] V. Acquaviva, N. Bartolo, S. Matarrese and A. Riotto, *Second order cosmological perturbations from inflation*, *Nucl. Phys. B* **667** (2003) 119 [astro-ph/0209156].

[48] Planck collaboration, *Planck 2013 Results. XXIV. Constraints on primordial non-Gaussianity*, *Astron. Astrophys.* **571** (2014) A24 [1303.5084].

[49] J.M. Maldacena, *Non-Gaussian features of primordial fluctuations in single field inflationary models*, *JHEP* **05** (2003) 013.

[50] S. Weinberg, *Adiabatic modes in cosmology*, *Phys. Rev. D* **67** (2003) 123504 [astro-ph/0302326].

[51] Y. Akrami and others, *Planck 2018 results. X. Constraints on inflation*, *Astron. Astrophys.* **641** (2020) A10.

[52] S. Renaux-Petel and K. Turzynski, *On reaching the adiabatic limit in multi-field inflation*, *JCAP* **06** (2015) 010 [1405.6195].

[53] A.A. Starobinsky, *Spectrum of relict gravitational radiation and the early state of the universe*, *JETP Lett.* **30** (1979) 682.

[54] A.H. Guth, *The Inflationary Universe: A Possible Solution to the Horizon and Flatness Problems*, *Phys. Rev.* **D23** (1981) 347.

[55] A.A. Starobinsky, *A New Type of Isotropic Cosmological Models Without Singularity*, *Phys. Lett.* **B91** (1980) 99.

[56] K. Sato, *First Order Phase Transition of a Vacuum and Expansion of the Universe*, *Mon. Not. Roy. Astron. Soc.* **195** (1981) 467.

[57] A.D. Linde, *A New Inflationary Universe Scenario: A Possible Solution of the Horizon, Flatness, Homogeneity, Isotropy and Primordial Monopole Problems*, *Second Seminar on Quantum Gravity Moscow, USSR, October 13-15, 1981* **B108** (1982) 389.

[58] V.F. Mukhanov and G.V. Chibisov, *Quantum Fluctuations and a Nonsingular Universe*, *JETP Lett.* **33** (1981) 532.

[59] A.H. Guth and S.Y. Pi, *Fluctuations in the New Inflationary Universe*, *Phys. Rev. Lett.* **49** (1982) 1110.

[60] A. Albrecht and P.J. Steinhardt, *Cosmology for Grand Unified Theories with Radiatively Induced Symmetry Breaking*, *Phys. Rev. Lett.* **48** (1982) 1220.

[61] A.A. Starobinsky, *Dynamics of Phase Transition in the New Inflationary Universe Scenario and Generation of Perturbations*, *Phys. Lett.* **B117** (1982) 175.

[62] S.W. Hawking, *The Development of Irregularities in a Single Bubble Inflationary Universe*, *Phys. Lett.* **B115** (1982) 295.

[63] A.D. Linde, *Chaotic Inflation*, *Phys. Lett.* **B129** (1983) 177.

[64] J.M. Bardeen, P.J. Steinhardt and M.S. Turner, *Spontaneous Creation of Almost Scale - Free Density Perturbations in an Inflationary Universe*, *Phys. Rev.* **D28** (1983) 679.

[65] V.F. Mukhanov, *Quantum Theory of Gauge Invariant Cosmological Perturbations*, *Sov.Phys.JETP* **67** (1988) 1297.

[66] G. D'Amico, J. Gleyzes, N. Kokron, K. Markovic, L. Senatore, P. Zhang et al., *The Cosmological Analysis of the SDSS/BOSS data from the Effective Field Theory of Large-Scale Structure*, *JCAP* **05** (2020) 005.

[67] G. D'Amico, Y. Donath, M. Lewandowski, L. Senatore and P. Zhang, *The one-loop bispectrum of galaxies in redshift space from the Effective Field Theory of Large-Scale Structure*, 2211.17130.

[68] G. D'Amico, Y. Donath, M. Lewandowski, L. Senatore and P. Zhang, *The BOSS bispectrum analysis at one loop from the Effective Field Theory of Large-Scale Structure*, 2206.08327.

[69] O.H.E. Philcox, M.M. Ivanov, G. Cabass, M. Simonović, M. Zaldarriaga and T. Nishimichi, *Cosmology with the redshift-space galaxy bispectrum monopole at one-loop order*, *Phys. Rev. D* **106** (2022) 043530.

[70] M.M. Ivanov, O.H.E. Philcox, G. Cabass, T. Nishimichi, M. Simonović and M. Zaldarriaga, *Cosmology with the Galaxy Bispectrum Multipoles: Optimal Estimation and Application to BOSS Data*, 2302.04414.

[71] J. Fumagalli, M. Pieroni, S. Renaux-Petel and L.T. Witkowski, *Detecting primordial features with LISA*, *JCAP* **07** (2022) 020 [2112.06903].

[72] D.K. Hazra, A. Antony and A. Shafieloo, *One spectrum to cure them all: signature from early Universe solves major anomalies and tensions in cosmology*, *JCAP* **08** (2022) 063 [2201.12000].

[73] G. Galloni, N. Bartolo, S. Matarrese, M. Migliaccio, A. Ricciardone and N. Vittorio, *Updated constraints on amplitude and tilt of the tensor primordial spectrum*, *JCAP* **04** (2023) 062 [2208.00188].

[74] A. Kalaja, N. Bellomo, N. Bartolo, D. Bertacca, S. Matarrese, I. Musco et al., *From Primordial Black Holes Abundance to Primordial Curvature Power Spectrum (and back)*, *JCAP* **10** (2019) 031 [1908.03596].

[75] Y. Akrami and others, *Planck 2018 results. IX. Constraints on primordial non-Gaussianity*, *Astron. Astrophys.* **641** (2020) A9.

[76] G. Cabass, M.M. Ivanov, O.H.E. Philcox, M. Simonović and M. Zaldarriaga, *Constraints on Single-Field Inflation from the BOSS Galaxy Survey*, *Phys. Rev. Lett.* **129** (2022) 021301.

[77] G. D'Amico, M. Lewandowski, L. Senatore and P. Zhang, *Limits on primordial non-Gaussianities from BOSS galaxy-clustering data*, 2201.11518.

[78] G. Cabass, M.M. Ivanov, O.H.E. Philcox, M. Simonović and M. Zaldarriaga, *Constraints on multifield inflation from the BOSS galaxy survey*, *Phys. Rev. D* **106** (2022) 043506 [2204.01781].

[79] G. Cabass, M.M. Ivanov, O.H.E. Philcox, M. Simonovic and M. Zaldarriaga, *Constraining single-field inflation with MegaMapper*, *Phys. Lett. B* **841** (2023) 137912 [2211.14899].

[80] A. Krolewski et al., *Constraining primordial non-Gaussianity from DESI quasar targets and Planck CMB lensing*, 2305.07650.

[81] O.H.E. Philcox, J. Hou and Z. Slepian, *A First Detection of the Connected 4-Point Correlation Function of Galaxies Using the BOSS CMASS Sample*, 2108.01670.

[82] O.H.E. Philcox, *Probing parity violation with the four-point correlation function of BOSS galaxies*, *Physical Review D: Particles and Fields* **106** (2022) 063501.

[83] J. Hou, Z. Slepian and R.N. Cahn, *Measurement of parity-odd modes in the large-scale 4-point correlation function of Sloan Digital Sky Survey Baryon Oscillation Spectroscopic Survey twelfth data release CMASS and LOWZ galaxies*, *Mon. Not. Roy. Astron. Soc.* **522** (2023) 5701 [2206.03625].

[84] G. Cabass, S. Jazayeri, E. Pajer and D. Stefanyszyn, *Parity violation in the scalar trispectrum: no-go theorems and yes-go examples*, *JHEP* **02** (2023) 021.

[85] G. Cabass, M.M. Ivanov and O.H.E. Philcox, *Colliders and ghosts: Constraining inflation with the parity-odd galaxy four-point function*, *Physical Review D: Particles and Fields* **107** (2023) 023523.

[86] G. Domènech, *Scalar Induced Gravitational Waves Review*, *Universe* **7** (2021) 398 [2109.01398].

[87] K. Schutz, E.I. Sfakianakis and D.I. Kaiser, *Multifield Inflation after Planck: Isocurvature Modes from Nonminimal Couplings*, *Phys. Rev. D* **89** (2014) 064044.

[88] J.M. Ezquiaga, J. García-Bellido and V. Vennin, *The exponential tail of inflationary fluctuations: consequences for primordial black holes*, *JCAP* **03** (2020) 029.

[89] A.D. Gow, H. Assadullahi, J.H.P. Jackson, K. Koyama, V. Vennin and D. Wands, *Non-perturbative non-Gaussianity and primordial black holes*, *EPL* **142** (2023) 49001 [2211.08348].

[90] T. Cohen, D. Green and A. Premkumar, *Large deviations in the early Universe*, *Phys. Rev. D* **107** (2023) 083501 [2212.02535].

[91] J.M. Ezquiaga, J. García-Bellido and V. Vennin, *Massive Galaxy Clusters Like El Gordo Hint at Primordial Quantum Diffusion*, *Phys. Rev. Lett.* **130** (2023) 121003 [2207.06317].

[92] R. Brandenberger and P. Peter, *Bouncing Cosmologies: Progress and Problems*, *Found. Phys.* **47** (2017) 797.

[93] V. Kamali, M. Motaharfar and R. O. Ramos, *Recent developments in warm inflation*, 2302.02827.

[94] J.W. Henning and others, *Measurements of the temperature and E-mode polarization of the CMB from 500 square degrees of SPTpol data*, *Astrophysical Journal* **852** (2018) 97.

[95] K. Abazajian and others, *CMB-S4: Forecasting Constraints on Primordial Gravitational Waves*, *Astrophys. J.* **926** (2022) 54.

[96] LiteBIRD collaboration, *Probing Cosmic Inflation with the LiteBIRD Cosmic Microwave Background Polarization Survey*, *PTEP* **2023** (2023) 042F01 [2202.02773].

[97] DESI collaboration, *The DESI Experiment, a whitepaper for Snowmass 2013*, 1308.0847.

[98] R. Maartens, F.B. Abdalla, M. Jarvis and M.G. Santos, *Overview of Cosmology with the SKA*, *PoS* **AASKA14** (2015) 016.

[99] R. Scaramella and others, *Euclid preparation - I. The Euclid Wide Survey*, *Astron. Astrophys.* **662** (2022) A112.

[100] B. Blum et al., *Snowmass2021 Cosmic Frontier White Paper: Rubin Observatory after LSST*, in *Snowmass 2021*, 3, 2022 [2203.07220].

[101] Z. Arzoumanian and others, *The NANOGrav 12.5-year Data Set: Search for Non-Einsteinian Polarization Modes in the Gravitational-wave Background*, *Astrophys. J. Lett.* **923** (2021) L22.

[102] A. Finke, S. Foffa, F. Iacovelli, M. Maggiore and M. Mancarella, *Cosmology with LIGO/Virgo dark sirens: Hubble parameter and modified gravitational wave propagation*, *JCAP* **08** (2021) 026 [2101.12660].

[103] A. Mitra, J. Mifsud, D.F. Mota and D. Parkinson, *Cosmology with the Einstein Telescope: No Slip Gravity Model and Redshift Specifications*, *Mon. Not. Roy. Astron. Soc.* **502** (2021) 5563 [2010.00189].

[104] LISA Cosmology Working Group collaboration, *Cosmology with the Laser Interferometer Space Antenna*, 2204.05434.

[105] B. Bonga, S. Brahma, A.-S. Deutsch and S. Shandera, *Cosmic variance in inflation with two light scalars*, *JCAP* **05** (2016) 018.

[106] D. Campo and R. Parentani, *Inflationary spectra and violations of Bell inequalities*, *Phys. Rev. D* **74** (2006) 025001.

[107] J. Maldacena, *A model with cosmological Bell inequalities*, *Fortsch. Phys.* **64** (2016) 10.

[108] S. Choudhury, S. Panda and R. Singh, *Bell violation in the Sky*, *Eur. Phys. J. C* **77** (2017) 60.

[109] J. Martin and V. Vennin, *Bell inequalities for continuous-variable systems in generic squeezed states*, *Phys. Rev.* **A93** (2016) 062117.

[110] J. Martin and V. Vennin, *Obstructions to Bell CMB Experiments*, *Phys. Rev.* **D96** (2017) 063501.

[111] K. Ando and V. Vennin, *Bipartite temporal Bell inequalities for two-mode squeezed states*, *Phys. Rev. A* **102** (2020) 052213.

[112] L. Espinosa-Portalés and V. Vennin, *Real-space Bell inequalities in de Sitter*, *JCAP* **07** (2022) 037.

[113] V. Vennin, *Stochastic inflation and primordial black holes*, Ph.D. thesis, U. Paris-Saclay, 6, 2020. 2009.08715.

[114] L. Grishchuk and Y. Sidorov, *Squeezed quantum states of relic gravitons and primordial density fluctuations*, *Phys. Rev.* **D42** (1990) 3413.

[115] L. Grishchuk, H. Haus and K. Bergman, *Generation of squeezed radiation from vacuum in the cosmos and the laboratory*, *Phys. Rev.* **D46** (1992) 1440.

[116] A. Albrecht, P. Ferreira, M. Joyce and T. Prokopec, *Inflation and squeezed quantum states*, *Phys. Rev. D* **50** (1994) 4807.

[117] D. Polarski and A.A. Starobinsky, *Semiclassicality and decoherence of cosmological perturbations*, *Class. Quant. Grav.* **13** (1996) 377.

[118] J. Lesgourgues, D. Polarski and A.A. Starobinsky, *Quantum to classical transition of cosmological perturbations for nonvacuum initial states*, *Nucl. Phys.* **B497** (1997) 479.

[119] C. Kiefer, D. Polarski and A.A. Starobinsky, *Quantum to classical transition for fluctuations in the early universe*, *Int. J. Mod. Phys.* **D7** (1998) 455.

[120] J. Martin and V. Vennin, *Quantum Discord of Cosmic Inflation: Can we Show that CMB Anisotropies are of Quantum-Mechanical Origin?*, *Phys. Rev.* **D93** (2016) 023505.

[121] J. Grain and V. Vennin, *Squeezing formalism and canonical transformations in cosmology*, *JCAP* **2002** (2020) 022.

[122] J. Martin, A. Micheli and V. Vennin, *Comparing quantumness criteria*, *EPL* **142** (2023) 18001 [2211.10114].

[123] J. Martin, C. Ringeval and V. Vennin, *Encyclopædia Inflationaris*, *Phys. Dark Univ.* **5-6** (2014) 75.

[124] F.L. Bezrukov and M. Shaposhnikov, *The Standard Model Higgs boson as the inflaton*, *Phys. Lett. B* **659** (2008) 703.

[125] F. Bezrukov, A. Magnin, M. Shaposhnikov and S. Sibiryakov, *Higgs inflation: consistency and generalisations*, *JHEP* **01** (2011) 016 [1008.5157].

[126] J. Rubio, *Higgs inflation*, *Front. Astron. Space Sci.* **5** (2019) 50 [1807.02376].

[127] M. Shaposhnikov, A. Shkerin, I. Timiryasov and S. Zell, *Higgs inflation in Einstein-Cartan gravity*, *JCAP* **02** (2021) 008 [2007.14978].

[128] E. Palti, *The Swampland: Introduction and Review*, *Fortsch. Phys.* **67** (2019) 1900037 [1903.06239].

[129] M. van Beest, J. Calderón-Infante, D. Mirfendereski and I. Valenzuela, *Lectures on the Swampland Program in String Compactifications*, *Phys. Rept.* **989** (2022) 1 [2102.01111].

[130] A. Barrau, C. Renevey and K. Martineau, *The String Theory Swampland in the Euclid, Square Kilometer Array, and Vera Rubin Observatory Era*, *Astrophys. J.* **912** (2021) 99 [2101.02942].

[131] E. Pajer and M. Peloso, *A review of Axion Inflation in the era of Planck*, *Class. Quant. Grav.* **30** (2013) 214002.

[132] A. Achúcarro and G.A. Palma, *The string swampland constraints require multi-field inflation*, *JCAP* **02** (2019) 041 [1807.04390].

[133] J. Khoury, B.A. Ovrut, P.J. Steinhardt and N. Turok, *The Ekpyrotic universe: Colliding branes and the origin of the hot big bang*, *Phys. Rev. D* **64** (2001) 123522.

[134] I. Agullo and P. Singh, *Loop Quantum Cosmology*, in *Loop Quantum Gravity: The First 30 Years*, A. Ashtekar and J. Pullin, eds., pp. 183–240, WSP (2017), DOI [1612.01236].

[135] C.J. Fewster and K. Rejzner, *Algebraic Quantum Field Theory – an introduction*, 1904.04051.

[136] C.J. Fewster, *A generally covariant measurement scheme for quantum field theory in curved spacetimes*, in *Progress and Visions in Quantum Theory in View of Gravity: Bridging foundations of physics and mathematics*, 4, 2019 [1904.06944].

[137] C.J. Fewster and R. Verch, *Measurement in quantum field theory*, 2304.13356.

[138] F. Piazza and F. Vernizzi, *Effective Field Theory of Cosmological Perturbations*, *Class. Quant. Grav.* **30** (2013) 214007 [1307.4350].

[139] R. Allahverdi, K. Enqvist, J. Garcia-Bellido, A. Jokinen and A. Mazumdar, *MSSM flat direction inflation: Slow roll, stability, fine tunning and reheating*, *JCAP* **06** (2007) 019 [hep-ph/0610134].

[140] G. Weymann-Despres, S. Henrot-Versillé, G. Moultaka, V. Vennin, L. Duflot and R. von Eckardstein, *MSSM-inflation revisited: Towards a coherent description of high-energy physics and cosmology*, 2304.04534.

[141] S. Mohanty and A. Nautiyal, *Natural inflation at the GUT scale*, *Phys. Rev. D* **78** (2008) 123515 [0807.0317].

[142] D. Baumann and L. McAllister, *Inflation and String Theory*, Cambridge Monographs on Mathematical Physics, Cambridge University Press (May, 2015), 10.1017/CBO9781316105733.

[143] M. Cicoli and F. Quevedo, *String moduli inflation: An overview*, *Class. Quant. Grav.* **28** (2011) 204001.

[144] D.H. Lyth and D. Wands, *Generating the curvature perturbation without an inflaton*, *Phys. Lett.* **B524** (2002) 5.

[145] C. Gordon, D. Wands, B.A. Bassett and R. Maartens, *Adiabatic and entropy perturbations from inflation*, *Phys. Rev. D* **63** (2000) 023506 [astro-ph/0009131].

[146] F. Vernizzi and D. Wands, *Non-gaussianities in two-field inflation*, *JCAP* **0605** (2006) 019.

[147] X. Chen and Y. Wang, *Quasi-Single Field Inflation and Non-Gaussianities*, *JCAP* **04** (2010) 027.

[148] A. Achucarro, J.-O. Gong, S. Hardeman, G.A. Palma and S.P. Patil, *Features of heavy physics in the CMB power spectrum*, *JCAP* **01** (2011) 030.

[149] S. Cespedes, V. Atal and G.A. Palma, *On the importance of heavy fields during inflation*, *JCAP* **05** (2012) 008.

[150] A. Achucarro, J.-O. Gong, S. Hardeman, G.A. Palma and S.P. Patil, *Effective theories of single field inflation when heavy fields matter*, *JHEP* **05** (2012) 066.

[151] X. Chen and Y. Wang, *Quasi-Single Field Inflation with Large Mass*, *JCAP* **09** (2012) 021.

[152] S. Pi and M. Sasaki, *Curvature Perturbation Spectrum in Two-field Inflation with a Turning Trajectory*, *JCAP* **10** (2012) 051.

[153] L. Pinol, *Multifield inflation beyond $N_\mathrmfield=2$: non-Gaussianities and single-field effective theory*, *JCAP* **04** (2021) 002.

[154] T. Colas, J. Grain and V. Vennin, *Quantum recoherence in the early universe*, *EPL* **142** (2023) 69002 [2212.09486].

[155] V. Assassi, D. Baumann, D. Green and L. McAllister, *Planck-Suppressed Operators*, *JCAP* **01** (2014) 033.

[156] N. Arkani-Hamed and J. Maldacena, *Cosmological Collider Physics*, 1503.08043.

[157] A.A. Starobinsky, *Stochastic de Sitter (inflationary) stage in the early universe*, *Lect.Notes Phys.* **246** (1986) 107.

[158] Y. Nambu and M. Sasaki, *Stochastic Stage of an Inflationary Universe Model*, *Phys.Lett.* **B205** (1988) 441.

[159] Y. Nambu and M. Sasaki, *Stochastic Approach to Chaotic Inflation and the Distribution of Universes*, *Phys.Lett.* **B219** (1989) 240.

[160] H.E. Kandrup, *Stochastic inflation as a time dependent random walk*, *Phys.Rev.* **D39** (1989) 2245.

[161] K.-i. Nakao, Y. Nambu and M. Sasaki, *Stochastic Dynamics of New Inflation*, *Prog.Theor.Phys.* **80** (1988) 1041.

[162] Y. Nambu, *Stochastic Dynamics of an Inflationary Model and Initial Distribution of Universes*, *Prog.Theor.Phys.* **81** (1989) 1037.

[163] D.S. Salopek and J.R. Bond, *Nonlinear evolution of long wavelength metric fluctuations in inflationary models*, *Phys. Rev.* **D42** (1990) 3936.

[164] S. Mollerach, S. Matarrese, A. Ortolan and F. Lucchin, *Stochastic inflation in a simple two field model*, *Phys.Rev.* **D44** (1991) 1670.

[165] R.H. Brandenberger, V.F. Mukhanov and T. Prokopec, *Entropy of a classical stochastic field and cosmological perturbations*, *Phys. Rev. Lett.* **69** (1992) 3606.

[166] A.A. Starobinsky and J. Yokoyama, *Equilibrium state of a selfinteracting scalar field in the De Sitter background*, *Phys. Rev.* **D50** (1994) 6357.

[167] F. Finelli, G. Marozzi, A. Starobinsky, G. Vacca and G. Venturi, *Generation of fluctuations during inflation: Comparison of stochastic and field-theoretic approaches*, *Phys.Rev.* **D79** (2009) 044007.

[168] B. Garbrecht, G. Rigopoulos and Y. Zhu, *Infrared correlations in de Sitter space: Field theoretic versus stochastic approach*, *Phys. Rev. D* **89** (2014) 063506.

[169] T. Fujita, M. Kawasaki and Y. Tada, *Non-perturbative approach for curvature perturbations in stochastic δN formalism*, *JCAP* **1410** (2014) 030.

[170] V. Vennin and A.A. Starobinsky, *Correlation Functions in Stochastic Inflation*, *Eur. Phys. J.* **C75** (2015) 413.

[171] J. Grain and V. Vennin, *Stochastic inflation in phase space: Is slow roll a stochastic attractor?*, *JCAP* **1705** (2017) 045.

[172] L. Pinol, S. Renaux-Petel and Y. Tada, *A manifestly covariant theory of multifield stochastic inflation in phase space: solving the discretisation ambiguity in stochastic inflation*, *JCAP* **04** (2021) 048.

[173] C. Burgess, R. Holman and G. Tasinato, *Open EFTs, IR effects & late-time resummations: systematic corrections in stochastic inflation*, *JHEP* **01** (2016) 153.

[174] C.P. Burgess, R. Holman, G. Tasinato and M. Williams, *EFT Beyond the Horizon: Stochastic Inflation and How Primordial Quantum Fluctuations Go Classical*, *JHEP* **03** (2015) 090.

[175] S. Brahma, O. Alaryani and R. Brandenberger, *Entanglement entropy of cosmological perturbations*, *Phys. Rev. D* **102** (2020) 043529.

[176] J. Weenink and T. Prokopec, *On decoherence of cosmological perturbations and stochastic inflation*, 1108.3994.

[177] T.J. Hollowood and J.I. McDonald, *Decoherence, discord and the quantum master equation for cosmological perturbations*, *Phys. Rev. D* **95** (2017) 103521.

[178] J. Oppenheim, C. Sparaciari, B. Šoda and Z. Weller-Davies, *The two classes of hybrid classical-quantum dynamics*, 2203.01332.

[179] J. Oppenheim, C. Sparaciari, B. Šoda and Z. Weller-Davies, *Gravitationally induced decoherence vs space-time diffusion: testing the quantum nature of gravity*, 2203.01982.

[180] I. Layton, J. Oppenheim and Z. Weller-Davies, *A healthier semi-classical dynamics*, 2208.11722.

[181] P. Creminelli and M. Zaldarriaga, *Single field consistency relation for the 3-point function*, *JCAP* **0410** (2004) 006.

[182] C. Cheung, A.L. Fitzpatrick, J. Kaplan and L. Senatore, *On the consistency relation of the 3-point function in single field inflation*, *JCAP* **02** (2008) 021.

[183] L. Hui, A. Joyce, I. Komissarov, K. Parmentier, L. Santoni and S.S.C. Wong, *Soft theorems for boosts and other time symmetries*, *JHEP* **02** (2023) 123 [2210.16276].

[184] W. Zhao and Q.-G. Huang, *Testing inflationary consistency relations by the potential CMB observations*, *Class. Quant. Grav.* **28** (2011) 235003 [1101.3163].

[185] N.S. Sugiyama, D. Yamauchi, T. Kobayashi, T. Fujita, S. Arai, S. Hirano et al., *First test of the consistency relation for the large-scale structure using the anisotropic three-point correlation function of BOSS DR12 galaxies*, 2305.01142.

[186] N. Bartolo, S. Matarrese and A. Riotto, *Non-Gaussianity in the Cosmic Microwave Background Anisotropies at Recombination in the Squeezed limit*, *JCAP* **02** (2012) 017 [1109.2043].

[187] P. Creminelli, C. Pitrou and F. Vernizzi, *The CMB bispectrum in the squeezed limit*, *JCAP* **11** (2011) 025 [1109.1822].

[188] H.P. Breuer and F. Petruccione, *The theory of Open Quantum Systems*, Oxford University Press (2002), 10.1093/acprof:oso/9780199213900.001.0001.

[189] D. Sudarsky, *Shortcomings in the Understanding of Why Cosmological Perturbations Look Classical*, *Int. J. Mod. Phys. D* **20** (2011) 509 [0906.0315].

[190] J. Martin, V. Vennin and P. Peter, *Cosmological Inflation and the Quantum Measurement Problem*, *Phys. Rev.* **D86** (2012) 103524.

[191] W.H. Zurek, *Pointer Basis of Quantum Apparatus: Into What Mixture Does the Wave Packet Collapse?*, *Phys. Rev. D* **24** (1981) 1516.

[192] W.H. Zurek, *Environment induced superselection rules*, *Phys. Rev. D* **26** (1982) 1862.

[193] E. Joos and H. Zeh, *The Emergence of classical properties through interaction with the environment*, *Z. Phys. B* **59** (1985) 223.

[194] W.H. Zurek, *Quantum darwinism*, *Nature Physics* **5** (2009) 181.

[195] W.H. Zurek, *Emergence of the Classical World from Within Our Quantum Universe*, *Fundam. Theor. Phys.* **204** (2022) 23 [2107.03378].

[196] C. Bloch and A. Messiah, *The Canonical form of an antisymmetric tensor and its application to the theory of superconductivity*, *Nucl. Phys.* **39** (1962) 95.

[197] R. Schnabel, *Squeezed states of light and their applications in laser interferometers*, *Phys. Rept.* **684** (2017) 1.

[198] V.V. Dodonov, *'Nonclassical' states in quantum optics: a 'squeezed' review of the first 75 years*, *J. Opt. B* **4** (2002) R1.

[199] C. Kiefer and D. Polarski, *Why do cosmological perturbations look classical to us?*, *Adv. Sci. Lett.* **2** (2009) 164.

[200] W.B. Case, *Wigner functions and Weyl transforms for pedestrians*, *American Journal of Physics* **76** (2008) 937.

[201] R. Simon, E.C.G. Sudarshan and N. Mukunda, *Gaussian Wigner distributions: A complete characterization*, *Physics Letters A* **124** (1987) 223 .

[202] S. Kanno, J.P. Shock and J. Soda, *Quantum discord in de Sitter space*, *Phys. Rev. D* **94** (2016) 125014.

[203] J.S. Bell, *On the einstein podolsky rosen paradox*, *Physics Physique Fizika* **1** (1964) 195.

[204] A. Aspect, P. Grangier and G. Roger, *Experimental realization of Einstein-Podolsky-Rosen-Bohm Gedankenexperiment: A New violation of Bell's inequalities*, *Phys. Rev. Lett.* **49** (1982) 91.

[205] M. Walschaers, *Non-Gaussian Quantum States and Where to Find Them*, *PRX Quantum* **2** (2021) 030204.

[206] J.F. Clauser, M.A. Horne, A. Shimony and R.A. Holt, *Proposed experiment to test local hidden-variable theories*, *Phys. Rev. Lett.* **23** (1969) 880.

[207] D.I. Kaiser, *Tackling Loopholes in Experimental Tests of Bell's Inequality*, 2011.09296.

[208] J. Handsteiner et al., *Cosmic Bell Test: Measurement Settings from Milky Way Stars*, *Phys. Rev. Lett.* **118** (2017) 060401 [1611.06985].

[209] D. Rauch et al., *Cosmic Bell Test Using Random Measurement Settings from High-Redshift Quasars*, *Phys. Rev. Lett.* **121** (2018) 080403 [1808.05966].

[210] K. Banaszek and K. Wódkiewicz, *Testing quantum nonlocality in phase space*, *Phys. Rev. Lett.* **82** (1999) 2009.

[211] J. Martin and V. Vennin, *Leggett-Garg Inequalities for Squeezed States*, *Phys. Rev.* **A94** (2016) 052135.

[212] J.e. Martin and V. Vennin, *Real-space entanglement in the Cosmic Microwave Background*, *JCAP* **10** (2021) 036 [2106.15100].

[213] J. Martin and V. Vennin, *Real-space entanglement of quantum fields*, *Phys. Rev. D* **104** (2021) 085012 [2106.14575].

[214] I. Agullo, B. Bonga, P. Ribes-Metidieri, D. Kranas and S. Nadal-Gisbert, *How ubiquitous is entanglement in quantum field theory?*, 2302.13742.

[215] R.H. Brandenberger, R. Laflamme and M. Mijic, *Classical Perturbations From Decoherence of Quantum Fluctuations in the Inflationary Universe*, *Mod. Phys. Lett. A* **5** (1990) 2311.

[216] A.O. Barvinsky, A.Y. Kamenshchik, C. Kiefer and I.V. Mishakov, *Decoherence in quantum cosmology at the onset of inflation*, *Nucl. Phys. B* **551** (1999) 374.

[217] F.C. Lombardo and D. Lopez Nacir, *Decoherence during inflation: The Generation of classical inhomogeneities*, *Phys. Rev. D* **72** (2005) 063506.

[218] C. Kiefer, I. Lohmar, D. Polarski and A.A. Starobinsky, *Pointer states for primordial fluctuations in inflationary cosmology*, *Class. Quant. Grav.* **24** (2007) 1699.

[219] P. Martineau, *On the decoherence of primordial fluctuations during inflation*, *Class. Quant. Grav.* **24** (2007) 5817.

[220] C.P. Burgess, R. Holman and D. Hoover, *Decoherence of inflationary primordial fluctuations*, *Phys. Rev. D* **77** (2008) 063534.

[221] T. Prokopec and G.I. Rigopoulos, *Decoherence from Isocurvature perturbations in Inflation*, *JCAP* **11** (2007) 029.

[222] E. Nelson, *Quantum Decoherence During Inflation from Gravitational Nonlinearities*, *JCAP* **03** (2016) 022.

[223] J. Martin and V. Vennin, *Observational constraints on quantum decoherence during inflation*, *JCAP* **05** (2018) 063.

[224] J. Martin and V. Vennin, *Non Gaussianities from Quantum Decoherence during Inflation*, *JCAP* **06** (2018) 037.

[225] S. Kanno, J. Soda and J. Tokuda, *Noise and decoherence induced by gravitons*, *Phys. Rev. D* **103** (2021) 044017.

[226] J. Martin, A. Micheli and V. Vennin, *Discord and decoherence*, *JCAP* **04** (2022) 051.

[227] A. Daddi Hammou and N. Bartolo, *Cosmic decoherence: primordial power spectra and non-Gaussianities*, *JCAP* **04** (2023) 055 [2211.07598].

[228] C.P. Burgess, R. Holman, G. Kaplanek, J. Martin and V. Vennin, *Minimal decoherence from inflation*, *JCAP* **07** (2023) 022 [2211.11046].

[229] S. Ning, C.M. Sou and Y. Wang, *On the Decoherence of Primordial Gravitons*, 2305.08071.

[230] D. Koks, A. Matacz and B. Hu, *Entropy and uncertainty of squeezed quantum open systems*, *Phys. Rev. D* **55** (1997) 5917.

[231] D. Campo and R. Parentani, *Decoherence and entropy of primordial fluctuations. I: Formalism and interpretation*, *Phys. Rev. D* **78** (2008) 065044 [0805.0548].

[232] D. Campo and R. Parentani, *Decoherence and entropy of primordial fluctuations II. The entropy budget*, *Phys. Rev. D* **78** (2008) 065045 [0805.0424].

[233] C. Anastopoulos and B.L. Hu, *A Master Equation for Gravitational Decoherence: Probing the Textures of Spacetime*, *Class. Quant. Grav.* **30** (2013) 165007.

[234] M. Fukuma, Y. Sakatani and S. Sugishita, *Master equation for the Unruh-DeWitt detector and the universal relaxation time in de Sitter space*, *Phys. Rev. D* **89** (2014) 064024.

[235] S. Akhtar, S. Choudhury, S. Chowdhury, D. Goswami, S. Panda and A. Swain, *Open Quantum Entanglement: A study of two atomic system in static patch of de Sitter space*, *Eur. Phys. J. C* **80** (2020) 748.

[236] G. Kaplanek and C.P. Burgess, *Qubits on the Horizon: Decoherence and Thermalization near Black Holes*, *JHEP* **01** (2021) 098.

[237] G. Kaplanek and C.P. Burgess, *Hot accelerated qubits: decoherence, thermalization, secular growth and reliable late-time predictions*, *Journal of High Energy Physics* **2020** (2020) 8.

[238] S. Brahma, A. Berera and J. Calderón-Figueroa, *Universal signature of quantum entanglement across cosmological distances*, *Class. Quant. Grav.* **39** (2022) 245002.

[239] C.P. Burgess, R. Holman and G. Kaplanek, *Quantum Hotspots: Mean Fields, Open EFTs, Nonlocality and Decoherence Near Black Holes*, *Fortsch. Phys.* **2022** (2021) 2200019.

[240] S. Brahma, A. Berera and J. Calderón-Figueroa, *Quantum corrections to the primordial tensor spectrum: open EFTs & Markovian decoupling of UV modes*, *JHEP* **08** (2022) 225.

[241] A. Matsumura, *Reduced dynamics with Poincaré symmetry in open quantum system*, 2301.01451.

[242] J.J. Halliwell and T. Yu, *Alternative derivation of the Hu-Paz-Zhang master equation of quantum Brownian motion*, *Phys. Rev. D* **53** (1996) 2012.

[243] D. Boyanovsky, *Effective field theory during inflation: Reduced density matrix and its quantum master equation*, *Phys. Rev.* **D92** (2015) 023527.

[244] T. Colas, J. Grain and V. Vennin, *Benchmarking the cosmological master equations*, *Eur. Phys. J. C* **82** (2022) 1085.

[245] L. Diósi, *A universal master equation for the gravitational violation of quantum mechanics*, *Physics Letters A* **120** (1987) 377.

[246] R. Penrose, *On gravity's role in quantum state reduction*, *Gen. Rel. Grav.* **28** (1996) 581.

[247] S.A. Salcedo, M.H.G. Lee, S. Melville and E. Pajer, *The Analytic Wavefunction*, 2212.08009.

[248] F. Minganti, A. Biella, N. Bartolo and C. Ciuti, *Spectral theory of Liouvillians for dissipative phase transitions*, *Physical Review A* **98** (2018) .

[249] I. Agullo, B. Bonga and P.R. Metidieri, *Does inflation squeeze cosmological perturbations?*, *JCAP* **09** (2022) 032 [2203.07066].

[250] A. Serafini, F. Illuminati and S. De Siena, *Von Neumann entropy, mutual information and total correlations of Gaussian states*, *J. Phys. B* **37** (2004) L21.

[251] T. Colas, J. Grain and V. Vennin, *Four-mode squeezed states: two-field quantum systems and the symplectic group $\mathrm Sp(4,\mathbb R)$*, *Eur. Phys. J. C* **82** (2022) 6.

[252] P.C. Martin, E.D. Siggia and H.A. Rose, *Statistical dynamics of classical systems*, *Phys. Rev. A* **8** (1973) 423.

[253] D. Manzano, *A short introduction to the Lindblad master equation*, *AIP Advances* **10** (2020) 025106.

[254] R. Feynman and F. Vernon, *The theory of a general quantum system interacting with a linear dissipative system*, *Annals of Physics* **24** (1963) 118.

[255] A. Kamenev and A. Levchenko, *Keldysh technique and non-linear sigma model: basic principles and applications*, *Advances in Physics* **58** (2009) 197.

[256] D. Boyanovsky, *Effective Field Theory out of Equilibrium: Brownian quantum fields*, *New J. Phys.* **17** (2015) 063017.

[257] H.-P. Breuer, A. Ma and F. Petruccione, *Time-local master equations: influence functional and cumulant expansion*, quant-ph/0209153.

[258] L. Diósi and L. Ferialdi, *General Non-Markovian Structure of Gaussian Master and Stochastic Schrödinger Equations*, *Physical Review Letters* **113** (2014) .

[259] L. Ferialdi, *Exact Closed Master Equation for Gaussian Non-Markovian Dynamics*, *Physical Review Letters* **116** (2016) .

[260] W. Shi, Y. Chen, Q. Ding, J. Wang and T. Yu, *Positivity Preserving non-Markovian Master Equation for Open Quantum System Dynamics: Stochastic Schrödinger Equation Approach*, 2212.13362.

[261] D. Boyanovsky, *Effective field theory during inflation. II. Stochastic dynamics and power spectrum suppression*, *Phys. Rev. D* **93** (2016) 043501.

[262] G. Kaplanek, C.P. Burgess and R. Holman, *Qubit heating near a hotspot*, *JHEP* **08** (2021) 132.

[263] S. Chaykov, N. Agarwal, S. Bahrami and R. Holman, *Loop corrections in Minkowski spacetime away from equilibrium. Part II. Finite-time results*, *JHEP* **02** (2023) 094 [2206.11289].

[264] S. Chaykov, N. Agarwal, S. Bahrami and R. Holman, *Loop corrections in Minkowski spacetime away from equilibrium. Part I. Late-time resummations*, *JHEP* **02** (2023) 093 [2206.11288].

[265] F. Shibata, Y. Takahashi and N. Hashitsume, *A generalized stochastic liouville equation. Non-Markovian versus memoryless master equations*, *Journal of Statistical Physics* **17** (1977) 171.

[266] N.G. Van Kampen, *A cumulant expansion for stochastic linear differential equations. I*, *Physica* **74** (1974) 215.

[267] N.G. Van Kampen, *A cumulant expansion for stochastic linear differential equations. II*, *Physica* **74** (1974) 239.

[268] G. Kaplanek and E. Tjoa, *Effective master equations for two accelerated qubits*, *Phys. Rev. A* **107** (2023) 012208 [2207.13750].

[269] S. Shandera, N. Agarwal and A. Kamal, *Open quantum cosmological system*, *Phys. Rev. D* **98** (2018) 083535.

[270] S. Prudhoe and S. Shandera, *Classifying the non-time-local and entangling dynamics of an open qubit system*, .

[271] C.A. Brasil, F.F. Fanchini and R.d.J. Napolitano, *A simple derivation of the Lindblad equation*, *Revista Brasileira de Ensino de Física* **35** (2013) 01.

[272] R. Simon, E.C.G. Sudarshan and N. Mukunda, *Gaussian-Wigner distributions in quantum mechanics and optics*, *Phys. Rev. A* **36** (1987) 3868.

[273] G. Lindblad, *On the Generators of Quantum Dynamical Semigroups*, *Commun. Math. Phys.* **48** (1976) 119.

[274] M.-D. Choi, *Completely positive linear maps on complex matrices*, *Linear Algebra and its Applications* **10** (1975) 285.

[275] W. Cottrell, B. Freivogel, D.M. Hofman and S.F. Lokhande, *How to Build the Thermofield Double State*, *JHEP* **02** (2019) 058 [1811.11528].

[276] C. Käding and M. Pitschmann, *New method for directly computing reduced density matrices*, *Phys. Rev. D* **107** (2023) 016005 [2204.08829].

[277] R.S. Whitney, *Staying positive: going beyond Lindblad with perturbative master equations*, *Journal of Physics A Mathematical General* **41** (2008) 175304.

[278] G. Théret and D. Sugny, *Complete positivity, positivity and long-time asymptotic behavior in a two-level open quantum system*, 2304.01748.

[279] H.-P. Breuer, E.-M. Laine, J. Piilo and B. Vacchini, *Colloquium: Non-Markovian dynamics in open quantum systems*, *Rev. Mod. Phys.* **88** (2016) 021002.

[280] P. Ehrenfest, *Bemerkung über die angenäherte Gültigkeit der klassischen Mechanik innerhalb der Quantenmechanik*, *Zeitschrift für Physik* **45** (1927) 455.

[281] M. Dias, J. Frazer, D.J. Mulryne and D. Seery, *Numerical evaluation of the bispectrum in multiple field inflation—the transport approach with code*, *JCAP* **12** (2016) 033 [1609.00379].

[282] J.W. Ronayne and D.J. Mulryne, *Numerically evaluating the bispectrum in curved field-space— with PyTransport 2.0*, *JCAP* **01** (2018) 023 [1708.07130].

[283] D. Werth, L. Pinol and S. Renaux-Petel, *Cosmological Flow of Primordial Correlators*, 2302.00655.

[284] R.N. Raveendran and S. Chakraborty, *Distinguishing cosmological models through quantum signatures of primordial perturbations*, 2302.02584.

[285] T.-H. Lee and J.K. Korbicz, *Bound information in the environment: Environment learns more than it will reveal*, 2304.12222.

[286] D. Barral, M. Isoard, G. Sorelli, M. Gessner, N. Treps and M. Walschaers, *Metrological detection of purely-non-Gaussian entanglement*, 2301.03909.

[287] M. Scandi, P. Abiuso, J. Surace and D. De Santis, *Quantum Fisher Information and its dynamical nature*, 2304.14984.

[288] C. Cheung, T. He and A. Sivaramakrishnan, *On entropy growth in perturbative scattering*, 2304.13052.

[289] D. Boyanovsky, H.J. de Vega, R. Holman and M. Simionato, *Dynamical renormalization group resummation of finite temperature infrared divergences*, *Phys. Rev. D* **60** (1999) 065003.

[290] C.P. Burgess, L. Leblond, R. Holman and S. Shandera, *Super-Hubble de Sitter Fluctuations and the Dynamical RG*, *JCAP* **03** (2010) 033.

[291] D. Green and A. Premkumar, *Dynamical RG and Critical Phenomena in de Sitter Space*, *JHEP* **04** (2020) 064.

[292] F. Gautier and J. Serreau, *Infrared dynamics in de Sitter space from Schwinger-Dyson equations*, *Phys. Lett. B* **727** (2013) 541.

[293] V. Gorbenko and L. Senatore, $\lambda\phi^4$ *in dS*, 1911.00022.

[294] T. Cohen, D. Green, A. Premkumar and A. Ridgway, *Stochastic Inflation at NNLO*, *JHEP* **09** (2021) 159.

[295] S.P. Miao, N.C. Tsamis and R.P. Woodard, *Summing inflationary logarithms in nonlinear sigma models*, *JHEP* **03** (2022) 069 [2110.08715].

[296] R.P. Woodard and B. Yesilyurt, *Unfinished Business in A Nonlinear Sigma Model on de Sitter Background*, 2302.11528.

[297] M. Crossley, P. Glorioso and H. Liu, *Effective field theory of dissipative fluids*, *JHEP* **09** (2017) 095 [1511.03646].

[298] D. Lopez Nacir, R.A. Porto, L. Senatore and M. Zaldarriaga, *Dissipative effects in the Effective Field Theory of Inflation*, *JHEP* **01** (2012) 075 [1109.4192].

[299] P. Creminelli, S. Kumar, B. Salehian and L. Santoni, *Dissipative Inflation via Scalar Production*, 2305.07695.

[300] A. Berera, *Warm inflation*, *Phys. Rev. Lett.* **75** (1995) 3218.

[301] J. Yokoyama and A.D. Linde, *Is warm inflation possible?*, *Phys. Rev. D* **60** (1999) 083509 [hep-ph/9809409].

[302] G. Adesso, S. Ragy and A.R. Lee, *Continuous variable quantum information: Gaussian states and beyond*, *arXiv e-prints* (2014) arXiv:1401.4679.

[303] H. Poincaré, *Sur le problème des trois corps et les équations de la dynamique*, *Acta Mathematica* **13** (1890) 1.

[304] S.A. Sato, U.D. Giovannini, S. Aeschlimann, I. Gierz, H. Hübener and A. Rubio, *Floquet states in dissipative open quantum systems*, *Journal of Physics B: Atomic, Molecular and Optical Physics* **53** (2020) 225601.

[305] T. Mori, *Floquet States in Open Quantum Systems*, 2203.16358.

[306] M.J. Jacquet, S. Weinfurtner and F. König, *The next generation of analogue gravity experiments*, *Phil. Trans. Roy. Soc. Lond. A* **378** (2020) 20190239 [2005.04027].

[307] V.S. Barroso, A. Geelmuyden, Z. Fifer, S. Erne, A. Avgoustidis, R.J.A. Hill et al., *Primary thermalisation mechanism of Early Universe observed from Faraday-wave scattering on liquid-liquid interfaces*, 2207.02199.

[308] V.S. Barroso, C.R.D. Bunney and S. Weinfurtner, *Non-linear effective field theory simulators in two-fluid interfaces*, *J. Phys. Conf. Ser.* **2531** (2023) 012003 [2305.00226].

[309] J.-T. Hsiang and B.-L. Hu, *Fluctuation–dissipation relation for a quantum Brownian oscillator in a parametrically squeezed thermal field*, *Annals Phys.* **433** (2021) 168594 [2107.13343].

[310] P. Creminelli, O. Janssen and L. Senatore, *Positivity bounds on effective field theories with spontaneously broken Lorentz invariance*, *JHEP* **09** (2022) 201 [2207.14224].

[311] S. Brahma, J. Calderón-Figueroa, M. Hassan and X. Mi, *Momentum-space entanglement entropy in de Sitter*, 2302.13894.

[312] A.Y. Kamenshchik, A.A. Starobinsky and T. Vardanyan, *Massive scalar field in de Sitter spacetime: a two-loop calculation and a comparison with the stochastic approach*, *Eur. Phys. J. C* **82** (2022) 345 [2109.05625].

[313] M. Honda, R. Jinno, L. Pinol and K. Tokeshi, *Borel resummation of secular divergences in stochastic inflation*, 2304.02592.

[314] S. Jazayeri and S. Renaux-Petel, *Cosmological bootstrap in slow motion*, *JHEP* **12** (2022) 137 [2205.10340].

[315] G.L. Pimentel and D.-G. Wang, *Boostless cosmological collider bootstrap*, *JHEP* **10** (2022) 177 [2205.00013].

[316] D.-G. Wang, G.L. Pimentel and A. Achúcarro, *Bootstrapping multi-field inflation: non-Gaussianities from light scalars revisited*, *JCAP* **05** (2023) 043 [2212.14035].

[317] E. Pajer, F. Schmidt and M. Zaldarriaga, *The Observed Squeezed Limit of Cosmological Three-Point Functions*, *Phys. Rev.* **D88** (2013) 083502.

[318] Z. Kenton and D.J. Mulryne, *The squeezed limit of the bispectrum in multi-field inflation*, *JCAP* **1510** (2015) 018.

[319] X. Tong, Y. Wang, C. Zhang and Y. Zhu, *BCS in the Sky: Signatures of Inflationary Fermion Condensation*, 2304.09428.

[320] E. Dimastrogiovanni, M. Fasiello, M. Michelotti and L. Pinol, *Primordial Gravitational Waves in non-Minimally Coupled Chromo-Natural Inflation*, 2303.10718.

[321] N. Arkani-Hamed, D. Baumann, H. Lee and G.L. Pimentel, *The Cosmological Bootstrap: Inflationary Correlators from Symmetries and Singularities*, *JHEP* **04** (2020) 105.

[322] E. Pajer, D. Stefanyszyn and J. Supel, *The Boostless Bootstrap: Amplitudes without Lorentz boosts*, *JHEP* **12** (2020) 198.

[323] H. Goodhew, S. Jazayeri and E. Pajer, *The Cosmological Optical Theorem*, *JCAP* **04** (2021) 021 [2009.02898].

[324] J. Armas and A. Jain, *Effective field theory for hydrodynamics without boosts*, *SciPost Phys.* **11** (2021) 054 [2010.15782].

[325] M.J. Landry, *Higher-form and (non-)Stückelberg symmetries in non-equilibrium systems*, 2101.02210.

[326] N.D. Birrell and P.C.W. Davies, *Quantum Fields in Curved Space*, Cambridge University Press, Cambridge (1982), 10.1017/CBO9780511622632.

[327] A. Berera and L.-Z. Fang, *Thermally induced density perturbations in the inflation era*, *Phys. Rev. Lett.* **74** (1995) 1912.

[328] J. Martin, *Inflationary perturbations: The Cosmological Schwinger effect*, *Lect. Notes Phys.* **738** (2008) 193.